LAKE TAHOE ATMOSPHERIC DEPOSITION STUDY (LTADS)

Final Report

September 2006

Prepared for

Lahontan Regional Water Quality Control Board
Nevada Division of Environmental Protection
Tahoe Regional Planning Agency

Prepared by

Atmospheric Processes Research Section
Research Division
Air Resources Board
California Environmental Protection Agency

California Environmental Protection Agency
AIR RESOURCES BOARD

This page blank intentionally.

State of California
AIR RESOURCES BOARD

Staff Report: Lake Tahoe Atmospheric Deposition Study

Date of Release: September 29, 2006

Prepared by:

Leon Dolislager, Research Division
Ash Lashgari, Dr. Env., J.D., Research Division
Jim Pederson, Research Division
Tony VanCuren, Ph.D., Research Division

Reviewed by:

Professor Emeritus Thomas Cahill, UC Davis
Professor Keith Stolzenbach, UC Los Angeles
Professor Gail Tonnesen, UC Riverside
Professor Akula Venkatram, UC Riverside
Professor Anthony Wexler, UC Davis

Eileen McCauley, Ph.D., Manager, Research Division
Richard Corey, Branch Chief, Research Division
Bart E. Croes, P.E., Division Chief, Research Division
Michael H. Scheible, Deputy Executive Officer

Disclaimer

This report was prepared by the staff of the California Air Resources Board. Publication does not signify that the contents reflect the views and policies of the Air Resources Board, nor does mention of trade names or commercial products constitute endorsement or recommendation for use.

Acknowledgements

The Lake Tahoe Atmospheric Deposition Study (LTADS) enlisted the support of many collaborators inside and outside of the Air Resources Board (ARB). The ARB efforts were spearheaded by the Atmospheric Processes Research Section under the direction of Eileen McCauley. Her staff members that contributed substantially to the LTADS include Leon Dolislager, Ash Lashgari, Dongmin Luo, James Pederson, William Vance, and Tony VanCuren. Several students contributed outstanding efforts including Yatiraj Bhumkar, Marisa Bolander, Charles Cozad, Sarah Connelly, Wendy Griffe, Joseph Linn Galan, and Peter Ruibal.

Major supporting contributions were received from other ARB groups, including Ms. Debora Popejoy, manager of the Air Quality Monitoring North Section, and Mr. Michael Fitzgibbon, manager of the Emission Inventory Analysis Section. Their staff members devoted a substantial amount of time and effort in addition to their routine responsibilities to help LTADS be a success. The staff in these groups included Jerry Freeman, Ken Breitwieser, Jamie Vandermast, Joe Cruz, Morris Erickson, and Eric Walton from the Monitoring & Laboratory Division and Ying Hsu from the Planning & Technical Support Division. The Atmospheric Processes Research Section is also extremely grateful for the design, construction, training, audits, trouble-shooting, etc. provided by Steve Mara and Clint Taylor of the Research Division in support of the Two-Week-Sampler program.

Many groups outside of the ARB contributed guidance, funding, and personnel to assist with the LTADS. These groups and primary coordinators included:

1) Lahontan Regional Water Quality Control Board – Dave Roberts and Jacque Landy
2) Tahoe Regional Planning Agency – Jennifer Quashnick
3) Tahoe Research Group – John Reuter
4) Nevada Division of Environmental Protection – Jason Kuchnicki
5) US Environmental Protection Agency – John Kennedy
6) USDA Forest Service – Rich Platt and Lorraine Gerchas
7) Contractors: – DRI, NOAA, UC-Berkeley, UC-Davis, UC-Riverside, UC-San Diego

For being ARB's "eyes, hands, and legs" in the Tahoe Basin by supporting our sampling and monitoring objectives, we especially thank Bob Richards, Scott Hackley, and Patricia Bucknell of TRG, Jennifer Quashnick, Melissa Blake, and Rita Whitney of TRPA, Jacque Landy, Shannon Horgan, Ginnie Chu, and Kim Gorman of LRWQCB. Also, we gratefully acknowledge the cooperation of the following in the siting our monitoring equipment on their property or at their facilities: California State Parks, CARB/MLD (Deborah Popejoy, Dennis Goodenow), Incline Village General Improvement District, Lake Tahoe Airport (Michael Dikun), NASA (Simon Hook), Nevada State Parks (Allen Newberry), Placer County (Robert Costa), SMUD (Chris Moffit), TRPA/California Nature Conservancy (Jennifer Quashnick), TRG (Bob Richards, Geoff Schladow), Thunderbird Lodge (University of Nevada), Timber Cove Properties (Bob Hassett), US Coast Guard, USDA Forest Service (Rich Platt), Wallis Residence (Harvey Wallis family), and Zephyr Cove Resort (Chris Burke).

This page blank intentionally.

Abstract

The world-famous water clarity of Lake Tahoe decreased dramatically during the last several decades. To address the water clarity concern California's Lahontan Regional Water Quality Board (LRWQCB) and the Nevada Division of Environmental Protection (NDEP) are developing the Lake Tahoe Nutrient and Sediment Total Maximum Daily Load (TMDL) for Lake Tahoe. A TMDL is a water quality restoration plan to achieve a specific water quality standard or goal. To meet the need of the TMDL for estimates of atmospheric deposition to Lake Tahoe, the California Air Resources Board (CARB) conducted the Lake Tahoe Atmospheric Deposition Study (LTADS). The primary goal of this study was to quantify the contribution of dry atmospheric deposition to the nitrogen, phosphorus, and particulate matter loading of Lake Tahoe. This report presents CARB's estimates of direct atmospheric deposition to Lake Tahoe. The information resulting from LTADS and similar studies of other pathways inputting materials into Lake Tahoe will be used by the LRWQCB, NDEP, and the Tahoe Regional Planning Agency (TRPA) to develop programs to restore the water clarity of Lake Tahoe.

This page blank intentionally.

Executive Summary

Between the 1960s and the 1990s, the water clarity of Lake Tahoe decreased from 100 feet to 65 feet of visibility into the water at mid-lake. Much of the decreased clarity may be due to increased algal growth. To address the water clarity concern California's Lahontan Regional Water Quality Board (LRWQCB) and the Nevada Division of Environmental Protection (NDEP) are developing the Lake Tahoe Nutrient and Sediment Total Maximum Daily Load (TMDL) for Lake Tahoe. A TMDL is a water quality restoration plan designed to determine the ability of a body of water to accept contaminants without resulting in a reduction in water quality. Materials that can adversely impact water clarity enter the Lake via water runoff, groundwater seepage, shoreline erosion, on-lake activities, and direct atmospheric deposition.

To meet the need of the TMDL for estimates of atmospheric deposition to Lake Tahoe, the California Air Resources Board (CARB) conducted the Lake Tahoe Atmospheric Deposition Study (LTADS). The primary goal of this study was to quantify the contribution of dry atmospheric deposition to the nitrogen (N), phosphorus (P), and particulate matter (PM) loading of Lake Tahoe. Of specific interest are N and P that serve as nutrients to phyto- and zoo-plankton growth and the inert component of PM that scatters or absorbs light. This effort entailed measurement of these materials in the air over the lake and estimation of the airborne material that deposits directly onto the lake surface.

This report presents CARB's methods and estimates of dry and wet atmospheric deposition of N, P, and PM directly to the surface of Lake Tahoe. Potential indirect atmospheric input to the lake (i.e., deposition to the watershed and subsequent transfer to the water) was part of the watershed modeling effort and not directly addressed by LTADS. The LRWQCB, NDEP, and the Tahoe Regional Planning Agency (TRPA) will use the information resulting from LTADS and the other research programs to develop programs to restore the water clarity of Lake Tahoe.

LTADS was a multi-million dollar effort with contributions of funds and effort by the United States Environmental Protection Agency, USDA Forest Service, Tahoe Research Group (TRG), NDEP, LRWQCB, and TRPA, as well as CARB's Monitoring & Laboratory, Planning & Technical Support, and Research Divisions. Research groups from the Berkeley, Davis, Riverside, and San Diego campuses of the University of California, the Desert Research Institute (DRI), and the National Oceanic & Atmospheric Administration also contributed their expertise. Planning for the study began in the Fall of 2001. By the end of 2002, several new air quality or meteorological monitoring sites had been set up in the Lake Tahoe Basin and at Big Hill, a well-exposed site on the western slope of the Sierra Nevada to the west-southwest of Lake Tahoe. Collection of gaseous and particulate ambient air quality and meteorological data continued through the end of 2003 at all sites and a subset of parameters at some sites into the spring of 2004. Air quality and meteorological measurements have routinely been made for many years at a limited number of locations in the Tahoe Basin and enhanced sampling has occurred during short-term field studies. However, the combined sampling efforts

of the ARB, TRG, TRPA, DRI, etc. during LTADS resulted in a large set of contemporaneous air quality and meteorological data representing conditions in the Lake Tahoe region during four seasons. In addition, to support the development of an improved emission inventory for the Tahoe Basin, studies were conducted to measure emission activity factors critical sources such as road dust and smoke (from residential and prescribed wood burning).

The LTADS approach for estimating dry atmospheric deposition to Lake Tahoe was based on seasonal-average N, P, and PM mass concentrations being apportioned, based on mass, to hourly concentrations, which then were merged with day- and hour-specific deposition velocities to provide deposition estimates. The wet deposition estimates were based on a simple conceptual model that used seasonal air quality concentrations in four quadrants of the Tahoe Basin, precipitation frequency, and various assumptions regarding mixing heights, washout efficiency, etc. The estimate of wet deposition is for the year 2003, which allows direct comparison with field measurements obtained with surrogate surface deposition samplers and with the LTADS dry deposition estimate. However, precipitation frequency data indicate that the number of days with measurable precipitation were greater than normal during 2003, although the total precipitation amounts were less than normal. *Based on the precipitation frequency in 2003 compared to the climatological norm, wet deposition in a normal year would be about 70% of the 2003 estimate presented in this report.*

The LTADS estimates of annual direct atmospheric deposition of N, P, and PM to Lake Tahoe (central with upper and lower bounds) are presented for both dry and wet deposition in **Tables ES-1 and ES-2**, respectively. CARB staff prepared these final estimates of direct atmospheric deposition to Lake Tahoe based on comments from peer reviewers and additional refined analyses. The updated analyses included improved formulation of the deposition velocity equations and improved characterization of depletion of PM over the Lake, etc. The seasonal deposition estimates (summarized in **Figure ES-1**) and the characterization of the emission sources and atmospheric processes at work in the Tahoe Basin will help to guide the development of potential control measures to reverse the declining water clarity for which Lake Tahoe is famous. Background information, approaches, assumptions, and analyses leading to these atmospheric deposition estimates are presented primarily in Chapters 4 and 5 of this report.

Table ES-1. LTADS Estimates of Annual Dry Atmospheric Deposition to Lake Tahoe
(metric tons/year)

Pollutant	Lower Bound	Central Estimate	Upper Bound
N (NH_3, NH_4^+, HNO_3, NO_3^-)	70	120	170
P (P, PO_4^{-3})	1	2	3
PM (in 3 size ranges)	360	590	860

Table ES-2. LTADS Estimates of Annual Wet Atmospheric Deposition to Lake Tahoe*
(metric tons/year)

Pollutant	Lower Bound	Central Estimate	Upper Bound
N (NH_3, NH_4^+, HNO_3, NO_3^-)	30	70	150
P (P, PO_4^{-3})	0	1	2
PM	70	165	315

* The wet deposition estimates are based on a simple analysis with realistic but unvalidated assumptions.

Figure ES-1. LTADS Central Estimates of Seasonal Total Atmospheric Deposition to Lake Tahoe
(metric tons/year)*

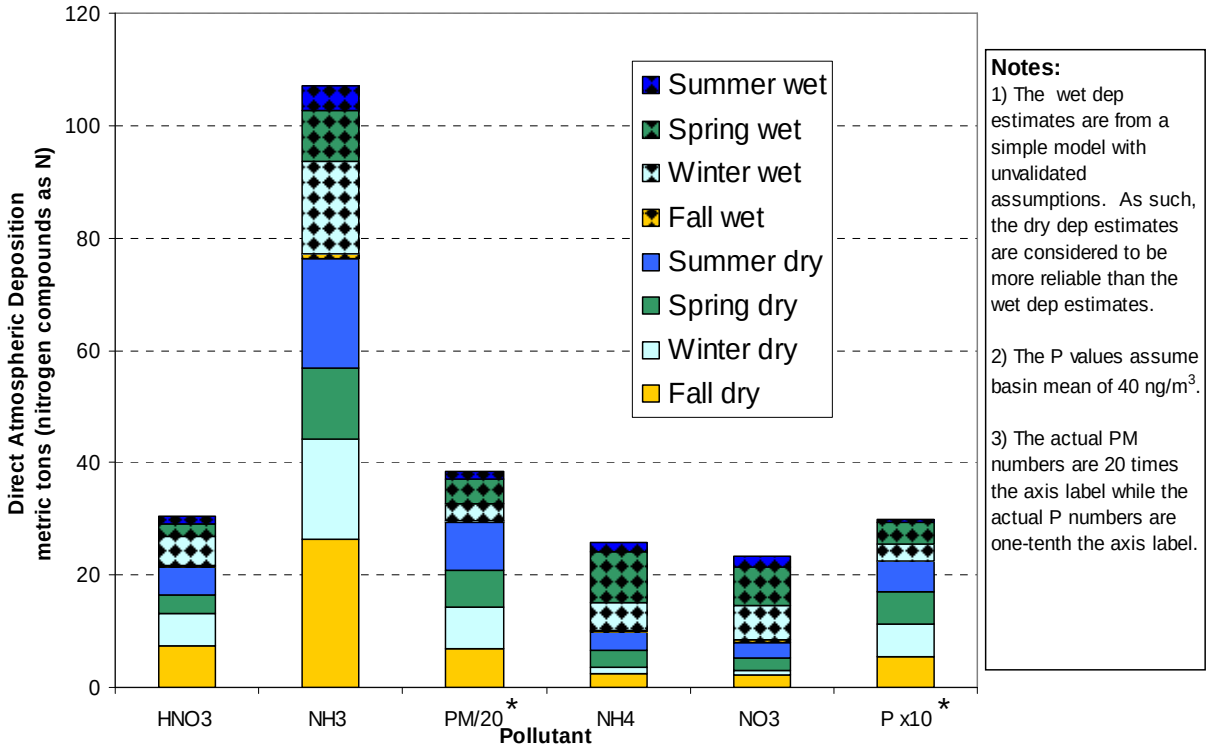

* Note adjustment to PM and P values. Actual PM dep is 20 times greater and actual P dep is 10 times less than indicated on Y-axis.

The LTADS total annual atmospheric deposition estimate for nitrogen is comparable with previous deposition estimates from water-based surrogate surface deposition samplers operated by TRG.

Due to the difficulty and large uncertainties associated with the measurement of phosphorus in particulate matter, the CARB analysis provides phosphorus deposition estimates that are conservatively based on assuming a spatially and temporally constant phosphorus concentration of 40 ng/m^3. The central estimate from LTADS of total annual phosphorus deposition to the Lake is less than that based on surrogate surface samplers operated by TRG. A factor in the discrepancy between the CARB and TRG P deposition estimates is that CARB's air quality measurements do not include the very largest particles, such as those associated with soil, plant detritus, and pollen near sources, which the TRG surrogate surface deposition sample would include. The phosphorus measurements from TRG's dry bucket samples, when the field notes indicated pollen was present, suggest that natural sources may be a significant source of phosphorus input to the lake. With adjustment for these highly impacted samples, the TRG estimate of total phosphorus deposition is comparable to, but still higher than, the LTADS estimate.

The LTADS estimate for the atmospheric deposition of PM is the first ever developed for Lake Tahoe. The estimates of direct atmospheric deposition of PM mass to the lake include three size fractions: PM_fine (diameter < 2.5 µm), PM_coarse (2.5 µm < diameter < 10 µm), and PM_large (diameter > 10 µm). The estimates are for atmospheric PM. *Because about 20% of the PM mass is water soluble, it will be necessary for water quality scientists to account for subsequent losses and changes in particle size and composition prior to considering their optical effects on water clarity*.

The following list summarizes the major findings from LTADS. Some findings are new but many are confirmatory of previous measurements, hypotheses, conceptual models, and findings.

1) Atmospheric deposition is difficult to estimate precisely. It is somewhat reassuring that different approaches have yielded comparable results for the direct atmospheric deposition of biological nutrients in 2003, nitrogen (~200 metric tons) and phosphorus (~5 metric tons). The wet/dry bucket (surrogate surface) sampler at the Wallis Tower site is not a representative sampling location due to extensive and nearby presence of trees.
2) About three-fourths of the deposited N is in gaseous form (~150 metric tons in 2003), primarily ammonia but also nitric acid. The differences in ammonia concentrations measured at two nearby sites but on opposite sides of Highway 50 indicate that motor vehicles could be a major local source of ammonia emissions.
3) Phosphorus is very difficult to measure at the low concentrations (and with interfering pollutants) found at Lake Tahoe.
4) The mass of atmospheric PM directly deposited into Lake Tahoe in 2003 was conservatively estimated at ~1200 metric tons (includes soluble ions).
5) PM larger than 10 µm tends to deposit near its sources as evidenced by the small difference in ambient PM10 and TSP concentrations at sites not impacted by local sources and by road dust experiments making particle count measurements at various distances from a roadway source.

6) PM2.5 concentrations tend to be relatively low and uniform around the Basin while larger particles exhibit a much larger spatial and diurnal variation associated with population and motor vehicle activity.
7) Uncertainties remain regarding transport of materials aloft, above the surface layer. Ozone data collected during LTADS confirm that surface layer transport of ozone and other reactive species (e.g., HNO_3, NH_3, nitrates) is infrequent and of relatively low magnitude due to meteorological processes (e.g., wind flow reversals, transport speeds, mountain barrier, limitations on vertical mixing, deposition, chemical reactions). However, limited measurements of conditions aloft by an aircraft indicate an enhanced background level of ozone and a relatively uniform vertical distribution of ammonia concentrations.

The data, estimates, conclusions, and implications from the Lake Tahoe Atmospheric Deposition Study are now informing the development of the Lake Tahoe Water Clarity TMDL by the California and Nevada water quality planners as well as the environmental threshold planning by the Tahoe Regional Planning Agency.

This page blank intentionally.

Table of Contents

Appendices

Report Authors/Contacts

Executive Summary – Eileen McCauley, Leon Dolislager

Chapter 1 (Background) – Leon Dolislager, Ash Lashgari

Chapter 2 (Atmospheric Processes) – Leon Dolislager, Jim Pederson

Chapter 3 (Data Quality and Ambient Concentrations) – Ash Lashgari, Leon Dolislager

Chapter 4 (Dry Deposition) – Jim Pederson

Chapter 5 (Wet Deposition) – Leon Dolislager

Chapter 6 (Air Pollution Transport) – Ash Lashgari

Chapter 7 (Characterization of PM and Nutrient Sources) – Tony VanCuren, Leon Dolislager, Ash Lashgari

Chapter 8 (Conclusions and Recommendations) – Eileen McCauley, Ash Lashgari

Appendix A (Comparison of Surrogate Surface Methods of Measuring Dry Deposition) – Leon Dolislager

Appendix B (Analysis of Historical Aerosol Data) – Tony VanCuren

Appendix C (Comparison of PM Sampling Methods) – Leon Dolislager

Appendix D (Additional Meteorological Data Summaries) – Leon Dolislager

Appendix E (Java Code used in Dry Deposition Model) – Jim Pederson

Appendix F (Details of Calculating Monin-Obhukov Length) – Jim Pederson

Appendix G (Summary of UC Peer Review Comments on Work Plan with Staff Responses) – Leon Dolislager

Appendix H (Summary of UC Peer Review Comments on Interim Report with Staff Responses) – Leon Dolislager

Appendix I (UC Peer Review Comments on Draft Final Report) – Leon Dolislager

Appendix J (Summary of UC Peer Review Comments on Final Report with Staff Responses) – Leon Dolislager and Jim Pederson

Appendix K (Additional Reading and Resources) – Leon Dolislager

Appendix L (Estimates of Dry Deposition without Depletion over Lake Tahoe) – Jim Pederson

This page blank intentionally.

List of Figures

List of Tables

This page blank intentionally.

1. Background

1.1 Context

Lake Tahoe is a beautiful lake ringed by mountains. The lake surface covers 191 square miles (501 square kilometers) and is at an elevation of 6225 feet (1886 meters) MSL. The average water depth is 1000 feet and the maximum depth is 1645 feet, making it the 2nd deepest lake in the U.S. and the 10th deepest in the world. This unique alpine lake is world-renowned for its rich blue color. The unique color of the lake is due to its high altitude and pristine water clarity. At one time, objects more than 100 feet deep could be seen through the water. The water clarity is so good because 40% of the precipitation within the Lake Tahoe watershed falls directly on the Lake; furthermore, the remaining precipitation in the basin drains through granitic soil, which is relatively nutrient sterile and filters material flowing in subsurface water toward the streams and eventually the Lake.

However, the water clarity of this once pristine lake has been declining (see **Figure 1-1**). Between the mid-1960s and the mid-1990s, the water clarity decreased from 100 feet to 65 feet, a decrease averaging over one foot per year. Data for recent years suggest an improvement but additional study is needed to clearly understand the factors impacting water clarity and to ensure environmental thresholds are attained.

Biologically accessible forms of phosphorus (P) and nitrogen (N) contribute to algal growth, which is a major factor in the decline of water clarity in most bodies of water. The sources of these nutrients entering Lake Tahoe are not easily differentiated and the amounts entering via air or water are not well quantified. Water runoff containing fertilizers, seepage of contaminated groundwater into the Lake, and direct atmospheric deposition are all likely contributors to the phosphorus and nitrogen loading of Lake Tahoe. Estimates prior to LTADS indicated that about half of the total N loading and one-quarter of the P loading to the Lake enters via atmospheric deposition (**Table 1-1**). Note however, that the table does not indicate the relative certainty of the individual estimates or of the total loading. Thus, there are no reported error bounds on the percentages assigned to the various media and sources.

More recently, the Tahoe Research Group (TRG), which has studied Lake Tahoe during the last five decades, also identified insoluble (inert) particles as a significant year-round contributor to the reduced water clarity of Lake Tahoe. Because of the growing concern about the potential impact of particles, LTADS featured a diverse and comprehensive measurement program related to the atmospheric deposition of particles in addition to nutrients.

Likely atmospheric sources of PM and nutrients (N and P) include smoke from planned and unplanned vegetative fires, wood stoves, and fireplaces; vehicle exhaust, roadway dust (e.g., dirt, sanding material), and potential transport from global and regional sources (e.g., Asian dust, ammonia and fine particles from the Central Valley). These emissions may be in the form of PM or gases that deposit directly to the Lake or gases that convert to PM in the atmosphere and then deposit.

Figure 1-1. Lake Tahoe Water Clarity Trend.

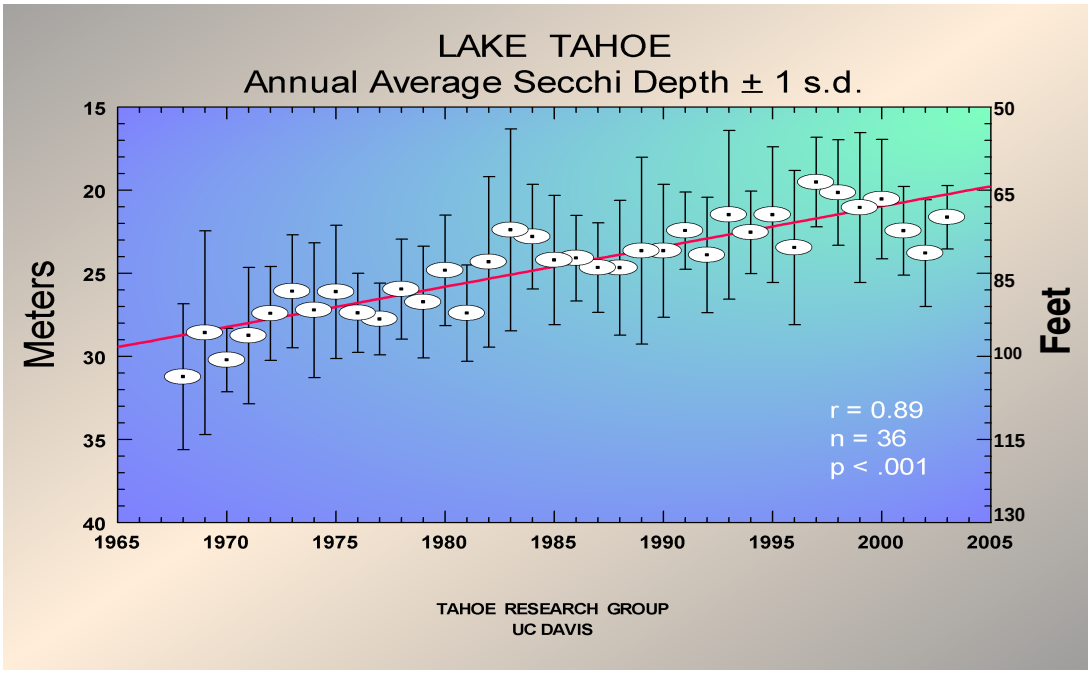

The California Air Resources Board (CARB) is collaborating with the Tahoe Regional Planning Agency (TRPA), the US Department of Agriculture Forest Service (USFS), the US Environmental Protection Agency (USEPA – Region IX) to support the Lahontan Regional Water Quality Control Board (LRWQCB) and the Nevada Division of Environmental Protection (NDEP) in the development of the Lake Tahoe Nutrient and Sediment Total Maximum Daily Load (TMDL). The CARB effort focused on the contribution of dry atmospheric deposition directly to the Lake to the total loading of nutrients and sediments to Lake Tahoe. The atmospheric nutrients can be deposited as gases, aerosols, or soluble ions in rain and snow. The particles by definition are deposited as aerosols but many particles include ionic salts that dissolve when in contact with water. A goal of LTADS was to address the relative contribution of local (within basin) and regional (transport into the basin) sources of nutrients and PM. A watershed analysis (separate from LTADS) will provide information on the atmospheric deposition to the Lake Tahoe watershed where runoff from rain storms and snow melt contribute to the total atmospheric contribution of the nutrients and PM loading to the Lake. CARB staff developed a research plan, which was reviewed by experts in the University of California, to address, within the constraints imposed by the regulatory timeline and the funding available, the informational needs in the Basin.

Table 1-1. Pre-LTADS matrix of annual nutrient loading to Lake Tahoe (metric tons).

INPUTS	NITROGEN	PHOSPHORUS
Atmospheric Deposition	234 (56%)	12 (26%)
Stream Loading	82 (19%)	13 (28%)
Direct Runoff	42 (10%)	16 (33%)
Groundwater	60 (14%)	4 (8%)
Shoreline Erosion	2 (<1%)	2 (4%)
TOTAL	419 (100%)	47 (100%)

Source: Murphy and Knopp (2000)

Note: The LTADS analysis summarized in this report results in the following updated central estimates for atmospheric deposition of N & P: 185 and 6 metric tons, respectively, or approximately 30% and 50% lower than the earlier estimates based on surrogate surface samplers. The LTADS direct deposition estimates have uncertainties characterized by upper and lower bounding assumptions. The lower and upper bounds of deposition are 100 to 320 metric tons for N and 2 to 12 metric tons for P. The revised percent contribution by atmospheric deposition will depend on how the inputs from the other pathways change due to the recent research.

The specific informational needs of the LRWQCB and NDEP for the TMDL (and related information needed for the TRPA 20-year Environmental Improvement Program plan update) addressed by this report are: 1) improved estimates of the annual and seasonal loading of phosphorus, nitrogen, and particulate matter from atmospheric deposition directly to Lake Tahoe (including confidence levels), 2) improved attribution of the in-basin and out-of-basin contributions of these materials, and 3) assessment of the effect of ozone concentrations on forest health.

The air quality improvement that has occurred in the Tahoe basin during the last two decades is summarized in **Table 1-2**. As shown, CO concentrations have declined over 80%, NOx concentrations have declined about 25%, and PM10 concentrations have declined over 30%. Ozone concentrations have remained steady near the California ambient air quality standards for ozone.

Table 1-2. Maximum ambient air quality concentrations observed in the Lake Tahoe Air Basin (1980 – 2000).

Pollutant (avg. period, units)	1980	2000	Δ (%)
CO (8-hr, ppm)	13.7	2.1	-85
O_3 (1-hr, ppm)	0.089	0.089	0
O_3 (8-hr, ppm)	0.080	0.079	-1
NO_2 (1-hr, ppm)	0.077	0.058	-25
NO_2 (annual, ppm)	0.015	0.011	-27
PM10 (24-hr, $\mu g/m^3$)	95	50	-47
PM10 (annual, $\mu g/m^3$)	26.0	17.6	-32

1.2 Total Maximum Daily Load Concept for Water Clarity

The LRWQCB and NDEP are working together to develop the Lake Tahoe Nutrients and Sediment TMDL to protect and restore the water clarity of Lake Tahoe (see index of activities - http://www.swrcb.ca.gov/rwqcb6/TMDL/Tahoe/Tahoe_Index.htm). A TMDL, or Total Maximum Daily Load, is a watershed-based tool for eliminating water quality impairments. A TMDL is the amount of a specific pollutant that a specific body of water can receive and maintain applicable water quality standards. TMDLs are the sum of the allowable loads of a single pollutant from all contributing point and non-point sources. They include a margin of safety and consider seasonal variations. They provide an analytical basis for planning and implementing pollution controls, land management practices, and restoration projects needed to protect water quality. States are required to include approved TMDLs and associated implementation measures in State water quality management plans or basin plans. Because of this responsibility, each state, along with their associated territorial water quality agencies, is responsible for implementing the TMDL process.

The purpose of a TMDL is to identify and mitigate all significant stressors that cause, or threaten to cause, impairment of the uses of a water body. To this end, a TMDL:

1. Identifies “Quality Limited Waters”. Currently, California has almost 700 water bodies on this list; almost 100 of these are in the Lahontan region.
2. Establishes “Priority Waters and Watersheds”. Lake Tahoe is considered a Priority Watershed.
3. Outlines a plan to achieve water quality standards. A TMDL is a quantitative assessment of water quality problems, contributing sources, and load reductions or control actions needed to restore and protect individual water bodies.

A TMDL will determine the causes and extent of impairment. It creates a flexible assessment and planning framework for identifying load reductions or other actions needed to attain water quality standards. A typical TMDL will account for all individual waste load allocations for point and non-point sources, natural background pollutants, and an appropriate margin of safety.

Typical components of a TMDL include the following:

Problem Statement: A description of the waterbody/watershed setting, beneficial use impairments of concern, and pollutants or stressors causing the impairment.

- **Numeric Target(s)**: For each stressor addressed in the TMDL, appropriate measurable indicators and associated numeric target(s) based on numeric or narrative water quality standards which express the target or desired condition for designated beneficial uses of water.

Loading Capacity Estimate: An estimate of the assimilative capacity of the water body that assures attainment of the standards for the pollutant(s) of concern.

Source Analysis: Identifies the amount, timing, and origin of the pollutant. It includes point, non-point and natural sources. Each source is then evaluated to assess its contribution to the problem. Analytical tools are often used for this including Geographic Information System (GIS) overlays and models, and watershed landscape models.

Linkage Analysis: Establishes the cause-and-effect relationship between the selected targets and the identified pollution sources. This is the "heart" of the analytical discussion.

Load Allocations: Allocation of allowable loads or load reductions among different sources of concern. These allocations are usually expressed as waste load allocations to point sources and load allocations to non-point sources. Allocations can be expressed in terms of mass loads or other appropriate measures. The TMDL equals the sum of allocations and cannot exceed the loading capacity.

Margin of Safety: This is similar to all health and safety rulemaking. A margin of safety must be allowed. This is provided as part of the load allocated to account for uncertainties of models and analytical procedures used. This can be done explicitly, i.e., 10% below target, or implicitly through conservative assumptions.

Implementation Elements: Description of best management practices, point source controls or other actions necessary to implement TMDL. Usually a plan describing how and when necessary controls and restoration actions will be accomplished, and who is responsible for implementation. Other issues of the plan address waste discharge prohibitions; state/local laws, regulations, and ordinances; and local/regional watershed management programs.

Monitoring Plan: Plan to monitor effectiveness of TMDL and schedule for reviewing and (if necessary) revising TMDL and associated implementation elements.

Complete TMDL programs include implementation plans and require basin plan amendments. These amendments would comply with requirements of a scientific peer review, CEQA, public participation and approvals by the regional water board, SWRCB, Office of Administrative Law, and U.S. EPA.

The Lake Tahoe Nutrients and Sediment TMDL will set "the number" for allowable loads, determine sources by category and general location, outline general options for load reductions, and give direction and act as the basis for all water quality related plans in the Basin (208 Plan, Forest Plan, etc.). This LTADS report supports the development of the Tahoe TMDL program by addressing critical informational needs regarding direct atmospheric deposition to Lake Tahoe.

1.3 Atmospheric Deposition Estimates

Understanding the impacts of air quality on nutrient loading of the Lake requires quantification of the deposition of both particles and gases under both wet and dry conditions. To be most useful, the estimates must be accompanied by a measure of their numerical uncertainty. The goal is to provide the rate of nutrient loading (total mass entering the lake surface per unit time, e.g., kg/month). But the rate of deposition to the Lake is highly variable by location, time of day, season, and likely year.

Particles and soluble gases are both removed by wet deposition. Compared to dry deposition, wet deposition is relatively easy to observe and quantify, subject only to the ability to measure the volume of precipitation and it's chemical composition. Two obvious simple concerns are that 1) some methods and siting situations will not provide representative volume collection and 2) contamination of samples during collection must be considered.

On the other hand, dry deposition is much more difficult to measure directly. Quantification by indirect methods is also complicated. Indirect methods relate the amount deposited to the observed concentrations, meteorological conditions, and surface characteristics. For quantification of dry deposition, a suite of approaches is possible. Convergence of the results from different approaches provides confidence in the results.

Some definitions are needed for meaningful discussion. The term deposition rate defines the nutrient loading at a specific location and time. Deposition rate has units of mass, area, and time, e.g., grams/m^2/second. The deposition rate of a specific substance divided by its atmospheric concentration is simply the deposition rate normalized for concentration. Because the deposition rate divided by concentration has units of velocity (distance/time; e.g., m/sec) it is known as the deposition velocity. The deposition velocity depends on the substance of interest in the atmosphere and the underlying surface. In addition the deposition velocity usually depends strongly on the meteorological conditions.

When considering larger particles of specified size and density we also calculate a settling velocity, which is the rate of fall for that particle resulting from the balance between frictional and gravitational forces. Although deposition and settling velocities may share common units (e.g., cm/second) a clear distinction should be made between these two terms. Deposition velocity and settling velocity are generally not equivalent nor are they physically analogous. Deposition rates and deposition velocities change with time and location because they depend strongly on many environmental factors, including the efficiency of the surface for removal of the substance of interest and the degree of meteorological mixing that either permits or denies surface contact for air originating from a particular height above ground level. Settling velocity however, is relatively insensitive to environmental conditions, depending mainly on particle size and the density difference between the particle and the air.

Observation (direct measurement) of deposition (and parameters used to estimate deposition) requires considerable care in site selection and choice of instrument heights. Spatial homogeneity of the surface over sufficient upwind fetch is essential. The best opportunity for direct measurements will be over water or at the water's edge during periods of onshore wind direction (airflow from the Lake toward land). For large bodies of water sufficient fetch is available for the development of breaking waves and spray. This is significant, because the presence of breaking waves and spray constitutes an entirely different regime for deposition as compared to a smooth water surface. (Jielun Sun, 2001 personal communication)

Deposition velocities are highly variable with meteorological conditions and thus they will vary with time of day as do concentrations of most chemical species of interest. For that reason, concentrations and meteorological parameters used to estimate deposition rates were measured or estimated on an hourly basis to the extent possible. The Lake itself provides some benefits to the calculations because it provides 1) a long upwind and spatially homogeneous fetch, and 2) well-defined surface temperatures for contrast with hourly air temperatures in the estimation of atmospheric stability.

The California Acid Deposition Monitoring Program (Watson et al., 1991) provided deposition estimates for a variety of locations in California (Blanchard et al., 1996). A summary of dry deposition estimates of selected nitrogenous species during 1988-1992 is shown in **Figure 1-2**. The results for Yosemite and Sequoia were anticipated to be most likely to represent the situation at Lake Tahoe because they are sites in the Sierra Nevada and include local effects as well as regional transport from upwind urban areas. At these two sites, the nitrogen deposition is primarily from nitric acid (HNO_3) and ammonia (NH_3) and totals less than 2 kilograms/hectare/year (about half of the deposition estimate shown in **Figure 1-2**). The LTADS results indicate that ammonia (NH_3) is the major nitrogen source in the Tahoe Basin.

Figure 1-2. Annual Dry Deposition Rates of Major Nitrogenous Species in California. (1988-1993)
(based on *Blanchard et al.*, 1996)

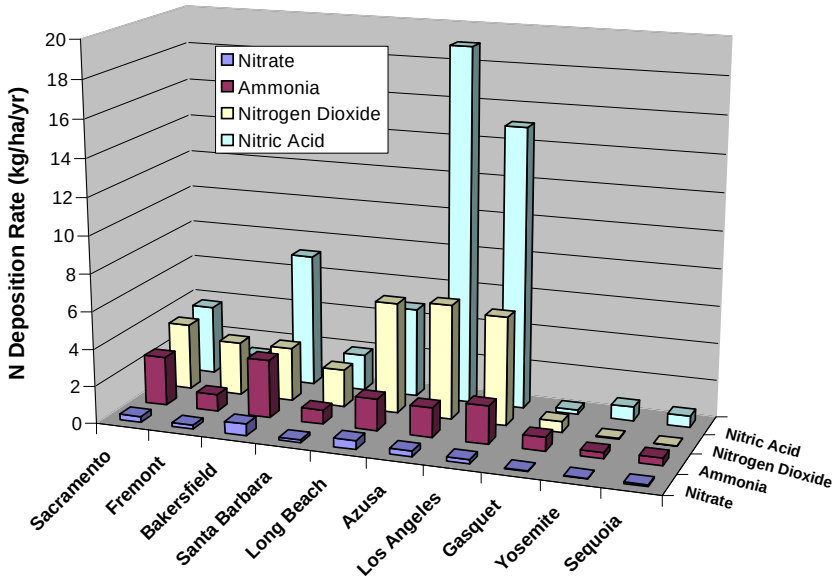

1.4 LTADS Objectives

The primary goal of the Lake Tahoe Atmospheric Deposition Study (LTADS) was to quantify the atmospheric dry deposition of substances thought to be significant to declining water clarity of Lake Tahoe. The LTADS focus was on direct deposition to Lake Tahoe. Because the Lake Tahoe occupies a large portion (~60%) of the watershed, the soils are nutrient deficient, and much of the precipitation falls as snow (slow runoff), it is anticipated that direct deposition predominates over the indirect deposition of material. The LTADS measurements made to support quantification of dry deposition included observations of ambient concentrations of particles and gases having water clarity implications in the air near and over the Lake and environmental variables needed for calculating the temporally and spatially resolved deposition velocities for these substances to the Lake. Because the prior estimates of wet and dry deposition with surrogate surfaces did not include particulate matter, which is a significant water clarity concern, staff used data collected during LTADS and a simple conceptual model to estimate direct wet deposition to Lake Tahoe. This enabled quantification of total PM (also sized in 3 bins) deposition directly to Lake Tahoe. The reader is reminded that deposition estimates via models or surrogate surfaces have significant uncertainties and unknowns that mean even the best deposition estimates probably have a precision no better than about 50%.

A secondary goal was to provide qualitative information on the major sources of emissions influencing pollutant concentrations in the air and subsequent atmospheric deposition. Identification and characterization of sources of atmospheric deposition

required using additional types of information and inferences beyond those solely needed to quantify deposition. The data analysis process for source identification and source characterization is recursive – the historical data establish a regional-decadal context and portray a conceptual image of the major sources and processes controlling deposition to Lake Tahoe. Building on this historical resource, the LTADS data (both routine and special measurements) refined the understanding of the spatial and temporal dynamics of atmospheric processes influencing air quality near and within the Tahoe basin.

The challenge for LTADS was to balance available resources and multiple time sensitive regulatory informational needs of TRPA and LRWQCB with respect to air quality and atmospheric deposition of phosphorus, nitrogen, and particulate matter to Lake Tahoe. After quantification of deposition of these materials, the foremost general need was for analyses of the meteorological and air quality measurements useful for better understanding the atmospheric processes at work in the Tahoe Basin and estimating the contributions to the N, P, and PM deposition in the LTAB from local sources relative to the regional and global sources creating background concentrations.

The general objectives were:

1. To reach a technical consensus on the monitoring/sampling methods sufficient and necessary to meet the foremost informational needs within the constraints of available resources and the schedules (determined by regulatory timelines) for use of the results by TRPA and the LRWQCB.

2. To represent conditions under all seasons by enhancing the monitoring/sampling network for at least a one-year study period and to do so in a manner that would enable scientists to collect and analyze the appropriate emissions, meteorological, and air quality data to meet the following priorities:
    - Quantify deposition of N, P, and PM to Lake Tahoe at least seasonally,
    - Qualitatively refine out-of-basin and in-basin contributions to the seasonal loading, and
    - Qualitatively identify and characterize the source categories; and

3. To assess forest damage possibly related to air quality (i.e., ozone and nitric acid).

The specific approaches taken to implement the strategies evolved in the context of new information regarding specific needs, limitations, and resources. There is always tension between an ideal approach with unlimited time and resources and the prioritization and sacrifices necessitated by fiscal and staffing constraints. However, in the case of LTADS the schedule was a major constraint. A phased approach to monitoring and analysis that would sequentially address the priorities listed above was not feasible because neither the funding mechanisms nor the schedule of regulatory informational needs would support a lengthy program.

1.5 LTADS Design and Rationale

Although the regulatory program is called a total maximum daily loading plan, the cumulative annual (not the daily) loading of the Lake is thought to control the trend of water clarity in Lake Tahoe. Thus, improved estimates of the annual atmospheric deposition were requested of LTADS for input into the lake clarity and watershed models used to estimate the effects of the various emission sources on Lake. A difficulty with developing annual and seasonal loading estimates is that potentially significant emissions sources do not contribute in a constant or uniform manner, either spatially or temporally. Furthermore, meteorological conditions that affect the deposition of these emissions are not constant. Thus, an episodic field study to characterize deposition would be fraught with uncertainties about the representativeness of the specific episodes studied and how that information can be applied to generate an annual estimate.

Ideally, to address the deposition issues, one would prefer hourly-resolved air quality and meteorological data because the emission sources and meteorological conditions vary seasonally and diurnally. However, representing the chemical nature and sizes of particles with both spatial and temporal resolution sufficient to represent individual source types, physical and chemical transformation of the material, and meteorological redistribution for an annual study would be extremely expensive and even with funding would not be logistically feasible because of limitations in instrumentation and laboratory analytical capabilities. In addition, the generally clean air in the Tahoe Basin challenges the detection limits of many monitoring/sampling methods. The combination of low concentrations, harsh sampling conditions (e.g., wind, snow, cold temperatures) and the desire for fine temporal resolution created a unique field study challenge in the Tahoe Basin.

To address the particulate data needs, the CARB strategy was to make the Two-Week-Sampler (TWS) the cornerstone of its sampling program. The TWS has a simple design, has participated in previous field studies, and has been validated against federal reference methods (Taylor et al., 1998; Motallebi et al., 2003). The TWS can continuously collect PM samples in three size ranges (PM2.5, PM10, and TSP) during a two-week period. With the long sampling period, it is practical to collect samples for laboratory analysis throughout the one-year field study. By essentially sampling every hour of every day, the TWS eliminates the uncertainties and complexities raised by intermittent sampling and extrapolating to estimate total seasonal and annual loadings of pollutants. By using a two-week-sampler, ARB sacrificed temporal resolution of concentrations for the sake of collecting samples characterizing an entire year and avoided the problems associated with episodic sampling, while staying within budgetary constraints for laboratory analyses.

One difficulty associated with the use of the TWS was its relatively low flow rate of about 1.3 liters/minute, requiring relatively strict tolerances on flow rate to avoid invalidation of samples. Icing or heavy loading of particles on the filter could restrict air flow and thereby invalidate a sampling period. Given the relatively pristine air quality at Lake Tahoe except during periods of local stagnation, heavy loading would rarely be a

problem. However, on the other extreme, at times sufficient mass might not be collected to ensure detection or quantification of some elements/compounds. This was a problem for some species, including phosphorus, during LTADS.

Another limitation associated with the use of the TWS is that the sampling period spans the much shorter variations in source activities and in meteorological processes. Thus, each sample represents a gross average of the many details needed to investigate atmospheric processes and to isolate the major sources of emissions contributing to the presence and deposition of materials adversely impacting the water clarity of Lake Tahoe. To refine the TWS measurements temporally, collocated continuous Beta Attenuation Monitors (BAM) provided hourly total mass measurements of PM2.5, PM10, and TSP at multiple sites. Site-specific hourly BAM measurements were averaged over each season to provide a seasonal diurnal mass profile. Assuming the relative mix of emission sources does not change significantly during the two-week period, the chemical species can be prorated using the diurnal profiles and the hourly data can be compared with the meteorological data to improve deposition estimates and implicate potential source areas and categories. Knowing the average composition in each two-week period and the daily and diurnal variations in total mass, and the concurrent meteorology will enable refined estimates of seasonal loading and the relative contribution of different sources.

Time-and size-resolved ambient concentrations are combined with continuous meteorological data to refine estimates of the temporal variations in deposition amounts and origins. In addition to surface meteorological sites, three mini-sodar sites were located around the Lake to enable refined estimates of the convergence and divergence of air flows over the Lake. In addition to characterizing conditions around the Lake, measurements near the upwind boundary of the Basin helped characterize the composition and frequency of air being transported to the Tahoe Basin. Measurements on buoys, piers, and a research vessel on the Lake helped characterize horizontal variations in conditions on the Lake.

The total mass of N and P nutrients being deposited to the Lake is important in assessing the impact on water clarity via algal growth. Particles are important because they can scatter and absorb light in addition to serving as surfaces for algae to attach to. The exact nature of the particles has implications concerning the potential impacts. For example, the larger particles (e.g., diameters > 10 μm) are important because of their large mass and light absorption characteristics. However, the smaller particles (e.g., diameters < 1 μm) are also of interest because of their light scattering characteristics. Furthermore, the physical structure of the particle can be important. Once an atmospheric particle is deposited to a water surface, a number of significant transformations can occur that affect the light scattering and absorption characteristics of the original particle. For example, the original particles could disintegrate into smaller particles when deposited in the water, they could aggregate together and grow in size via various physical and biological processes, they could dissolve, they could undergo chemical transformations, they could be eaten, etc. Clearly, the particle size distribution in the air could be very different from the size distribution of the same particles once

they have entered the water and begin transformations. Settling velocity, which depends on a particle's size, shape, and density, is also a factor in water clarity. Thus, in addition to the total mass of particles and the fractions that serve as bio-available nutrients, the number of particles and the size distribution also affect water clarity. To address this concern, LTADS included experiments with optical particle sizing counters to characterize the spatial variations in particle numbers and sizes near sources. In addition, a particle sizing counter was installed on a boat (during winter) to provide critical information on the horizontal variations in particle counts and sizes. **Figure 1-3** provides an example of the particle size distributions observed in air and in the water of Lake Tahoe. The number of particles in water is roughly 10,000 times greater than the same size particle in air for particles less than 1 micron. This ratio of the number of particles in water to the number of particles in air decreases to about 1500 for particle diameters of 5 microns, to about 150 for particle diameters of 10 microns, to about 100 for particle diameters of 20 microns. The greater ratio of particle counts in water to air, especially for the smaller particles could be due to a combination of longer residence time in water than air (slower deposition rate in a thicker fluid), the breaking of aerosols into smaller particles as ionic bonds holding particles together dissolve in water, and additional sources of particles (e.g., runoff, turbulent resuspension by waves).

Analyses by TRG staff indicate that algal growth in Lake Tahoe was N-limited initially but that it has become P-limited in the last decade or two. It remains important though to understand the atmospheric nitrogen balance in case nitrogen again becomes the limiting nutrient. Knowing the N-balance is also an important tool for validating any airshed model performance to ensure it is getting reasonable results for the correct reasons. To this end, ammonia, nitric acid, organic nitrogenous compounds, and nitrates were significant components of the field measurement program. A laser-induced-fluorescence instrument for nitrogen dioxide, nitric acid, and organic nitrates as well as a continuous nitrate analyzer operated at the site upwind of the Basin. In addition, an instrument measuring oxides of nitrogen (NO_X) or total reactive oxides of nitrogen (NO_Y) was operated at most sites. Lastly, in addition to PM2.5, PM10, and TSP measures of N and NO_3^-, the TWSs were equipped with denuders to provide measurements of ammonia and nitric acid concentrations.

Analytical assessments and interpretations of the ambient data and modeling results will be highly dependent and enhanced by a good understanding of the complex meteorological processes associated with the unique Tahoe Basin. A large lake surrounded by mountains is an ideal setting for meso-scale meteorological processes to exert a significant role in the movement of pollutants from sources to the Lake. To this end, the existing meteorological network was enhanced by additional surface stations and continuous remote sensing systems for characterizing the wind and temperature conditions above ground level. The thickness of the surface layers into which the pollutants are emitted is a critical factor in the concentrations of materials and the probability of contact with the lake surface. Radar wind profilers that can detect the winds from a few hundred meters above ground level to above the Sierra crest were critical for understanding the dynamics of the air flow over the Sierra and mixing with the air inside the Tahoe Basin.

Figure 1-3. Particle size distributions observed in the air and water in the Tahoe Basin
Note that the units of the Y-axis are in terms of the number of particles per cubic centimeter (air unit) or milliliter (water unit), which are equivalent, per micron of diameter size (µm).

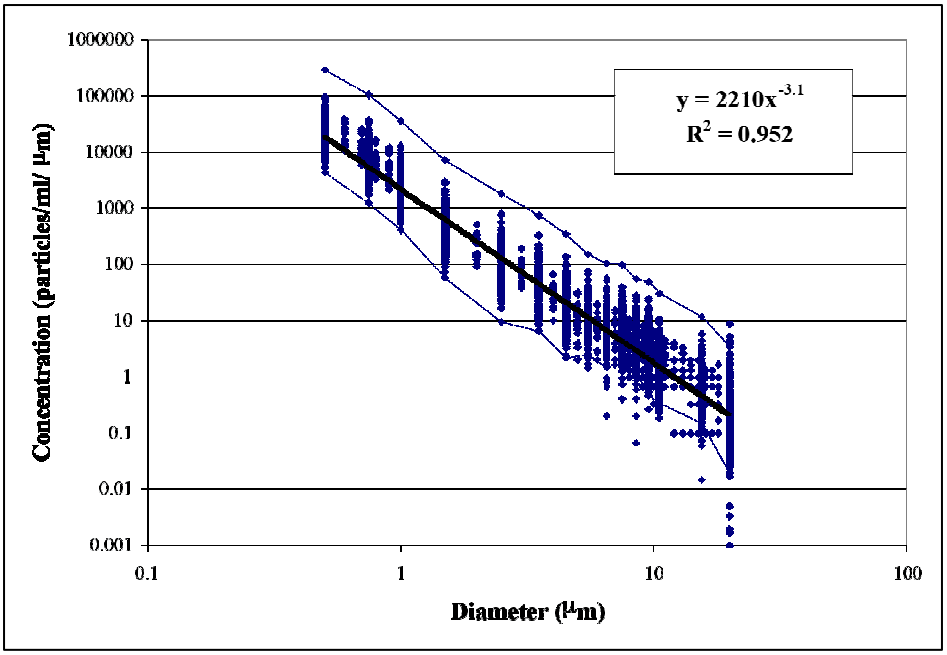

Mid-lake water particle counts during 1999-2000 (Source: TRG)

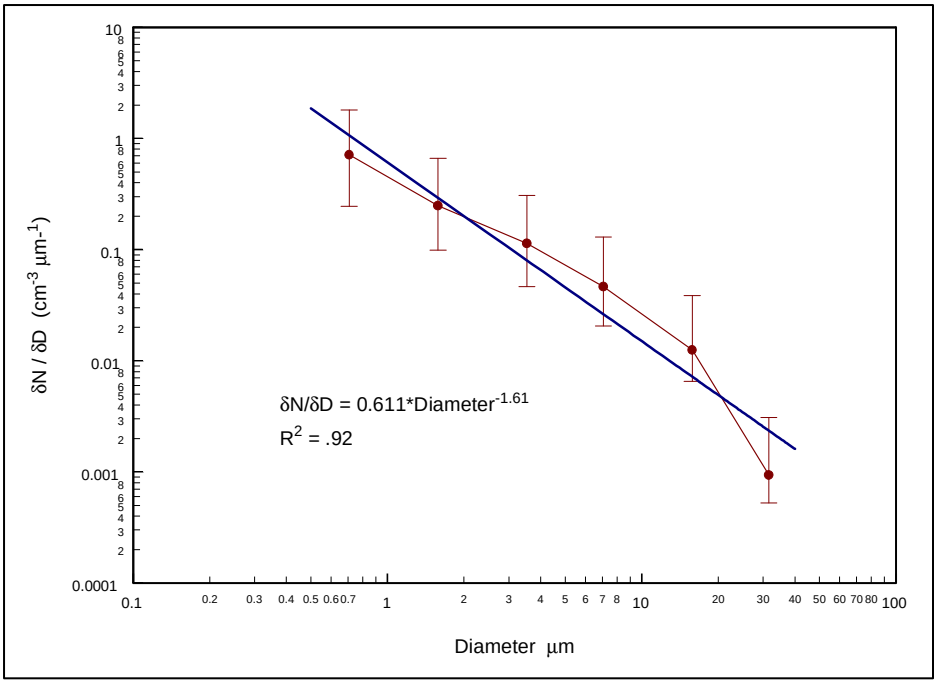

LTADS air particle counts at SOLA for September 2-9, 2003

1.5.1 Overview of Monitoring Network

The monitoring network was designed to provide information on the spatial variations in the ambient concentrations of pollutants around the Lake and upwind of the Basin. The sites allow characterization of the spatial variations in local air quality due to variations in local emissions and meteorological conditions but also potentially the impact due to transport from emissions sources upwind of the Basin. The monitoring network needed to be sufficiently comprehensive to characterize the major source categories of N, P, and PM and the predominant meteorological processes. The unique setting of the Tahoe Basin created additional challenges compared to typical field studies conducted by the ARB. For example, the number of potential monitoring sites is greatly reduced by the limited number of facilities in many areas, limited access to power and phone lines, restrictions on site access and use by land owners, an extensive pine forest that causes many sites not to meet air quality monitoring guidelines, harsh winter conditions that potentially adversely impact instrument performance, power supply, ease of servicing the equipment, etc. Many of the monitoring sites do not fully meet the U.S. EPA criteria for siting equipment to be representative of neighborhood conditions but are the best options possible. In several cases, staff went to great efforts and costs to establish reasonable monitoring sites.

The air quality and aloft meteorological monitoring networks are summarized in **Tables 1-3 and 1-4**, respectively. Most of the air quality sites also had meteorological monitoring equipment. The locations of the monitoring sites are identified in **Figure 1-4**. The study “cornerstone” sites (Big Hill, South Lake Tahoe – Sandy Way, Lake Forest, and Thunderbird Lodge) were those collecting the two-week-samples, and are shown in bold type in the figure. They are also located near the mini-sodar sites characterizing low level air movements. Meso-scale meteorological processes are likely to have a major influence on air flow patterns and the deposition of materials influencing water clarity. To capture the magnitude of the convergence or divergence of air over the lake surface, a network of three mini-sodars, was distributed around the Lake.

Additional intermittent monitoring, including particle counters, was conducted with aircraft, boat, and ground-based studies to provide more information regarding spatial variations in ambient conditions. The aircraft flights occurred primarily during summer and fall 2002 while the UCD boat trips were conducted primarily during early 2003. Each of these intermittent monitoring episodes (4-5 during each season) consisted of two days, each with morning and afternoon sampling. The aircraft flight plan called for sampling during the transits between Davis and Lake Tahoe (beginning of first day and end of second day), spirals over the Sierra Nevada in the general vicinity of Big Hill and over Lake Tahoe itself, and horizontal orbits at ~600’ and 1600’ above lake level.

The network of air quality monitoring/sampling stations also represented different categories of sources and provides spatial coverage. Because deposition of material into the Lake was the primary focus of the study, particulate monitoring sites are distributed around the edge of the Lake to capture the full impact of materials that could be advected over the Lake. The three “super” monitoring sites established around the Lake were: South Lake Tahoe, Lake Forest (NW shore), and Thunderbird Lodge (NE

shore). Air quality and meteorological monitoring on a buoy near the center of the Lake would be ideal for characterizing the spatial variations in concentrations (particularly particulate matter) and the convergence of down slope air flows. Although meteorological data are being collected on several buoys and locations around the Lake, the power requirements for extensive air quality monitoring on the Lake limited air quality sampling to occasional PM sampling on two buoys.

Although an existing monitoring station was in operation near the Sierra crest at Echo Summit to document any pollutants being transported up the Sierra and into the Tahoe Basin, it was also exposed to local influences (i.e. idling trucks and equipment). An effort was made to reduce the local impacts by raising the sampling inlet. However, another monitoring site in a more pristine and better exposed location (representing general air flow into the Sierra Nevada) was needed to investigate the amount and frequency of significant transport up the Sierra slopes. To meet that need, a transport site was established on Big Hill (elevation 6200') about 30 miles west-southwest of Lake Tahoe. This isolated hilltop location is ideally suited for exposure to transported material coming up the slope of the Sierra. This area was burned during the Cleveland Fire and was salvage logged subsequently. The site included a mini-sodar to better characterize the depth of the airflow up the Sierra slope toward the Sierra crest.

Because the long-term record of dry deposition data at Tahoe is based on an non-validated method, CARB staff conducted a 4-way dry deposition method comparison experiment in Sacramento. Staff collocated two traditional wet/dry deposition samplers (one with water (standard TRG method) and one without (standard acid deposition method)) and a snow tube bulk deposition sampler with a water surface dry deposition sampler (WSS) designed to minimize the disturbance of the air flowing over the sampler. The WSS design was used in the Lake Michigan Ozone Study (Yi, 1997). It was hoped that a comparison of data from the four dry deposition sampling methods would indicate whether any sampling biases might exist and, if so, under what general conditions they occur. Assuming any bias is method dependent and not site dependent, the results could be used to adjust historical data and trends and to serve as a reference point for the calculations (estimates) of dry deposition from the collocated TWS.

The text in the following sub-sections focuses on modifications to existing monitoring sites and the set-up of new monitoring sites.

Figure 1-4. Air Quality & Meteorology Aloft Monitoring Network. The four "cornerstone" sites of LTADS are shown in bold type.

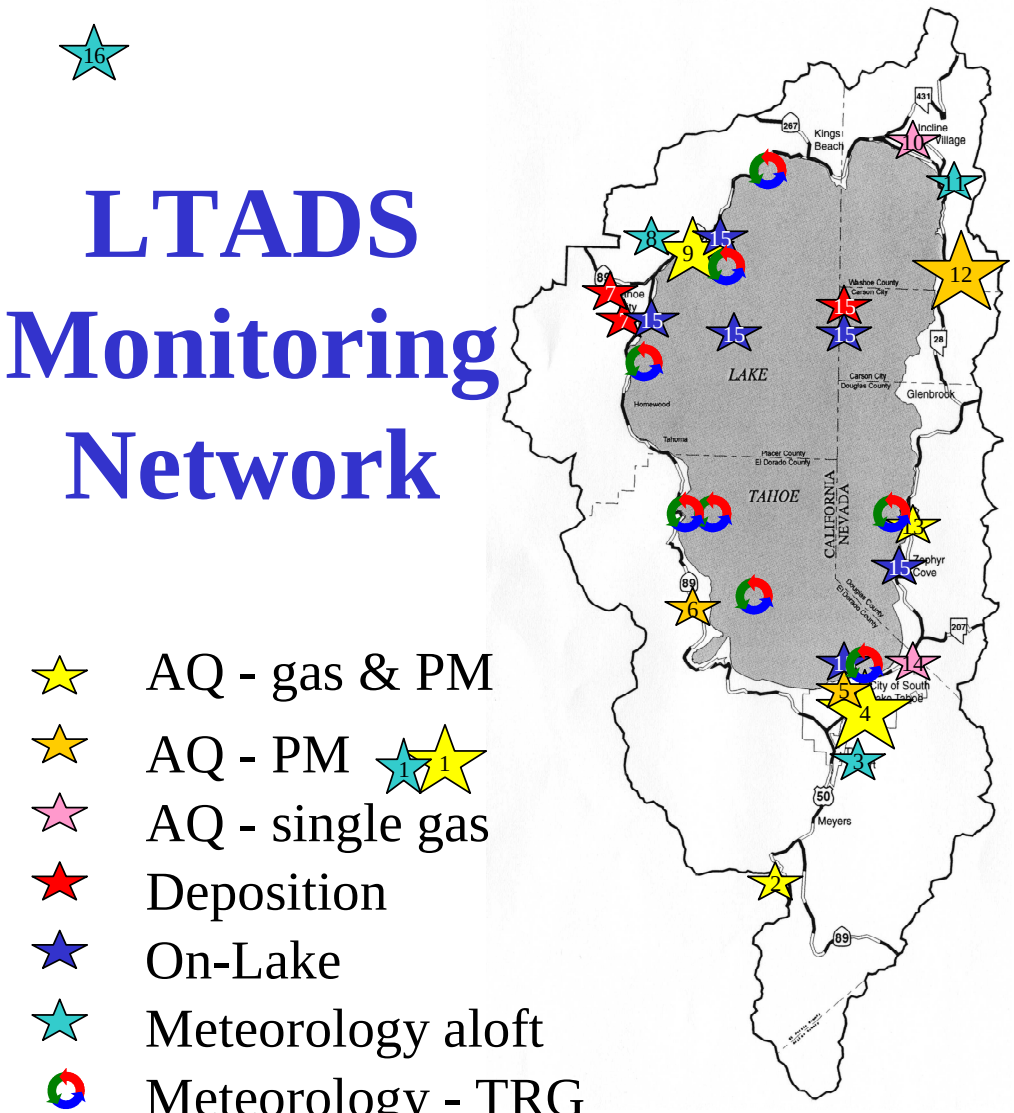

1. **Big Hill**
2. Echo Summit
3. Tahoe Airport
4. **SLT-Sandy Way**
5. SLT-SOLA
6. DL Bliss SP
7. Ward Creek
8. Tahoe City
9. **Lake Forest**
10. Incline Vlg - AQ
11. Incline Vlg - Met
12. **Thunderbird Ldg**
13. Cave Rock SP
14. Stateline - Harvey
15. Buoys/Piers
16. Grass Valley

Table 1-3. Monitoring Matrix

LAKE TAHOE ATMOSPHERIC DEPOSITION STUDY MEASUREMENTS - Air Quality & Surface Meteorology																						
Region:		**Regional**		**In-Basin**																		
Location relative to Lake Tahoe:		**SW**	**SW**	**S**	**S**	**S**	**W**	**W**	**NW**	**NW**	**NW**		**N**	**NE**	**E**	**SE**	**SE**	**L**	**L-N**	**L-S**	**L-N**	**L-N**
Parameter	**Equipment**	**Big Hill - Sierra slope**	**Echo Summit - SN crest**	**SLT - Sandy Way**	**SOLA - beach**	**Timber Cove Pier**	**DL Bliss SP - IMPROVE**	**Rubicon Bay**	**Ward Crk (3)- Hi/Lo/Pier**	**Tahoe City**	**Lake Forest** TRG lab	**Lake Forest** CG Pier	**Incline Village**	**Thunderbird Lodge**	**Cave Rock**	**Zephyr Cove Pier**	**Harvey's**	**Plane (summer,fall) Boat (winter,spring)**	**Boat North (Kings Beach/Tahoe**	**Boat South (Tahoe City/ Zephyr Cove/Camp**	**Mid-Lake buoy TB4 (off Dollar Point)**	**Mid-Lake buoy TB1 (off Nevada Stateline)**
CO	Dasibi 3008			*													*					
	API 300	*									*											
	API 300 (NV)		*																			
O_3	API Model 400	*	*	*							*		*		*			I		I		
NO_X	TECO 42		*	*																		
NO_Y	TECO 42CY	*		*							*							I	I	I		
NO_2	Laser Induced Fluorescence	*																				
Nitric Acid	Laser Induced Fluorescence; denuder (on plane)	*																I				
Total Org. Nitrates	Laser Induced Fluorescence	*																				
TWS (PM2.5, PM10, TSP; HNO3; NH3) (spec)	filters; denuders	*		*	*						*			*								
PM2.5 filter	R&P FRM			*																		
PM10 filter	Anderson SSI		*	*																		
TSP filter (spec)	mini-vol				W I	W I	W I		W I[1]			W I				W I					D I	D I
IMPROVE filter (spec)	PM2.5 species; PM10 mass only				*		*							*								
PM2.5 Continuous	Met One BAM2.5	*		*							*			*								
PM10 Continuous	Met One BAM10	*		*							*			*								
TSP Continuous	Met One BAM w/o head			*	*						*			*	*							
Particle Counter[2]	Climet CI-500				S	S	S									S		I	S	S		
Nephelometer	Met One CS-840		*		*									*								
Deposition[3] (w/d/b)	wet bucket; TRG modified dry bucket; TRG bulk tube								b w/d												b	b
Atmospheric Resistance[4]								*		*				*		*						
Wind Speed		*	*	*	*	*	*				*	*		*	*						*	*
Wind Direction		*	*	*	*	*	*				*	*		*	*						*	*
Temperature		*	*	*	*	*	*				*	*		*	*				*	*	*	*
Water Temperature																					*	*
Relative Humidity		*	*	*	*	*	*				*	*		*					*	*		
Solar Radiation				*			*					*		*	*							
Net Radiation																					*	*
Pressure			*	*			*							*	*			I			*	*

Notes:

Deposition is assessed through understanding of ambient concentrations, deposition velocity, size distribution, and time resolution:

shaded cell = no measurement

* = data were collected routinely

shaded parameter cell = included speciated analysis of aerosol filter

spec = aerosol speciation: X Ray Fluorescence, Ion Chromatography, Colorimetry, Flame Ionization Detection for elemental & organic carbon

I = intermittent sampling

D = 24-hour sampling

S = short-term special study

W = weekly sampling

[1] 2 sites on Wallis Residence (deposition platform & pier)

[2] multiple optical particle counters were used in studies associated with these sites and additional locations. Contact Research Division staff for details.

[3] various samplers (NADP dry, TRG dry, TRG snow tube, & water surface sampler) were used in a dry dep. methods comparison study in Sacramento

[4] atmospheric resistance is related to deposition velocity & collected through flux measurements by Professor Gayle Dana of DRI

Table 1-4. List of Meteorology Aloft Measured during LTADS

LAKE TAHOE ATMOSPHERIC DEPOSITION STUDY MEASUREMENTS - Meteorology Aloft					
Region:	**Up-Basin**		**In-Basin**		
Location relative to Lake Tahoe:	**NW**	**W**	**S**	**NW**	**NE**
Equipment (parameter)	**Grass Valley - Sierra Nevada slope**	**Big Hill[#] - Sierra Nevada slope**	**South Lake Tahoe Airport**	**Tahoe City - Wetlands Treatment Center**	**Incline Village - Sewage Treatment Plant**
Radar Wind Profiler (WS/WD)	*		*		
Radio Acoustic Sounding System (T)	*		*		
Mini-Sodar (WS/WD)		*	*	*	*
Surface wind speed & direction (WS/WD)	*	*	*	*	*
Surface temperature (T)	*	*	*	*	*
Surface relative humidity (RH)	*	*	*	*	*
UCD Aircraft (WS/WD, T, RH)[1]		I	I		

Notes:

= see air quality table for listing of air quality measurements also being made at this site

shaded cell = no meteorological measurement made by this method

* = data were collected

I = intermittent sampling

[1] multiple flights per day (ten 2-day and two 1-day sampling periods during summer and fall)
Flight paths include:
1) traverses to & from Davis and Tahoe Basin,
2) spirals over western Sierra slope and Lake Tahoe,
3) traverses over Lake at 300' & 1000' above lake level, and
4) excursion over SLT-AP

abbreviations: WS=wind speed, WD=wind direction, T=temperature, RH=relative humidity

1.5.1.1 Existing Monitoring Sites

- **Echo Summit**

The height of the inlet probe was raised to reduce the impact of nearby idling vehicles.

- **South Lake Tahoe – Sandy Way**

Branches from a nearby pine tree likely impact the meteorological and PM2.5 measurements at this site. Permission to trim the branches was denied by local authorities. A NOy instrument, a TWS, and 3 beta attenuation monitors (BAM; for measuring PM2.5, PM10, and TSP) were installed.

- **SOLA**

A TWS and a BAM for TSP were added to the existing platform (IMPROVE Program).

- **DL Bliss**

Occasional TSP samples (by mini-volume sampler) were collected at this site in addition to the standard IMPROVE Program (PM2.5 and PM10).

- **Upper Ward Creek**

No changes were made to this site.

- **Lower Ward Creek (Wallis Residence)**

The only change made to this site was the intermittent collection of TSP samples by mini-vol samplers. It should be noted however that the deposition measurements at this long-term site are being impacted by the presence of an adjacent, growing, deciduous tree and almost certainly being impacted by the presence of nearby coniferous trees. TSP samples (mini-vols) were collected routinely. In addition, TSP mini-vol samples were frequently collected on the boat pier of the Wallis residence.

- **Incline Village**

No changes were made to this site

- **Thunderbird Lodge**

TWS and BAMs (PM2.5, PM10, & TSP) were added to the existing IMPROVE-equivalent sampling program. The site required an additional power upgrade. Wet/dry bucket deposition sampler was dropped from monitoring plans due to insufficient space for all the instruments.

- **Cave Rock**

A BAM instrument measuring TSP was added.

- **Stateline – Harvey's**

No changes were made to this site.

1.5.1.2 New monitoring sites

- **Big Hill**

This was a fully instrumented monitoring site established to help quantify the magnitude and frequency of transport up the slopes of the Sierra Nevada toward the Lake Tahoe Basin. The equipment trailer was blown over by 100+ mph winds in November 2002 after the instruments were installed but before monitoring began. The trailer was righted and secured in December 2002. The electricity was reinstalled in January 2003 but had frequent power failures until March. With the exception of the BAMs (May), most air quality instruments were reporting data of good quality by March. The mini-sodar was installed in January 2003 but instrument failure delayed data collection for several weeks. The equipment was repaired and reinstalled in May but was then shut off several days later due to concerns about the level of noise. During the fire season, the mini-sodar was only operated from 7 am to 8 pm to allow USFS fire lookouts to sleep.

- **South Lake Tahoe – Airport**

A radar wind profiler with a radio acoustic sounding system (RWP/RASS) was installed to continuously monitor wind and temperature conditions aloft. A mini-sodar system was also installed to monitor winds less than 200 meters above ground level.

- **Timber Cove pier**

Filter samples (24 – 36 hour periods) with a mini-vol sampler were collected at the end of the pier on occasion. Vandalism resulted in two samplers being tossed into the lake and the effective termination of sampling due to the lack of site security to reduce the possibility of future vandalism.

- **Tahoe City Wetlands Treatment Center**

A mini-sodar was set up at this site.

- **Lake Forest**

A “cornerstone” monitoring site was established on the grounds of the TRG lab (Old Fish Hatchery) to monitor PM in three size fractions (both TWS and BAM) and multiple gases (i.e., 2-week averages for NH_3 and HNO_3, and hourly averages for CO, O_3, and NO_y).

- **Coast Guard pier**

Filter samples (7-day period) with a mini-vol sampler were collected approximately weekly near the end of the pier.

- **Mid-lake buoys**

Battery-operated mini-volume samplers were deployed on two buoys to collect TSP samples (24-hour period). The goal was to collect approximately one sample per month at each buoy given that servicing by boat would be constrained by operator schedule, weather, and lake conditions.

- **Zephyr Cove Pier**

A mini-vol sampler (1-week samples) was established at this site during LTADS.

1.5.2 Overview of Measurements

Ambient measurements of air pollutants potentially associated with water clarity degradation or transport from sources outside the Tahoe Basin were the focus of this field study. ARB staff compared its deposition estimates with historical estimates made with surrogate surface deposition samplers and air quality field studies in the Basin. Because direct measurements of deposition are difficult and subjective, the ARB applied an indirect approach to estimating atmospheric deposition in the Tahoe Basin. This approach included direct measurement of important pollutant species and meteorological conditions. These data were used to calculate seasonal hourly deposition in four quadrants of the Lake. Source-specific emissions, improvement of the emission inventory, the use of a variety of data analysis techniques to elucidate the atmospheric processes in various locations in the Basin improve the understanding of factors that contribute to atmospheric deposition to Lake Tahoe.

Water clarity can be reduced by nitrogen and phosphorus species (biologically available forms) because they contribute to the growth of algae. Water clarity can also be reduced by the presence of particles, particularly in the one micrometer (µm) size. Most of the air pollutant monitoring effort focused on PM and nitrogen species to help identify the relative roles of the various contributing factors. Nitrogen containing compounds measured included nitric oxide (NO), oxides of nitrogen (NO_X, primarily NO and NO_2), total reactive oxides of nitrogen (NO_Y, primarily NO, NO_2, HNO_3, HONO, PAN, N_2O_5), ammonia (NH_3), nitric acid (HNO_3), and particulate nitrates (NO_3). Unlike nitrogen, atmospheric sources of phosphorus are limited and only in particulate form. Particulate samples were analyzed for elemental phosphorus (P) and phosphate (PO_4^{-2}). Particulate matter was generally measured in 3 size classes - <2.5 µm, <10 µm and total suspended particulate (TSP). Two particle-sizing counters (size cuts of 0.3, 0.5, 1, 2.5, 10, and 20 µm) were deployed in various short-term studies to characterize the spatial and seasonal variations in particle counts by size.

As discussed earlier, the objective of sampling with the Two-Week-Sampler was to make continuous measurement of particulate matter (PM) throughout the year so that the air quality impact of all emission sources, regardless of temporal scale of influence, is included. Details as to the specific parameters measured at each site can be found in **Table 1-5**.

Although ozone (O_3) and carbon monoxide (CO) are not critical components of the water clarity issue, they do provide insights into the relative impacts of transport and local emissions sources. Being components of a typical air monitoring program, these parameters were maintained at existing monitoring sites and included in new monitoring sites. Furthermore, as part of an assessment of ozone impacts on forest health, several temporary (summer season) sites were established with passive ozone samplers (2-week sampling period).

Table 1-5. LTADS Particulate Matter Air Quality Network

Site	Location	Network	Sample Duration	Pollutants	Comments
Big Hill	western Sierra slope	TWS BAM	2-weeks hour	TSP, PM10, PM2.5, HNO_3, NH_3 PM10, PM2.5	remote location at ~6000' elevation
SLT-Sandy Way	SLT - south of Hwy 50	TWS BAM FRM	2-weeks hour 24-hour	TSP, PM10, PM2.5, HNO_3, NH_3 TSP, PM10, PM2.5 PM10, PM2.5	roof of 1-story building; 1 block south of Hwy 50
SOLA	SLT - north of Hwy 50	TWS IMPROVE BAM	2-weeks 24-hour hour	TSP, PM10, PM2.5, HNO_3, NH_3 PM10 (m), PM2.5 TSP	~30 m north of Hwy 50 and ~40 m from shore
Timber Cove	SLT - pier	MVS	24-hour	TSP	~100 m from shore
Zephyr Cove	SELT - pier	MVS	1-week	TSP	~30 m from shore
Cave Rock	ELT – shore	BAM	hour	TSP	~10 m from shore
Thunderbird Lodge	NELT – shore	TWS IMPROVE BAM	2-weeks 24-hour hour	TSP, PM10, PM2.5, HNO_3, NH_3 PM10 (m), PM2.5 TSP, PM10, PM2.5	back of Elephant House
Coast Guard	NLT - shore	MVS	1-week	TSP	~100 m from shore
Lake Forest	NLT – south of Hwy 28	TWS BAM	2-weeks hour	TSP, PM10, PM2.5, HNO_3, NH_3 TSP, PM10, PM2.5	~25 m south of Hwy 28
Wallis Tower	NWLT – dep site	MVS	1-week	TSP	~20 m east of Hwy 89
Wallis Pier	NWLT – pier	MVS	1-week	TSP	~20 m from shore; ~120 m east of tower
Bliss State Park	WLT – west of Hwy 89	MVS IMPROVE	1-week 24-hour	TSP PM10 (m), PM2.5	~25 m above and ~50 m west of Hwy 89
Buoy TB1	on-lake northeast	MVS	24-hour	TSP	~6 km east of TB4 and ~5 km west of eastern shore
Buoy TB4	on-lake northwest	MVS	24-hour	TSP	~5 km SE of Coast Guard

TWS - Two-Week-Sampler
MVS - Mini-Volume Sampler
BAM – Beta Attenuation Monitor
FRM – Federal Reference Method
IMPROVE – Interagency Monitoring of PROtected Visual Environments (or equivalent)
(m) – mass only

1.6 Special Studies

CARB contracted with several groups to conduct specialized measurements useful in addressing atmospheric processes related to atmospheric deposition and emissions. The abstract for each project is listed below, and, where available, an electronic link to the full report.

1.6.1 Aircraft and Boat Measurements of Air Quality and Meteorology

UC Davis (ARB Contract No. 01-326)

During the summer and fall of 2002, aircraft measurements of meteorological and air quality variables were obtained over the western Sierra Nevada and the Lake Tahoe Basin. During the winter of 2003, similar measurements were made close to the lake's surface using a small research vessel on the lake. Aircraft air quality sampling included real-time monitoring of ozone, NO, NOy, and particulate concentrations plus grab samples of gaseous and particulate nitrogen species using annular denuder-filter pack (DFP) assemblies. Boat sampling involved the same instrumentation except that no ozone monitor was aboard. The primary objective of these field efforts was to document the concentrations of nitrogen-containing species as well as other pollutants in the air over and upwind of the lake, as these species can deposit into the lake and act as nutrients that accelerate eutrophication. This report describes the techniques used to acquire the data, assure their quality and summarizes the general conditions encountered. Descriptions of instrument calibrations and of the formats used for the QA/QC-ed data sets transferred to the ARB are also included.

Sampling was conducted on 20 days during the summer and fall with an aircraft and on 6 days during the winter with a boat. Two additional days were devoted to joint aircraft-boat sampling in the fall. Data recovery for the continuous real time measurements was nearly 100 percent. Analyses of the DFP samples from the aircraft also went well, although there were issues with blank levels for several chemical species. During our sampling days, the concentration of atmospheric N over Lake Tahoe ranged from 33 to 360 nmol-N/m^3-air, with an average value of 120 nmol-N/m^3-air. Gaseous ammonia was typically the dominant component, accounting for an average of 55% of total N, while particulate ammonium contributed an additional 10% of total N on average. Nitric acid/nitrate and organic nitrogen (gaseous and particulate) were also significant components that, on average, accounted for 20% and 14% of the total atmospheric N burden. In contrast, levels of nitrous acid and nitrite were generally insignificant.

A variety of weather conditions were encountered which clearly affect pollutant levels measured both in the Tahoe Basin and over the mountains to the west. On most days, late afternoon air quality was slightly to significantly worse to the west of the basin than in the basin. In the mornings, the variations among locations were more random. A preliminary analysis of our DFP measurements, in conjunction with meteorological data, suggests that nitrogen levels in the air above Lake Tahoe can be affected by a number of sources and factors including the regional "background" pollution level, in-basin emissions, local and distant forest fires, and pollution from the Central Valley.

Full Report (ftp://ftp.arb.ca.gov/carbis/research/apr/past/01-326.pdf)

1.6.2 Improvement of the PM Emission Inventory for the Lake Tahoe Region

CE-CERT (ARB Contract No. 0004-AP-ARB-01)
Lake Tahoe is a beautiful lake located in California and Nevada. The lake is well known for its pristine water clarity and color, and is a popular vacation destination. However, since the 1960's, the water clarity of the lake has been steadily declining. It is believed that the degradation in the water clarity is due to increases in the input of particles and biologically available phosphorus and nitrogen. A significant fraction of this input is estimated to be through the atmosphere. Possible sources of particles, phosphorus and nitrogen deposition from the atmosphere include smoke from residential wood burning, prescribed files, wildfires, vehicle exhaust, roadway dust, and regional transport. Currently, the quantity and impact from these and other sources are not well understood. This project explores characterizing the emissions contained in wood burning activities and quantifying the amount and type of wood burning in the Tahoe region. In addition, the type and amount of on-road vehicle activity is better characterized. This information will aid in understanding the magnitude and sources of nutrients and particulate matter deposited to Lake Tahoe, to enable the development of a plan for reducing emissions and improving water quality.

Full Report (ftp://ftp.arb.ca.gov/carbis/research/apr/past/01-733.pdf)

1.6.3 Lake Tahoe Source Characterization Study

Desert Research Institute (ARB Contract No. 01-734)
PM samples directly relevant to major PM sources in Lake Tahoe were collected and analyzed as part of this study. Sources sampled included residential wood combustion (RWC), motor vehicle exhaust, and entrainment of road dust, traction control material, and road deicing material.

In addition, several new emission measurement technologies were applied during this study. A portable emission test stand measured both gases and particles at 1 s resolution from RWC appliances and on-road motor vehicles. Measurements of plume concentrations were used to determine fuel-based emission factors based on the ratio of pollutant concentrations to CO_2, CO, and hydrocarbons. A background subtraction technique was applied to fast-response PM measurements to estimate the fraction of PM emitted by a source and collected on a filter.

A tower instrumented with fast-response PM monitors was erected downwind of a highway. The flux of particles past the tower was related to the number of vehicles traveling on the road to calculate a vehicle and distance-based emission factor for typical wintertime, post-storm, post-street sweeping, and post-deicing conditions.

An onboard road dust sampling system was operated on more than 2000 km of paved road in the Lake Tahoe Basin. The instrumented vehicle was operated on fixed routes around the lake and over Mt. Rose Pass to monitor the change in road dust emission factors between winter and summer. Onboard measurements were also related to the

flux of PM downwind of the road to provide the first paved road calibration point for the mobile system. This data set permitted the extrapolation of fleet average emission factors to all areas surveyed by the mobile system.

Full Report (ftp://ftp.arb.ca.gov/carbis/research/apr/past/01-734.pdf)

1.6.4 Keeping Tahoe Blue: Quantifying Atmospheric Nitrogen Oxides in the Lake Tahoe Basin

UC Berkeley (ARB Contract No. 01-327)

The motivation for collecting data at Big Hill and the focus for this analysis has been to quantify the distribution of reactive nitrogen oxides at a site upwind of Lake Tahoe and use those measurements to assess the role of transport along the western slope of the Sierra in contributing to nitrogen deposition in Lake Tahoe. By combining the data we obtained at Big Hill with corresponding measurements at Blodgett Forest, we have developed a highly constrained model of the processes that govern reactive nitrogen distribution during the summer months in the region. Data collected during winter months shows that the meteorology does not favor net transport of pollutants from west to east in the surface layer. Plumes from several prescribed burns were measured, often containing higher concentrations of reactive nitrogen than the urban plume, but likely having significantly reduced geographical influence. Total reactive nitrogen in the region is likely at a maximum during the summer, though observations from more sites would be necessary to quantify the importance of burning events as a source of reactive nitrogen to Lake Tahoe. Based on our analyses of the observations made, we can draw the following conclusions:

- During summer months, the Sacramento region is the dominant source of reactive nitrogen in the plume on the western slope of the Sierra Nevada
- HNO_3 deposition is sufficiently fast that very little remains in the plume by the time it reaches high elevation sites near the western rim of the Lake Tahoe Basin
- At Big Hill, similar concentrations of HNO_3 are found in airmasses coming from the west and the east, suggesting that urban areas to the west of Lake Tahoe cannot be identified as important sources
- Organic nitrates are significantly elevated in the plume compared to background conditions but their contribution to nitrogen deposition is poorly understood
- During winter months, total reactive nitrogen is lower, net flow at the surface is downhill and the urban plume rarely reaches the western rim of the Basin
- Individual winter episodes of high NO_2 and inorganic nitrates associated with small-scale burning events along the western slope and may generate HNO_3 that can reach Tahoe.

Full Report (ftp://ftp.arb.ca.gov/carbis/research/apr/past/01-327.pdf)

1.6.5 Evaluation of Ozone and HNO_3 Vapor Distribution and Ozone Effects on Conifer Forests in the Lake Tahoe Basin and Eastern Sierra Nevada

US Dept. of Agriculture, Forest Service (ARB Contract No. 01-334)
Two-week average concentrations of ambient ozone (O_3), nitric acid vapor (HNO_3), and ammonia (NH_3) were measured during the 2002 smog season in selected areas of the Sierra Nevada, California (i.e., Lake Tahoe Basin, San Joaquin River Drainage, portions of the eastern and southern Sierra Nevada). High O_3 concentrations were present along the San Joaquin River Drainage and southern Sierra Nevada throughout the summer. Ozone levels were also elevated in the eastern Sierra Nevada, although they were lower than in the San Joaquin River Drainage. The transport of nitrogen oxides, carbon monoxide, and volatile organic compound emissions generated by the McNalley fire is postulated to have contributed to the very high O_3 concentrations that occurred in August. In the San Joaquin River Drainage, ambient concentrations of HNO_3 and NH_3 were highest near the San Joaquin Valley and decreased gradually toward the east. In addition, an evaluation of O_3 injury symptoms was conducted on ponderosa pines in the Lake Tahoe Basin and along the San Joaquin River Drainage. At 25-sites in the Lake Tahoe Basin, 23 percent of the trees evaluated had symptoms of foliar O_3 injury, but only slight injury to the pines occurred in this area. Ozone injury was, on average, only slight along the San Joaquin River Drainage.

Full Report (ftp://ftp.arb.ca.gov/carbis/research/apr/past/01-334.pdf)

1.6.6 Radar Wind Profiler Support for the CARB Lake Tahoe Pollution Studies: 2002-2003

NOAA (ARB Contract No. 01-342)
As part of this contract, the NOAA Environmental Technology Laboratory (ETL) performed system audits at the four CARB Doppler SODAR/wind profiler sites in the Lake Tahoe area and at the ETL Grass Valley wind profiler site during June 2003. ETL used both radiosonde and tethered-balloon systems for the audit of the radar and sodar systems.

Full Report (ftp://ftp.arb.ca.gov/carbis/research/apr/past/01-342.pdf)

1.6.7 Sampling and Analysis for Lake Tahoe Atmospheric Deposition Study

Desert Research Institute (ARB Contract No. 01-351)
The CARB initiated the LTADS in 2002 to quantify the contribution of atmospheric deposition to the declining water clarity of Lake Tahoe. The initial study design, which was described in a June 10, 2002 draft work plan for LTADS, included two major components: 1) a monitoring network in the Lake Tahoe Basin and 2) supplemental special studies. The monitoring network used two-week integrated samples from the five key sites in the TWS network and shorter term (generally 1-week) TSP samples with Mini-Vol samplers deployed at remote sites and on-board buoys. Field blanks were collected to subtract the background contribution from the sampling environment and field operation; however, TWS field blanks were only collected at SOLA and only three field blanks were collected from the Mini-Vol samplers. The limited and site-specific

field blanks may affect the results of the ambient samples. The chemical data were evaluated for internal consistency by examining the physical consistency and balance of reconstructed mass, based on chemical species versus measured mass. In general, the samples collected met the criteria of internal physical consistency.

Full Report (ftp://ftp.arb.ca.gov/carbis/research/apr/past/01-351_app.pdf)

1.6.8 Literature Review and Summary of Previous Work Related to the Transformation of Nitrogen Emissions during Transport

UC Berkeley (ARB Contract No. 02-331)
In addition to local sources of reactive nitrogen to the Tahoe Basin, other potential upwind sources include emissions from the Sacramento urban area, industrial and agricultural activity in the Central Valley, transportation along highway corridors, biomass burning and biogenic emissions from ecosystems within the western Sierra Nevada. The ability of these emissions to affect the water quality of Lake Tahoe depends on their chemical processing and on the transport pathways that bring the air toward the Tahoe Basin. Analysis of long term ground level observations suggest that most HNO_3 within the urban plume deposits prior to reaching Lake Tahoe, though organic nitrates may persist. Short-term aircraft studies attempting to identify transport pathways for pollutants have occasionally observed higher concentrations of photochemical products lofted above the mixed layer. Downwind of biomass burning episodes, elevated levels of reactive nitrogen in both the gaseous and particulate phase have been observed [Zhang, 2002]. If these burning events occur within five hours transit time to the Tahoe Basin, they may be capable of delivering additional nitrogen to the atmosphere above the Lake.

Full Report (ftp://ftp.arb.ca.gov/carbis/research/apr/past/02-331.pdf)

1.6.9 The Use of Multi-Isotope Ratio Measurements as a New and Unique Technique to Resolve NOx Transformation, Transport, and Nitrate Deposition in the Lake Tahoe Basin

UC San Diego (ARB Contract No. 03-317)
This work is not yet completed but a final report is expected in 2006.

The objectives of this project are to evaluate the isotopic composition of nitrate in Lake Tahoe and in aerosols and deposition collections obtained within the basin and on transects outside the region. Evaluating the isotopic composition of atmospherically produced nitrate and comparing it with that found in the Lake will quantify the flux of atmospheric N deposited on the Lake and can be used as tracer of nutrient fluxes over the course of the year.

1.6.10 LTADS s-XRF Filter Analysis QA Report - Enhanced Measurements with Synchrotron-XRF

UC Davis (ARB Contract No. 03-334)
As part of the LTADS 71 ambient filter samples from various collection sites throughout the Lake Tahoe Basin were analyzed. The sample subset from the large LTADS sample base was selected from those with high reported phosphorous values from other analyses combined samples collected on the same dates at corresponding sites. In addition, several source and other specialized samples were analyzed. In this preliminary report we discuss only the ambient samples. Each of these samples was previously analyzed by the analytical facility at the DRI and the DRI data were shared. The samples were analyzed at the analytical facility at beam line 10.3.1 at the Advanced Light Source-Lawrence Berkeley National Laboratory (ALS-LBL). The analysis technique is commonly known as synchrotron x-ray fluorescence (S-XRF), but it is distinguished from traditional XRF (such as that employed by the analytical facility at DRI) by the source of the incident x-rays. The primary goals for understanding the LTADS filter QA study were to 1) determine the range of phosphorous concentration in the Lake Tahoe Basin, and 2) determine the statistical significance of reported phosphorous data from the S-XRF and DRI analyses as an additional quality assurance of the LTADS sampling and analytical program.

Full Report (ftp://ftp.arb.ca.gov/carbis/research/apr/past/03-344.pdf)

1.6.11 Shore Zone Dispersion Study

CARB staff
The LTADS Shore Zone Dispersion Study was a limited set of short-term field projects designed to provide anecdotal data on air flow and pollutant distribution in close proximity to major pollutant sources. The experiments of the study were broken into four different categories:

- Exploratory measurements
- Source-oriented dispersion experiments
- Shore zone process experiments
- Particle size distribution characterization experiments

Exploratory measurements consisted of short field experiments, primarily using portable particle counters. The goal was to gather enough data about particular sampling environments to allow for the development of sampling plans for later controlled experiments. Source-oriented dispersion experiments were designed to evaluate near source deposition and primary aerosols to calibrate dispersion estimation schemas applied to the long-term monitoring data. Shore zone experiments were designed to identify the spatial and temporal extent of near shore pollutant concentrations. Finally, particle size distribution experiments were used to develop particle size distribution curves to apply to the bulk chemical data collected by the TWS and mini-vols and to parse the concentrations collected by the BAMs into appropriate “bins” for deposition calculations.

Staff resource constraints limited the number of experiments to a few exploratory measurement efforts. Two Climet CI-500 particle counters (the main portable particle counter in use) have proven to produce comparable results. After the particle counters were proven to produce similar readings, they were dispersed at Sacramento and at Zephyr Cove Resort in Lake Tahoe. Preliminary data from the Zephyr Cove and Sacramento comparison experiment show that the Tahoe Basin does have significant local aerosol sources and that local aerosol is generally larger in size than urban aerosol in California and thus more prone to deposit in the lake. Data from another deployment shows that the particle counters are able to detect the tail end of the nighttime inversion and midmorning shift of night and morning offshore flow to midday lake breeze. The particle counter was also able to detect a morning episode of road transport caused by the morning traffic peak. Other experiments conducted on the UC Davis boat and aircraft show promising correlation with land-based particle counts and have been successful in tracking aerosol episodes.

Summaries of these measurements can be found in Chapter 3 of this report.

1.6.12 Comparison of Surrogate Surface Methods of Measuring Dry Deposition

CARB staff

Measurement of the deposition of gases and aerosols from the atmosphere to surfaces is difficult and fraught with complexities associated with disturbances during sampling, reaction/transformation/contamination during sampling and before chemical analysis, analytical detection of small quantities, etc. Measurement of deposition to a water surface is further complicated by access and logistical challenges. Questions have historically been raised about the representativeness of deposition measurements associated with surrogate surface deposition samplers like the bucket sampler, particularly for dry deposition. It is believed that the wet bucket measurements are reasonably realistic, assuming proper siting of the equipment away from buildings and trees. CARB staff conducted a dry deposition methods comparison study to better characterize the potential differences between surrogate surface sampling methods that are or could be used for dry deposition measurements. In general, the relationships between the methods are not well defined and tend to have significant scatter. However, the alternative methods all tend to “see” more nitrogen species and comparable phosphorus species than the standard dry deposition method.

The details of this comparison can be found in Appendix A of this report.

1.7 References

Blanchard, C., Michaels, H., and Tanenbaum, S. (1996), Regional Estimates of Acid Deposition Fluxes in California for 1985-1994, report prepared for California Air Resources Board, Sacramento, CA, Contract No. 93-332, April.

Carroll, J.J., Anastasio, C., Dixon, A.J., (2004), Keeping Tahoe Blue through Atmospheric Assessment: Aircraft and Boat Measurements of Air Quality and Meteorology near and on Lake Tahoe, report prepared for California Air Resources Board, Contract No. 01-326, Sacramento, CA, June.

Motallebi, N., Taylor, C.A. Jr., Turkiewicz, K., and Croes, B.E. (2003), Particulate Matter in California: Part 1—Intercomparison of Several PM2.5, PM10-2.5, and PM10 Monitoring Networks, *J. Air & Waste Manage. Assoc.* **53**:1509-1516, December.

Murphy DD, Knopp CM (eds.) (2000), Lake Tahoe Watershed Assessment: Vol. I. USDA Forest Service, Pacific Southwest Research Station, Albany, CA, Gen Tech Rep No. PSW-GTR-175, 736 p.

Sun, J., (2001), personal communication with James Pederson.

Tahoe Research Group (TRG), Lake Tahoe Particle Characterization, 1999-2000, http://trg.ucdavis.edu/research/annualreport/contents/lake/article6.html

Taylor, C.A. Jr., Stover, C.A., and Westerdahl, F.D. (1998), Speciated Fine Particle (<2.5 μm aerodynamic diameter) and Vapor-Phase Acid Concentrations in Southern California. Presented at the 91st Annual Conference & Exhibition of A&WMA, San Diego, CA, June, Paper 98-WA74.01 (A825).

Watson, J.G. and Chow, J.C., (1991), Measurements of Dry Deposition Parameters for the California Acid Deposition Monitoring Program, report prepared for California Air Resources Board, Contract No. A6-076-32, Sacramento, CA, June.

Yi, S.M., Holsen, T., and Noll, K. (1997), Comparison of Dry Deposition Predicted from Models and Measured with a Water Surface Sampler, *Environmental Science & Technology* **31**(1):272-278.

2. Atmospheric Processes

The Lake Tahoe Basin lies between crests of the Sierra Nevada and Carson mountain ranges. The surface of Lake Tahoe is 1,900 meters (6230 feet) above mean sea level and has an irregular oval shape, 35 kilometers (22 miles) long by 19 kilometers (12 miles) wide, comprising an area of 500 square kilometers (193 square miles). Lake Tahoe is a deep lake (as deep as 505 meters or 1645 feet) and contains a large volume of water – factors which keep the water temperature relatively stable throughout the year. The Lake itself dominates the watershed (almost 40% of the surface area). The alpine features encircling the Lake create a bowl appearance. These topographic features have a significant influence on the meteorology of the Basin.

The meteorological characteristics of the Tahoe Basin are largely determined by its geographic setting. On the large or synoptic scale, its location near the eastern edge of the semi-permanent eastern Pacific high pressure system influences the seasonal patterns of temperature and precipitation. On the regional scale, its alpine topography strongly influences the spatial patterns of winds, temperature, and precipitation. On the local scale, the different interactions of the air with the ground and Lake result in the formation of complex temperature inversion layers and local winds which create perceptible differences in meteorological conditions over short distances. All of these different meteorological scales contribute to the unique meteorology of the Tahoe Basin.

Not only do meteorological processes determine the weather at a particular location, they also help to determine the air quality. Emission sources and activities add materials to the air. Depending on the nature of the material (e.g., gas, aerosol, reactive, “sticky”, size), these materials can move long distances with the wind or can “disappear” rapidly; they can be very concentrated at one location and non-detectable a short distance away. Because the meteorology strongly influences the emission, transformation, dissipation, and deposition of materials, ARB staff has made meteorological measurements a major component of the Lake Tahoe Atmospheric Deposition Study. Without detailed knowledge of the temporal and spatial (horizontal and vertical) variations in temperature and wind, the characterization of the relative impacts of various global, regional, and local sources of nutrients and aerosols contributing to the declining water clarity in Lake Tahoe would be compromised.

2.1 Precipitation Patterns

Precipitation is a factor in the annual deposition of materials to the Tahoe Basin. Precipitation is generally associated with good air quality due to enhanced dispersion and deposition of pollutant emissions. However, anthropogenic emissions of very small particles can also serve as condensation nuclei and deposit to the Lake. More importantly, the falling precipitation can “wash” the lower atmosphere of pollutants and stabilize soils, reducing windblown dust. In general, the first period of precipitation during a storm contributes the bulk of the total wet deposition of pollutants from the storm. When the precipitation falls as snow, an additional source of nutrients and aerosols is created by the application of road sanding materials. The air quality and

depositional impacts of road sanding will vary, depending on the composition and size of the sanding material as well as the efficiency of road sweeping operations.

Tahoe's proximity to the Pacific Ocean provides it with a source of moisture for precipitation. The eastern Pacific high pressure system creates a Mediterranean type of climate with most of the precipitation occurring during relatively mild winters (November through March). At an elevation greater than 6,000 feet, much of the precipitation in the Basin occurs as snow. When synoptic scale weather systems are not present, the regional topography (alpine basin) influences the diurnal wind and temperature patterns via up-slope and down-slope breezes. The orographic lift provided by the Sierra Nevada to the air arriving from the west causes much of the precipitation to occur just west of the basin (**Figure 2-1**). Although the amount of precipitation during the winter varies from year to year, on average, over 60 inches (") of precipitation falls along the Sierra crest, about 30" along the western shore of the Lake, 20-30" over the Lake itself (less on the eastern side), and increasing to about 30" near the top of the Carson Range on the eastern side of the Tahoe Basin.

A map identifying the locations of many meteorological monitoring sites discussed in this report is provided in **Figure 2-2**. As illustrated in **Figure 2-3**, precipitation amounts on the eastern side of the Lake are similar to that on the western side during the summer when showers provide most of the meager precipitation. During winter months when synoptic storms dominate precipitation patterns, precipitation is approximately double on the western side of the Lake as that on the eastern side.

As illustrated in **Figure 2-4**, the frequency of precipitation is more similar throughout the region than are precipitation amounts. The normal number of days with measurable precipitation in the Tahoe Basin is indicated by the dashed line in **Figure 2-4** and is the mean of the three sites in the Basin (i.e., Tahoe City, Stateline, and Glenbrook). In fact, the frequency of precipitation in 2003 exhibited more spatial uniformity than normal during the winter and spring (**Figure 2-5**). Because of the relative infrequency and scatter nature of thundershowers during the summer, it is not unusual that Incline Village experienced twice the summer norm while Meyers experienced slightly fewer than normal.

Precipitation data for Incline Village were readily available during LTADS and were used to estimate wet deposition to Lake Tahoe. Hourly and daily precipitation totals at Incline Village during 2003 are shown in **Figures 2-6 and 2-7**. **Figure 2-6**, which presents hourly precipitation totals at Incline Creek during 2003, indicates like the other sites with long-term precipitation records in the Basin that the most intense precipitation is associated with summer thunderstorms. The 2003 precipitation data for Incline Village also indicate that most of the annual precipitation was associated with organized storm systems in the winter and early spring (**Figure 2-7**). This pattern is consistent with the seasonal norms (**Figure 2-8**), although 2003 exhibited some deviations from normal. Although storms were relatively frequent in January and February of 2003 (equal to long-term norm), they were not as strong as normal and so did not deliver as much

Figure 2-1. Annual Precipitation (inches) in Northern California-1691-90 Mean.
(Source: www.wrcc.dri.edu/pcpn/ca_north.gif. Note the enhanced precipitation along the western slope of the Sierra Nevada due to orographic lifting of the air. Storm systems typically move from the west southwest toward the east northeast. The Tahoe Basin is on the lee side of the Sierra where annual precipitation amounts decline.)

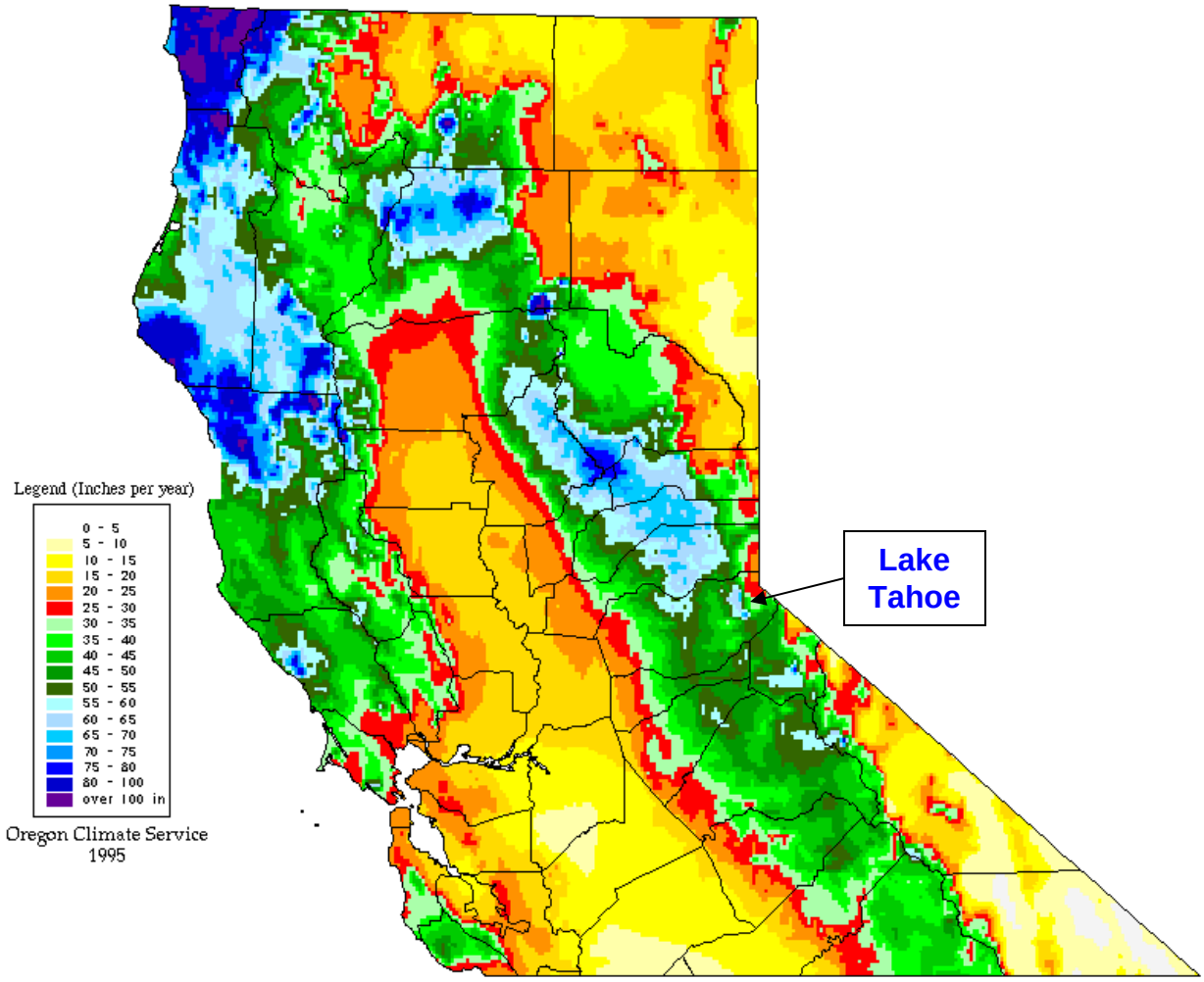

precipitation as normal. However, December of 2003 saw a steady procession of storms that delivered above normal precipitation amounts. Overall, both the northern and southern portions of the Basin experienced a normal number of precipitation days but less than normal amounts of precipitation during the winter season. The number of precipitation days in spring was well above normal (particularly for April) but the amount of precipitation during the spring was slightly above normal. Precipitation during the summer was spotty due to the absence of strong frontal storms and the occasional development of isolated thunderstorms. Overall, the frequency and amount of precipitation during the summer was near normal. Precipitation in the fall however was about half of normal both in terms of frequency and amount. Of course, it should be remembered that although the frequency of frontal storms typically increases in November, the frequency and total amount of precipitation during the fall season is

Figure 2-2. Map Showing Locations of Selected Meteorological Sites in the Vicinity of Lake Tahoe.

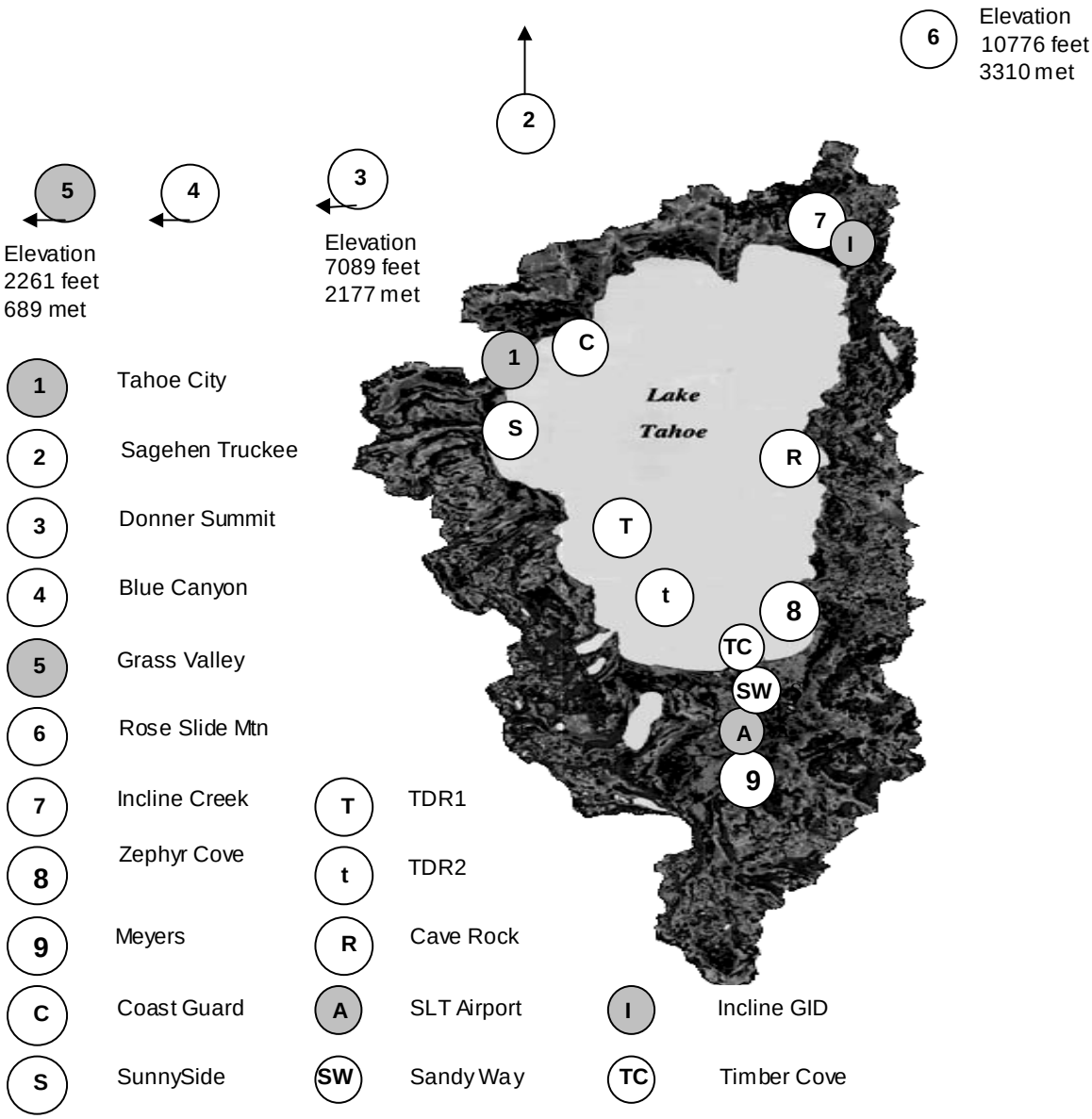

Upper Air Meteorological Sites are shaded.
SLT Airport & Grass Valley were Radar Wind Profiler RASS Sites.

Figure 2-3. Long-term (≥ 30 years) Monthly Mean Precipitation Amounts in Lake Tahoe Basin.
(Source: AccuWeather, 2004)

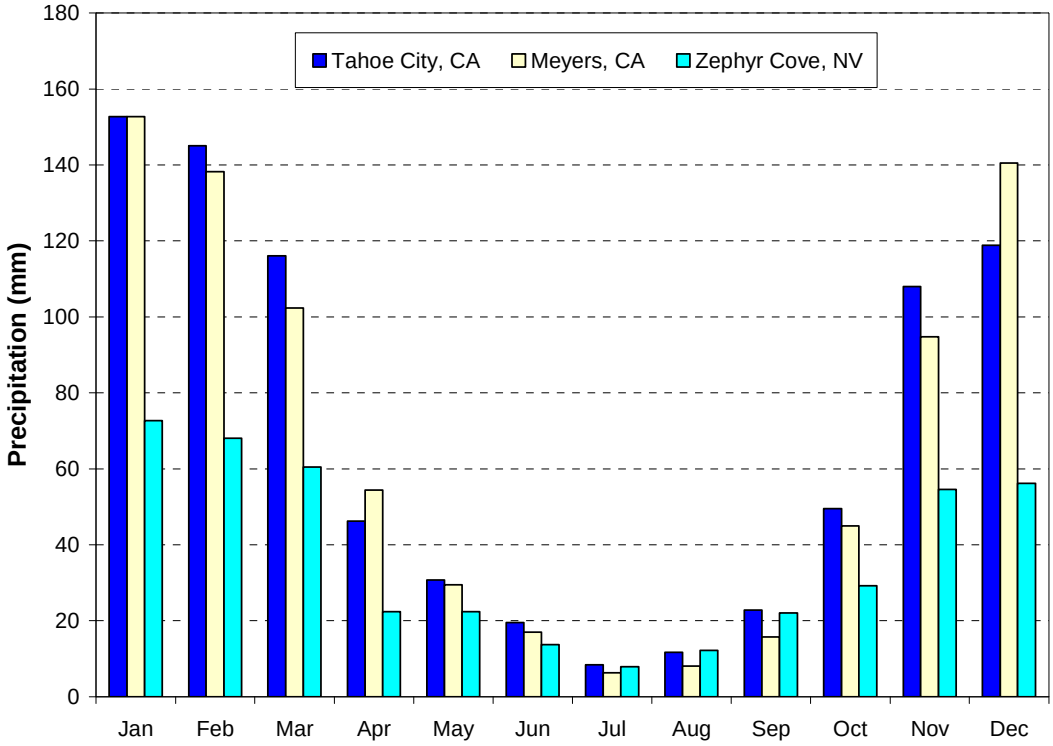

relatively limited – significantly greater than in summer but still significantly less than in winter and even spring.

When the precipitation frequencies during 2003 at Incline Creek and Meyers are compared with the Tahoe Basin norm (developed in **Figure 2-4**), it can be seen from **Figure 2-9** that the fall was drier than normal and that the precipitation frequency abnormalities in winter and spring were driven primarily by the frequent precipitation in December and April, respectively. Seasonal representations of normal precipitation frequencies and the frequency in 2003 are shown in **Figures 2-10 and 11**, respectively. For the year, both Incline Creek and Meyers experienced about 45% more days of precipitation than normal despite precipitation amounts being less than normal. Thus, the 2003 wet deposition estimates will also be higher than normal. Based on the number of days with measurable precipitation at Meyers and Incline Creek in 2003 compared to normal in the Tahoe Basin, wet deposition in a year with a normal precipitation frequency could be as low as 70% of the 2003 values reported in Chapter 5. However, the exact discount amount for a year with a "normal" precipitation frequency would depend not only on the seasonal precipitation frequencies but would also be ameliorated by the higher precipitation frequency likely causing lower ambient concentrations.

Figure 2-4. Normal (long-term average) Precipitation Frequencies (# of days with precipitation > 0.01 inches) at Selected Near-Tahoe Locations* in the Sierra Nevada.

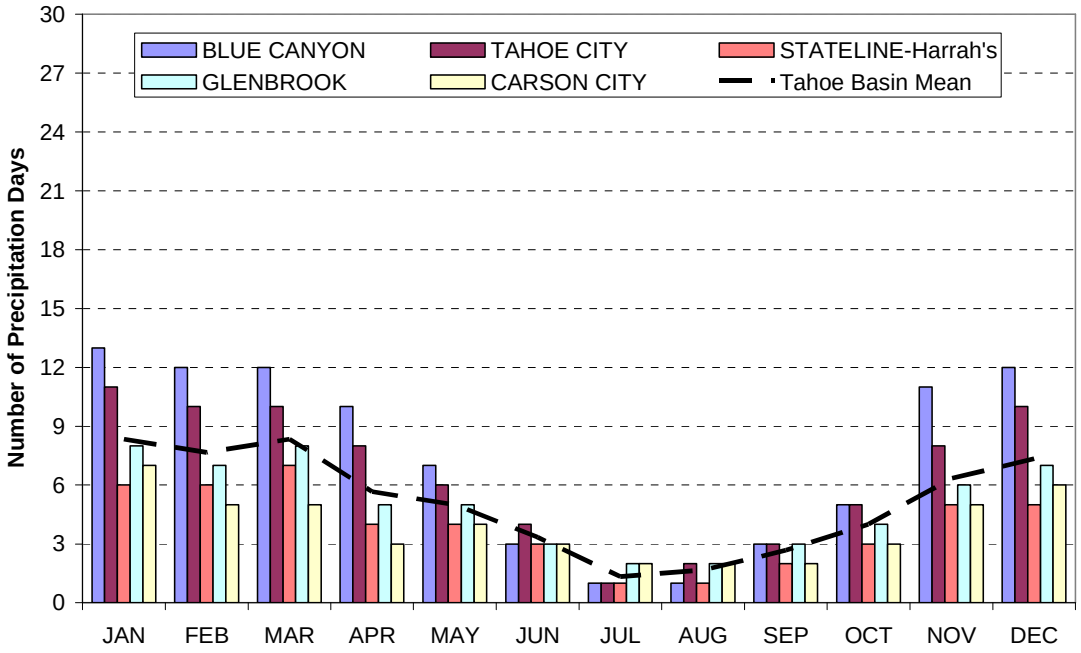

* **Note:** Precipitation data are no longer collected at Stateline, NV (mean is based on 1984-98 data). Precipitation data for Glenbrook, NV (in-basin) and Carson City, NV (outside of Tahoe Basin) represent 1948-2005 means. Additional hourly or summarized meteorological data for these sites were not accessed or retrieved for LTADS.

Figure 2-5. Precipitation Frequencies (# of days with precipitation > 0.01 inches) during 2003 at Selected Near-Tahoe Locations in the Sierra Nevada. (Source: WRCC, 2005)
(Note: the long-term (30-year) annual mean precipitation amounts are shown in parentheses.)

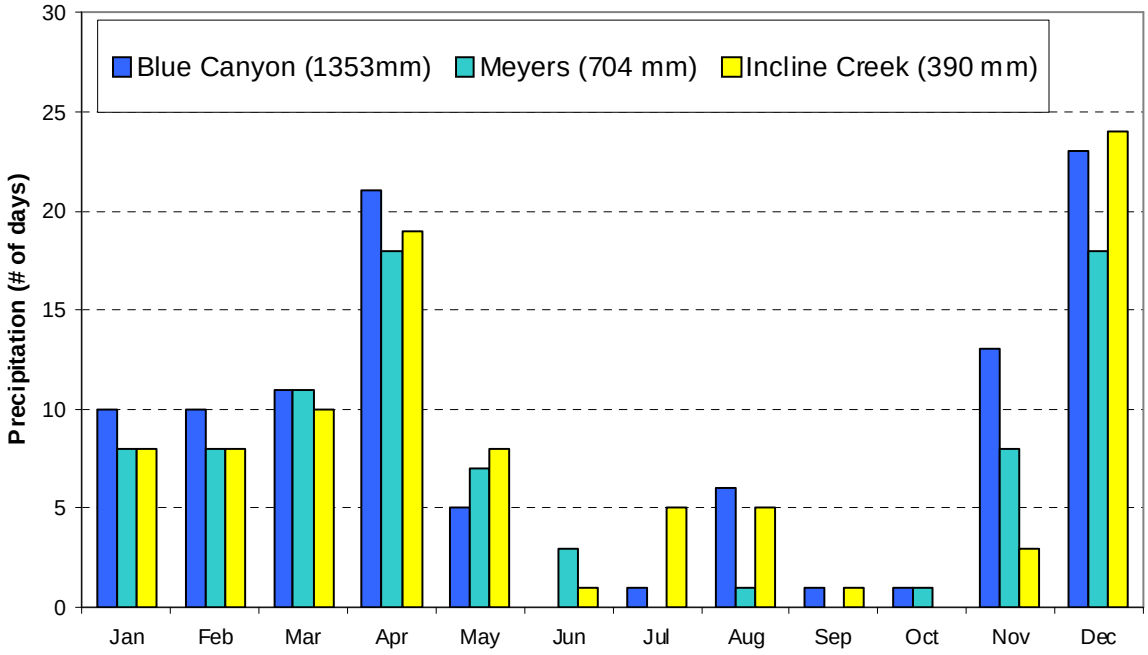

Figure 2-6. Hourly Precipitation Amounts at Incline Creek in 2003.

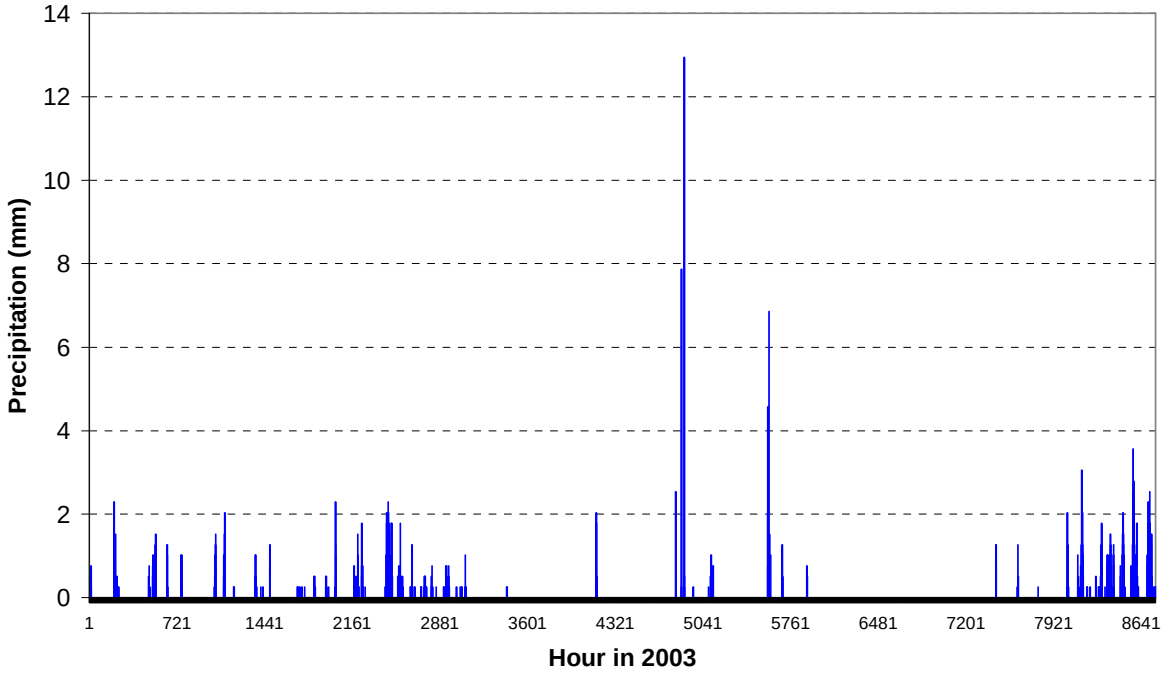

Figure 2-7. Daily Precipitation Amounts at Incline Creek in 2003.

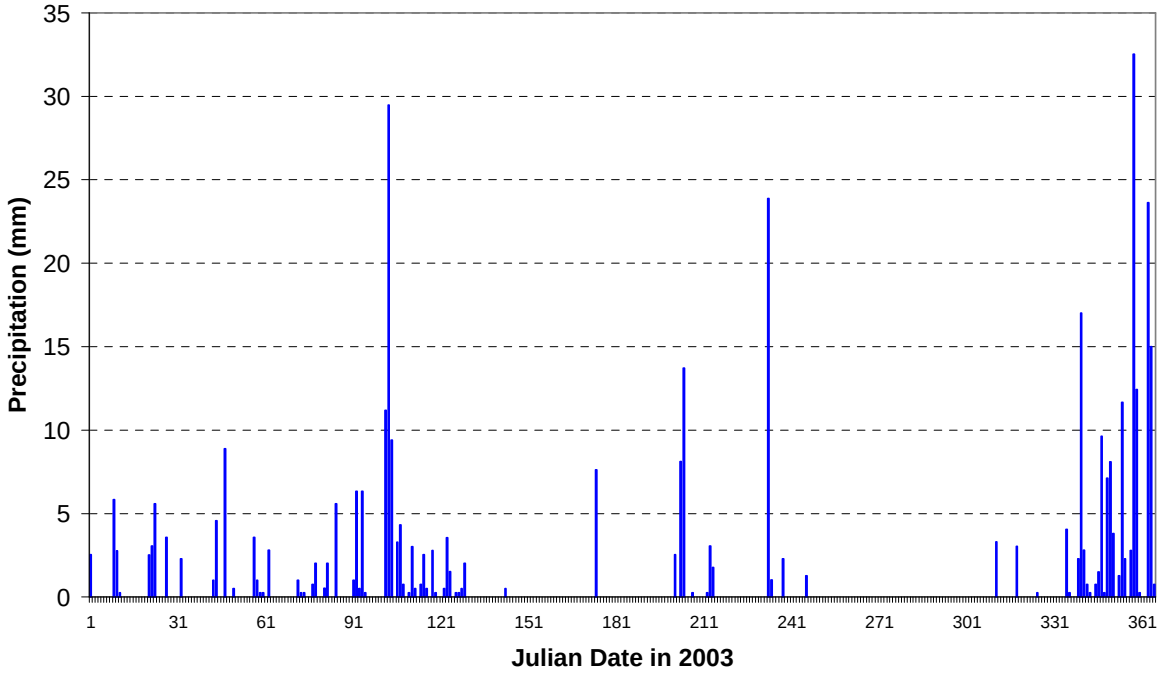

What might all of this mean with respect to atmospheric deposition in 2003 compared to an average (climatologically normal) year? More frequent storms would tend to decrease pollutant concentrations by increasing turbulence and atmospheric mixing. However, increased turbulence could also increase the dry deposition rate of gaseous pollutants that are water soluble (e.g., ammonia and nitric acid). Wet deposition, on the other hand, would always be expected to increase with increasing frequency of precipitation. As indicated in **Figure 2-8**, the number of days with precipitation (≥0.01") was almost twice normal for the winter and spring seasons, approximately normal for the summer, and almost half normal for the fall. Overall, 2003 experienced about 50% more precipitation days than in the average year (~90 vs. 60). Because atmospheric mixing is reduced during winter (except during storms) and pollutants are trapped near ground-level by frequently occurring surface inversions, the staff's dry deposition estimates for winter could be lower than in average years due to likely lower ambient concentrations than normal as a result of the more frequent storms. On the other hand, this potential underestimation of dry deposition is partially offset by staff not discounting the dry deposition during the periods of precipitation when ambient concentrations would be lower than the seasonal average. The wet deposition estimates might not be affected significantly because the estimate is based on the product of concentrations and precipitation frequency. Thus, the wet deposition increase due to more frequent precipitation would be counter balanced by the lower concentrations (amount of material) available for wet deposition.

Figure 2-8. Precipitation Amounts in 2003 versus Seasonal Normals.

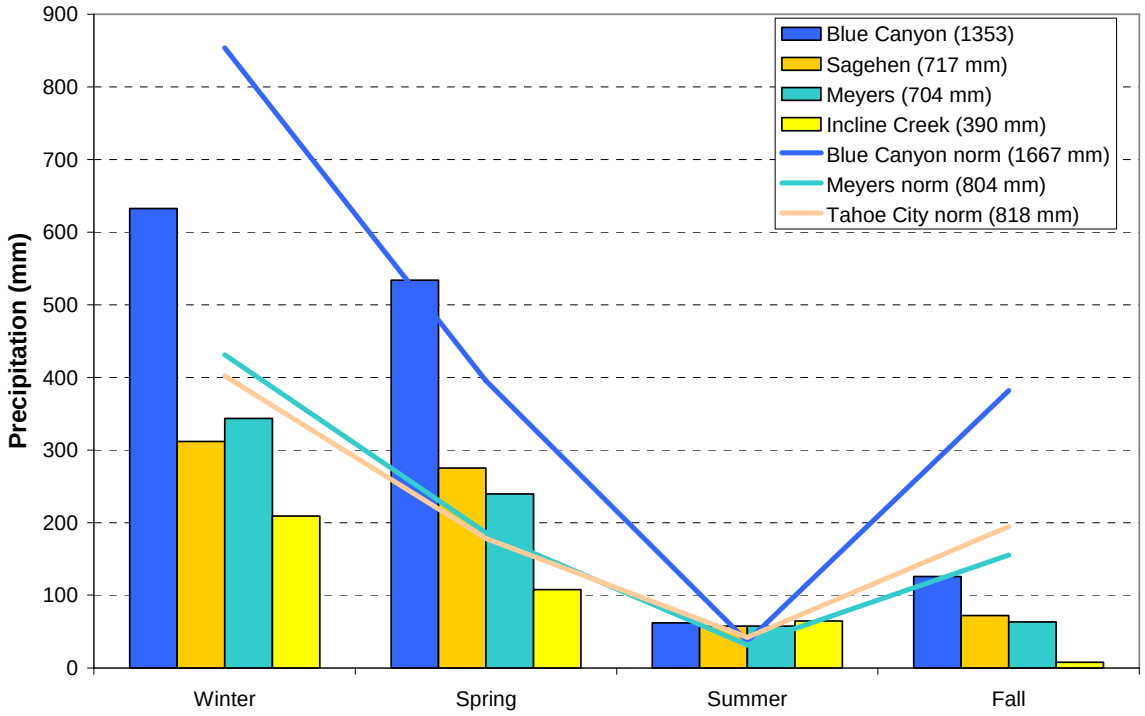

Figure 2-9. Comparison of Precipitation Frequencies (# of days with precipitation > 0.01 inches) during 2003 at Two Tahoe Locations with the Climatological Mean for the Tahoe Basin. (**Note:** Tahoe Basin mean is based on long-term results for Stateline (1948-1998), Glenbrook (1948-2005), and Tahoe City (1914-2005).)

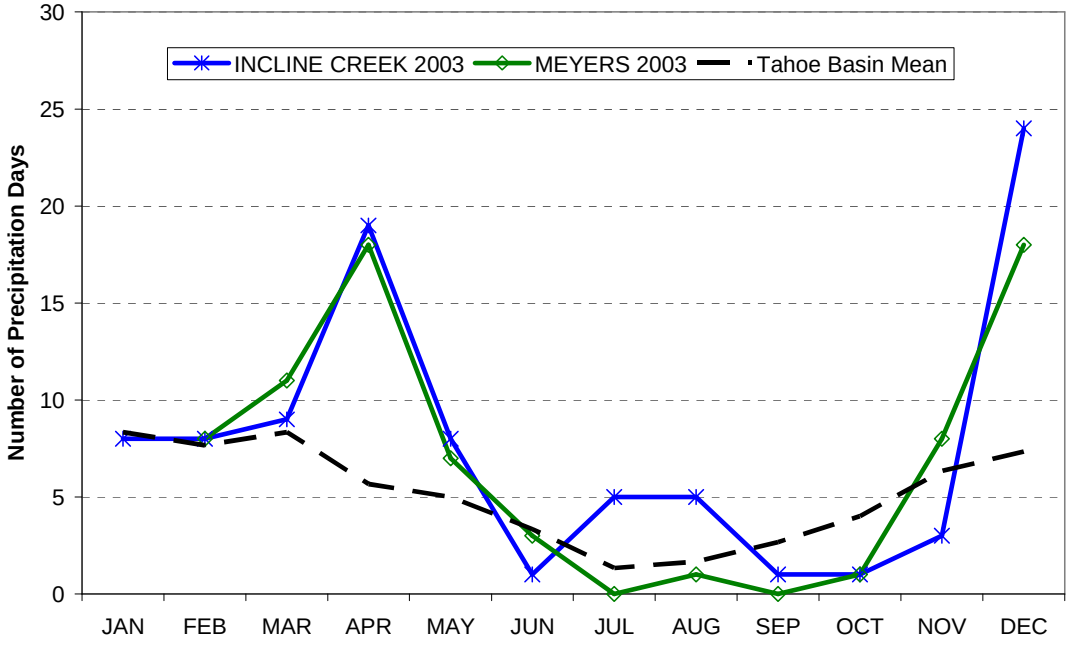

Figure 2-10. Climatologically Normal Number of Days per Season with Precipitation Amounts greater than 0.01 inches. (Note: Tahoe Basin mean is based on long-term results for Stateline (1948-1998), Glenbrook (1948-2005), and Tahoe City (1914-2005).)

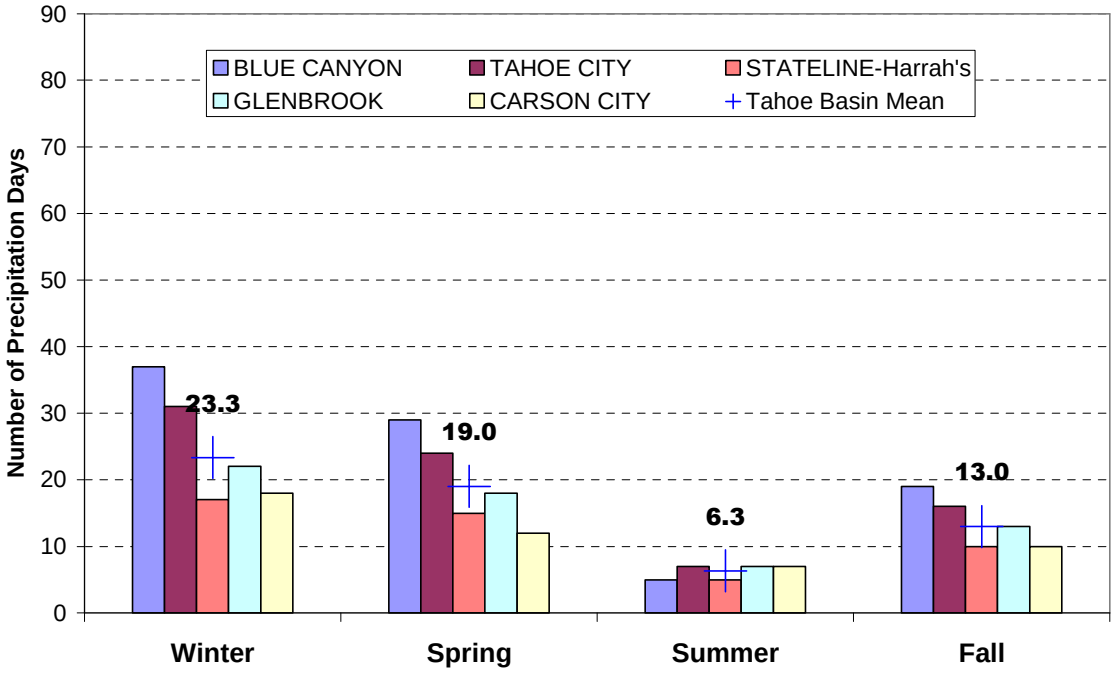

Figure 2-11. Comparison of 2003 against Climatologically Normal Number of Days per Season with Precipitation greater than 0.01 inches. (**Note:** Tahoe Basin mean is based on long-term results for Stateline (1948-1998), Glenbrook (1948-2005), and Tahoe City (1914-2005).)

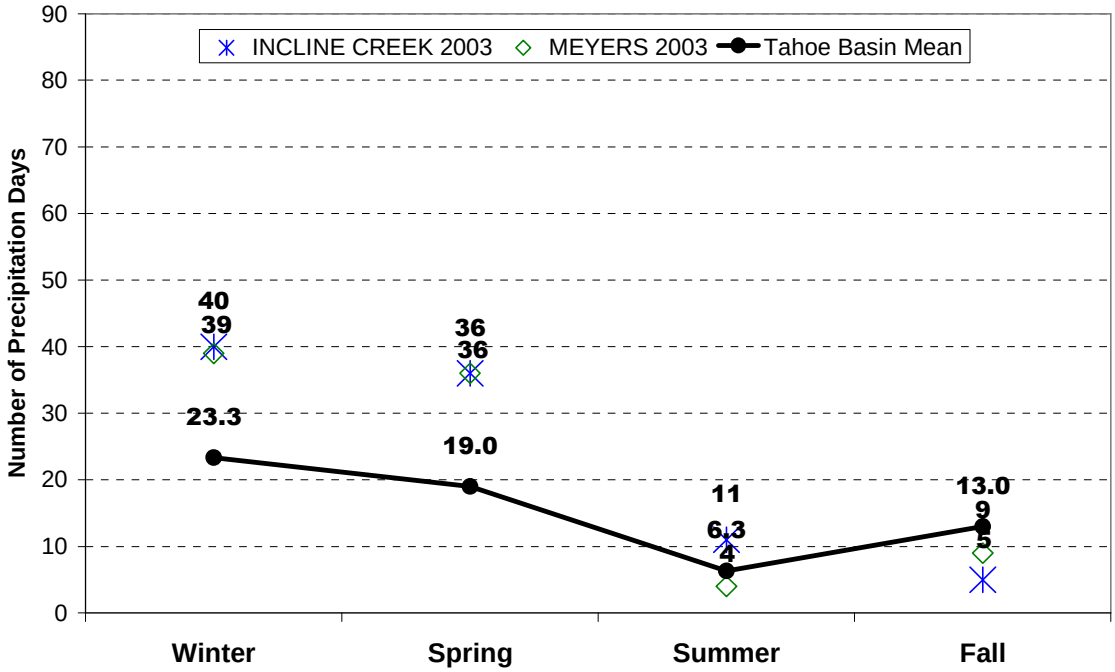

2.2 Temperature Patterns

The distinctive patterns of temperature in the Tahoe Basin provide a framework for broad understanding of horizontal winds and vertical mixing, and their variations by time of day and season. The winds, obviously responsible for horizontal transport of any pollutants, water vapor, or nutrients that they contain, are driven primarily by gradients of air density and air pressure. Those gradients are caused by the differences in air temperature that will be described here. Furthermore, the variation in air temperature with altitude above the ground or water surface is critical to the vertical dispersion of pollutants.

Thus, temperature patterns provide a foundation for understanding the potential for transport and dispersion, and ultimately deposition of substances emitted into the atmosphere. Likewise, because those temperature patterns give insight into the potential for horizontal and vertical movement of atmospheric constituents, they also provide insight into the likely spatial representativeness of the observed concentrations that will be described in Chapter 3. The next sections describe the patterns of temperature, and their implications for locally generated winds and for enhancing or suppressing vertical mixing.

2.2.1 Surface Air Temperatures

As illustrated in **Figures 2-12 through 2-14**, average temperatures near lake level in the Tahoe Basin in the summer (July) range from daily maximums in the low 80s (^{O}F; ~28 ^{O}C) to daily minimums in the 40s (^{O}F; ~7 ^{O}C); in the winter (January), temperatures range from highs around 40 ^{O}F (4 ^{O}C) to lows around 20 ^{O}F F (-7 ^{O}C). The diurnal ranges in temperature in July are about 30 ^{O}F (17 ^{O}C) (at Zephyr Cove (east), 35 ^{O}F (19 ^{O}C) at Tahoe City (northwest), and 40 ^{O}F (22 ^{O}C) at S. Lake Tahoe (south). The diurnal variations in temperature during January are smaller, 20 ^{O}F - 25 ^{O}F (~12 ^{O}C) (greatest at S. Lake Tahoe). In general, temperatures decrease with increasing altitude but local temperatures also depend on humidity, exposure to sunlight, and terrain-following air flow.

Figure 2-15 provides a daily trace of the maximum and minimum temperatures during 2003 at the ARB air quality monitoring site in South Lake Tahoe. The dominant feature, particularly from the daily maximum temperature trend, was the rapid transitions between winter and summer. The effect of the stormy April is also evident. In general, the difference between the daily maximum and daily minimum temperatures are greater during dry periods (e.g., summer) and little smaller during wet periods (e.g., December). However, when the temperatures in 2003 are compared to the monthly climatological temperature norms for sites around the Basin (**Figure 2-16**), 2003 appears quite normal except for the months of April and November, which were cooler than typical, and January, which was slightly warmer than normal. Because the deposition estimates are made on the basis of seasonal air quality and meteorological conditions, the seasonal temperatures for 2003 are compared with seasonal norms in **Figure 2-17**. Once again, the 2003 temperatures appear representative of typical temperatures experienced in previous years.

Figure 2-12. Monthly Mean and Record Temperatures at Zephyr Cove, NV.
(Source: AccuWeather, 2004)

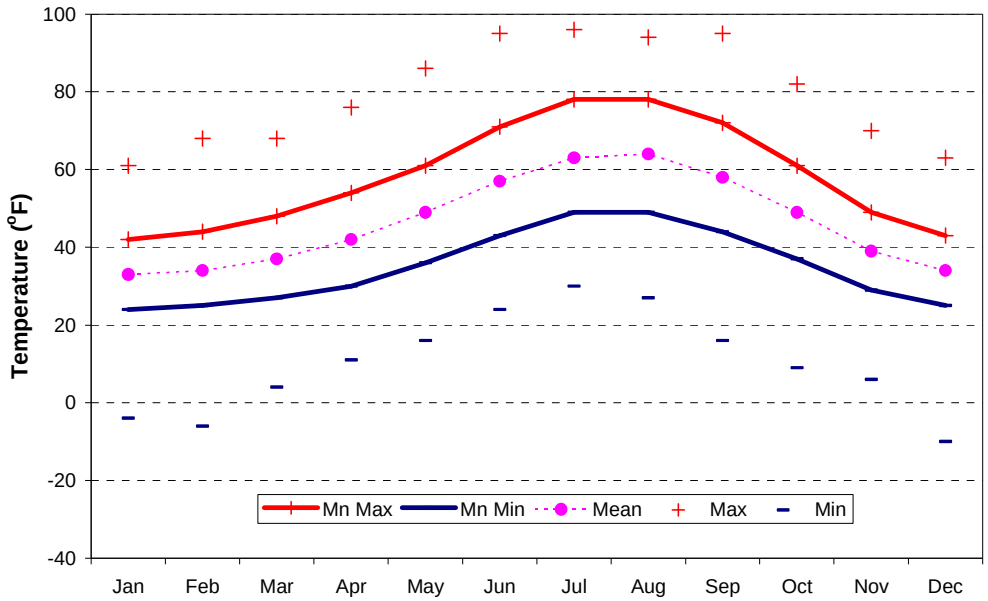

Figure 2-13. Monthly Mean and Record Temperatures at Tahoe City, CA.
(Source: AccuWeather, 2004)

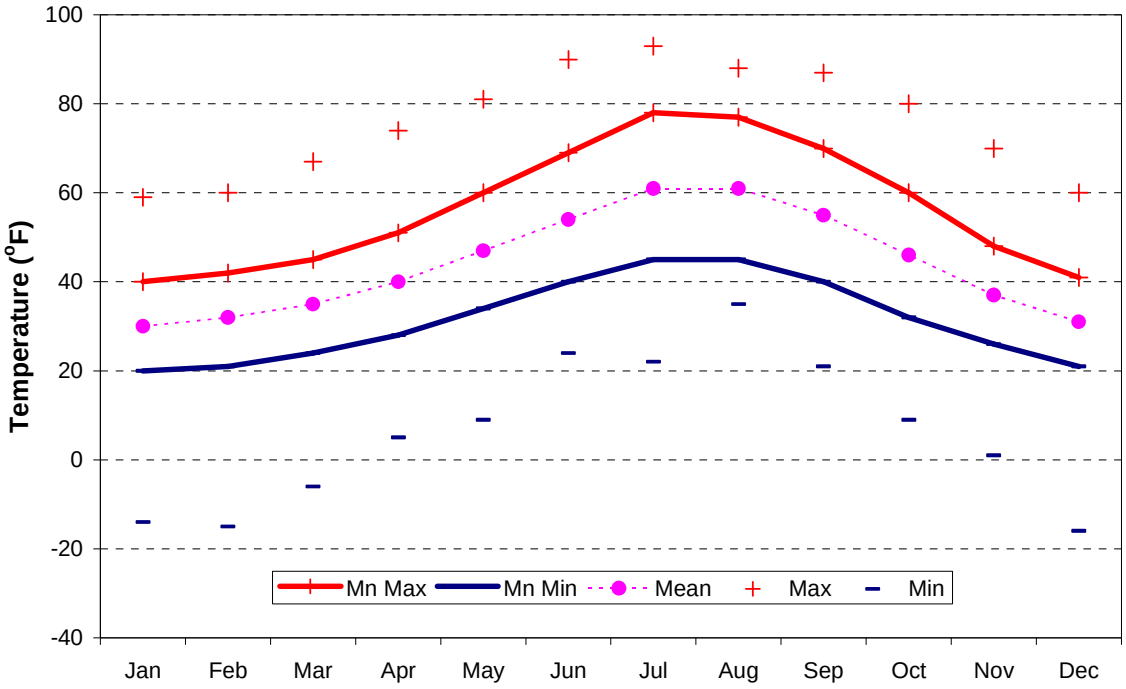

Figure 2-14. Monthly Mean and Record Temperatures at South Lake Tahoe, CA.
(Source: AccuWeather, 2004)

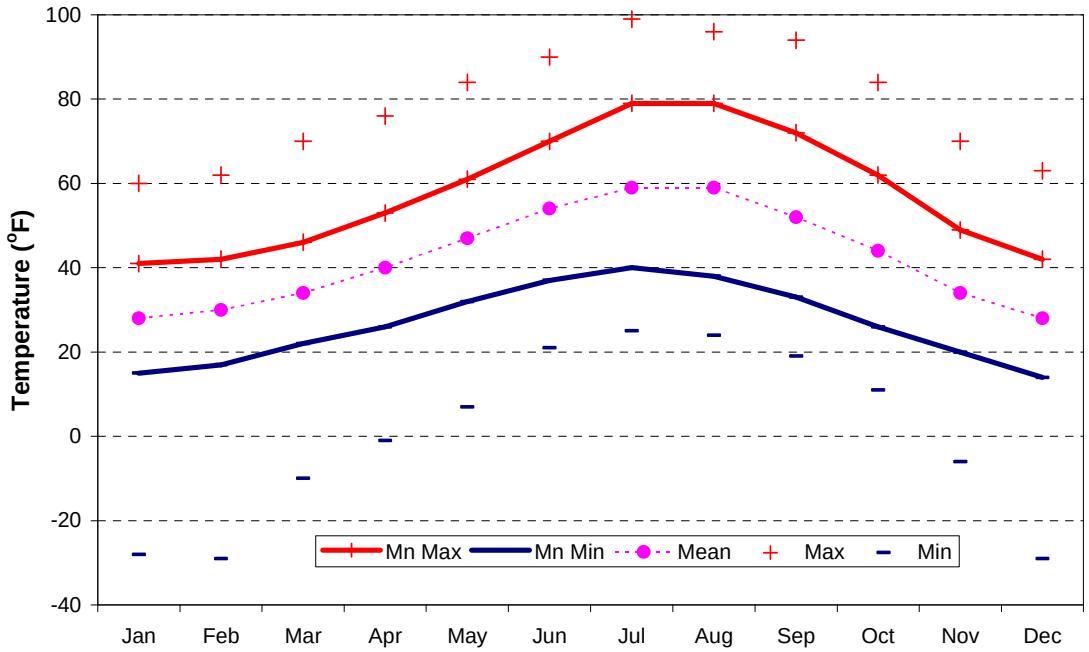

Figure 2-15. Daily Maximum and Minimum Temperatures during 2003 at South Lake Tahoe (Sandy Way).

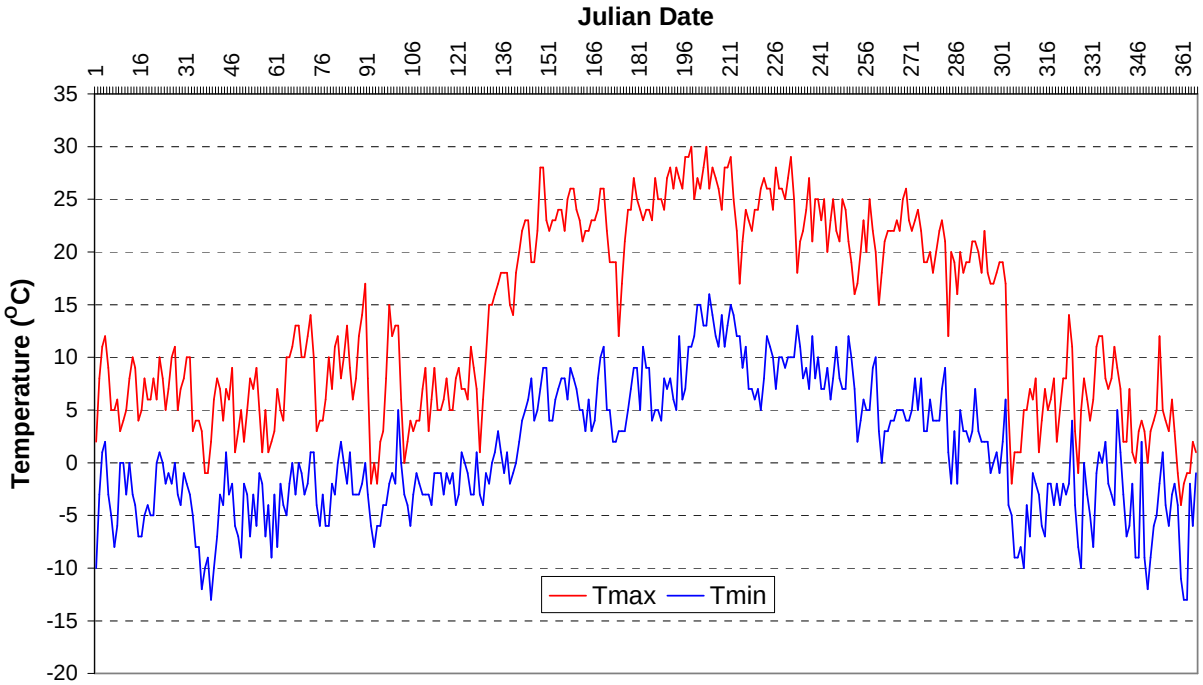

Figure 2-16. Comparison of 2003 Temperatures at SLT – Sandy Way with Climatological Normal Temperatures at Long-Term Sites in the Tahoe Basin.

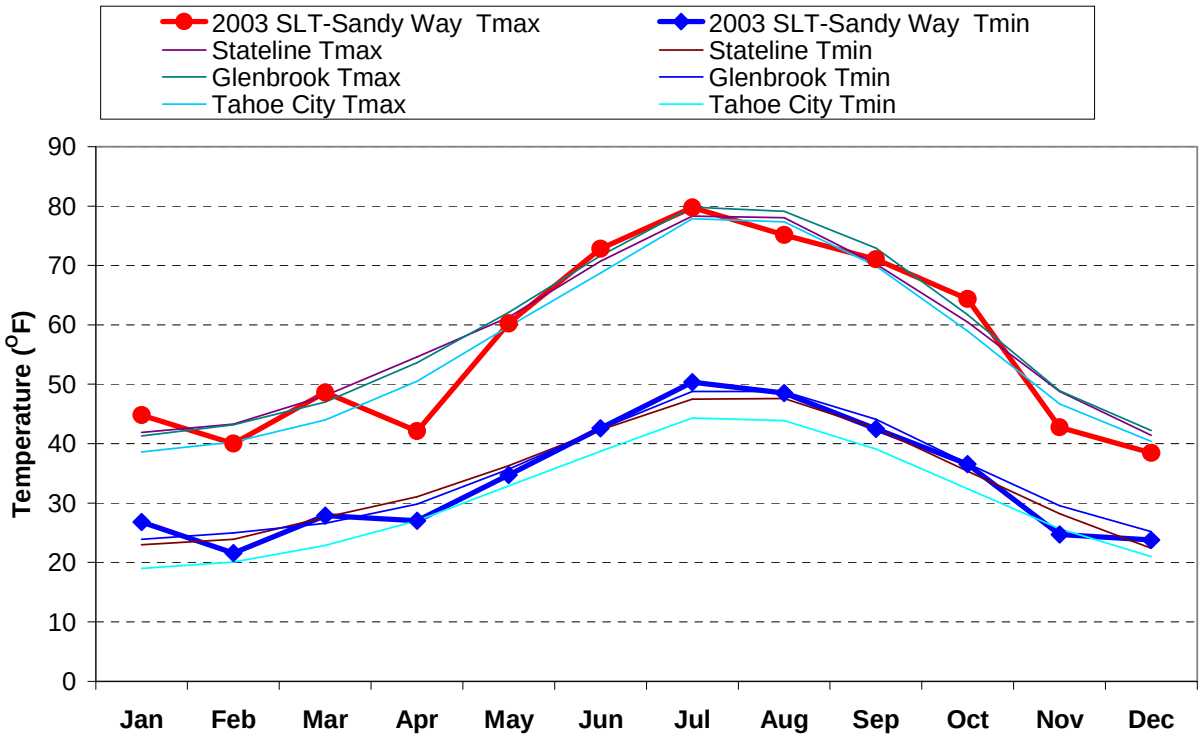

Figure 2-17. Comparison of Seasonal 2003 Temperatures with Seasonal Normals.

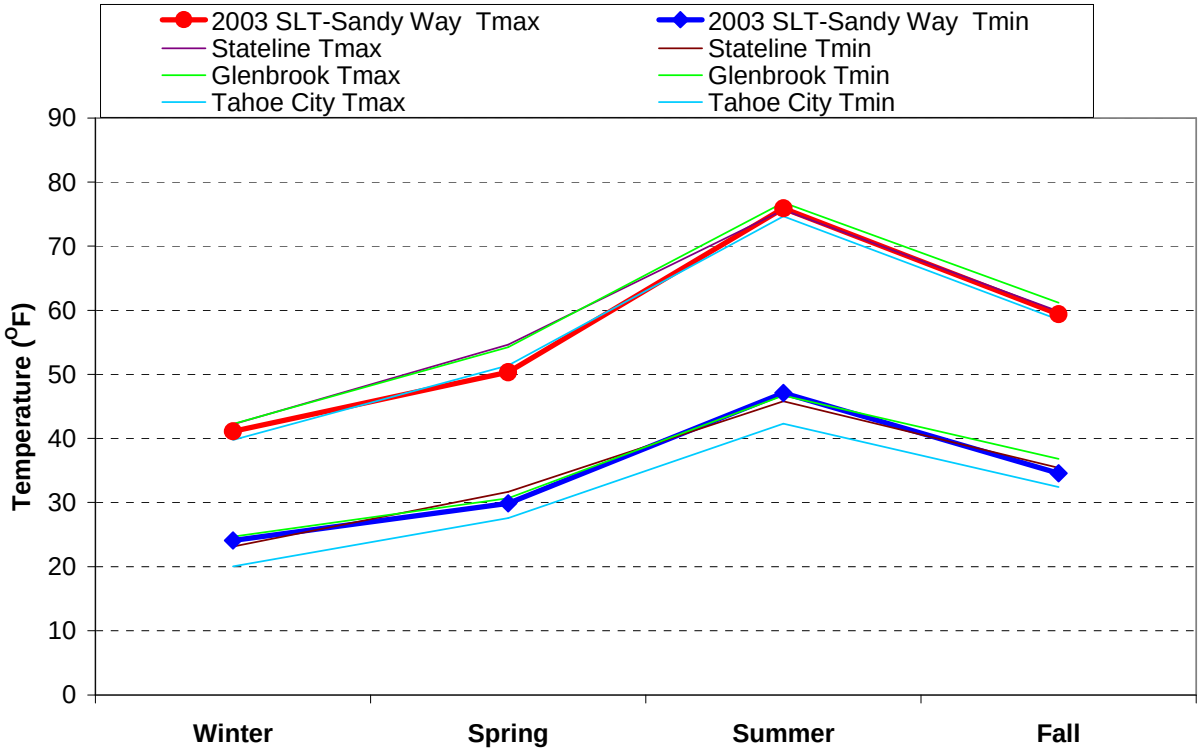

With increasing altitude, the air is less dense and holds less water vapor, two factors that help air retain its heat. Land surfaces at altitude cool rapidly at night and thereby also cool the lowest layer of the atmosphere. Because cold air is heavier (more dense) than warm air, the bowl-like shape of the Basin facilitates the accumulation of the cold air draining off the mountain slopes. Thus, nocturnal temperature inversions frequently form during all seasons and have great potential to accumulate air pollutants (Twiss et al., 1971). The months of June through October have the most frequent inversions, averaging 15 to 20 days per month. Surface-based inversions influence when and how deeply local emissions are mixed vertically and diluted (assuming cleaner air aloft, away from local emissions). In addition, temperature inversions inhibit vertical mixing between air aloft (that may transport material over the mountains) and the surface air that is in contact with the ground and water surfaces.

Due to the alpine location of the basin, the greater intensity of solar radiation relative to lower elevations has the potential to accelerate ozone and nitrogen photochemistry (Twiss et al., 1971). Generally more solar radiation reaches the Lake Tahoe Basin because the thinner and less polluted atmosphere scatters and absorbs less solar radiation. However, although scattering and absorption both tend to decrease the incident radiation at the surface, they may have opposite effects on rates of photolysis because those rates depend not on the incident radiation (i.e., on a surface) but on the actinic flux. The actinic flux is the spherically integrated radiative flux (i.e., the sum of the incoming radiation from any and all directions) that is intercepted by each

atmospheric molecule. Although absorption decreases both incident radiation and actinic flux, generally scattering decreases incident radiation but increases actinic flux. The relative changes in the actinic flux and resulting rates of photolysis depend on the size and chemical composition of particles and their vertical distribution.

2.2.2 Vertical Distribution of Temperature

A layer of the atmosphere in which the air temperature increases with height is an effective barrier to vertical mixing. Such a layer (referred to as a temperature inversion or thermally stable layer) is typically caused by various predictable and observable atmospheric processes. If observations are available, layers with or without vertical mixing can be differentiated by examining how the temperatures change with altitude above the surface and by comparing observed air temperatures near the surface and with those aloft.

Temperature inversions (in the most simple sense, where warmer air overlies cooler air) greatly restrict the exchange of air and the pollutants between the different layers. Inversions can be formed by a variety of methods – subsidence (sinking air associated with high pressure systems), advection (e.g., sea/lake breeze), radiative cooling, cold air drainage, etc. Inversions that form at ground level are of particular interest as they will trap most pollutant emissions and keep them near ground level where people can be impacted by them and where surfaces are available for deposition.

2.2.2.1 Subsidence Inversions

A region of high pressure generally creates a temperature inversion aloft (as a result of subsiding air) and thereby restricts vertical mixing across the subsidence inversion. The position and strength of the eastern Pacific high pressure zone varies seasonally and daily, and thus it has an intermittent effect on temperatures aloft and vertical mixing of the atmosphere over the western states including the Tahoe Basin. The restriction of vertical mixing due to the Eastern Pacific High is generally greatest in the late summer and early fall. When present, the area of high pressure creates divergent (i.e., net outward) horizontal air flow over a broad area (i.e., spanning hundreds to thousands of kilometers) and continuity of mass requires a compensating weak downward motion of the air aloft in response. Intuitively, one might expect downward motion of the air aloft to cause downward mixing of air from aloft, but it does not. The downward motion is very slow and thus extends only very short vertical distances, but it creates a persistent temperature inversion near 9-10 thousand feet MSL. As the air moves downward, it is compressed by the increasing air pressure it encounters and is heated by that compression. Thus, the Eastern Pacific High can create a relatively persistent temperature inversion over a large area that is an effective barrier to vertical mixing of surface air with air above it.

Some subsidence and heating of air is also expected in the lee of the Sierra crest and that downward motion will also induce compressional heating of a layer of air and possibly generating another temperature inversion. However, a lee inversion would likely be of limited spatial extent and may only intermittently block vertical mixing. Also, it is common for shallow atmospheric waves to develop in this inversion layer that are

analogous to water waves. The atmospheric lee waves may intermittently cause mixing of air above and below the inversion. However, observations relevant to documenting such processes were outside the scope of LTADS.

Another weak type of subsidence inversion occurs (primarily in the summer and fall) when winds are weak and the solar heating of the land draws air off the Lake and up the mountain slopes. The air moving off the Lake is replaced by descending air above which warms due to compressional heating. This descending air can evaporate haze and fog layers from above while creating a subsidence inversion trapping particles and other pollutants below it. Again however, observations relevant to documenting such processes were outside the scope of LTADS.

2.2.2.2 Surface-Based Inversions

Surface processes are also important to determining vertical mixing and their effects vary over smaller areas. In considering mixing depths in the Tahoe Basin, it is especially important to understand the processes that may cause the mixing depth to differ over the Lake as compared to over the land.

The typical diurnal evolution of the surface mixing depth over land is discussed first. Over land at night and in the early morning, there is usually only shallow vertical mixing (especially with clear sky conditions) because a surface-based inversion forms due to radiative cooling of land surfaces and advection (e.g., drainage of cooler air off the mountain slopes). Around sunrise, it is common for concentrations of pollutants at the surface to be relatively high because local emissions (e.g., from wood combustion or traffic) are usually mixed only through a shallow layer of air. Under these conditions (especially with light winds and a low sun angle), it is frequently possible to visually observe a relatively polluted surface layer and a sharp transition to cleaner air above the inversion.

As the ground is heated by the sun, the air at the land surface is warmed; over flat areas, the depth of mixing increases while upslope flows are generated in more complex terrain. Frequently, it is possible to visually observe the depth of the surface layer increase during the morning hours as land surfaces are heated by the sun and in turn heat the lower atmosphere. As the mixing depth increases through the day, pollutants emitted at the surface are diluted through a deeper volume and concentrations at the surface generally decrease. However, it is also possible for higher concentrations of some pollutants to occur above the mixed layer. In this case, the increasing depth of the mixed layer of air near the surface will mix some of the air aloft into the surface layer and the resulting concentrations will reflect a mixture of the concentrations previously observed at the surface and aloft.

By mid-day, vertical mixing can be vigorous through a moderately deep surface layer as the sun warms the ground and the air in contact with the ground, creating thermal plumes that rise until they reach a layer of warmer air aloft. The maximum depth of the surface mixed layer usually occurs approximately the time of daily maximum air temperature at the surface, typically between 1300 and 1600 local time. As the sun

drops toward the horizon, the earth's surface and the air near it, begin to cool and over a period of hours (and generally before sunset), a nocturnal surface-based inversion is formed. The surface cooling typically begins before sunset because the net radiation balance at the surface becomes negative before sunset (as the incoming short-wave solar radiation decreases quickly and outgoing long-wave infrared radiation decreases slowly).

Thus, over land with clear skies, periods of vertical mixing through moderate or deep layers are generally limited to the daylight hours and mixing is deepest from about noon to mid-afternoon. Clouds may moderate this cycle by decreasing both daytime heating and nocturnal cooling of the ground surface. Deep mixing will also be present over both land and water during the passage of low-pressure storm systems, the formation of cumulonimbus clouds, and possibly the presence of high winds.

2.2.2.3 Deep Mixing

During periods of deep mixing, concentrations are generally low both at the surface and aloft. Deep vertical mixing occurs during the passage of low-pressure storm systems. Deep mixing will also occur where cumulonimbus clouds develop (either with or without thunderstorms). High winds can also occur without a low pressure system or cumulonimbus and will generally disperse emissions and result in lower concentrations.

2.2.2.4 Differences in the Vertical Mixing of Air Over the Lake and Land

The vertical mixing of air over the Lake differs from that over the land because the day-to-night change in water surface temperature is small compared to that of the land surface. During most hours of the year, the temperature of the Lake water is warmer than the temperature of the air, with the greatest differential occurring at night and in the early morning. Thus, when cold down-slope drainage winds flow onto the Lake, we also expect some warming of air near the water and as a result, some vertical mixing due to weak convection. On the other hand, conductive cooling of the air by a colder Lake surface occurs during some seasons and hours, e.g., during summer mainly from mid-day to mid-afternoon. At these times, there is also a tendency for onshore flow so that the cooler air from over the Lake surface is advected over the land area, creating an inversion. However, such an inversion will likely not persist very far inland from the Lake due to heating of the land by the sun and enhanced mixing.

Rawinsondes, balloon-borne instruments for measuring temperature (humidity and winds aloft, are routinely launched at 00Z and 12Z (Zulu or Greenwich Meridian Time) from locations around the world. Zulu time is 8 hours ahead of Pacific Standard Time. Thus, the 00Z launch time corresponds to 1600 Pacific Standard Time (PST) of the prior day and the 12Z launch time corresponds to 0400 PST on the same day. The rawinsonde launch location in northern California is Oakland International Airport. Sondes are also launched at Reno, NV. Monthly mean temperatures observed at 00Z at the 850 millibar (mb) pressure level, about 4800 feet above mean sea level (MSL), above Oakland during the summers of 1991-2000 are plotted in **Figure 2-18**. Compared to temperatures observed at the surface, temperatures observed aloft are representative of those over a broad area. As one might expect, the temperatures over

Oakland at 850 mb are warmest during the summer and mean monthly temperatures exceed 60 ^{O}F (15.5 ^{O}C) during July, August, and September. Also shown in the figure are the monthly mean surface temperatures observed at South Lake Tahoe (6200 feet MSL). Comparison of the temperatures at South Lake Tahoe and at 850 mb pressure altitude over Oakland provides an indication of the seasonal tendency for temperature inversions (with inversions associated with relatively warmer temperatures over Oakland). Assuming a dry adiabatic lapse rate for the change in temperature with pressure altitude, the Oakland 850 mb temperature would be almost 5 ^{O}F colder at the elevation of Lake Tahoe. The temperature inversion analysis can be made by visually sliding the seasonal 850 mb temperature line downward 5 ^{O}F (to correspond to the equivalent temperature at the elevation of South Lake Tahoe). The tendency for warmer air over Oakland (and potential for subsidence-induced temperature inversions aloft over Tahoe) is lower in May and June, moderate in July and August, and greatest in September and October.

Figure 2-18. 850mb Temperatures at 4 a.m. PST at Oakland, CA. (Source: AccuWeather, 2004; Bennett, 2004)

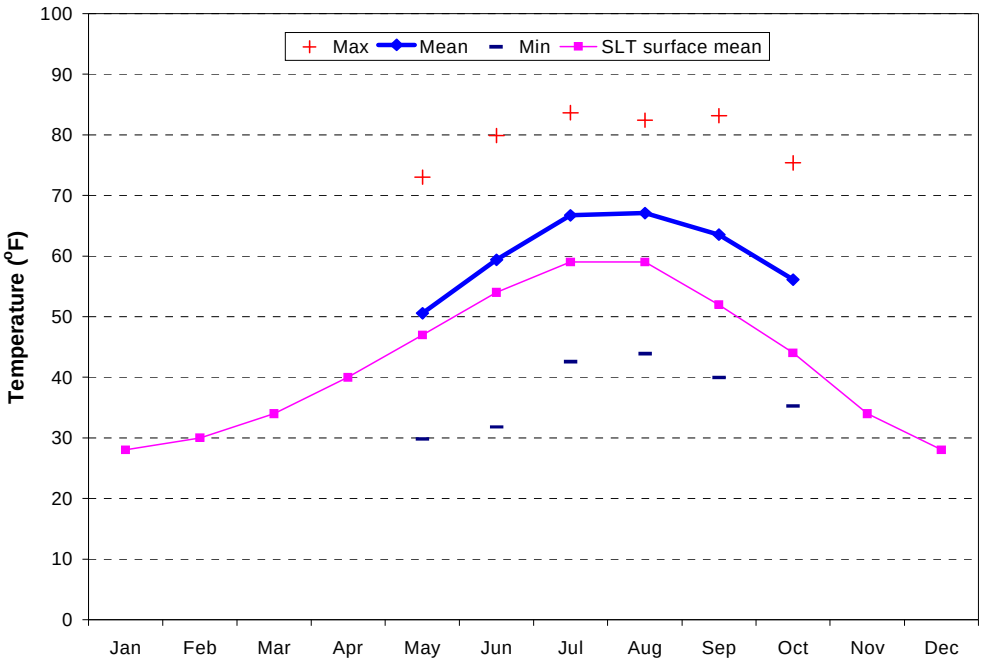

A limited number of temperature soundings have been made over Lake Tahoe (Barone, 1979; Unger, 1979; Carroll, 2004). The data often indicate a subsidence inversion around 10,000 feet MSL and frequently another inversion is noted near 8,000 feet (') MSL (see **Figure 2-19**). Because most of the summer temperature soundings have been made with aircraft, less is known about the frequency and strength of low level (surface) inversions. Basic meteorological principles and the limited available information (e.g., balloons during winter) suggest that surface-based inversions may be quite common. Limited measurements of the mixing depths at the South Lake Tahoe Airport averaged 150 to 400 feet (Barone, 1979). An example of temperature profiles

observed concurrently over land and Lake during a winter day is provided in **Figure 2-20**. In this example, a strong surface-based inversion is present in the morning over the Airport up to 7000' with another inversion layer between 7250' and 7750'. A couple of potential weak inversion layers might exist near 8000' and 9600'. The subsidence temperature inversion is present from 10,500' to at least 11,250'. Note that the morning temperature profile over the Lake indicates a surface-based inversion up to about 7500' but it is much warmer and more isothermal than the surface inversion on land because the large thermal mass of the Lake moderates overnight decreases in air temperature. In the afternoon soundings, it is evident that solar heating and increased air movement raised the air temperatures throughout the atmosphere in the Basin. Although much weaker, temperature inversions still appear to be present at the surface and 7500' at the Airport. Note too that the subsidence associated with a high pressure system also caused the base of the subsidence inversion to drop below 10,000' during the day.

The LTADS aloft measurements included hourly remote sensing of temperature with the radar acoustic sounder system (RASS) operated in conjunction with the radar wind profiler at the South Lake Tahoe Airport. Although the RASS has less vertical range than the balloon borne rawinsondes, the ability to obtain hourly observations provides a great benefit for understanding the climatology of mixing in the Tahoe Basin. The data have been utilized by comparison of simultaneous hourly observations of air temperatures aloft (from the RASS) and near the surface as measured both at land sites and on the Lake itself.

Figure 2-19. Sample Temperature Profiles during Summer from Aircraft Soundings. (Unger, 1979)

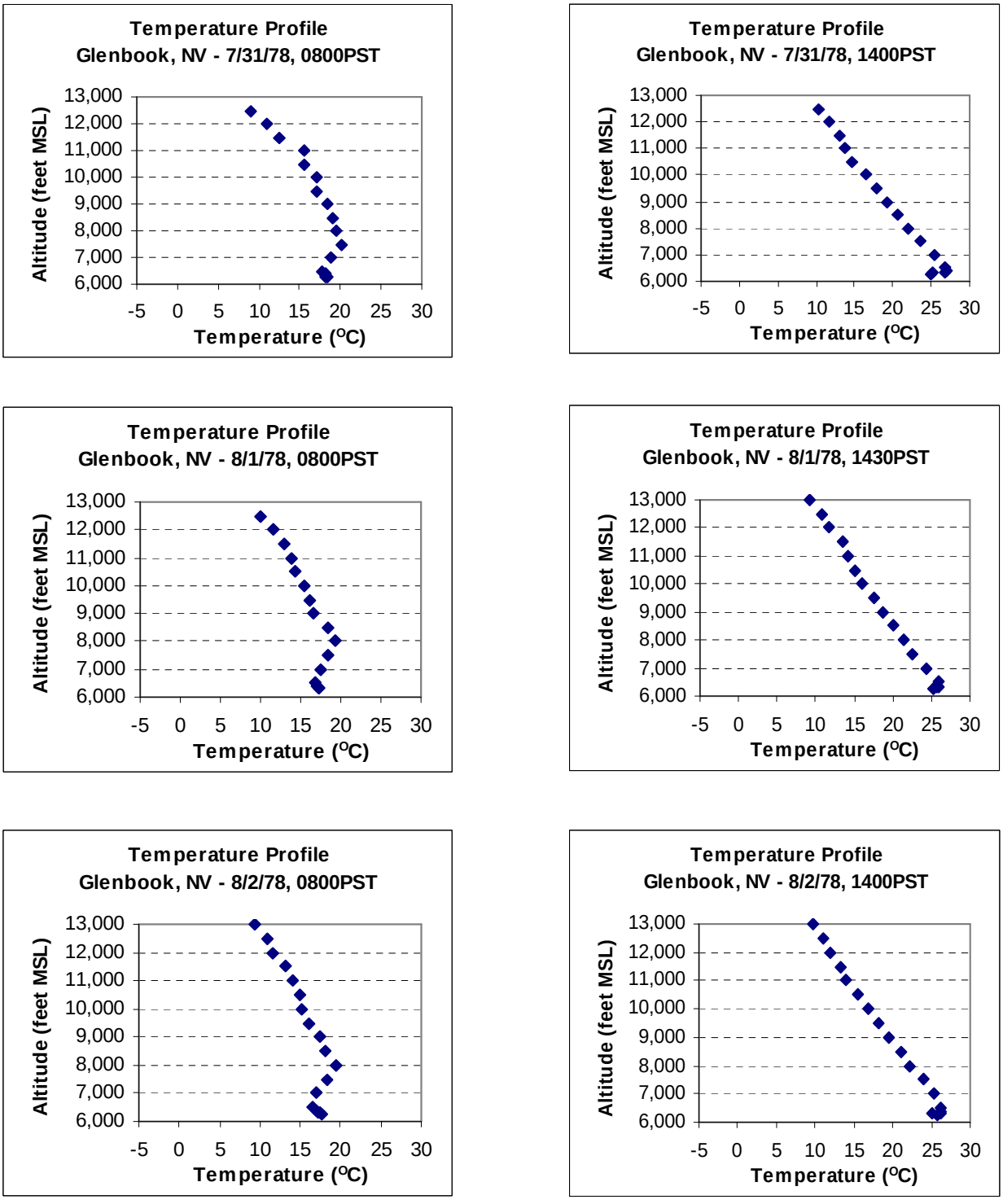

Figure 2-20. Sample Temperature Profiles During Winter (1/22/79) from Balloon Soundings Released in the Morning and Afternoon from the South Lake Tahoe Airport (AP) and from Lake Tahoe (L). (Unger, 1979)

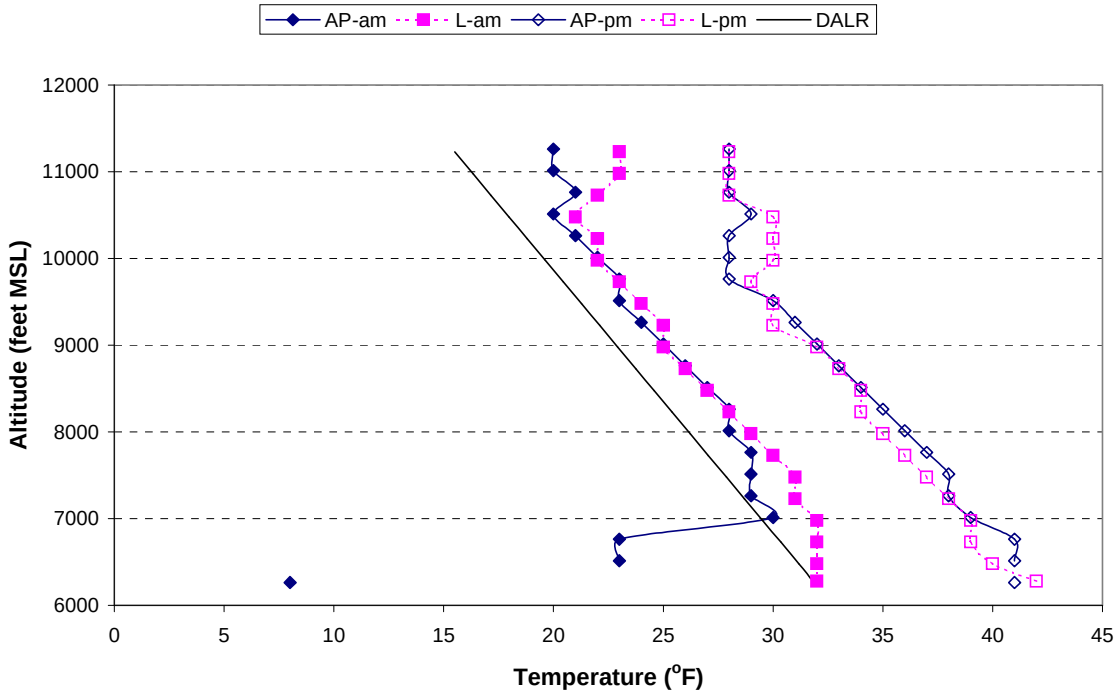

Note: The dry adiabatic lapse rate (DALR) is shown as a solid straight line and indicates the rate that an air parcel would cool (warm) due solely to expansion (compaction) as the parcel might rise (descend) through the atmosphere. The parcel of air would tend to cease changing altitude when its temperature becomes the same as the ambient air around it. In general, a temperature inversion is present if the slope of the ambient temperature is greater (more vertical or even left to right) than the DALR slope.

2.2.3 Air and Water Temperatures

At Tahoe, because of the high altitude, steep terrain, and thermal inertia of the Lake, temperature patterns (and thus wind speed and direction) typically vary in predictable daily patterns. The thinner and often drier atmosphere at higher altitudes allows rapid cooling at night and results in larger day-night swings in land surface temperatures at Tahoe than at lower elevations. In contrast to the large temperature swings over land, the temperature of the Lake surface and the air temperature immediately above its surface are moderated by the large thermal mass of the deep Lake. Despite cold air temperatures during the night at altitude and sometimes deep snow fall, the depth of the Lake creates sufficient thermal inertia that the Lake surface does not freeze except for small areas near the shoreline and only during periods of extreme cold.

Figures 2-21 illustrate the seasonal average temperature of air (solid symbols) and water (open symbols) measured at 2-cm depth by time of day on Lake Tahoe. At the U.S. Coast Guard pier at night, during all seasons, the air is colder than the water temperature by about 6-8 ^{O}C. During fall and winter the air is colder than the water even during the warmest hours of the day. During spring and summer the air

temperature exceeds the 2-cm water temperature during some daytime hours but by only a few degrees. Also note the very large increase in temperatures between the spring and summer seasons. In comparison to temperatures nearer the shoreline, the air temperatures observed 3 km offshore at the TDR1 buoy appear to be moderated by the Lake to a greater extent, but that moderation is also attributable in part to a lower measurement height. The TDR1 observations at 3 m above the Lake surface are about one half the height on the pier sites. As will be presented in Chapter 4, the air-water temperature difference is used as an indicator of atmospheric stability as part of the calculation of deposition velocity. **Figures 2-22** present the differences between observed air and water temperatures for the same sites.

The skin temperature of the water generally differs from the water temperature at 2-cm depth during relatively calm conditions, but the differences are small. The largest deviation will be under cloudless summer conditions due to stronger positive net radiation during the day and stronger negative net radiation at night.

Hook et al. (2003) discuss and plot bulk and skin water temperatures and associated meteorological variables at Lake Tahoe. Given low or moderate wind speeds (< 4 m/s), nighttime skin temperatures are cooler by 0.2 - 1.0 ^{O}C than bulk temperatures at 2-cm depth. Daytime skin temperatures can range from 0.2 ^{O}C cooler to >1.0 ^{O}C warmer than bulk water temperatures. The skin temperature is generally warmer than the bulk temperature as the net radiation approaches its maximum, and cooler than the bulk as net radiation decreases. During elevated (> 4 m/s) wind conditions, the difference between skin and bulk temperature can vanish, but will reappear within seconds of relaxation of the wind (Steissberg, 2005).

Figure 2-21. Seasonal Air and Water Temperatures at the U.S. Coast Guard Pier and TDR1 Buoy.

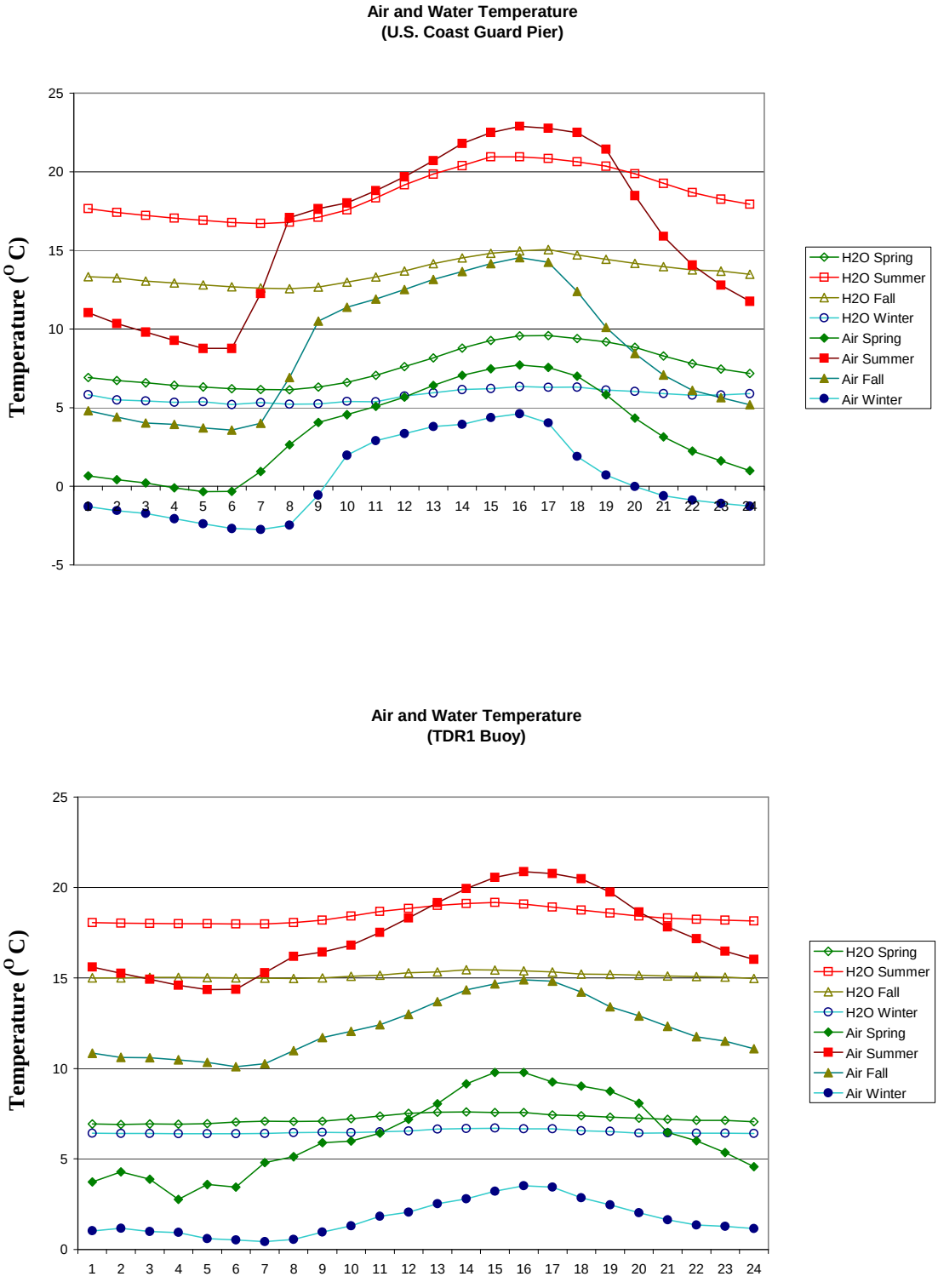

Figure 2-22. Seasonal Differences between Air and Water Temperature by Time of Day at the U.S. Coast Guard Pier and TDR1 Buoy.

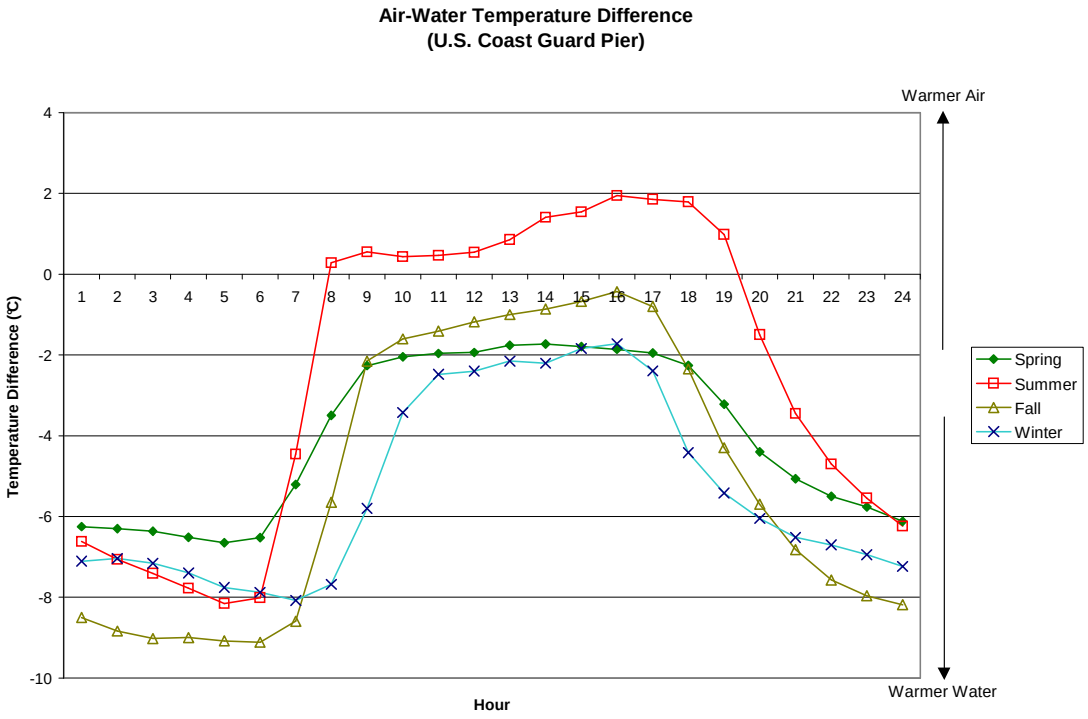

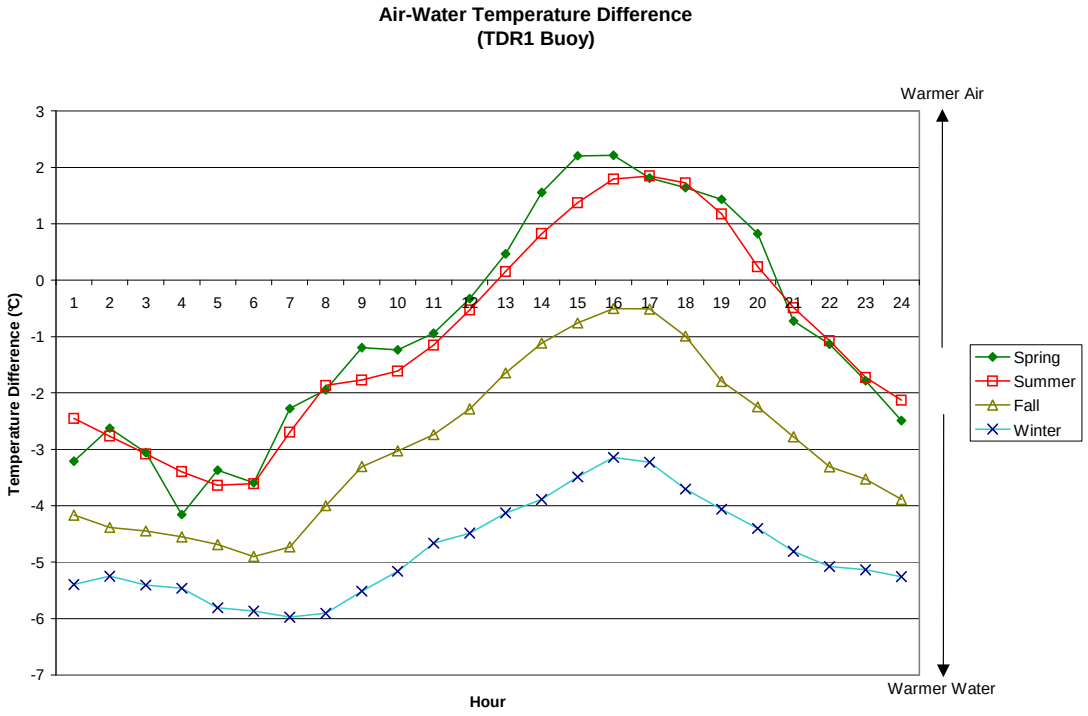

The depth of atmospheric mixing is predicted from the simple concept that, when the surface air is cooler and denser than the air aloft, vertical mixing is suppressed. The comparison of surface and aloft temperatures allows determination of whether vertical mixing extends to the height of each of the range gates of the RASS during that hour. The comparisons require and included adjustments for differences in humidity and pressure elevation. The results can be summarized as the frequency of mixing to a given depth during any hour of day or season. **Table 2-1** presents estimated frequencies of mixing to the various range gate elevations based on hourly air and water temperatures at buoy TDR1 and air temperatures at Sandy Way. Consideration of these estimates should include review of the nature and limitations of the observations on which they are based, which are described below.

The RASS remotely measured average air density through 60-meter layers (range gates) and reported those densities as hourly values of virtual temperature, meaning the temperature of dry air having the observed density. Virtual temperature is a variable used by meteorologists to uniquely describe the density of air due to the combined influences of temperature and water vapor content. Because the air always contains some water vapor and the molecular weight of water is less than the average molecular weight of air, the virtual temperature is slightly higher than actual temperature. The RASS observed virtual temperatures for range gates spanning 90 to more than 1000 m above ground level (AGL). The lowest data recovery rates were in the higher range gates. Data recovery also suffered somewhat in the lowest (90-150 m AGL) range gate. The maximum range for collecting reliable temperature data averaged a little less than 1 km and varied depending on environmental conditions. Note also that there were seasonal differences in data recovery rates, with lower recovery rates for RASS data during summer. The variations in RASS data recovery rates for higher range gates and during certain periods are reflected in **Table 2-1** as “counts” of the pairs of valid surface and aloft observations used to estimate mixing at that elevation.

Because the comparisons of surface versus aloft temperatures were made with observations from different locations, it is also necessary to consider under what conditions the RASS observations are a reasonable representation of temperatures aloft over the surface sites. The RASS was located at SLT Airport nearly 5 km south of the Lake; Sandy Way is a few hundred meters from the shore; and TDR1 buoy is 3 km east of Meeks Bay. For hours of downslope flow the surface air temperatures at the airport and Sandy Way are representative of larger land areas. During onshore flow temperatures at Sandy Way are strongly influenced by the Lake but the airport is influenced by the Lake to a lesser extent.

Heating or cooling of the air in the lower range gates of the RASS (due to differences in upwind surfaces or advection) has the potential to differ from processes over the Lake. During late morning through afternoon, with onshore flows (driven by surface heating of the land) some excess heating of the air in the lower range gates over SLT Airport is expected as compared to conditions over the Lake. These conditions could cause some under estimation of mixing depth over the Lake during daytime hours. Conversely, during night and early morning hours drainage flows over the airport will likely cool air in the lower range gates compared to temperatures at the same altitudes

over the Lake. Under these conditions comparison of the RASS observations with surface temperatures measured at land sites near the Lake shore should provide reasonable estimates of mixing depth. However, use of RASS observations of temperature obtained during drainage flows to represent temperatures over the Lake during those same periods are expected to result in overestimates of the maximum mixing depth on the Lake. An alternative analysis might include compensation for the expected biases in aloft temperature observed over SLTahoe Airport as compared to temperatures expected aloft over the Lake.

Tables 2-1 contrasts estimates of the potential maximum mixing over the Lake (based on observations at the TDR1 buoy and assumptions discussed above) and expected mixing over a land site near the shoreline (based on observations at Sandy Way). Estimates of the maximum mixing depth over the Lake are summarized in **Table 2-1a**. Seasonal frequency distributions of mixing to specified heights by time of day are provided in the column labeled “Freq“. These estimates of mixing are based on a surface air temperature assumed to equal the larger of either the hourly air temperature or the hourly water temperature (adjusted to mimic skin temperature) at TDR1. This assumption maximizes the estimated mixing depth over the Lake and presumes that, for some location over the Lake, the air temperature is warmed to the water temperature observed at TDR1 buoy. The count is the number of simultaneous hourly temperature observations at the surface and the specified height. The counts generally decrease with height and thus estimates of the frequency of mixing at the upper levels are uncertain. Physical principles suggest that the percent frequency values should decrease or remain constant with increasing height. Instances in which the percent frequency values increase with height are indicative of uncertainty in RASS observations of virtual temperature.

The results suggest deep mixing is possible over the Lake during winter and spring. In spring the apparent variation in mixing depth from morning to mid day is probably an artifact of warming of the surface layer over the airport that is not occurring to nearly the same extent over the Lake. Mixing over the Lake, even the maximum mixing per this estimate presented here, is apparently limited during fall and especially during summer as compared to the mixing depths over the Lake in winter and spring.

The similarly constructed estimates of mixing over Sandy Way, summarized in **Table 2-1b** are easier to interpret. They are based upon the air temperature and humidity at the surface as observed at Sandy Way. The resulting estimates of mixing depth for Sandy Way are qualitatively quite different from those suggested over the Lake (**Table 2-1a**). Over land the night and early morning mixing depths are very low during all seasons and maximum mixing depths occur during mid day or afternoon. The estimated daytime mixing depths increase in height through the day as expected. During the summer, the depths of mixing over land exceed those predicted for over the Lake.

Table 2-1a. Seasonal frequency of an estimated maximum potential mixing depth over Lake Tahoe reaching specified heights is shown in column labeled "Freq". Count is the number of hourly data pairs utilized. See text for description of caveats, and assumptions. Shading indicates median of estimated mixing depth values.

Season: Winter

ELEV	Freq	Count	Freq	Count	Freq	Count	Freq	Count	Freq	Count	Freq	Count
3480		0		0		0		0	0%	1		0
3420		0		0		0	0%	1	0%	2		0
3359		0		0		0	33%	3	0%	3	0%	1
3299	67%	3	100%	1	100%	1	50%	4	13%	8	100%	1
3240	71%	7	100%	2	100%	1	60%	5	20%	10	25%	4
3180	33%	6	100%	2	67%	3	64%	11	27%	11	57%	7
3119	63%	8	50%	4	25%	4	47%	15	36%	14	45%	11
3059	59%	27	33%	9	50%	8	63%	16	21%	19	39%	18
3000	46%	41	38%	13	50%	10	55%	22	34%	32	50%	22
2940	44%	50	50%	14	57%	14	48%	29	32%	37	47%	30
2880	43%	67	54%	24	50%	20	39%	36	43%	42	50%	30
2819	45%	78	33%	30	62%	29	48%	46	41%	54	50%	42
2759	42%	104	48%	46	56%	32	54%	57	49%	71	53%	51
2700	53%	118	59%	54	63%	41	61%	74	50%	80	51%	57
2640	60%	124	63%	59	77%	44	66%	90	53%	93	63%	63
2579	62%	144	66%	61	69%	52	71%	95	61%	99	63%	65
2519	68%	156	69%	61	71%	59	71%	99	60%	108	63%	70
2460	67%	163	73%	64	74%	70	71%	101	61%	109	70%	74
2400	72%	179	80%	75	75%	76	76%	107	62%	117	69%	74
2339	76%	188	85%	82	83%	75	78%	116	73%	120	79%	81
2279	84%	205	86%	83	84%	80	83%	120	78%	116	87%	79
2220	89%	210	91%	81	85%	86	84%	120	80%	114	86%	88
2160	93%	221	96%	83	87%	85	87%	123	82%	119	92%	85
2099	97%	221	99%	70	91%	86	90%	128	86%	127	98%	86
2039	99%	206	99%	69	90%	82	91%	127	87%	126	99%	86
1980	99%	186	100%	55	91%	75	91%	115	93%	120	100%	84
Winter 200	0000-0659		0700-0959		1000-1259		1300-1659		1700-2059		2100-2359	

Season: Spring

ELEV	Freq	Count	Freq	Count	Freq	Count	Freq	Count	Freq	Count	Freq	Count
3480		0		0		0		0		0		0
3420		0		0		0		0	0%	3		0
3359		0		0		0		0	29%	7	0%	1
3299	100%	1		0		0		0	30%	10	0%	3
3240	33%	3		0		0	100%	1	50%	16	33%	6
3180	86%	7		0		0	100%	1	47%	19	50%	8
3119	80%	10	100%	1		0	33%	3	50%	18	53%	15
3059	70%	23	83%	6	40%	5	0%	3	44%	25	50%	26
3000	63%	32	91%	11	50%	10	25%	8	50%	32	38%	40
2940	59%	54	65%	23	57%	14	38%	13	47%	43	42%	38
2880	53%	70	59%	32	52%	23	57%	23	51%	53	38%	42
2819	54%	102	61%	44	51%	41	55%	33	52%	62	40%	50
2759	53%	129	62%	65	54%	46	43%	47	56%	90	37%	57
2700	49%	147	59%	71	45%	60	42%	59	57%	116	37%	71
2640	51%	179	65%	86	47%	75	51%	77	57%	127	40%	83
2579	51%	196	65%	102	51%	87	51%	91	56%	139	37%	87
2519	52%	213	65%	108	51%	93	51%	105	54%	155	39%	104
2460	51%	235	65%	111	56%	93	51%	111	52%	152	41%	113
2400	53%	253	65%	117	49%	100	53%	113	52%	155	38%	118
2339	55%	255	70%	120	58%	99	54%	114	57%	159	46%	121
2279	56%	264	73%	123	56%	99	55%	119	56%	161	45%	126
2220	58%	279	67%	128	56%	100	57%	129	57%	164	45%	128
2160	61%	268	68%	127	57%	115	59%	135	57%	159	45%	130
2099	64%	269	71%	133	66%	116	62%	127	56%	154	54%	139
2039	70%	260	74%	130	72%	108	62%	125	61%	157	62%	134
1980	81%	213	81%	111	74%	88	62%	104	63%	135	65%	118
Spring 200	0000-0659		0700-0959		1000-1259		1300-1659		1700-2059		2100-2359	

Table 2-1a (continued). Seasonal frequency of an estimated maximum potential mixing depth over Lake Tahoe.

Season: Summer

ELEV	Freq	Count	Freq	Count	Freq	Count	Freq	Count	Freq	Count	Freq	Count
3480		0		0		0		0		0		0
3420	0%	1		0		0		0	0%	1	0%	1
3359	0%	2		0		0		0	0%	1	0%	2
3299	0%	3		0		0		0	0%	2	0%	4
3240	0%	6		0		0		0	0%	3	0%	4
3180	0%	8		0		0		0	0%	4	0%	8
3119	0%	12		0		0		0	0%	5	0%	11
3059	0%	17	0%	1	0%	1	0%	1	0%	5	0%	10
3000	0%	21	0%	4	0%	1	0%	1	0%	7	0%	13
2940	0%	28	0%	5	0%	2	0%	2	0%	15	0%	17
2880	0%	32	0%	9	0%	4	17%	6	0%	19	5%	19
2819	0%	42	0%	13	0%	5	14%	7	3%	31	4%	28
2759	0%	49	6%	17	0%	7	10%	10	3%	35	0%	30
2700	0%	57	6%	16	0%	12	10%	10	2%	41	0%	37
2640	1%	67	5%	21	5%	19	9%	11	7%	41	2%	44
2579	1%	75	6%	33	5%	20	13%	15	9%	45	10%	41
2519	2%	101	12%	41	5%	22	25%	16	11%	47	6%	48
2460	5%	91	7%	41	17%	24	13%	16	7%	56	15%	52
2400	6%	98	11%	44	19%	26	26%	19	6%	53	11%	55
2339	14%	102	18%	56	41%	22	40%	15	13%	54	18%	56
2279	18%	107	26%	61	48%	23	64%	22	18%	51	19%	58
2220	18%	105	33%	64	50%	32	64%	22	20%	54	23%	62
2160	25%	114	50%	64	67%	39	79%	19	34%	56	29%	65
2099	43%	123	68%	62	86%	43	94%	17	69%	55	55%	69
2039	55%	128	74%	58	91%	45	96%	25	83%	54	69%	68
1980	93%	76	79%	33	83%	24	93%	15	87%	39	82%	38
ummer 200	0000-0659		0700-0959		1000-1259		1300-1659		1700-2059		2100-2359	

Season: Fall

ELEV	Freq	Count	Freq	Count	Freq	Count	Freq	Count	Freq	Count	Freq	Count
3480		0		0		0		0		0		0
3420		0		0		0		0	0%	2	0%	1
3359	0%	2		0		0		0	0%	2	0%	2
3299	0%	1		0		0		0	0%	5	0%	3
3240	0%	7	0%	1		0		0	0%	5	0%	3
3180	11%	9	0%	2	0%	1	0%	1	0%	9	0%	5
3119	8%	13	0%	5	0%	3	0%	3	0%	13	0%	7
3059	0%	20	0%	7	0%	4	0%	6	0%	16	0%	7
3000	0%	28	18%	11	27%	11	0%	10	0%	24	0%	12
2940	4%	45	20%	15	27%	11	20%	15	8%	36	5%	20
2880	10%	59	17%	23	23%	13	24%	25	10%	42	11%	36
2819	15%	72	23%	35	38%	26	21%	34	13%	55	20%	45
2759	20%	98	22%	45	31%	36	21%	47	16%	63	16%	57
2700	23%	137	26%	58	35%	52	35%	66	21%	89	19%	67
2640	33%	158	42%	71	39%	66	36%	83	36%	111	37%	78
2579	38%	185	42%	76	48%	80	45%	96	37%	121	36%	95
2519	42%	234	49%	91	52%	96	42%	119	39%	136	34%	110
2460	50%	260	48%	95	56%	107	48%	130	42%	151	38%	115
2400	50%	271	50%	111	53%	118	48%	145	43%	155	41%	112
2339	59%	279	62%	117	57%	122	51%	153	48%	168	53%	118
2279	64%	291	66%	119	61%	129	49%	154	51%	179	53%	123
2220	65%	295	71%	118	61%	127	47%	149	48%	156	59%	126
2160	67%	297	68%	126	63%	126	52%	161	57%	179	61%	117
2099	74%	297	72%	127	65%	124	51%	157	64%	171	73%	122
2039	81%	302	78%	120	63%	128	55%	158	69%	179	77%	124
1980	94%	267	83%	110	66%	120	53%	140	76%	156	87%	110
Fall 2003	0000-0659		0700-0959		1000-1259		1300-1659		1700-2059		2100-2359	

Table 2-2b. Seasonal frequency of estimated mixing through specified depths over Sandy Way.

Season: Winter

ELEV	Freq	Count	Freq	Count	Freq	Count	Freq	Count	Freq	Count	Freq	Count
3480		0		0		0		0	0%	1		0
3420		0		0		0	0%	1	0%	2		0
3359		0		0		0	0%	3	0%	3	0%	1
3299	0%	3	0%	1	0%	1	0%	4	0%	8	0%	1
3240	0%	9	0%	2	0%	1	0%	5	0%	10	0%	5
3180	0%	10	0%	2	0%	3	9%	11	0%	13	0%	9
3119	0%	14	0%	4	0%	4	0%	15	6%	17	0%	12
3059	0%	34	0%	9	13%	8	6%	16	0%	24	0%	22
3000	0%	49	0%	13	0%	10	0%	22	3%	39	0%	28
2940	0%	61	0%	14	13%	15	14%	29	2%	47	0%	37
2880	0%	76	0%	24	9%	22	8%	36	2%	51	0%	38
2819	0%	93	3%	30	10%	30	9%	47	2%	66	0%	54
2759	0%	121	4%	47	12%	33	12%	58	1%	85	0%	65
2700	0%	140	6%	54	12%	43	12%	77	1%	95	0%	73
2640	1%	149	10%	60	21%	47	18%	97	1%	110	0%	79
2579	0%	168	9%	65	23%	57	17%	104	1%	116	0%	82
2519	1%	186	15%	66	26%	69	16%	110	2%	128	0%	87
2460	2%	198	13%	68	27%	79	16%	114	2%	128	0%	91
2400	0%	217	13%	80	20%	86	17%	121	1%	137	0%	91
2339	0%	225	22%	85	31%	84	22%	131	1%	143	0%	99
2279	1%	244	20%	89	33%	88	23%	136	2%	137	0%	96
2220	2%	250	21%	86	36%	96	26%	134	3%	135	3%	104
2160	2%	263	27%	88	33%	92	28%	137	3%	143	4%	102
2099	4%	259	38%	74	53%	91	40%	141	9%	150	6%	105
2039	6%	241	42%	74	60%	89	40%	141	12%	146	7%	106
1980	8%	222	57%	61	71%	83	46%	128	13%	135	10%	99
Winter 200	0000-0659		0700-0959		1000-1259		1300-1659		1700-2059		2100-2359	

Season: Spring

ELEV	Freq	Count	Freq	Count	Freq	Count	Freq	Count	Freq	Count	Freq	Count
3480		0		0		0		0		0		0
3420		0		0		0		0	0%	6	0%	1
3359		0		0		0		0	11%	9	0%	2
3299	0%	1	0%	1		0		0	8%	12	0%	5
3240	0%	3	0%	2		0	100%	1	5%	19	0%	7
3180	0%	8	0%	2		0	100%	1	17%	24	0%	10
3119	0%	16	0%	4	0%	1	33%	3	13%	23	0%	19
3059	0%	35	20%	10	14%	7	0%	4	13%	30	0%	32
3000	0%	48	27%	15	14%	14	11%	9	10%	41	0%	48
2940	0%	71	41%	27	21%	19	35%	17	13%	55	0%	49
2880	0%	92	25%	36	21%	28	45%	29	16%	70	0%	53
2819	0%	129	24%	49	33%	48	47%	43	13%	80	0%	66
2759	1%	161	27%	74	37%	54	44%	57	16%	110	1%	77
2700	1%	184	31%	83	45%	73	48%	73	16%	141	3%	100
2640	2%	231	42%	103	45%	92	56%	94	20%	157	5%	114
2579	1%	257	40%	121	46%	111	53%	108	18%	176	4%	119
2519	2%	272	42%	130	48%	118	53%	123	18%	194	5%	133
2460	2%	292	46%	134	52%	120	53%	129	20%	194	3%	146
2400	2%	316	43%	146	50%	127	53%	132	18%	198	5%	151
2339	4%	324	55%	148	63%	126	56%	134	26%	200	6%	151
2279	4%	332	58%	151	65%	126	58%	139	26%	202	4%	157
2220	5%	349	59%	154	62%	127	58%	150	26%	210	8%	159
2160	5%	336	58%	150	66%	142	57%	158	26%	206	9%	170
2099	8%	330	70%	157	79%	140	68%	145	32%	206	16%	175
2039	10%	319	75%	150	82%	132	68%	141	33%	200	18%	171
1980	14%	251	88%	128	82%	105	70%	115	36%	167	23%	141
Spring 200	0000-0659		0700-0959		1000-1259		1300-1659		1700-2059		2100-2359	

Table 2-1b (continued). Seasonal frequency of estimated mixing through specified depths over Sandy Way.

Season: Summer

ELEV	Freq	Count	Freq	Count	Freq	Count	Freq	Count	Freq	Count	Freq	Count
3480		0		0		0		0		0		0
3420	0%	1		0		0		0	0%	1	0%	1
3359	0%	2		0		0		0	0%	1	0%	2
3299	0%	3		0		0		0	0%	2	0%	4
3240	0%	6		0		0		0	0%	3	0%	4
3180	0%	8		0		0		0	0%	4	0%	8
3119	0%	12		0		0		0	0%	5	0%	11
3059	0%	17	0%	1	0%	1	100%	1	0%	5	0%	10
3000	0%	21	25%	4	0%	1	100%	1	0%	7	0%	13
2940	0%	28	20%	5	0%	2	100%	2	0%	15	0%	17
2880	0%	32	44%	9	0%	4	83%	6	0%	19	0%	19
2819	0%	42	38%	13	0%	5	71%	7	10%	31	0%	28
2759	0%	49	41%	17	29%	7	70%	10	11%	35	0%	30
2700	0%	57	38%	16	27%	11	80%	10	10%	41	0%	37
2640	0%	67	38%	21	50%	18	100%	11	12%	41	0%	44
2579	0%	75	36%	33	63%	19	93%	15	16%	45	0%	41
2519	0%	101	32%	41	62%	21	94%	16	15%	47	0%	48
2460	0%	91	29%	41	74%	23	87%	15	14%	56	0%	52
2400	0%	98	36%	44	80%	25	83%	18	13%	53	0%	55
2339	0%	102	49%	55	86%	21	93%	14	19%	54	0%	56
2279	2%	107	56%	61	91%	22	95%	21	22%	51	0%	58
2220	2%	105	62%	63	97%	31	95%	21	22%	54	0%	62
2160	2%	114	70%	64	97%	38	100%	18	29%	56	0%	65
2099	5%	123	84%	62	100%	42	100%	17	44%	55	6%	69
2039	8%	128	90%	58	100%	44	100%	25	52%	54	7%	68
1980	18%	76	94%	33	100%	23	93%	15	62%	39	5%	38
ummer 200	0000-0659		0700-0959		1000-1259		1300-1659		1700-2059		2100-2359	

Season: Fall

ELEV	Freq	Count	Freq	Count	Freq	Count	Freq	Count	Freq	Count	Freq	Count
3480		0		0		0		0		0		0
3420		0		0		0		0	0%	2	0%	1
3359	0%	2		0		0		0	0%	2	0%	2
3299	0%	1		0		0		0	0%	5	0%	3
3240	0%	8	0%	1		0		0	0%	5	0%	3
3180	0%	10	0%	2	0%	1	0%	1	0%	9	0%	5
3119	0%	17	0%	7	0%	3	0%	3	0%	13	0%	7
3059	0%	26	0%	9	0%	4	0%	6	0%	16	0%	7
3000	0%	36	0%	13	0%	12	0%	10	0%	24	0%	12
2940	0%	51	12%	17	27%	11	7%	15	0%	36	0%	21
2880	0%	67	4%	25	27%	15	8%	25	0%	42	0%	38
2819	0%	84	5%	38	24%	29	11%	35	0%	56	0%	47
2759	0%	112	6%	49	18%	40	8%	48	0%	66	0%	59
2700	0%	152	6%	63	25%	57	9%	69	0%	95	0%	71
2640	0%	178	14%	78	38%	73	17%	88	1%	119	0%	81
2579	0%	207	20%	83	40%	87	17%	103	1%	131	1%	100
2519	0%	253	24%	98	40%	104	21%	127	1%	149	1%	117
2460	0%	278	26%	101	43%	115	19%	140	3%	163	2%	122
2400	0%	289	24%	118	41%	126	17%	153	2%	167	3%	117
2339	0%	298	32%	125	53%	130	22%	162	2%	179	3%	126
2279	1%	308	33%	129	54%	138	24%	164	4%	189	3%	129
2220	2%	310	35%	129	54%	134	22%	158	4%	162	5%	133
2160	2%	317	40%	136	51%	134	27%	172	4%	189	5%	122
2099	3%	317	53%	135	60%	131	35%	166	8%	180	9%	127
2039	5%	318	54%	128	63%	136	38%	167	13%	189	8%	130
1980	6%	283	67%	118	64%	128	32%	148	13%	166	15%	117
Fall 2003	0000-0659		0700-0959		1000-1259		1300-1659		1700-2059		2100-2359	

2.3 Wind Patterns

Winds are of interest when addressing atmospheric deposition because they can move emissions of pollutants from one area to another and the associated turbulence can affect the rates of deposition.

2.3.1 Surface Winds

2.3.1.1 Outside the Tahoe Basin

Winds in northern California tend to have a westerly (west to east) component due to its mid-latitude location in the northern hemisphere where westerly winds dominate the global circulation patterns. This typical pattern is perturbed near ground level however by the presence of mountain ranges (Coastal Ranges and Sierra Nevada) separated by the Great Central Valley of California. Furthermore, the valleys and mountain slopes create strong diurnal mesoscale variations in the global wind pattern. The diurnal and seasonal variations in wind speed and direction are graphically summarized for the Blue Canyon Airport in **Figure 2-23**. Blue Canyon is at an approximate elevation of 5200 feet MSL (about 1000 feet lower than Lake Tahoe). Several wind features typical of mountain settings can be seen in the figure. First, average wind speeds are greatest about mid-day and tend to be stronger in summer than in other seasons. Second, the winds tend to have a westerly component during the day and an easterly component during the night. This pattern is consistent with up-slope air flow during the day and down-slope or drainage flows during the night. As the sun warms the western slopes of the Sierra, the air tends to rise and flow eastward. After the sun sets, the surface layer of air cools and flows downhill.

Closer to the crest of the Sierra Nevada, readily available meteorological data for Donner Summit (NW of Lake Tahoe) in the Sierra Nevada are summarized in **Tables 2-2 and 2-3**. At Donner Summit, the two predominant wind directions are WSW and ENE. The westerly-enhanced up-slope flows occur primarily during the day and slower, down-slope ENE flows occur primarily during the night. The up-slope flows occur during about 2/3rds of the time and down-slope flows occur about 25% of the time. Thus, calm winds and wind directions other than WSW or ENE are relatively rare. Resultant winds, shown in **Table 2-3**, represent the net movement of air. The net movement is from the SW in all seasons and is strongest and most persistent during winter and summer. Presented in **Figure 2-24** are seasonal wind roses for Donner Summit that demonstrate the upslope/downslope wind pattern is present in all seasons with relatively minor variations. It is likely that channeling of the winds through the pass may enhance the consistency of wind directions at this location.

Further east and at a higher altitude, winds are also measured near the peak of Slide Mountain in Nevada. Slide Mountain is located NNE of Lake Tahoe at an elevation of 9,650 feet MSL. This elevation is typically about 1000 feet below the subsidence inversion associated with the eastern Pacific high pressure system. A wind rose is presented for Slide Mountain in **Figure 2-25**. The predominant wind directions are similar to those at Donner Summit, although the flows are less channeled, and are probably the best land-based measurements of the free air flow over the Sierra Nevada. Winds have a southwesterly component (i.e., transport potential from the Sacramento

metropolitan region) over 40 percent of the time. The annual average wind speed is 18.7 mph at this elevation (**Figure 2-26**), considerably higher than surface wind speeds at lower altitude sites. Peak wind speeds are over 100 mph.

Table 2-2. Summary of Predominant Winds at Donner Summit. (CARB, 1984)

Statistic \ Season:	Winter	Spring	Summer	Fall	Annual
Primary Direction					
Direction	WSW	WSW	WSW	WSW	WSW
Mean Speed (mph)	20.0	16.0	12.6	15.9	16.2
Frequency (%)	69.3	63.2	70.3	63.7	66.6
Secondary Direction					
Direction	ENE	ENE	ENE	ENE	ENE
Mean Speed (mph)	13.6	11.5	8.0	11.0	11.3
Frequency (%)	26.8	28.1	19.6	29.9	26.2

Table 2-3. Resultant Winds at Donner Summit. (CARB, 1984)

Statistic \ Season:	Winter	Spring	Summer	Fall	Annual
Direction (degrees)[+]	241	241	236	242	240
Speed (mph)	10.1	6.9	7.4	6.8	7.8
Persistance*	0.57	0.50	0.67	0.49	0.55

[+] Compass degrees (0 or 360 indicates wind from North, 90 indicates wind from East, 180 indicates wind from South, and 270 indicates wind from West)

* Ratio of resultant wind speed to mean wind speed (values can vary between 0 to 1 with "1" indicating that the wind is always from the resultant wind direction)

Figure 2-23. Diurnal and Seasonal Variations in Wind Patterns at Blue Canyon. (CARB, 1984)

BLUE CANYON (Blue Canyon Airport)

LATITUDE: 39° 17' N **LONGITUDE:** 120° 42' W

PERIOD: December 1974 - November 1979 **LEVEL:** Surface

MONTHLY THREE HOURLY RESULTANT WIND DIAGRAM
Direction (shown by arrows), Speed (mph)

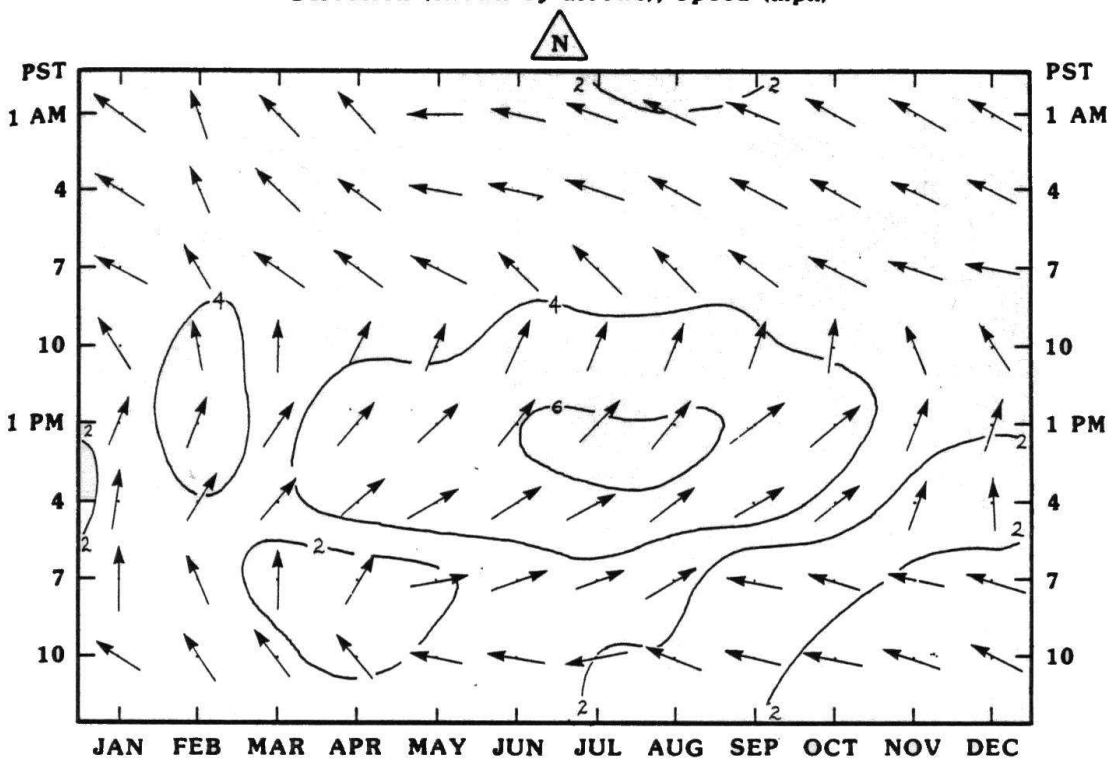

SEASONAL THREE HOURLY, DAILY AND YEARLY RESULTANT WIND SUMMARY

	WINTER (Dec, Jan, Feb)		SPRING (Mar, Apr, May)		SUMMER (Jun, Jul, Aug)		FALL (Sep, Oct, Nov)		ANNUAL	
Time (PST)	Direction (deg)	Speed (mph)	Direction (deg)	Speed (mph)	Direction (deg)	Speed (mph)	Direction (deg)	Speed (mph)	Direction (deg)	Speed (mph)
1 AM	140	2.6	125	2.4	105	2.2	118	2.3	123	2.3
4 AM	135	2.6	121	2.7	107	2.3	118	2.2	121	2.4
7 AM	126	2.7	130	3.0	138	2.9	118	2.5	128	2.8
10 AM	159	3.3	191	3.6	200	5.1	183	3.6	185	3.8
1 PM	202	3.4	222	4.4	222	6.1	220	4.3	218	4.5
4 PM	198	2.3	229	4.3	236	5.4	228	3.2	227	3.7
7 PM	126	2.4	216	1.4	246	2.5	105	1.2	180	1.0
10 PM	130	2.7	128	2.1	098	2.0	110	2.3	117	2.2
DAILY	149	2.4	180	2.3	196	2.3	161	1.8	172	2.1

CALIFORNIA AIR RESOURCES BOARD
AEROMETRIC DATA DIVISION 4/84

Figure 2-24. Seasonal Wind Roses for Donner Summit. (based on CARB, 1984)

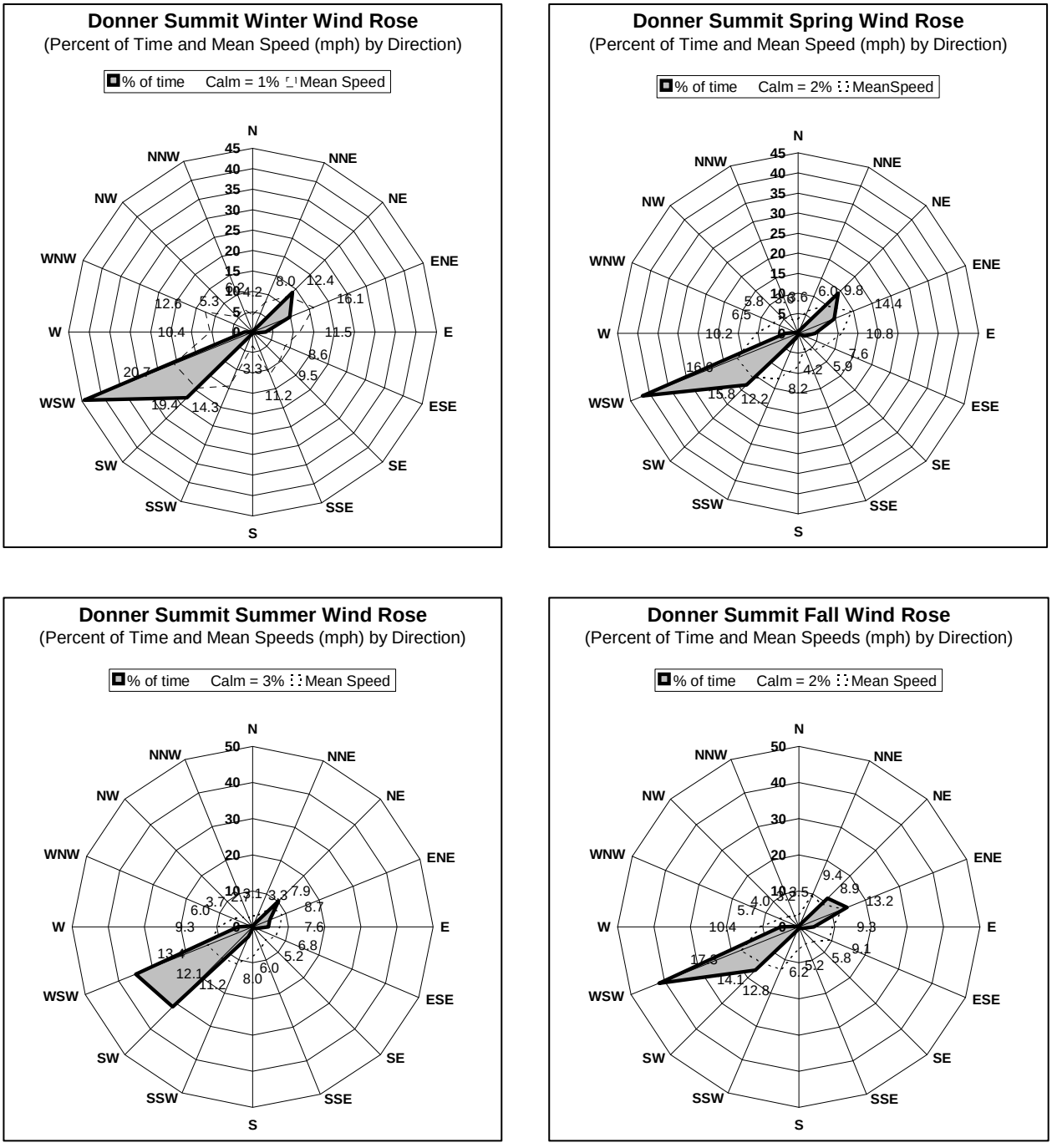

Figure 2-25. Wind Rose for Slide Mountain, NV based on 1968-1970 data. (WRCC, 2004)

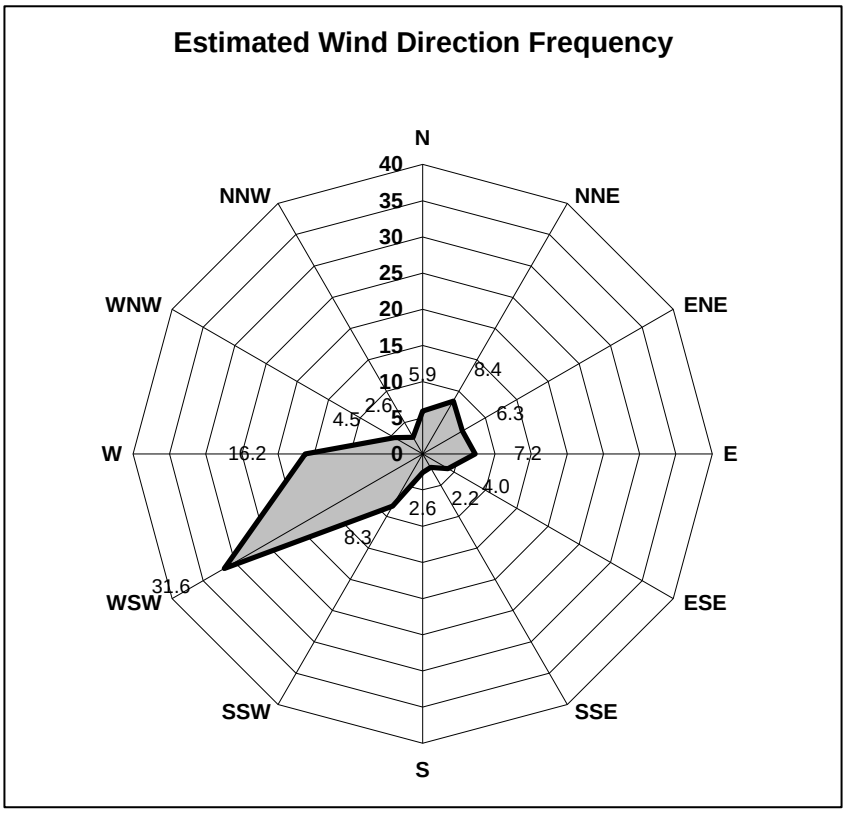

Figure 2-26. Cumulative Wind Speed Frequency for Slide Mountain, NV based on 1968-1970 data. (WRCC, 2004)

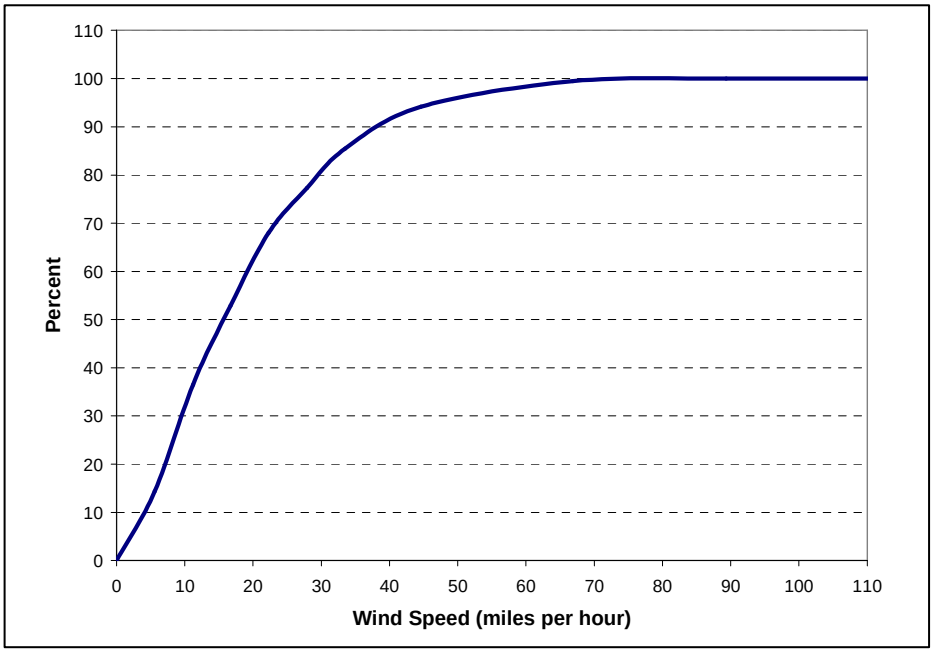

2.3.1.2 Inside the Tahoe Basin

In the Tahoe Basin itself, mesoscale weather strongly influences local air flow patterns. Resultant and predominant wind data are readily available for South Lake Tahoe (**Tables 2-4 and 2-5**) and are presented by season. Winds tend to be channeled at this site (airport) and are generally from the south or southwest. The resultant wind speeds are highest during summer (a factor of two greater than the spring or fall resultant speeds). The resultant wind speed in winter is enhanced by the routine passage of storm systems.

Table 2-4. Resultant Wind Data Summary for South Lake Tahoe. (CARB, 1984)

Statistic \ Season:	Winter	Spring	Summer	Fall	Annual
Direction (degrees)[+]	187	225	215	213	208
Speed (mph)	3.8	2.1	4.5	2.1	3.0
Persistance*	0.52	0.26	0.53	0.31	0.39

[+] Compass degrees (0 or 360 indicates wind from North, 90 indicates wind from East, 180 indicates wind from South, and 270 indicates wind from West)

* Ratio of resultant wind speed to mean wind speed (values can vary between 0 to 1 with "1" indicating that the wind is always from the resultant wind direction)

Table 2-5. Predominant Wind Data Summary for South Lake Tahoe. (CARB, 1984)

Statistic \ Season:	Winter	Spring	Summer	Fall	Annual
Primary Direction					
Direction	S	SSW	SSW	S	SSW
Mean Speed (mph)	11.9	12.1	11.9	10.2	12.0
Frequency (%)	41.7	32.0	43.6	29.1	35.2
Secondary Direction					
Direction	NNE	N	N	N	N
Mean Speed (mph)	8.1	9.4	9.0	8.1	8.8
Frequency (%)	15.6	25.7	17.2	20.0	19.5

Wind roses (showing the directional frequency of surface winds) for the South Lake Tahoe Airport are presented by season in **Figure 2-27**. The bi-directional nature of the surface wind is of immediate note and is associated with down-slope drainage flows of cold air at night and up-slope flows during the day. The percentage of time with calm winds is significantly higher at the SLT-Airport than at other mountain sites shown earlier. Similarly, in the aloft wind measurements described in the following paragraphs, a higher frequency of calm winds was observed above the ground at SLT-Airport

compared to over the western slope of the Sierra Nevada near the Grass Valley Radar Wind Profiler with Radio Acoustic Sounding System (RWP/RASS) site.

The mesoscale processes in the Tahoe Basin create a tendency for the winds to vary diurnally and to often be oriented perpendicular to the shoreline (i.e., up and down the mountain slopes). Thus, categorizing wind direction relative to the shoreline (onshore, offshore, or sideshore) can be more useful than compass wind direction when comparing the diurnal timing and orientation of the winds on different sides of the Lake. Seasonal bar charts of the proportion of each air flow type (i.e., calm, offshore, onshore, sideshore) by hour are provided for three sites representing different sectors of the Lake (South - SLT-Sandy Way, East – Cave Rock, and Northwest – USCG) in **Figures 2-28 through 2-31**. Downslope flow dominates during the night at all three sites and upslope flow dominates during most daylight hours. Obviously, downslope flows prevail during more hours in winter due to the longer nights and upslope flows are more prevalent in summer. When considering atmospheric deposition to the Lake, the periods of downslope air flows are likely to be a primary contributor to the temporal loading of the Lake. This pattern implies low-level convergence of air over the Lake at night and low-level divergence over the Lake during the day. Such a pattern suggests that local emissions would primarily contribute to deposition during the night and the potential for in-basin and out-of-basin emission sources to impact deposition during the day as air descends over the Lake to replace the low level air moving up the mountain slopes.

Figure 2-27. Seasonal wind roses for South Lake Tahoe. (based on CARB, 1984)

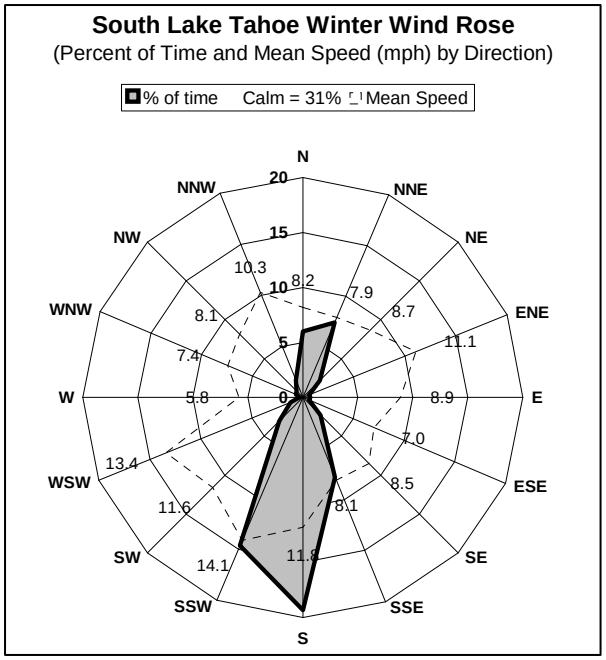

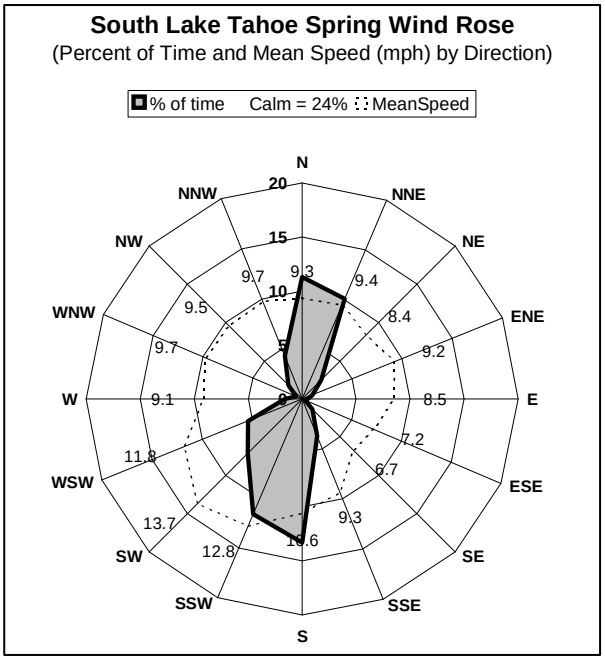

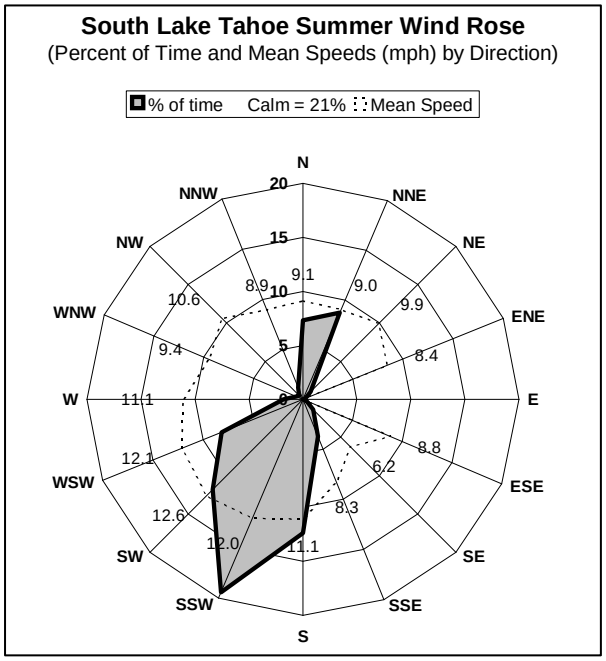

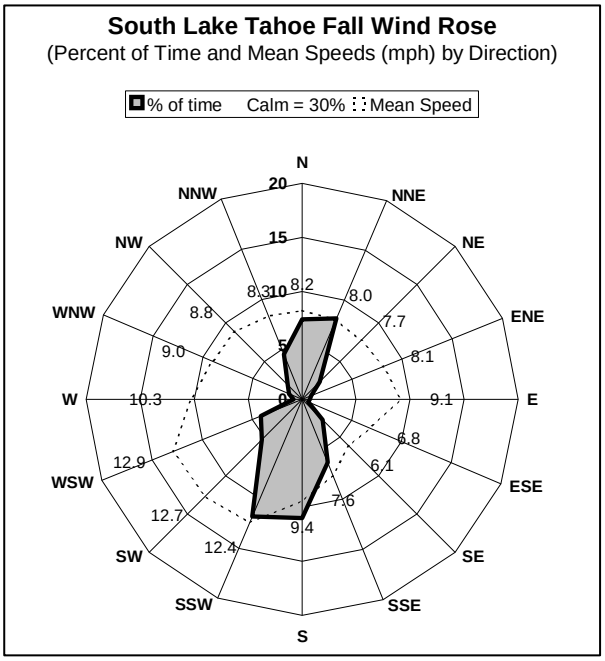

Figure 2-28. Winter Wind Patterns for SLT-Sandy Way (top), Cave Rock (middle), and Lake Forest - USCG (bottom) in 2003.

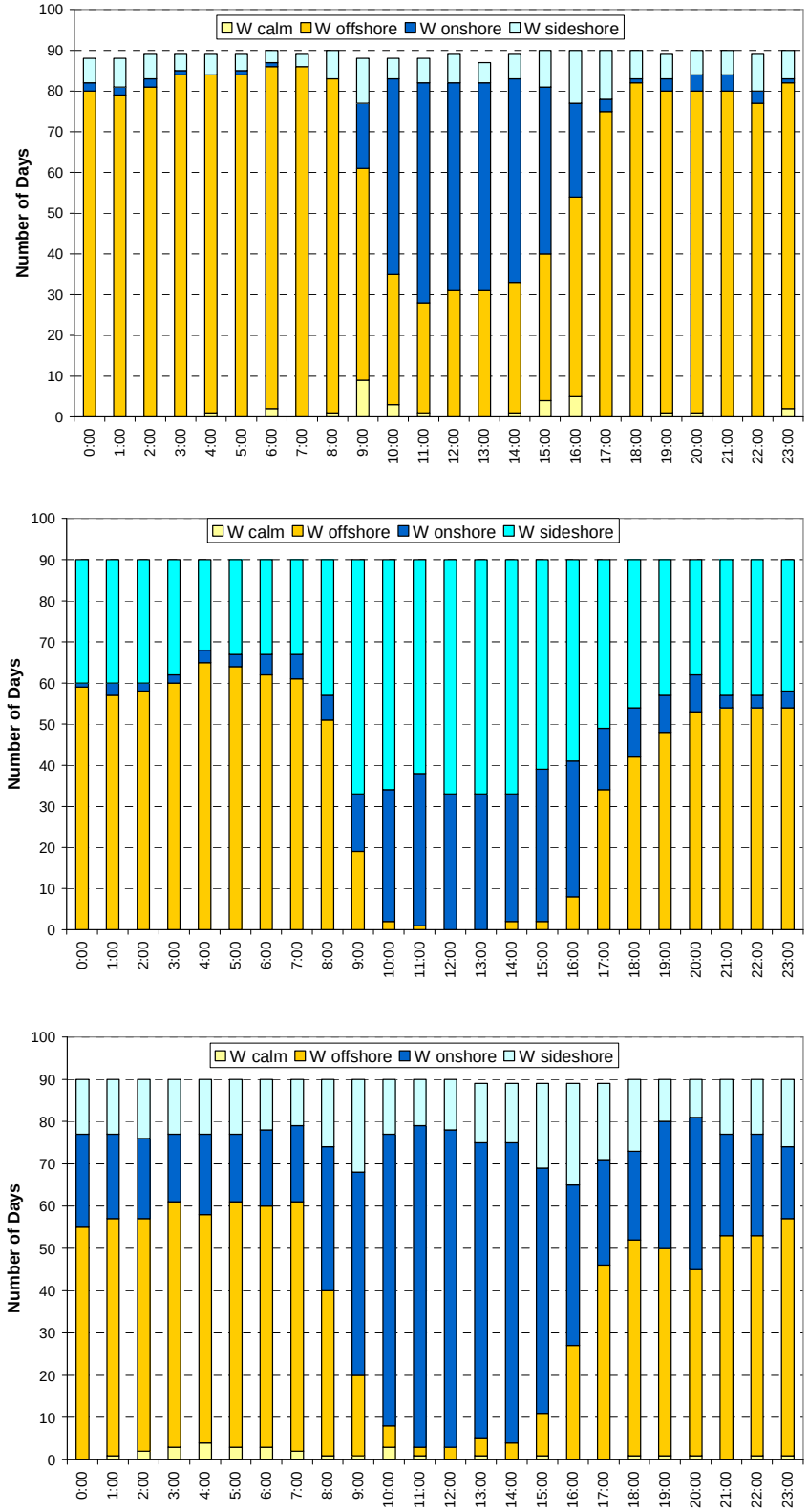

Figure 2-29. Spring Wind Patterns for SLT-Sandy Way (top), Cave Rock (middle), and Lake Forest - USCG (bottom) in 2003.

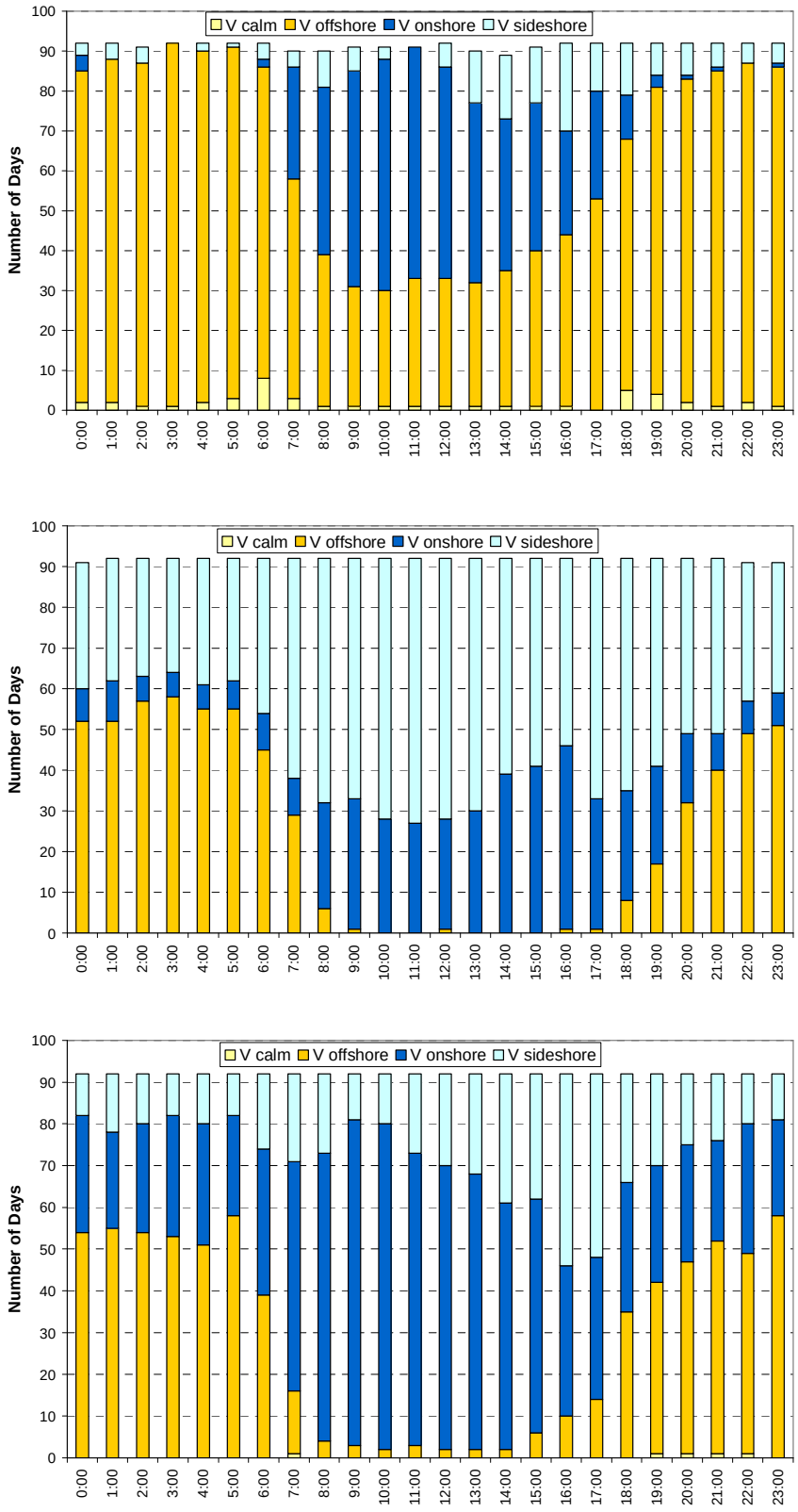

Figure 2-30. Summer Wind Patterns for SLT-Sandy Way (top), Cave Rock (middle), and Lake Forest - USCG (bottom) in 2003.

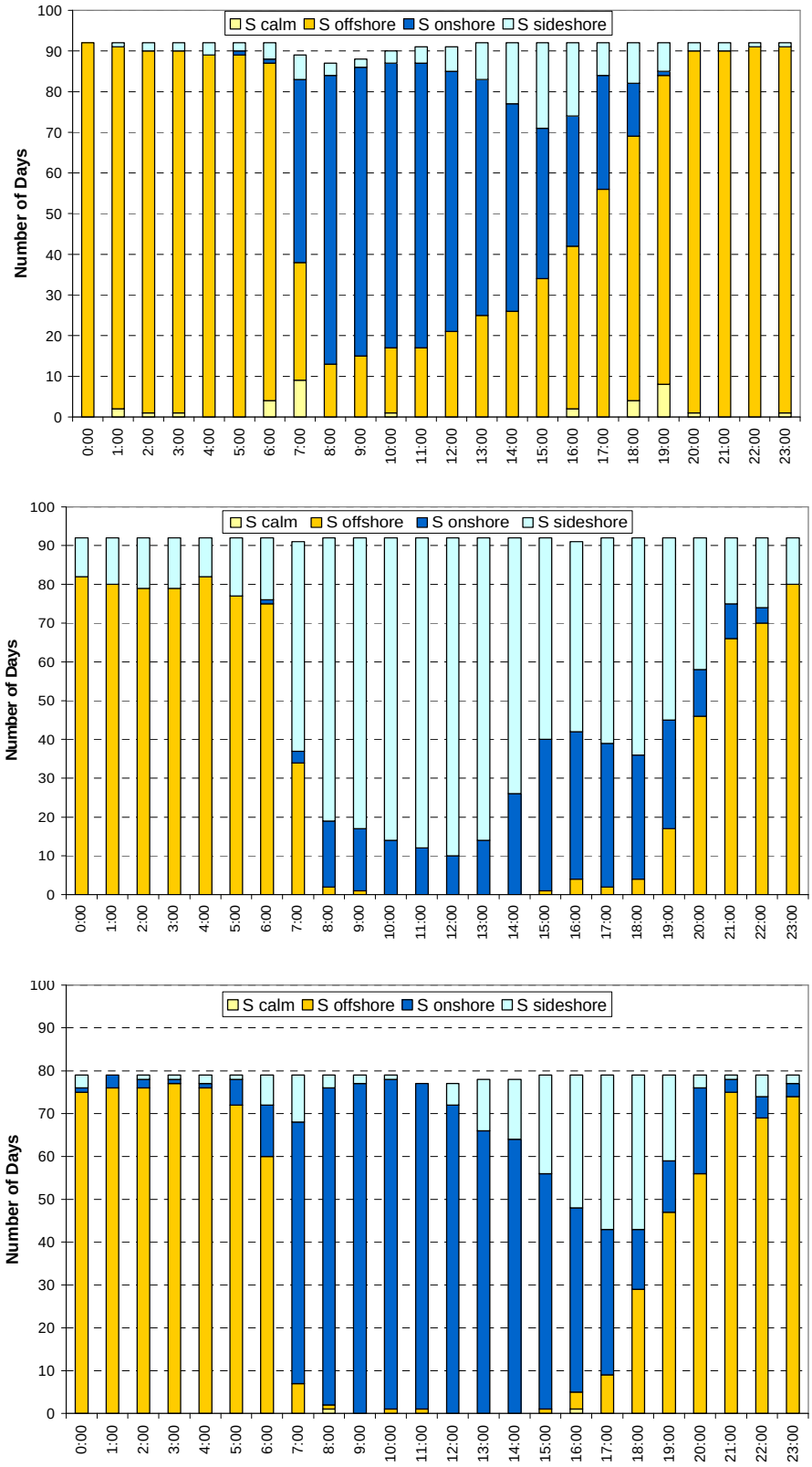

Figure 2-31. Fall Wind Patterns for SLT-Sandy Way (top), Cave Rock (middle), and Lake Forest - USCG (bottom) in 2003.

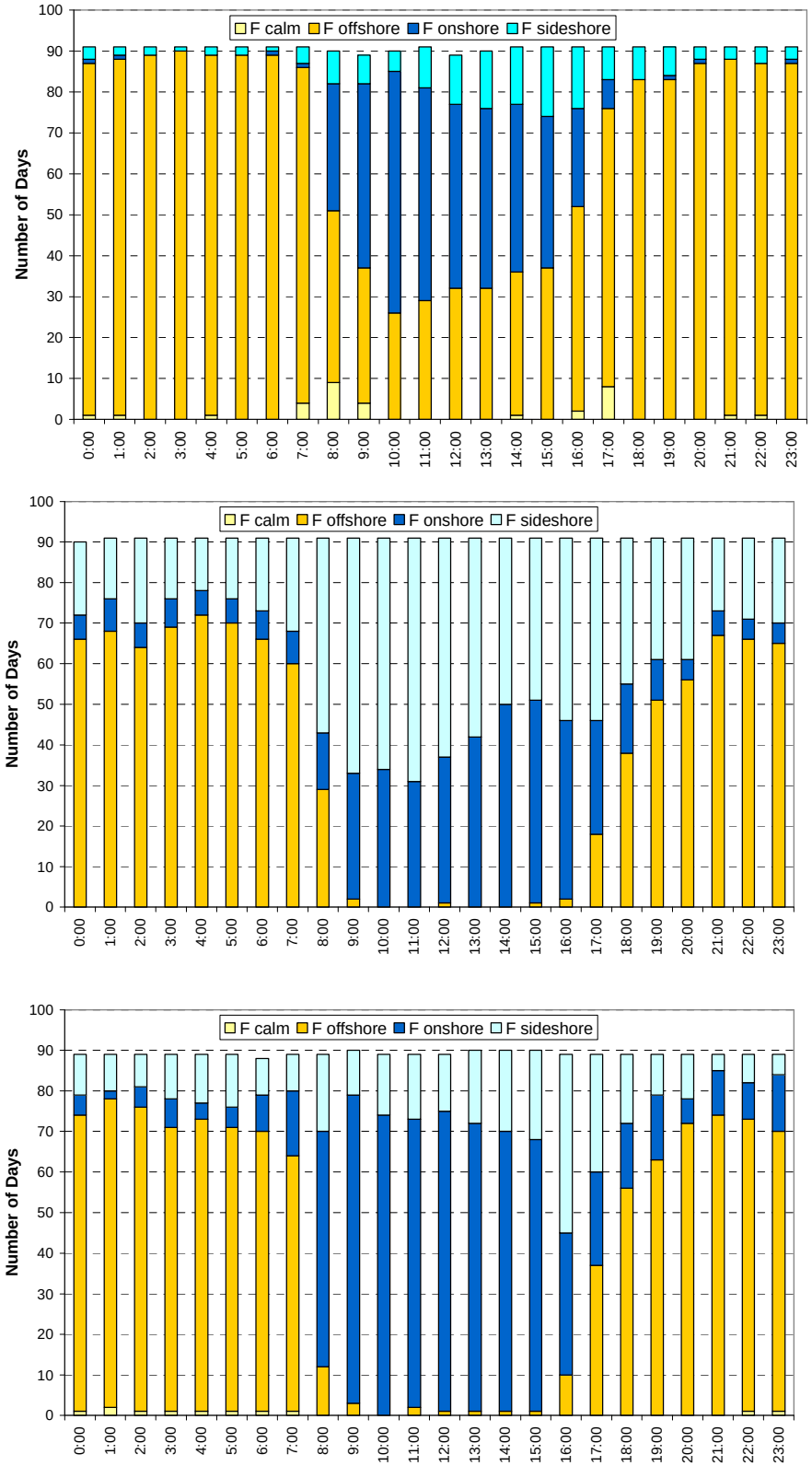

2.3.2 Winds Aloft

A limited number of balloon soundings and aircraft flights have been conducted where wind speeds and wind directions aloft have been measured. Twice-daily balloon soundings at Oakland, CA and Reno, NV provide the nearest long-term consistent observations of meteorological conditions aloft. Balloon soundings use to be conducted in Sacramento, CA to support daily decisions by the Air Resources Board regarding agricultural burning. A summary of the winds observed aloft during these soundings provide an indication of the potential frequency for transport of pollutants from the Central Valley to the Tahoe Basin. Seasonal summaries of the wind speeds and directions at 1000 and 3000 feet AGL are provided for 4 a.m., 10 a.m., and 4 p.m. PST in **Figures 2-32 and 2-33**. The seasonal frequencies of wind directions with the potential to transport material from the Central Valley to the Tahoe Basin are summarized in **Table 2-6**. These data show the greatest propensity for winds from the southwest through the west during the summer and the lowest propensity during the winter. Also, the frequency of winds from these "transport" directions is greater during the afternoon than during the morning. These data represent the maximum potential frequency for transport as they do not consider the wind speeds and persistence of the wind direction to effectively move material from the Valley to the Tahoe Basin. Furthermore, vertical mixing processes in the Valley, Sierra Nevada, and the Tahoe Basin would further act to reduce the impact of pollutant transport.

Table 2-6. Percent Frequency of Wind Directions above Sacramento with the potential* for transporting polluted air to the Tahoe Basin. (CARB, 1979)

Time (PST)	Winter	Spring	Summer	Fall	Annual
at 3000 feet above ground					
4 a.m.	13.6	28.6	38.5	28.2	29.1
10 a.m.	21.6	25.3	37.2	22.0	27.5
4 p.m.	19.4	46.2	70.2	39.1	45.1
at 1000 feet above ground					
4 a.m.	14.9	39.3	59.5	38.0	41.6
10 a.m.	18.3	37.4	63.6	25.8	39.3
4 p.m.	17.1	56.0	84.1	41.8	51.6

* wind direction from the west or southwest (i.e., between 195 and 285^{O}); for transport to occur, the temporal persistence of the wind speeds and directions must also be sufficient for the air mass to traverse the distance between Sacramento and the Sierra crest.

As seen from the annual summary graphs, Sacramento winds aloft are in the direction of the Tahoe Basin about 40% of the time during the morning and 50% of the time during the afternoon at the 1000 foot altitude and somewhat lower (30% and 45% of the time) at the 3000 foot altitude.

To provide better understanding of the winds above ground level, LTADS included radar wind profilers operated in the Tahoe Basin at the South Lake Tahoe Airport, elevation 1909 m (6263 feet) MSL, and on the western slope of the Sierra Nevada near Grass

Valley, elevation 689 m (2261 feet) MSL. As configured for LTADS, the radar wind profilers provided hourly averaged observations of wind speed and direction for vertical intervals (range gates) of about 60 meters. The lowest range gate provided the average winds between 90 and 150 m AGL. The maximum range varied with environmental conditions and was usually several kilometers AGL. Generally, rates of data recovery increase a little with height through the first few range gates and then decrease with height through the upper range gates.

The hourly LTADS wind observations observed above the South Lake Tahoe Airport were summarized by time of day and season. **Figure 2-34** is an example figure illustrating wind observations during summer as a time height cross section. Each of the small wind roses shows the mean speed and frequency of wind direction for a specific height and time interval. Each of the three lowest height intervals represents observations from two 60-meter range gates of the RASS. The fourth interval represents data from four range gates (~240 meters). The percent frequency of calms (defined in this figure as speed < 1 m/s) and the number of hours of observations available are noted for each time-height interval.

The dominant wind direction over South Lake Tahoe Airport is from the SW quadrant during all seasons for nearly all times of day and elevations. During daylight hours, a secondary direction from the N develops due to onshore, up-valley flow. The vertical extent and frequency of the N wind is greatest in summer and fall when it is evident as high as 2400 m MSL (about 500 m above lake-level). Even during winter when storms tend to occur and when the diurnal variation in temperature is least, the frequency of N winds remains higher during daylight hours than during the night. During winter, although the higher range gates detect northerly winds less frequently than during summer, it appears that the depth of up-valley flow over SLT-Airport may reach to 2400 m MSL during some days and hours.

Mini-SODARs were operated at three sites in the Tahoe Basin and one site on the western slope of the Sierra Nevada during LTADS. The mini-SODARs provide fine (5-meter) vertical resolution of wind speed and direction near the surface, providing vertical coverage that is complementary to the radar wind profilers. Their vertical range depends upon humidity conditions. During LTADS their range extended from near ground level into the first range gate of the radar wind profiler and did not consistently extend through the second range gate of the radar wind profiler.

The in-basin mini-SODAR sites were Tahoe City Wetlands, Incline Village General Improvement District, and the SLT Airport (collocated with the radar wind profiler). The western Sierra slope site was located at Big Hill, about 25 miles SW of Lake Tahoe at about the 6000’ MSL elevation. The hours of operation were restricted at Big Hill to limit noise near sleeping quarters for fire lookouts and fire fighters.

As an example of the observations obtained with the mini-SODAR, summer frequency distributions of wind speed and direction at SLT Airport are summarized in **Figure 2-35**. As in **Figure 2-34**, each wind rose represents the seasonal frequency distribution of wind speed and direction over a height interval during specified hours of the day.

Figure 2-32a. Seasonal Summary of 0400 PST Winds at 1000 Feet AGL at Sacramento Executive Airport. (based on CARB, 1979)

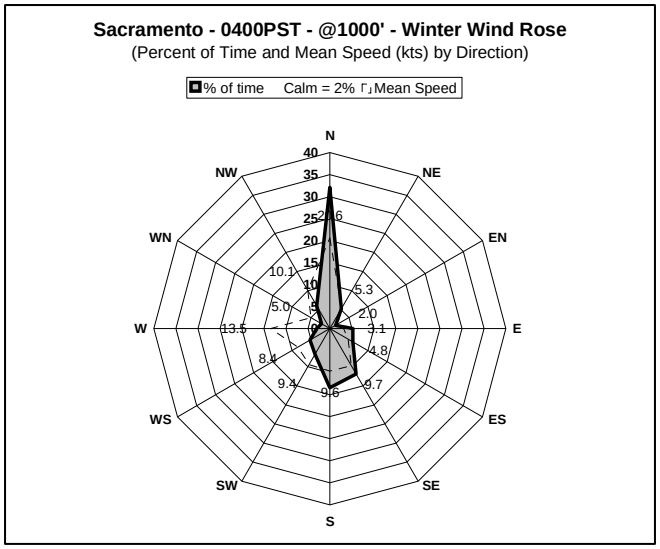

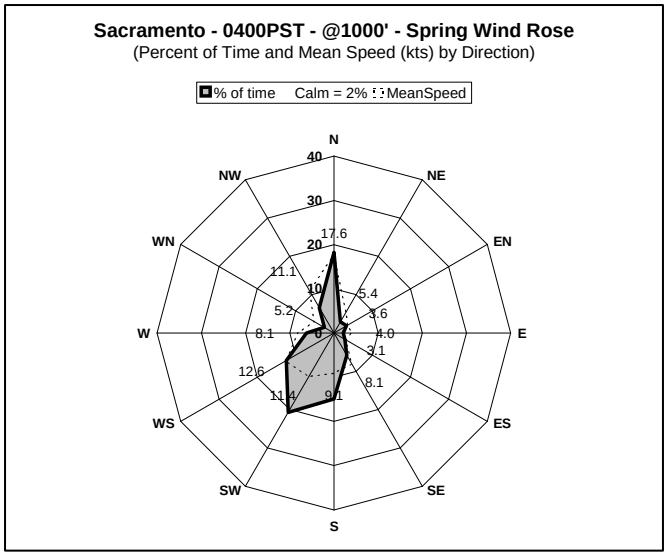

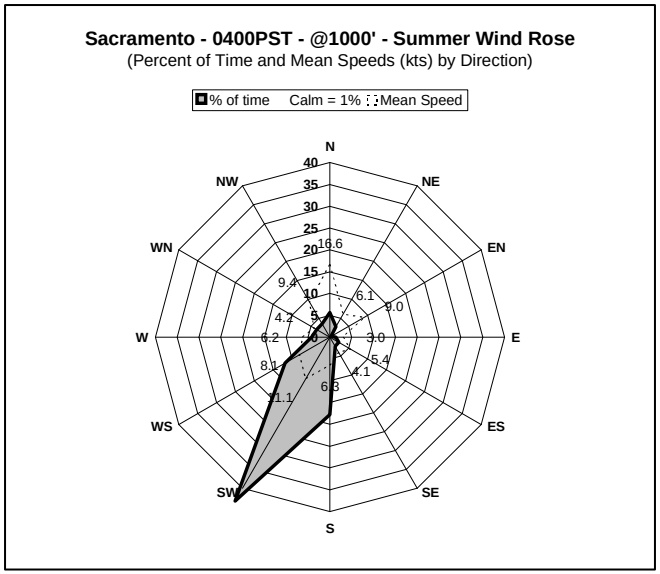

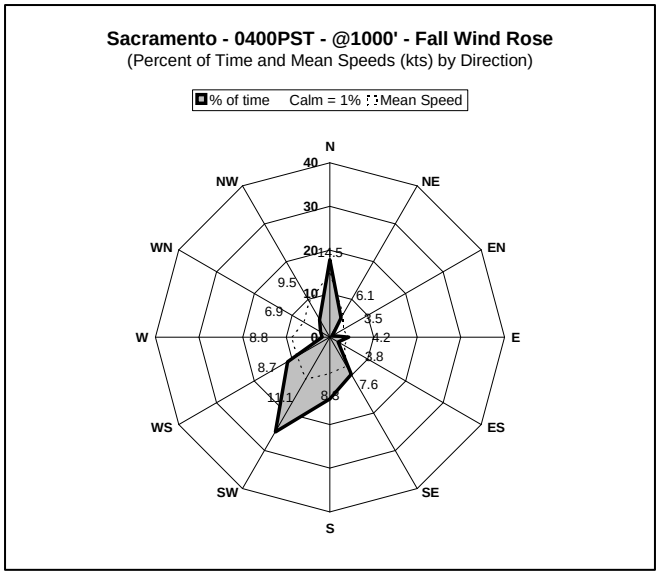

Figure 2-33b. Seasonal Summary of 1000 PST Winds at 1000 Feet AGL at Sacramento Executive Airport. (based on CARB, 1979)

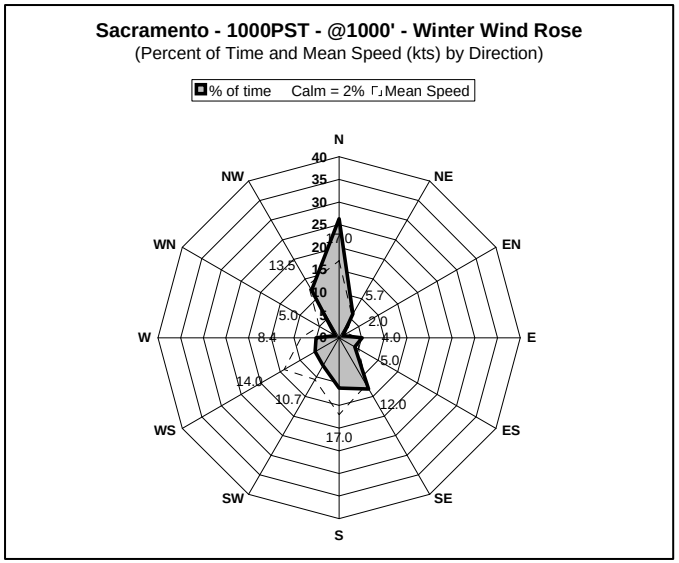

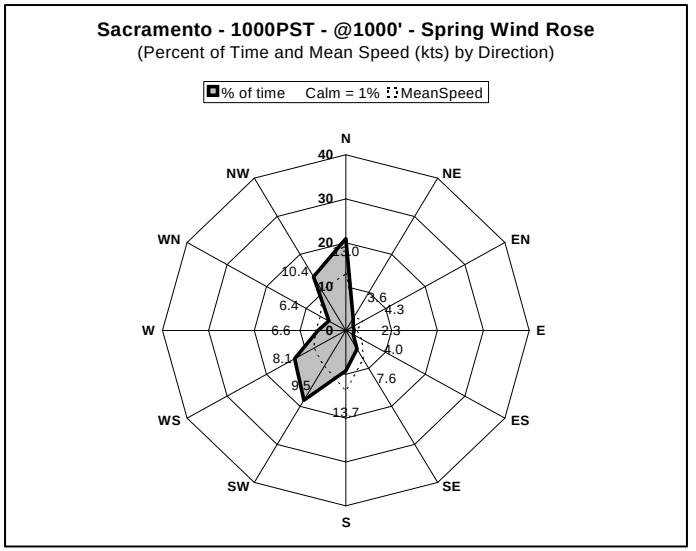

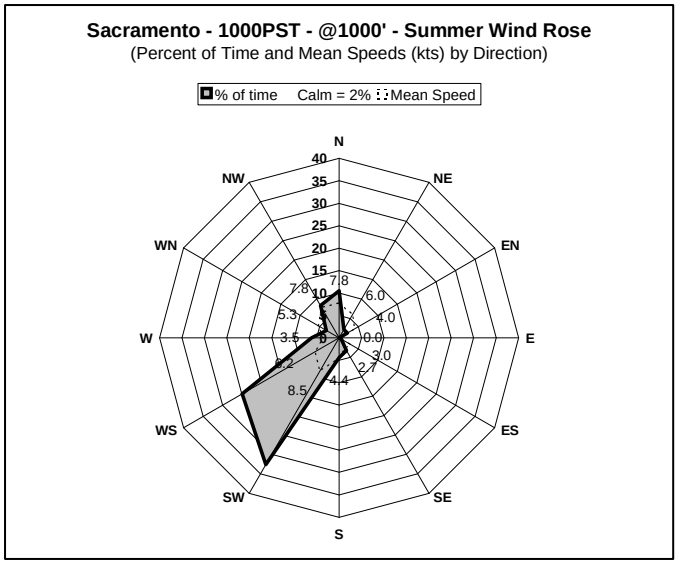

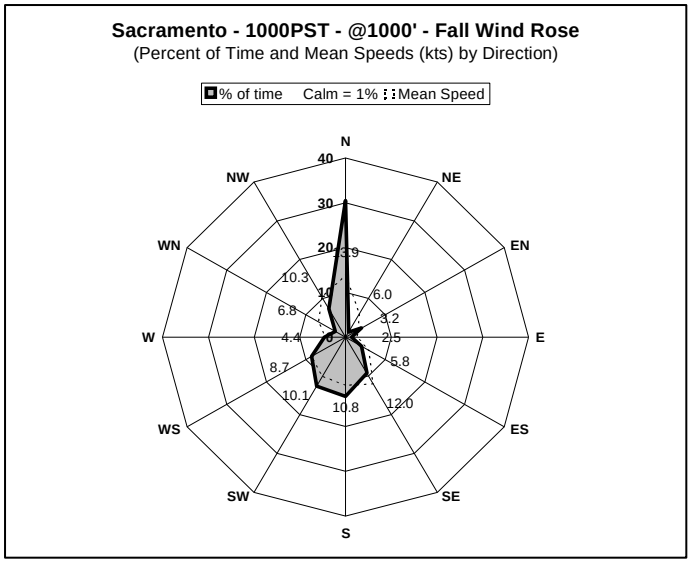

Figure 2-34c. Seasonal Summary of 1600 PST Winds at 1000 Feet AGL at Sacramento Executive Airport. (based on CARB, 1979)

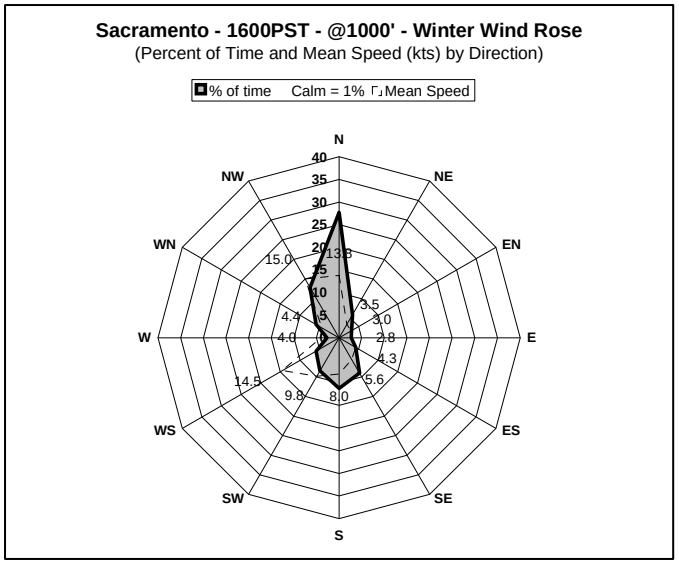

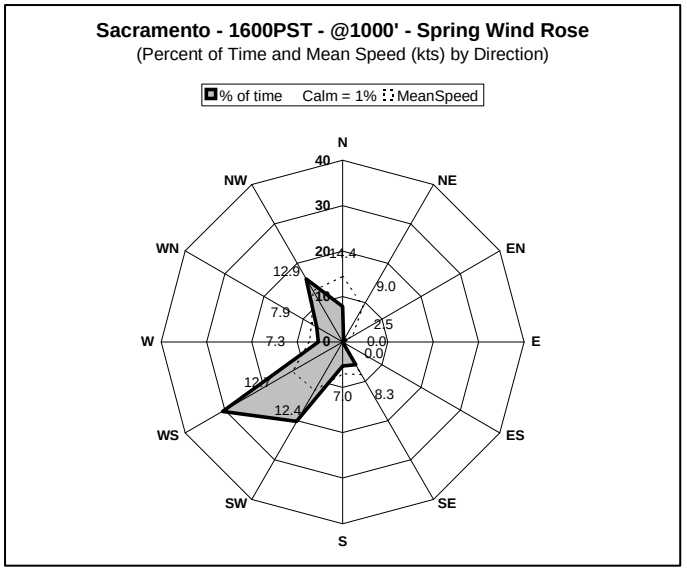

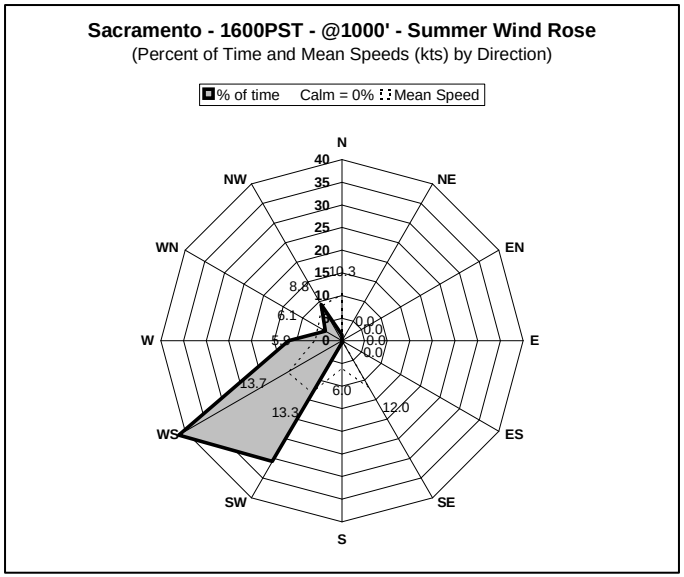

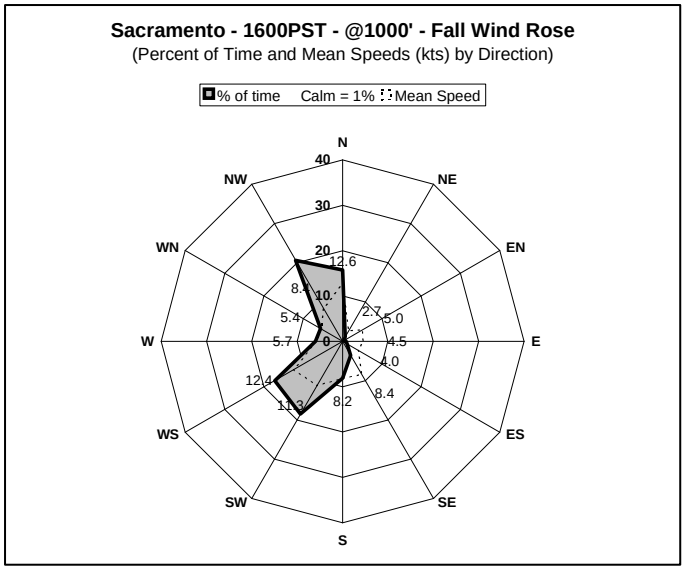

Figure 2-35a. Seasonal Summary of 0400 PST Winds at 3000 Feet AGL at Sacramento Executive Airport. (based on CARB, 1979)

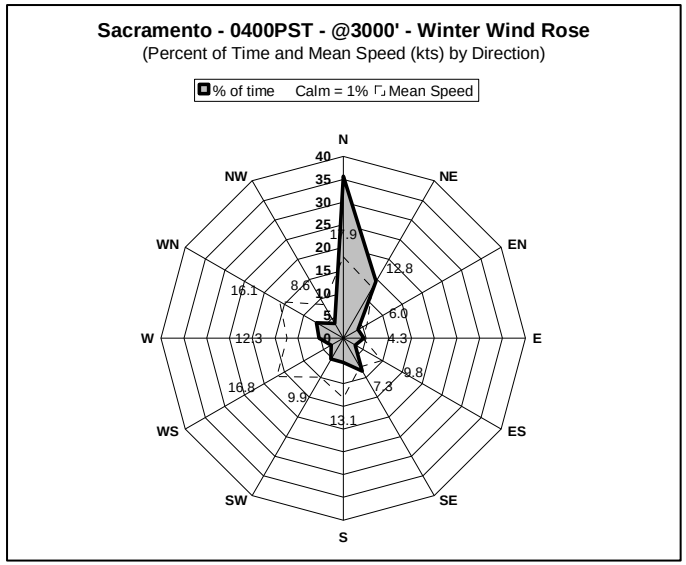

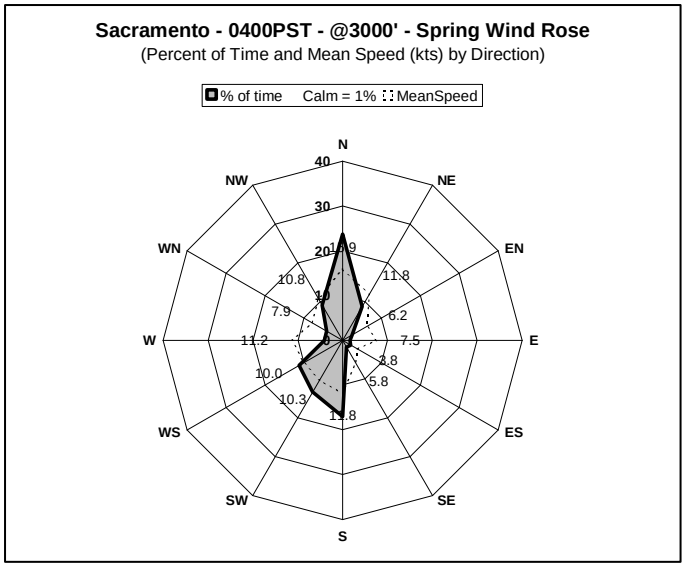

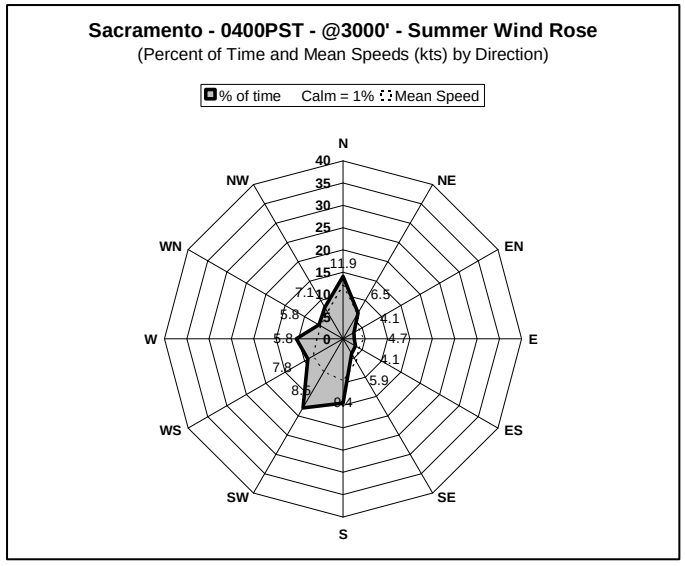

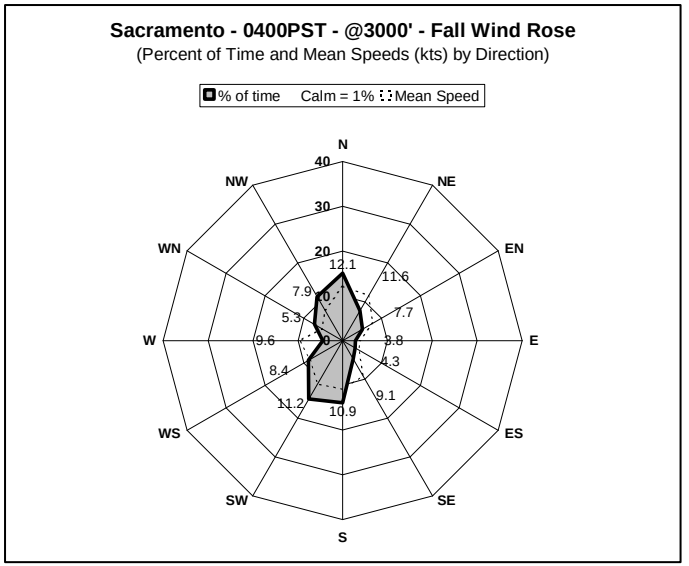

Figure 2-36b. Seasonal Summary of 1000 PST Winds at 3000 Feet AGL at Sacramento Executive Airport. (based on CARB, 1979)

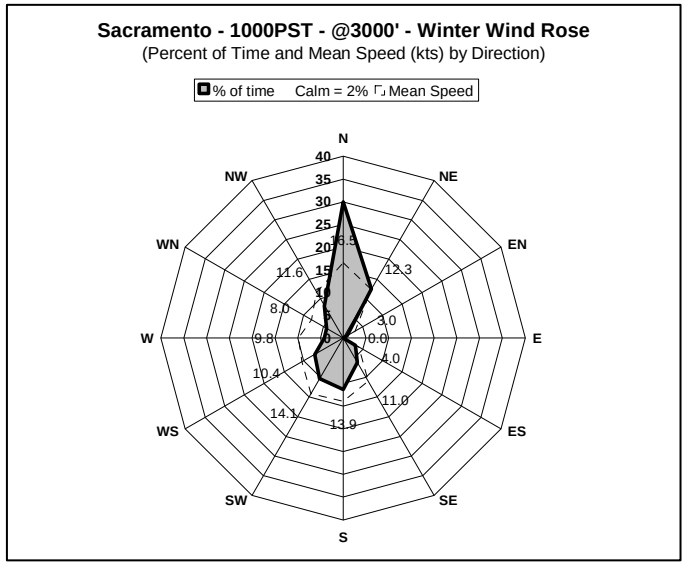

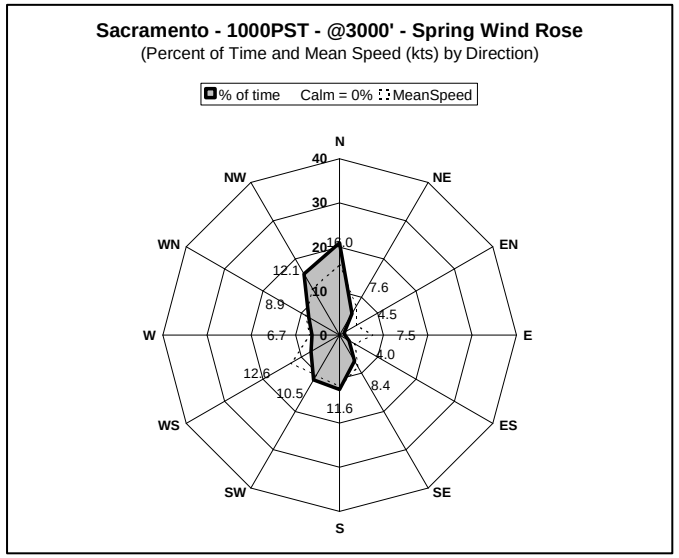

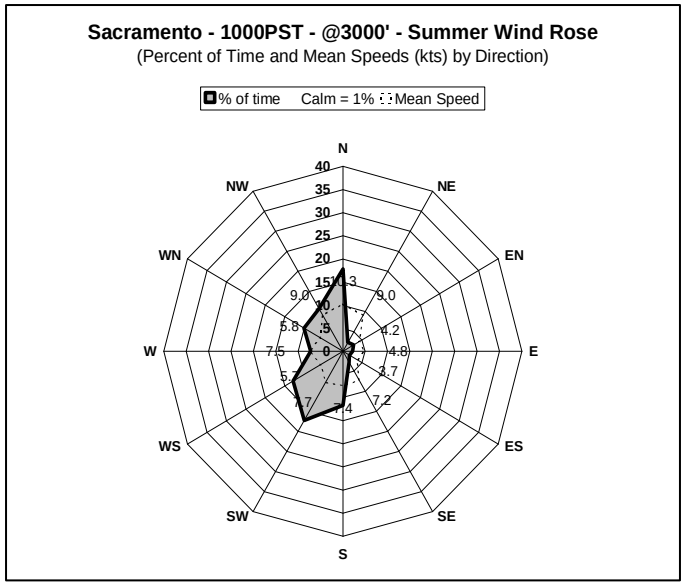

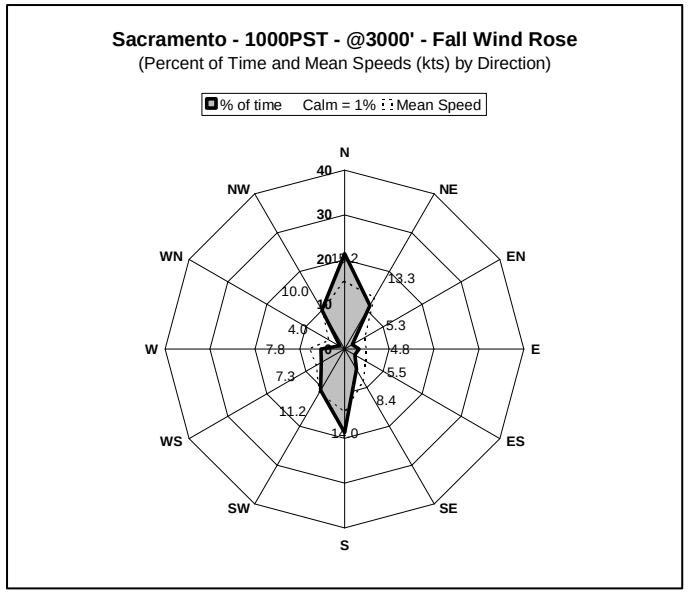

Figure 2-37c. Seasonal Summary of 1600 PST Winds at 3000 Feet AGL at Sacramento Executive Airport. (based on CARB, 1979)

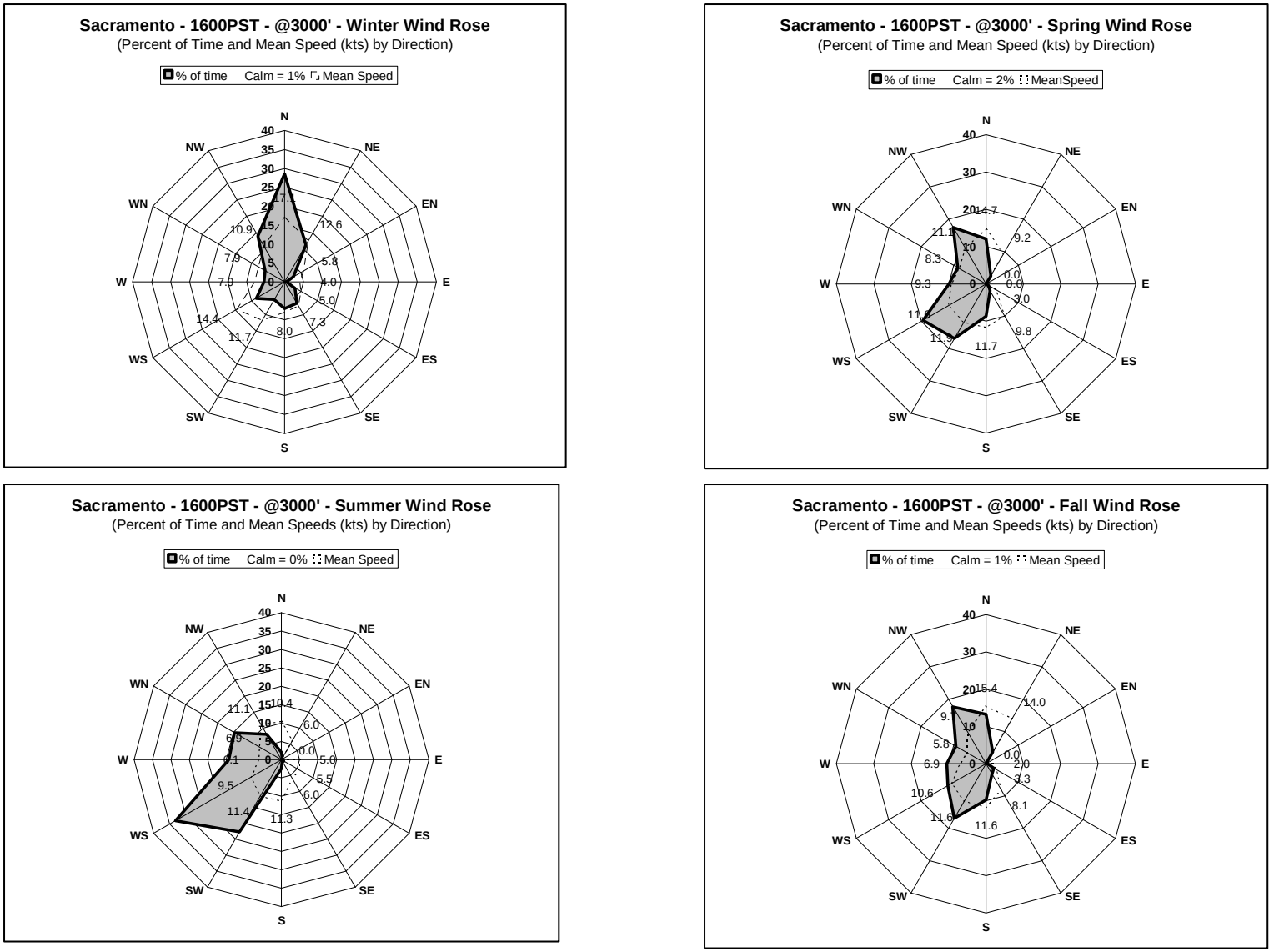

Figure 2-34. Altitude-Time Cross-Section of Wind Roses, SLT-Airport Radar Wind Profiler Lower Range Gates, Summer 2003.

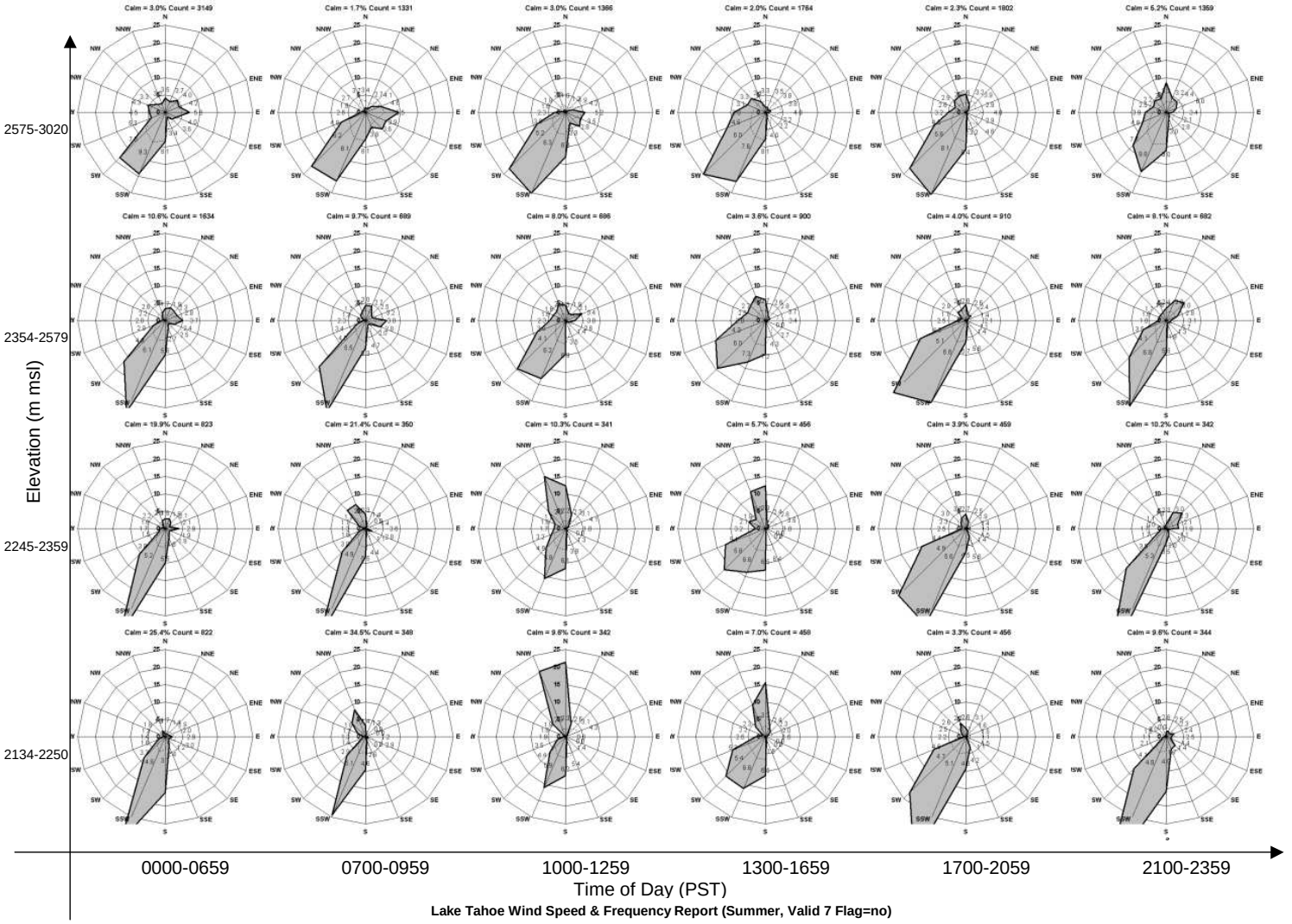

Figure 2-35. Altitude Time Cross-Section of Wind Roses for SLT-Airport Mini SODAR Lower Range Gates, Summer 2003.

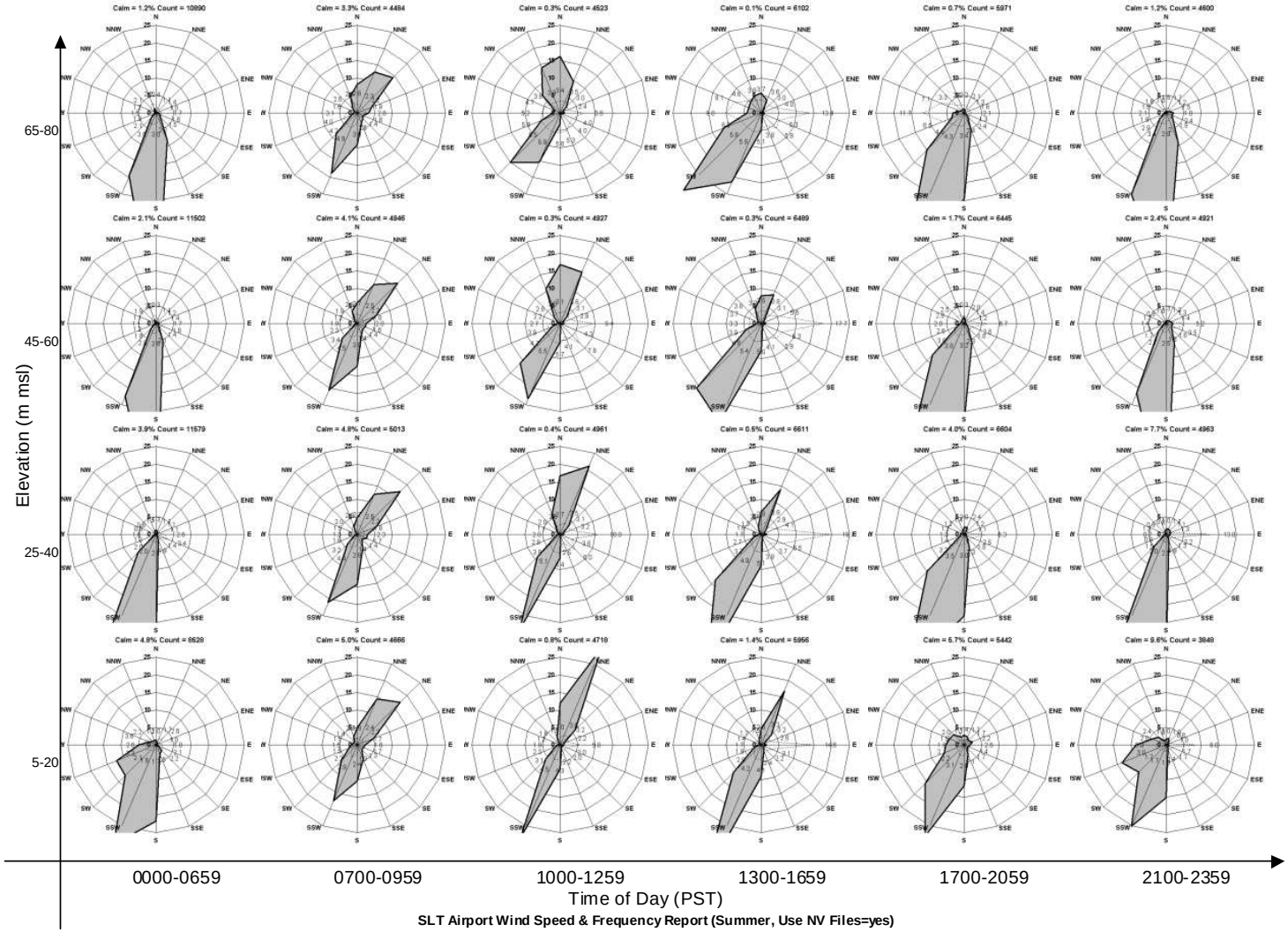

2.4 Meteorological Impact on Air Quality

Emissions of natural and anthropogenic materials can vary diurnally, by day of week, seasonally, and annually. Depending on the meteorological conditions when they are emitted, the ultimate impact of the emissions can vary dramatically. Whether pollutants are of local or regional origin, once present over the Lake, the rates of deposition of the gases and particles will be strongly influenced by meso- and micro-scale meteorological conditions (e.g., turbulence, temperature gradients). These factors and the prediction of the hourly deposition rates are laid out in detail in Chapter 4.

Various scales of meteorological influences are at work in the Tahoe Basin and each can impact the air quality of the Basin. Global and synoptic scale meteorological processes can transport dust and gases from Asia to the Sierra Nevada in detectable amounts, especially during the spring (Appendix B; VanCuren, 2003). Synoptic scale meteorological processes can move air from the Pacific coast over the populated areas of the San Francisco Bay, Stockton, Sacramento, and the Sierra foothills into and over the Sierra Nevada. Ozone concentrations increase as air flows east from the San Francisco Bay Area, to the Central Valley, and to the foothills. Ozone concentrations decline over the Sierra Nevada and drop to just below the California health-based standard in the Tahoe Basin. Thus, the potential exists for impacts in the Tahoe Basin from global and synoptic scale movement of air contaminated by human and natural emissions (e.g., motor vehicles, smoke).

As is illustrated in **Figures 2-28 through 2-31**, the transition from down-slope to up-slope air flow in the Sierra Nevada tends to occur a few hours later during the winter than during the summer while the transition from up-slope to down-slope flow tends to occur a few hours later during summer than winter. The night-time down-slope flows tend to be stronger in winter than in other seasons while the up-slope flows during summer tend to be much stronger than during other seasons. Thus, the potential for transport of materials up the Sierra slopes toward Tahoe is greatest during the summer. Generously assuming westerly winds for 10 hours at 6 miles per hour during the summer yields a typical one-day transport distance of 60 miles. Typically, surface winds then generally will not result in direct transport from the Sacramento urban area to the Tahoe Basin in one day.

The potential for pollutants generated upwind to affect air quality in the Tahoe Basin requires both horizontal transport, which can be characterized by wind directions and speeds, and also vertical transport, whereby air that flows over the Sierra crest must mix down to lake level. Vertical mixing is limited by thermal stability of the atmosphere (i.e., temperature inversions, either aloft or surface-based). Over land areas, in the absence of storms or waves formed on the lee side of the Sierra, this mixing, as indicated by the vertical profiles of temperature and the comparisons of surface and aloft temperatures is generally limited to the daylight hours between a few hours after sunrise and a few hours before sunset. However, during winter and spring relatively warm Lake temperatures compared to air temperatures suggest that median mixing depths (for limited areas over the Lake) could potentially reach to between 500 and

1000 m above the Lake level. During summer and fall the median values of maximum mixing depth over the Lake are likely less than about 300 and 400 meters respectively.

What happens to contaminants originating from outside the Tahoe Basin when they arrive at Tahoe? Transported air parcels must pass over the Sierra Nevada (ridgeline at ~2500-3000 meters) and then descend to the lake surface at ~1900 meters. Thus, vertical downmixing of air must occur over at least 600 meters to reach the Lake's surface and 700-1000 meters if the transport is to be significant. Historical temperature soundings over Lake Tahoe (though relatively limited in number) consistently indicate a temperature inversion between about 3,000 and 3,300 feet MSL. Any air pollutants transported above that altitude would take special circumstances (e.g., deep convective mixing) to be transported through the inversion and to the lake.

Furthermore, surface-based inversions frequently occur at night and during winter. The presence of surface-based inversions due to radiative cooling, conductive cooling (e.g., shallow layer of air cooled from direct contact with cold water of Lake Tahoe), or advection (e.g., drainage of cooler air off the mountain slopes, movement onshore of the relatively cooler air over the lake surface) can have a very significant impact. Not only can they prevent material transported aloft from coming into contact with the lake, they also trap local emissions near the ground and, if advected over the Lake, near the Lake surface. However, the lake's warmth during these periods would tend to prevent surface inversions from occurring over the lake itself. Conversely, during summer days, the lake's coolness relative to the air temperature could cause shallow inversions over the lake. Thus, the complex meteorology associated with a large alpine bowl located in the eastern Pacific high pressure zone frequently creates temperature inversions (both near ground-level and above the crest of the Sierra) that inhibit the vertical exchange of pollutants.

The soundings of temperature and winds (rawinsondes and flights) available prior to LTADS suggested that nocturnal inversions are most common during the summer months, averaging 15 to 20 days per month. The depths of the surface-based inversions were generally between 150 and 350 feet. The LTADS observations confirm limited mixing over land sites due to nocturnal inversions in all seasons.

Additional LTADS observations of temperatures aloft provide an indication of the climatology of mixing depth. The temporal and spatial details of the vertical mixing are complex and thus limited measurements at a few locations cannot fully characterize the mixing. However, based on the available measurements and various assumptions previously discussed, the following characteristics of mixing are predicted. Over land persistent low level inversions dominate during hours of darkness during all seasons and deep mixing is generally limited to midday hours during summer and fall. Over the Lake, the maximum extent of vertical mixing over the Lake is probably similar during night and day and may be fairly deep during winter and spring. Generally however, maximum mixing depth over the Lake is probably about 300 meters or less during summer and 400 m or less during fall.

What happens to contaminants originating from within the Tahoe Basin? Emissions of natural and anthropogenic materials can vary diurnally, heptdominally (day of week), seasonally, and annually. Depending on the meteorological conditions when they are emitted, the ultimate impact of the emissions can vary dramatically. Based upon the dominant pattern of limited vertical mixing and downslope flows shortly before, during, and immediately following hours of darkness, local emissions occurring between late afternoon and mid morning the next day will have the greatest impact on the Lake. Deeper mixing over land and upslope/onshore flow between mid morning and late afternoon of fall and summer suggest that local emissions during those hours will have less impact on the Lake.

Emissions originating from outside the basin will have much less opportunity to interact with the Lake than local emissions do because the meso-scale wind patterns and inversions in and over the Tahoe Basin tend to keep local emissions near the ground and the transported emissions aloft or diluted. Mixing depths over the Lake will likely be greatest in winter and to a lesser extent in spring. Under these conditions of enhanced vertical mixing, concentrations are relatively dilute, but meteorological conditions alone do not necessarily preclude impacts from upwind sources. Although some emissions from upwind might be entrained into shallow downslope flows, the observations of diurnal variations in particle concentrations near the shoreline indicate otherwise. The downslope flows were relatively clean during early morning hours but particle counts were observed to increase quickly with the onset of local morning activity. An improved understanding of the spatial and temporal variations in both emissions and meteorological processes will greatly enhance our understanding of the spatial and temporal representativeness of measurements of ambient concentrations and atmospheric deposition to the Lake Tahoe.

Chapter 2 has described key meteorological factors that impact spatial and temporal patterns of pollutant concentrations in order to provide a foundation for interpreting the spatial and temporal variations in the observed concentrations reported in Chapter 3. Meteorological information is also used in predicting the rates of deposition of concentrations from the atmosphere to the Lake surface. These rates are determined in large part by the wind speed, surface roughness immediately upwind, and the rate of change of temperature with elevation immediately above the water surface. These relationships and the algorithms for prediction of the deposition rates are laid out in detail in Chapter 4. Additional summaries of meteorological data are also presented in Appendix D.

2.5 References and Data Sources

AccuWeather (2004), www.accuweather.com.

Barone, John B., L.L. Ashbaugh, R.A. Eldred, and T.A. Cahill (1979), "Further Investigation of Air Quality in the Lake Tahoe Basin", report prepared for the California Air Resources Board under Contract No. A6-219-30 by the University of California, Davis, CA, March.

Bennett, Chuck (2004), personal communication regarding NOAA rawinsonde data retrieved from the National Climate Data Center.

California Air Resources Board (1979). Summary of California Upper Air Meteorological Data, Sacramento, CA, December.

California Air Resources Board (1984). California Surface Wind Climatology, Sacramento, CA, (reprinted January 1992).

California Department of Transportation (1979). South Lake Tahoe Cold Weather Carbon Monoxide and Hydrocarbon Study, Report No. CA-TL-79-11, Sacramento, CA, May.

California Department of Water Resources (1978). Wind in California, Bulletin No. 185, Sacramento, CA, January.

Carroll, John J., C. Anastasio, A.J. Dixon (2004). "Keeping Tahoe Blue through Atmospheric Assessment: Aircraft and Boat Measurements of Air Quality and Meteorology near and on Lake Tahoe", report prepared for California Air Resources Board by University of California, Contract No. 01-326, Davis, CA, June.

Hook, S. J., F. J. Prata, R. E. Alley, A. Abtahi, R. C. Richards, S. G. Schladow, and S. O. Palmarsson (2003). "Retrieval of lake bulk and skin temperatures using Along-Track Scanning Radiometer (ATSR-2) data: A case study using Lake Tahoe, California". *Journal of Atmospheric and Oceanic Technology*, **20**(4):534–548.

Shultz, Herbert B. (1974). "Meso-climatic Wind Patterns and their Application for Abatement of Air Pollution in the Central California Valley", draft report prepared for California Air Resources Board by University of California, Davis, CA, June.

Steissberg, T. (2005). University of California, Davis. Personal communication with Jim Pederson, 6/7/2005.

Tahoe Regional Planning Agency (1982), 1982 Air Quality Plan for the Lake Tahoe Basin, Draft Environmental Impact Statement, March.

Twiss, Robert H. et al. (1971). “Climate and Air Quality of the Lake Tahoe Region, A Guide to Planning”, report prepared for the Tahoe Regional Planning Agency and the U.S. Forest Service, South Lake Tahoe, CA, September.

Unger, Chuck (1979). “Meteorology and Air Quality in the Tahoe Basin, Part II – The Potential for Urban Air Pollution at Lake Tahoe during the Winter”, draft report prepared for the California Air Resources Board, Sacramento, CA, April.

VanCuren, Richard A. (2003). “Asian Aerosols in North America: Extracting the chemical composition and mass concentration of the Asian continental aerosol plume from long term aerosol records in the western United States”, J. Geophys. Res., 108 (D20), 4623, doi:10.1029/2003JD003459.

Western Regional Climatic Center (2004). www.wrcc.dri.edu, Reno, NV.

THIS PAGE BLANK INTENTIONALLY

3. Ambient Air Quality

This chapter is intended to provide background and documentation of the ambient concentrations used in estimating the direct atmospheric deposition of nitrogen, phosphorus, and particles to Lake Tahoe. A description of the LTADS deposition methodologies and the deposition estimates themselves are presented in Chapters 4 (dry) and 5 (wet). The level of detail and analysis presented in each section varies depending on the use of that data in constructing the deposition estimates. Some material presented initially in previous LTADS documents might only be summarized or referenced herein but the complete material is included as an appendix.

Six general types of air quality data were used to support the development of the LTADS deposition estimates. They were:

1) Historical and current regulatory air quality gas and aerosol data: intermittent 24-hour integrated TSP, PM10, PM2.5 aerosol mass and chemistry, and hourly gaseous pollutant data collected by the States of California and Nevada,
2) Historical and current visibility monitoring data: 24-hour integrated PM10 and PM2.5 filter samples collected by the federal IMPROVE Network and TRPA (following IMPROVE protocols),
3) 24^{+}-hour integrated aerosol filter samples collected during LTADS using portable "Mini-volume" samplers (MVS) around the basin and on buoys anchored on the Lake,
4) Two-week integrated aerosol and gas chemical speciation samples collected during LTADS with Two-Week Samplers (TWS) deployed at selected monitoring sites,
5) Hourly TSP, PM10, and PM2.5 mass concentrations collected during LTADS by Beta Attenuation Monitors (BAMs), and
6) Minute to hourly, size-resolved ambient particle counts (in six size ranges) collected in specialized short-term "dust" experiments during LTADS.

A description of the TWS and MVS sampling networks for LTADS is provided in **Table 3-1**. **Figure 3-1** shows the locations of air quality and aloft meteorological monitoring sites used as part of LTADS. The locations of the surface meteorological sites are shown in Figure 2-2.

Table 3-1. Lake Tahoe Atmospheric Deposition Study (LTADS) Two-Week-Sampler (TWS) and Mini-Volume Sampler (MVS) Networks.

Site Name (*)	Setting	Description	Sampling Network	PM Size Cuts	Sample Duration
Lake Forest (8)	Tahoe City North Lake Shore	20 meters S from Hwy 28	TWS	TSP, PM10, PM2.5	2 Weeks
Coast Guard Pier (14)	Tahoe City North Lake Shore	Pier 300 meters SSE from LF	MVS	TSP	1 Week
Thunderbird (11)	East Lake Shore - Distant from Hwy 28	Elephant House 10 meters E	TWS	TSP, PM10, PM2.5	2 Weeks
Zephyr Cove (14)	Zephyr Cove Marina, East Lake Shore	Pier 200 meters W from Hwy 50	MVS	TSP	1 Week
Timber Cove (14)	South Lake Tahoe, South Lake Shore	Pier 200 meters N from SOLA	MVS	TSP	48 Hours
SLT - SOLA (5)	South Lake Tahoe, South Lake Shore	30 meters N from Hwy 50	TWS	TSP, PM10, PM2.5	2 Weeks
SLT - Sandy Way (4)	South Lake Tahoe, South Lake Inland	40 meters S from Hwy 50	TWS	TSP, PM10, PM2.5	2 Weeks
Bliss State Park (6)	West Lake Shore Inland Mountain	20 meters W from Hwy 89	MVS	TSP	1 Week
Wallis Res - Tower (7)	West Lake Shore	20 meters E from Hwy 89	MVS	TSP	1 Week
Wallis Res - Pier (17)	West Lake Shore	Pier 50 meters E from Tower	MVS	TSP	1 Week
Buoy TB1 East (14)	Mid Lake North East	-	MVS	TSP	24 Hours
Buoy TB4 West (14)	Mid Lake North West	-	MVS	TSP	24 Hours
Big Hill (1)	Outside the Basin Near Loon Lake	25 miles SW of DL Bliss	TWS	TSP, PM10, PM2.5	2 Weeks

* (#) indicates number of site as depicted on map in Figure 3-1.

Figure 3-1. Map of LTADS study sites and activities at each site - November 2002 to March 2004.

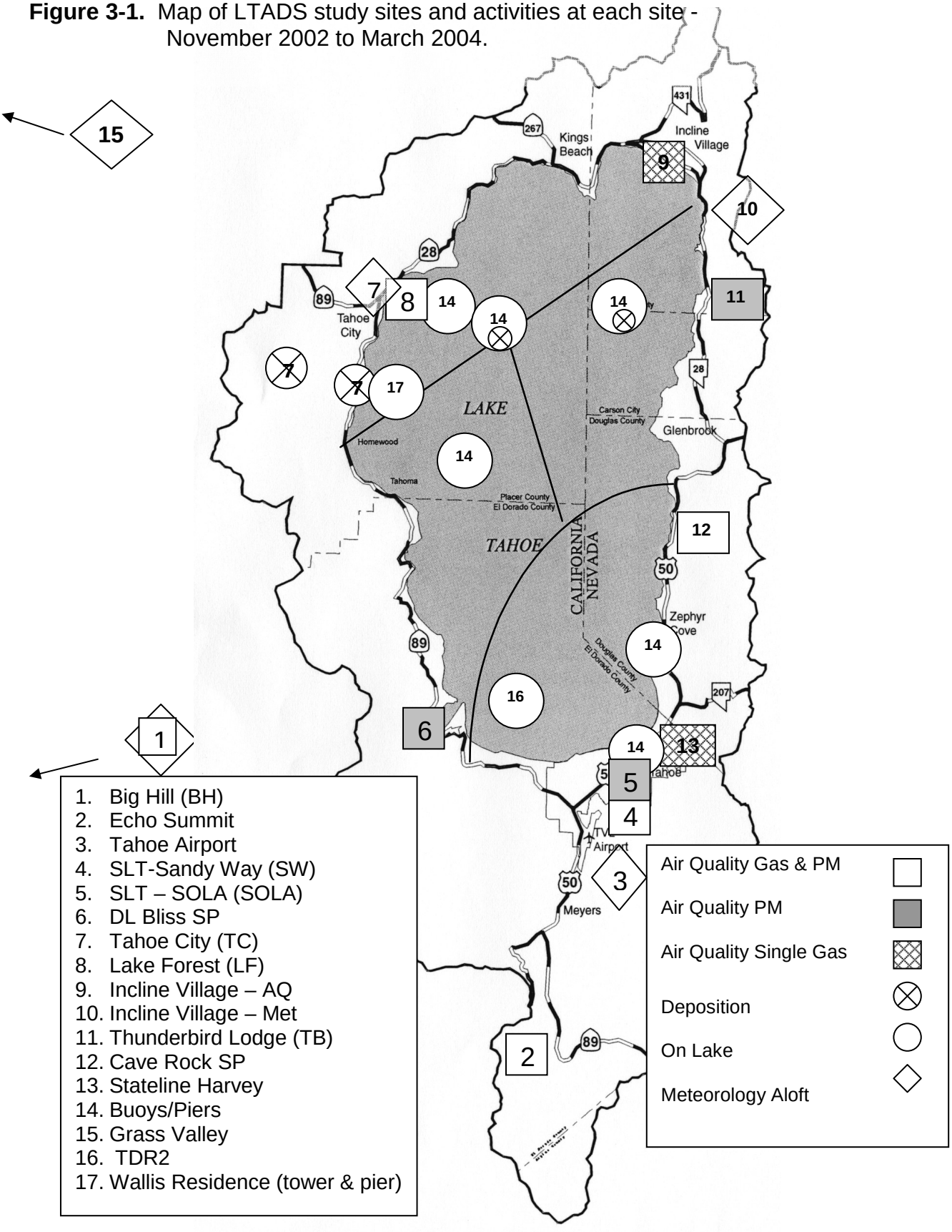

3.1 Data Quality

The monitoring programs in place before the initiation of LTADS have standard, established quality assurance protocols. The quality assurance for these two programs can be examined at websites identified in the following paragraphs.

The federal Environmental Protection Agency's Aerometric Information Retrieval System (AIRS) quality assurance programs have set guidelines for historical and current regulatory air quality gas and aerosol data. These guidelines apply to such data collected at Tahoe and are discussed in full detail at the following world wide web location: http://www.epa.gov/oar/oaqps/qa/.

Quality Assurance activities for the federal IMPROVE network and the associated TRPA sampling programs, applicable to samples collected at Tahoe, can be found in section 2.8 of "Semi-Annual Data Summary Report for Chemical Speciation of PM2.5 Filter Samples Project, July 8 to December 31, 2003, RTI." This report completed on August 26, 2004 can be found at the following world wide web location: http://www.epa.gov/ttn/amtic/files/ambient/pm25/spec/datsumspec.pdf.

The focus of this chapter is quality assurance of the remaining four general types of air quality sampling programs used to develop the LTADS deposition estimates. This section is also intended to provide sufficient analytical detail to give other researchers and interested scientists a fuller understanding of the strengths and weaknesses of the LTADS database. Please refer to the CARB LTADS website (http://www.arb.ca.gov/research/ltads/ltads.htm) or the TRPA TIIMS website (http://www.tiims.org/) for guidance on accessing the data collected during LTADS.

3.1.1 TWS and MVS Data

LTADS established a network of Two Week Samplers (TWS) whose performance during the Children's Health Study (CHS) showed ruggedness, reliability, and the ability to accommodate a nearly complete suite of chemical species measurements (Fitz, et al., 1996). This system was operated at a flow rate of 1.3 liter per minute (lpm). TWS included gaseous denuders for ammonia and nitric acid and filter collections for mass, ions, elements, and organic species for three size cuts of total suspended particulate matter (TSP), PM below 10 micrometers in aerodynamic diameter (PM10), and PM below 2.5 micrometers in aerodynamic diameter (PM2.5).

The TWS filter system likely converted peroxy and alk-oxy acetyl nitrates (PAN type species), which are also recognized as organic nitrates, into nitrate either through the Teflon filter itself or through the back-up filter. LTADS nitrates concentrations should therefore be treated as an upper limit of true nitrate concentrations at Tahoe.

The TWS denuder system has also been tested and found reliable for nitric acid (Fitz, et al., 1996). However, nitrous acid (HONO) is recognized to be an artifact included in this measurement approach. As such, LTADS nitric acid concentration data should be treated as an upper limit of true nitric acid concentrations at Tahoe. The ammonia TWS denuder system followed the standard methodologies developed for ammonia

extraction from annular denuder. The same measurement technique, used onboard the airplane for measurements aloft, experienced problems with high blank values (Carroll et al., 2004 and Zhang et al., 2002). Although field blank values for NH_3 were comparable to the minimum measurements at Thunderbird Lodge, the cleanest TWS site during LTADS, most of the NH_3 measurements by TWS were well above the field blank amounts.

The Mini-Volume Sampler (MVS) network used the standard Air Metrics Mini-Volume Sampler, which operates at 5.0 lpm. These were generally equipped with the same type of Teflon filters as for the TWS network. Unlike the TWS filter network that was equipped with a back-up filter to sequester volatilized nitric acid and nitrates, the MVS network had no back-up filters.

3.1.2 DRI TWS and MVS Data Validation

TSP, PM10, and PM2.5 samples were gravimetrically analyzed for total mass concentration and detailed chemical speciation profiles. A total of 129 sets of TWS samples, including TSP, PM10, and PM2.5, 36 sets for buoy Mini-Vol TSP samples, and 129 sets for non-buoy Mini-Vol TSP samples were collected in LTADS. Replicate analysis was performed on 10% of the ambient samples.

Field blanks were collected to subtract the background contribution from the sampling environment and field operation. TWS field blanks were only collected at SOLA. MVS field blanks were collected at the Wallis Tower and Zephyr Cove. The limited, variable, and site-specific field blanks increase the uncertainty of ambient sample concentrations.

The chemical data were evaluated for internal consistency by examining the physical consistency and balance of reconstructed mass, based on chemical species versus measured mass. In general, the samples collected met the criteria of internal physical consistency. A few TWS samples were suspected to be outliers; however, no field flag was noted for these samples (with the exception of one laboratory flag).

The annual average mass concentrations and chemical species were the highest in TSP and the lowest in PM2.5 at the same site; however such physical consistency was not necessarily observed for TWS samples in every sampling period. Such sampling artifacts can result from a number of factors: 1) the TWS design and low sampling flow rate of 1.3 liters per minute, which can contribute to an undersampling of TSP, 2) the frequently low mass concentration of ambient particulate matter in the Tahoe Basin, 3) the random bounce and penetration of particles larger than the 50% cutpoint of the sampling inlet, and 4) the potential sampling artifacts of semi-volatile species associated with the long sampling duration (2-weeks).

Scatter plots of duration showed that Mini-Vol samples were poorly correlated spatially and temporally; therefore, temporal and spatial variations were only examined for TWS samples. The highest annual average TSP (21.9 $\mu g/m^3$) and PM10 (18.8 $\mu g/m^3$) mass concentrations were observed at the SOLA site and the highest annual average PM2.5 mass concentration (9.0 $\mu g/m^3$) was observed at the SW site. The lowest TSP, PM10, and PM2.5 mass concentration were 6.2, 6.0, and 3.6 $\mu g/m^3$, respectively, and were

observed at the TB site. Similar annual averages of organic carbon (OC), elemental carbon (EC), ammonium, and sulfate in TSP, PM10, and PM2.5 were observed. PM10 mass comprised 80-90% of TSP mass and was approximately twice that of PM2.5 mass. The most abundant chemical species were OC (16.5%-29.8%), silicon (10.8%-16.0%), and aluminum (3.9%-4.7%) for TSP; OC (16.2%-27.8%), silicon (10.0%-21.1%), and aluminum (3.5%-6.6%) for PM10; and OC (42.1%-52.0%), EC (4.9%-16.4%), and ammonium (3.1%-5.8%) for PM2.5.

The lowest TWS TSP, PM10, and PM2.5 mass concentrations were observed from March to April 2003 at all five sites. TWS TSP, PM10, and PM2.5 mass concentrations observed at the BH, TB, and LF sites from May to October 2003 were twice as high as those observed from November 2002 to February 2003; however, TWS TSP, PM10, and PM2.5 mass concentrations were comparable during these two periods at the SOLA and SW sites. The elevated TWS TSP, PM10, and PM2.5 mass concentrations at the SOLA and SW sites from November 2002 to February 2003 were due to elevated OC and EC concentrations, which were likely the result of increased traffic volume for winter activities. Wood smoke also contributed to elevated PM2.5 mass concentrations during winter.

3.1.3 Sample Preparation, Shipment, Receiving, and Analysis

3.1.3.1 Sample Preparation

3.1.3.1.1 Configurations of TWS and Mini-Volume Samplers in the LTADS

Filter-based measurements of atmospheric pollutants were obtained using two types of samplers: Two Week Samplers (TWS) and AirMetrics Mini-Vol samplers. The TWS were operated for two-week durations and collected integrated samples representing total suspended particulate (TSP), PM10 and PM2.5 (particles with aerodynamic diameters less than 10 and 2.5 µm, respectively), and nitric acid and ammonia via denuder measurements. The TWS were operated at a nominal flow rate of 1.3 lpm from 11/20/02 to 01/06/04 at five sites (four sites in the Tahoe Basin and one site upwind of the Basin).

The Mini-Vol samplers without PM2.5 or PM10 inlets (i.e., TSP samples) were deployed on lake buoys, piers, and at some land-based sites. All of the buoy samples and a few of the pier samples were collected for the duration of the sampler battery (typically 24-30 hours). The duration of the non-buoy samples that operated on AC power varied due to sampler malfunctions; typically, the sampling filters were replaced on a weekly schedule. The Mini-Vol samplers were operated at a nominal flow rate of 5.0 lpm from 09/26/02 to 04/26/04.

Each TWS had eight channels: three channels contained Teflon-membrane filters to measure TSP, PM10 and PM2.5 mass and elements; three channels contained quartz filters to measure TSP, PM10, and PM2.5 ions and carbon; and two channels were used to collect ammonia and nitric acid denuder samples. Mini-Vol samplers were run in pair, where one sampler contained a Teflon-membrane filter and the other contained a quartz-fiber filter. All sampling media collected by the TWS and Mini-Vol samplers

were prepared and chemically analyzed by the Desert Research Institute's Environmental Analysis Facility.

3.1.3.1.2 Sampling Media

Teflon-membrane filters were equilibrated for weighing after passing acceptance testing by X-ray flourescence (XRF). Initial weights were performed after the filters equilibrated for a minimum of four weeks. A minimum of two filters per lot (approximately 100 filters per lot) received from the manufacturer were analyzed for chemical species to verify that pre-established specifications had been met. The lot was rejected if the verification filters did not pass this acceptance test. Each filter was individually examined over a light table prior to use for discoloration, pinholes, creases, or other defects. In addition to laboratory blanks, 5 to 10% of all filters were designated as field blanks per standard operating procedures.

Quartz-fiber filters absorb organic gases from ambient air and organic artifacts from the manufacturing process. By pre-firing the quartz-fiber filters, these absorbed gases and artifacts are reduced to constant, insignificant, levels. The filters were pre-fired in preparation for thermal/optical reflectance carbon (TOR) analysis, which is a thermal desorption process subjecting the filters to temperatures between 25 to 800^{o} C; therefore, the filters were pre-fired at 900^{o} C to remove all possible TOR analysis interferences. Sets of filters with levels that exceeded 1.5 µg/cm^{2} for organic carbon (OC) and 0.5 µg/cm^{2} for elemental carbon (EC) were re-fired or rejected. Pre-fired filters were sealed and stored in a freezer prior to preparation for field sampling.

Cellulose fiber filters were impregnated with a solution of sodium chloride (5% NaCl, 5% glycerol and 90% distilled de-ionized water [DDW]) and used for the collection of volatilized nitrate. These filters were prepared in batches and subjected to acceptance testing prior to use in accordance with DRI SOP #2-104.3. Filter packs for the TWS were prepared in accordance with the CARB standard operating procedures (SOP) for TWS. Glass denuders were coated and handled according to the CARB SOP for TWS. Filter packs for the Mini Vol samplers were prepared in accordance with DRI's SOP # 2-110.4.

3.1.3.1.3 Sample Shipping and Receiving

The TWS filter packs were packaged and shipped to two locations for deployment. Filter packs for the Lake Forest (LF) and Big Hill (BH) sites were shipped to the CARB in Sacramento, CA; filter packs for the South Lake Tahoe (SL), Thunderbird (TB), and Sandy Way (SW) sites were shipped to the Tahoe Regional Planning Agency (TRPA) in South Lake Tahoe, CA. Each sampling set of eight filter packs was sealed in large, re-closable freezer bags (with the site marked on the outside of each bag and the associated field data sheet enclosed).

Mini-Vol sampler filter packs were packaged and shipped to two locations for deployment at the request of the operator. Due to sampler variation, two types of holders were deployed. The filters for use at the North Shore (NS) site were loaded into blue cassettes and shipped to the Tahoe Research Group, Tahoe City, CA. The filters

for use at the South Shore (SS) site were loaded into nucleopore holders and shipped to the TRPA, South Lake Tahoe, CA. Mini-Vol sampler filter packs were sealed in reclosable bags with a field data sheet for each set of filters (paired Teflon-membrane and quartz-fiber filter packs).

All filter packs were placed in coolers refrigerated with blue ice for shipment. The coolers were then shipped by second-day service for arrival by Tuesday of the designated sample change-out week. Entries of the shipment and the sample ID of the filter packs were made in the DRI/EAF shipping logbook.

3.1.3.2 Analysis Methods

3.1.3.2.1 Gravimetric Analysis

Unexposed and exposed Teflon-membrane filters were equilibrated at a temperature of 21.5 ± 1.5^{o} C and a relative humidity of 35 ± 5% for a minimum of 24 hours prior to weighing (Chow et al., 2005). Weighing was performed on a Mettler MT-5 electro microbalance with ±0.001 mg sensitivity. The charge on each filter was neutralized by exposure to a polonium-210 source for 30 seconds before the filter was placed on the balance pan. The balance was calibrated with a 200 mg Class S weight and the tare was set prior to weighing each batch of filters. After every 10 filters were weighed, the calibration and tare were re-checked. If the results of these performance tests deviated from specifications by more than ±5 µg, the balance was re-calibrated.

All initial filter weights were checked by an independent technician. Samples were re-weighed if these check-weights did not agree with the original weights within ±0.010 mg. At least 30% of the exposed filter weights were checked by an independent technician. Samples were re-weighed if these check-weights did not agree with the original weights within ±0.015 mg. Pre- and post-weights, check weights, and re-weights (if required) were recorded on data sheets and directly entered into a data base via an RS232 connection. All weights were entered by filter number into the DRI aerosol data base.

3.1.3.2.2 Elements by XRF

After gravimetric analysis, a Kevex model 700 energy dispersive X-ray fluorescence analyzer (EDXRF) (Watson, et al, 1999) was used to quantify sodium (Na), magnesium (Mg), aluminum (Al), silicon (Si), phosphorus (P), sulfur (S), chlorine (Cl), potassium (K), calcium (Ca), titanium (Ti), vanadium (V), chromium (Cr), manganese (Mn), iron (Fe), cobalt (Co), nickel (Ni), copper (Cu), zinc (Zn), gallium (Ga), arsenic (As), selenium (Se), bromine (Br), rubidium (Rb), strontium (Sr), yttrium (Y), zirconium (Zr), molybdenum (Mo), palladium (Pd), silver (Ag), cadmium (Cd), indium (In), tin (Sn), antimony (Sb), barium (Ba), gold (Au), mercury (Hg), thallium (Tl), lead (Pb), lanthanum (La), and uranium (U) on Teflon-membrane samples. Calibration was performed using thin film standards from Micromatter Inc. A multi-element thin film standard was analyzed with each run to monitor for calibration drift and was used as the indicator for routine calibrations.

3.1.3.2.3 Organic and Elemental Carbon

The thermal/optical reflectance (TOR) method measures total carbon (TC), organic carbon (OC) and elemental carbon (EC). The TOR method is based on the principle that different types of carbon-containing particles are converted to gases under designated temperature and oxidation conditions. These specific carbon fractions also help to distinguish between seven carbon fractions reported by TOR, following the Interagency Monitoring of Protected Visual Environments (IMPROVE) protocol (Chow, et al, 1993):

- The carbon evolved in a helium (He) atmosphere at temperatures between ambient (~25^{o} C) and 120^{o} C (OC1)
- The carbon evolved in a He atmosphere at temperatures between 120^{o} C and 250^{o} C (OC2)
- The carbon evolved in a He atmosphere at temperatures between 250^{o} C and 450^{o} C (OC3)
- The carbon evolved in a He atmosphere between 450^{o} C and 550^{o} C (OC4)
- The carbon evolved in an oxidizing atmosphere at 550^{o} C (EC1)
- The carbon evolved in an oxidizing atmosphere between 550^{o} C and 700^{o} C (EC2)
- The carbon evolved in an oxidizing atmosphere between 700^{o} C and 800^{o} C (EC3)

The thermal/optical reflectance carbon analyzer consists of a thermal system and an optical system. The thermal system consists of a quartz tube placed inside a coiled heater. Current through the heater is controlled to attain and maintain pre-set temperatures for given time periods. A portion of a quartz-fiber filter is placed in the heating zone and heated to designated temperatures under non-oxidizing and oxidizing atmospheres. The optical system consists of a He-Ne laser, a fiber optic transmitter and receiver, and a photocell. The filter deposit faces a quartz light tube so that the intensity of the reflected laser beam can be monitored throughout the analysis.

As the temperature is increased from ambient (~25^{o} C) to 550^{o} C in a non-oxidizing He atmosphere, OC compounds are volatilized from the filter while EC is not oxidized. When oxygen (O_2) is added to the He at temperatures greater than 550^{o} C, the EC burns and enters the sample stream. The evolved gases pass through an oxidizing bed of heated manganese dioxide, where they are oxidized to carbon dioxide (CO_2), and then across a heated nickel catalyst that reduces the CO_2 to methane (CH_4). The CH_4 is then quantified with a flame ionization detector (FID).

The reflected laser light is continuously monitored throughout the analysis cycle. The negative change in reflectance is proportional to the degree of pyrolytic conversion from OC to EC that occurs during OC analysis. After O_2 is introduced, the reflectance increases rapidly as the light-absorbing carbon is burned off of the filter. The carbon measured after the reflectance attains the value it had at the beginning of the analysis cycle is classified as EC. This adjustment for pyrolysis can be as high as 25% of OC or EC and therefore cannot be ignored.

The instrument was calibrated by analyzing samples of known amounts of CH_4, CO_2 and potassium hydrogen phthalate (KHP). The FID response was compared to a reference level of CH_4 injected at the end of each sample analysis. Performance tests of the instrument's calibration were conducted at the beginning and end of each day's operation. Intervening samples were re-analyzed when calibration changes greater than ±10% are found.

Known amounts of American Chemical Society (ACS) certified reagent grade crystal sucrose and KHP were committed to TOR as a verification of the OC fractions. Fifteen different standards were used for each calibration; however, widely accepted primary standards for EC and OC are still lacking. Results of the TOR analysis of each filter were entered into the DRI data base.

3.1.3.2.4 Inorganic Ion Analyses

Water-soluble chloride, nitrate, sulfate, ammonium, sodium, magnesium, calcium, and potassium were obtained by extracting the quartz-fiber particle filter in 15 ml of DDW. The extraction vials were capped and sonicated for 60 minutes, shaken for 60 minutes, then aged overnight to assure complete extraction of the deposited material in the solvent. The ultrasonic bath water was monitored to prevent temperature increases from the dissipation of ultrasonic energy in the water. After extraction, these solutions were stored under refrigeration prior to analysis.

3.1.3.2.5 Ion Chromatographic Analysis for Chloride, Nitrate, and Sulfate

Water-soluble chloride (Cl^-), nitrate (NO_3^-), and sulfate ($SO_4^=$) were measured with the Dionex 2020i (Sunnyvale, CA) ion chromatograph (IC) (Chow and Watson, 1999). The IC uses an ion-exchange column to separate the sample ions in time for individual quantification by a conductivity detector. Prior to detection, the column effluent enters a suppressor column where the chemical composition of the component is altered and results in a matrix of low conductivity. The ions are identified by their elution/retention times, and are quantified by the conductivity peak area. Approximately 2.0 ml of the filter extract are injected into the IC. The resulting peaks are integrated and the peak integrals are converted to concentrations using calibration curves derived from solution standards. The Dionex system for the analysis of Cl^-, NO_3^-, and $SO_4^=$ contains a guard column (AG4a column, Cat. No. #37042), an anion separator column (AS4a column, Cat. No. #37041) with a strong basic anion exchange resin, and an anion micro-membrane suppressor column (250 ´ 6 mm ID) with a strong acid ion exchange resin. The anion eluent consists of sodium carbonate (Na_2CO_3) and sodium bicarbonate ($NaHCO_3$) prepared in DDW. The DDW is verified to have a conductivity of less than 1.8 ´ 10-5 ohm/cm prior to preparation of the eluent. For quantitative determinations, the IC is operated at a flow rate of 2.0 ml per minute.

The primary standard solution containing NaCl, $NaNO_3$, and $(Na)_2SO_4$ were prepared with reagent-grade salts dried in an oven for one hour at 105^o C and then brought to room temperature in a desicator. The anhydrous salts were weighed to the nearest 0.10 mg on a routinely calibrated analytical balance under controlled temperature (~20

^{O}C) and relative humidity (±30%). The salts were then diluted in precise volumes of DDW. Calibration standards were prepared at least once per month by diluting the primary standard solution to concentrations covering the range expected in the filter extracts. The standards were then stored in a refrigerator. Calibration concentrations of 0.1, 0.2, 0.5, 1.0, and 2.0 mg/ml were prepared or each of the analysis species.

Calibration curves were performed weekly. Chemical compounds were identified by matching the retention time of each peak in the unknown sample with the retention times of peaks in the chromatograms of the standards. A DDW blank was analyzed after every 20 samples and a calibration standard was analyzed after every 10 samples. These quality control checks verified the baseline and the calibration, respectively. Environmental Research Associates (ERA, Arvada, CO) standards were used daily as an independent quality assurance (QA) check. These standards (ERA Wastewater Nutrient and ERA Mineral WW) are traceable to the National Institute of Standards and Technology (NIST) simulated rainwater standards. If the values obtained for these standards did not coincide within a pre-specified uncertainty level (typically three standard deviations of the baseline level, or ±5%), the samples analyzed between that standard and the previous calibration standards were re-analyzed.

After analysis, the printout for each sample in the batch was reviewed for the following: 1) proper operational settings, 2) correct peak shapes and integration windows, 3) peak overlaps, 4) correct background subtraction, and 5) quality control sample comparisons. When values for replicates differed by more than ±10% or values for standards differed by more than ±5%, samples before and after these quality control checks were designated for re-analysis in a subsequent batch. Individual samples with unusual peak shapes, background subtractions, or deviations from standard operating parameters were also designated for re-analysis.

Water soluble nitrate and nitric acid concentrations were obtained from the cellulose backup filter and the nitric acid denuder, respectively, using the same IC analysis procedure. IC analysis procedures are detailed in DRI SOP # 2-203.5.

3.1.3.2.6 Ammonium Analysis

An Astoria 2 Automated Colorimetry (AC) system (Astoria–Pacific, Clackamas, OR) was used to measure ammonium concentrations by the indolphenol method. Each sample was mixed with reagents and subjected to appropriate reaction periods before submission to the colorimeter. Beer's Law relates the liquid's absorbency to the amount of the ion in the sample. A photomultiplier tube measured this absorbency through an interference filter specific to ammonium. Two ml of extract in a sample vial were placed in a computer-controlled auto-sampler. Calibration curves were produced with each daily batch of samples.

Ammonia concentrations from the citric acid denuders were determined using the same analysis method.

3.1.3.2.7 Atomic Absorption Analysis for Soluble Metals

Soluble sodium, magnesium, potassium and calcium were measured using a Varian Spectra AA-880 atomic absorption spectrophotometer. In atomic absorption spectrophotometry, the sample is aspirated into a flame and atomized. A light beam from a hollow cathode lamp is directed through the flame into a monochromator, and then onto a photoelectric detector that measures the amount of light absorbed by the atomized element in the flame. The cathode of a hollow cathode lamp contains the pure metal which results in a line source emission spectrum. Since each element has its own characteristic absorption wavelength, the source lamp composed of that element is used. The amount of energy of the characteristic wavelength absorbed in the flame is proportional to the concentration of the element in the sample. Calibration curves were produced with each daily batch of samples.

3.1.3.2.8 Nitric Acid & Ammonia – TWS Limits of Detection and Uncertainties

For various reasons, the first seven samples at Big Hill and 13 samples at other sites failed to properly collect any material for analysis. Additionally, two nitric acid and three ammonia cassettes failed leak checks; the concentrations are reported with the proper warnings attached. Nitric acid and ammonia concentrations were above uncertainty levels 99% and 96% of the time, respectively:

Tarnay et al. (2001) reported minimum detection limits of approximately 0.30 ug/m^3 for nitric acid and ammonia for a field study in the Tahoe Basin. Adjusting for different flow rates and sampling duration (Tarnay et al. (2001) sampled at 10 lpm for 12 hours while LTADS TWS sampled at 1.3 lpm for two weeks), an equivalent detection limit (using same laboratory equipment and procedures) for the LTADS TWS measurements is about 0.08 ug/m^3. This detection value is comparable to the minimum nitric acid concentration of 0.08 ug/m^3 but twice the minimum ammonia concentration reported during LTADS with the TWS sampler.

3.1.4 Database Management and Data Validation

Numerous air quality studies have been conducted over the past decade, but the data are not often available or applicable to analysis and modeling because the databases lack documentation with regard to sampling and analysis methods, quality control/quality assurance procedures, accuracy specifications, precision calculations, and data validity. Lioy et al. (1980), Chow and Watson (1989), Watson and Chow (1992), and Chow and Watson (1994a) summarized the requirements, limitations, and current availability of ambient and source databases in the United States. The data sets for LTADS intend to meet these requirements. The data files for this study have the following attributes:

- They contain the ambient observables needed to assess source and receptor relationships.
- They are available in a well-documented, computerized form accessible by personal computers and over the Internet.
- Measurement methods, locations, and schedules are documented.

- Precision and accuracy estimates are reported.
- Validation flags are assigned.

This section introduces the features, data structures, and contents of the LTADS data archive. **Figure 3-2** illustrates the approach followed to obtain the final data files. These data are available on floppy diskettes in Microsoft Excel format for convenient distribution to data users. The file extension identifies the file type according to the following definitions:

- TXT = ASCII text file
- DOC = Microsoft Word document
- XLS = Microsoft Excel spreadsheet

The assembled aerosol database for filter pack measurements taken during LTADS is fully described in the Microsoft Excel file (see **Table 3-2**), which documents variable names, descriptions, and measurement units.

Figure 3-2. Flow diagram of the database management system.

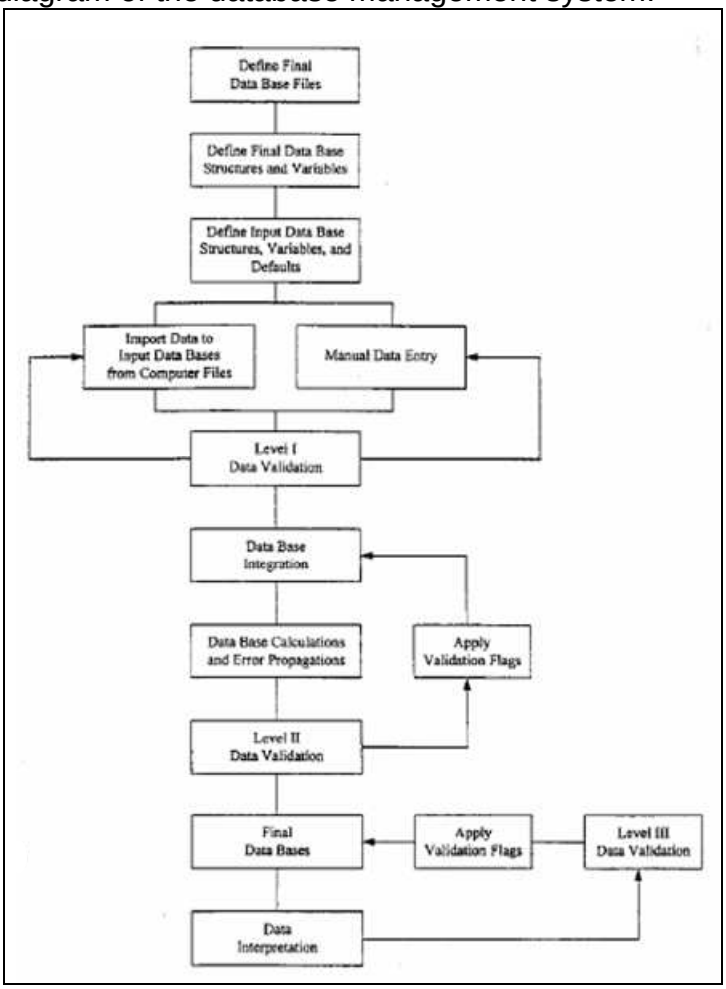

Table 3-2. Variable names, descriptions, and measurement units in the assembled aerosol database for filter pack measurements taken during the study.

Field Code Description Measurement Unit

SITE - Sampling site
DATE - Sampling date
SIZE - Sample particle size cut, µm
DATEI - Sample start date
DATEF - Sample end date
TID - Teflon filter pack ID
QID - Quartz filter pack ID
TFFLG - Teflon filter pack field flag
QFFLG - Quartz filter pack field flag
MSGF - Gravimetry analysis flag
NHCF - Ammonia analysis flag
HNIF - Volatilized nitrate analysis flag
ANIF - Anion analysis flag
N4CF - Ammonium analysis flag
KPAF - Soluble potassium analysis flag
OETF - Carbon analysis flag
ELXF - XRF analysis flag
TVOC - Teflon filter volume, m^3
TVOU - Teflon filter volume uncertainty, m^3
QVOC - Quartz filter volume, m^3
QVOU - Quartz filter volume uncertainty, m^3
MSGC - Mass concentration, $\mu g/m^3$
MSGU - Mass concentration uncertainty, $\mu g/m^3$
NHCC - Ammonia (NH_3) concentration, $\mu g/m^3$
NHCU - Ammonia (NH_3) concentration uncertainty, $\mu g/m^3$
HNIC - Volatilized nitrate concentration, $\mu g/m^3$
HNIU - Volatilized nitrate concentration uncertainty, $\mu g/m^3$
CLIC - Chloride concentration, $\mu g/m^3$
CLIU - Chloride concentration uncertainty, $\mu g/m^3$
N3IC - Nitrate concentration, $\mu g/m^3$
N3IU - Nitrate concentration uncertainty, $\mu g/m^3$
S4IC - Sulfate concentration, $\mu g/m^3$
S4IU - Sulfate concentration uncertainty, $\mu g/m^3$
N4CC - Ammonium concentration, $\mu g/m^3$
N4CU - Ammonium concentration uncertainty, $\mu g/m^3$
KPAC - Soluble Potassium concentration, $\mu g/m^3$
KPAU - Soluble Potassium concentration uncertainty, $\mu g/m^3$
O1TC - Organic Carbon fraction one concentration, $\mu g/m^3$
O1TU - OC fraction one concentration uncertainty, $\mu g/m^3$
O2TC - Organic Carbon fraction two concentration, $\mu g/m^3$
O2TU - OC fraction two concentration uncertainty, $\mu g/m^3$
O3TC - Organic Carbon fraction three concentration, $\mu g/m^3$

Table 3-2 (continued)

O3TU - OC fraction three concentration uncertainty, µg/m^3
O4TC - Organic Carbon fraction four concentration, µg/m^3
O4TU - OC fraction four concentration uncertainty, µg/m^3
OPTC - Pyrolyzed Organic carbon concentration, µg/m^3
OPTU - Pyrolyzed OC concentration uncertainty, µg/m^3
OCTC - Organic Carbon concentration, µg/m^3
OCTU - Organic Carbon concentration uncertainty, µg/m^3
E1TC - Elemental Carbon fraction one concentration, µg/m^3
E1TU - EC fraction one concentration uncertainty, µg/m^3
E2TC - Elemental Carbon fraction two concentration, µg/m^3
E2TU - EC fraction two concentration uncertainty, µg/m^3
E3TC - Elemental Carbon fraction three concentration, µg/m^3
E3TU - EC fraction three concentration uncertainty, µg/m^3
ECTC - Elemental Carbon concentration, µg/m^3
ECTU - Elemental Carbon concentration uncertainty, µg/m^3
TCTC - Total Carbon concentration, µg/m^3
TCTU - Total Carbon concentration uncertainty, µg/m^3
NAXC - Sodium concentration, µg/m^3
NAXU - Sodium concentration uncertainty, µg/m^3
MGXC - Magnesium concentration, µg/m^3
MGXU - Magnesium concentration uncertainty, µg/m^3
ALXC - Aluminum concentration, µg/m^3
ALXU - Aluminum concentration uncertainty, µg/m^3
SIXC - Silicon concentration, µg/m^3
SIXU - Silicon concentration uncertainty, µg/m^3
PHXC - Phosphorous concentration, µg/m^3
PHXU - Phosphorous concentration uncertainty, µg/m^3
SUXC - Sulfur concentration, µg/m^3
SUXU - Sulfur concentration uncertainty, µg/m^3
CLXC - Chlorine concentration, µg/m^3
CLXU - Chlorine concentration uncertainty, µg/m^3
KPXC - Potassium concentration, µg/m^3
KPXU - Potassium concentration uncertainty, µg/m^3
CAXC - Calcium concentration, µg/m^3
CAXU - Calcium concentration uncertainty, µg/m^3
TIXC - Titanium concentration, µg/m^3
TIXU - Titanium concentration uncertainty, µg/m^3
VAXC - Vanadium concentration, µg/m^3
VAXU - Vanadium concentration uncertainty, µg/m^3
CRXC - Chromium concentration, µg/m^3
CRXU - Chromium concentration uncertainty, µg/m^3
MNXC - Manganese concentration, µg/m^3
MNXU - Manganese concentration uncertainty, µg/m^3
FEXC - Iron concentration, µg/m^3

Table 3-2 (continued)

FEXU - Iron concentration uncertainty, µg/m^3
COXC - Cobalt concentration, µg/m^3
COXU - Cobalt concentration uncertainty, µg/m^3
NIXC - Nickel concentration, µg/m^3
NIXU - Nickel concentration uncertainty, µg/m^3
CUXC - Copper concentration, µg/m^3
CUXU - Copper concentration uncertainty, µg/m^3
ZNXC - Zinc concentration, µg/m^3
ZNXU - Zinc concentration uncertainty, µg/m^3
GAXC - Gallium concentration, µg/m^3
GAXU - Gallium concentration uncertainty, µg/m^3
ASXC - Arsenic concentration, µg/m^3
ASXU - Arsenic concentration uncertainty, µg/m^3
SEXC - Selenium concentration, µg/m^3
SEXU - Selenium concentration uncertainty, µg/m^3
BRXC - Bromine concentration, µg/m^3
BRXU - Bromine concentration uncertainty, µg/m^3
RBXC - Rubidium concentration, µg/m^3
RBXU - Rubidium concentration uncertainty, µg/m^3
SRXC - Strontium concentration, µg/m^3
SRXU - Strontium concentration uncertainty, µg/m^3
YTXC - Yttrium concentration, µg/m^3
YTXU - Yttrium concentration uncertainty, µg/m^3
ZRXC - Zirconium concentration, µg/m^3
ZRXU - Zirconium concentration uncertainty, µg/m^3
MOXC - Molybdenum concentration, µg/m^3
MOXU - Molybdenum concentration uncertainty, µg/m^3
PDXC - Palladium concentration, µg/m^3
PDXU - Palladium concentration uncertainty, µg/m^3
AGXC - Silver concentration, µg/m^3
AGXU - Silver concentration uncertainty, µg/m^3
CDXC - Cadmium concentration, µg/m^3
CDXU - Cadmium concentration uncertainty, µg/m^3
INXC - Indium concentration, µg/m^3
INXU - Indium concentration uncertainty, µg/m^3
SNXC - Tin concentration, µg/m^3
SNXU - Tin concentration uncertainty, µg/m^3
SBXC - Antimony concentration, µg/m^3
SBXU - Antimony concentration uncertainty, µg/m^3
BAXC - Barium concentration, µg/m^3
BAXU - Barium concentration uncertainty, µg/m^3
LAXC - Lanthanum concentration, µg/m^3
LAXU - Lanthanum concentration uncertainty, µg/m^3
AUXC - Gold concentration, µg/m^3

Table 3-2 (continued)

AUXU - Gold concentration uncertainty, µg/m^3
HGXC - Mercury concentration, µg/m^3
HGXU - Mercury concentration uncertainty, µg/m^3
TLXC - Thallium concentration, µg/m^3
TLXU - Thallium concentration uncertainty, µg/m^3
PBXC - Lead concentration, µg/m^3
PBXU - Lead concentration uncertainty, µg/m^3
URXC - Uranium concentration, µg/m^3
URXU - Uranium concentration uncertainty, µg/m^3
COMMENT - Sampling and/or analysis comments

3.1.5 Database Structures and Features

The raw LTADS data were processed with Microsoft FoxPro 2.6 for Windows (Microsoft Corp., 1994), a commercially available relational database management system. FoxPro can accommodate 256 fields of up to 4,000 characters per record and up to one billion records per file. This system can be implemented on most IBM PC-compatible desktop computers. The database files (*.DBF) can also be read directly into a variety of popular statistical, plotting, database, and spreadsheet programs without requiring any specific conversion software. After processing, the final LTADS data were converted from FoxPro to Microsoft Excel format for reporting purposes.

In FoxPro, one of five field types (character, date, numerical, logical, or memo) was assigned to each observable. Sampling sites and particle size fractions were defined as "character" fields, sampling dates were defined as "date" fields, and measured data were defined as "numeric" fields, "logical" fields were used to represent a "yes" or "no" value applied to a variable, and "memo" fields accommodated large blocks of text and were used to document the data validation results.

Data contained in different database files can be linked by indexing on and relating to common attributes in each file. Generally, sampling site, sampling hour, sampling period, particle size, and sampling substrate IDs were the common fields used to relate the data between files.

To assemble the final data files, information was merged from many data files derived from field monitoring and laboratory analyses by relating information on the common fields cited above.

3.1.6 Measurement and Analytical Specifications

Every measurement consists of: 1) a value; 2) a precision; 3) an accuracy; and 4) a validity (Hidy, 1985; Watson et al., 1989, 1995). The measurement methods described in this chapter were used to obtain the value. Performance testing via regular submission of standards, blank analysis, and replicate analysis were used to estimate precision. The submission and evaluation of independent standards through quality audits were used to estimate accuracy. Validity applied to both the measurement

method and to each measurement taken with that method. The validity of each measurement was indicated by appropriate flagging within the database and the validity of the methods used in this study has been evaluated.

3.1.7 Definitions of Measurement Attributes

The precision, accuracy, and validity of the LTADS aerosol measurements are defined as follows (Chow et al., 1993):

- A **measurement** is an observation at a specific time and place that possesses: 1) value – the center of the measurement interval; 2) precision – the width of the measurement interval; 3) accuracy – the difference between measured and reference values; and 4) validity – the compliance with assumptions made in the measurement method.
- A **measurement method** is the combination of equipment, reagents, and procedures that provides the value of a measurement. The full description of the measurement method requires substantial documentation. For example, two methods may use the same sampling systems and the same analysis systems; however, they are not identical if one method performs acceptance testing on the filter media and the other does not. Seemingly minor differences between methods can result in major differences in measurement values.
- **Measurement method validity** is the identification of measurement method assumptions, the quantification of the effects of deviations from those assumptions, the evaluation that deviations are within reasonable tolerances for the specific application, and the creation of procedures to quantify and minimize those deviations during a specific application.
- **Sample validation** is accomplished by procedures that identify deviations from measurement assumptions and the assignment of flags to individual measurements to indicate for potential deviations from assumptions.
- The **comparability and equivalence of sampling and analysis methods** are established by the comparison of values and precisions for the same measurement obtained by different measurement methods. Inter-laboratory and intra-laboratory comparisons are usually made to establish this comparability. Simultaneous measurements of the same observable are considered equivalent when more than 90% of the values differ by no more than the sum of two one-sigma precision intervals for each measurement.
- **Completeness** measures how many environmental measurements with specified values, precisions, accuracies, and validities were obtained out of the total number attainable. It measures the practicability of applying the selected measurement processes throughout the measurement period. Databases which have excellent precision, accuracy, and validity may be of little use if they have so many missing values that data interpretation is impossible. A database with numerous data points, such as the one used in this study, requires detailed documentation of precision, accuracy, and validity of the measurements. This and following sections address the procedures followed to define these quantities and present the results of those procedures.

3.1.8 Definitions of Measurement Precision

Measurement precisions were propagated from precisions of the volumetric measurements, the chemical composition measurements, and the field blank variability using the methods of Bevington (1969) and Watson et al. (1995).

Dynamic field blanks were periodically placed in each sampling system without air being drawn through them to estimate the magnitude of passive deposition for the period of time during which the filter packs remained in a sampler. Field blanks for the TWS were collected only at the SOLA site. Field blanks for the MVS were collected at two sites - Wallis Tower and Zephyr Cove. No statistically significant differences in field blank concentrations were found for any species after removal of outliers (i.e., concentration exceeding three times the standard deviations of the field blanks). The average field blank concentrations (with outliers removed) were calculated for each species on each substrate (e.g., Teflon-membrane, quartz-fiber).

3.1.9 Analytical Specifications

Blank precisions (σBi) are defined as the higher value of the standard deviation of the blank measurements (STDBi) or the square root of the averaged squared uncertainties of the blank concentrations (SIGBi). If the average blank for a species was less than its precision, the blank was set to zero. The precisions (σMi) for XRF analysis were determined from counting statistics unique to each sample; therefore, the σMi is a function of the energy-specific peak area, the background, and the area under the baseline.

3.1.10 Quality Assurance

Quality control (QC) and quality auditing establish the precision, accuracy, and validity of measured values. Quality assurance (QA) integrates QC, quality auditing, measurement method validation, and sample validation into the measurement process. The results of quality assurance are data values with specified precisions, accuracies, and validities.

For TWS, field blanks were only acquired at SOLA; and only field blanks were acquired for Mini-Vol TSP samplers at Wallis Residence Platform and Zephyr Cove, as shown in **Table 3-3**. Replicate analyses were performed for ~10% of all ambient samples.

Quality audits of sample flow rates were conducted at the beginning, middle, and end of the study period, and these audits determined that flow rates were within ±10% of specifications. Data were submitted to three levels of data validation (Chow et al., 1994b; Watson et al., 2001). Detailed data validation processes are documented in the following subsections.

Table 3-3. Field blanks collected in LTADS (reported as concentration for typical air sample volume).

SITE	Start Date	End Date	Size	Period	Mass Concentration (ug)	Uncertainty of [mass] (ug)
Two Week Samplers						
SOLA	2002/12/4	2002/12/18	TSP	2	12.00	4.92
SOLA	2002/12/4	2002/12/18	PM10	2	9.00	4.92
SOLA	2002/12/4	2002/12/18	PM2.5	2	1.00	4.92
SOLA	2003/5/21	2003/6/4	TSP	14	30.00	7.40
SOLA	2003/5/21	2003/6/4	PM10	14	5.00	7.40
SOLA	2003/5/21	2003/6/4	PM2.5	14	5.00	7.40
SOLA	2003/7/16	2003/7/30	TSP	18	8.00	7.98
SOLA	2003/7/16	2003/7/30	PM10	18	1.00	7.98
SOLA	2003/7/16	2003/7/30	PM2.5	18	13.00	7.98
Mini-Vol Samplers						
Wallis Tower	2003/7/25	2003/8/1	TSP		15.00	7.24
Wallis Tower	2003/8/1	2003/8/8	TSP		6.00	7.24
Zephyr Cove	2003/7/8	2003/7/15	TSP		4.00	7.24

* Field blank samples set 2 and set 14 are used for the background subtraction for two week samplers from 12/4/2002 to 6/4/2003

** Field blank sample set 18 is used for the background subtraction for two week samplers from period 6/18/2003 to 1/6/2004

*** Average of Mini-vol sampler field blanks is used for the background subtraction for all mini-vol samples.

3.1.11 Data Validation

Ambient measurements can be sequentially subjected to four levels of data validation:

- Level 0 sample validation: designates data as they come off the instrument. This process ascertains that the field or laboratory instrument is functioning properly.
- Level I sample validation: 1) flags samples where significant deviation from measurement assumptions have occurred, 2) verifies computer file entries against data sheets, 3) eliminates values for measurements that are known to be invalid because of instrument malfunctions, 4) replaces data from a backup data acquisition system in the event of failure of the primary system, and 5) adjusts values for quantifiable calibration or interference biases.
- Level II sample validation applies consistency tests to the assembled data based on known physical relationships between variables.
- Level III sample validation is part of the data interpretation process. The first assumption upon finding a measurement that is inconsistent with physical expectations is that the unusual value is due to a measurement error. If, upon

tracing the path of the measurement, nothing unusual is found, then it may be assumed the value was the result of a valid environmental cause. Unusual values are identified during the data interpretation process as: 1) extreme values, 2) values which would otherwise normally track the values of other variables in a time series, and 3) values for observables which would normally follow a qualitatively predictable spatial or temporal pattern.

Air quality data acquired during LTADS were submitted to three data validation levels: 0, I, and II. Level I validation flags and comments are included with each data record in the database. Level II validation tests and results are described in the following subsections. Level II tests evaluate the chemical data for internal consistency. In this study, Level II data validations were made for: 1) physical consistency and 2) balance of reconstructed mass based on chemical species versus measured mass. Correlations and linear regression statistics were computed and scatter plots prepared to examine the data.

3.1.12 Physical Consistency

The compositions of chemical species concentrations measured by different chemical analysis methods were examined. Physical consistency was tested for: 1) sum of chemical species vs. measured mass, 2) $SO_4^=$ versus total sulfur (S), 3) ammonium balance, 4) anion/cation balance, and 5) K^+ versus total potassium (K).

3.1.12.1 Sum of chemical species vs. measured mass

Chemical species, including elements, ions, and cations analyzed by XRF, IC, and AA, respectively, and OC and EC, were summed and compared to mass measured by gravimetric analysis. Oxygen was not considered in the form of metal oxides and organic carbon; therefore, it was expected that the slope and ratio of the sum of chemical species to measured mass would be less than 1. The correlation (r^2) and intercept vary by site and sampling period and are dependent on chemical compositions in particulates; therefore, they are not used for data QA/QC. **Figure 3-3(a-c)** shows that the slopes between the sum of chemical species and measured mass at all five sites for TWS TSP, PM10, and PM2.5 were 0.40, 0.54, and 0.65, respectively. The average ratios between the sum of chemical species and measured mass for TWS TSP, PM10, and PM2.5 were 0.65, 0.68, and 0.84, respectively. The slopes in the scatter plots of sum of species to measured mass (**Figures 3-3d,e**) are 0.40 and 0.45, for TSP collected by Mini-vol sampler on lake shore (non-buoy Mini-vol samplers) and TSP collected by Mini-vol sampler on buoys (buoy Mini-vol sampler), respectively. The average ratio between the sum of chemical species and measured mass are generally less than one, except that for the buoy TSP Mini-vol samplers. The sampling duration for buoy TSP Mini-vol sampler is generally less than 24 hours with low TSP mass concentrations. In addition, the samples were left on the buoy till the scheduled collection date may results in high uncertainty of the sample quality. These slopes and ratios met the expected criteria. A lab flag was noted on 12/04/02 for the measured mass (fiber or fuzz observed on filter) at the Lake Forest site, which may explain the high measured mass but low sum of chemical species.

3.1.12.2 Sulfate ($SO_4^=$) versus total sulfur (S)

Sulfate was measured by IC analysis on quartz-fiber filters and S was measured by XRF analysis on Teflon-membrane filters. The mass ratio of $SO_4^=$:S should equal 3:1 if all S is present as $SO_4^=$. **Figure 3-4**(a-c) shows scatter plots of $SO_4^=$ versus S concentrations at five sites for TSP, PM10, and PM2.5. The average $SO_4^=$:S ratios for TSP, PM10, and PM2.5 were 2.1 ± 0.93, 2.3 ± 1.1, and 2.3 ± 1.0, respectively, which were lower than the 3:1 ratio. This suggests that a significant amount of S in particulate matter (PM) consists of non-soluble S compounds. The regression statistics gave slopes of 1.883 with an intercept of.0.033 µg/m^3 for TSP, 1.618 with an intercept of 0.117 µg/m^3 for PM10, and 1.651 with an intercept of 0.099 µg/m^3 for PM2.5. The correlation (r^2) between $SO_4^=$ and S increased from 0.60 to 0.76 as particle size range decreased from TSP to PM2.5, which agrees with the expectation that most of the S in PM2.5 is in the form of $SO_4^=$ and therefore better correlated. For the buoy TSP Mini-vol samplers, the average $SO_4^=$:S ratio in **Figure 3-4d** is 3.05 ± 2.41.and the slope is 2.17 with intercept of 0.04 µg/m^3 and high r^2 of 0.82; the average ratio is 2.83 ± 8.44 and the slope is 1.26 with intercept of 0.15 µg/m^3 and high r^2 of 0.41, for non-buoy TSP Mini-vol samplers (**Figure 3-4e**). The high standard deviation of the average $SO_4^=$:S ratio for the non-buoy TSP Mini-Vol samplers is probably due to the various sampling durations and locations. Nevertheless, the slopes of $SO_4^=$:S and average $SO_4^=$:S ratio are less than 3:1, which suggests that a significant amount of sulfur in PM consists of non-soluble sulfur compounds.

Figure 3-3. Comparisons of Sum of Chemical Species and Measured Mass at Five Sites for (a) TSP, b) PM10, and c) PM2.5, d) Buoy Mini-Vol TSP, and e) Non-buoy Mini-Vol TSP.

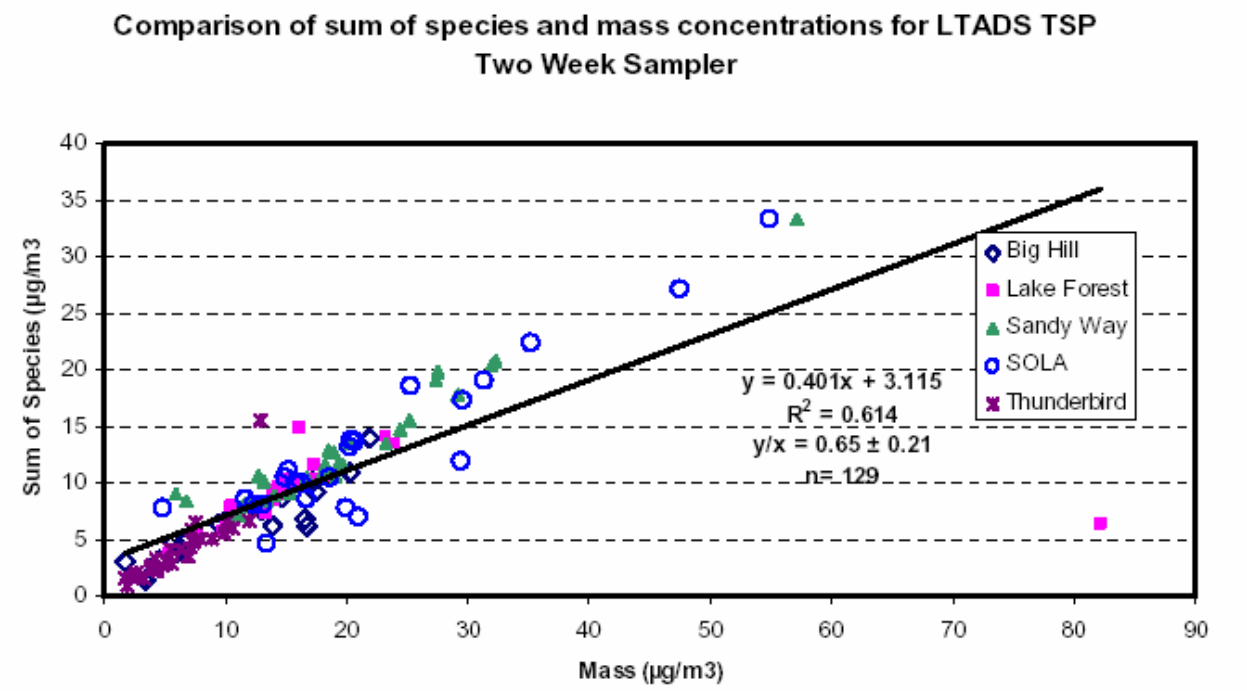

(a)

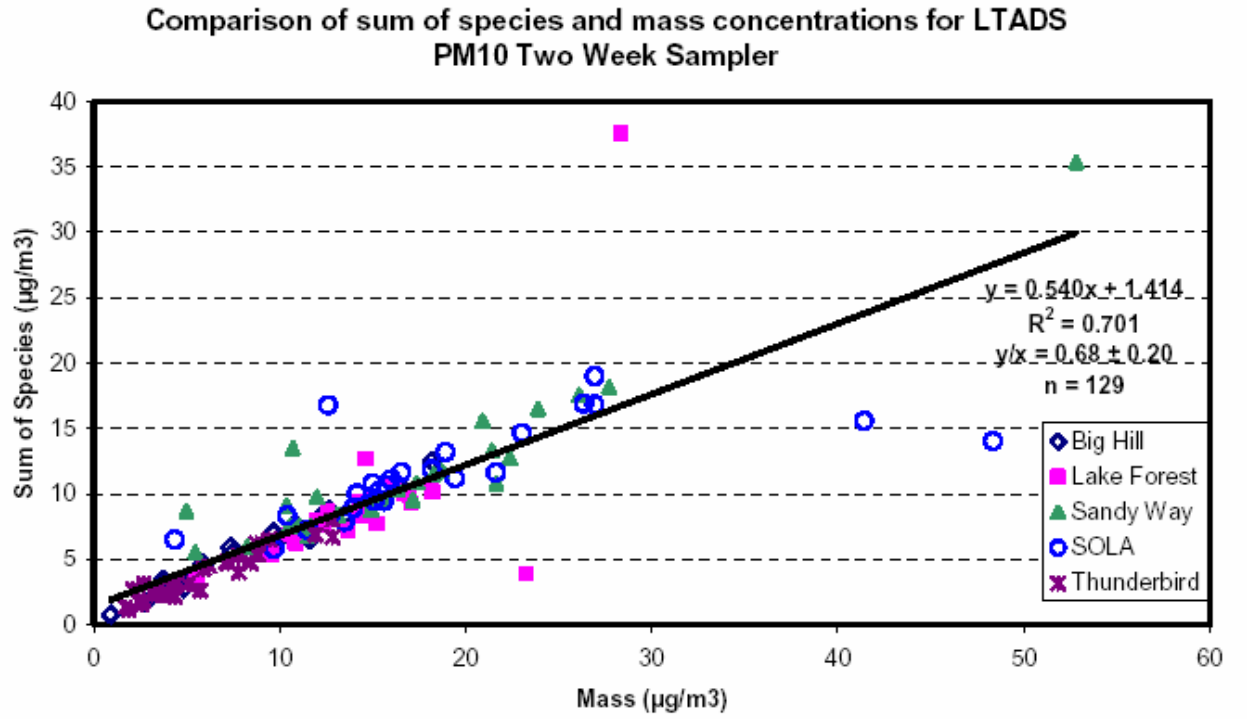

(b)

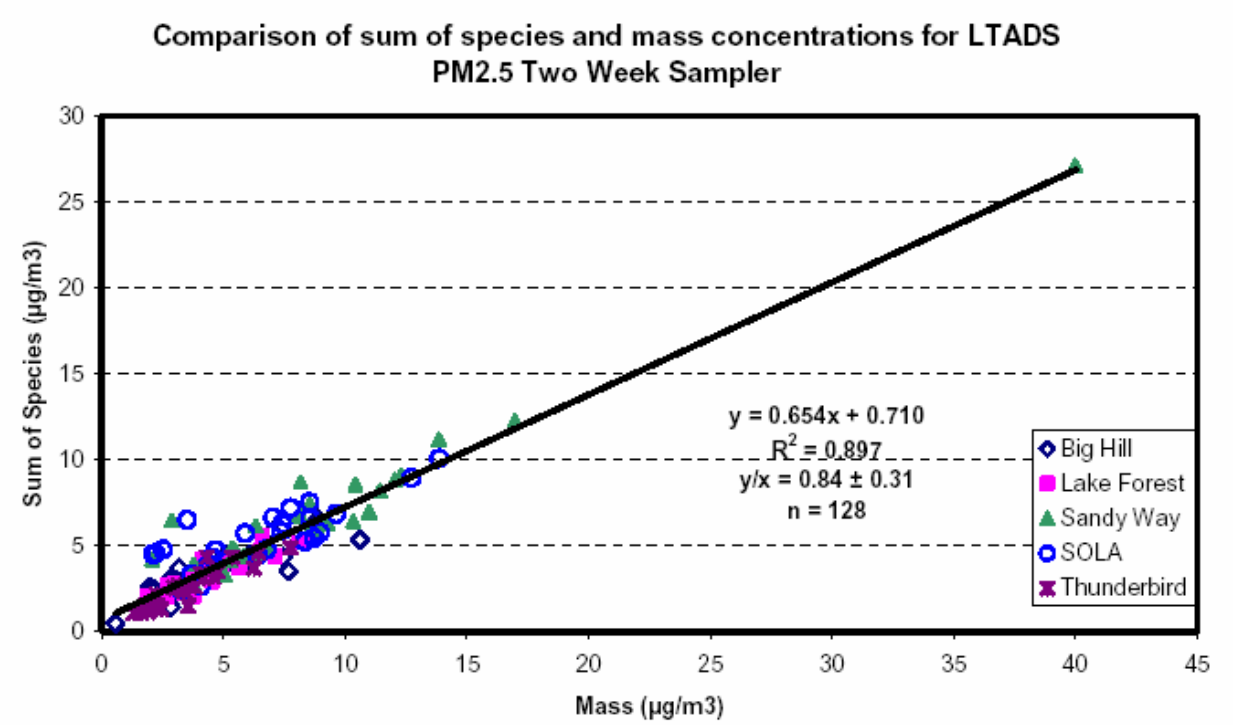
Comparison of sum of species and mass concentrations for LTADS
PM2.5 Two Week Sampler
Sum of Species (µg/m3)
Mass (µg/m3)
y = 0.654x + 0.710
R2 = 0.897
y/x = 0.84 ± 0.31
n = 128
Big Hill
Lake Forest
Sandy Way
SOLA
Thunderbird

(c)

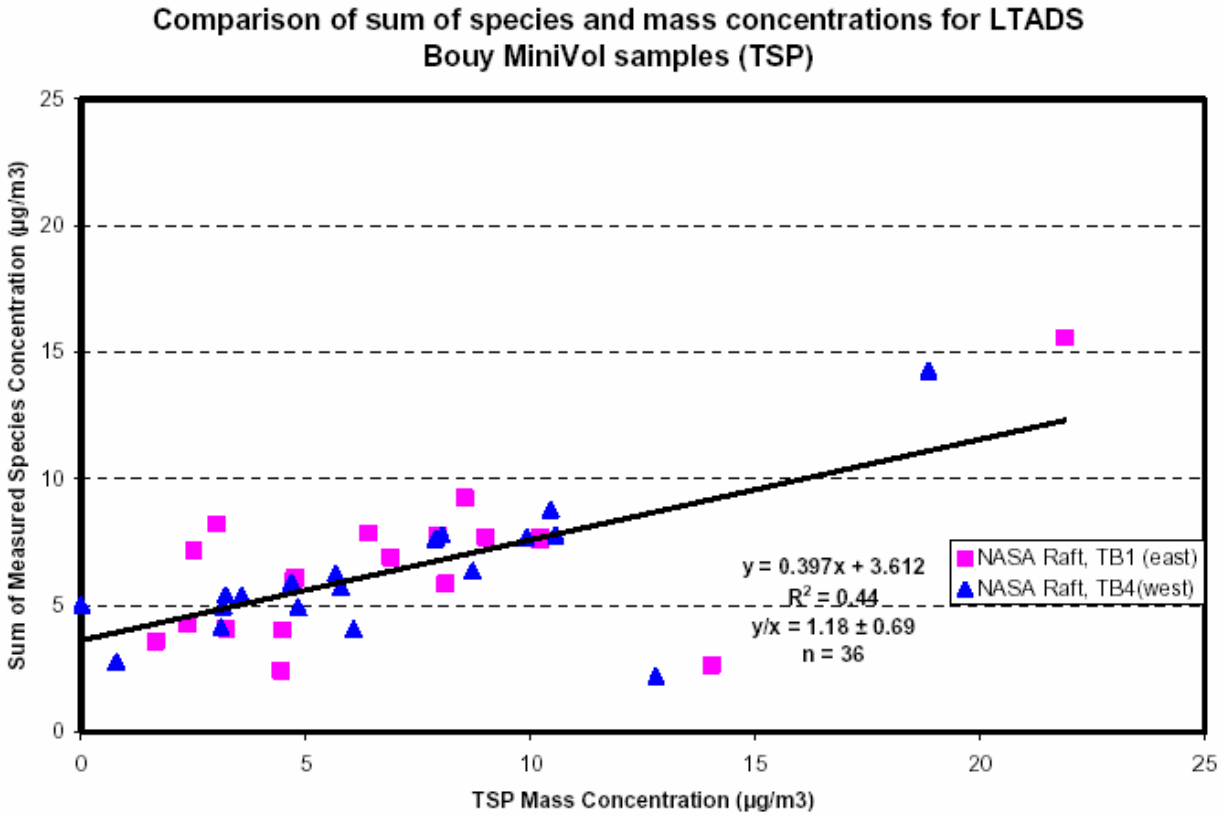
Comparison of sum of species and mass concentrations for LTADS
Bouy MiniVol samples (TSP)
Sum of Measured Species Concentration (µg/m3)
TSP Mass Concentration (µg/m3)
y = 0.397x + 3.612
R2 = 0.44
y/x = 1.18 ± 0.69
n = 36
NASA Raft, TB1 (east)
NASA Raft, TB4(west)

(d)

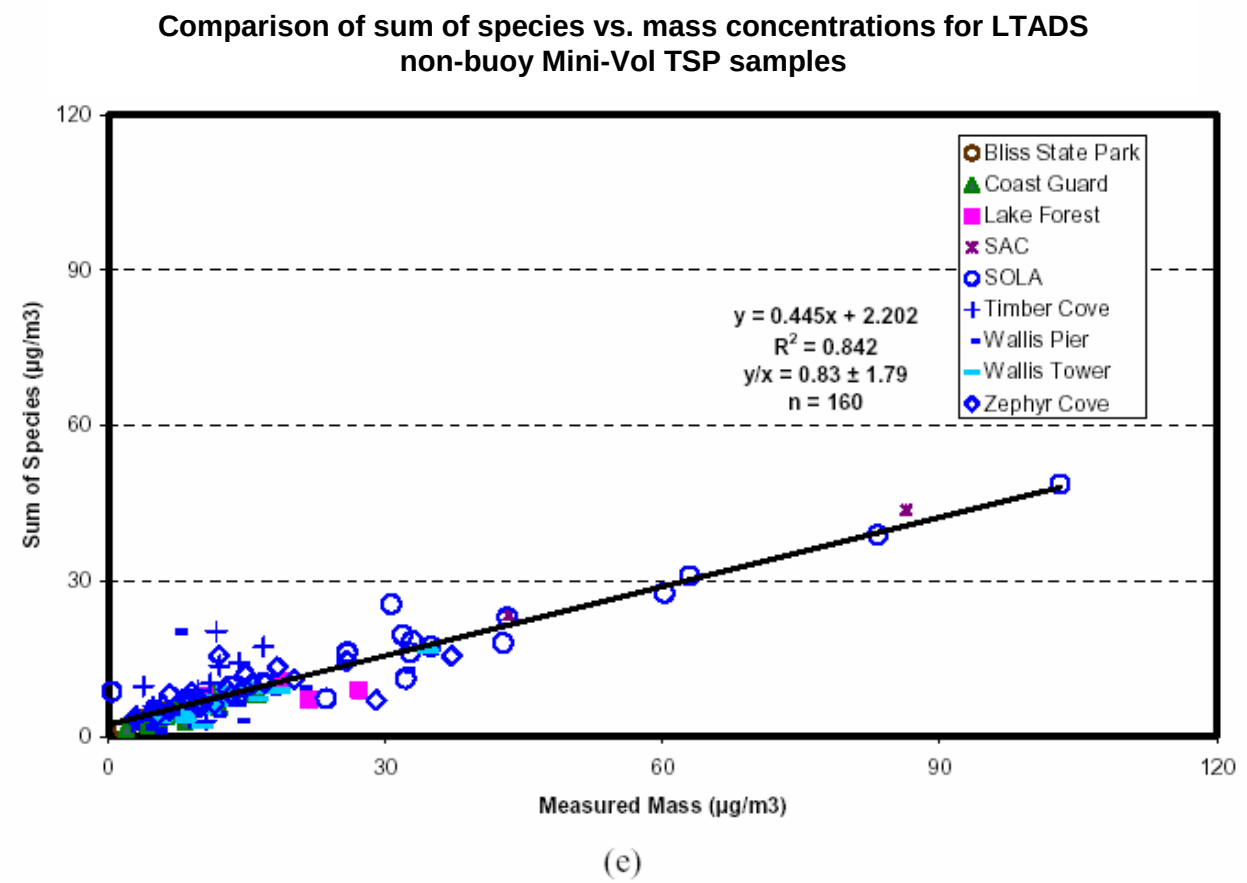
Comparison of sum of species vs. mass concentrations for LTADS non-buoy Mini-Vol TSP samples
Sum of Species (µg/m3)
Measured Mass (µg/m3)
0
30
60
90
120
y = 0.445x + 2.202
R2 = 0.842
y/x = 0.83 ± 1.79
n = 160
Bliss State Park
Coast Guard
Lake Forest
SAC
SOLA
Timber Cove
Wallis Pier
Wallis Tower
Zephyr Cove

(e)

Figure 3-4. Scatter Plot of Sulfate Versus Sulfur Concentrations at the Five Sites for a) TSP, b) PM10, and, c) PM2.5, d) Buoy Mini-Vol TSP, and e) Non-buoy Mini-Vol TSP.

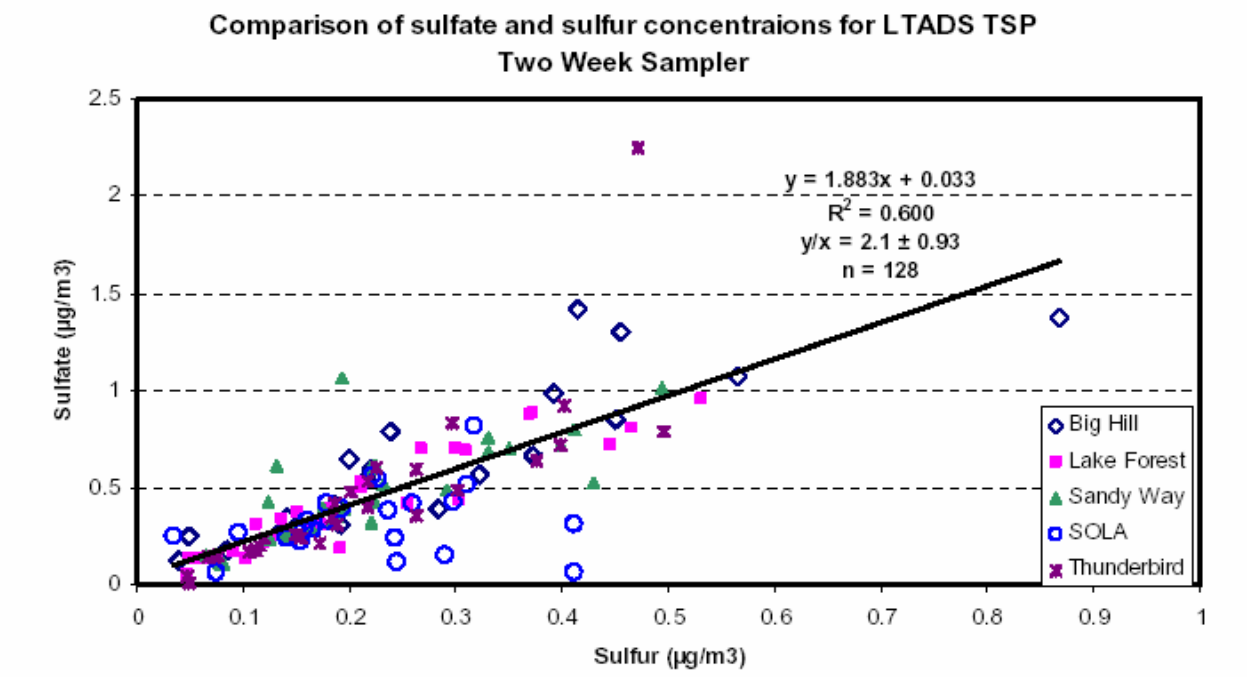

(a)

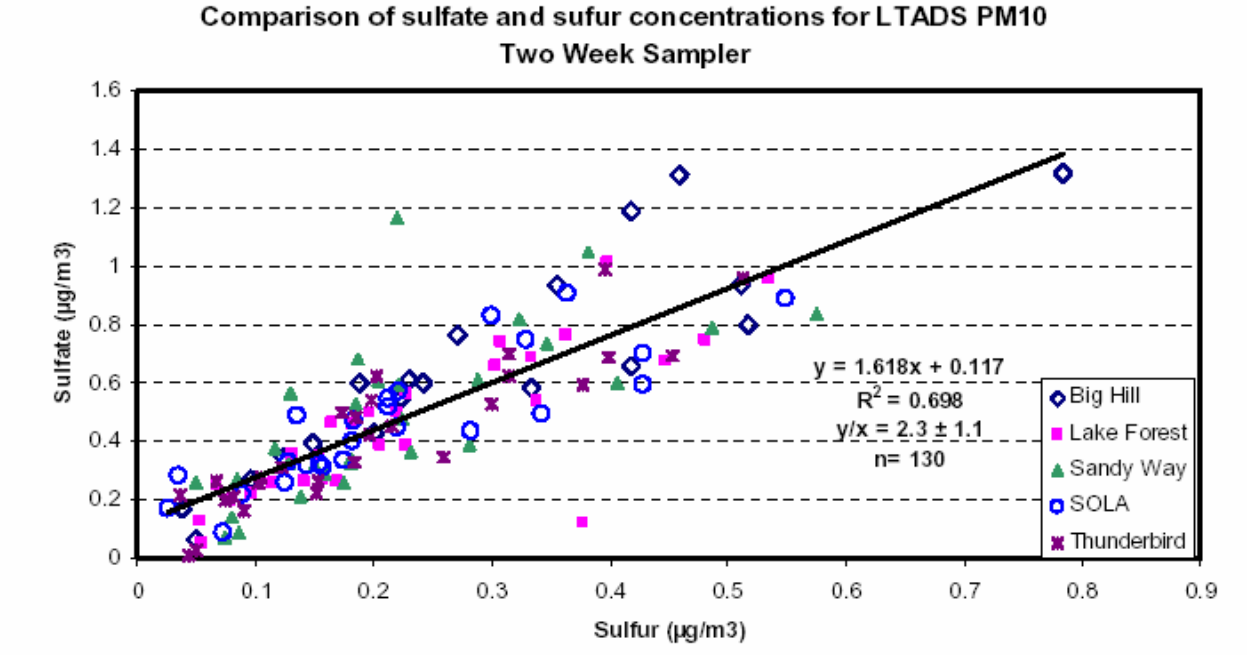

(b)

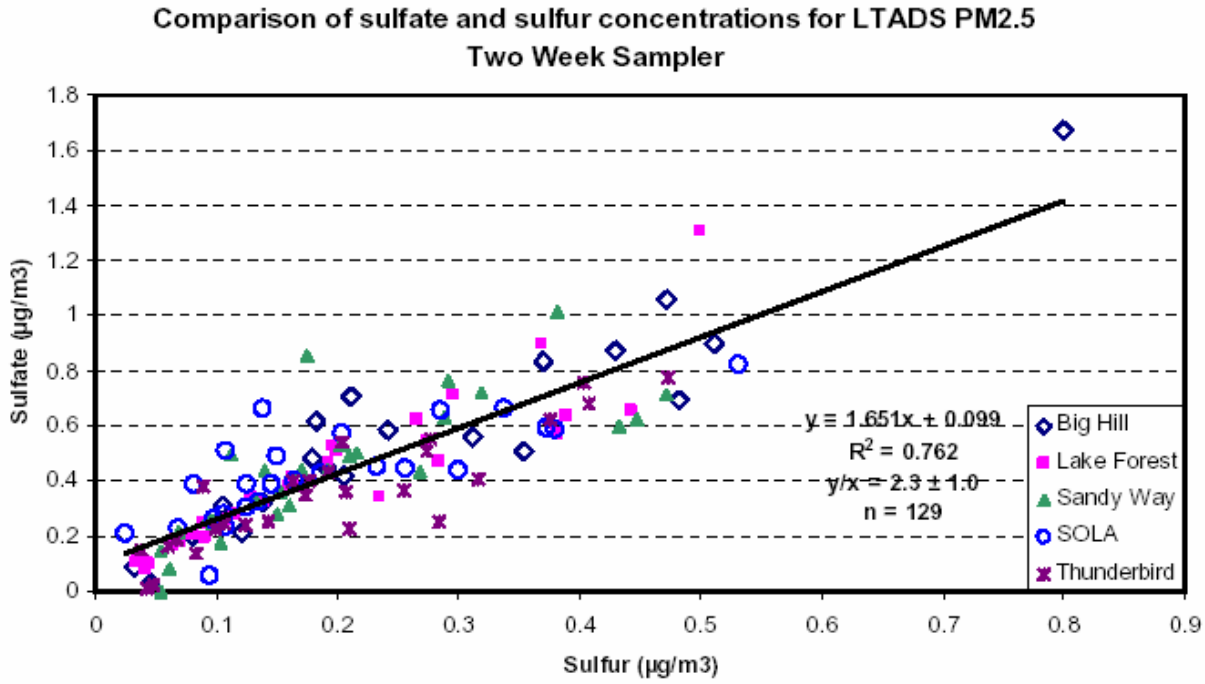
Comparison of sulfate and sulfur concentrations for LTADS PM2.5
Two Week Sampler
Sulfate (µg/m3)
Sulfur (µg/m3)
y = 1.651x + 0.099
R2 = 0.762
y/x = 2.3 ± 1.0
n = 129
Big Hill
Lake Forest
Sandy Way
SOLA
Thunderbird

(c)

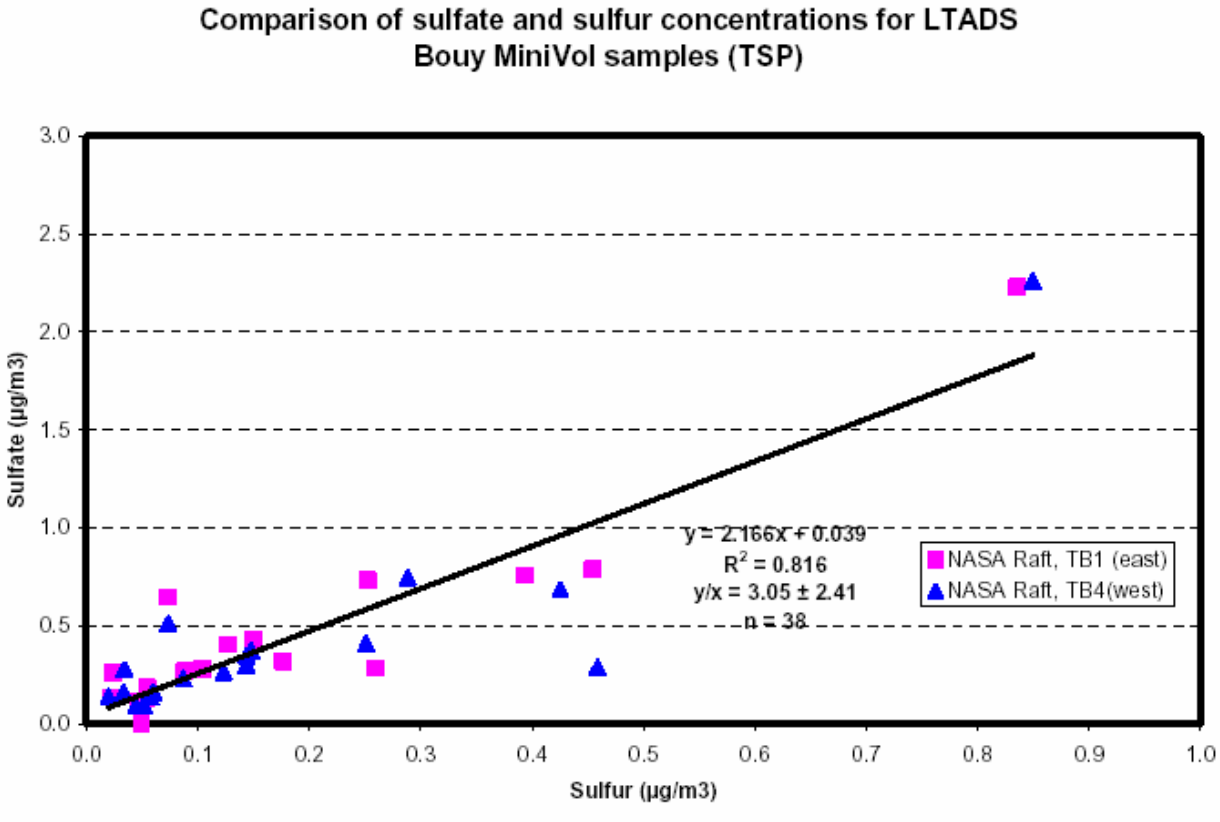
Comparison of sulfate and sulfur concentrations for LTADS
Bouy MiniVol samples (TSP)
Sulfate (µg/m3)
Sulfur (µg/m3)
y = 2.166x + 0.039
R2 = 0.816
y/x = 3.05 ± 2.41
n = 38
NASA Raft, TB1 (east)
NASA Raft, TB4(west)

(d)

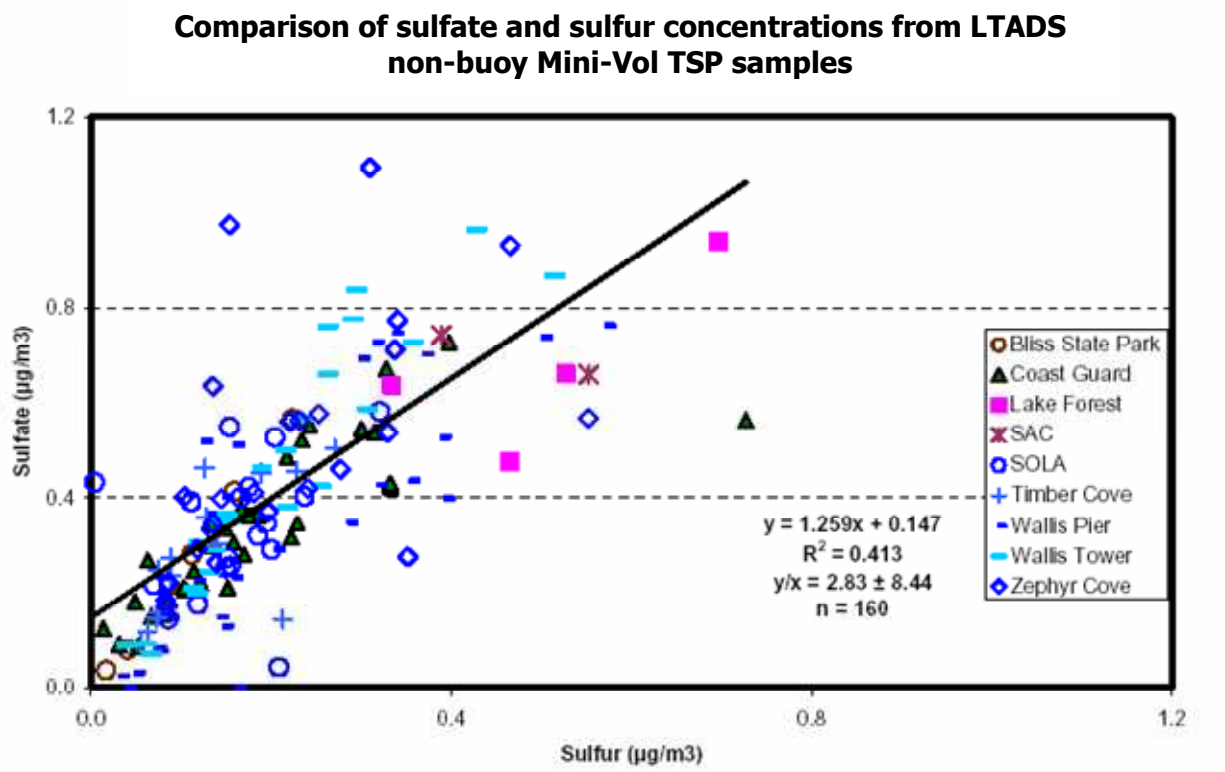

(e)

3.1.12.3 *Ammonium balance*

Ammonium in particles occurs most commonly as ammonium nitrate (NH_4NO_3), ammonium sulfate [$(NH_4)_2SO_4$], ammonium bisulfate [$(NH_3)HSO_4$], and ammonium chloride (NH_4Cl). Measured ammonium can be compared to calculated ammonium, which is the sum of ammonium assumed to be associated with nitrate and sulfate ($0.29 \times NO_3^- + 0.192 \times HSO_4^-$) or nitrate and bisulfate ($0.29 \times NO_3^- + 0.3 \times SO_4^=$). NH_4Cl was not used for ammonium balance because Lake Tahoe is generally not influenced by sea salt. The slopes between sulfate based ammonium and measured ammonium are shown in **Figure 3-5** (a-c) and were 0.92, 0.85, and 0.71 for TWS TSP, PM10, and PM2.5, respectively. These slopes were higher than the bisulfate based ammonium slopes of 0.57, 0.49, and 0.40 for TWS TSP, PM10, and PM2.5, respectively. The regression slopes between sulfate and bisulfate based ammonium and measured ammonium (**Figure 3-5d**) are 0.89 and 0.44 for buoy Mini-Vol TSP samples with poor correlation (<0.35). The slopes for non-buoy Mini-Vol TSP samples (**Figure 3-5e**) are close to unity with moderate correlation. This agrees with atmospheric chemistry, where ammonium sulfate is more stable than ammonium bisulfate. The slopes of measured ammonium and sulfate based ammonium were less than unity, which suggests potential excess ammonia in the atmosphere was absorbed onto the quartz-fiber filter. The decreasing slopes between calculated ammonium and measured ammonium as particle size fraction decreases from TSP to PM2.5 can be attributed to the sampling artifacts of volatilized ammonium nitrate, which becomes ammonia and nitric acid gas. The

disassociated ammonia is absorbed onto the quartz-fiber filter media. Such sampling artifacts are more pronounced at low ammonium nitrate particulate concentrations (Chang et al., 2000a; Pathak et al., 2004).

Figure 3-5. Scatter Plot of Calculated and Measured Ammonium Concentrations for: a) TSP, b) PM10, and, c) PM2.5, d) Buoy Mini-Vol TSP, and e) Non-Buoy Mini-Vol TSP.

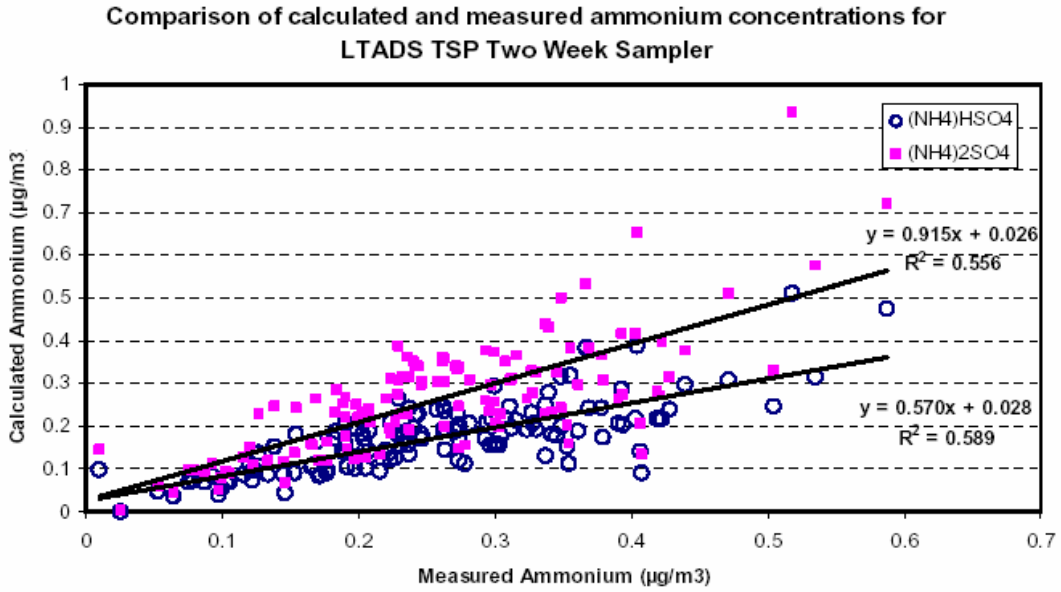

(a)

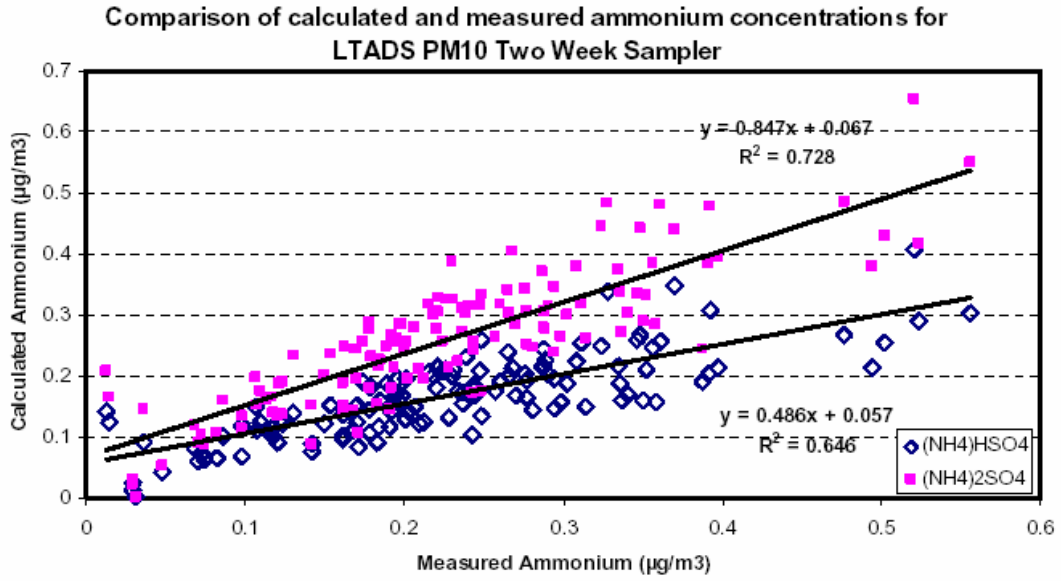

(b)

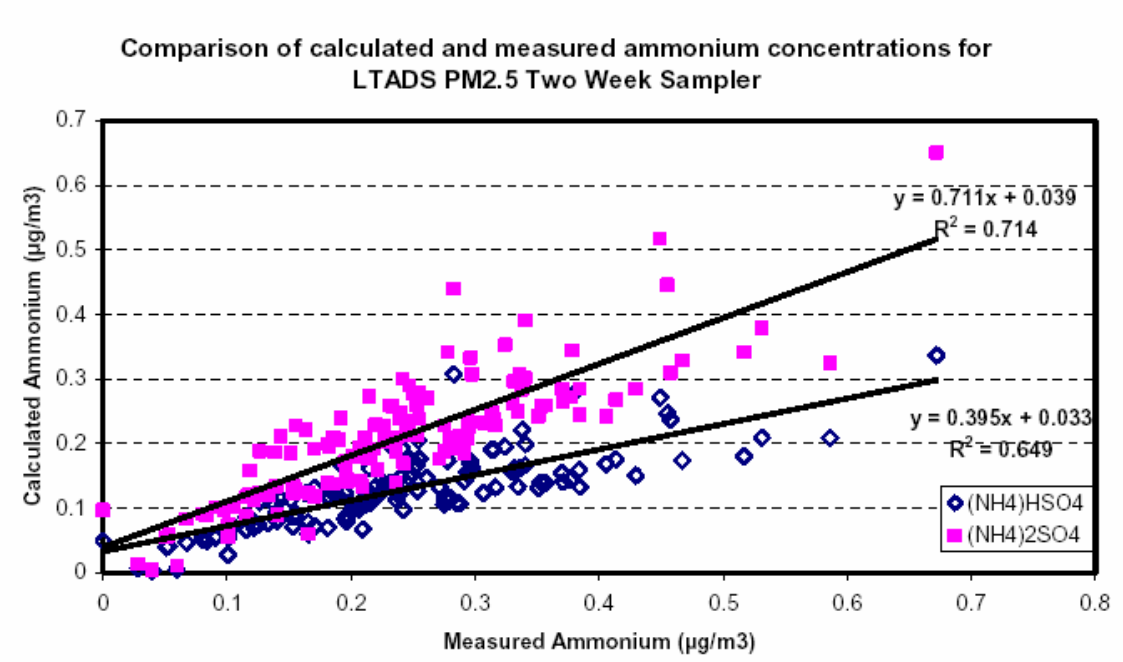
Comparison of calculated and measured ammonium concentrations for LTADS PM2.5 Two Week Sampler
Calculated Ammonium (µg/m3)
Measured Ammonium (µg/m3)
y = 0.711x + 0.039
R2 = 0.714
y = 0.395x + 0.033
R2 = 0.649
(NH4)HSO4
(NH4)2SO4
0
0.1
0.2
0.3
0.4
0.5
0.6
0.7
0.8

(c)

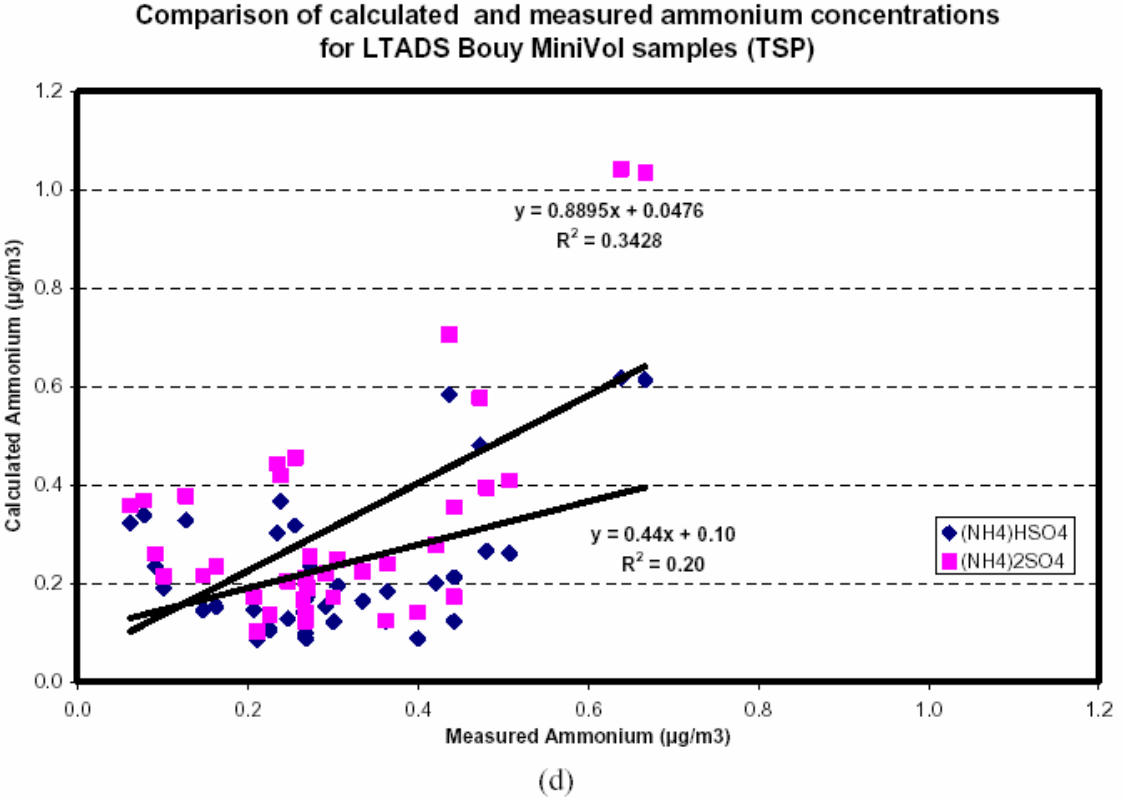
Comparison of calculated and measured ammonium concentrations for LTADS Bouy MiniVol samples (TSP)
Calculated Ammonium (µg/m3)
Measured Ammonium (µg/m3)
y = 0.8895x + 0.0476
R2 = 0.3428
y = 0.44x + 0.10
R2 = 0.20
(NH4)HSO4
(NH4)2SO4
0.0
0.2
0.4
0.6
0.8
1.0
1.2

(d)

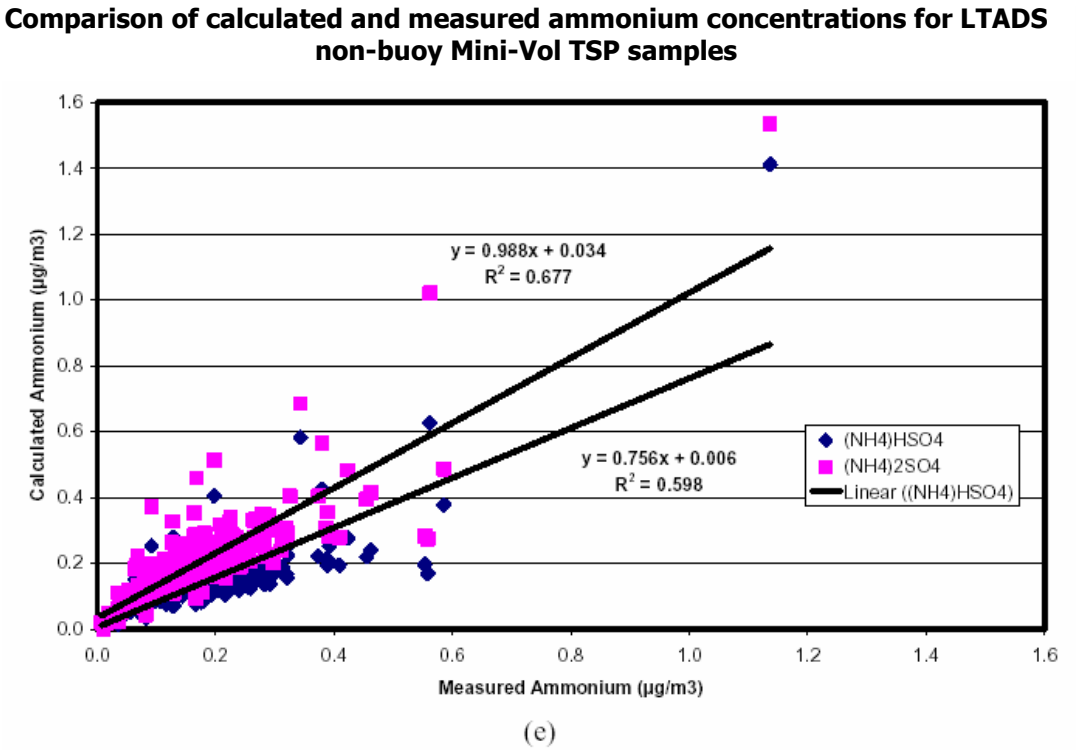

(e)

3.1.12.4 Anion and cation balance

The balance of anions and cations was calculated by comparing the sum of Cl^-, NO_3^-, and $SO_4^=$ to the sum of NH_4^+, K^+, and Na^+ in microequivalence/m^3. Microequivalence/m^3 of each species is calculated as the product of mass concentration (Cm) (in µg/m^3) divided by the atomic weight of the chemical species multiplied by the species' charge. Therefore, microequivalence/m^3 for anion = Cm,Cl^-/35.453 + Cm,NO_3^- /62 + Cm, $SO_4^=$/96x2 microequivalence/m^3 for cations = Cm,$NH4^+$/18 + Cm,K^+/39.1 + Cm,Na^+/23. **Figure 3-6 (a-c)** shows plots of anion and cation balance in microequivalence/m^3 for TWS TSP, PM10, and PM2.5. The slopes are within the range of 0.65-0.68 for all particle sizes, and have moderate correlation (r^2=0.65-0.70). The ratios between anions and cations for TWS TSP, PM10, and PM2.5 were 0.92±0.98, 0.94±0.27, and 0.84±0.23, respectively. The slopes between anions and cations are 1.07 (r^2=0.61) and 1.08 (r^2=0.82), and average ratios are 1.1±0.41, 0.98±0.0.25, for buoy and non-buoy Mini-Vol TSP samples, respectively. The slightly difference between the average ratio of anion and cations versus slopes for TWS samples were because the slopes are more sensitive to high and low concentrations in the data. However, each pair of anion and cation data was weighed equally in ratio. The average PM2.5 anion and cation ratio was 11.6 measured at the TB site on 05/07/03, which is suspected to be an outlier.

Figure 3-6. Scatter Plot of Anion and Cation Balance in Microequivalence/m^3 for: a) TSP, b) PM10, and, c) PM2.5, d) Buoy Mini-Vol TSP, and e) Non-buoy Mini-Vol TSP.

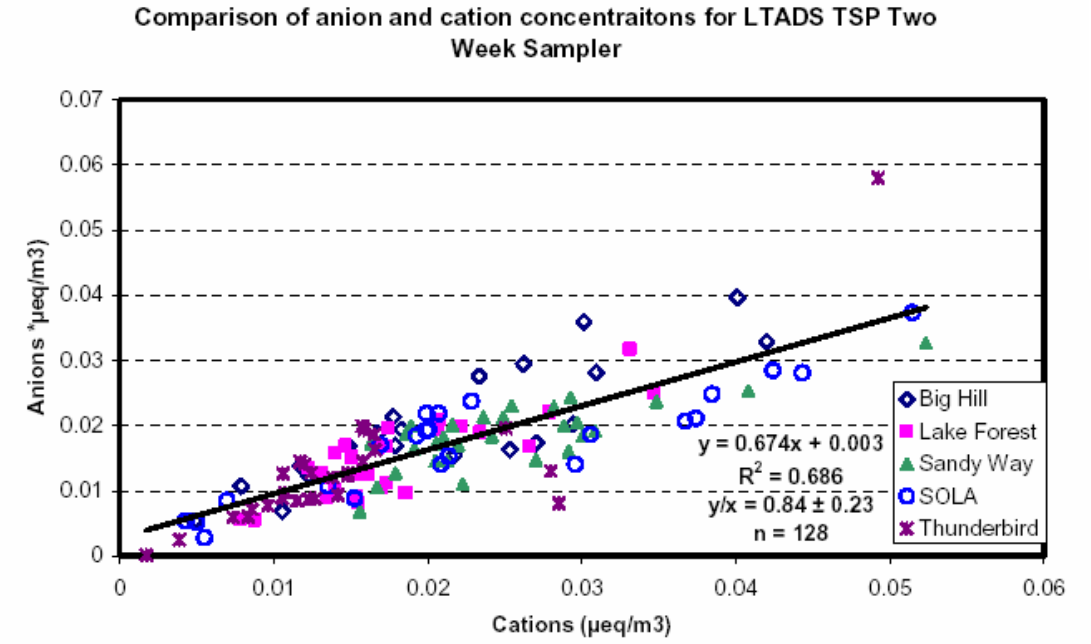

(a)

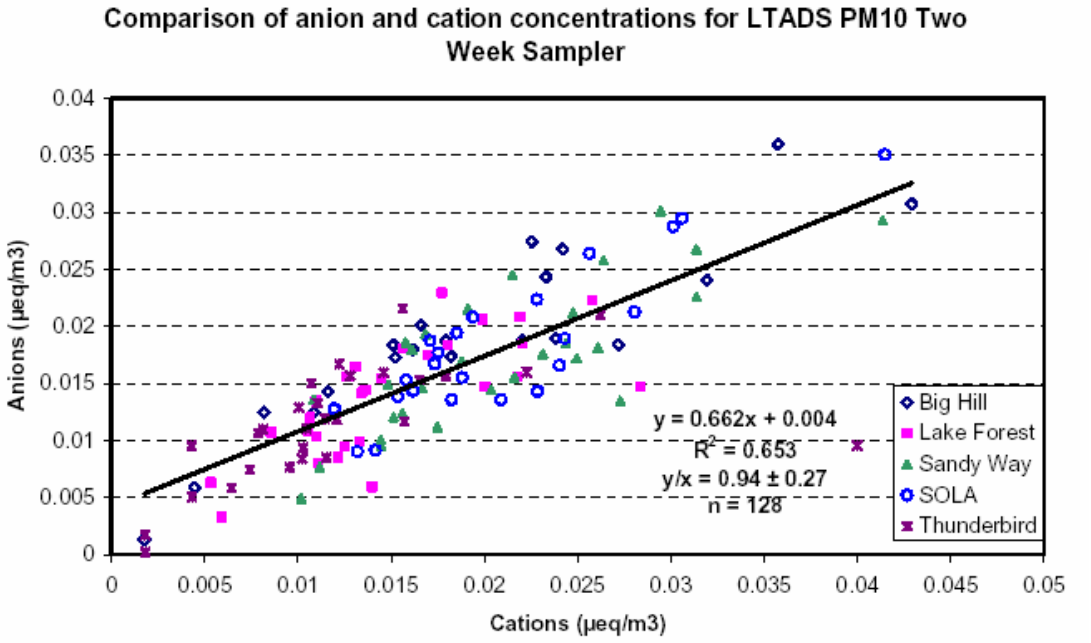

(b)

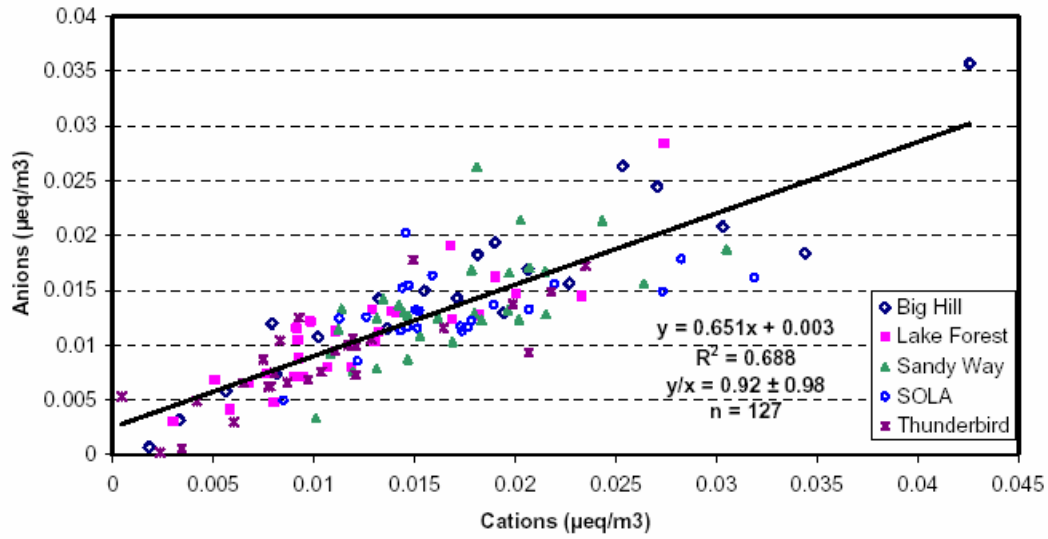
Comparison of anion and cation concentrations for LTADS PM2.5
Two Week Sampler
Anions (µeq/m3)
Cations (µeq/m3)
0.04
0.035
0.03
0.025
0.02
0.015
0.01
0.005
0
0
0.005
0.01
0.015
0.02
0.025
0.03
0.035
0.04
0.045
y = 0.651x + 0.003
R2 = 0.688
y/x = 0.92 ± 0.98
n = 127
Big Hill
Lake Forest
Sandy Way
SOLA
Thunderbird

(c)

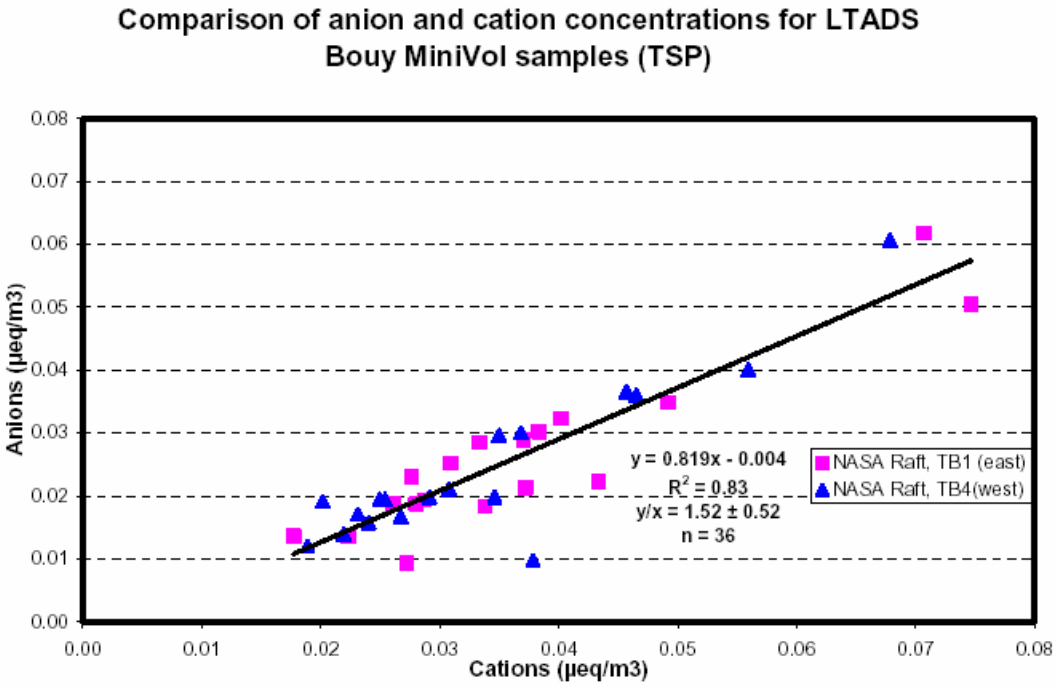
Comparison of anion and cation concentrations for LTADS
Bouy MiniVol samples (TSP)
Anions (µeq/m3)
Cations (µeq/m3)
0.08
0.07
0.06
0.05
0.04
0.03
0.02
0.01
0.00
0.00
0.01
0.02
0.03
0.04
0.05
0.06
0.07
0.08
y = 0.819x - 0.004
R2 = 0.83
y/x = 1.52 ± 0.52
n = 36
NASA Raft, TB1 (east)
NASA Raft, TB4(west)

(d)

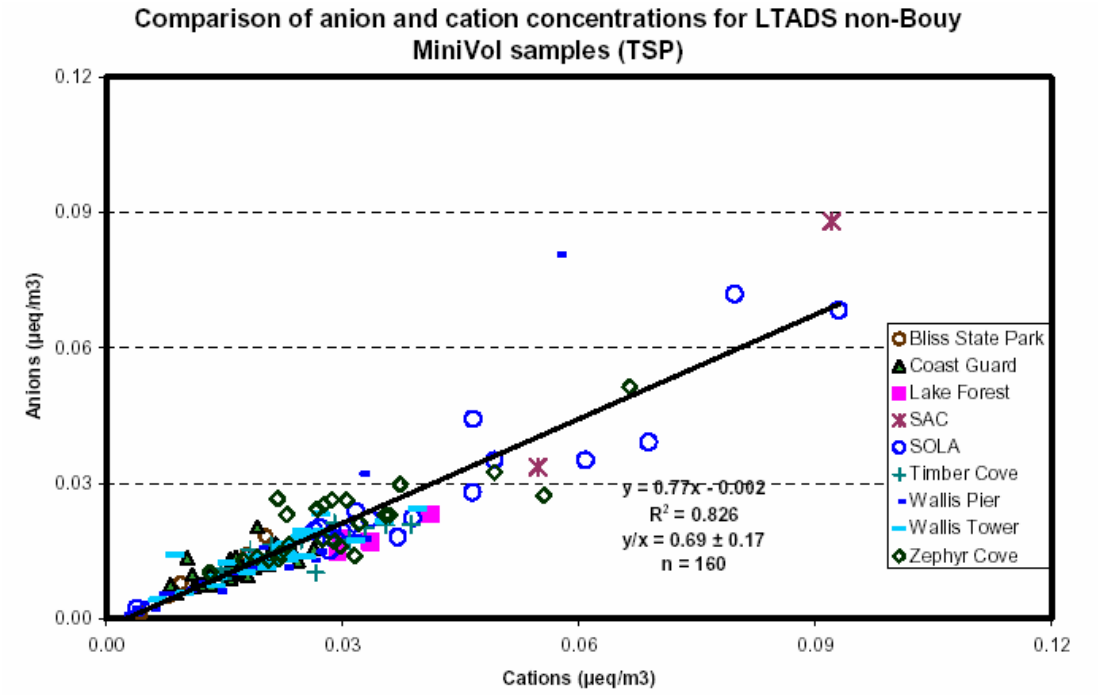

(e)

3.1.12.5 Water-soluble potassium (K^+) versus potassium (K)

K^+ was measured by atomic adsorption spectrophotometry (AAS) analysis on quartz-fiber filter and K was measured by XRF on Teflon-membrane filters. **Figure 3-7 (a-c)** shows scatter plots of K^+ versus K concentrations for TWS TSP, PM10, and PM2.5; and **Figure 3-7 (d, e)** show those for buoy and non-buoy Mini-Vol TSP samples. Very weak correlations between K^+ and K were observed in TWS TSP and PM10, buoy Mini-Vol TSP, and non-buoy Mini-Vol TSP. A high K concentration (1.544 µg/m^3) in PM10 and much lower K^+ concentrations (0.061 µg/m^3 and 0.043 µg/m^3 in TSP and PM2.5, respectively) were observed on 11/15/03. It is suspected that the sample was contaminated. The regression statistics show moderate correlations (r^2 = 0.62) between K^+ and K measured in PM2.5. This suggests the major sources of K^+ in PM2.5 in the Lake Tahoe area are wood smoke from residential cooking and heating processes or from biomass burning.

Figure 3-7. Scatter plot of water-soluble potassium versus potassium concentrations for: a) TSP, b) PM10, c) PM2.5, d) Buoy Mini-Vol TSP, and e) Non-buoy Mini-Vol TSP.

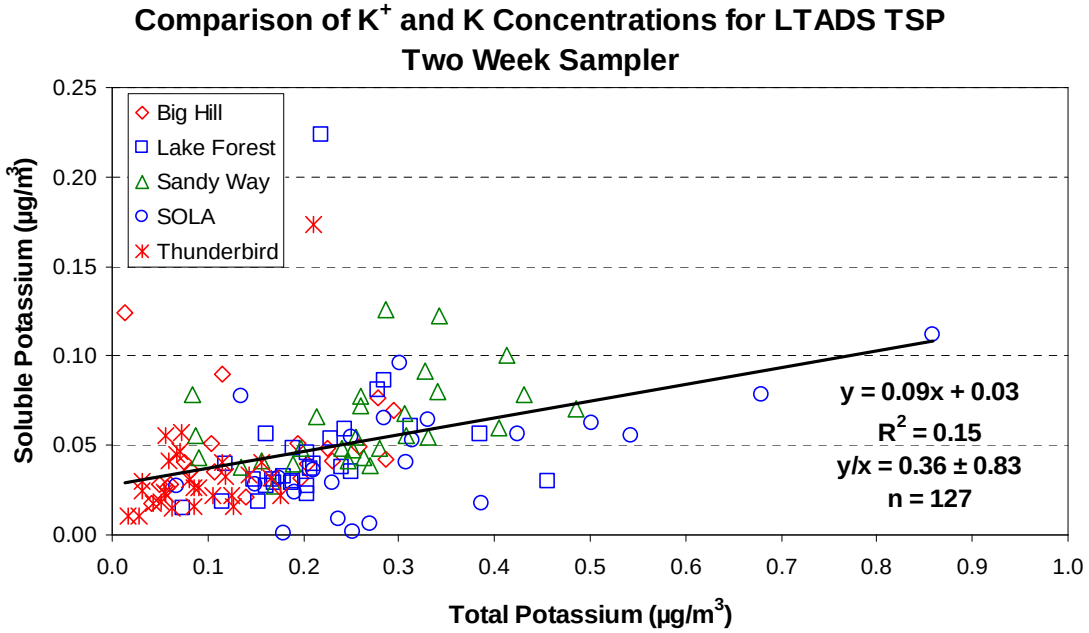

(a)

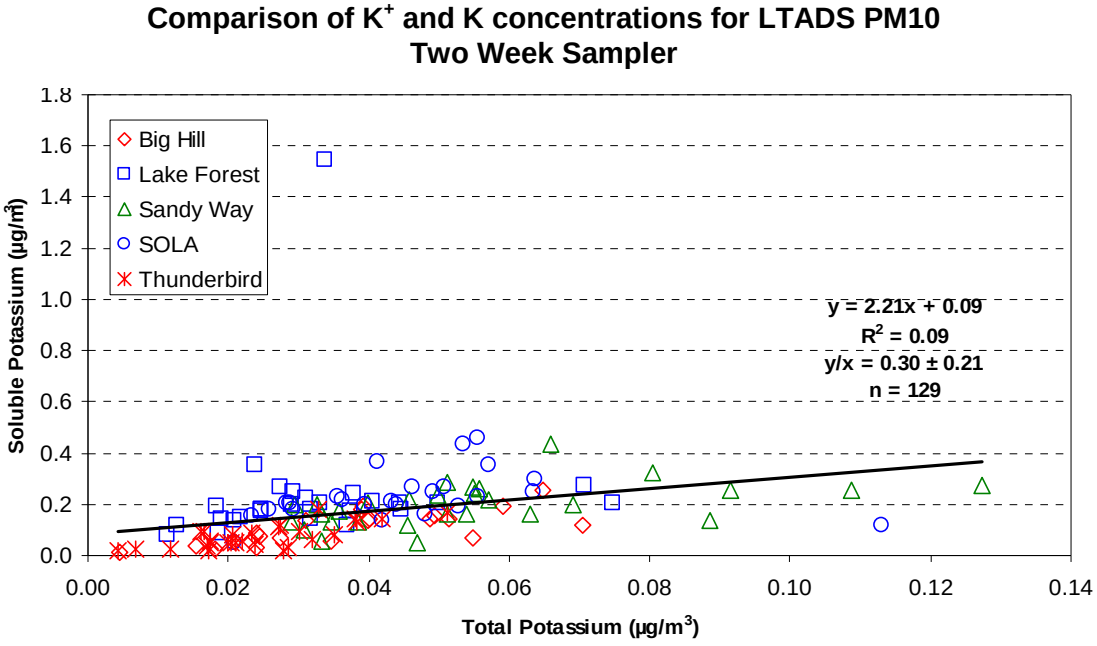

(b)

Comparison of K^+ and K concentrations for LTADS PM2.5 Two-Week-Sampler

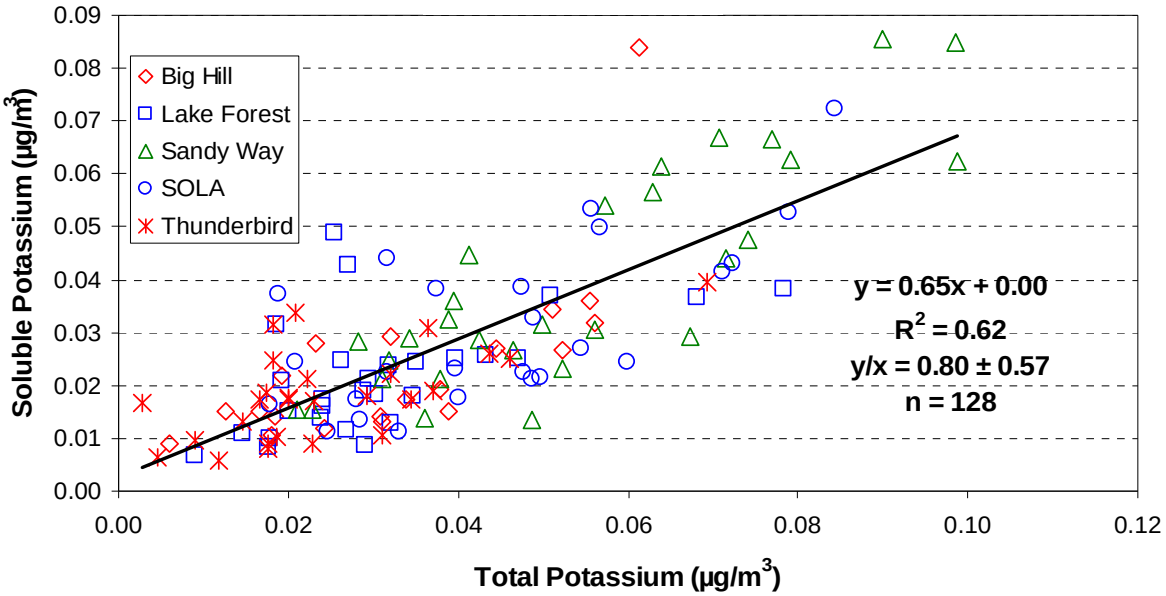

(c)

Comparison of K^+ and K concentrations for LTADS buoy Mini-Vol TSP samples

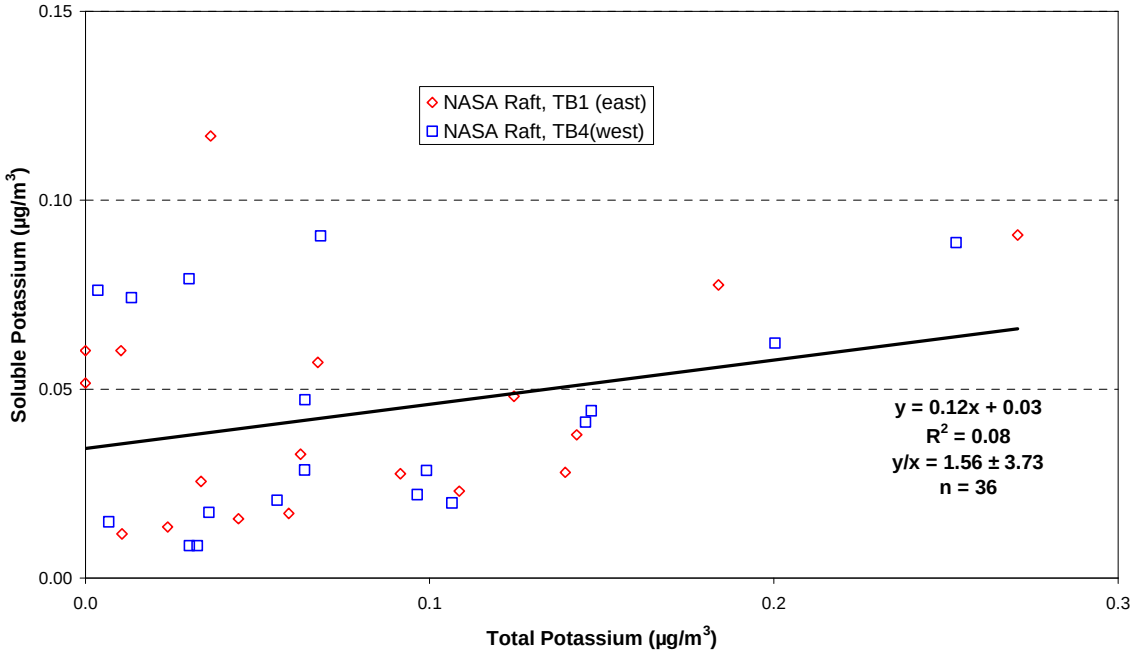

(d)

Comparison of K^+ and K concentrations for LTADS non-buoy Mini-Vol TSP samples

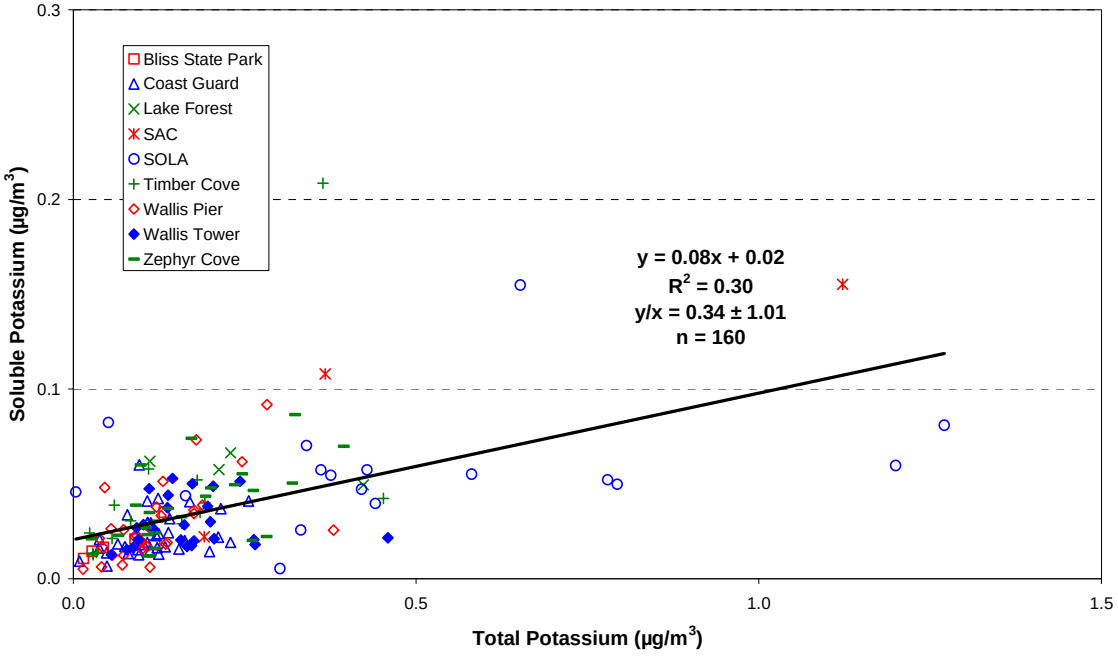

(e)

3.1.13 BAM, TWS, MVS, and FRM Equivalency Demonstrations

Several different instruments and sampling/monitoring technologies for measuring particulate matter were used during LTADS. Because some of these instruments have seldom been used in such a clean, high-altitude, and cold location as Lake Tahoe before, the concentration measurements from different collocated instruments were compared to confirm the assumed equivalency of the measurement methods.

In **Figure 3-8**, hourly TSP data from the Beta Attenuation Monitor (BAM) at SOLA were averaged over the comparable sampling periods of TSP with a collocated mini-volume sampler (MVS). Discounting the two periods when the MVS malfunctioned (data indicated with red circles), the TSP concentrations as measured with the BAM and MVS compared very well (m=1.06, b=0.7 ug/m^3, and r^2=0.97).

TSP concentrations when an MVS was collocated with the TWS at SOLA are plotted in **Figure 3-9**. Only four contemporaneous samples are available but the data indicate a consistent bias toward lower TSP concentrations with the TWS (~5-7 ug/m^3 lower). This low TSP bias with the TWS is very likely due to its design (low flow rate, large precipitation shield, and, to a lesser extent, its inverted sampler inlet (drawing air up to the filter face rather than down to the filter)).

PM data were collected in PM2.5 and PM10 sizes with both a BAM (continuous hourly measurement) and a Federal Reference Method (24-hour filter sample) at the SLT –

Sandy Way site. The BAM data were temporally matched with the FRM samples during 2003. The 24-hour averaged BAM measurements for PM2.5 and PM10 are compared with the FRM measurements in **Figure 3-10**. The relationship between the methods is excellent for PM2.5 (m=0.997; b=0.59 ug/m^3; r^2=0.81) and good for PM10 (m=0.892; b=2.84 ug/m^3; r^2=0.87). It appears that some type of offset that occurred during six sampling periods might be biasing the PM10 regression line toward a higher intercept and a lower slope than normally would exist between the two measurement methods at low concentrations. In general, the BAM measurements corresponded well with the standard (official) FRM measurements. Matched 2-week average PM concentrations by TWS and BAM are shown by site and measurement size in **Figure 3-11**. In almost all cases, the measurement methods are comparable for PM2.5 and PM10 with differences less than 5 ug/m^3. On average, the [PM2.5] was 0.5 ug/m^3 higher and the [PM10] was 1.0 ug/m^3 lower with the TWS than with the BAM measurement; these differences are approximately 10% of the means. The [TSP]s by the two methods exhibited more scatter, particularly at the more polluted locations. On average, the [TSP] was 4.1 ug/m^3 higher by BAM than by TWS; this difference is about 20% of the BAM mean.

Figure 3-8. TSP Concentrations: Mini-Volume Sampler vs. BAM at South Lake Tahoe – SOLA.

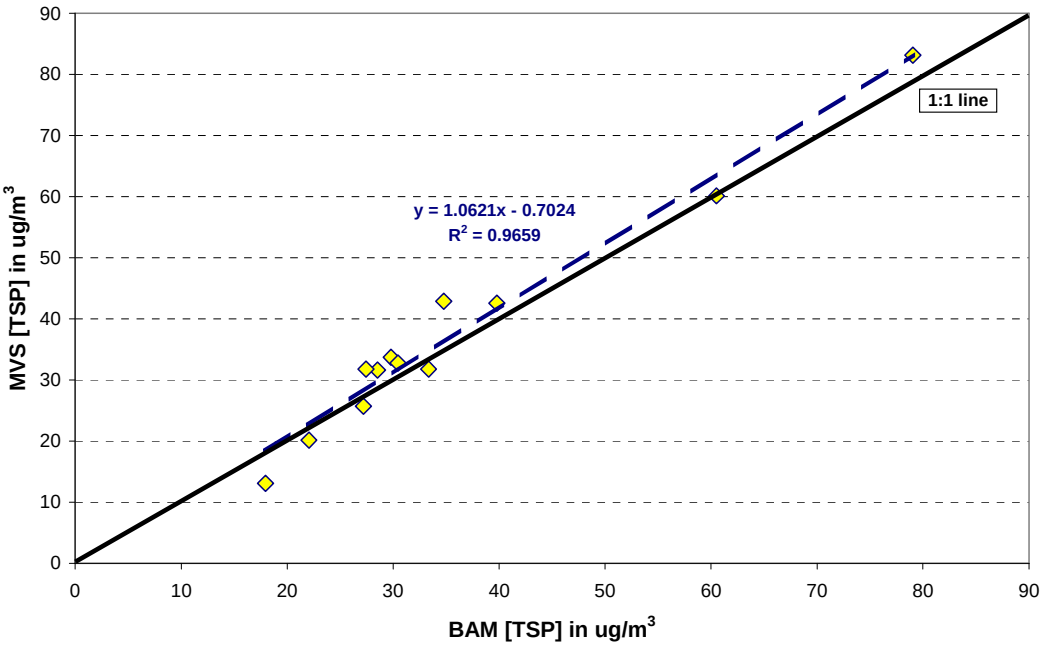

Figure 3-9. TSP Concentrations: Mini-Volume Sampler vs. Two-Week-Sampler at South Lake Tahoe – SOLA.

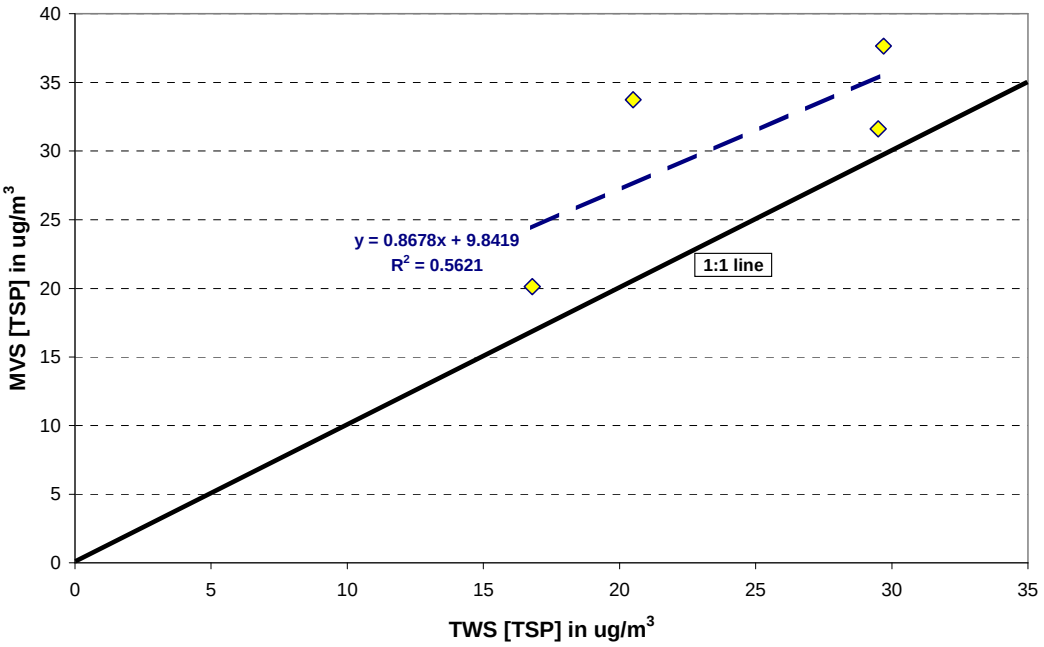

Figure 3-10. BAM PM versus Federal Reference Method PM at SLT-Sandy Way Site in 2003.

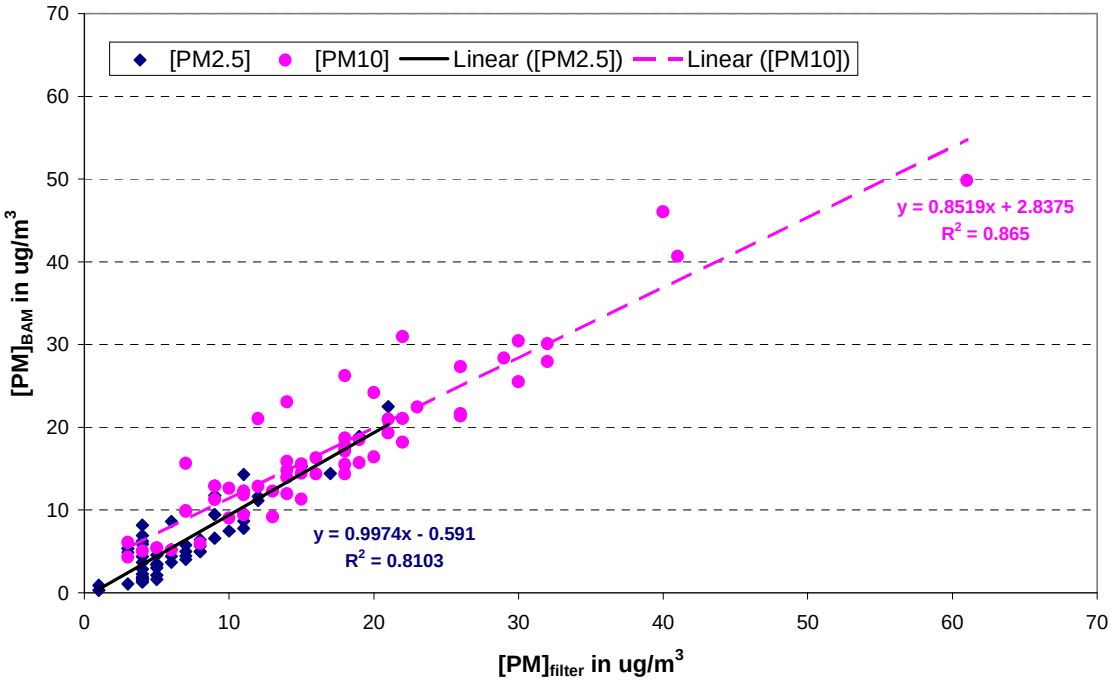

Figure 3-11. Matched 2-week average particulate matter concentrations by collocated TWS and BAM. (Note: all outliers > 10 µg/m^3 from the 1:1 relationship, and the lone case when the [TWS] was > 5 µg/m^3 above the 1:1 relationship, were associated with the two SLT sites.)

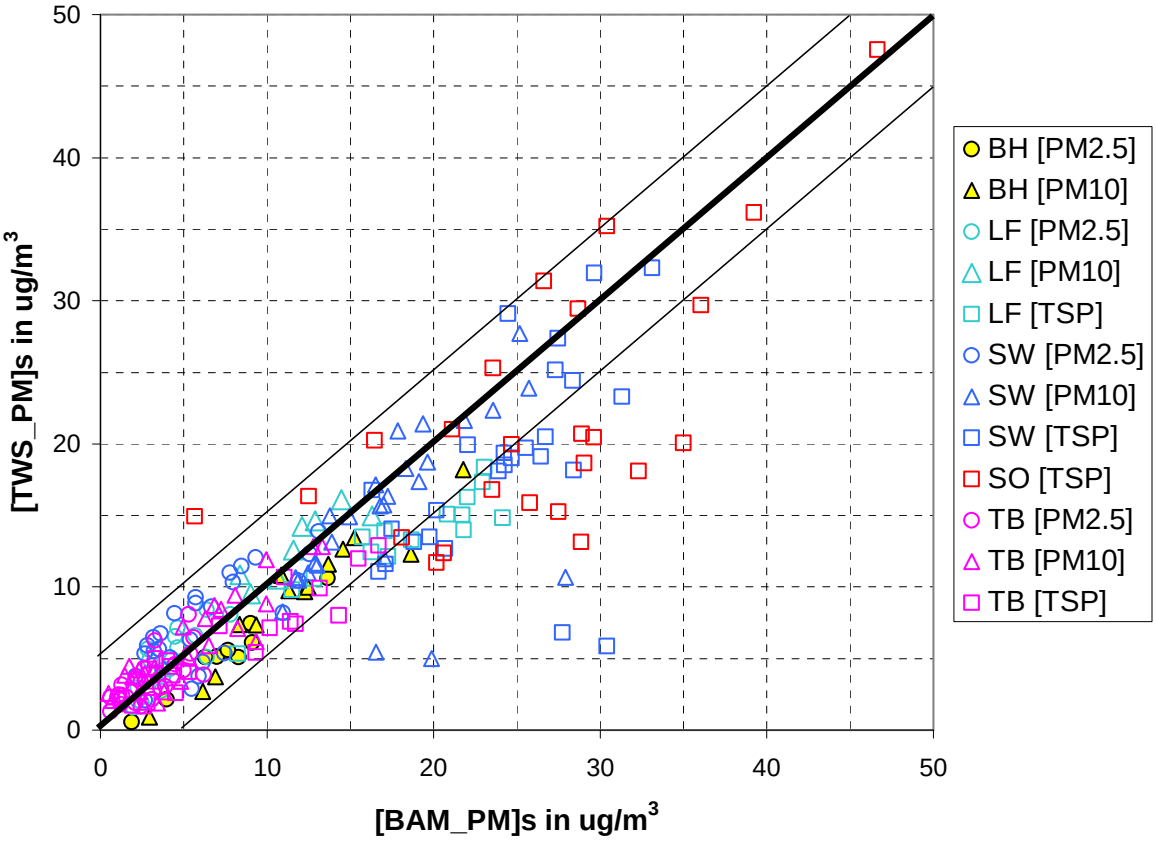

3.1.14 Comparison of Optical Particle Counts to Mass Measurements

The principal instrumentation used in the dust experiments was a set of Climet CI-500 optical particle counters. These counters draw a stream of air through an optical chamber where, one-at-a-time, particles in the air stream pass through the beam of a solid-state laser. Light scattered by a particle is sensed photoelectrically, with the strength of the scattering converted into particle size based on scattering cross-section, and the number of particles in each size "bin" is recorded over a standard sampling period (typically one to a few minutes). There is a maximum count rate, beyond which multiple particles are sensed together (causing miss-sizing), but concentrations observed in the Tahoe region never exceeded the count-rate capability of the instruments.

These instruments are calibrated at the factory, and cannot be adjusted by the user. Validation of calibration was determined by side-by-side testing of multiple instruments, and comparison of estimated aerosol mass with BAM data. Examples are shown in **Figure 3-12a-g**.

Figure 3-12. Cross-Comparison of Optical Particle Counter Instruments by Size Bin.

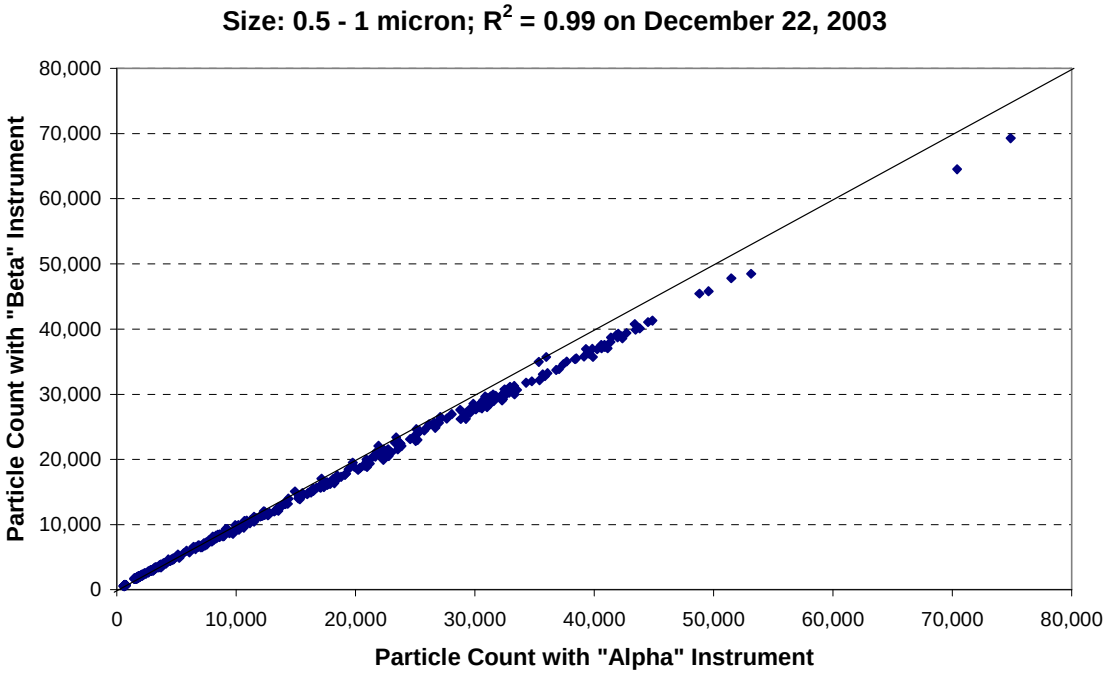

a)

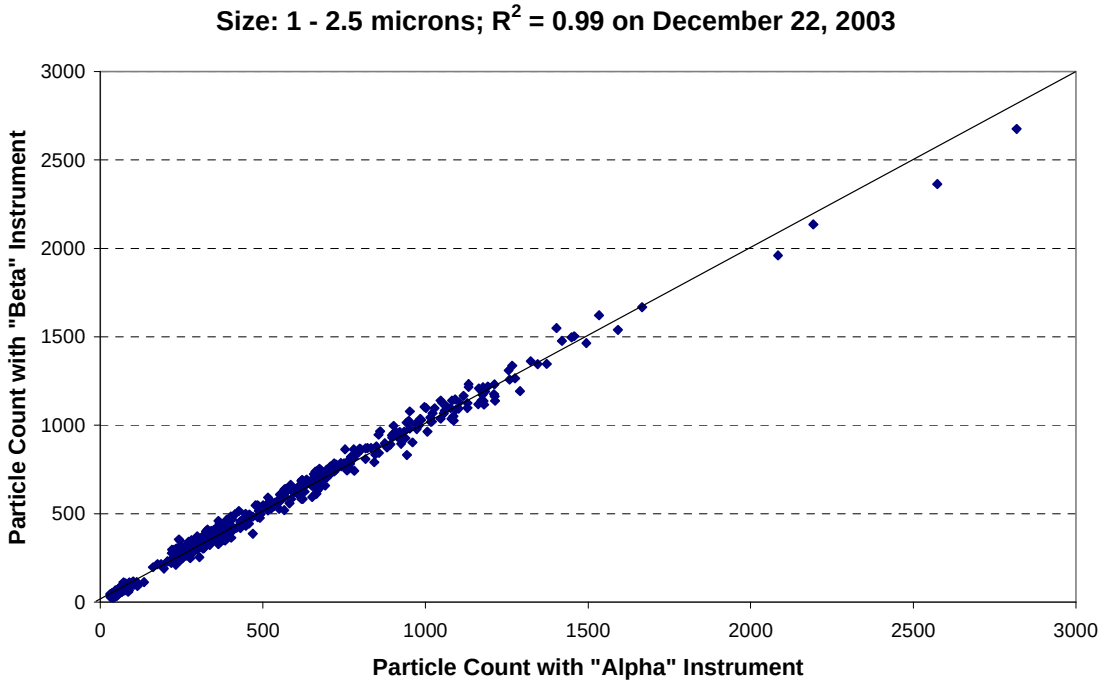

b)

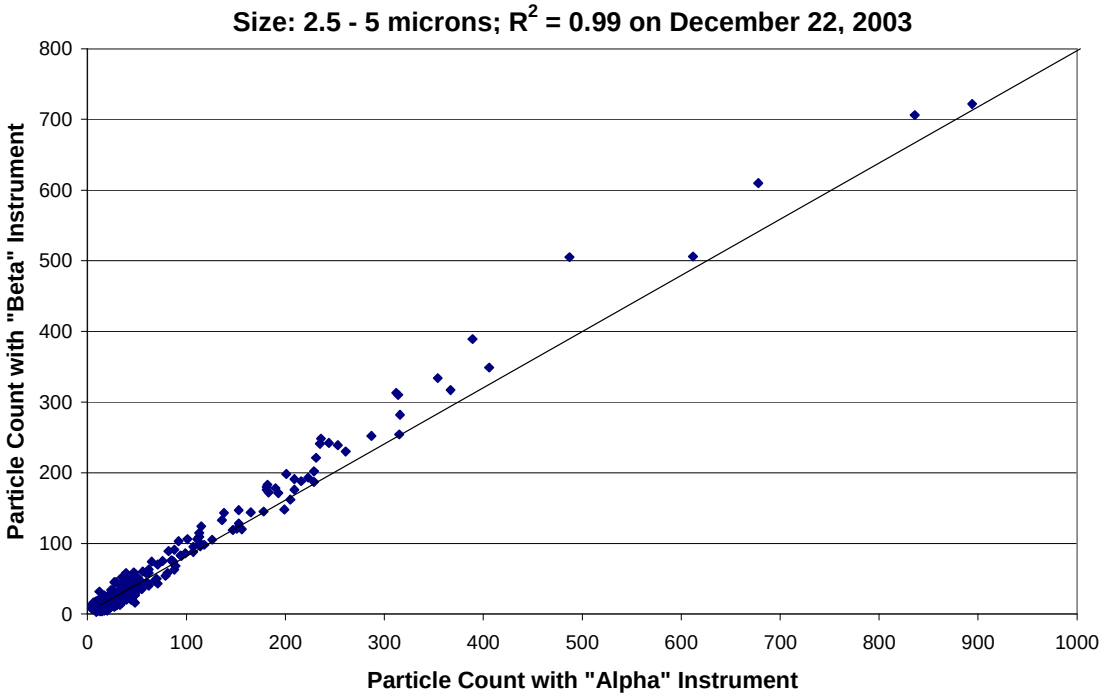
Size: 2.5 - 5 microns; R2 = 0.99 on December 22, 2003
Particle Count with "Beta" Instrument
Particle Count with "Alpha" Instrument
0
100
200
300
400
500
600
700
800
900
1000

c)

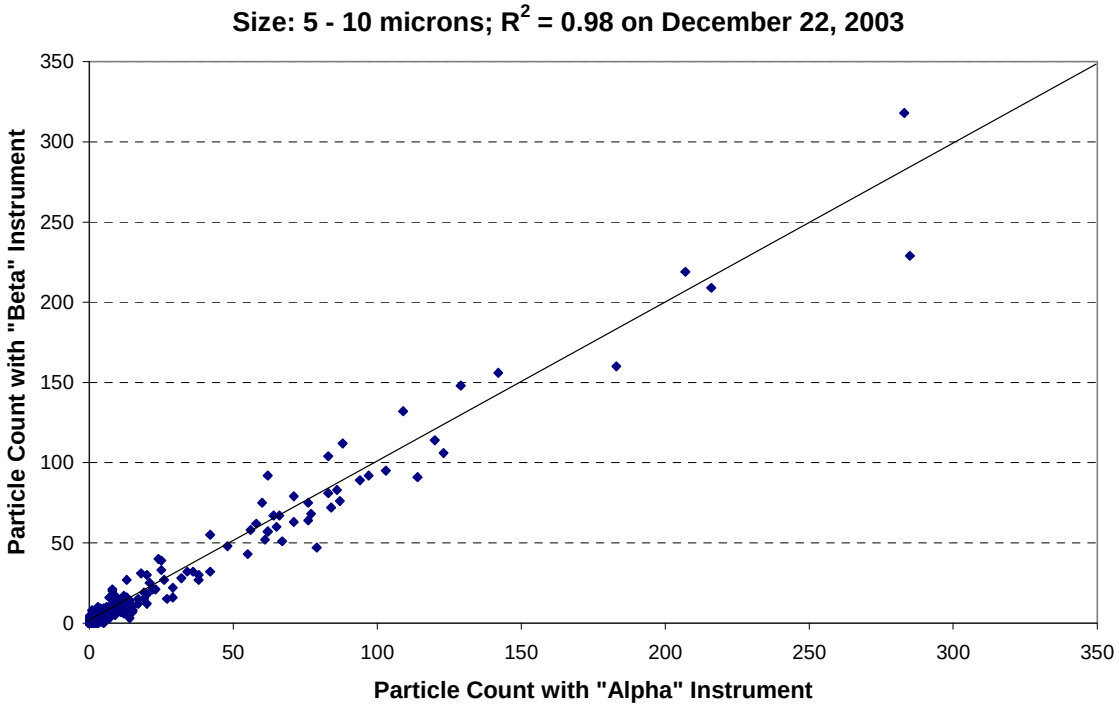
Size: 5 - 10 microns; R2 = 0.98 on December 22, 2003
Particle Count with "Beta" Instrument
Particle Count with "Alpha" Instrument
0
50
100
150
200
250
300
350

d)

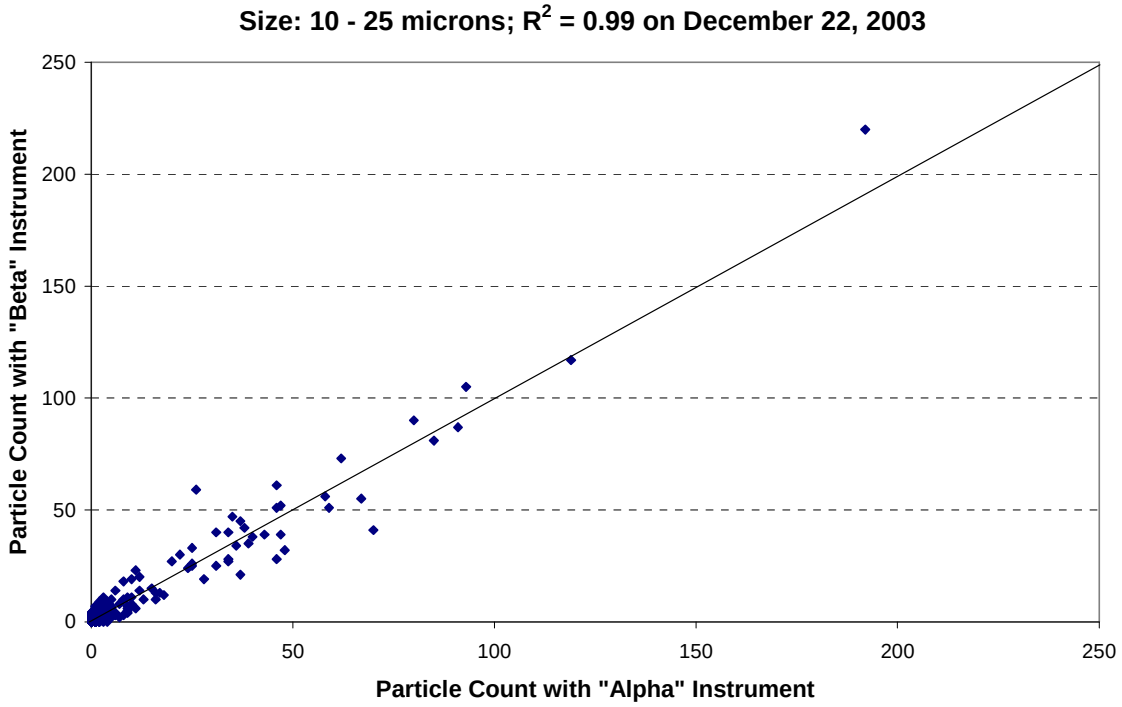
Size: 10 - 25 microns; R2 = 0.99 on December 22, 2003
Particle Count with "Beta" Instrument
Particle Count with "Alpha" Instrument
0
50
100
150
200
250

e)

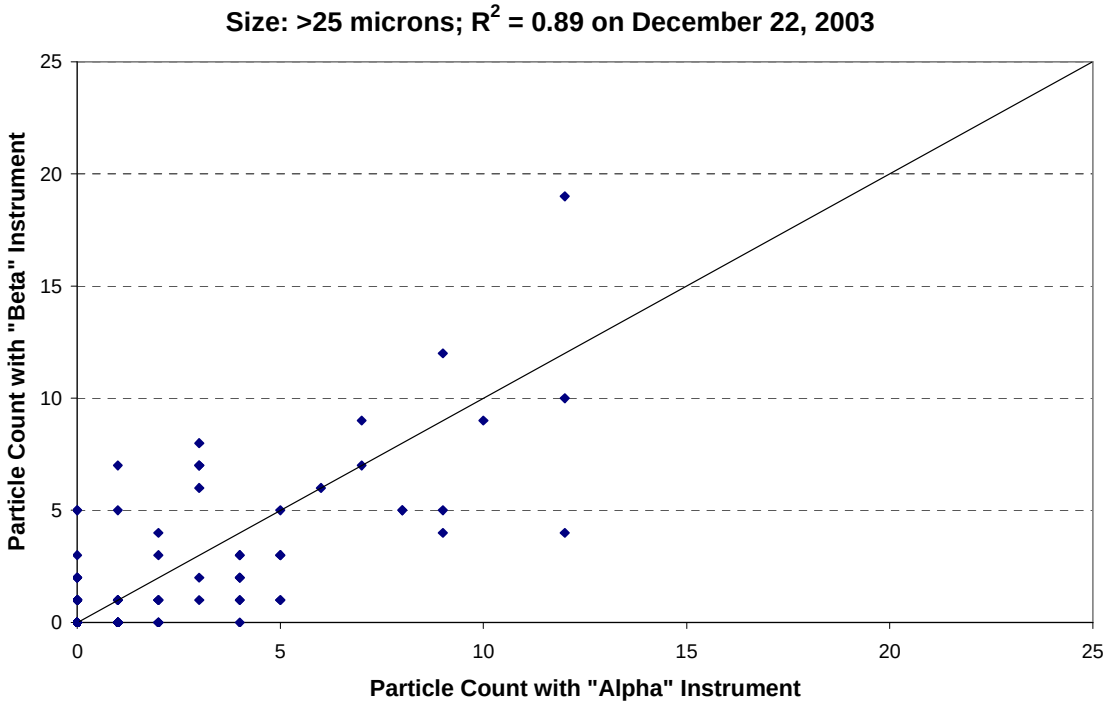
Size: >25 microns; R2 = 0.89 on December 22, 2003
Particle Count with "Beta" Instrument
Particle Count with "Alpha" Instrument
0
5
10
15
20
25

f)

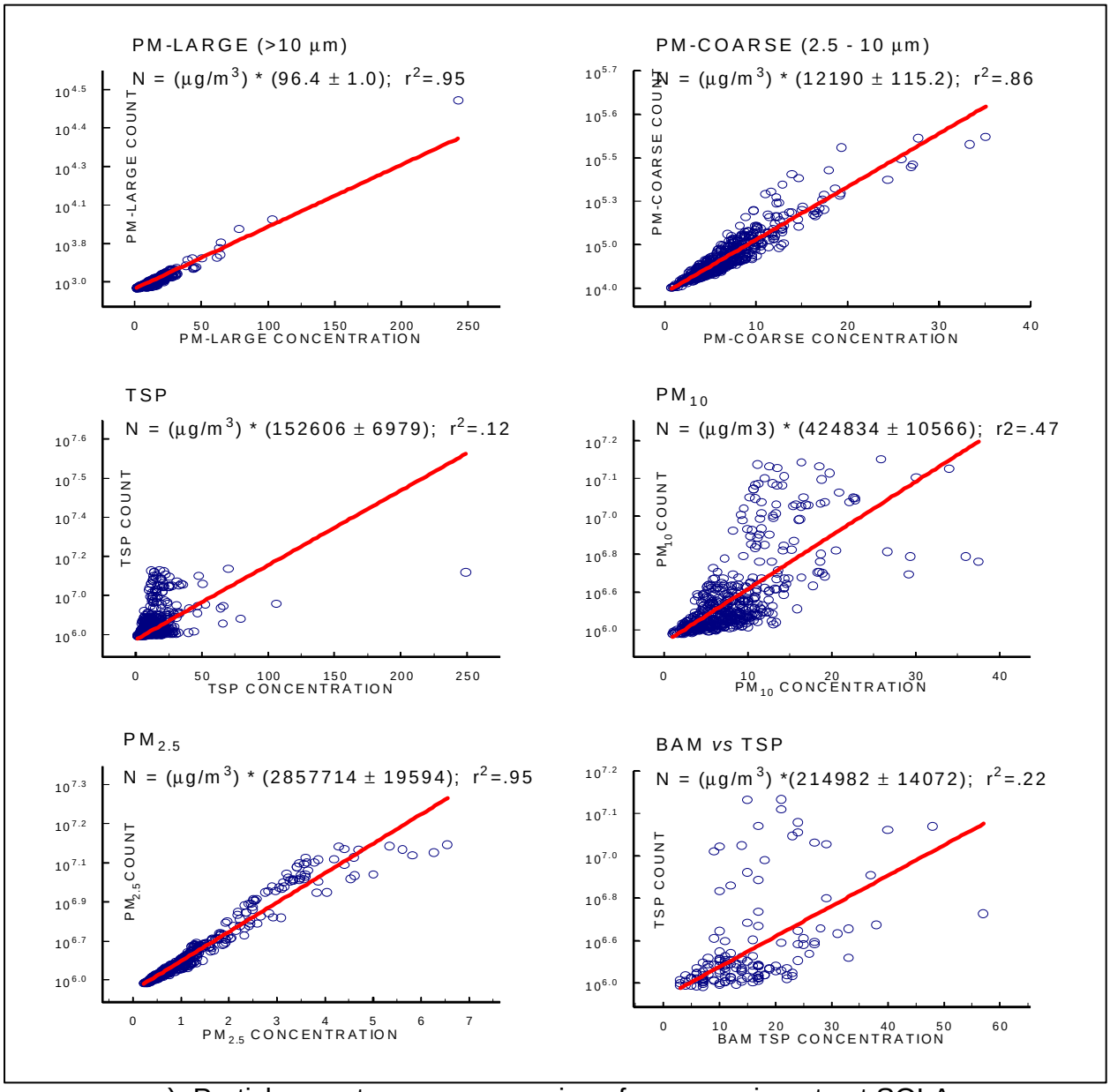

g) Particle count - mass regressions from experiments at SOLA.

3.2 Ambient Concentrations

Various data summaries of the LTADS measurements are presented and discussed in this section.

3.2.1 Particulate Matter

3.2.1.1 Variations in the Sampling Durations of Particulate Measurements

In general, good contemporaneous TWS sampling occurred at BH, LF, TB, SW, and SOLA sites due to a formal sampling schedule. A modification was made to the initial shipping schedule to ensure that refrigerated sampling filters were always available for deployment on the scheduled days. Winter storms and power outages caused most of the deviations from the planned 2-week sampling periods early in the field study. The most severe problem was wind damage that delayed the initiation of sampling at the BH site about three months, until late February 2003.

The sampling schedule with the Mini-Vol samplers was less formal and varied due to differences in power availability, limited access due to weather conditions, sampler malfunctions, etc. The number of Mini-Vol samples and sample duration statistics are summarized by sampling location in **Table 3-4**. The average sampling duration and the number of samples collected were similar for the five primary MVS sites: Coast Guard Pier, Wallis Pier, Zephyr Cove Pier, Wallis Tower, and SOLA. The typical sampling duration was about 170 hours (1 week) and more than 20 samples were collected at these five sites. Sampler malfunctions and occasional two-week samples created a wide range of sampling durations. Fewer than 10 MVS samples were collected at Lake Forest, Bliss State Park, Timber Cove Pier (battery power only), and Sacramento (part of the dry deposition methods comparison study). Of particular interest and effort was the collection of MVS samples on two buoys. These samplers operated on battery power only and sampling durations were typically about 30 hours. The variable sampling durations and pattern of contemporaneous measurements with the MVS network limit spatial and temporal analyses to case studies. However, the TSP mass and major specie measurements are plotted by sample start_date later in this chapter to provide an indication of seasonal and spatial patterns.

Table 3-4. Number of samples and sample duration statistics for Mini-Vol samplers.

Site Name	Number of Samples Collected	Average Sampling Duration (hours)	Minimum Sampling Duration (hours)	Maximum Sampling Duration (hours)
Coast Guard Pier	45	174.9	0.0	338.5
Wallis Pier	41	141.7	0.0	341.9
Zephyr Cove Pier	39	152.0	0.0	394.0
Wallis Tower	32	157.6	0.0	368.0
SOLA	21	233.8	0.0	368.0
Timber Cove Pier	14	43.2	11.5	60.3
Lake Forest	8	182.6	117.1	298.6
Bliss State Park	7	141.5	0.0	283.5
Sacramento	6	115.5	0.0	240.3
TB4 (west) buoy	21	29.3	14.8	48.2
TB1 (east buoy)	21	30.0	24.0	47.1

3.2.1.2 Annual Summary of TWS Aerosol Mass and Chemical Concentrations

Table 3-5 (a-c) presents the annual averages for TWS TSP, PM10, and PM2.5 mass and chemical fractions concentrations from November 2002 to December 2003 at the BH, TB, LF, SW, and SOLA sites. The highest annual average TSP mass concentration was found at the SOLA site (21.9 µg/m^3), followed by the SW (20.1 µg/m^3), LF (14.5 µg/m^3), BH (11.4 µg/m^3), and TB (6.2 µg/m^3) sites. The most abundant chemical species (>1%) in TSP were OC (16.5-29.8%), silicon (10.8-16.0%), aluminum (3.9-4.7%), EC (2.5- 6.2%), calcium (1.7-2.4%), iron (2.1-2.7%), potassium (1.3-1.4%), nitrate (1.2-3.5%), ammonium (1.2-3.3%), and sulfur (1.1-3.4%).

The annual average PM10 mass concentration was highest at the SOLA site (18.8 µg/m^3), followed by the SW (16.8 µg/m^3), LF (14.0 µg/m^3), BH (8.8 µg/m^3), and TB (6.0 µg/m^3) sites. The most abundant chemical species in PM10 were OC (16.2-27.8%), silicon (10.0- 21.1%), aluminum (3.5-6.6%), EC (3.0-7.0%), iron (1.8-3.3%), calcium (1.6-2.9%), nitrate (1.3-3.6%), ammonium (1.3-3.2%), potassium (1.2-1.7%), and sulfur (1.2%-3.5%). The highest annual average PM2.5 mass concentration was found at the SW site (9.0 µg/m^3), followed by the SOLA (6.5 µg/m^3), BH (5.0 µg/m^3), LF (4.3 µg/m^3), and TB (3.6 µg/m^3) sites. The most abundant chemical species in PM2.5 were OC (42-51%), EC (4.9- 16.4%), ammonium (3.1-5.8%), sulfur (2.2-5.7%), nitrate (1.6-3.4%), and silicon (1.3- 2.6%).

The lowest annual average PM10 and PM2.5 mass concentrations were observed at the TB site and the highest PM10 and PM2.5 mass concentrations were observed at the SOLA and SW sites. Mass concentrations of TSP, PM10 and PM2.5 at the BH site were higher than those at the TB site. Similar trends were found for OC, EC, nitrate, ammonium, and sulfate concentrations in PM10 and PM2.5. PM10 and PM2.5 OC and EC concentrations at the SW and SOLA sites were two to three times greater than

those at the LF and TB sites, which could be explained by the influence of increased vehicle emissions at the SOLA and SW sites.

These results agree with the assumed characteristics of the sites identified for the LTADS: the TB site represents a local background site and the SOLA and SW sites represent heavy urban sites. PM2.5 mass and chemical concentrations were lower at the TB site than those at the BH site, which suggests that PM losses due to deposition and settling during transportation from the BH site to the Lake Tahoe region. Silicon and aluminum concentrations at these sites were high in PM10 but low in PM2.5, which suggests a significant contribution of re-suspended dust to coarse particles. The re-suspended dust contribution could be the result of vehicle traffic and wind.

3.2.1.3 Temporal and Spatial Variations in TWS Aerosol Mass and Composition

The temporal and spatial variations of the TWS mass and chemical compositions are presented in this section. When data are summarized by particle size, the following definitions are applied: PM_fine = PM2.5; PM_coarse = PM10 minus PM2.5; PM_large = TSP minus PM10.

An abbreviated summary of the TWS measurements is presented by TWS sampling period in **Figures 3-13 through 3-15**. TWS sampling periods 1-3 include data collected near the end of 2002; all the other TWS sampling periods include data collected during 2003. These figures show the contributions of particle size (PM_fine, PM_coarse, and PM_large) to total mass, nitrate, and ammonium at each site. Samples collected when events occurred that could impact the analytical results are identified as "**uncertain**". These sampling events include sampling durations different than planned, flow rate abnormalities, filter damage, etc. The events themselves do not necessarily invalidate the results but do indicate that non-standard sampling conditions occurred; data analysts should review the data for appropriate usage in specific applications. PM_coarse and PM_large data are derived from the PM2.5, PM10, and TSP measurements. Negative concentrations for PM_coarse or PM_large indicate that one or both of the source measurements may be invalid or, in the case of small negative values, that the difference in concentrations is less than the accuracy of the measurements. In general, PM_large contributed the least to the TSP mass. The rural sites (Big Hill and Thunderbird Lodge) tended to have PM_fine as a significant component of the TSP while the more urban sites (SW, SOLA, and Lake Forest) tended to have the greatest contribution to TSP in the PM_coarse size fraction. As might be expected, most of the ammonium, and much of the nitrate, was in the PM_fine fraction.

Figures 3-16, 3-17, and 3-18 show the variation of the relative contribution of each major component to TSP, PM10, and PM2.5, respectively, at each site. The dates in these figures indicate the start of TWS sampling. The BH site was selected to evaluate the transportation of atmospheric pollutants from areas outside the Lake Tahoe region. The TWS TSP mass concentrations measured at the BH site from 05/21/03 to 10/22/03 ranged from 10-22 $\mu g/m^3$, which were more than twice the TSP mass concentrations (1.8-6.7 $\mu g/m^3$) measured at this site from 02/26/03 to 04/23/03 and 12/03/03 to

Table 3-5a. Annual average TSP mass and chemical fractions for Two-Week Samplers

	Big Hill		Thunderbird		Lake Forest		Sandy Way		SOLA	
	Average Concentration (ug/m3)	% Mass	Average Concentration (ug/m3)	% Mass	Average Concentration (ug/m3)	% Mass	Average Concentration (ug/m3)	% Mass	Average Concentration (ug/m3)	% Mass
Number in Average	19		28		28		29		25	
Mass	11.355	100.000	6.206	100.000	16.466	100.000	20.118	100.000	21.895	100.000
Volatalized Nitrate	0.833	7.340	0.429	6.907	0.345	2.093	0.671	3.335	0.446	2.037
Chloride	0.009	0.079	0.026	0.415	0.090	0.549	0.089	0.444	0.167	0.761
Nitrite	0.000	0.000	0.000	0.000	0.000	0.000	0.000	0.000	0.000	0.000
Nitrate	0.394	3.470	0.171	2.753	0.205	1.246	0.382	1.899	0.373	1.705
Phosphate	0.000	0.000	0.000	0.000	0.000	0.000	0.000	0.000	0.000	0.000
Sulfate	0.655	5.768	0.452	7.285	0.435	2.643	0.470	2.335	0.331	1.512
Ammonium	0.305	2.689	0.206	3.314	0.214	1.302	0.318	1.579	0.258	1.178
Soluble Sodium	0.075	0.663	0.056	0.905	0.111	0.671	0.137	0.683	0.187	0.856
Soluble Magnesium	0.012	0.107	0.010	0.161	0.012	0.074	0.015	0.072	0.012	0.057
Soluble Potassium	0.047	0.417	0.034	0.549	0.046	0.282	0.063	0.311	0.045	0.204
Soluble Calcium	0.109	0.958	0.080	1.296	0.117	0.708	0.144	0.717	0.165	0.752
O1TC	0.106	0.934	0.063	1.010	0.097	0.586	0.420	2.087	0.280	1.277
O2TC	0.304	2.677	0.213	3.432	0.321	1.951	0.920	4.572	0.661	3.021
O3TC	1.170	10.304	0.846	13.628	1.437	8.728	3.269	16.247	2.468	11.274
O4TC	0.487	4.289	0.350	5.644	0.588	3.572	1.157	5.749	0.869	3.967
OPTC	0.241	2.125	0.185	2.987	0.277	1.682	0.240	1.194	0.205	0.935
OCTC	2.308	20.329	1.657	26.701	2.720	16.518	6.005	29.849	4.483	20.473
E1TC	0.342	3.012	0.265	4.268	0.481	2.919	1.129	5.610	0.986	4.503
E2TC	0.171	1.505	0.156	2.521	0.270	1.642	0.340	1.690	0.321	1.464
E3TC	0.016	0.138	0.009	0.150	0.018	0.108	0.028	0.138	0.016	0.074
ECTC	0.287	2.531	0.245	3.953	0.492	2.988	1.256	6.243	1.118	5.106
TCTC	2.596	22.860	1.902	30.654	3.212	19.506	7.261	36.093	5.601	25.580
Sodium	0.029	0.258	0.019	0.303	0.053	0.323	0.042	0.211	0.050	0.227
Magnesium	0.012	0.106	0.017	0.270	0.024	0.144	0.011	0.054	0.016	0.071
Aluminum	0.529	4.658	0.255	4.102	0.839	5.096	0.779	3.873	1.006	4.595
Silicon	1.230	10.830	0.767	12.356	2.643	16.049	2.556	12.703	3.472	15.859
Phosphorus	0.000	0.001	0.000	0.005	0.001	0.008	0.001	0.003	0.001	0.003
Sulfur	0.291	2.561	0.211	3.403	0.215	1.305	0.222	1.103	0.236	1.079
Chlorine	0.004	0.037	0.006	0.099	0.084	0.512	0.119	0.591	0.203	0.928
Potassium	0.151	1.328	0.089	1.432	0.212	1.289	0.263	1.307	0.307	1.403
Calcium	0.180	1.586	0.121	1.943	0.388	2.359	0.334	1.661	0.460	2.101
Titanium	0.024	0.210	0.011	0.181	0.047	0.288	0.043	0.214	0.050	0.227
Vanadium	0.001	0.005	0.000	0.007	0.001	0.006	0.001	0.006	0.001	0.004
Chromium	0.001	0.005	0.000	0.004	0.001	0.004	0.001	0.004	0.001	0.004
Manganese	0.008	0.067	0.003	0.050	0.009	0.053	0.009	0.044	0.011	0.049
Iron	0.263	2.315	0.130	2.100	0.446	2.708	0.458	2.276	0.596	2.724
Cobalt	0.002	0.017	0.001	0.015	0.004	0.023	0.004	0.018	0.005	0.022
Nickel	0.000	0.003	0.000	0.003	0.000	0.002	0.000	0.002	0.000	0.002
Cupper	0.009	0.077	0.002	0.028	0.003	0.019	0.007	0.033	0.006	0.027
Zinc	0.008	0.067	0.004	0.063	0.008	0.046	0.017	0.083	0.019	0.085
Gallium	0.000	0.001	0.000	0.002	0.000	0.000	0.000	0.000	0.000	0.000
Arsenic	0.000	0.001	0.000	0.002	0.000	0.001	0.000	0.002	0.000	0.001
Selenium	0.000	0.001	0.000	0.001	0.000	0.000	0.000	0.000	0.000	0.000
Bromine	0.001	0.013	0.001	0.021	0.001	0.009	0.002	0.008	0.002	0.008
Rubidium	0.001	0.006	0.000	0.005	0.001	0.004	0.001	0.005	0.001	0.005
Strontium	0.001	0.010	0.001	0.015	0.006	0.039	0.004	0.021	0.006	0.028
Yttrium	0.000	0.003	0.000	0.005	0.000	0.002	0.000	0.002	0.000	0.002
Zirconium	0.000	0.004	0.000	0.004	0.002	0.010	0.001	0.006	0.002	0.007
Molybdenum	0.000	0.003	0.000	0.002	0.000	0.002	0.000	0.001	0.000	0.001
Palladium	0.000	0.002	0.000	0.003	0.000	0.001	0.000	0.001	0.000	0.001
Silver	0.000	0.002	0.000	0.003	0.000	0.002	0.000	0.001	0.000	0.002
Cadmium	0.000	0.001	0.000	0.003	0.000	0.002	0.000	0.002	0.000	0.001
Indium	0.001	0.007	0.000	0.006	0.000	0.002	0.001	0.003	0.001	0.003
Tin	0.001	0.013	0.001	0.023	0.001	0.009	0.001	0.007	0.002	0.007
Antimony	0.001	0.011	0.001	0.019	0.001	0.007	0.001	0.006	0.001	0.005
Barium	0.005	0.046	0.006	0.097	0.013	0.080	0.013	0.063	0.021	0.095
Lanthanum	0.008	0.071	0.007	0.118	0.006	0.038	0.005	0.023	0.006	0.028
Gold	0.000	0.001	0.000	0.002	0.000	0.001	0.000	0.001	0.000	0.001
Mercury	0.000	0.001	0.000	0.002	0.000	0.001	0.000	0.000	0.000	0.001
Thallium	0.000	0.001	0.000	0.001	0.000	0.001	0.000	0.000	0.000	0.001
Lead	0.001	0.010	0.001	0.015	0.001	0.008	0.002	0.008	0.001	0.006
Uranium	0.000	0.001	0.000	0.003	0.000	0.001	0.000	0.001	0.000	0.001

Table 3-5b. Annual average PM10 mass and chemical fractions for Two Week

	Big Hill		Thunderbird		Lake Forest		Sandy Way		SOLA	
	Average Concentration (ug/m3)	% Mass	Average Concentration (ug/m3)	% Mass	Average Concentration (ug/m3)	% Mass	Average Concentration (ug/m3)	% Mass	Average Concentration (ug/m3)	% Mass
Number in Average	19		28		28		29		25	
Mass	8.814	100.000	5.957	100.000	13.981	100.000	16.762	100.000	18.822	100.000
Volatalized Nitrate	0.519	5.885	0.243	4.082	0.270	1.933	0.559	3.332	0.482	2.560
Chloride	0.022	0.254	0.016	0.275	0.050	0.360	0.065	0.387	0.111	0.591
Nitrite	0.007	0.076	0.000	0.000	0.000	0.000	0.000	0.000	0.000	0.000
Nitrate	0.313	3.556	0.131	2.205	0.182	1.304	0.329	1.963	0.346	1.838
Phosphate	0.004	0.041	0.000	0.000	0.004	0.027	0.000	0.000	0.000	0.000
Sulfate	0.644	7.301	0.425	7.142	0.458	3.274	0.486	2.897	0.467	2.479
Ammonium	0.282	3.197	0.157	2.636	0.182	1.300	0.272	1.621	0.261	1.388
Soluble Sodium	0.066	0.747	0.067	1.126	0.095	0.679	0.097	0.582	0.135	0.718
Soluble Magnesium	0.010	0.117	0.006	0.107	0.010	0.070	0.012	0.070	0.011	0.057
Soluble Potassium	0.038	0.431	0.025	0.412	0.032	0.231	0.055	0.329	0.046	0.244
Soluble Calcium	0.074	0.842	0.054	0.906	0.093	0.668	0.117	0.700	0.146	0.778
O1TC	0.352	3.998	0.255	4.284	0.267	1.910	0.673	4.013	0.388	2.062
O2TC	0.296	3.362	0.194	3.259	0.281	2.010	0.844	5.034	0.604	3.211
O3TC	1.067	12.104	0.723	12.137	1.167	8.346	2.869	17.114	2.414	12.826
O4TC	0.484	5.490	0.310	5.202	0.470	3.359	1.037	6.186	0.905	4.807
OPTC	0.225	2.552	0.172	2.895	0.221	1.583	0.216	1.290	0.194	1.030
OCTC	2.424	27.506	1.655	27.777	2.406	17.209	5.638	33.636	4.505	23.936
E1TC	0.298	3.386	0.237	3.974	0.381	2.725	1.009	6.017	1.018	5.408
E2TC	0.178	2.018	0.152	2.557	0.267	1.907	0.357	2.128	0.382	2.028
E3TC	0.015	0.168	0.016	0.269	0.016	0.111	0.032	0.190	0.021	0.112
ECTC	0.266	3.020	0.233	3.906	0.442	3.161	1.181	7.046	1.227	6.518
TCTC	2.691	30.527	1.887	31.682	2.848	20.369	6.819	40.682	5.732	30.454
Sodium	0.045	0.506	0.017	0.287	0.052	0.371	0.032	0.190	0.038	0.201
Magnesium	0.018	0.206	0.017	0.280	0.019	0.135	0.010	0.061	0.023	0.123
Aluminum	0.371	4.206	0.208	3.496	0.928	6.636	0.590	3.519	0.799	4.244
Silicon	0.881	9.992	0.623	10.456	2.955	21.137	1.837	10.962	2.594	13.781
Phosphorus	0.000	0.002	0.001	0.017	0.001	0.007	0.000	0.002	0.001	0.005
Sulfur	0.287	3.251	0.206	3.451	0.233	1.666	0.217	1.294	0.220	1.169
Chlorine	0.002	0.025	0.006	0.096	0.130	0.928	0.080	0.480	0.123	0.656
Potassium	0.112	1.276	0.075	1.258	0.236	1.691	0.198	1.179	0.232	1.235
Calcium	0.137	1.551	0.098	1.649	0.402	2.876	0.237	1.413	0.340	1.805
Titanium	0.015	0.175	0.008	0.142	0.045	0.325	0.028	0.165	0.038	0.201
Vanadium	0.001	0.008	0.000	0.006	0.001	0.005	0.001	0.005	0.001	0.006
Chromium	0.000	0.005	0.001	0.019	0.001	0.005	0.001	0.003	0.001	0.003
Manganese	0.005	0.061	0.003	0.046	0.009	0.062	0.006	0.038	0.008	0.041
Iron	0.218	2.476	0.108	1.808	0.462	3.303	0.324	1.934	0.443	2.354
Cobalt	0.002	0.019	0.001	0.014	0.004	0.028	0.003	0.016	0.003	0.019
Nickel	0.000	0.004	0.000	0.007	0.000	0.002	0.000	0.002	0.000	0.002
Cupper	0.002	0.022	0.001	0.021	0.003	0.024	0.007	0.041	0.004	0.023
Zinc	0.003	0.033	0.002	0.032	0.009	0.065	0.013	0.076	0.014	0.072
Gallium	0.000	0.001	0.000	0.001	0.000	0.001	0.000	0.001	0.000	0.000
Arsenic	0.000	0.001	0.000	0.003	0.000	0.002	0.000	0.001	0.000	0.001
Selenium	0.000	0.001	0.000	0.002	0.000	0.001	0.000	0.001	0.000	0.000
Bromine	0.002	0.018	0.001	0.022	0.002	0.011	0.002	0.009	0.002	0.008
Rubidium	0.000	0.003	0.000	0.004	0.001	0.006	0.001	0.004	0.001	0.004
Strontium	0.001	0.010	0.001	0.013	0.006	0.045	0.003	0.016	0.004	0.023
Yttrium	0.000	0.002	0.000	0.004	0.000	0.003	0.000	0.001	0.000	0.002
Zirconium	0.000	0.005	0.000	0.004	0.002	0.012	0.001	0.005	0.001	0.007
Molybdenum	0.000	0.001	0.000	0.003	0.000	0.003	0.000	0.002	0.000	0.001
Palladium	0.000	0.001	0.000	0.002	0.000	0.001	0.000	0.001	0.000	0.001
Silver	0.000	0.003	0.000	0.004	0.000	0.002	0.000	0.001	0.000	0.001
Cadmium	0.000	0.003	0.000	0.004	0.000	0.001	0.000	0.002	0.000	0.002
Indium	0.001	0.007	0.000	0.006	0.001	0.004	0.000	0.003	0.000	0.002
Tin	0.002	0.025	0.001	0.016	0.001	0.010	0.002	0.011	0.002	0.011
Antimony	0.001	0.008	0.001	0.011	0.001	0.008	0.001	0.007	0.001	0.006
Barium	0.004	0.045	0.006	0.105	0.015	0.110	0.011	0.064	0.013	0.067
Lanthanum	0.007	0.082	0.006	0.103	0.006	0.046	0.004	0.024	0.006	0.032
Gold	0.000	0.000	0.000	0.003	0.000	0.002	0.000	0.000	0.000	0.001
Mercury	0.000	0.002	0.000	0.001	0.000	0.001	0.000	0.001	0.000	0.001
Thallium	0.000	0.000	0.000	0.000	0.000	0.000	0.000	0.000	0.000	0.000
Lead	0.001	0.014	0.001	0.017	0.002	0.013	0.002	0.011	0.002	0.008
Uranium	0.000	0.002	0.000	0.001	0.000	0.002	0.000	0.001	0.000	0.001

Table 3-5c. Annual average PM2.5 mass and chemical fractions for Two Week

	Big Hill		Thunderbird		Lake Forest		Sandy Way		SOLA	
	Average Concentration (ug/m3)	% Mass	Average Concentration (ug/m3)	% Mass	Average Concentration (ug/m3)	% Mass	Average Concentration (ug/m3)	% Mass	Average Concentration (ug/m3)	% Mass
Number in Average	19		28		28		29		25	
Mass	4.950	100.000	3.629	100.000	4.307	100.000	8.952	100.000	6.530	100.000
Volatalized Nitrate	0.470	9.505	0.231	6.375	0.253	5.868	0.527	5.883	0.471	7.214
Chloride	0.015	0.299	0.009	0.252	0.015	0.348	0.036	0.404	0.031	0.469
Nitrite	0.004	0.090	0.000	0.000	0.000	0.000	0.000	0.000	0.005	0.080
Nitrate	0.167	3.381	0.059	1.630	0.099	2.288	0.218	2.438	0.222	3.405
Phosphate	0.004	0.082	0.000	0.000	0.000	0.000	0.000	0.000	0.004	0.055
Sulfate	0.579	11.696	0.360	9.926	0.428	9.944	0.436	4.872	0.433	6.625
Ammonium	0.285	5.762	0.172	4.743	0.204	4.732	0.277	3.093	0.288	4.405
Soluble Sodium	0.031	0.632	0.016	0.440	0.011	0.265	0.018	0.204	0.026	0.391
Soluble Magnesium	0.002	0.035	0.001	0.038	0.001	0.033	0.001	0.015	0.001	0.020
Soluble Potassium	0.024	0.478	0.018	0.506	0.022	0.508	0.040	0.446	0.031	0.477
Soluble Calcium	0.006	0.126	0.005	0.150	0.009	0.200	0.009	0.101	0.012	0.191
O1TC	0.589	11.893	0.386	10.644	0.384	8.906	0.603	6.741	0.455	6.968
O2TC	0.330	6.669	0.186	5.124	0.236	5.478	0.746	8.338	0.462	7.073
O3TC	0.873	17.638	0.574	15.814	0.755	17.529	2.171	24.254	1.486	22.760
O4TC	0.334	6.745	0.231	6.378	0.299	6.938	0.788	8.803	0.568	8.697
OPTC	0.179	3.625	0.163	4.495	0.174	4.036	0.265	2.957	0.232	3.559
OCTC	2.305	46.570	1.541	42.454	1.847	42.887	4.574	51.092	3.203	49.058
E1TC	0.260	5.250	0.195	5.367	0.271	6.289	0.976	10.905	0.819	12.550
E2TC	0.151	3.060	0.156	4.298	0.247	5.739	0.379	4.237	0.444	6.804
E3TC	0.008	0.170	0.017	0.469	0.026	0.605	0.039	0.441	0.042	0.639
ECTC	0.240	4.855	0.205	5.639	0.370	8.596	1.130	12.626	1.073	16.433
TCTC	2.545	51.425	1.746	48.093	2.217	51.483	5.704	63.718	4.276	65.491
Sodium	0.009	0.188	0.034	0.937	0.015	0.339	0.025	0.281	0.034	0.516
Magnesium	0.007	0.147	0.007	0.194	0.010	0.222	0.007	0.081	0.008	0.121
Aluminum	0.024	0.489	0.017	0.456	0.030	0.705	0.032	0.356	0.035	0.529
Silicon	0.066	1.333	0.060	1.650	0.113	2.619	0.117	1.305	0.121	1.853
Phosphorus	0.000	0.004	0.000	0.005	0.000	0.001	0.000	0.000	0.000	0.000
Sulfur	0.273	5.517	0.208	5.732	0.197	4.572	0.194	2.172	0.190	2.916
Chlorine	0.000	0.004	0.000	0.004	0.001	0.034	0.005	0.060	0.004	0.058
Potassium	0.033	0.670	0.025	0.696	0.031	0.724	0.054	0.605	0.045	0.691
Calcium	0.016	0.326	0.015	0.402	0.026	0.613	0.025	0.282	0.028	0.431
Titanium	0.002	0.032	0.001	0.041	0.002	0.054	0.001	0.014	0.003	0.053
Vanadium	0.000	0.006	0.000	0.008	0.000	0.006	0.000	0.002	0.000	0.006
Chromium	0.000	0.004	0.000	0.003	0.000	0.003	0.000	0.001	0.000	0.002
Manganese	0.001	0.013	0.001	0.015	0.001	0.020	0.001	0.009	0.001	0.014
Iron	0.024	0.491	0.023	0.629	0.043	1.005	0.043	0.477	0.054	0.831
Cobalt	0.000	0.008	0.000	0.008	0.001	0.012	0.001	0.006	0.000	0.007
Nickel	0.000	0.004	0.000	0.002	0.000	0.002	0.000	0.001	0.000	0.002
Cupper	0.001	0.011	0.002	0.041	0.001	0.029	0.007	0.079	0.002	0.036
Zinc	0.002	0.033	0.002	0.059	0.003	0.062	0.009	0.097	0.005	0.080
Gallium	0.000	0.001	0.000	0.001	0.000	0.002	0.000	0.000	0.000	0.002
Arsenic	0.000	0.002	0.000	0.004	0.000	0.001	0.000	0.003	0.000	0.002
Selenium	0.000	0.003	0.000	0.002	0.000	0.003	0.000	0.001	0.000	0.001
Bromine	0.001	0.029	0.002	0.043	0.001	0.028	0.001	0.015	0.001	0.021
Rubidium	0.000	0.003	0.000	0.003	0.000	0.002	0.000	0.003	0.000	0.003
Strontium	0.000	0.003	0.000	0.005	0.000	0.010	0.000	0.004	0.000	0.007
Yttrium	0.000	0.005	0.000	0.005	0.000	0.003	0.000	0.002	0.000	0.004
Zirconium	0.000	0.002	0.000	0.003	0.000	0.003	0.000	0.001	0.000	0.001
Molybdenum	0.000	0.003	0.000	0.006	0.000	0.007	0.000	0.002	0.000	0.002
Palladium	0.000	0.002	0.000	0.001	0.000	0.003	0.000	0.002	0.000	0.002
Silver	0.000	0.003	0.000	0.007	0.000	0.005	0.000	0.002	0.000	0.004
Cadmium	0.000	0.009	0.000	0.004	0.000	0.007	0.000	0.004	0.000	0.004
Indium	0.000	0.006	0.000	0.009	0.001	0.014	0.000	0.003	0.000	0.003
Tin	0.001	0.025	0.001	0.022	0.001	0.034	0.001	0.013	0.001	0.018
Antimony	0.001	0.025	0.001	0.022	0.001	0.022	0.001	0.009	0.001	0.012
Barium	0.008	0.161	0.005	0.125	0.006	0.131	0.007	0.083	0.006	0.087
Lanthanum	0.005	0.111	0.005	0.146	0.006	0.139	0.008	0.088	0.005	0.074
Gold	0.000	0.002	0.000	0.003	0.000	0.003	0.000	0.001	0.000	0.003
Mercury	0.000	0.002	0.000	0.002	0.000	0.003	0.000	0.001	0.000	0.002
Thallium	0.000	0.001	0.000	0.000	0.000	0.001	0.000	0.000	0.000	0.001
Lead	0.001	0.012	0.001	0.022	0.001	0.021	0.002	0.018	0.001	0.013
Uranium	0.000	0.001	0.000	0.004	0.000	0.003	0.000	0.002	0.000	0.003

12/17/03. Geological material and unidentified mass contributed more than 60% of TSP mass from 05/21/03 to 10/22/03 and less than 50% from 02/26/03 to 04/23/03 and from 12/03/03 to 12/17/03 (**Figure 3-16a**).

TSP mass concentrations at the TB site (**Figure 3-16e**), considered to be the local background site, were generally less than 5 $\mu g/m^3$ during winter and spring (11/20/02 to 04/10/03 and 11/05/03 to 12/17/03) but increased during the period from 05/07/03 to 10/22/03. The temporal variation of TSP mass concentrations observed at the TB site was similar to that observed at the BH site; however, a temporal pattern of geological and unidentified material contributions to TSP did not emerge at the TB location. **Figures 3-16c and d** confirm the expectation of higher PM concentrations in South Lake Tahoe. These figures show that similar temporal trends and comparable TSP mass concentrations were observed at the SOLA and SW sites. **Figure 3-16b** shows that, if the sample collected on 12/04/02 (sampling period 2, 82 $\mu g/m^3$) is excluded, PM concentrations at Lake Forest were generally lower than South Lake Tahoe. TSP mass concentration decreases from > 25 $\mu g/m^3$ in January to 10 $\mu g/m^3$ in March and April, with a slight increase to 15 $\mu g/m^3$ in summer and fall (05/07/03 to 11/19/03). In general, TSP mass concentrations observed at the LF, SOLA, and SW sites were approximately two to three times greater than those observed at the BH and LF sites.

For TSP, in addition to geological and unidentified material, organic matter (OC) and soot (EC) were the second and the third largest chemical species that contributed to the temporal variation observed at the sites. (Note: OC concentrations were multiplied by 1.2 to correct for pyrolysis of organic carbon compounds to elemental carbon. Without this correction, the organic carbon fraction of the sample would be underestimated and the elemental carbon fraction would be overestimated by including some pyrolyzed organic carbon. (DRI, 2000)) Contributions of organic matter and soot to TSP mass concentration increased at the SOLA and SW sites during the period from 11/20/02 to 03/12/03, which was likely the result of wood smoke and increased traffic volume for winter sport activities in the vicinity of the SOLA and SW sites. PM10 composed > 80% of TSP at the five sites in LTADS. **Figures 3-16 and 3-17** show that the temporal and spatial variations of PM10 mass concentrations, geological material, organic matter, and soot are similar to those of TSP.

Figure 3-18 shows the very large OC contribution to PM2.5 at all sites. No clear temporal variation of PM2.5 mass concentration (**Figure 3-18a**) was observed at the BH site. The PM2.5 mass concentrations at the TB site were generally < 3 $\mu g/m^3$ for measurements prior to 04/10/03, and increased by 50% or more from 05/07/03 to 10/08/03. Significant increases in PM2.5 mass concentrations (8-15 $\mu g/m^3$) were observed at the SOLA and SW sites from 11/20/02 to 02/26/03. This increase was due to the increased organic matter and EC concentrations, which were twice as high as those measured at the TB site. Concentrations of geological material in PM2.5 were similar at all five sites and temporal variation was not observed. Organic matter and EC contributed approximately 80% of PM2.5 mass at the SOLA and SW sites from 11/20/02 to 02/26/03.

Figure 3-13a. PM Size Contributions to Total Mass Observed with the TWS at Big Hill.

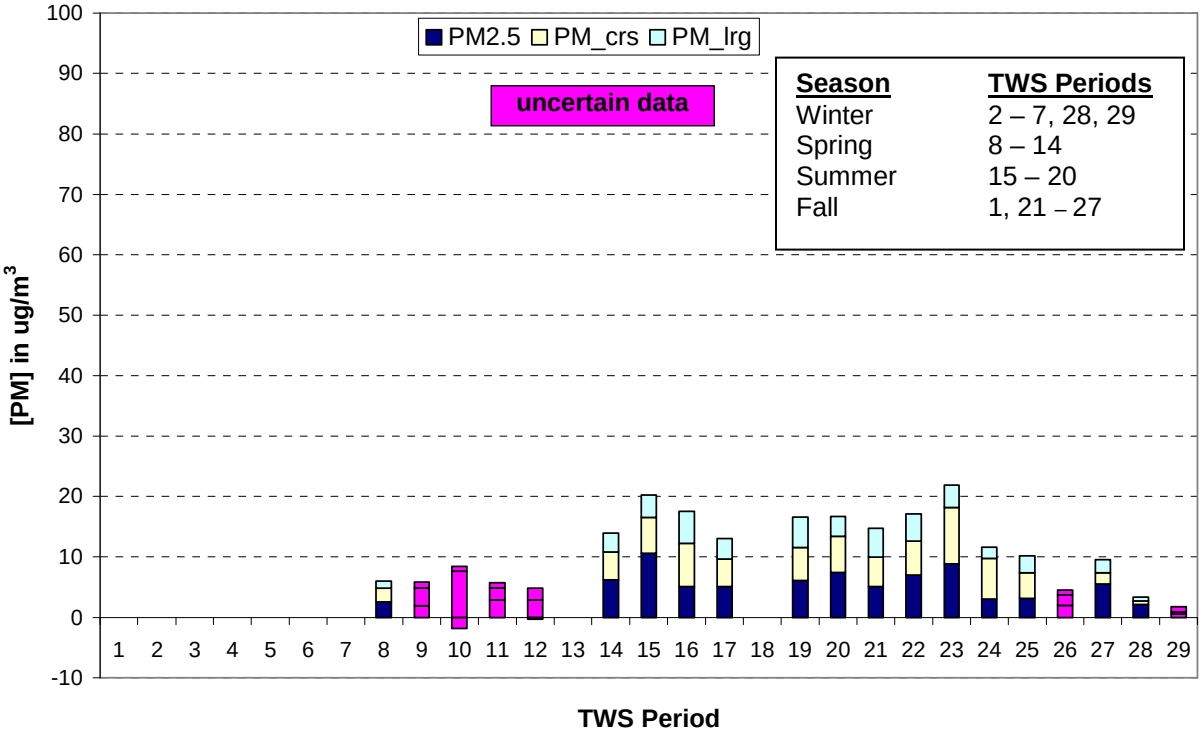

Figure 3-13b. PM Size Contributions to Total Mass Observed with the TWS at SLT-Sandy Way**.**

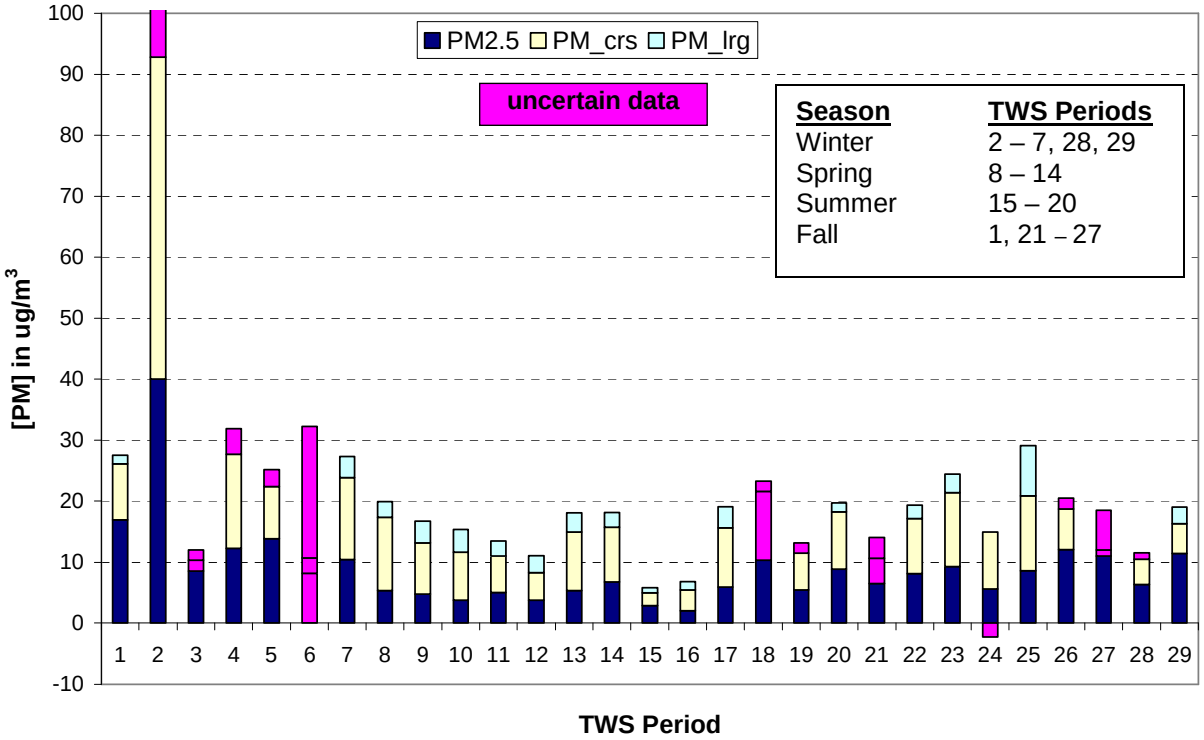

Figure 3-13c. PM Size Contributions to Total Mass Observed with the TWS at SLT-SOLA.

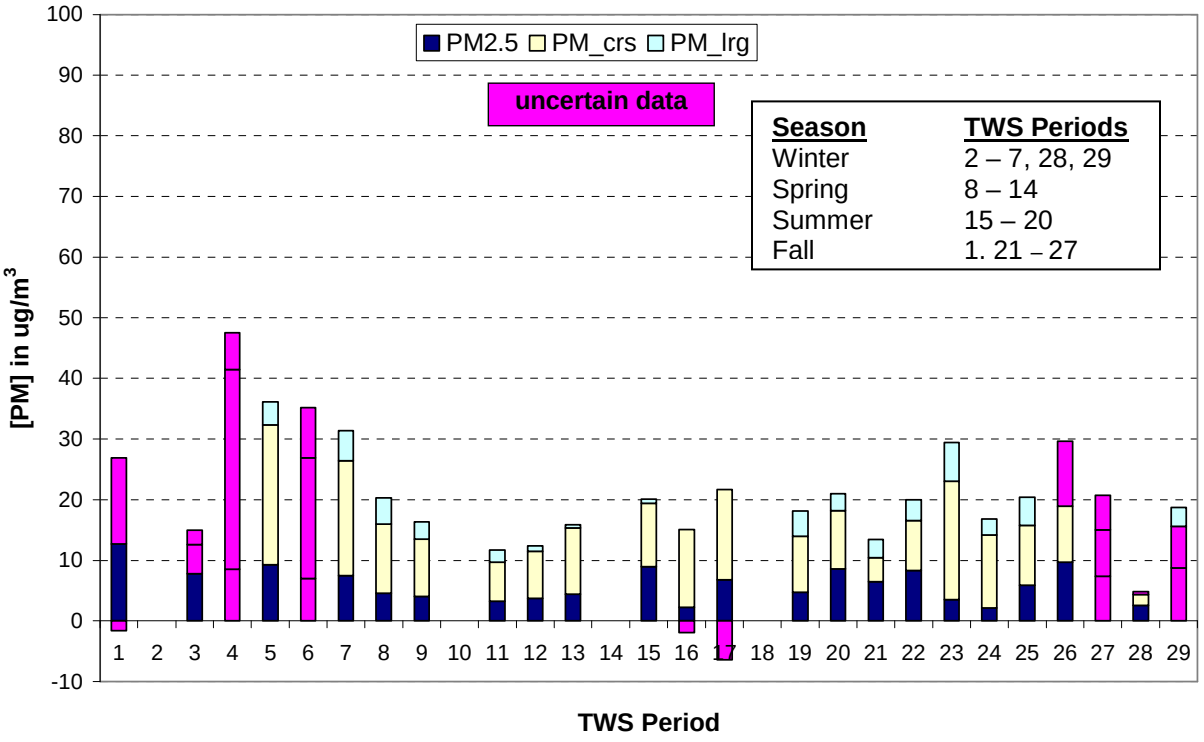

Figure 3-13d. PM Size Contributions to Total Mass Observed with the TWS at Thunderbird Lodge.

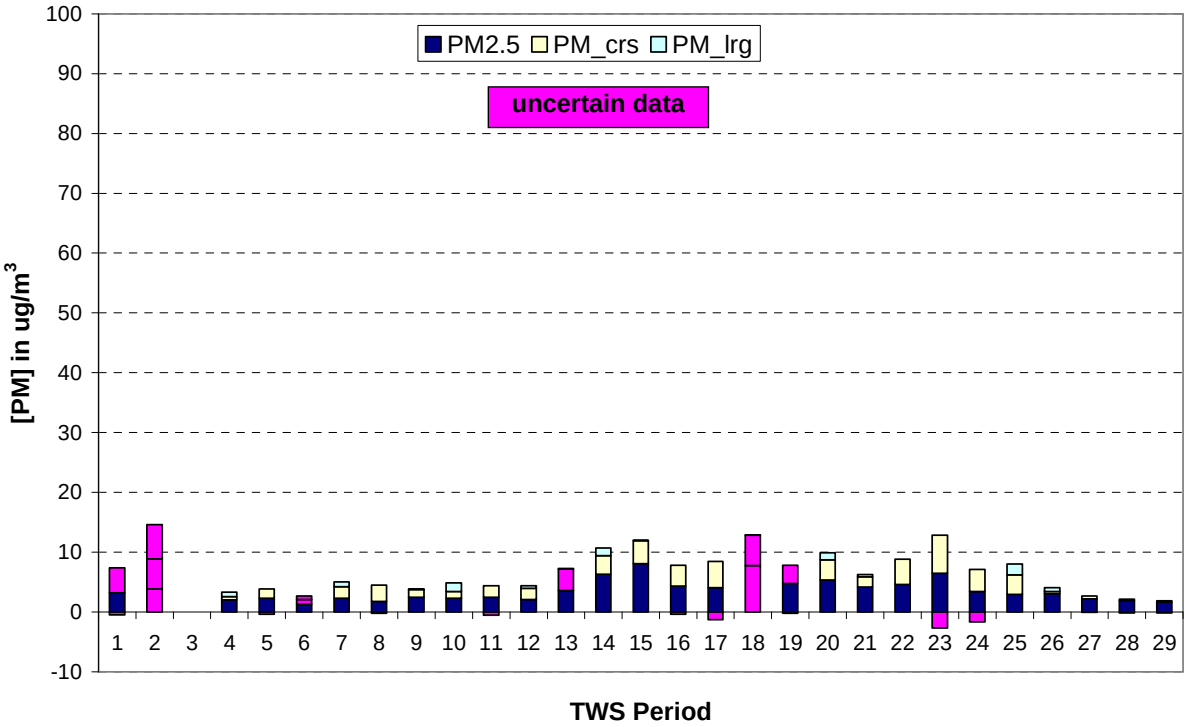

Figure 3-13e. PM Size Contributions to Total Mass Observed with the TWS at Lake Forest.

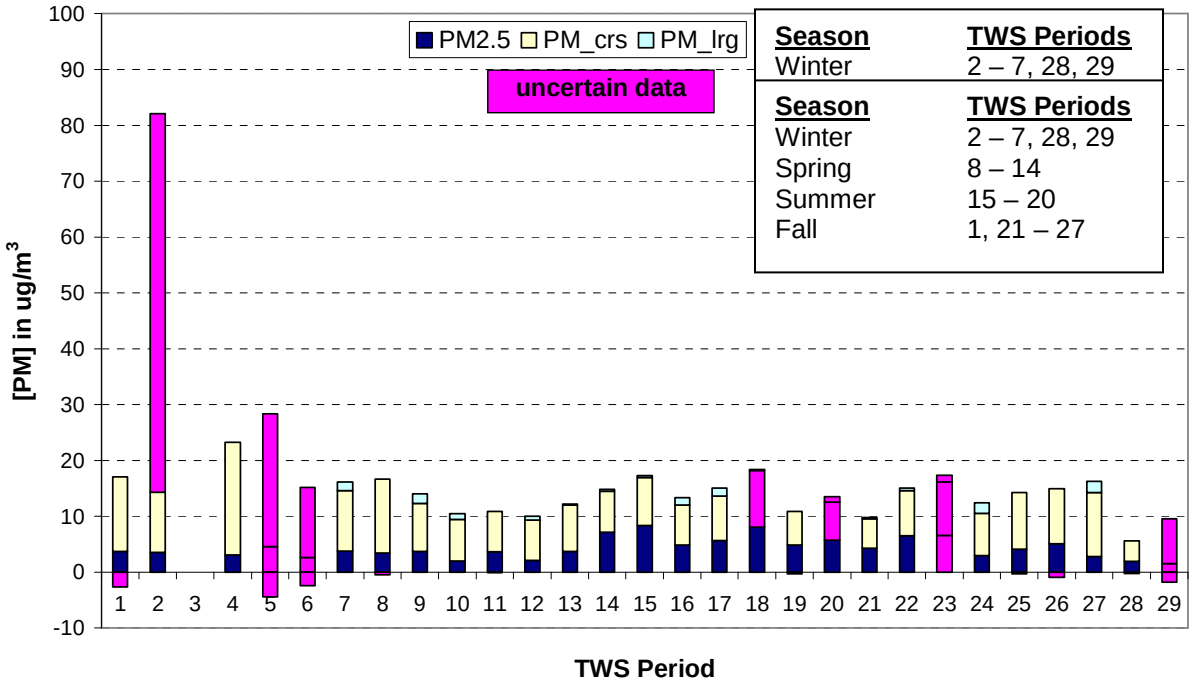

Figure 3-14a. PM Size Contributions to Nitrate Observed with the TWS at Big Hill.

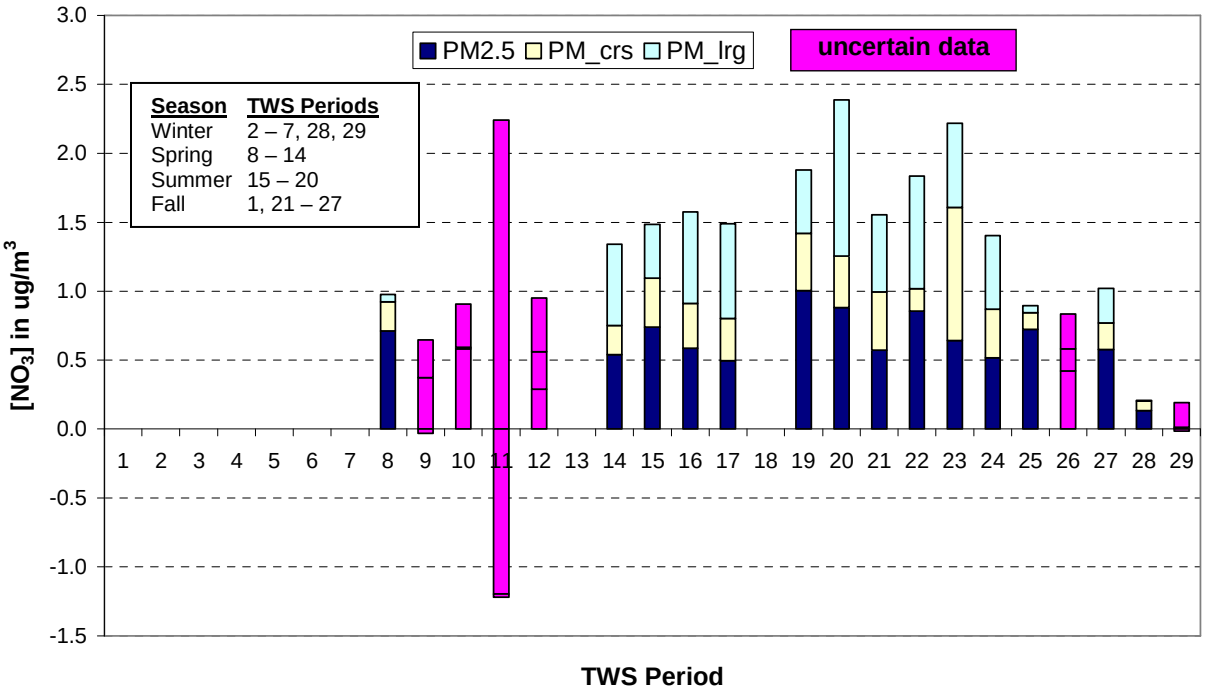

Figure 3-14b. PM Size Contributions to Nitrate Concentrations Observed with the TWS at SLT-Sandy Way.

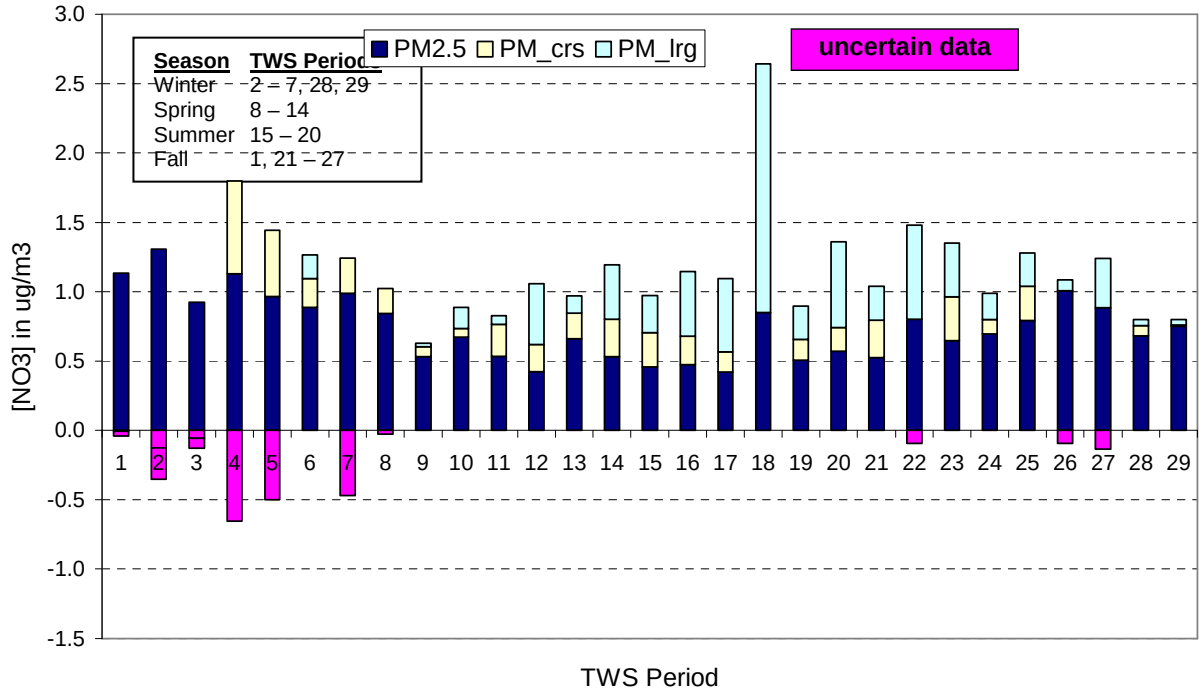

Figure 3-14c. PM Size Contributions to Nitrate Concentrations Observed with the TWS at SLT-SOLA.

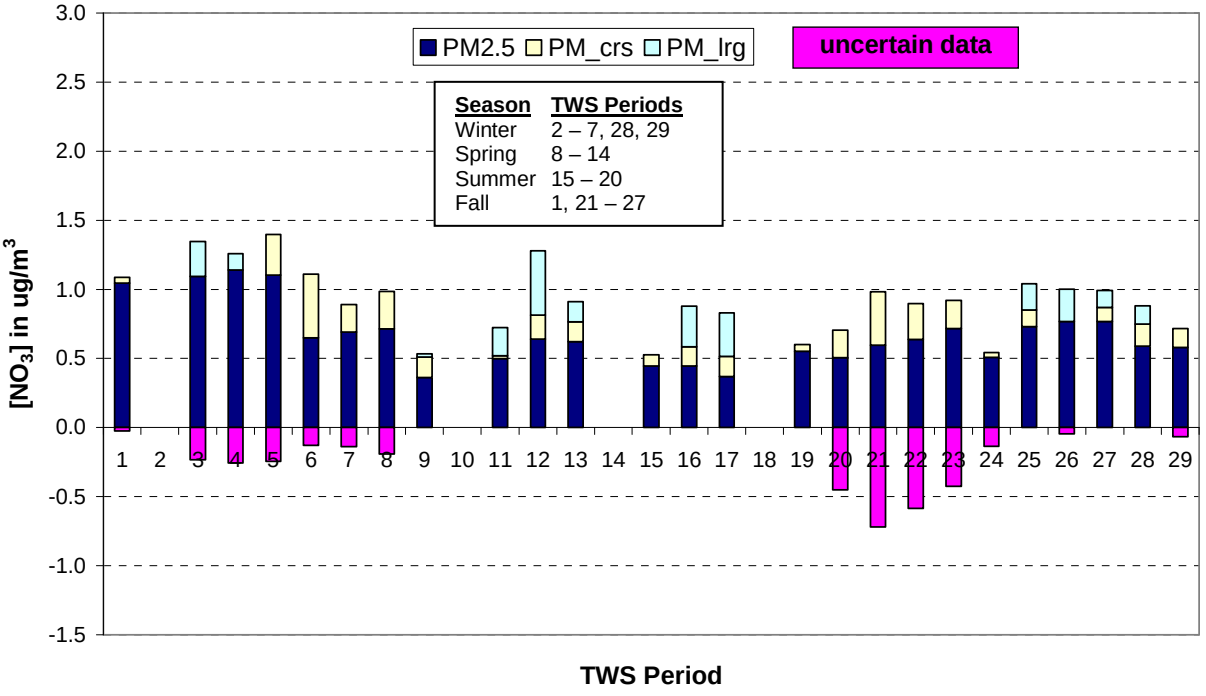

Figure 3-14d. PM Size Contributions to Nitrate Concentrations Observed with the TWS at Thunderbird Lodge.

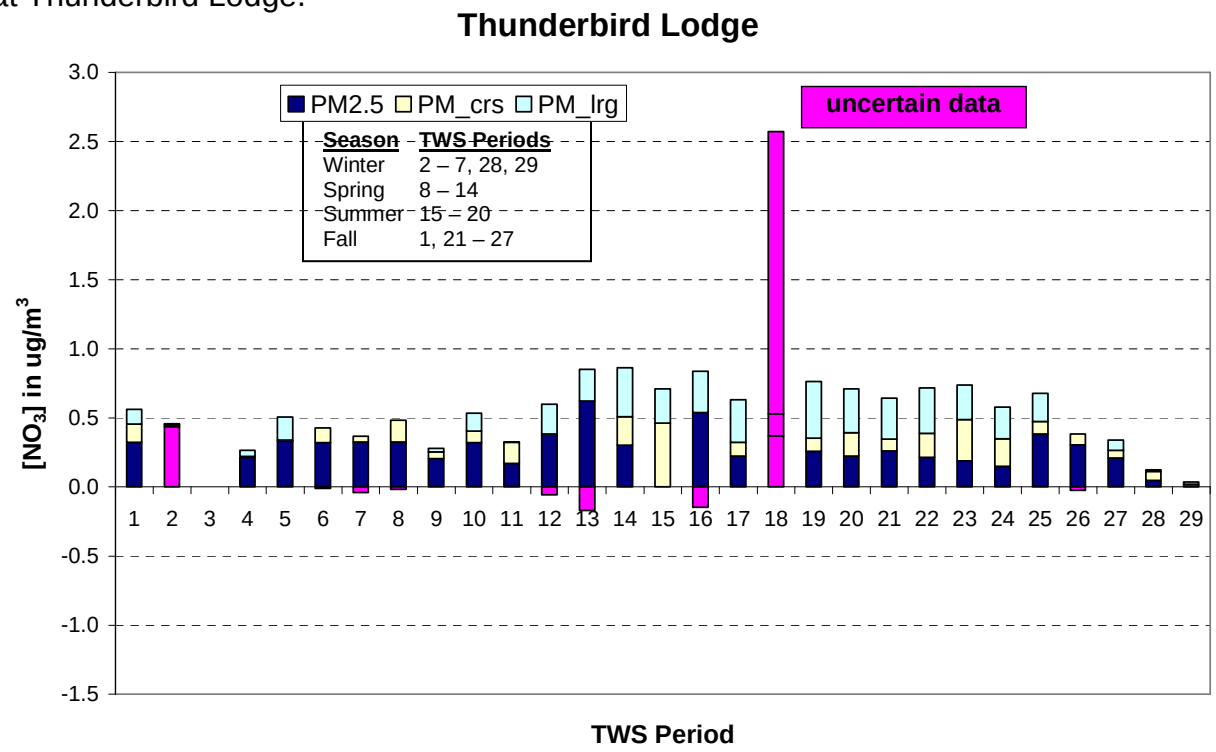

Figure 3-14e. PM Size Contributions to Nitrate Concentrations Observed with the TWS at Lake Forest.

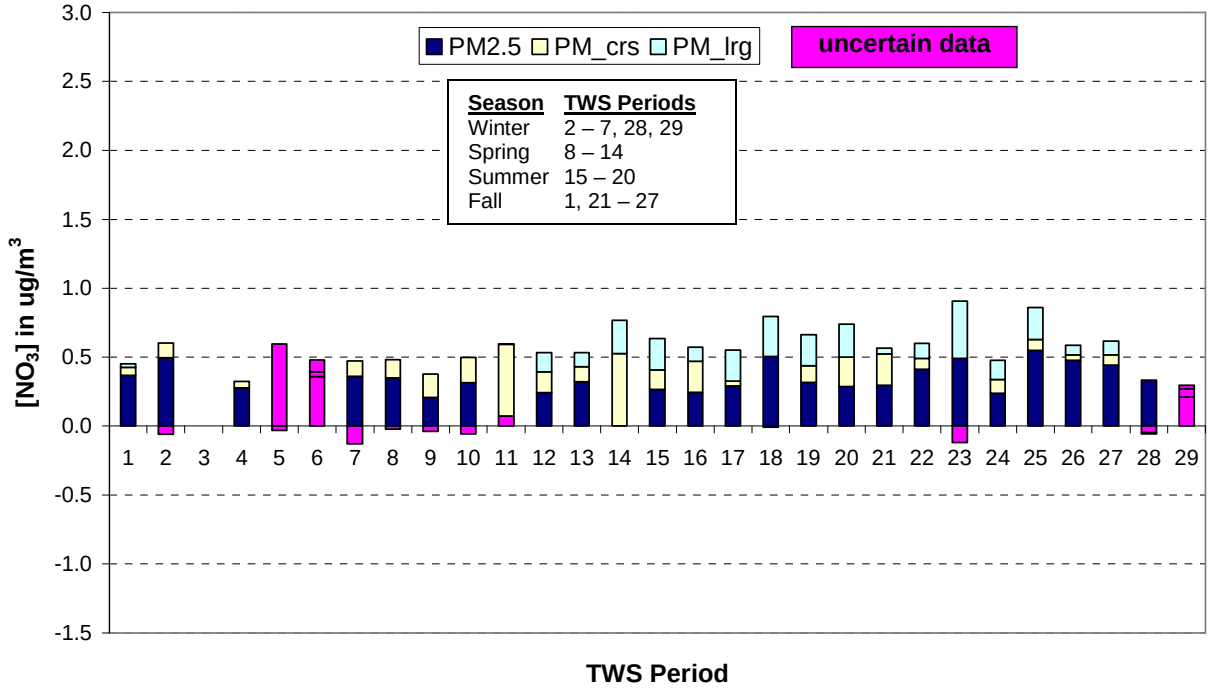

Figure 3-15a. PM Size Contributions to Ammonium Concentrations Observed with the TWS at Big Hill.

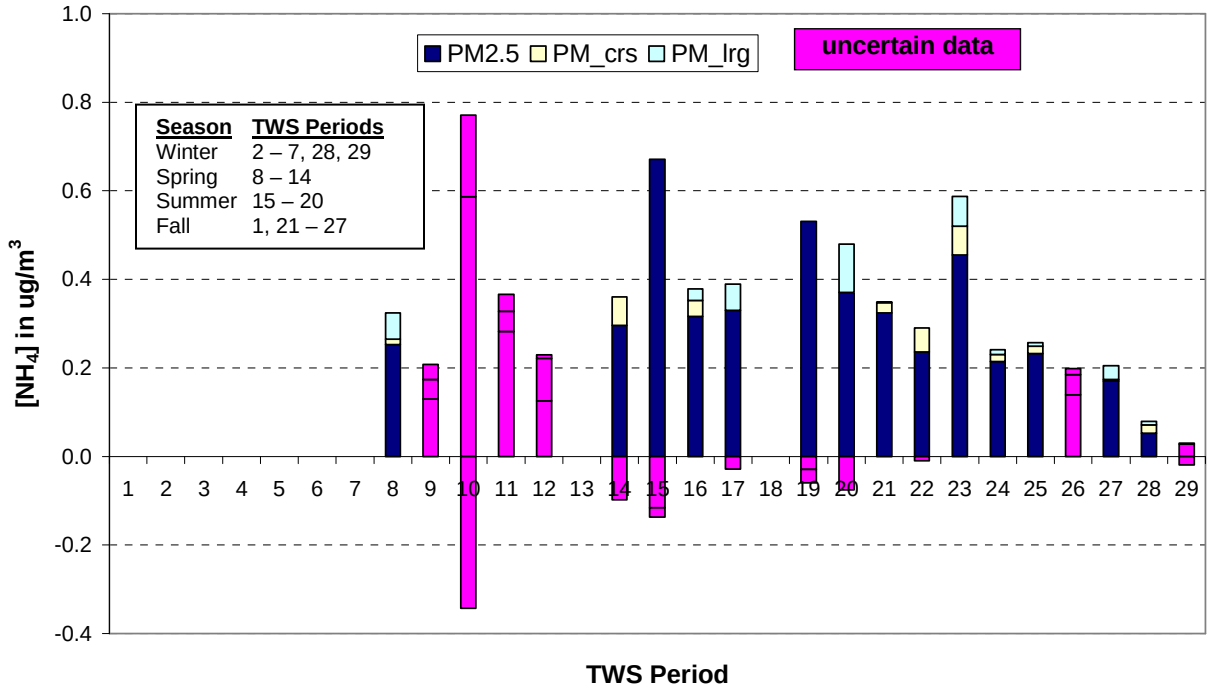

Figure 3-15b. PM Size Contributions to Ammonium Concentrations Observed with the TWS at SLT-Sandy Way.

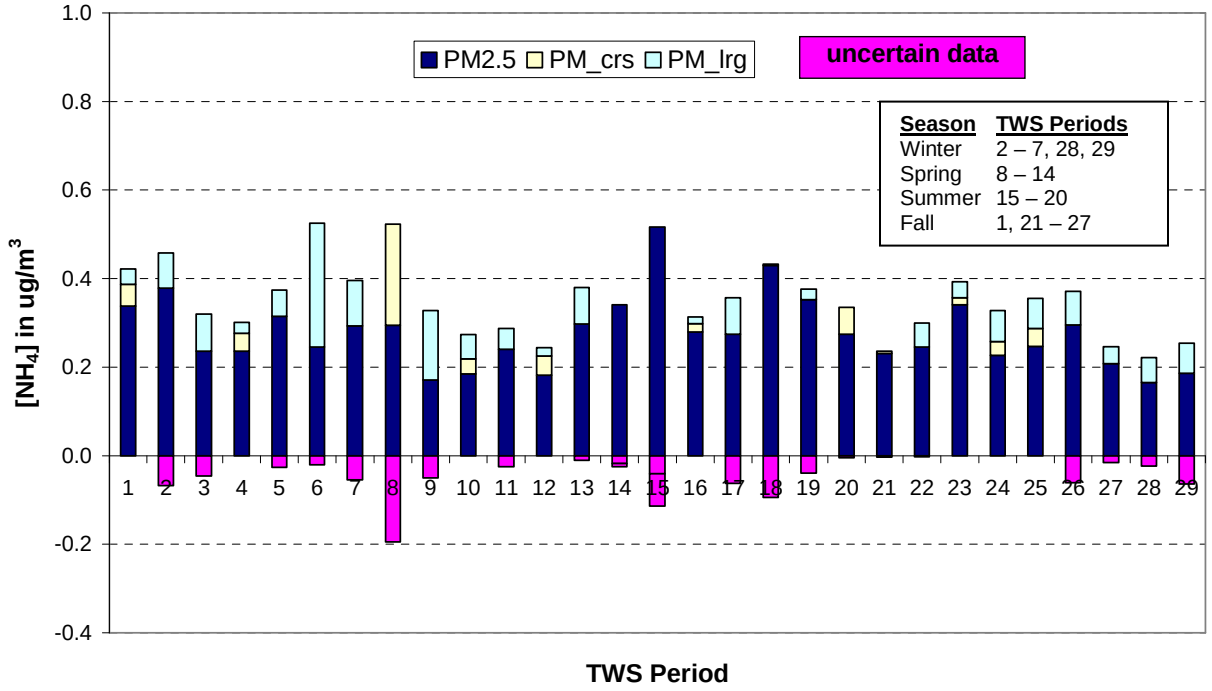

Figure 3-15c. PM Size Contributions to Ammonium Concentrations Observed with the TWS at SLT-SOLA.

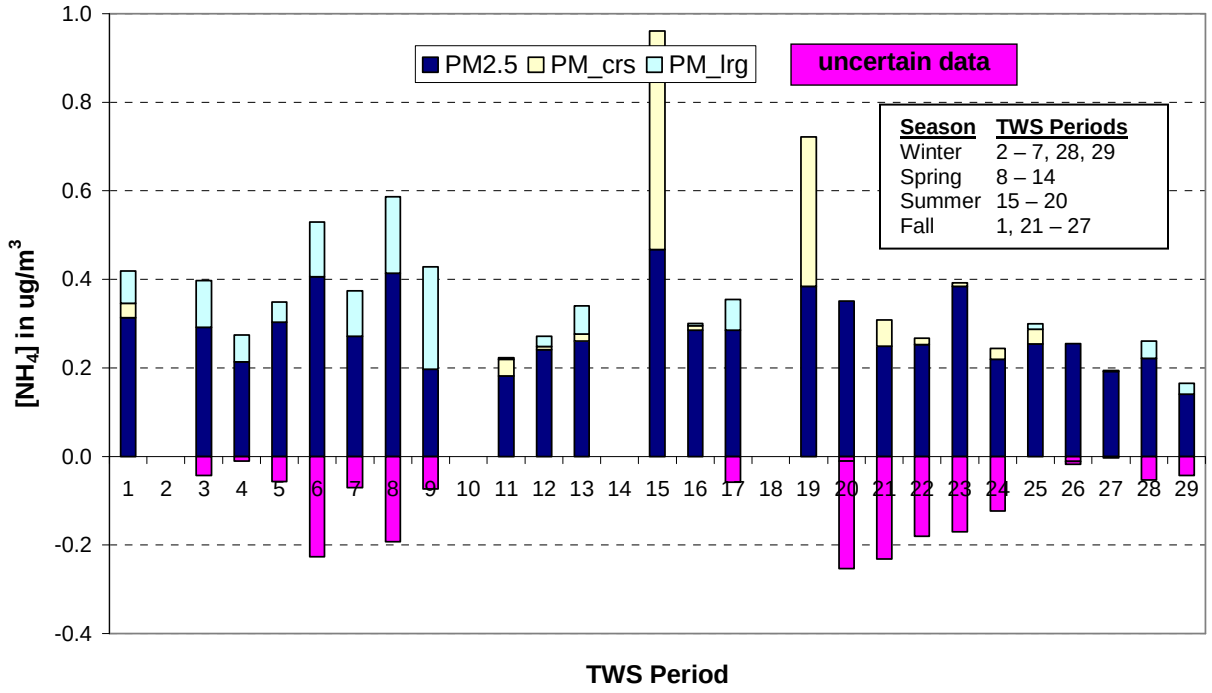

Figure 3-15d. PM Size Contributions to Ammonium Concentrations Observed with the TWS at Thunderbird Lodge.

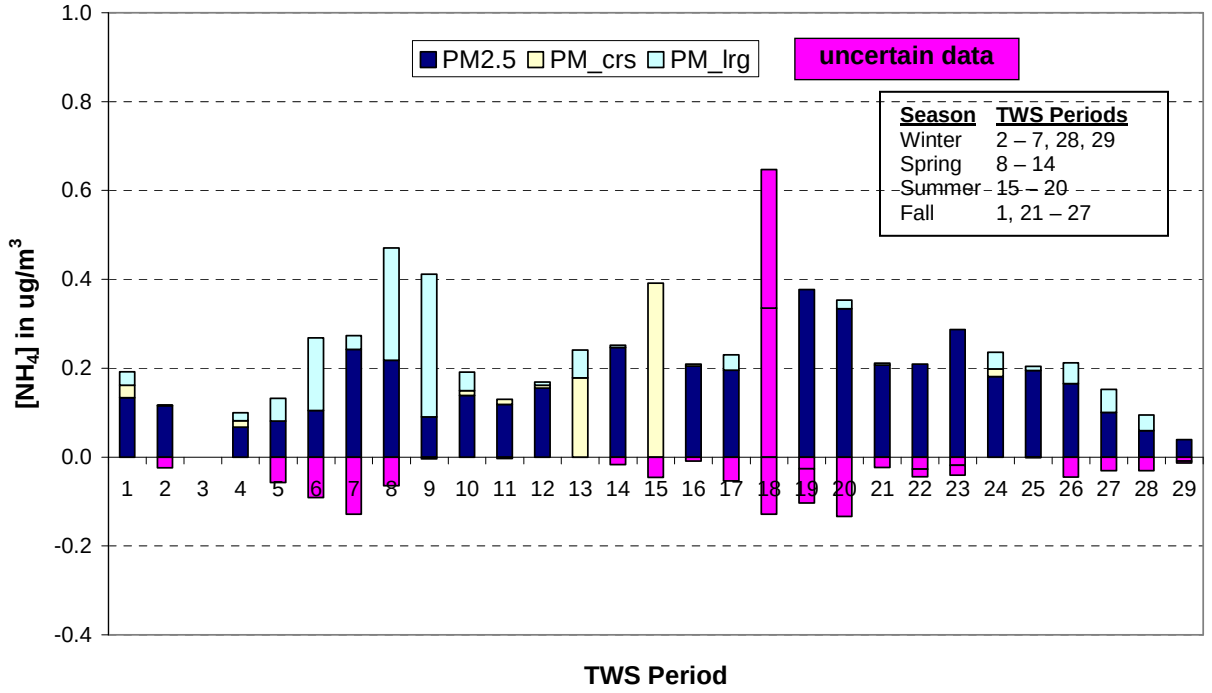

Figure 3-15e. PM Size Contributions to Ammonium Concentrations Observed with the TWS at Lake Forest.

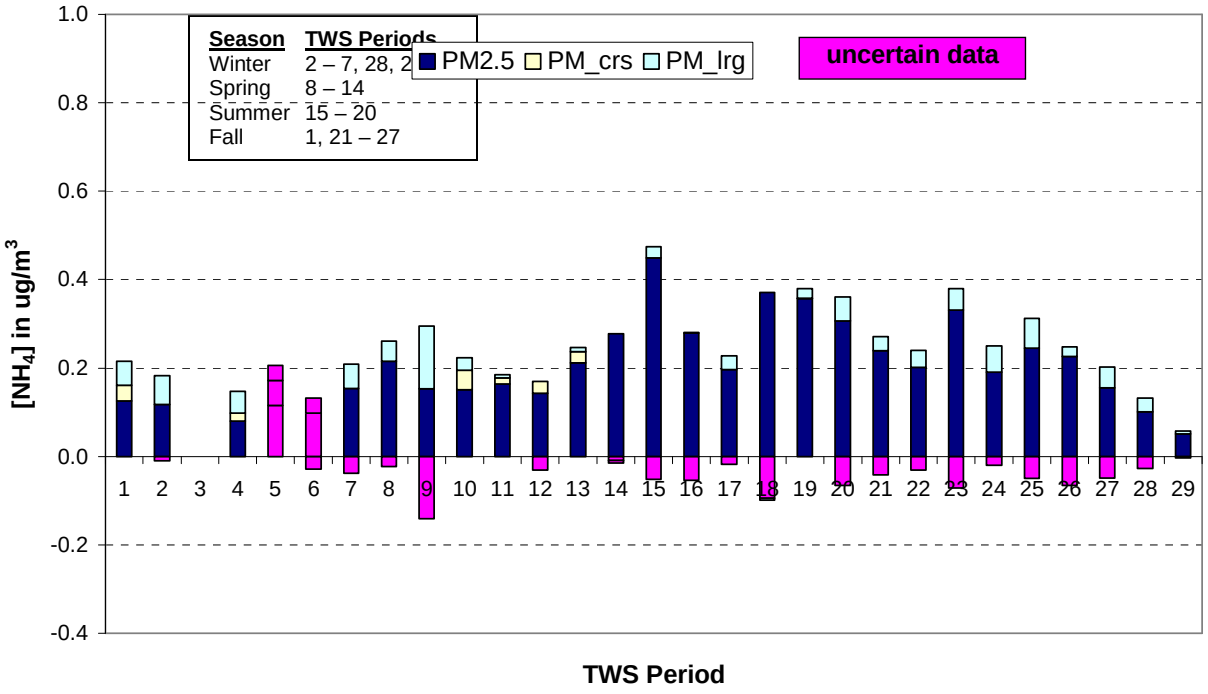

Figure 3-16. Time Series Plots of Contribution of Each Major Chemical Component to Fractional TSP Mass at a) Big HIll, b) Lake Forest, c) Sandy Way, d) SOLA, and e) Thunderbird.

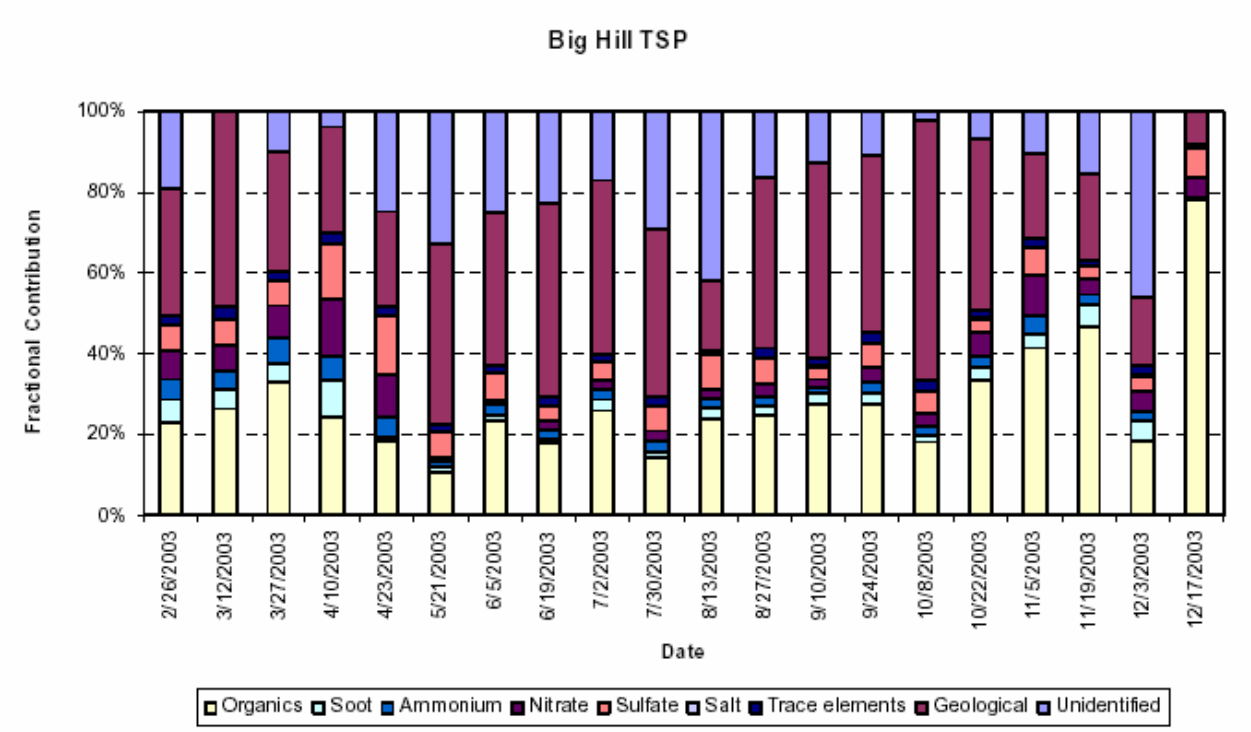

(a)

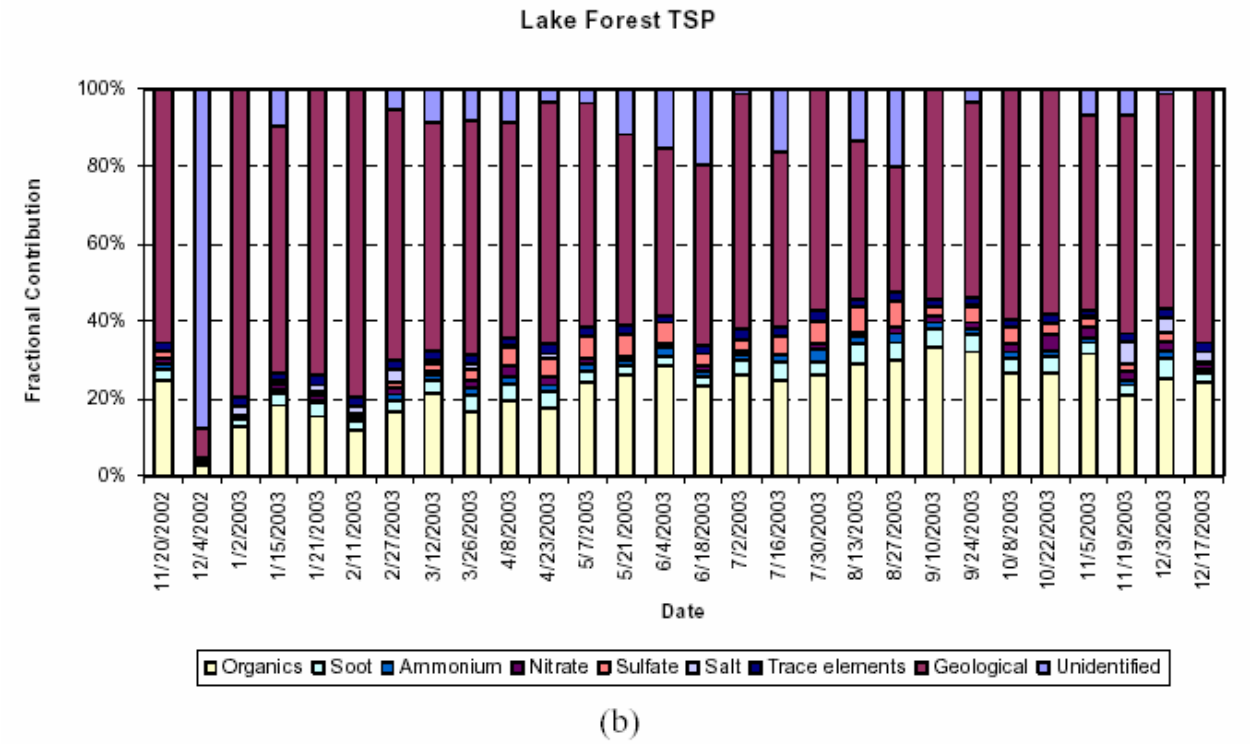

(b)

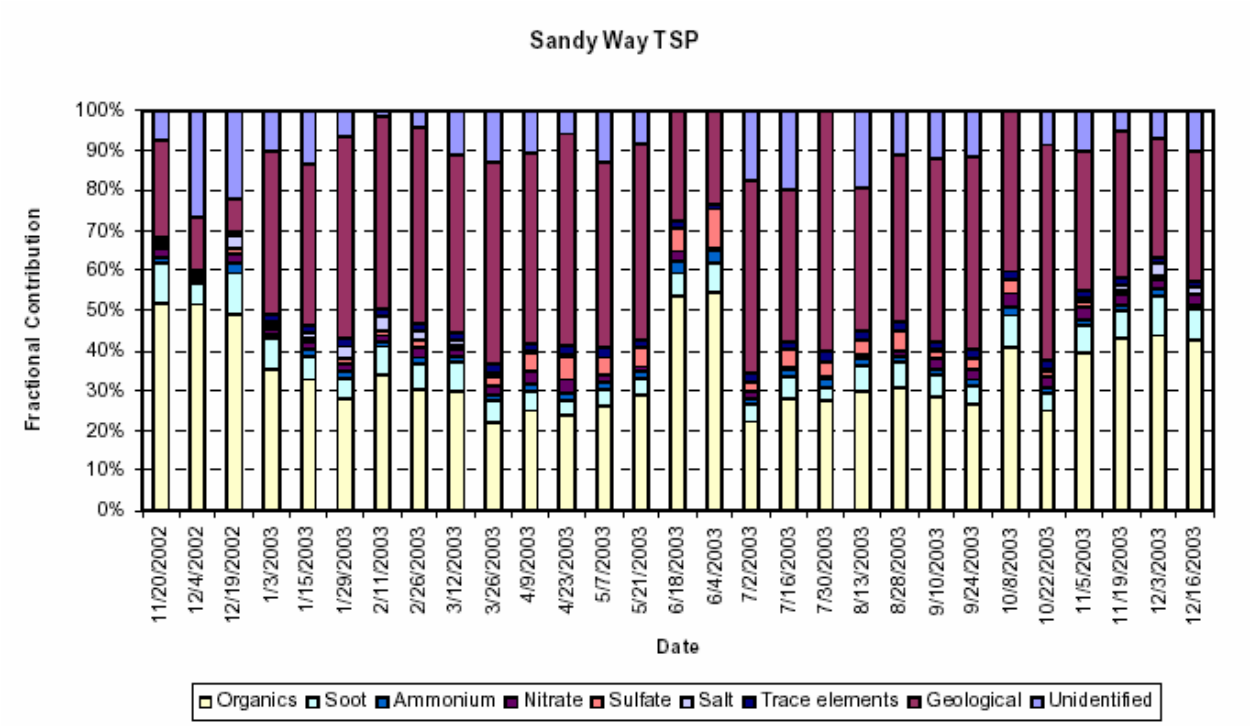
Sandy Way TSP
Fractional Contribution
100%
90%
80%
70%
60%
50%
40%
30%
20%
10%
0%
11/20/2002
12/4/2002
12/19/2002
1/3/2003
1/15/2003
1/29/2003
2/11/2003
2/26/2003
3/12/2003
3/26/2003
4/9/2003
4/23/2003
5/7/2003
5/21/2003
6/18/2003
6/4/2003
7/2/2003
7/16/2003
7/30/2003
8/13/2003
8/28/2003
9/10/2003
9/24/2003
10/8/2003
10/22/2003
11/5/2003
11/19/2003
12/3/2003
12/16/2003
Date
Organics
Soot
Ammonium
Nitrate
Sulfate
Salt
Trace elements
Geological
Unidentified

(c)

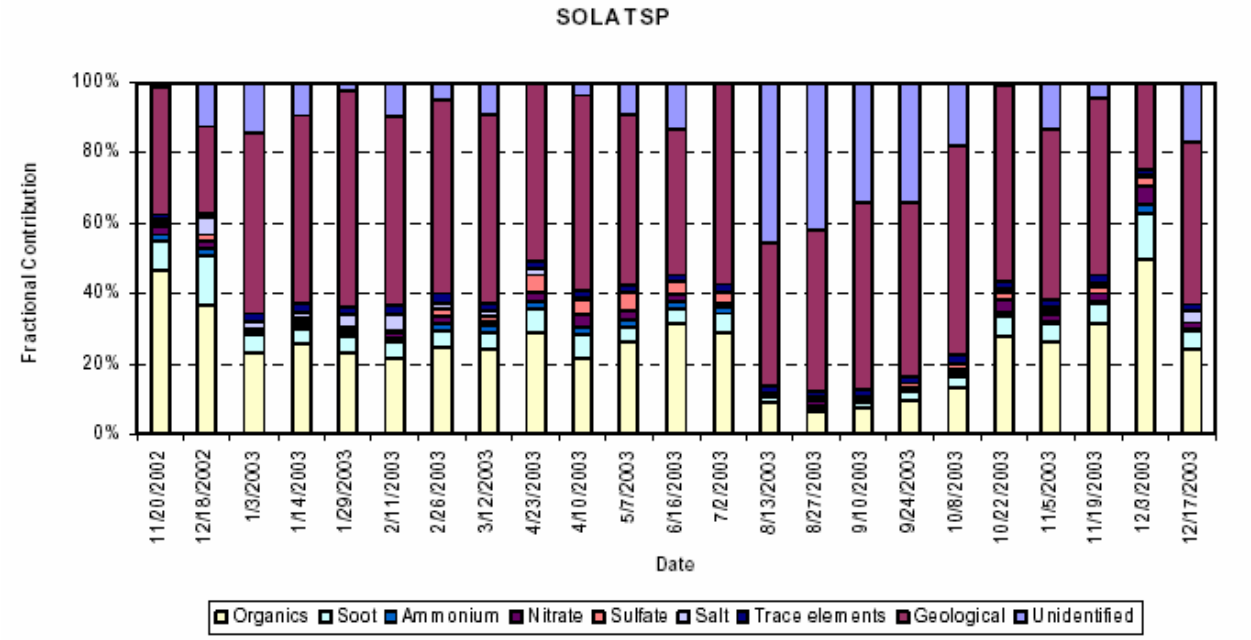
SOLA TSP
Fractional Contribution
100%
80%
60%
40%
20%
0%
11/20/2002
12/18/2002
1/3/2003
1/14/2003
1/29/2003
2/11/2003
2/26/2003
3/12/2003
4/23/2003
4/10/2003
5/7/2003
6/16/2003
7/2/2003
8/13/2003
8/27/2003
9/10/2003
9/24/2003
10/8/2003
10/22/2003
11/5/2003
11/19/2003
12/3/2003
12/17/2003
Date
Organics
Soot
Ammonium
Nitrate
Sulfate
Salt
Trace elements
Geological
Unidentified

(d)

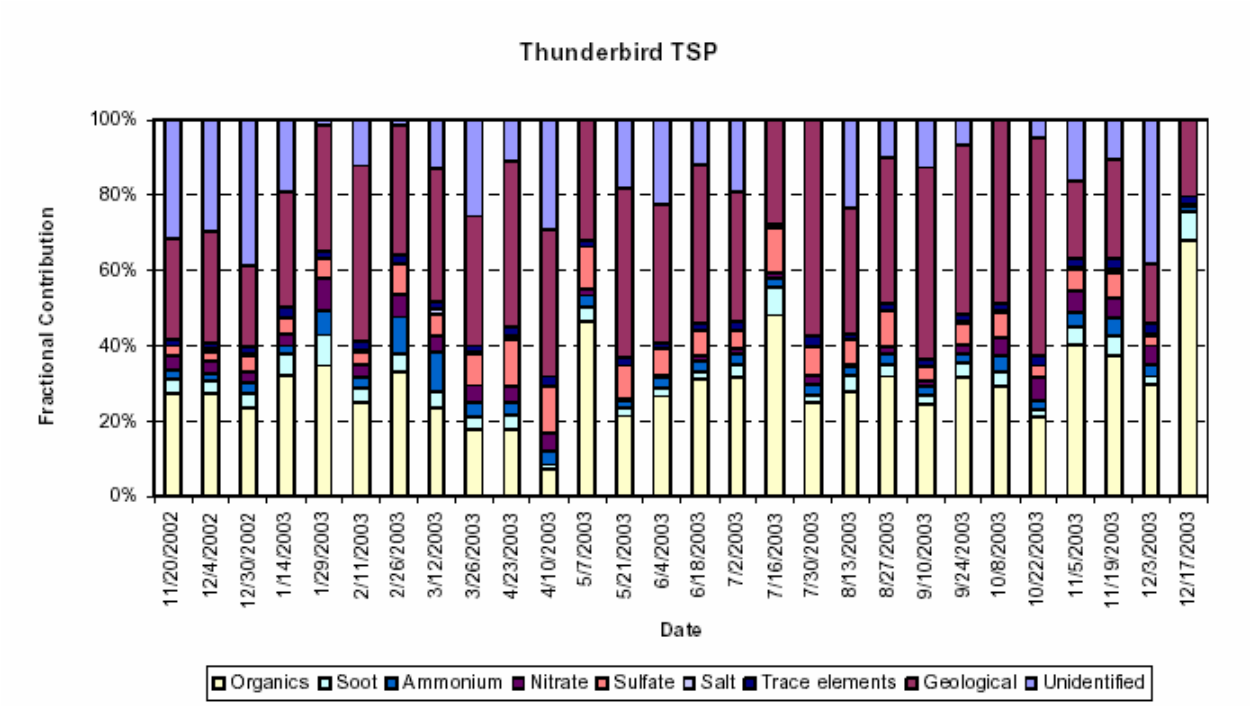
Thunderbird TSP
Fractional Contribution
100%
80%
60%
40%
20%
0%
11/20/2002
12/4/2002
12/30/2002
1/14/2003
1/29/2003
2/11/2003
2/26/2003
3/12/2003
3/26/2003
4/23/2003
4/10/2003
5/7/2003
5/21/2003
6/4/2003
6/18/2003
7/2/2003
7/16/2003
7/30/2003
8/13/2003
8/27/2003
9/10/2003
9/24/2003
10/8/2003
10/22/2003
11/5/2003
11/19/2003
12/3/2003
12/17/2003
Date
Organics
Soot
Ammonium
Nitrate
Sulfate
Salt
Trace elements
Geological
Unidentified

(e)

Figure 3-17. Time Series Plots of Contribution of Each Major Chemical Component to Fractional PM10 Mass at a) Big Hill, b) Lake Forest, c) Sandy Way, d) SOLA, and e) Thunderbird.

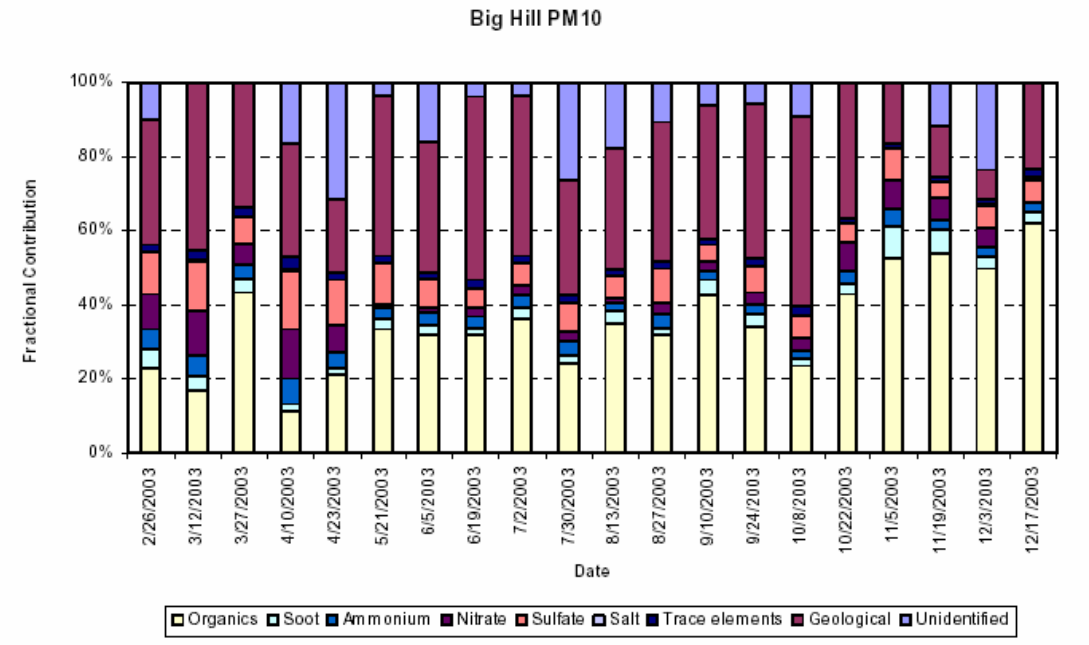

(a)

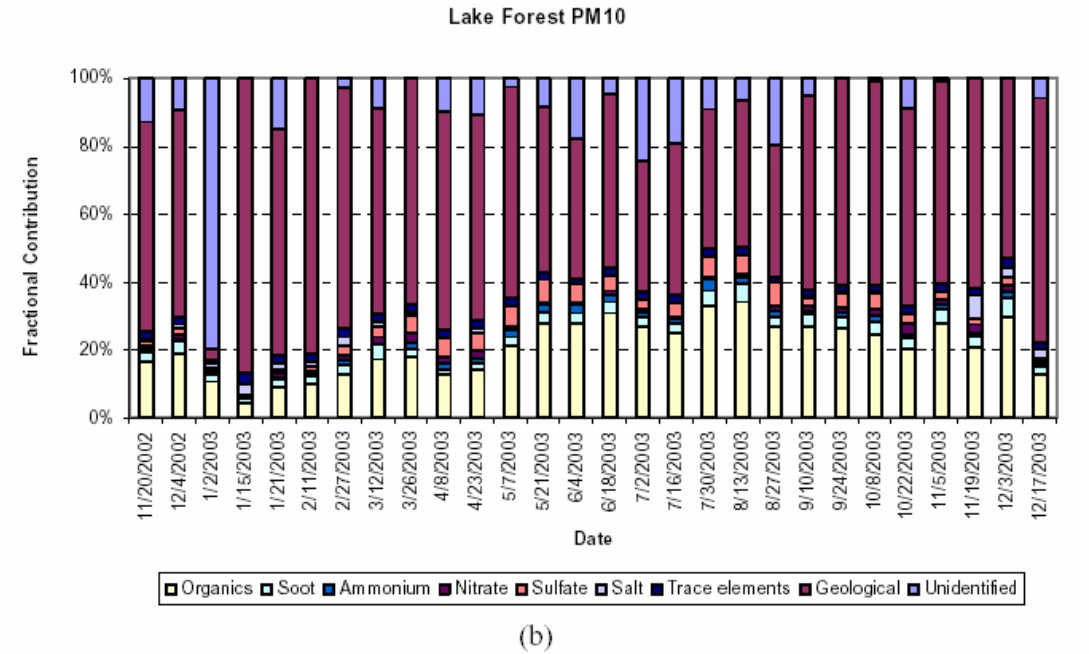

(b)

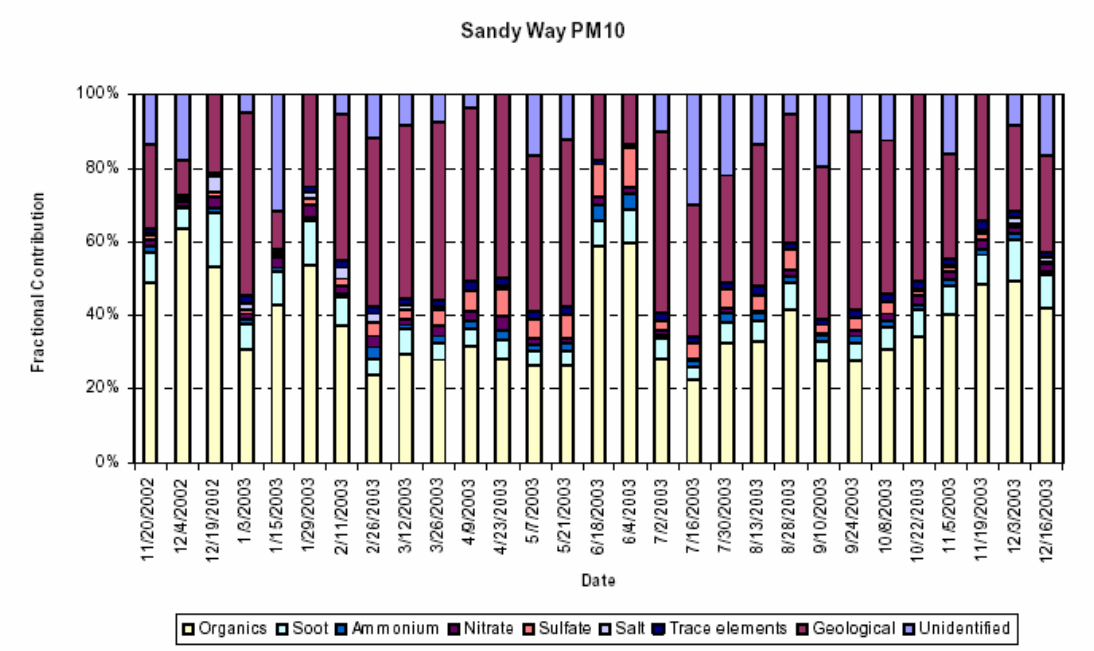
Sandy Way PM10
Fractional Contribution
100%
80%
60%
40%
20%
0%
11/20/2002
12/4/2002
12/19/2002
1/3/2003
1/15/2003
1/29/2003
2/11/2003
2/26/2003
3/12/2003
3/26/2003
4/9/2003
4/23/2003
5/7/2003
5/21/2003
6/18/2003
6/4/2003
7/2/2003
7/16/2003
7/30/2003
8/13/2003
8/28/2003
9/10/2003
9/24/2003
10/8/2003
10/22/2003
11/5/2003
11/19/2003
12/3/2003
12/16/2003
Date
Organics
Soot
Ammonium
Nitrate
Sulfate
Salt
Trace elements
Geological
Unidentified

(c)

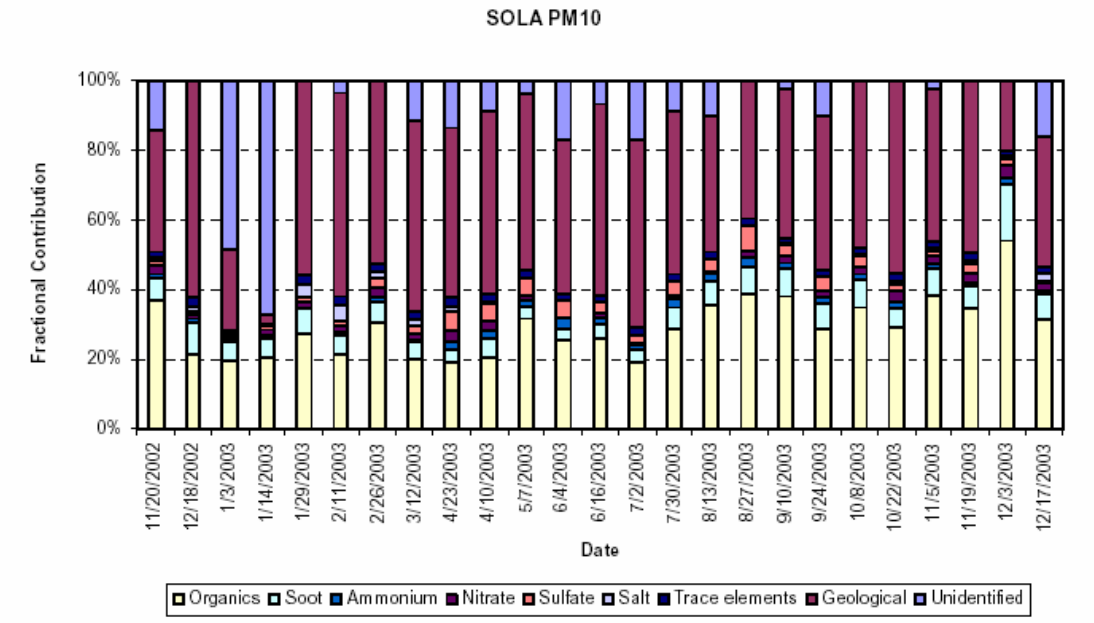
SOLA PM10
Fractional Contribution
100%
80%
60%
40%
20%
0%
11/20/2002
12/18/2002
1/3/2003
1/14/2003
1/29/2003
2/11/2003
2/26/2003
3/12/2003
4/23/2003
4/10/2003
5/7/2003
6/4/2003
6/16/2003
7/2/2003
7/30/2003
8/13/2003
8/27/2003
9/10/2003
9/24/2003
10/8/2003
10/22/2003
11/5/2003
11/19/2003
12/3/2003
12/17/2003
Date
Organics
Soot
Ammonium
Nitrate
Sulfate
Salt
Trace elements
Geological
Unidentified

(d)

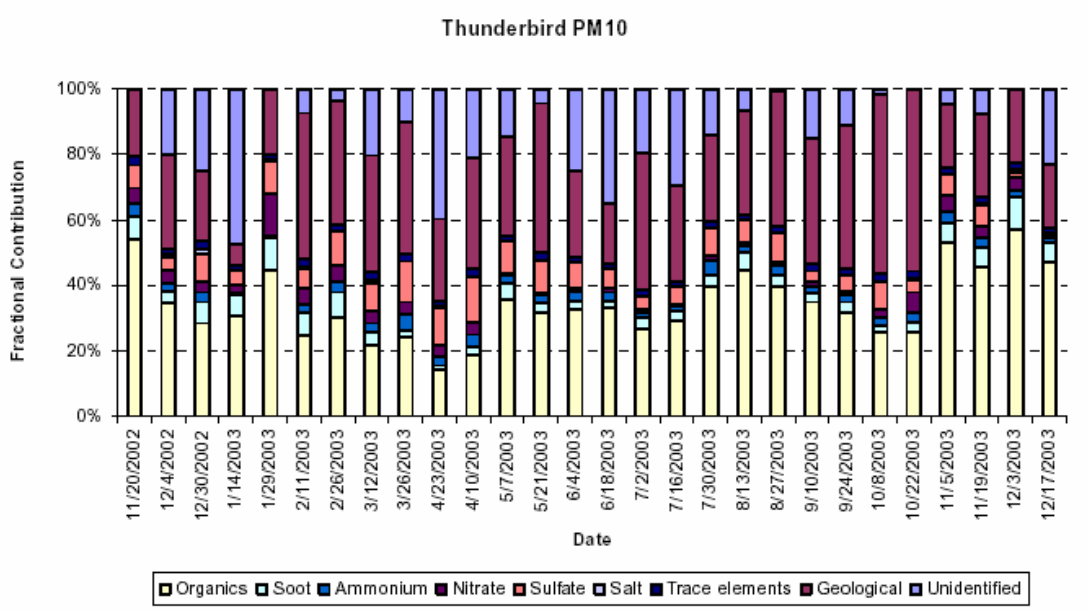
Thunderbird PM10
Fractional Contribution
100%
80%
60%
40%
20%
0%
11/20/2002
12/4/2002
12/30/2002
1/14/2003
1/29/2003
2/11/2003
2/26/2003
3/12/2003
3/26/2003
4/23/2003
4/10/2003
5/7/2003
5/21/2003
6/4/2003
6/18/2003
7/2/2003
7/16/2003
7/30/2003
8/13/2003
8/27/2003
9/10/2003
9/24/2003
10/8/2003
10/22/2003
11/5/2003
11/19/2003
12/3/2003
12/17/2003
Date
Organics
Soot
Ammonium
Nitrate
Sulfate
Salt
Trace elements
Geological
Unidentified

(e)

Figure 3-18. Time Series Plots of Contribution of Each Major Chemical Component to Fractional PM2.5 Mass at a) Big Hill, b) Lake Forest, c) Sandy Way, d) SOLA, and e) Thunderbird.

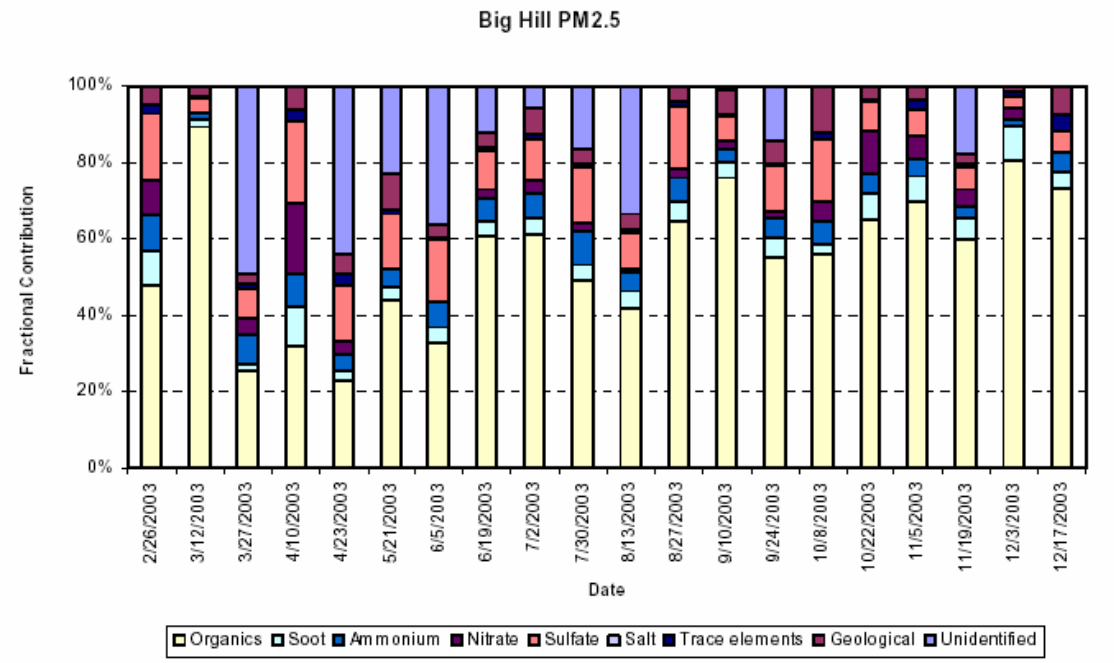

(a)

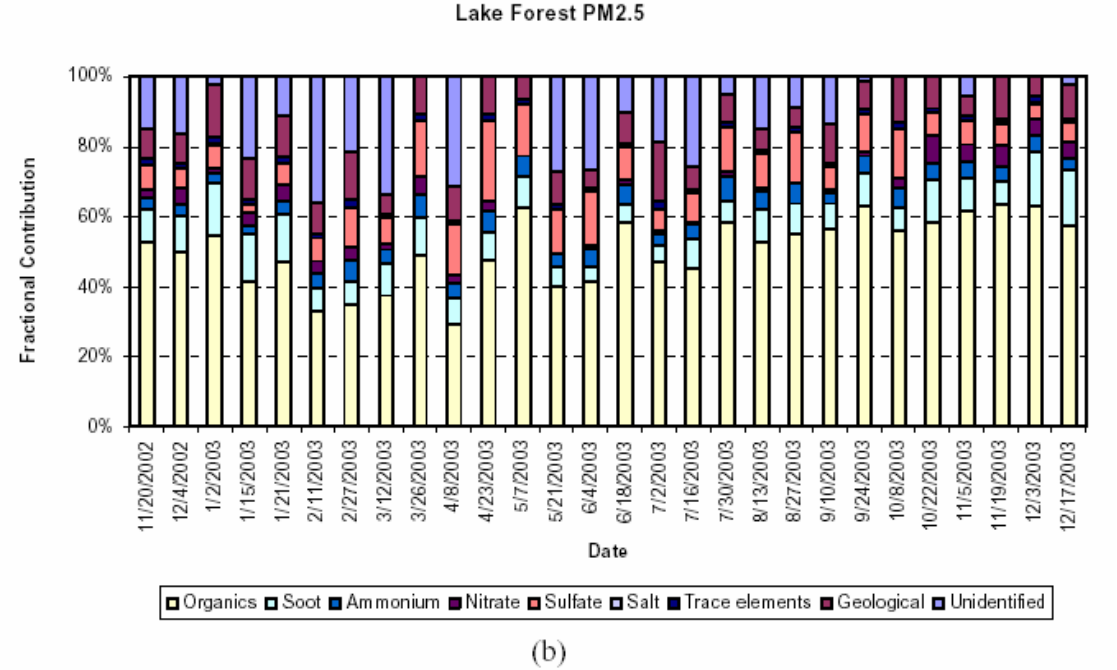

(b)

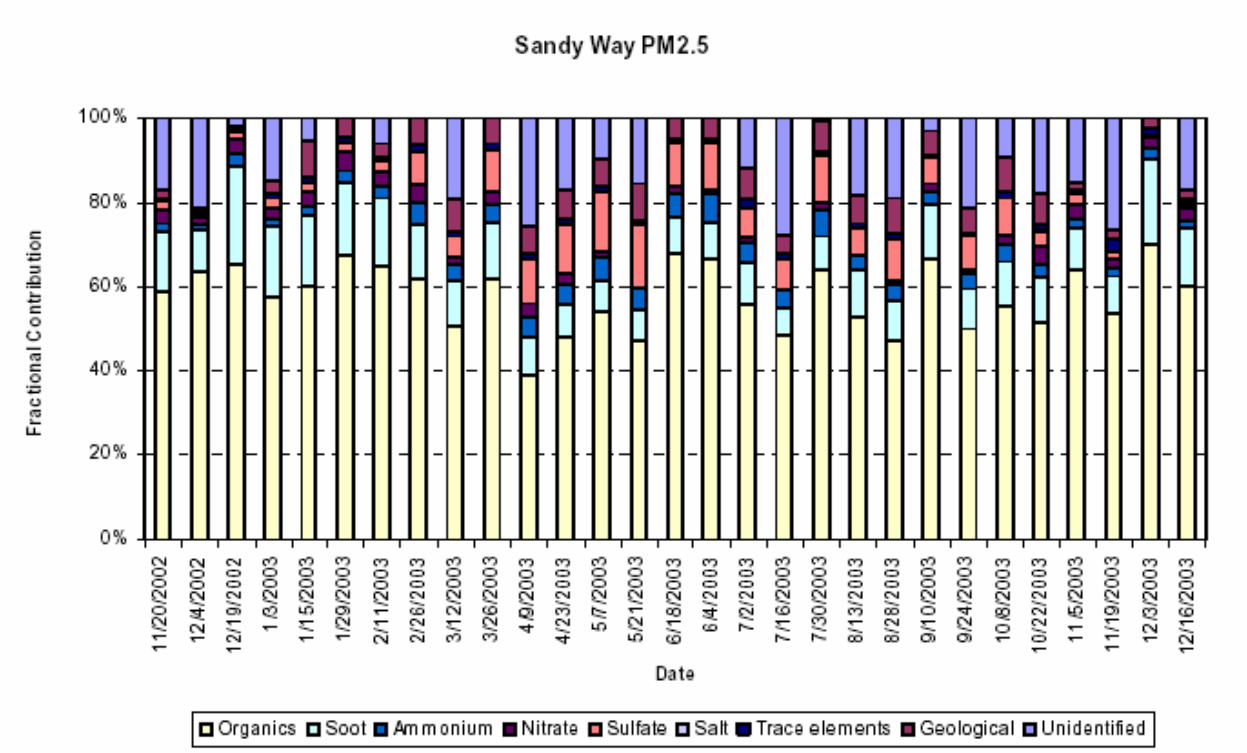
Sandy Way PM2.5
Fractional Contribution
100%
80%
60%
40%
20%
0%
11/20/2002
12/4/2002
12/19/2002
1/3/2003
1/15/2003
1/29/2003
2/11/2003
2/26/2003
3/12/2003
3/26/2003
4/9/2003
4/23/2003
5/7/2003
5/21/2003
6/18/2003
6/4/2003
7/2/2003
7/16/2003
7/30/2003
8/13/2003
8/28/2003
9/10/2003
9/24/2003
10/8/2003
10/22/2003
11/5/2003
11/19/2003
12/3/2003
12/16/2003
Date
Organics
Soot
Ammonium
Nitrate
Sulfate
Salt
Trace elements
Geological
Unidentified

(c)

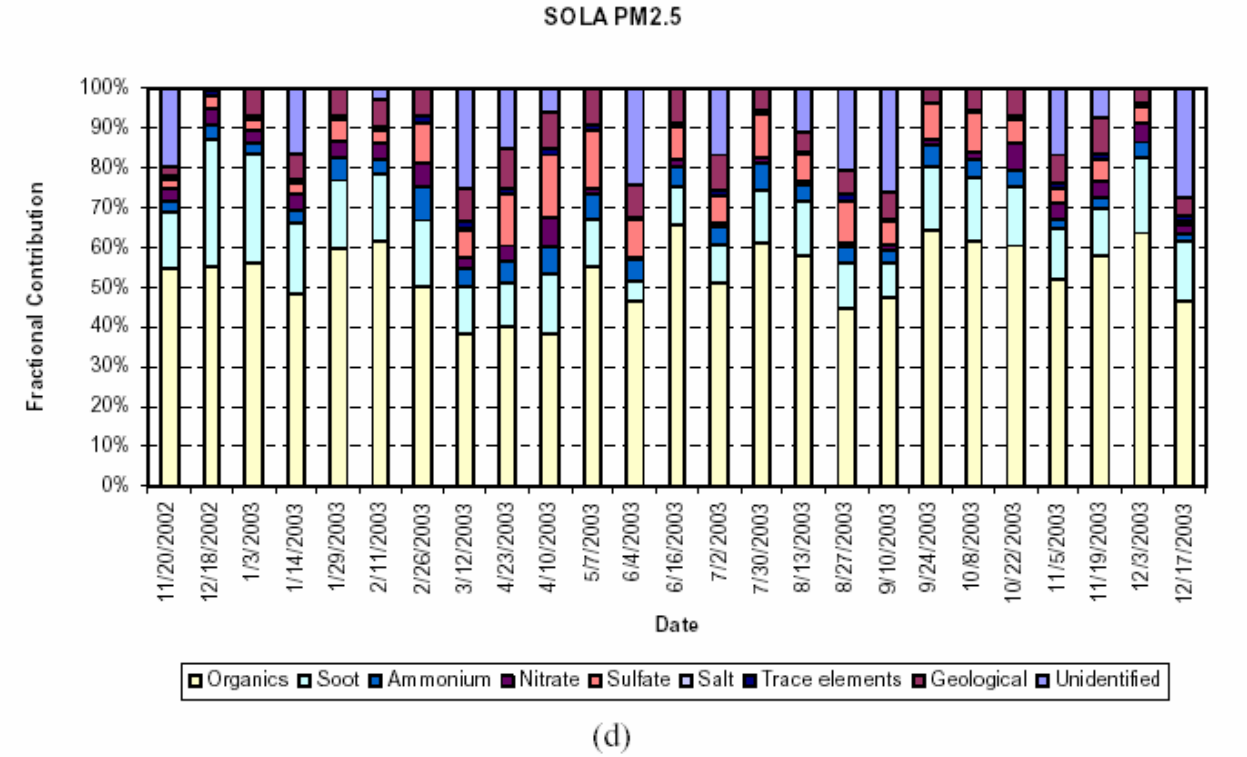
SOLA PM2.5
Fractional Contribution
100%
90%
80%
70%
60%
50%
40%
30%
20%
10%
0%
11/20/2002
12/18/2002
1/3/2003
1/14/2003
1/29/2003
2/11/2003
2/26/2003
3/12/2003
4/23/2003
4/10/2003
5/7/2003
6/4/2003
6/16/2003
7/2/2003
7/30/2003
8/13/2003
8/27/2003
9/10/2003
9/24/2003
10/8/2003
10/22/2003
11/5/2003
11/19/2003
12/3/2003
12/17/2003
Date
Organics
Soot
Ammonium
Nitrate
Sulfate
Salt
Trace elements
Geological
Unidentified

(d)

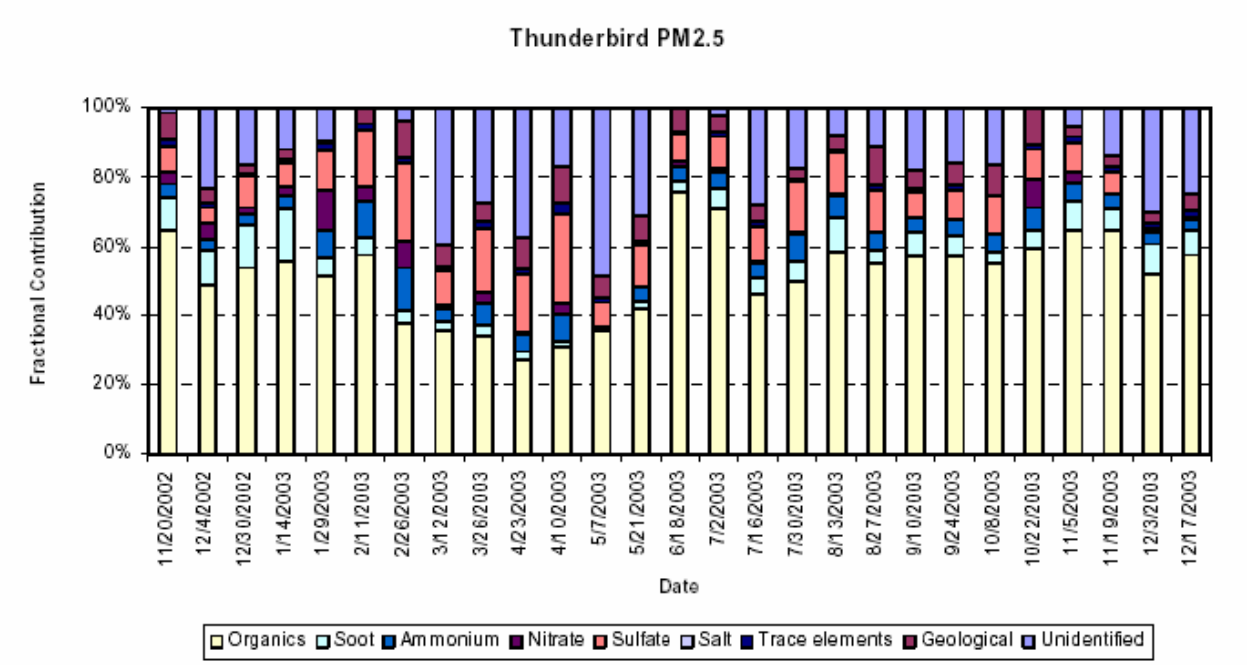

(e)

3.2.1.4 MVS Data

As noted earlier in **Table 3-4**, the MVS sampling network collected data for sampling periods as short as 24 hours and as long as two weeks for chemical composition data. Multi-site summaries of TSP and component concentrations collected with the mini-volume sampler (MVS) are provided in **Figure 3-19**. It should be noted that MVS samples were very infrequently made at the SOLA site during the first half of the field study. Although the MVS samples do not always have similar start or duration times, some seasonal and spatial variations can be inferred. For example, higher TSP concentrations were generally observed at the pier and shoreline sites than at the buoy sites but comparable concentrations of secondary pollutants (e.g., $SO_4^{=}$, NH_4^{+}, and NO_3^{-}) were observed on the buoys and piers. The measurements at the two buoy sites tended to be very similar. Interestingly, the highest sulfur concentrations tended to occur during the summer months. Almost all of the TSP concentrations greater than 20 µg/m^3 were associated with the SOLA and Zephyr Cove sites in the urbanized southeast quadrant of the basin. Lastly, non-zero measurements of phosphorus and phosphates were infrequent.

Although the sampling durations associated with the MVS and TWS networks varied, the seasonal results when combined generate a coherent summary of the seasonal and spatial pattern of TSP concentrations within the Tahoe Basin. The important concept to take from **Figure 3-20** is that PM concentrations are highest (15-25 µg/m^3) at the sites closest to emission sources (e.g., South Lake Tahoe and Lake Forest which are near busy roads), drop off (10-15 µg/m^3) at the sites that are near less busy roads or farther from the road (e.g., Wallis Tower or Zephyr Cove), and decline further (5-10 µg/m^3) at sites distant from local emission sources (e.g., buoys and Thunderbird Lodge).

Figure 3-19a. Total Suspended Particulate Matter (TSP) Concentrations Observed with the MVS Network.

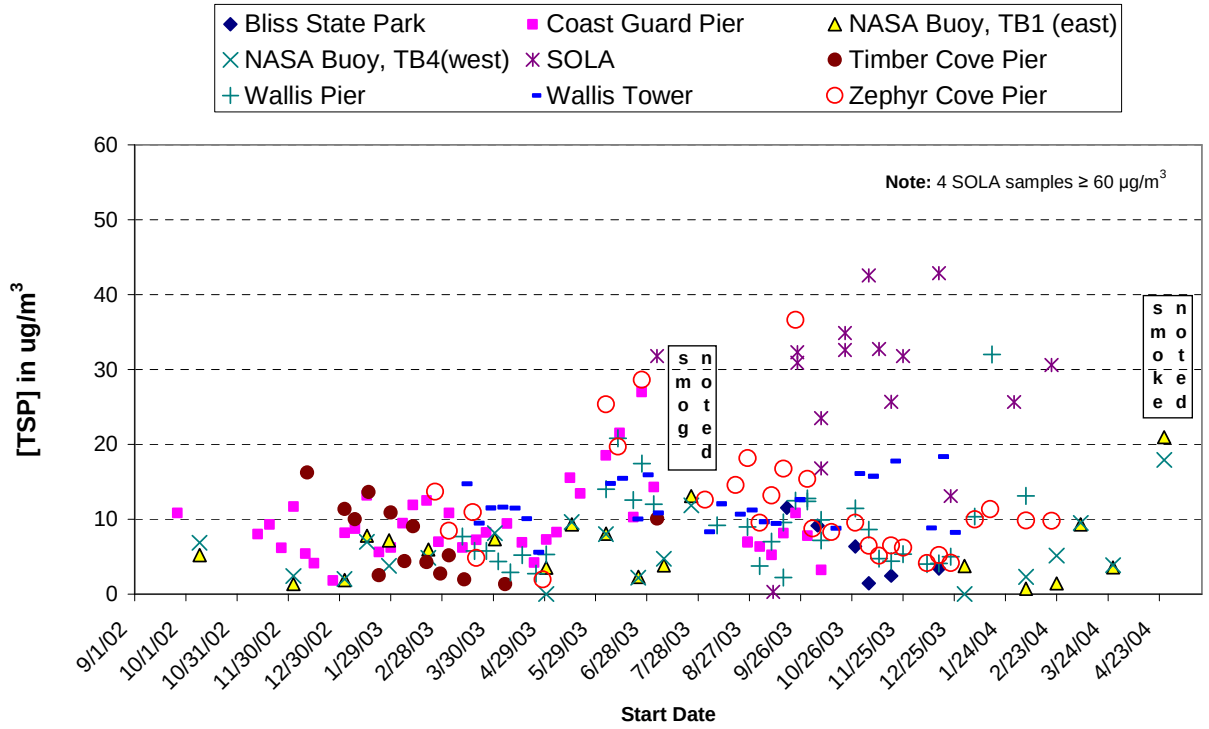

Figure 3-19b. TSP Sulfur (S) Concentrations Observed with the MVS Network.

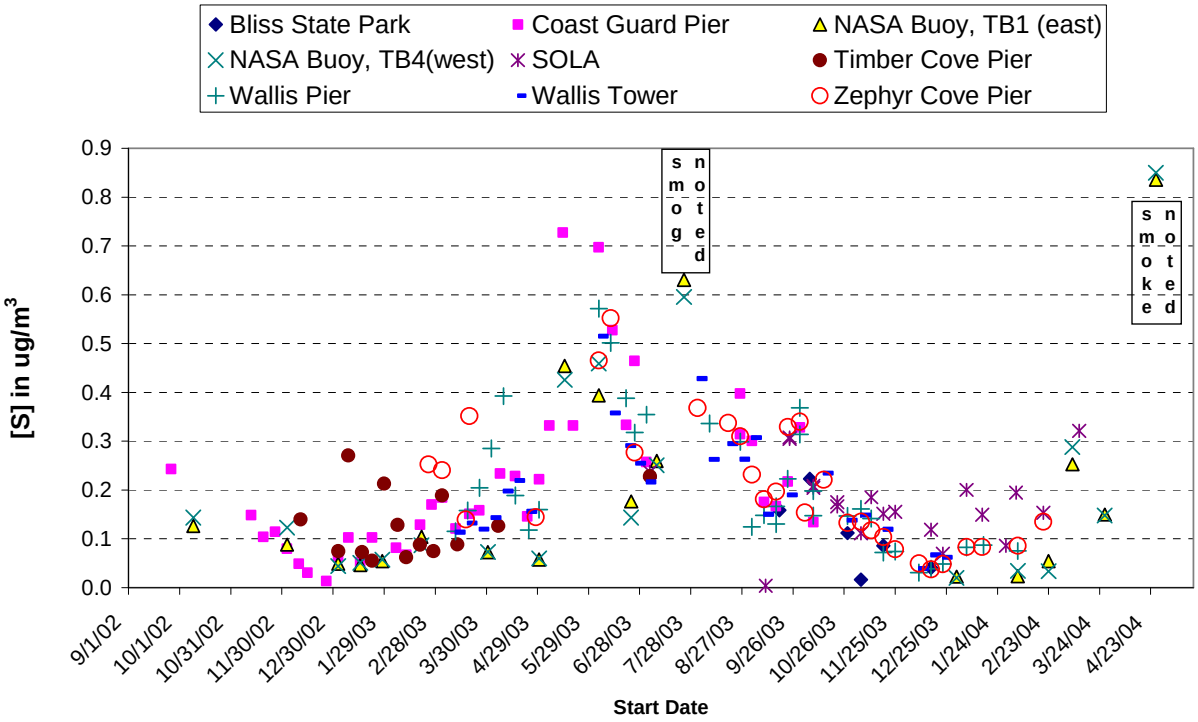

Figure 3-19c. TSP Sulfate (SO_4) Concentrations Observed with the MVS Network.

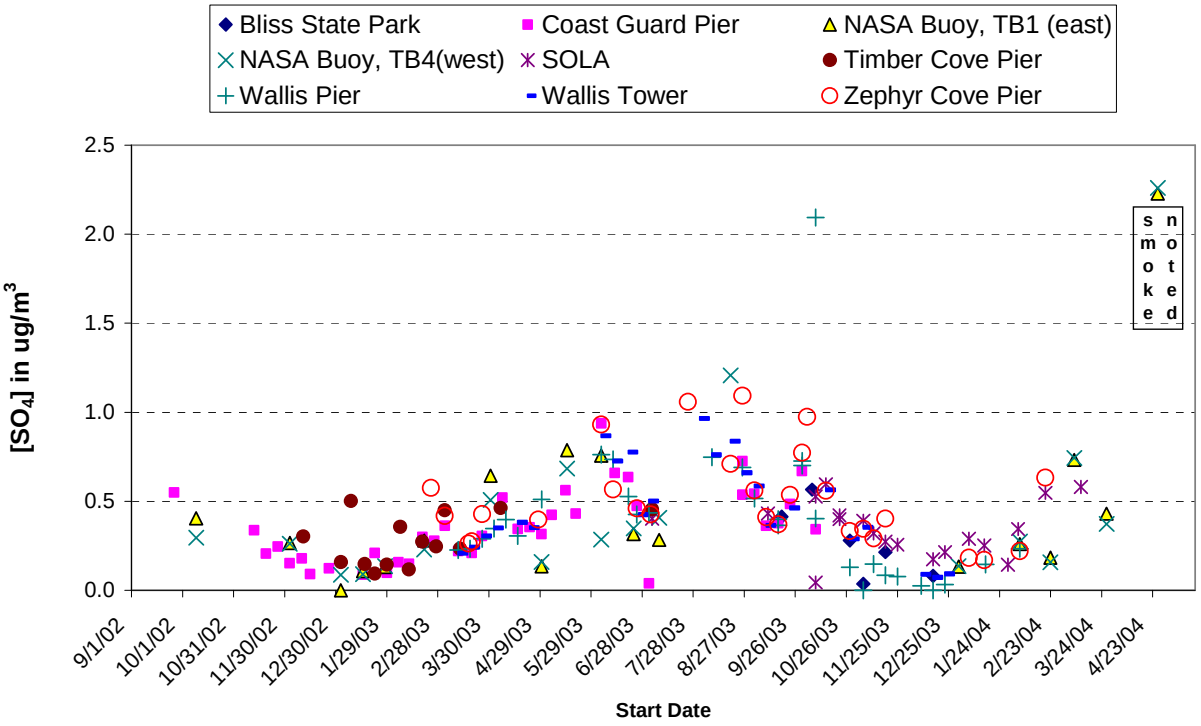

Figure 3-19d. TSP Phosphorus (P) Concentrations Observed with the MVS Network.

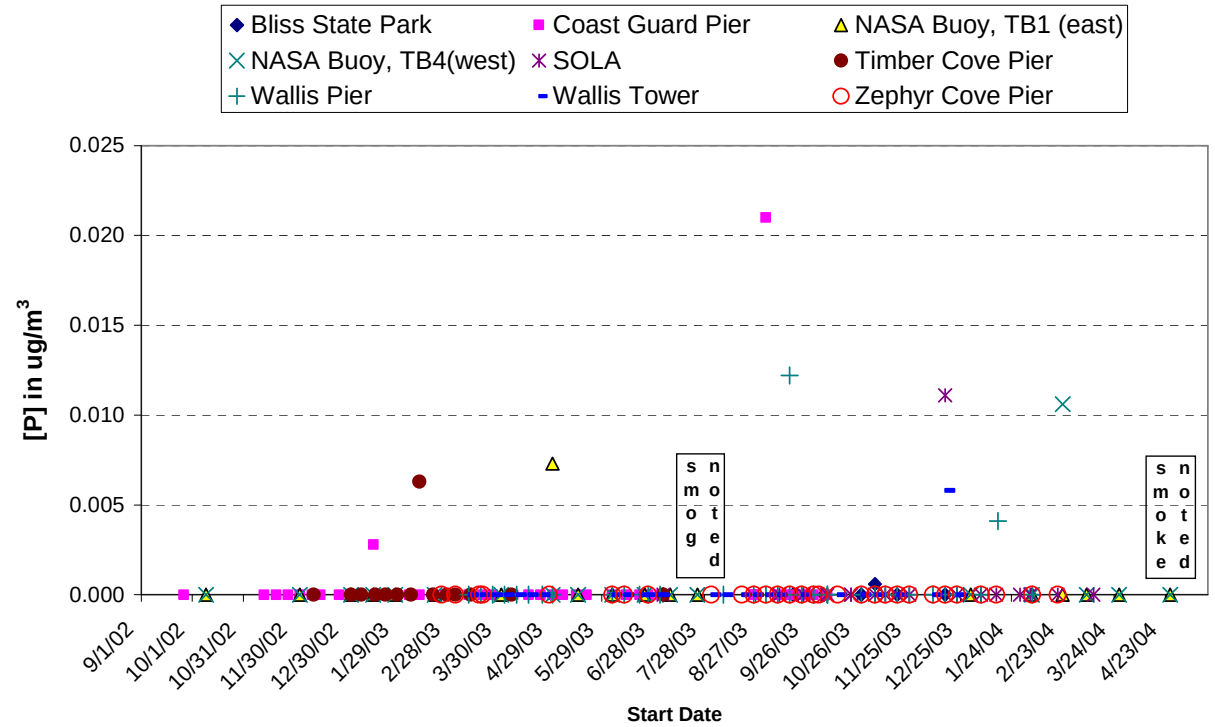

Figure 3-19e. TSP Phosphate (PO_4) Concentrations Observed with the MVS Network.

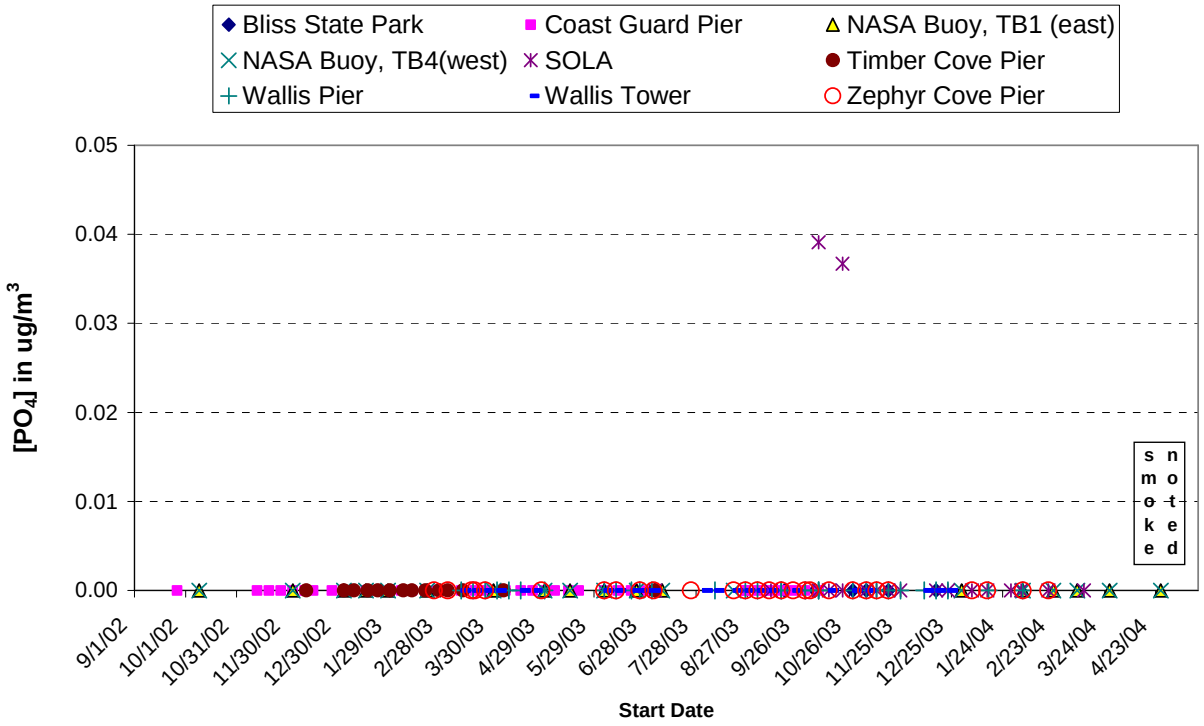

Figure 3-19f. TSP Nitrate (NO_3) Concentrations Observed with the MVS Network.

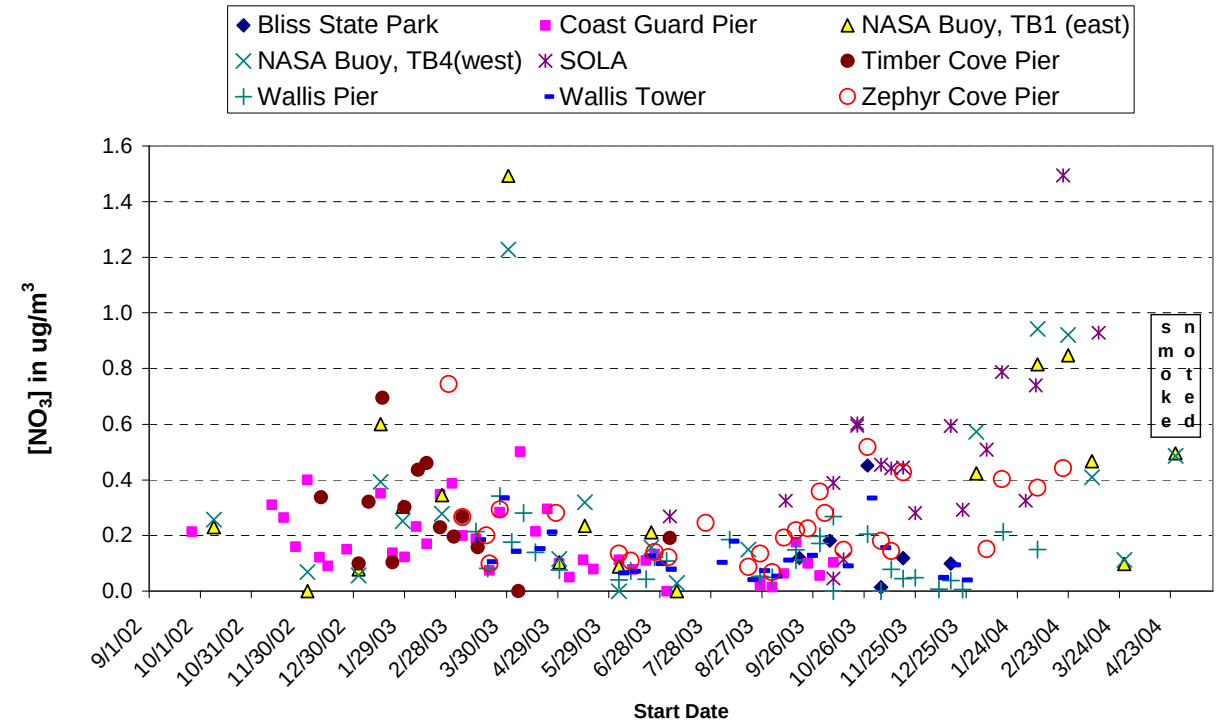

Figure 3-19g. TSP Ammonium (NH_4) Concentrations Observed with the MVS Network.

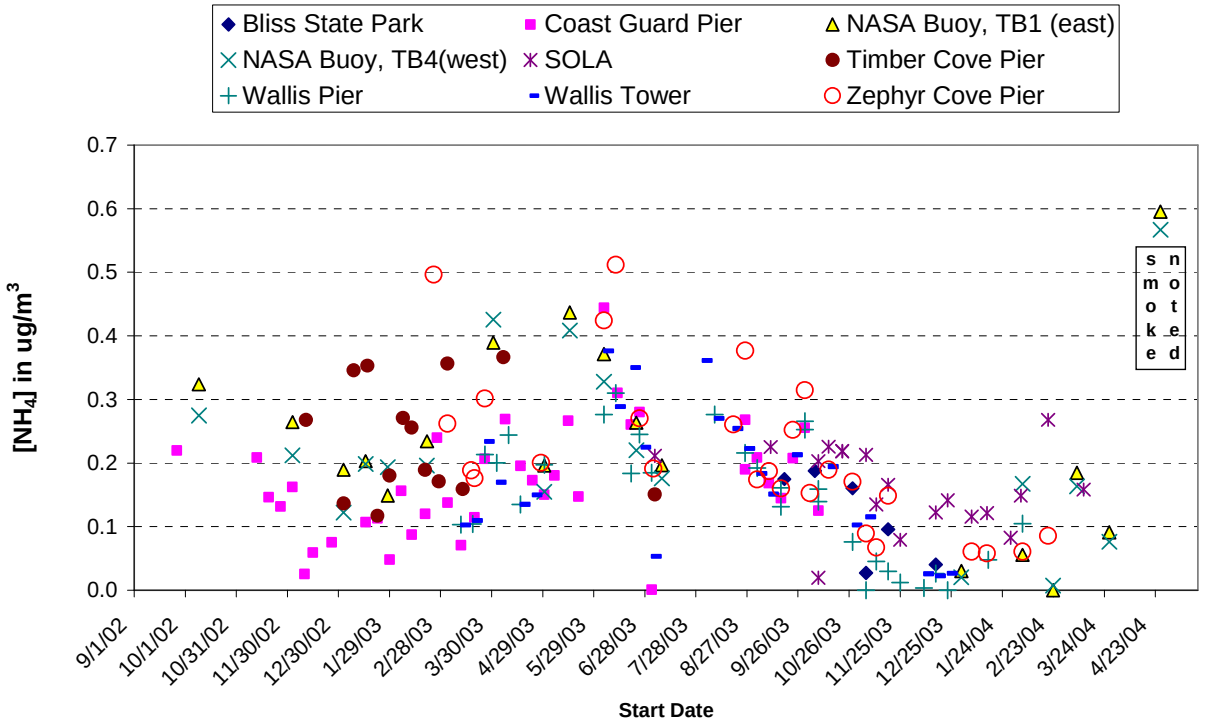

Figure 3-20. Seasonal TSP concentrations observed during LTADS with the TWS and MVS sampling networks.

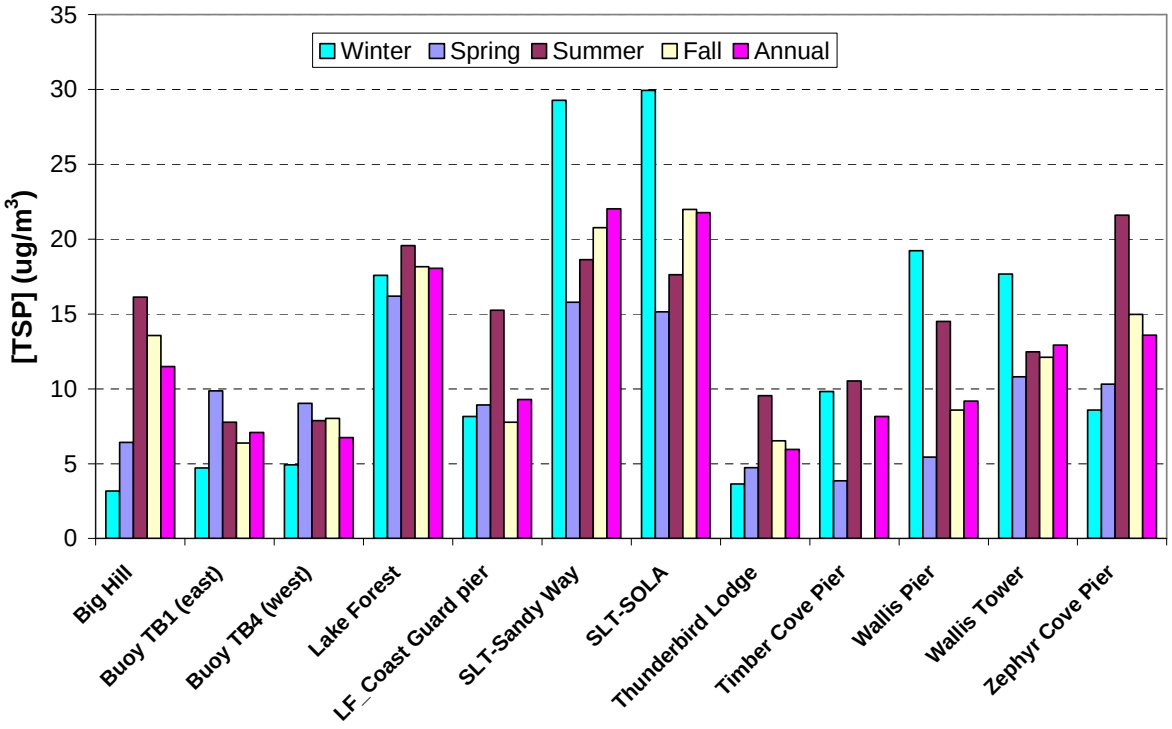

3.2.1.5 BAM Data

Deposition estimates require air pollutant concentration and deposition velocity data for the same time and general location. To develop deposition estimates that account for the dynamics of the meteorology in the Tahoe Basin, hourly deposition velocities are required. Consequently, hourly pollutant concentration profiles are needed to match with the temporal resolution of the meteorological data. The TWS provided ammonia, nitric acid, and detailed compositional information but on a two-week average. The BAMs provided not only some size information about aerosols but also the crucial hourly temporal information about aerosols. The hourly and sized aerosol data from the BAMs were used to construct hourly sized compositional estimates of the aerosols by season (see Chapter 4 for more detail). In a similar manner, the 2-week averages of nitric acid from the TWS network were scaled to seasonal hourly estimates based on the diurnal seasonal differences between NOy and NOx concentrations at SLT-Sandy Way. A limited number of day/night samples that were collected with a second TWS at the SOLA site but the results were inconclusive. Thus, a crude confirmation of the nitric acid by the difference method was not possible and the ammonia concentrations were assumed invariant during each season.

The BAM network collected hourly concentration data in TSP, PM10, and PM2.5 size fractions at several, though not all, stations. The BAM diurnal PM concentration profiles were used to parse seasonal TWS data into seasonal hourly concentration data for TSP, PM10, and PM2.5 and their compositional species. **Figure 3-21** provides a synopsis of BAM diurnal profiles for each of the four seasons at Big Hill (3-21a), Sandy Way (3-21b), SOLA (3-21c), Cave Rock (3-21d), Thunderbird Lodge (3-21e), and Lake Forest (3-21f). Because the BAM instruments collect all particles below a specified cut-point or size, the concentrations include overlapping measurements. For sites with all three size measurements the data can be segregated into three non-overlapping size fractions by subtracting the PM10 measurement from the TSP measurement to give the concentration of particles larger than PM10 (referred to as “PM_large”. In a similar manner, the PM2.5 concentration can be subtracted from the PM10 concentration to give the concentration of particles of size greater than 2.5 μm and smaller than 10 μm (referred to as “PM_coarse”).

The BAM data indicate that PM_coarse and PM_large both varied markedly with hour of day, being highest around sunrise and sunset when the air is more stable and traffic activities tend to be greatest. Ambient concentrations of PM_large and PM_coarse tend to decline from the early evening peaks at night when winds are lighter and anthropogenic activities are reduced. PM concentrations are often lower during mid-day when atmospheric mixing is greatest and winds tend to be onshore. This diurnal pattern is particularly pronounced during winter at monitoring sites located near roadways. In general, PM2.5 shows relatively small diurnal variation. The exception to this statement is a large nighttime increase in PM2.5 at the Sandy Way site in winter and fall. The evening peak in the diurnal pattern of fine PM (i.e., PM2.5) at the Sandy Way site is suggestive of wood smoke as the sample inlet is on the roof of a 1-story building that is located downwind of residential areas at that time of day. The magnitude and variation

in PM concentrations at Thunderbird Lodge are of interest because it is an in-basin site with limited local emissions (particularly during winter).

Because hourly chemical analysis would be prohibitively expensive, the PM chemical constituents were assumed to have diurnal variations similar to the variations in total mass.

3.2.1.6 Aerosol Nitrogen

Several nitrogen species contribute to the nutrient loading of Lake Tahoe and can deposit from the atmosphere in both aerosol and gaseous forms. This section discusses aerosol nitrogen species and the gaseous nitrogen components will be discussed in Section 3.2.2.1.

The most common nitrogen-containing aerosol species are ammonium nitrate (NH_4NO_3) and ammonium sulfate ($(NH_4)_2SO_4$). Both are water soluble and readily deposit to water. Ammonium (NH_4^+), nitrate (NO_3^-), and sulfate ($SO_4^=$) ionic concentrations in LTADS samples were measured by extracting a portion of an aerosol filter (quartz) in water, then analyzing the liquid by ion chromatography (IC).

Aerosol nitrate (NH_4NO_3) is not chemically stable; rather, it exists in equilibrium with the gas-phase concentrations of its precursors, ammonia (NH_3) and nitric acid (HNO_3) and water vapor. Collecting nitrate particles on a filter can produce a negative bias if the air flow through the filter causes some of the nitrate on the filter to return to the gas phase. On the other hand, if gas-phase precursors in the air stream condense on the filter, the measured nitrate on the filter will have a positive bias. In the TWS, it is assumed that any ammonium nitrate that volatilized as nitric acid vapor was captured by the nylon backup filter. Volatilized ammonia was estimated as the equal molar concentration of the volatilized nitrate captured on the backup. This assumption provides an upper estimate of ammonium because some of the particulate nitrates may be associated with other cations (i.e., calcium, magnesium, sodium).

Total nitrate was computed for the TWS network as the sum of nitrates on the primary and backup filters. Total ammonium was computed as the sum of primary filter ammonium and the estimated volatilized ammonium from the backup filter. NH_4^+ and NO_3^- data from the IMPROVE program are based on the same type of collection and lab analyses. Neither denuders nor backup filters can be used with the standard design of MVSs as they would decrease the airflow and change the particle size cutpoints when used for PM2.5 or PM10 sampling. Although the MVSs used during LTADS were for TSP sampling, which is less sensitive to airflow variations, the short study timeline precluded the design, construction, and testing of a more sophisticated MVS sampling system.

Figure 3-21a. Seasonal diurnal profiles of PM concentrations based on BAM data collected at Big Hill.

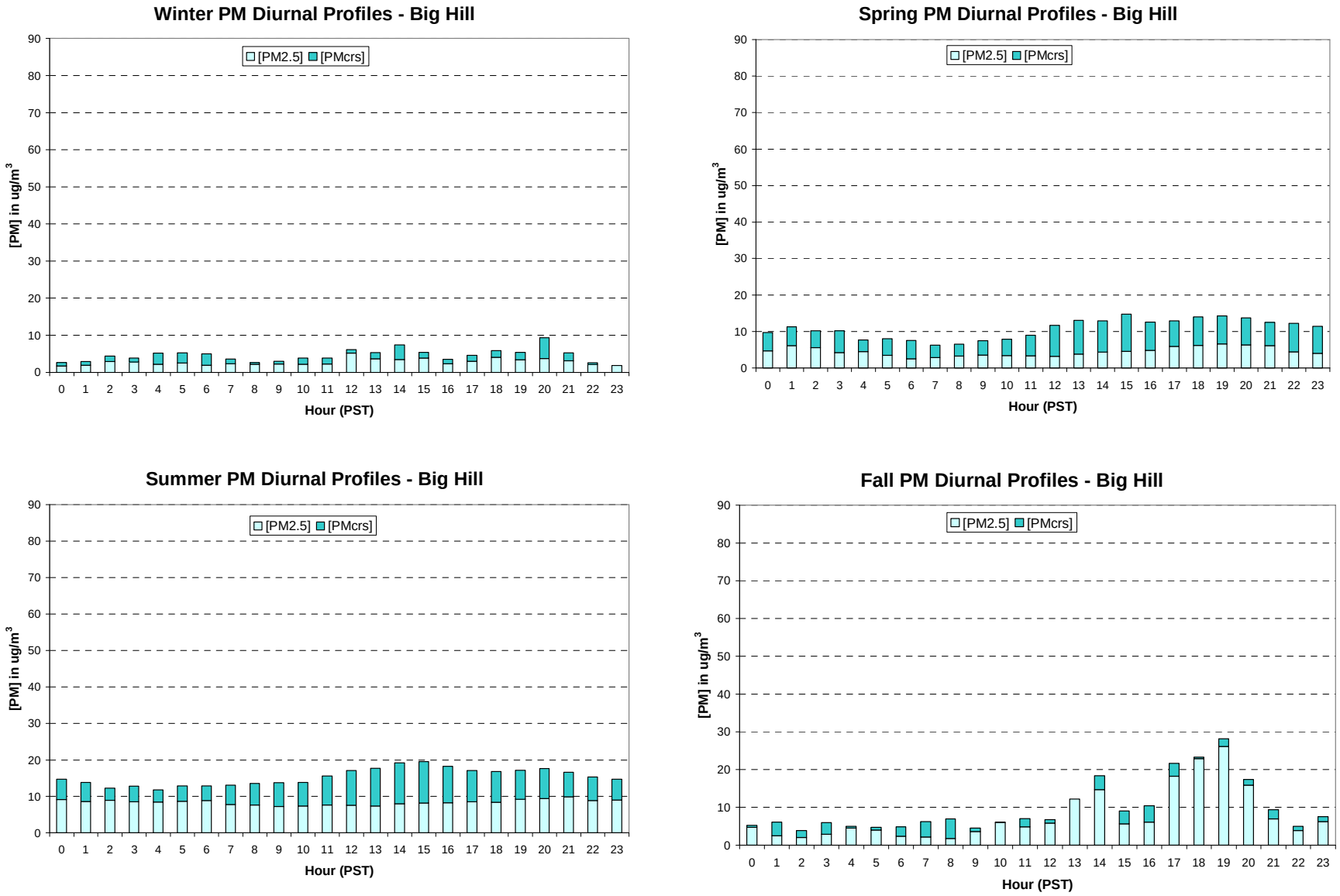

Figure 3-21b. Seasonal diurnal profiles of PM concentrations based on BAM data collected at SLT -Sandy Way.

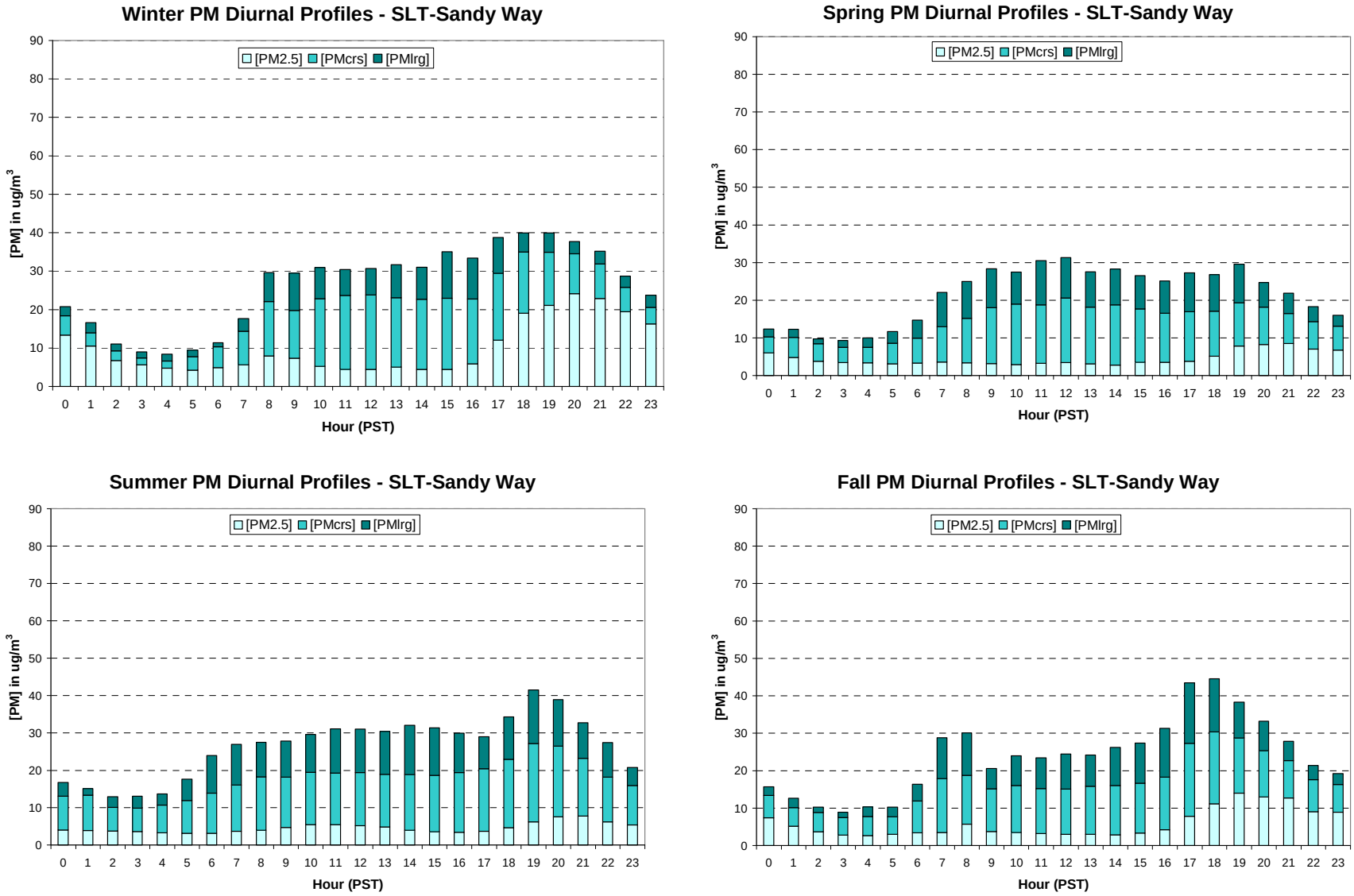

Figure 3-21c. Seasonal diurnal profiles of TSP concentration based on BAM data collected at SLT-SOLA.

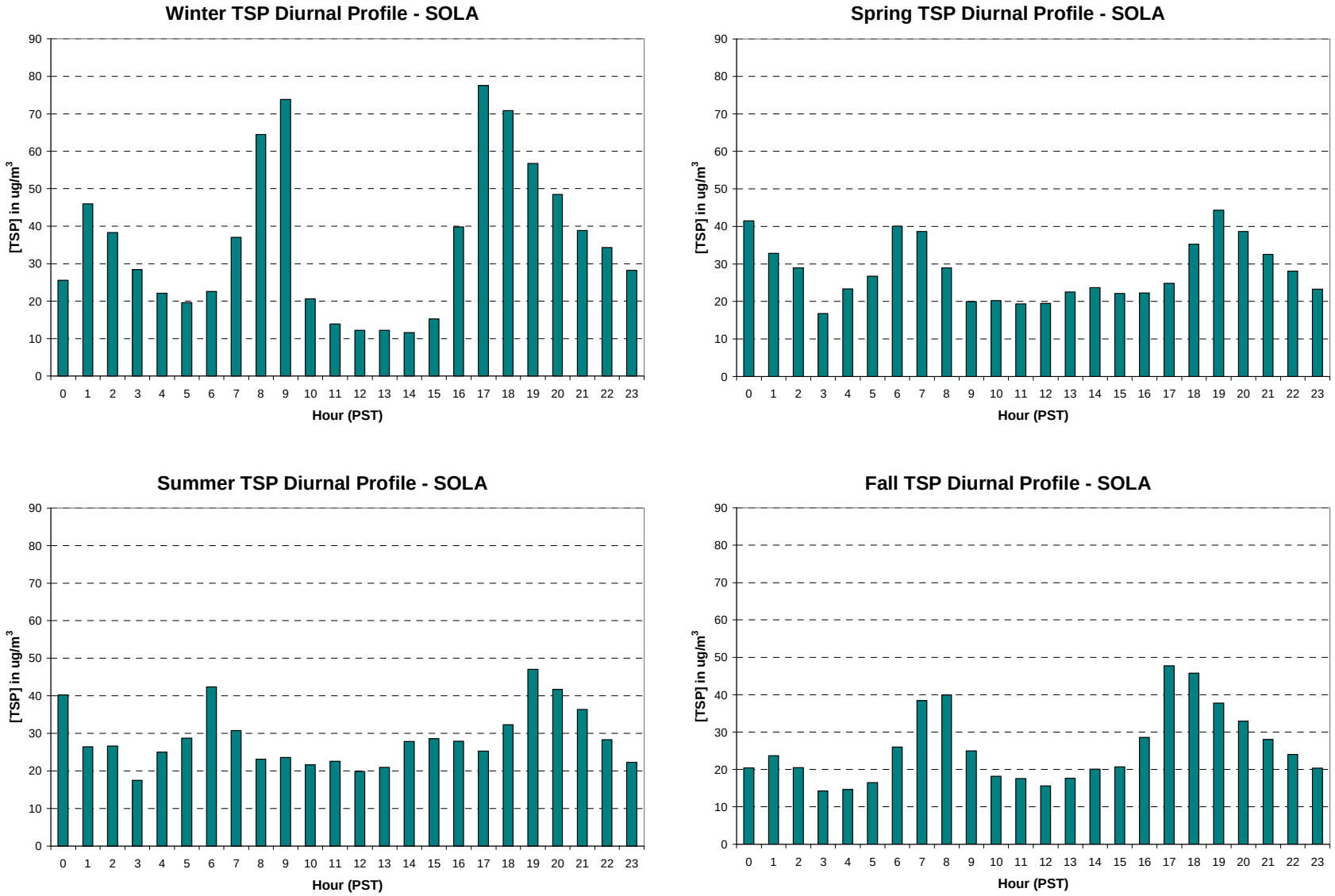

Figure 3-21d. Seasonal diurnal profiles of TSP concentration based on BAM data collected at Cave Rock.

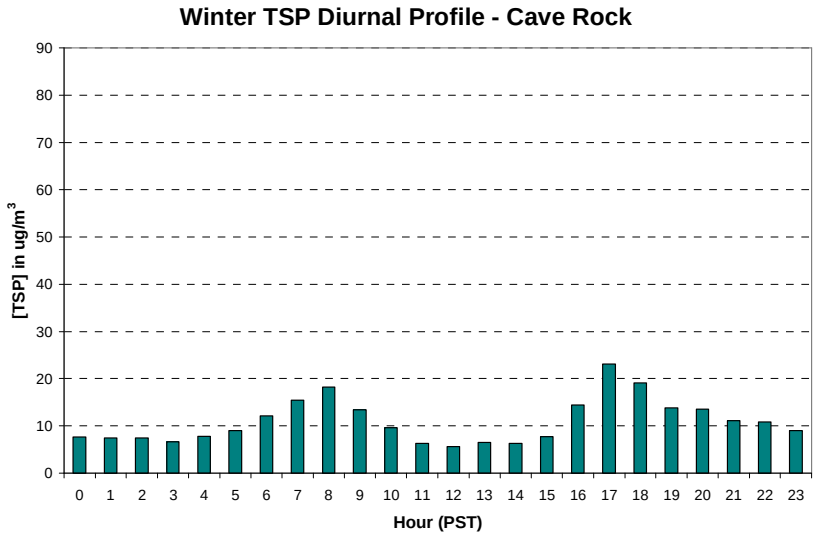

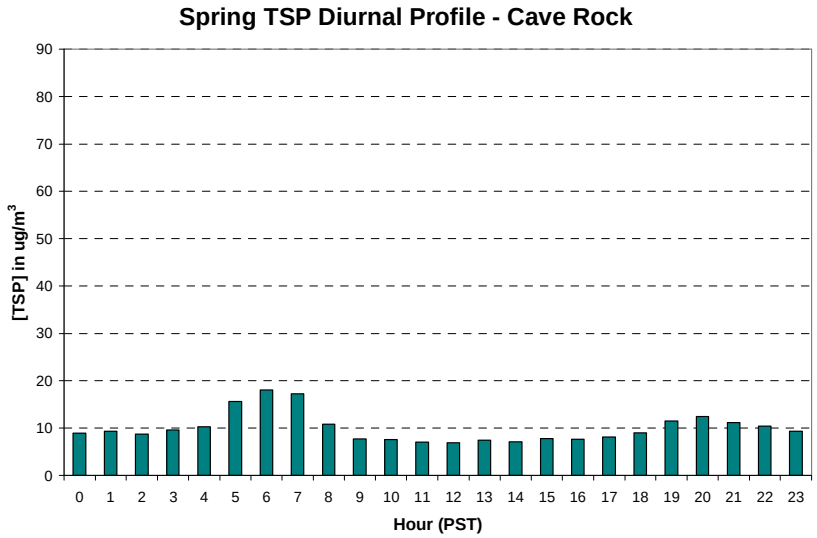

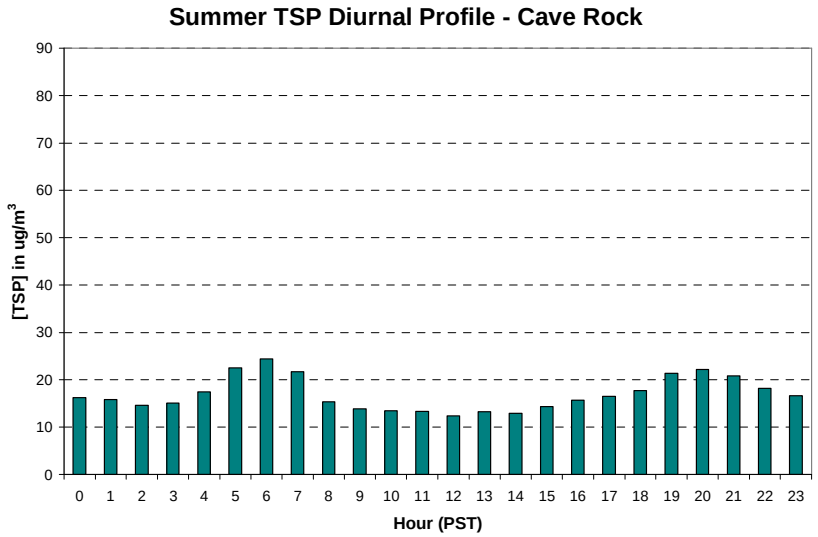

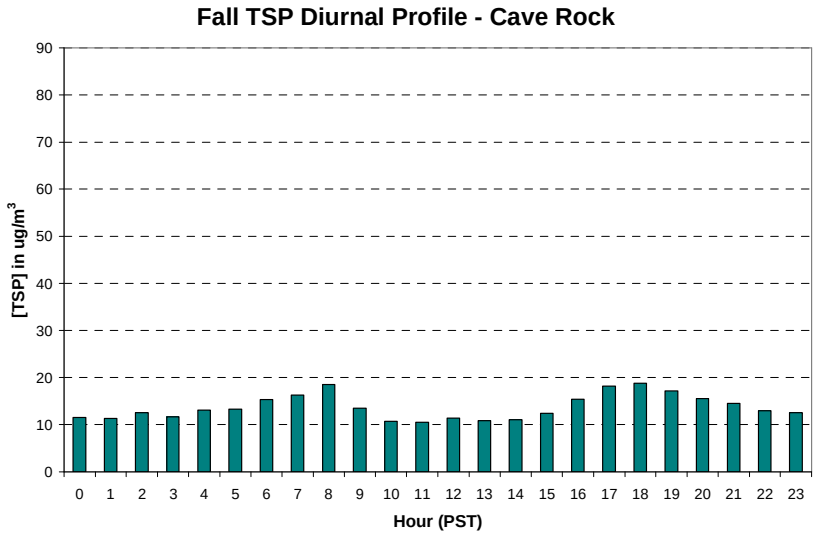

Figure 3-21e. Seasonal diurnal profiles of PM concentrations based on BAM data collected at Thunderbird Lodge.

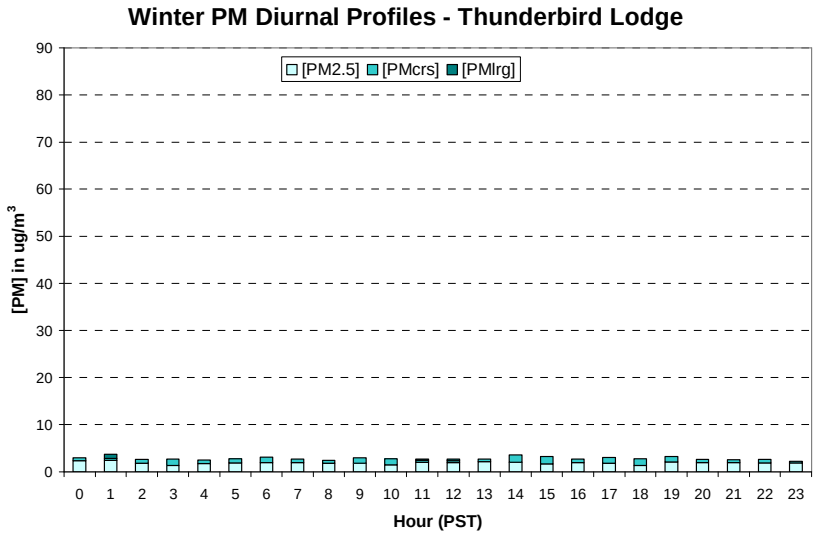

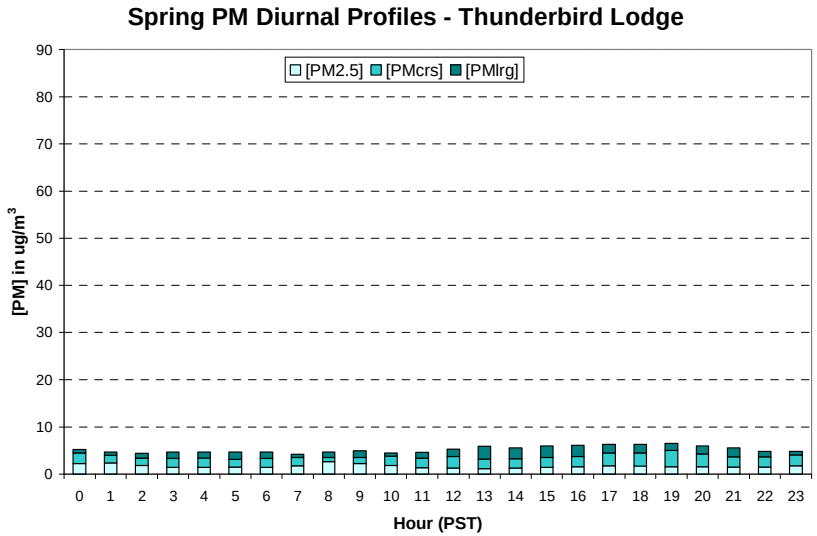

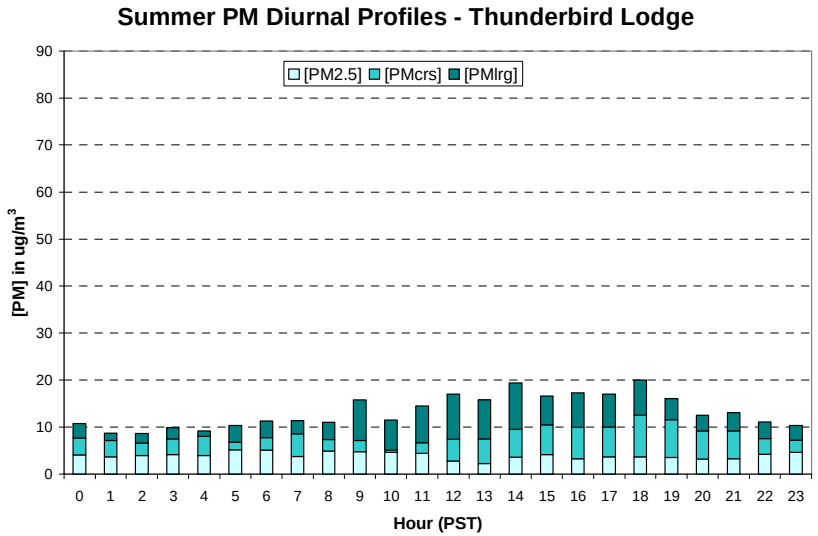

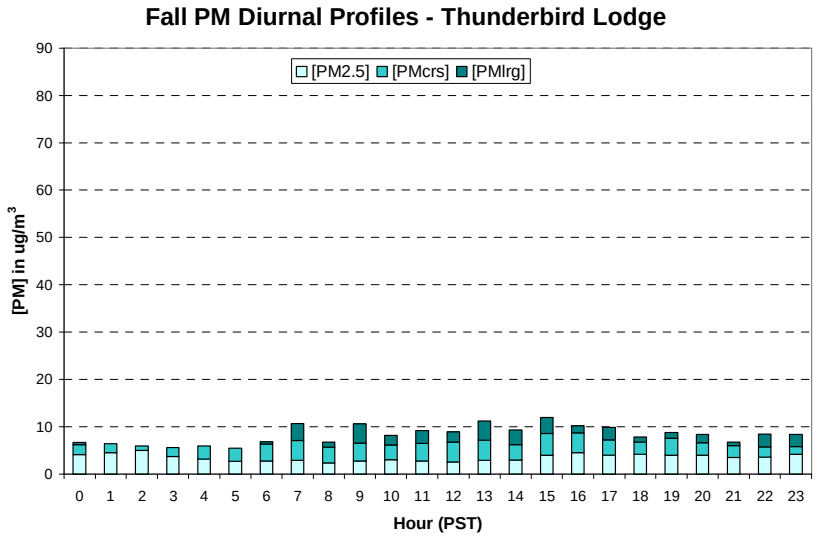

Figure 3-21f. Seasonal diurnal profiles of PM concentrations based on BAM data collected at Lake Forest.

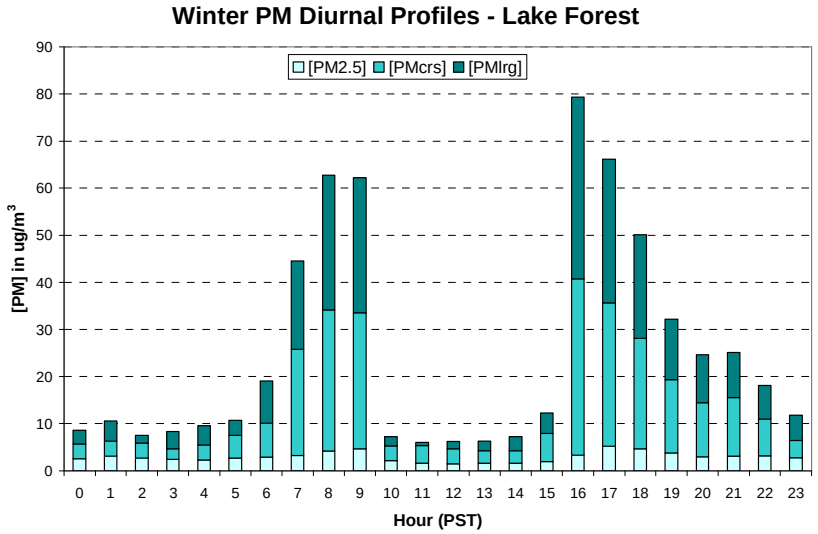

Lake Forest BAM had no matched size data during spring due to power and instrument failures.

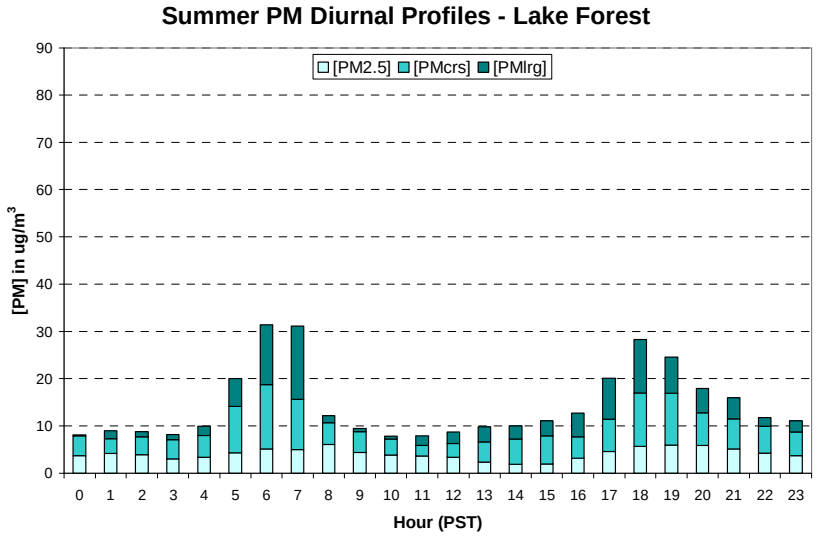

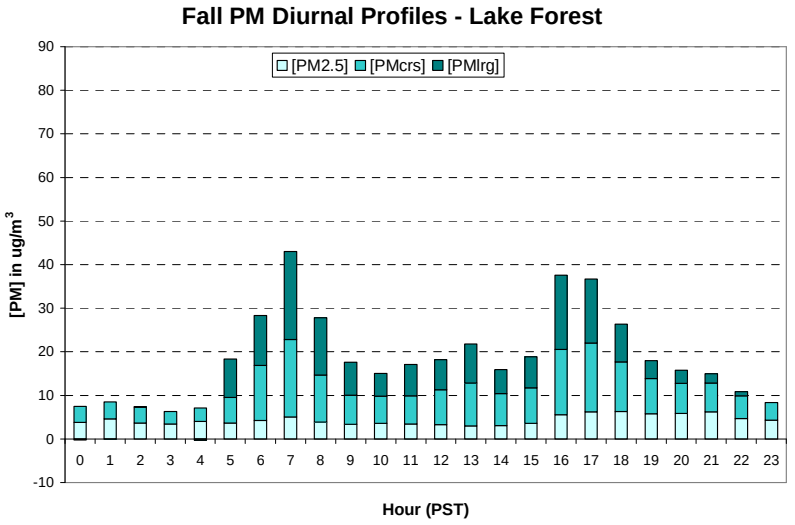

The nitrate/ammonium sampling and analytical procedures lead to six nitrogen measurement numbers, which are as follows:

1) Nitrate M: nitrate measured from the quartz filter on the TWS or MVS,
2) Nitrate V: volatilized nitrate measured from the backup nylon filter on the TWS,
3) Ammonium M: ammonium measured from the quartz filter on the TWS or MVS,
4) Ammonium V: volatilized ammonium estimated from Nitrate V,
5) Nitrate T: total nitrates (Nitrate M + Nitrate V), and
6) Ammonium T: total ammonium (Ammonium M + Ammonium V).

As stated earlier, it is unlikely that all volatilized nitrates are ammonium nitrate and therefore Ammonium V which assumes a mole of ammonium ion for every mole of volatilized nitrate ion overestimate Ammonium V and Ammonium T ambient concentrations.

An additional assumption is that ammonium nitrate does not dissociate to ammonia and nitric acid but remains at equilibrium. Because these are two-week average measurements, ammonium nitrate equilibrium is not maintained. Relative humidities above 62% (and cool temperatures) tend to promote aqueous instead of gas phase chemistry for ammonium nitrate. Further, within the proper relative humidity regimes, the gas/particulate phase partition coefficient (dissociation constant) is temperature dependent. Because substantial temperature swings occur daily and within a two-week sampling period, the ammonium-nitrate equilibrium varies throughout the sample collection period.

Ammonium T for the MVS was estimated from the ammonium measured by the MVS (Ammonium M) based on the Ammonium M to Ammonium T relationship observed with the TWS network. The difference between the estimated Ammonium T and Ammonium M for the MVS was then designated as Ammonium V. The Nitrate V was then estimated for the MVS by assuming it to be molar equal to the estimated Ammonium V. The Nitrate T estimate from the MVS was then the sum of the Nitrate M and the estimated Nitrate V. This approach allows the potential use of particulate nitrogen data from both of the TWS and MVS networks in estimating seasonal and annual deposition. However, the MVS flow rate was 5.0 liters per minute (lpm) compared to TWS flow rate of 1.3 lpm. In addition, the MVS samplers ran about 30 hours at mid-lake and 170 hours at piers while the TWS samplers ran for about 300 hours. Because of the potential difference in compound volatilization between the MVS and TWS systems, caution is recommended when comparing individually imputed Ammonium V and Nitrate V values between MVS and TWS. In the seasonal summary of particulate nitrogen measurements during LTADS shown in **Table 3-6**, the MVS Ammonium T, Nitrate T, and Total Particulate Nitrogen were calculated based on this treatment.

Table 3-6. Seasonal and Study Average NO_3^-, NH_4^+, and total particulate nitrogen concentrations from LTADS filter sampling.

LTADS Summary of Total Nitrogen Particulate, Nitrates, Ammonium							
	Nitrogen Particulate (as ug of N/m^3)					Nitrates	Ammonium
Site	Winter	Spring	Summer	Fall	Study Average	(ug/m^3)	(ug/m^3)
Big Hill PM2.5	*0.06*	0.49	0.62	0.42	0.47	0.64	0.42
Big Hill PM10	*0.07*	0.44	0.72	0.55	0.53	0.85	0.44
Big Hill TSP	*0.08*	0.54	1.00	0.74	0.71	1.25	0.55
Bliss State Park TSP	*0.07*	-	-	0.16	0.14	0.19	0.13
Coast Guard TSP	0.14	0.19	0.23	0.19	0.19	0.17	0.20
Lake Forest PM2.5	0.22	*0.21*	*0.35*	0.32	0.28	0.33	0.27
Lake Forest PM10	0.22	0.27	0.39	0.30	0.27	0.42	0.22
Lake Forest TSP	0.25	0.31	0.43	0.37	0.31	0.48	0.26
NASA Raft, TB1 (east) TSP	0.33	0.44	0.32	0.42	0.36	0.52	0.32
NASA Raft, TB1 (west) TSP	0.31	0.42	0.29	0.38	0.34	0.48	0.30
Sandy Way PM2.5	0.53	0.42	1.50	0.51	0.50	0.75	0.42
Sandy Way PM10	0.58	0.47	1.76	0.53	0.53	0.88	0.42
Sandy Way TSP	0.57	0.54	0.66	0.65	0.63	1.05	0.50
SOLA PM2.5	0.50	0.36	0.44	0.46	0.45	0.67	0.38
SOLA PM10	0.46	0.38	0.49	0.48	0.46	0.80	0.36
SOLA TWS TSP	0.59	0.54	0.43	0.38	0.48	0.81	0.39
SOLA MVS TSP*	0.53	*1.01*	*0.27*	0.21	0.41	0.58	0.17
Thunderbird PM2.5	0.13	0.18	0.16	0.13	0.15	0.30	0.10
Thunderbird PM10	0.15	0.25	0.36	0.27	0.26	0.38	0.22
Thunderbird TSP	0.20	0.37	0.48	0.35	0.35	0.53	0.29
Timber Cove TSP	0.31	0.34	*0.21*	-	0.32	0.39	0.30
Wallis Pier TSP	0.07	0.20	0.23	0.19	0.17	0.17	0.18
Wallis Tower TSP	0.10	0.18	0.25	0.18	0.19	0.16	0.19
Zephyr Cove TSP	0.14	0.35	0.35	0.23	0.26	0.28	0.25
Maximum Basinwide (excludes Big Hill)					2.57	2.57	1.04
2nd Maximum Lakewide (excludes Big Hill)					1.21	2.24	0.91
Average Lakewide (excludes Big Hill)					0.34	0.49	0.28
Median Basinwide (excludes Big Hill)					0.32	0.48	0.27
Minimum Basinwide (excludes Big Hill)					0.04	0.04	0.04

Underlined site names represent MVS measurements

Underlined data are estimates or rely on few data points; shaded cells indicate physically non-representative result

** SOLA MVS had higher flow & lower NH_4^+ than TWS (DRI ARB QA Review)*

Particulate nitrate and ammonium concentrations from the TWS network (i.e., Big Hill, SLT-Sandy Way, SLT-SOLA, Thunderbird Lodge, and Lake Forest) were summarized in **Figures 3-14 and 3-15**. During summer and fall (the seasons of greatest data capture at Big Hill), the nitrate concentrations at Big Hill are consistently higher than at sites within the Tahoe Basin. Comparing to the IMPROVE network, the Big Hill PM2.5 nitrate loadings are halfway between the averages for two transport-influenced sites in the southern Sierra Nevada - Yosemite (0.36 $\mu g/m^3$) and Sequoia (1.3 $\mu g/m^3$), suggesting that transport is an important component at Big Hill. The annual mean at Big Hill is somewhat uncertain. Most of the samples collected there are from the warm seasons when upslope transport from the Sacramento Valley is strongest (sampling began February 26, 2003), so much of the low nitrate winter period was likely missed. The Big Hill average is thus better viewed as an upper bound on the true annual average.

PM2.5 nitrate data from the TWS compare well with data from the IMPROVE network. At Bliss, IMPROVE nitrate averaged 0.22 $\mu g/m^3$, essentially the same as LTADS' limited MVS sampling of nitrate at Bliss, 0.19 $\mu g/m^3$. The Coast Guard, Wallis Tower, Wallis Pier, Thunderbird, and Lake Forest sites all show average nitrates concentrations of 0.2 to 0.9 $\mu g/m^3$, much lower than the 1.25 $\mu g/m^3$ observed at Big Hill. The SOLA and Sandy Way sites in South Lake Tahoe, with strong local motor vehicle and urban emissions, averaged about 1 $\mu g/m^3$ of nitrate. Although divorced from a more substantive meteorological assessment, aerosol nitrogen concentrations within the basin appear to be largely influenced by in-basin emissions, which is consistent with conclusions of Tarnay *et al*. (2002).

3.2.1.7 "Inert" Particles

Particles depositing from the atmosphere can dissolve in the lake water (the rate can vary) providing $SO_4^{=}$, PO_4^{-}, and NO_3^{-} that act as nutrients, stimulating biological growth, which can adversely impact water clarity and aesthetics. Insoluble particles depositing to the water will scatter and absorb light, thus also reducing visibility into the water. Little is quantitatively known at this time about the relative fates of atmospheric particles once they enter the water. As a crude estimate, the analysis of atmospheric particles by ion chromatography (water-soluble analysis of particulate matter) would provide an indication of the soluble fraction of particulate matter. An upper estimate of the inert particles would then be the difference between the total atmospheric PM and the soluble portion identified by ion chromatography. Furthermore, summation of the concentrations of $SO_4^{=}$, PO_4^{-}, NO_3^{-}, NH_4^{+}, Cl^{-}, Ca_2^{+}, K^{+}, Na^{+}, and a few other potentially soluble species permits an estimate of the total soluble fraction on a mass basis. An average of the LTADS data indicates that the soluble fraction is about 25% of the TSP mass at the transport site (i.e., Big Hill) and ranges from about 10 to over 20% of the TSP mass at the sites within the Tahoe Basin. As might be expected, the soluble fraction of PM2.5 is larger, being almost 30% at Big Hill and over 25% at all the TWS sites within the Tahoe Basin. Because large particles would deposit closer to their sources than small particles and some of the large particles would not be transported to the Lake, the direct atmospheric PM deposition estimates presented in later in Chapters

4 and 5 should be reduced by about 20% to better approximate the deposition of inert particles that truly affect the water clarity.

However, to begin a comprehensive assessment of inert particle light scattering and absorption for various water columns at Lake Tahoe, the LTADS information on the soluble fraction of PM is only a starting point. Very small particles produce Rayleigh scattering while larger particles undergo geometric scattering (Finlayson-Pitts and Pitts 1986) and particles in the middle of the size spectrum (comparable to the wavelength of visible light) may undergo Mie scattering. Rayleigh scattering occurs equally in the forward and backward directions, geometric scattering is about light refraction through large particles and is handled by classic optics, Mie scattering is non-uniform forward scattering and has a refraction index of 1.333 in water. In essence, to properly judge inert particle light scattering in the water column, very specific particle size (as many size cuts as possible), particle counts in each size, and particle concentration information in each size would be required. Particle composition and particle shape would also be extremely useful. The variable sunlight angle, the variable rates of particle accumulation (including disaggregation, conglomeration, chemical reaction), and the resultant particle settling within the water column would be additionally required information. Collecting these types of information was beyond the scope of LTADS.

3.2.1.8 Dust Experiments

A limited number of "dust experiments" were conducted to aid in understanding the mechanisms of emission, dispersion, deposition, and loss into and out of the air parcels as they traveled from sources on to the lake. Complete analyses of these experiments and publication of the results in a peer-reviewed journal is planned for the future. Nevertheless, preliminary analyses of three dust experiments are particularly noteworthy in describing these mechanisms. Additional discussion of these experiments can be found in Section 4.4.

3.2.1.8.1 July 2003, On-Lake, Northwest Shore Zone

During this experiment, the Tahoe Research Group's boat (R/V Frantz) was equipped with ozone, and NO_Y gaseous instruments, as well as CLIMET particle counters and a 2-stage particle counter limited to roughly 3 and 0.3-micrometer aerosol aerodynamic diameter bins. Information provided to the data logger included relative humidity and temperature, as well as boat's position. **Figure 3-22** provides a synopsis of the experiment.

In this instance, strong down-slope drainage airflow carried pollutants from the backshore areas onto the lake during the evening; as activities and pollutant emissions declined, the drainage air became cleaner during late night hours. On the next morning, pollutant flux over the lake increased as human activity began - NO_Y associated with vehicle exhaust was observed starting about 5 am. Particle counts, probably associated with chimney smoke and motor vehicle exhaust, increased after 6 am. The key finding from this experiment was that the night-time down-slope flow of air carried pollutants over the lake and was important in the dispersion and deposition of those

pollutants. The strong connection of shoreline activity, in particular motor vehicle traffic, with near-shore concentrations was also confirmed in this experiment. The most significant observation, however, was that concentrations over the lake declined rapidly (within a short distance of the shoreline and within a few hours), and implying that the effect of emission sources is largely confined to the near-shore environment.

3.2.1.8.2 August 2003, On-Lake, West and South Shore Zone

An evening sampling cruise aboard the R/V Frantz from Tahoe City to Zephyr Cove encountered an interesting combination of air pollutants transported into the Tahoe basin from the west and an accumulation of local "in-basin" emissions. This event may represent an archetype for "typical" summer meteorology and pollutant movement in the Tahoe region, and warrants a fuller discussion that the previous dust experiment. **Figure 3-23** presents the observations during this dust experiment.

3.2.1.8.2.1 On-Lake Conditions

Winds at Tahoe City at the start of this boat trip were light and from the west. Proceeding south along the west side of the lake toward Tahoma, in the area exposed to the Rubicon Gap (Loon Lake area of Sierra crest), the wind built to about 20 knots as estimated by the steep chop and whitecaps. Looking up at the crest there was a visible light haze associated with the air flowing over the crest. Farther south the course entered the wind shadow of the Rubicon Peak – Mount Tallac – Desolation Wilderness highlands and winds were lighter, but gusty, and from the west. Near the south end of the lake the winds turned southerly as the regional SW flow was turned by the terrain to follow the upper Truckee drainage. By late evening, approaching Zephyr Cove, down-slope flow brought air from the east shore onto the lake. This pattern of winds permitted the sampling of both the regional flow and local influences around the western and southern sides of the lake.

3.2.1.8.2.2 Gas Data

Figure 3-23 shows gas and aerosol data at 1-minute intervals. The ozone data indicate a depleted "urban" air mass, with steady concentration at 8-9 parts per hundred million per volume (pphm) coming through the Rubicon Gap. As the boat moved out of the direct exposure to the regional flow and into the wind shadow of the mountain peaks, ozone concentrations dropped to about 6 pphm; then, near Zephyr Cove, concentrations dropped again to about 3 pphm. Nitric oxide (NO) titration of ozone from motor vehicles along the south shore is suspected as the reason for this drop. NO_Y concentrations are low in the regional flow but increase in the sheltered areas of the south end of the lake. This suggests that much of reactive nitrogen in the regional flow is exhausted before the air parcel reaches the Tahoe Basin. Note the peaks in NO_Y when the Frantz' course ran near shore in the vicinity of Cascade Creek where Highway 89 runs along the shore, and approaching Zephyr Cove, where down-slope movement exposed the Frantz to fresh emissions along Highway 50. Occasional extreme NO_Y peaks are due to crossing wakes of motorboats – only spikes seen in successive

minutes should be considered due to terrestrial sources. Titration of regional ozone by local NO_X is the apparent cause of the drops in ozone concentrations.

3.2.1.8.2.3 Aerosol Data

The aerosol data are plotted here as "optical mass". This is estimated from particle counts by applying a correction factor of 2 for detection efficiency for sub-micron particles and using a sliding density scale of 1 for fines (assuming OC and water dominate the mass) to 2.5 (quartz) for coarse particles (assuming soil dominates the mass). This optical mass characterization provides a convenient scale for looking at these data, is internally consistent so that masses in different size bins can be compared, and is probably within a factor of 2 or so of real concentrations.

Fine aerosol data show regional material (PM2.5) accompanying the ozone in the regional flow below Rubicon Gap, then a modest enhancement from local sources around the southern end of the lake. Note that peaks near Cascade Creek and Zephyr Cove mimic the NO_Y data. The large (>2.5 μm) aerosol sizes show spotty effects along the west shore and stronger enhancement in the southern end of the lake, consistent with strong, localized sources. Some of the very large particles detected below the Rubicon gap may be spray.

These data track the regional/local split seen in the long term IMPROVE data. Although further work is needed to identify the source(s) of the regional ozone/fine PM, describe the synoptic and micro-scale meteorology, and quantify the local pollutant contributions, several key observations were made. Coarse particles (aerodynamic size>2.5 μm or larger than PM2.5) are significantly affected by local sources and their largest immediate impact is from sources in the southern end of the lake. NO_Y from local sources is sufficiently strong to reduce regional ozone concentrations. A large in-basin source region of reactive nitrogen is around South Lake Tahoe. Although meteorological processes indicate that summer is the primary season for potential transport of ozone and fine particles to the Tahoe Basin, these regional airflows are not likely to be the source of reactive nitrogen in the Tahoe Basin. A complete understanding of this event and the relevant local and regional contributions will require gathering all observational data for this time period, including synoptic and local meteorology and air quality data from upwind urban areas, western Sierra slope monitoring sites (Big Hill, Echo Summit, etc.), and in-basin sites.

Figure 3-22. On-Lake Dust Experiment, July 2003.

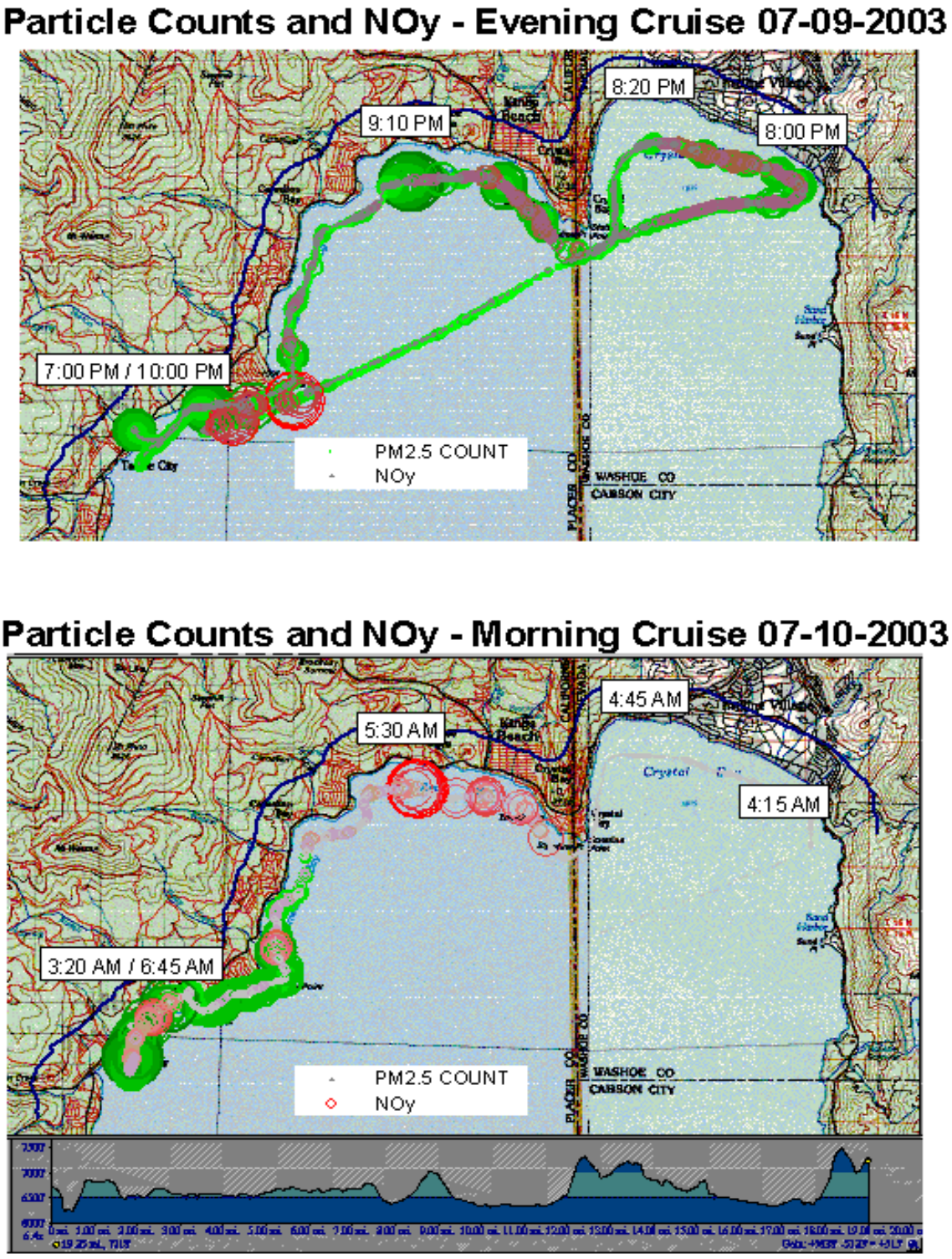

Note: Green circles denote PM2.5 and red circles denote total reactive nitrogen (NO_Y) concentrations with the size of any circle proportional to the amount of concentrations present.

Figure 3-23. On-Lake Dust Experiment, August 18, 2003 (6-9 pm).

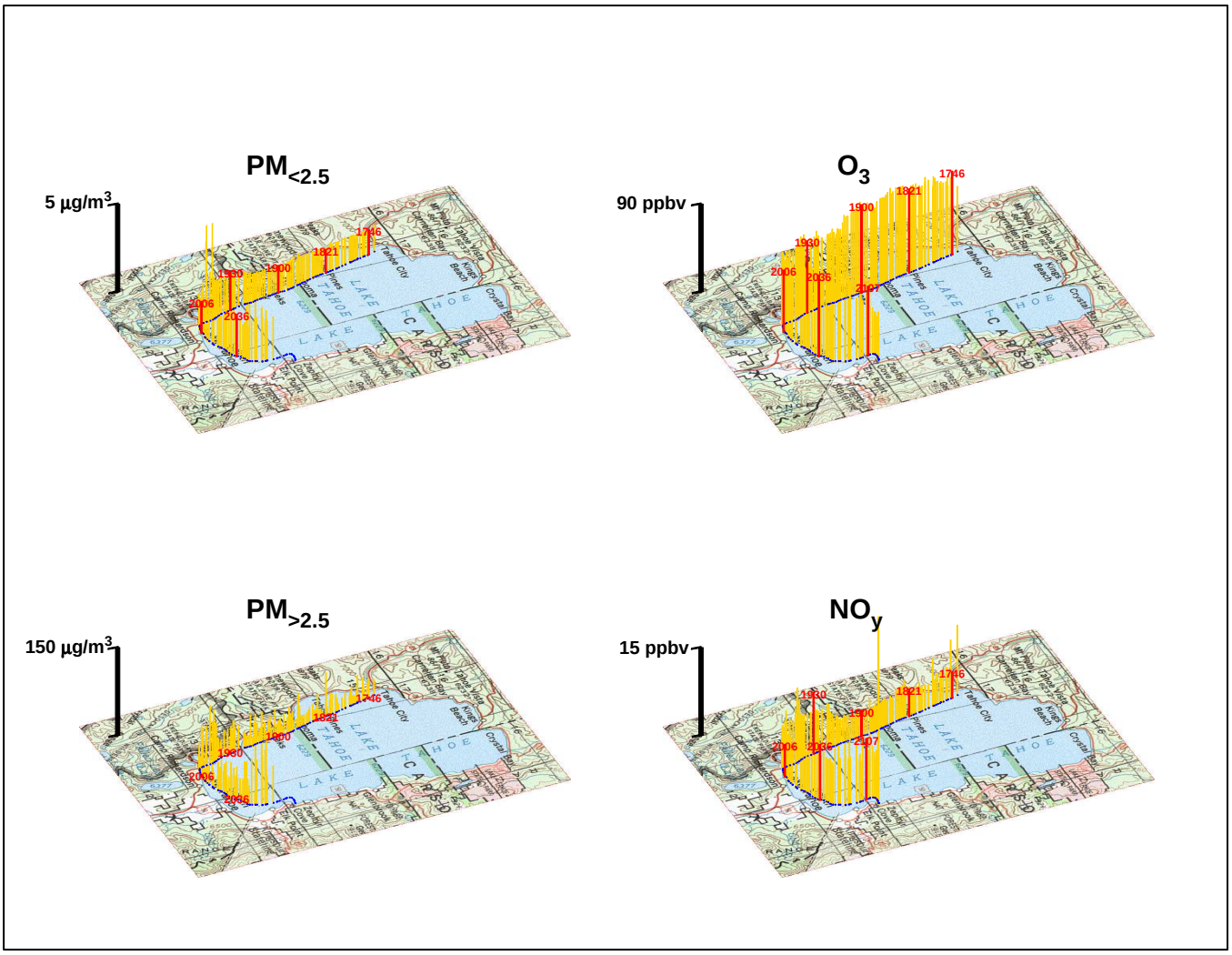

3.2.1.8.3 March 2004, SOLA Dust Experiments

To understand dispersion and loss as a function of distance from a likely source such as motor vehicle traffic, we designed and executed the SOLA Dust Experiments. SOLA site was situated roughly 50 feet away from the very busy Highway 50, also known as Lake Tahoe Boulevard in that stretch of the highway in South Lake Tahoe, and 100 feet away from the beach on the south shore. During Dust Experiments in March 2004, we placed CLIMET instruments at increasing distances from the road - a few feet away, 18 feet away, at SOLA, and one instrument roughly at the beach. **Figure 3-24** provides a synopsis of the experiment with S1 to S6 denoting 0.5 to 1, 1 to 2.5, 2.5 to 5, 5 to 10, 10 to 25, and >25 micrometer size fractions.

Even for particles in the smallest size fraction (0.5 to 1 micrometers in aerodynamic diameter), between the roadway, the emission sources, and the beach, there was nearly a 40% loss in number of particles due to dispersion, deposition, and interactions

with tree canopies. For the heavier particles (10 to 25 and >25 micrometers in diameter), there was a nearly 90% loss. The key lesson was that concentrations measured at our shoreline sites would almost always, and by a significant margin, overestimate concentrations near the middle of the lake. The monthly 24-hour TSP samples collected with MVS on two buoys were essentially identical with each other and remarkably similar to TSP concentrations at Thunderbird Lodge. The comments of peer reviewers and these insights led staff to account for depletion of particles over the Lake. Staff depleted PM_coarse and PM_large in the northern and southern quadrants of the Lake (primary source regions) by 25% of the difference between the PM concentrations at Lake Forest (north) and at SLT (south) and the PM concentrations at Thunderbird Lodge (east; basin background). Even with this depletion correction factor in the deposition estimates, the true (actual) deposition could be lower. Much more analysis is required to understand the full implications of dust experiments for mechanisms of air parcel transport within Tahoe Basin.

3.2.1.9 Phosphorus

Phosphorus (P) in either gaseous or aerosol form is not commonly a focus of air quality monitoring. We are not aware of any gaseous P measurements in California. California has a limited set of aerosol P data collected as part of the Toxic Air Contaminant (TAC) monitoring program. These TSP samples are collected on a 1-in-12 day schedule at urban sites throughout the state and are analyzed using X-ray fluorescence (XRF) by ARB staff. Phosphorus data were also reported by ARB's Dichot (PM10) network for PM2.5 and PM_coarse size fractions. The IMPROVE network also reports P concentrations in the PM2.5 size fraction. LTADS attempted to measure aerosol P, but had only limited success (see below). This section summarizes the P data available from the IMPROVE and LTADS sampling in the Tahoe Basin and, utilizing P data collected in other areas of California during other sampling programs, constructs a rough estimate of P concentrations in the basin.

3.2.1.9.1 Constraints on Aerosol Phosphorus Measurement

All of the sampling programs summarized here rely on XRF analysis of Teflon filters to measure aerosol P. In ambient aerosols, P detection is hampered by chronically low P concentrations and by strong interference from two common elements, sulfur (S) and silicon (Si).

The S interference is driven by three factors: 1) the strongest spectral fluorescence lines for P and S are separated by only a little more than the minimum energy resolution of typical fluorescence detectors (about 1.5 times the minimum resolution); allowing for some electronic "noise," the two peaks nearly overlie one another; 2) S fluoresces more strongly than P does; and finally, 3) S is usually present at several times the concentration of P. Together these factors often cause the S signal to overwhelm the P signal.

The Si interference is not as intrinsically strong, because the peak energies are more separated (nearly 3 times typical detector energy resolution). However, Si is generally

Figure 3-24. Normalized Particle Counts in Six Size Bins as Observed at SOLA during Early Morning Offshore Winds on March 12, 2004.

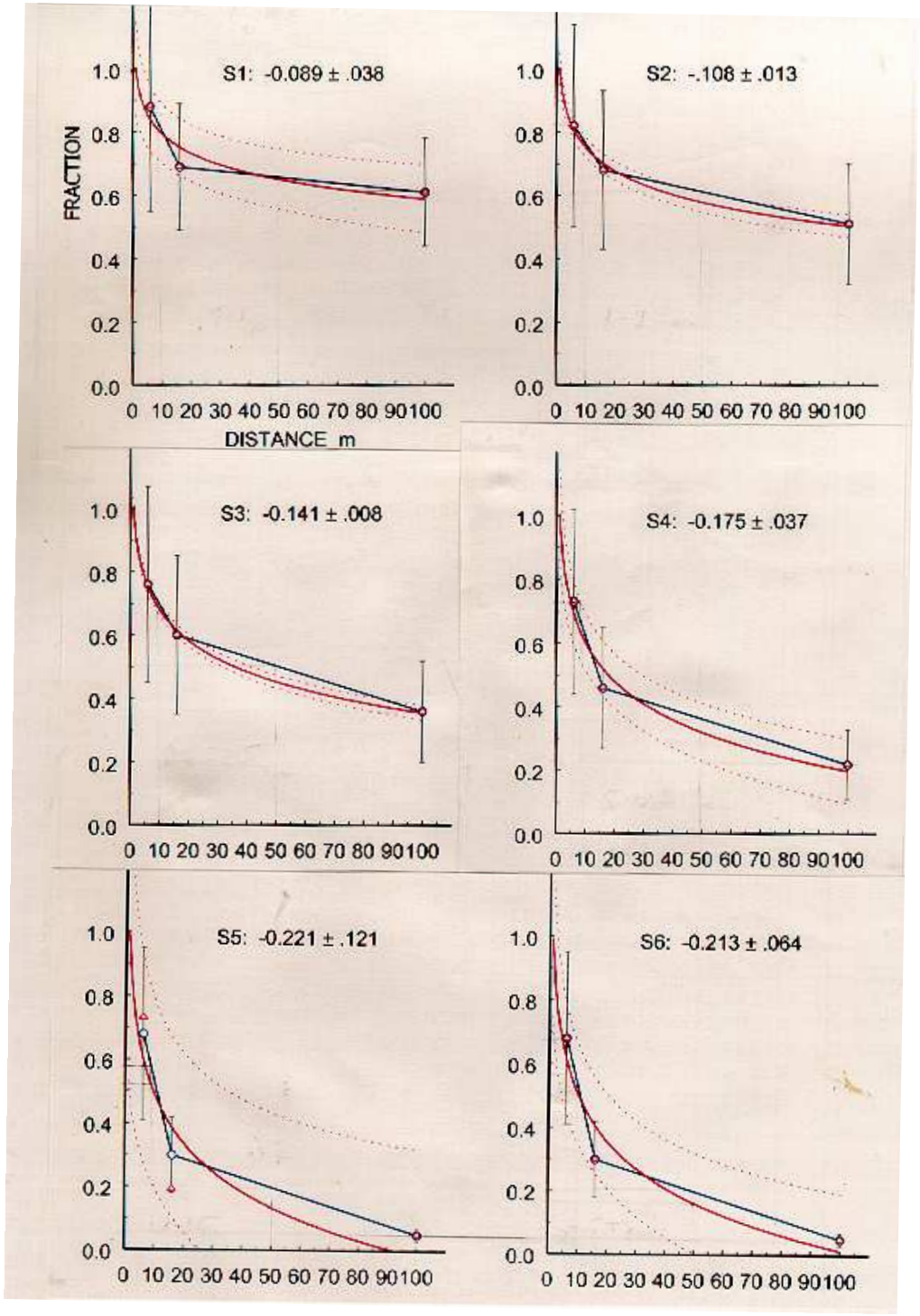

present in much higher concentrations than P, and the large concentration peaks have wider electronic “noise” footprints, so the net effect on the P peak is similar to that of S.

The relatively clean air in the Tahoe Basin accentuates the P detection problem. Although P can accurately be measured in pure standards, low P concentrations and interferences in ambient samples makes detecting P concentrations above measurement uncertainties in most XRF systems difficult to achieve in the best of circumstances. During the LTADS sampling program, 606 filters were analyzed by XRF. Of those filters, only 49 had P values greater than zero (i.e., there was a distinguishable P signal), and only ten of those were above measurement uncertainty limits (three other samples with [P] above uncertainty were compromised by other sampling problems and were invalidated). These measurements are presented in **Figure 3-25**. Most of the high [P]s were observed during winter with the other two cases occurring during late summer. The mean P concentration for the ten measurements was 11.1 ng/m^3 and the maximum observed was 21 ng/m^3. None of the phosphorus detections greater than measurement uncertainty were in the PM2.5 size fraction.

Figure 3-25. All 10 Occurrences When [P] Greater than Measurement Uncertainty.

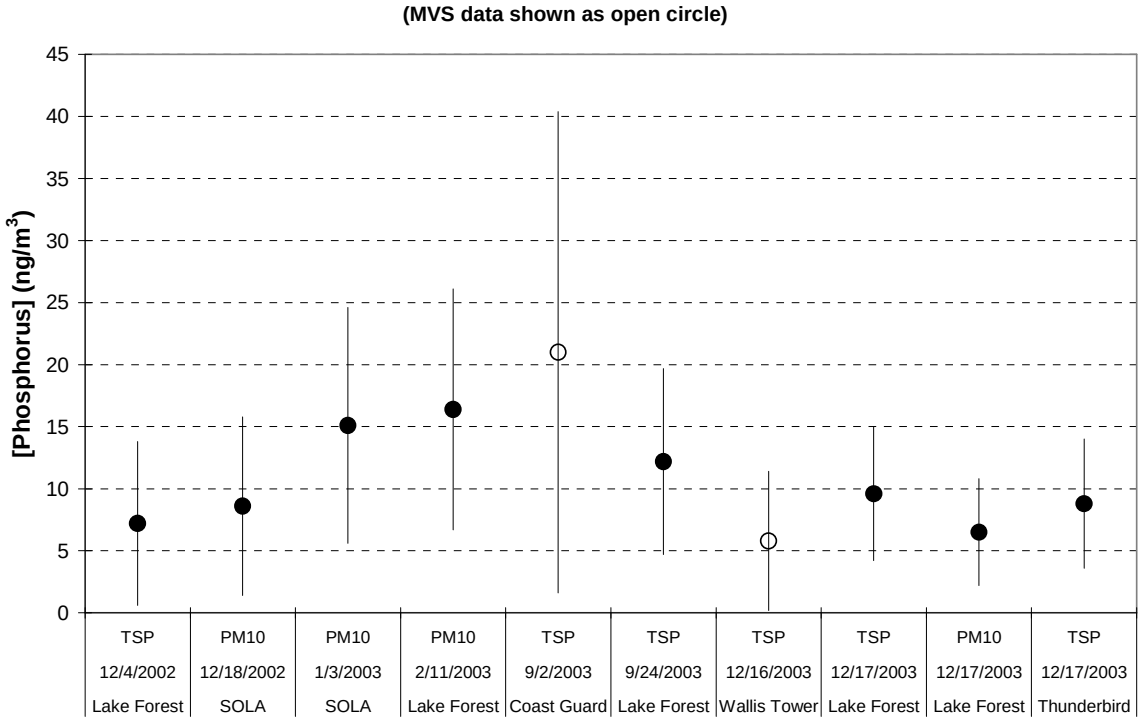

The average of the measurement uncertainties (i.e., the analytical uncertainties propagated from the counting statistics associated with each sample and background spectra) for the P non-detects indicates that the typical LTADS XRF limit of detection

(LOD) for P was about 10 ng/m^3. LOD denotes a statistical likelihood of detection. To increase confidence that the P was actually present, the operational limit of detection (O-LOD) is estimated by multiplying the standard deviation of the non-detect uncertainties by a factor of 3 (i.e., 97.5% confidence). For LTADS, the standard deviation of the P non-detect uncertainties, was 9.9 ng/m^3, providing an O-LOD of 30 ng/m^3. Note that although LODs in the range of 1 to 5 ng/m^3 have been reported by other studies, the analytical difficulties noted above result in an O-LOD of at least 20 ng/m^3. After careful review of data, staff believed that the O-LOD for detecting during LTADS was about 30 ng/m^3. However, as discussed later, peer review of the draft final report indicated other inherent P measurement problems with XRF in ambient settings that may make the O-LOD higher than 30 ng/m^3.

As noted before, P non-detects likely occur due to S and Si interference. The aerosol sample matrix may be the governing factor on whether or not XRF measurements successfully detect P. The fact that LTADS detected no P in the PM2.5 size fraction indicates that such concentrations were below the LOD. Furthermore, the phosphorus measurements of the source samples that were reanalyzed were variable and inconsistent. Therefore, conclusions regarding phosphorus concentrations in wood smoke and other combustion sources thought to dominate fine PM emissions are premature.

The LTADS P detection efficiency was about one-third that reported by the IMPROVE sampling. From 1989 to 2000, the IMPROVE sampling network collected 571 PM2.5 filters at Bliss State Park, reporting 30 P detects above uncertainty. Among 751 PM2.5 filters that were collected at SOLA over the same period, IMPROVE reported 31 P detects above uncertainty. The minimum detected P for IMPROVE appears to be around 1 ng/m^3. However, the IMPROVE LOD is likely much higher than 1 ng/m^3 because interferences from S and Si are expected. These data are summarized in **Table 3-7**.

In urban South Lake Tahoe, the IMPROVE data (PM2.5) reported a maximum P concentration of 21.5 ng/m^3 at SOLA. Similarly, the maximum P concentration observed during the 1-year LTADS was 21 ng/m^3 in a TSP sample (mini-vol sampler) at the US Coast Guard site in Lake Forest. In a more remote area in the basin (Bliss State Park, a site well above lake level and on western side of the Lake), the IMPROVE PM2.5 sampling recorded a maximum P concentration of 9.6 ng/m^3. LTADS only had six measurements (TSP by MVS) at Bliss and reported no P detects.

3.2.1.9.2 Phosphorus Measurement Difficulties in LTADS

In addition to the well-known overlap of the P x-ray emission spectrum with the tails of the emission spectra of the much more abundant sulfur (~20x) and silicon (~200x) atoms, the phosphorus x-rays can be self-absorbed within the particle. This self absorption effect is known to be relatively small (<10%) for fine (PM2.5) particles. Self absorption is potentially much greater in larger particles but depends on the amount and distribution of the P within the particle. The P data originally reported for LTADS included a 1.72 correction factor for the P measurements in PM10 and TSP samples.

One of the external peer reviewers of the draft version of this report, Professor Emeritus Tom Cahill of the University of California (Davis), whose expertise is in particulate matter measurements, pointed out that phosphorus x-rays in soil (an alumino-silica matrix) are strongly absorbed by Al and Si, which are abundant components of soil. A theoretical 3-layer particle model analysis indicated that large P correction factors may be necessary for particles larger than 2.5 µm. Assuming that PM_coarse particles (size between 2.5 and 10 µm) have an average diameter of 6.7 µm, their self absorption correction factor would be a factor of about 3.4; assuming that PM_large particles (size larger than 10 µm) have an average diameter of 12 µm, their self absorption correction factor would be a factor of about 6.8 (both estimates include a 1.42 factor for signal absorption within a silicon detector system that, in theory, should be accounted for during calibration of the analyzer response). Discounting the factor for absorption within a Si detector system, the self absorption correction factors for PM_coarse and PM_large would be about 2.4 and 4.8, respectively. Because the P data reported for PM10 and TSP samples in LTADS already included a 1.72 correction factor for self absorption within the particles, the P data in PM_coarse and PM_large sizes in the LTADS database would only require multiplicative factors of 1.4 and 2.8, respectively.

Table 3-7. Phosphorus concentration (ng/m^3) and S/P & Si/P ratio statistics based on 1989-2000 IMPROVE PM2.5 measurements in South Lake Tahoe (SOLA) and Bliss State Park (BLIS).

Statistic | Site \ Parameter:	[P]	S/P	Si/P
SOLA			
Minimum	5.39	2.48	2.63
Mean	11.84	12.38	16.25
Maximum	21.52	33.35	42.81
Median	10.99	9.91	16.25
Standard Deviation	4.06	7.85	10.76
Standard Error of Mean	0.73	1.43	1.96
# Samples detecting phosphorus	31	30	30
# Samples	751	751	751
BLISS			
Minimum	1.03	2.92	0.31
Mean	4.56	18.43	11.97
Maximum	9.61	57.62	72.09
Median	4.75	16.88	9.63
Standard Deviation	2.11	11.90	13.64
Standard Error of Mean	0.38	2.17	2.49
# Samples detecting phosphorus	30	30	30
# Samples	571	571	571

Nearly all XRF P data reported to date (not just LTADS) suffer from these particle size and soil matrix difficulties. However, additional research and peer review is necessary before the historical measurements could possibly be corrected for these measurement complexities. To understand these difficulties and to correct for their effects, a substantive knowledge of the particle sizes associated with the P measurements will be required. Knowledge of the chemical composition of the particles would also be necessary to account for absorption of P x-rays by other components. However, because detailed knowledge of particle size and composition is generally limited, it is clear that correcting the existing P data would be very challenging. The crude P corrections presented below assume that P atoms are uniformly distributed throughout the particle. In theory, the biologically available forms of P would more likely be near the surface of the particle. Thus, this approach of including large corrections for signal absorption deep within particles would significantly overestimate the P that is biologically available.

Because the number of P detections with the TWS (TSP, PM10, and PM2.5) and MVS (TSP only) PM networks was very limited with the standard XRF analysis, CARB contracted for a more sensitive analysis (synchrotron XRF) of 70 ambient samples at the Advanced Light Source (ALS) laboratory. The synchrotron XRF detected phosphorus in 49 of the samples while standard XRF detected phosphorus in only 15 of the samples. For the 11 matched "non-zero" measurements, the ALS results averaged over two times the standard XRF results (12 ng/m^3 vs. 5 ng/m^3).

The new theoretical absorption corrections were applied to the P data. Because the routine PM sampling during LTADS had limited PM size information, these corrections were necessarily constrained to estimates of the fraction of total PM mass (TSP) in the PM_fine (PM2.5), PM_coarse (PM10 minus PM2.5), and PM_large (TSP minus PM10) sizes with an assumed mean particle size in each size fraction. TSP measurements with the MVS were allocated among the three particle size bins based on the PM measurements from the Two Week Sampler network. These allocations were based on the general nature of the mini-vol sampling site as shown in **Table 3-8**. The SOLA, Sandy Way, Lake Forest, and Wallis Tower sites were classified as urban and the Thunderbird, Bliss, and buoy sites were classified as remote (i.e., limited influence from local emission sources). The sites on piers were assigned an intermediate classification.

Table 3-8. PM size fraction allocations to TSP samples from the mini-volume sampler program.

Sampling Sites	Exposure Type	PM_fine fraction	PM_coarse fraction	PM_large fraction
Thunderbird, Bliss, buoys	Remote	60%	35%	5%
Piers (US Coast Guard, Wallis, Timber Cove, Zephyr Cove)	Intermediate	50%	40%	10%
SOLA, Sandy Way, Lake Forest, Wallis Tower	Urban	40%	45%	15%

Because of the uncertainties in measuring P concentrations, a variety of information is relevant and necessary for estimating the range of central tendencies in P concentrations. Because P was not detected in many of the samples, an estimation is needed of the P concentration is needed for samples below the analytical detection limits (LOD). LTADS estimated an operational LOD for P measurements by the DRI and ALS systems by multiplying 3 times Standard Deviation of the P non-detect measurement uncertainties. For the ALS measurements, the O-LOD was 3 x 3 ng/m^3 or 9 ng/m^3. For the DRI measurements, the O-LOD was 3 x 9.9 ng/m^3 or ~30 ng/m^3. Typically, one-half of the O-LOD is used to estimate concentrations of substances below the analytical technique's detection limit.

The average P concentration of the 49 P detects with the ALS analysis was 61 ng/m^3 (after accounting for field blank values, the new self absorption correction factors, and the 1.42 silicon detector bias needed for the ALS data). Because 21 of the 70 ALS samples resulted in no detection of P, an estimate of the unknown P concentration in those samples is needed. Usually, one-half of the O-LOD is used for this estimate. However, the original P measurements do not account for the size-dependent self absorption and so the O-LOD also needs to be increased to account for the self absorption of the signal. Comparing average P concentrations originally reported by ALS for TWS TSP samples with the average P concentrations associated with the matched sized P corrections for self absorption (P_coarse * 2.4; P_large * 4.8) and the ALS correction factor for measuring P with a silicon detector (1.42) indicates a rather large P_TSP correction factor of 4.4 when accounting for the net impact of self absorption and calibration on the ALS P concentrations. Assuming the O-LOD is impacted in a similar proportion, the corrected O_LOD is 9 ng/m^3 * 4.4 or ~40 ng/m^3. Assuming one-half of the corrected O-LOD (½ x 40 ng/m^3) for the 21 samples without detection of P yields an average P concentration for the 70 ambient samples analyzed at the ALS of 49 ng/m^3. Assuming the 70 ALS samples were spatially and temporally representative of the 600+ total ambient samples collected during LTADS, an average P concentration of 49 ng/m^3 would be estimated for LTADS.

Although the ALS samples were selected on the basis of the highest P concentrations initially reported by DRI, the samples actually submitted to ALS for analysis included all of the available samples from other sites during the same sampling period (some filters were not available because they had been digested during a supplemental analysis by ICPMS). Consideration in the sample selection was also given to balance seasonal representation. Because the selection process for filters to be reanalyzed at ALS focused on the higher P concentrations reported by DRI, the possibility of a positive bias exists. However, the original DRI measurements of detectable phosphorus concentrations were infrequent and often unrelated in space and time. Thus, the ALS analysis of all associated samples (mostly P non-detect samples by DRI) and the consideration of seasonal balance in the sample selection process, the ALS phosphorus results are likely to be representative of the actual annual and seasonal concentrations.

However, if the ALS analytical set were assumed not to be temporally representative, the average LTADS phosphorus concentration could be estimated by assuming P concentrations equal to ½ of the DRI O-LOD for the ~540 samples with non-detects (assuming all the DRI P detects were analyzed by ALS) and averaging with the mean P concentration of the ALS samples (i.e., 49 ng/m^3). As noted above, staff conservatively estimated the O-LOD of the original DRI P measurements by using three times the standard deviation of the uncertainty associated with the reported "zero" P concentrations (9.9 ng/m^3) or ~ 30 ng/m^3. Based on the annual mean size fractions from the TWS data (10% in PM_large, 40% in PM_coarse, and 50% in PM_fine), the 30 ng/m^3 O-LOD for the original DRI data were adjusted upward to account for the larger self absorption correction factors in PM_coarse (x1.4) and PM_large (x2.8) particles. Thus, staff estimated a corrected O-LOD of 40 ng/m^3 for the DRI P measurements. Using the average P concentration of 49 ng/m^3 for the 70 ALS samples and ½ of the DRI self-absorption-corrected O-LOD (i.e., 20 ng/m^3) for the ~540 DRI samples with non-detects, this approach estimates an average P concentration of ~25 ng/m^3 during the LTADS sampling. This analysis is summarized in tabular form in **Table 3-9**. Based on the estimation approaches described above, the staff can confidently assume that the "true" annual average P concentration in the Tahoe Basin is not likely to be less than 25 ng/m^3 nor greater than 50 ng/m^3, including the large new theoretical correction factors.

Table 3-9. Estimation of LTADS average phosphorus concentration if assuming the mean P concentration from ALS subset of LTADS samples is not temporally representative. LTADS [P]avg = (sum of (# of samples x measurement or ½ x MDL))/total # of samples.

Analysis method	O-LOD (ng/m^3)	Number	x	Mean Measurement Or ½ x O-LOD (ng/m^3)	=	Product (ng/m^3)
ALS detects	---	49	x	61	=	2,989
ALS non-detects	40	21	x	20	=	420
DRI detects*	---	0	x	0	=	0
DRI non-detects	40**	536	x	20	=	10,720
Sum	---	606	x	---	=	14,129
LTADS [P] $_{avg}$	---	---	-	**23.3**	-	---

* Note: DRI detects were reanalyzed at ALS and so # of DRI detects is zero even though 10 were actually observed.

** estimated as 3 x StdDev of measurement uncertainty associated with DRI [P]s reported as 0 ng/m^3 (for TSP samples) and adjusted for updated size-specific self absorption correction factors (size distribution of P assumed to be the same as annual mean observed with TWS network: 10% in PM_large fraction (x 2.8), 40% in PM_coarse fraction (x 1.4), and 50% in PM_fine fraction (x 1.0)).

3.2.1.9.3 LTADS vs. Other Phosphorus Measurements

In addition to the LTADS and IMPROVE measurements within the Tahoe Basin, additional P measurements are available from the ARB'S Dichotomous (PM2.5 and PM_coarse) program for measuring PM10 and from ARB's Toxic Air Pollutants (TAC) monitoring network. Annual mean P concentrations for dichot sampling sites in the mountains are shown in **Table 3-10**. Note that no P was detected in the PM2.5 samples. Similarly, P was not detected in any LTADS PM2.5 samples. The IMPROVE sampling program has reported some P detects in the fine fraction (~4% of samples), however.

The mean annual P concentrations in the PM_coarse samples from the dichot network were roughly comparable (approximately 25 ng/m^3) among the four sampling locations in the mountains. Assuming that the PM_fine, PM_coarse, and PM_large fractions of TSP are 50%, 40%, and 10% respectively (based on average LTADS TWS results) and that P is uniformly distributed among PM sizes yields a 62 ng/m^3 annual mean concentration estimate of total P. However, no P was detected in any of the PM2.5 samples. Thus, 25 ng/m^3 serves as a lower bound and 60 ng/m^3 serves as an upper bound of annual average P concentrations. Assuming the updated size-dependent P self absorption correction factors (P_coarse * 1.4 and P_large * 2.8) creates a skewed corrected estimate of annual P concentrations of 35-85 ng/m^3.

The Toxic Air Contaminant (TAC) network samples in urban areas on a 1-in-12 day schedule. Median P concentrations from the TAC network seldom exceeded 60 ng/m^3. Stations not impacted by obvious agricultural or dairy impacts (e.g., Riverside-Rubidoux) have reported a P concentration exceeding 200 ng/m^3 only once, in Azusa in 2002 (ARB, 2002). The group median value of the eight site-specific annual median P concentrations is shown for each year (1996 through 2002) in **Table 3-11**. The annual median P concentrations ranged from 44 to 54 ng/m^3, based on standard XRF analysis. The minimum annual median P concentration at any site in the TAC (urban) network, a number more likely to be representative of less populated areas such as Lake Tahoe, ranged from 32 to 43 ng/m^3, with a multi-year mean of 36 ng/m^3. Based on a typical 10:40:50 split in PM_large:PM_coarse:PM_fine and accounting for the new, size-specific, theoretical self absorption correction factors (i.e., x 1.0 for P in PM2.5, x 1.4 for P in PM_coarse, and x 2.8 for P in PM_large), yields an absorption-corrected annual mean P concentration estimate of 1.34 x P_original or 43-58 ng/m^3 for the range of minimum concentrations in the TAC network and ambient concentrations in the Tahoe Basin. Based on the TAC data, annual mean P concentrations in the Tahoe Basin could be as low as 30 ng/m^3 and as high as 60 ng/m^3.

3.2.1.9.4 Phosphorus Estimated from PM Emission Inventory

As an alternative approach to estimating the phosphorus concentrations in the Tahoe Basin, staff also estimated seasonal average P concentrations from seasonal average PM concentrations by developing a P emission factor based on source profiles of P as a function of PM, weighted to the mix of PM sources in the Tahoe Basin. The PM

emissions were also divided into 3 sizes (PM_fine, PM_coarse, and PM_large) to apply the theoretical self absorption correction factors, which are not in the current P source profiles, to the PM_coarse and PM_large fractions. This analytical approach resulted in an average P concentration estimate of 22 ng/m^3 in the Tahoe Basin and is described in detail in **Table 3-12**.

Table 3-10. Annual mean P coarse concentrations (ng/m^3) from ARB's dichot PM10 (PM_fine & PM_coarse) monitoring network. All P measurements in the PM_fine fraction were non-detects. The dichot measurements are collected on a 1-in-6 day schedule.

Site \ Year:	1991	1992	1993	…	1998	1999	2000	Mean
Mammoth Lake	28.1	22.2						25.2
Truckee		24.6	31.2					27.9
Quincy		22.3	21.4					21.8
Portola					26.6	25.3	27.5	26.5

Table 3-11. Median annual P concentrations (ng/m^3) from ARB's toxic air contaminant monitoring network. The toxic network samples on a 1-in-12 day schedule.

Site \ Year:	1996	1997	1998	1999	2000	2001	2002	Mean
Azusa	---	---	---	---	59	68	54	60.3
Burbank-W Palm	57	65	62	64	54	55	63	60.0
Los Angeles-NM	53	---	56	56	47	---	51	52.6
N. Long Beach	32	44	43	51	36	35	37	39.7
Riverside-Rubidoux	210	---	---	250	220	240	230	230.0
Roseville-Sunrise	37	37	40	43	32	35	33	36.7
San Jose – 4th St	34	40	42	44	44	44	---	41.3
Stockton-Hazelton	46	53	56	52	51	50	54	51.7
MEDIAN	46	44	48	52	49	50	54	**49.0**
MINIMUM	32	37	40	43	32	35	33	**36.0**

Table 3-12. Estimation of LTADS average phosphorus concentration based on emission inventory P source profiles and ambient PM concentrations. LTADS [P]avg = (emissions-weighted source-specific P emission factor x PM emission estimate from that source measurement (or ½ x O-LOD))/total # of samples.

a) Phosphorus emission factors (i.e., P=f(PM)) based on ARB emission profiles.

Source	%TSP	%PM10	%PM2.5	Notes
Construct/demolition	0.1499	0.0979	0.2273	
Unpaved road dust	0.1225	0.1225	0.1225	
paved road dust	0.1372	0.1372	0.1372	
fireplaces & stoves	0.0288	0.0288	0.0196	based on orchard prunings as official inventory assumes 0.0000 for firewood
Waste burning	0.0295	0.0295	0.0205	
other (estimated)	0.0795	0.0795	0.0750	estimated as mean of P profiles for above 5 major PM sources

b) Estimated PM emissions (tons/day) based on ARB emission inventory.

(**Note:** The PM emission inventory does not include secondarily generated PM (e.g., NH_4NO_3) that can contribute significantly to ambient PM concentrations.)

Source	TSP	PM10	PM2.5	Notes
construct/demolition	0.85	0.42	0.09	
unpaved road dust	2.31	1.37	0.29	
paved road dust	2.16	0.99	0.17	
fireplaces & stoves	1.91	1.79	1.72	
waste burning	0.31	0.31	0.29	
other (estimated)	0.53	0.40	0.29	
TOTAL	8.07	5.28	2.85	

c) Development of PM source-weighted phosphorus emission factor based on ARB's PM emission inventory. Source-weighting multiplies equivalent cells in sub-tables a) and b) and divides by TOTAL PM emissions in sub-table b). The integrated source-weighted P emission factor by size is then the sum of the factors for each PM source.

	P fraction			
Source	**of TSP**	**of PM10**	**of PM2.5**	**Notes**
construct/demolition	0.000158	0.000078	0.000072	
unpaved road dust	0.000351	0.000318	0.000125	
paved road dust	0.000367	0.000257	0.000082	
fireplaces & stoves	0.000068	0.000098	0.000118	
waste burning	0.000011	0.000017	0.000021	
other (estimated)	0.000052	0.000060	0.000076	
Source-weighted P emission factor	**0.001007**	**0.000828**	**0.000494**	

d) Assuming that the ambient PM concentrations reflect the relative impact of PM emission sources and that the emission sources have the same average mix throughout the air basin, multiplying the integrated source-weighted average phosphorus emission factor in sub-table c) times the respective annual average PM concentrations observed during 2003 at each site in the Tahoe Basin yields the estimated annual [P]s. This analysis could also be done on a seasonal basis (provides more temporal detail but yields essentially the same annual results).

	$[PM]_{annual\ mean}$ in ng/m^3			$[P]_{annual\ mean}$* in ng/m^3		
PM Monitoring Site	**TSP**	**PM10**	**PM2.5**	**TSP**	**PM10**	**PM2.5**
SLT-Sandy Way	22,032	16,762	9,177	22.2	15.2	4.5
SLT_SOLA	21,773	18,551	7,270	21.3	16.5	3.6
Lake Forest	18,059	13,981	4,914	18.2	12.7	2.4
Thunderbird Lodge	5,958	5,957	3,629	6.2	5.3	1.8
Buoy-West (TB4)+	6,066	5,713	3,548	6.1	5.2	1.8
Buoy-East (TB1) +	6,251	5,887	3,656	6.3	5.3	1.8

* based on average P fraction: of TSP=0.001007, of PM10=0.000908, and of PM2.5=0.000494

+ because only TSP is sampled on buoys, PM10 and PM2.5 values are based on size relationships observed at Thunderbird.

e) Subtracting the P_PM10 estimate from the P_TSP estimate yields the [P] in PM_large; subtracting the P_PM2.5 estimate from the P_PM10 estimate yields the [P] in PM_coarse. P_fine equals P_PM2.5 and P_TSP equals the sum of P_fine plus P_coarse, and P_large.

	$[P]_{annual\ mean}$ in ng/m^3			
PM Monitoring Site	**P_large**	**P_coarse**	**P_fine**	**P_TSP**
SLT-Sandy Way	7.0	10.7	4.5	22.2
SLT_SOLA	4.9	12.9	3.6	21.3
Lake Forest	5.5	10.3	2.4	18.2
Thunderbird Lodge	0.9	3.5	1.8	6.2
Buoy-West (TB4)	0.9	3.4	1.8	6.1
Buoy-East (TB1)	1.0	3.5	1.8	6.3

f) Applying the updated self absorption correction factors for the DRI data, which already includes a 1.72 self absorption correction factor (x 2.8 for P_large, x 1.4 for P_coarse, and x 1.0 for P_fine), to the estimated annual average ambient P concentrations by particle size results in an enhanced estimate of ambient P concentrations (an annual mean 4-quadrant shoreline [P] estimate of 22 ng/m^3, all-site LTADS annual mean [P] of 20 ng/m^3, and, as shown in the table below, a mid-lake-weighted 4-quadrant annual mean [P] of 16 ng/m^3 (i.e., each quadrant's shoreline concentration averaged with the mid-lake concentration).

	Corrected $[P]_{annual\ mean}$ in ng/m^3			
PM Monitoring Site	**P_large**	**P_coarse**	**P_fine**	**P_TSP**
SLT-Sandy Way	19.4	14.9	4.5	38.8
SLT_SOLA	13.5	17.9	3.6	35.0
Lake Forest	15.3	14.3	2.4	32.0
Thunderbird Lodge	2.5	4.8	1.8	9.1
Buoy-West (TB4)	2.6	4.8	1.8	9.1
Buoy-East (TB1)	2.7	4.9	1.8	9.4
4-quad mean*	**9.2**	**10.1**	**2.5**	**21.8**
Mid-lake weighted 4-quad mean**	**5.9**	**7.5**	**2.2**	**15.5**

* 4-quadrant mean = ((SW+SOLA)/2 + LF + 2*TBL)/4

** mid-lake weighted 4-quadrant mean = {((SW+SOLA)/2 + LF + 2*TBL + 4*((TB4+TB1)/2)}/8

3.2.1.9.5 Selection of a phosphorus concentration for LTADS deposition estimates

Because ambient phosphorus concentrations were typically below the detection limits of the sampling and analysis protocols used in LTADS, staff was forced to estimate P concentrations for input into the analyses to estimate the direct dry and wet atmospheric deposition of P to Lake Tahoe. Because of all the uncertainties noted above, staff used a temporally and spatially constant P concentration of 40 ng/m^3 in both the dry and wet deposition modeling approaches to arrive at seasonal and annual estimates of phosphorus loading to Lake Tahoe. [Note: assuming that P is a consistent function of PM, one could generate seasonal and site-specific variations in P based on PM measurements.] The various measurements and insights that led to the selection of this concentration of phosphorus in the deposition analyses are summarized below.

a) DRI XRF measurements of P during LTADS. P detections during LTADS were limited (49 samples with [P] > 0 ng/m^3; only 10 samples with [P] > the measurement uncertainty and none of those were in the PM2.5 size). The average of the 49 detections of P was 5 ng/m^3 and the average of the 10 samples with concentrations greater than the measurement uncertainty was 11 ng/m^3, with a maximum of 21 ng/m^3. Assuming that the P O-LOD equals the 3 times the standard deviation of the "zero" P measurement uncertainties, the P O-LOD for MVS samples was ~30 ng/m^3 (3 x 9.9 ng/m^3). The estimated range of [P] was about 5 - 30 ng/m^3 given that the means are less than the O-LOD. Accounting for new self absorption correction factors, the range of the estimated annual [P] is approximately 10 – 45 ng/m^3. The best estimate of [P] from the DRI measurements is ½ of the O-LOD or ~20 ng/m^3.

b) Supplemental reanalysis of selected LTADS filters by synchrotron-XRF. Reanalysis of 70 ambient filter samples collected during LTADS by synchrotron_XRF analysis at the Advanced Light Source (ALS) laboratory detected P more frequently than the standard XRF method (ALS reported 54 detects out of 70 ambient samples). After correction for relatively high field blank values, the number of P detects dropped to 49 and the mean P concentration was 10 ng/m^3, with a maximum observed concentration of 38 ng/m^3. The mean P concentration of the samples where the [P] was greater than the measurement uncertainty was ~15 ng/m^3. Assuming that the P O-LOD equals the 3 times the standard deviation of the "zero" P measurement uncertainties, the P O-LOD for UCD samples was ~10 ng/m^3 (3 x 3 ng/m^3). Considering a recommended silicon detector calibration factor (x 1.42) for these data and also the self absorption correction factors, the mean P concentration would be on the order of 20-40 ng/m^3 with a maximum of ~95 ng/m^3. The corrected O_LOD would also be about 20 ng/m^3. Thus, the estimated range of [P]s is about 10 – 40 ng/m^3. The best estimate of [P] from the ALS measurements is ~30 ng/m^3 because of the improved measurement sensitivity and relatively high proportion of P detects.

c) Historical measurements of P from ARB's dichotomous sampler network. Although phosphorus has not been the focus of sampling programs, P measurements are available from various programs that have used XRF

analysis. Thus, these PM_coarse measurements would also be subject to the uncertainty associated with potentially large self absorption correction factors. In those that analyzed PM2.5 samples (e.g., dichot, IMPROVE), detection of P in PM_fine has been quite rare without special practices for higher sensitivity. In those programs that measure PM_coarse (i.e., dichot), the annual means of P concentrations in mountain settings (i.e., Truckee, Quincy, Portola, and Mammoth Lakes) were quite consistent at about 25 ng/m^3. The reported MDL for this XRF analytical technique was 15 ng/m^3. Based on the TWS results during LTADS, the following TSP size fractions were assumed: 50% in PM_fine, 40% in PM-coarse, and 10% in PM_large. Assuming the P is uniformly distributed, irrespective of the size of the PM particle, the P_coarse results from the dichot suggest that the total annual P concentration could be about 62 ng/m^3 (i.e., 25 ng/m^3/0.40). However, because no P detects were reported in the PM_fine samples and PM_large was not sampled, the estimated range of total P concentrations is 25 – 60 ng/m^3. Allowing for self absorption correction factors, the estimated range of total P concentrations expands to 35 to 85 ng/m^3.

d) Historical measurements of P from ARB's toxic air contaminant (TAC) sampler program. The TAC network collects TSP samples on a 1-in-12 day schedule in primarily urban areas. TAC data accessed by staff featured annual median P concentrations for 8 urban sites operating between 1996 and 2002. The TAC network average of the annual median P concentrations at the 8 sites was 49 ng/m^3. The minimum annual median P concentration among the 8 sites during each year ranged from 32 to 43 ng/m^3 and averaged 36 ng/m^3. Given the lower population and activity levels in the Tahoe Basin compared to an urban area, the minimum annual median P concentration is more likely than the average urban median P concentration to be representative of conditions in mountain communities such as South Lake Tahoe. Based on the minimum annual median TAC data, P concentrations in the Tahoe Basin are estimated to be 45 – 60 ng/m^3. Including adjustment for the theoretical self absorption correction factors, the estimated range of annual P concentrations in the Tahoe Basin becomes 60 – 80 ng/m^3.

e) Estimation of P as a function of PM concentrations. A limited number of PM samples for various emission sources result in emission source profiles for the PM constituents. Using the P fractions from these TSP, PM10, and PM2.5 source samples and assuming the mixture of P in ambient air is proportional to the mixture of P in source samples, an average P source profile, weighted to reflect the mixture of PM emission sources in the Tahoe Basin, can be applied to ambient PM concentrations measured during LTADS to estimate the concentration of P at the PM measurement sites within the Tahoe Basin. Thus, the spatial and temporal distribution of the P closely matches to PM distributions.

The P emission profiles for TSP, PM10, and PM2.5 were applied to the PM measurements to estimate P concentrations in those sizes. The sized P concentrations were differenced to yield P concentrations in PM_coarse and

PM_large sizes. The new theoretical self absorption correction factors were then applied to these sized P concentrations to yield the final estimate P concentrations at the measurement sites. The result of this analysis yielded a 4-quadrant (SLT + LF + BL + TB) average P concentration of 22 ng/m^3. The estimated annual [P] at the various monitoring sites ranged from 10 – 40 ng/m^3 with a best annual basin estimate of ~20 ng/m^3.

The variety of P estimation results highlight the uncertainty associated with phosphorus measurements and ultimately with estimates of its deposition to Lake Tahoe. From a strictly emission inventory perspective (P profiles and PM emissions), the P emissions within the Tahoe Basin are estimated to be 8 metric tons per year. The fraction of this emission total being deposited directly to the Lake would be appreciably less (less than half based on wind directions alone). Assuming a lake surface area of 500 km^2 and an average dry deposition velocity of 0.5 - 1 cm/sec, a 4 metric ton per year dry deposition estimate would require an average ambient P concentration of 25 - 50 ng/m^3 (assuming total deposition is equally comprised of wet deposition and dry deposition). This concentration analysis based on the emissions inventory yields an estimated annual P concentration range of 25 – 50 ng/m^3, which is comparable to the ambient concentration data analyses. Considering the range in estimates and the uncertainties in detection and self absorption correction factors (likely overestimating available P in larger particles), staff selected an intermediate phosphorus concentration value of 40 ng/m^3 for the LTADS depositional analyses.

3.2.2 Gases

3.2.2.1 Temporal and Spatial Variation of Ammonia and Nitric Acid

The TWS measurements also included denuder measurements of two important nitrogenous gases from a nutrient perspective, ammonia (NH_3) and nitric acid (HNO_3). **Figure 3-26** presents plots showing the variations in these gases. Nitric acid was measured via nitrate extraction from carbonate denuders while ammonia was measured via extraction of ammonium from citric acid denuders. Due to the long integration time of the TWS during variable conditions, stoichiometric balance among the gases and aerosols was not expected, and statistics only indicate weak relationships among the species. This lack of systematic relationships eliminates any basis for estimating nitric acid or ammonia for the MVS network. Gas-phase nitrogen calculations are therefore based entirely on data from the TWS network. Ammonia concentrations were highest at the SOLA site, which had concentrations noticeably higher than the nearby Sandy Way site. The concentrations of ammonia and nitric acid were lowest at the Thunderbird Lodge site. In general, concentrations were lowest during the spring. However, seasonal patterns were relatively weak with the exception of concentrations of both gases being higher in summer and fall at Big Hill and ammonia concentrations being higher during winter at the SOLA site.

Figure 3-26a. Ammonia and Nitric Acid Concentrations Observed with the TWS at Big Hill.

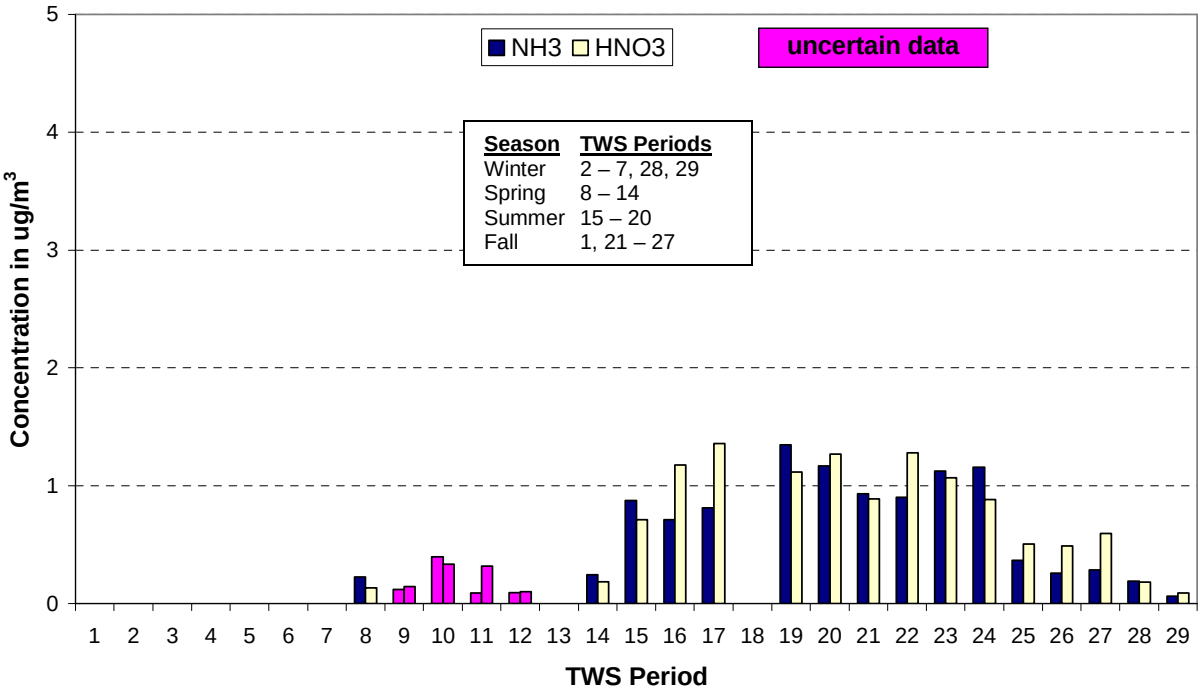

Figure 3-26b. Ammonia and Nitric Acid Concentrations Observed with the TWS at SLT-Sandy Way.

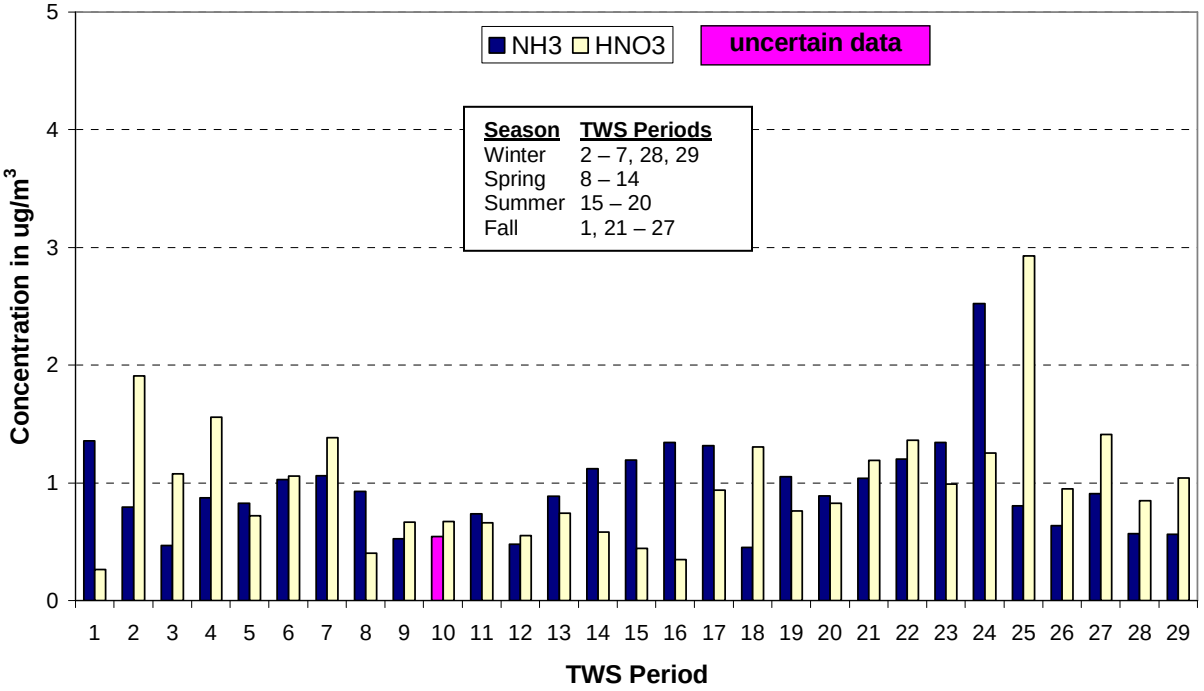

Figure 3-26c. Ammonia and Nitric Acid Concentrations Observed with the TWS at SLT-SOLA**.**

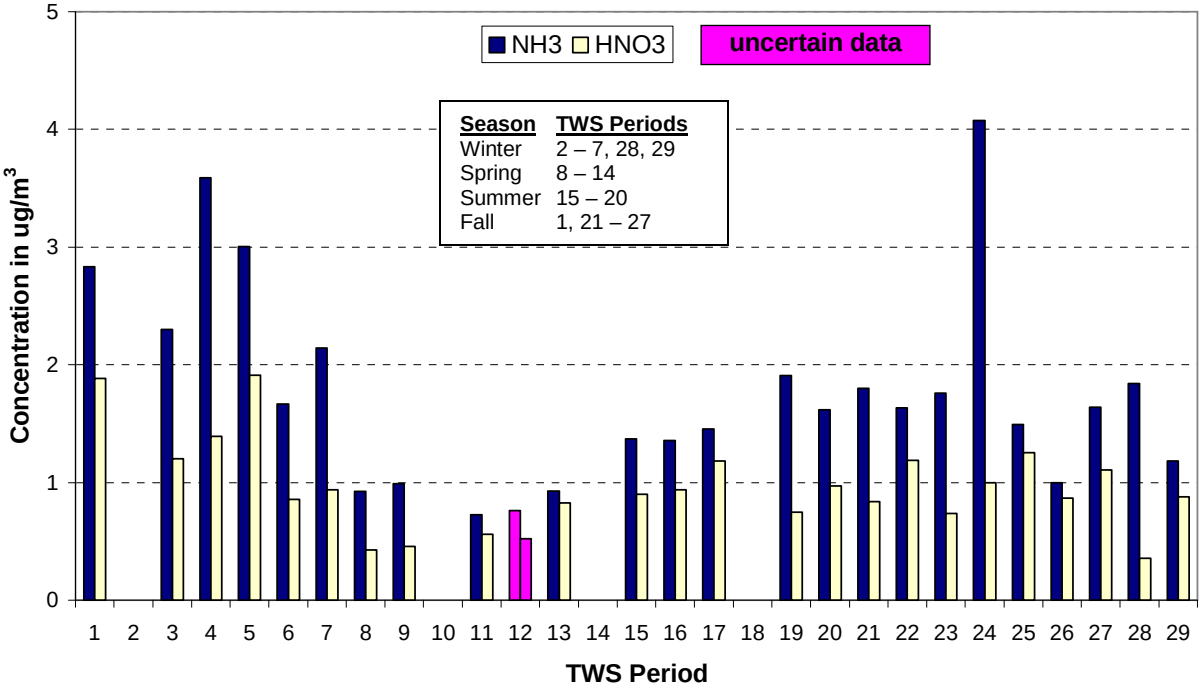

Figure 3-26d. Ammonia and Nitric Acid Concentrations Observed with the TWS at Thunderbird Lodge.

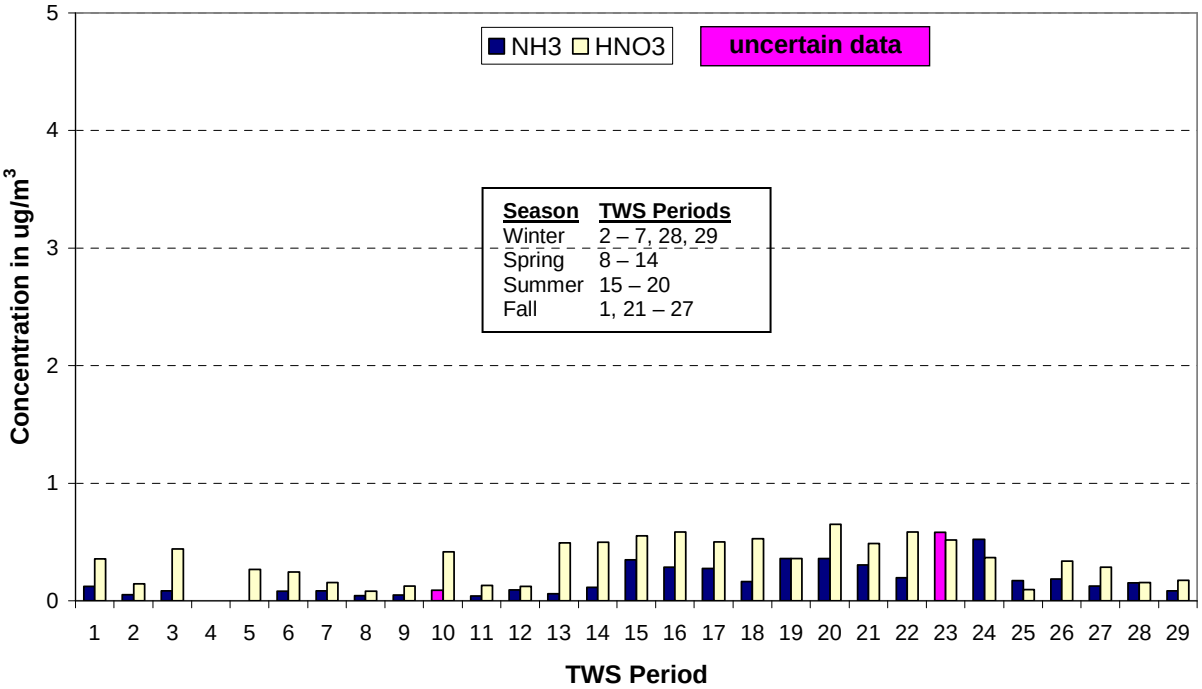

Figure 3-26e. Ammonia and Nitric Acid Concentrations Observed with the TWS at Lake Forest.

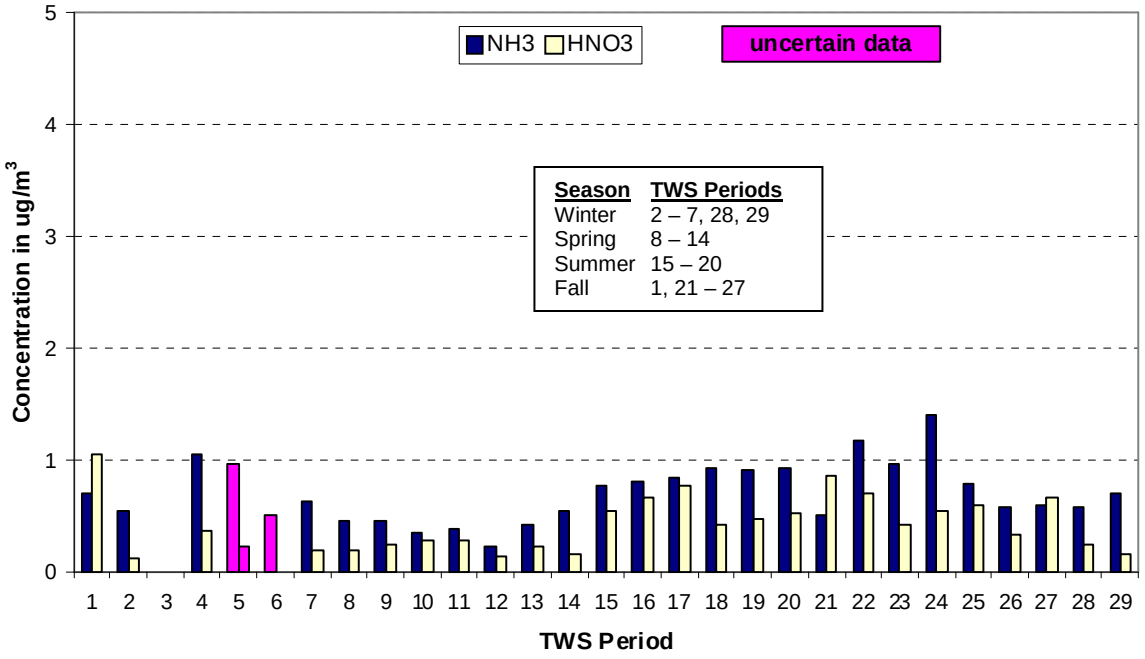

Difficulties in accurately measuring nitric acid were significantly enhanced due to positive artifacts for denuder samplers, and large uncertainties in the denuder method for the low ambient nitric acid concentrations present at all the LTADS sites. Denuder measurements can be biased upwards by conversion of nitrous acid into nitric acid within the denuder, and they also have significant uncertainties in nitric acid collection efficiency at low concentrations, in laboratory extraction efficiency, and the whole analytical process suffers from occasional high blank values. These uncertainties are usually small compared to ambient nitric acid levels in the urban areas where this technology was developed, but at very low concentrations, such as those in the Lake Tahoe Basin, they presented substantial challenges to achieving high data quality.

Review and analysis of the TWS data identified several occasions when nitric acid data were atypically low and deemed suspect. DRI reviewed the laboratory calculations, identified errors, and corrected the suspect values.

Gaseous nitrogen species were also measured using laser-induced fluorescence (LIF) at the Big Hill site by a research group from UC Berkeley. These measurements included alkyl nitrates, peroxy-acetyl nitrates, nitrogen dioxide, and nitric acid. Thus, measurements of nitrates and nitric acid by the LIF and TWS could be compared.

Thermal stability is of critical importance to LIF operations and generating high quality data. For a substantial amount of time at Big Hill, the power failed and the LIF unit was off line leading to difficulties in maintaining thermal stability. DRI has completed their QC work on the denuder database, while UC Berkeley believes that further work is

required to compare the two sets of data. Nevertheless, **Figure 3-27**, which compares data from the LIF and the TWS denuder (uncertainty bars represent the range of hourly concentrations), provides some confidence in the methods once operations stabilized by summer.

A review of the TWS ammonia data indicated fewer problems than was seen with nitric acid. Thus, the TWS-based seasonal and annual ammonia estimates are thought to be more reliable. Gaseous nitrogen measurements with the TWS are summarized in **Table 3-13**.

Using the ammonium nitrate equilibrium, ammonia concentrations, ambient temperature, and relative humidity, it is possible to estimate the dissociation constant K and consequently one could estimate nitric acid concentrations from the following equations (Stelson and Seinfeld, 1982):

$K = P_{HNO3} \times P_{NH3}$

$\text{Ln } K = 84.6 - (24{,}220/T) - 6.1\text{Ln } (T/298)$,

where T = Temperature in degrees Kelvin and RH is lower than 62%. The dissociation constant, K, is in units of $(\text{ppbV})^2$.

Table 3-13. Gaseous nitrogen from the LTADS TWS network.

Lake Tahoe Atmospheric Deposition Study Nitrogen Total Gas, Nitric Acid, Ammonia (ug/m^3)							
	Nitrogen Gas (N)					Nitric Acid	Ammonia
Site	Winter	Spring	Summer	Fall	Study Average	(Mass)	(Mass)
Big Hill	0.22	0.76	1.95	1.52	1.33	0.65	0.57
Lake Forest	0.93	0.67	1.17	1.20	0.97	0.47	0.67
Sandy Way	1.47	1.24	2.83	1.94	1.63	1.00	0.95
SOLA	2.73	1.38	1.88	2.30	2.13	0.96	1.73
Thunderbird	0.32	0.47	0.82	0.67	0.57	0.34	0.18
Maximum Basinwide (excludes Big Hill)					3.58	2.93	4.08
2nd Maximum Basinwide (excludes Big Hill)					3.26	1.91	3.59
Average Basinwide (excludes Big Hill)					1.32	0.69	0.88
Median Basinwide (excludes Big Hill)					1.30	0.71	0.81
Minimum Basinwide (excludes Big Hill)					0.04	0.08	0.00

However, a two-week sampling period invalidates the ammonium nitrate equilibrium assumption. Average two-week temperature and relative humidity data do not adequately describe second-to-second temperature and relative humidity profiles that likely govern nitric acid and ammonia concentrations, even if the ammonium nitrate equilibrium held. The 1997 Southern California Ozone Study data suggested that theoretical K values ought to consider dilution and the aerosol matrix of surfaces where ammonium nitrate reactions might take place. LTADS data do not include sufficient

time resolution and sufficient aerosol matrix and plume dilution information necessary for proper assessment of K.

As noted earlier, hourly concentration profiles are needed for integration with hourly meteorological data to estimate atmospheric deposition. Hourly BAM data were used to apportion the PM data. For nitric acid, the diurnal profile was estimated using gaseous NO_Y-NO_X concentration differences from South Lake Tahoe station at Sandy Way. Total reactive nitrogen (i.e., NO_Y) includes total oxides of nitrogen (i.e., NO_X) plus such species as peroxy acetyl and other organic nitrates, as well as, nitric and nitrous acids. Formulation of diurnal profiles presumes that nitric acid (plus nitrous acid, the positive artifact of nitric acid measurements) well exceeds other constituents of NO_Y. The seasonal mean diurnal HNO_3 concentrations are shown in **Figure 3-28**. Based on limited data from the day/night TWS denuder samples and no method during LTADS to estimate hourly concentrations of ammonia, no diurnal variation was assumed for ammonia concentrations.

3.2.2.2 LTADS vs. Other Tahoe Basin N-species Reports

Tarnay collected denuder gaseous nitric acid and ammonia data at remote forested locations in Bliss State Park and a high alpine forest near Incline Village (**Table 3-14**). Ammonium nitrate data reported in Tarnay *et al.* (2001) is from the IMPROVE network's Bliss site and is thus most relevant to rural, elevated, undeveloped regions of Tahoe Basin. In 2002, Tarnay expanded the network to several other stations but still only covered the summer months (July-September).

Please note that the different sampling years indicated opposite day/night relationships for ammonia. This is most likely the product of the difficulties we have noted in gaseous N species measurements using denuders. Nitric acid concentrations observed during LTADS are in the range of those reported by Tarnay *et al.* (2001 and 2003). However, despite similar sampling protocols, LTADS observed substantially higher ammonia concentrations than were reported by Tarnay *et al.* (2003). LTADS also reported substantially higher ammonium nitrate concentrations than those reported from IMPROVE network for Bliss State Park and at SOLA, for summer and fall seasons of 1990-96. LTADS data from the remote site at Bliss however do agree with ammonium nitrate concentrations reported by Tarnay *et al.* (2001).

Zhang *et al.* (2002) reported limited aircraft sampling in and near the Tahoe Basin. These show a wide range, but are within the range of LTADS reported concentrations. Note that ammonium plus ammonia concentrations reported in aircraft measurements are between LTADS reported median and maximum values (**Table 3-15**).

Figure 3-27. Comparison of nitric acid at Big Hill between LIF & Denuder Methods.
Note: Lighter colors represent the LIF measurements.

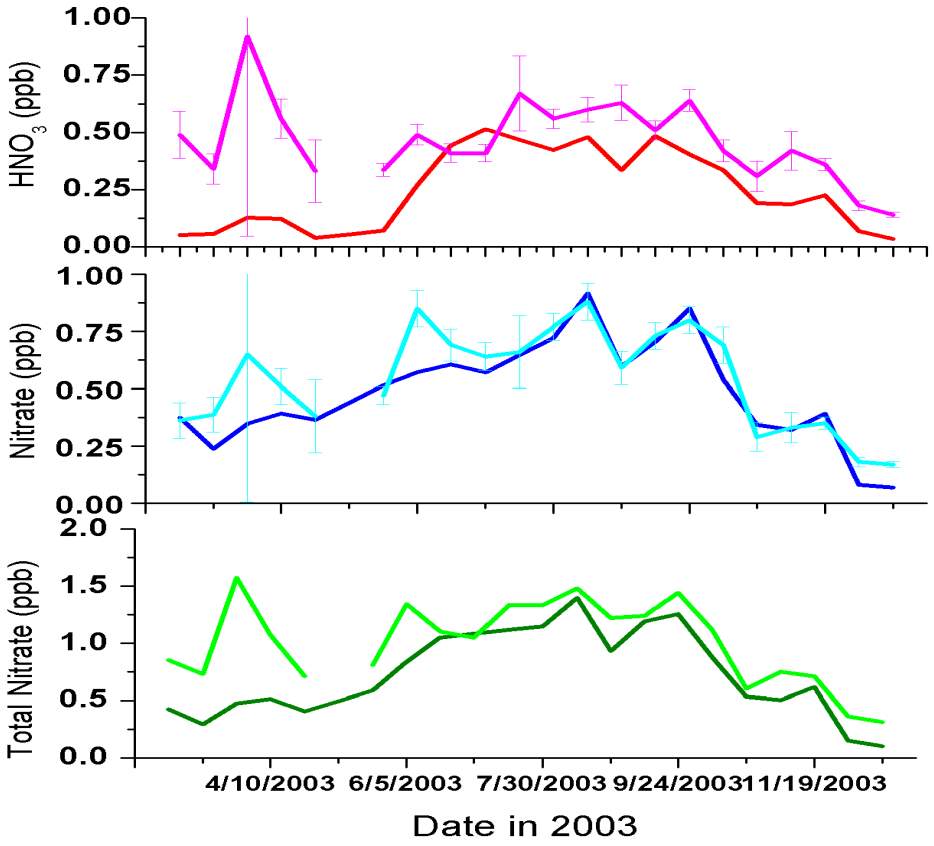

Figure 3-28. Estimated seasonal diurnal profiles of nitric acid (HNO_3) developed from NO_Y and NO_X measurements at SLT – Sandy Way monitoring station. The estimate method may include small amounts of nitrous acid (HONO) and nitrates (NO_3^-).

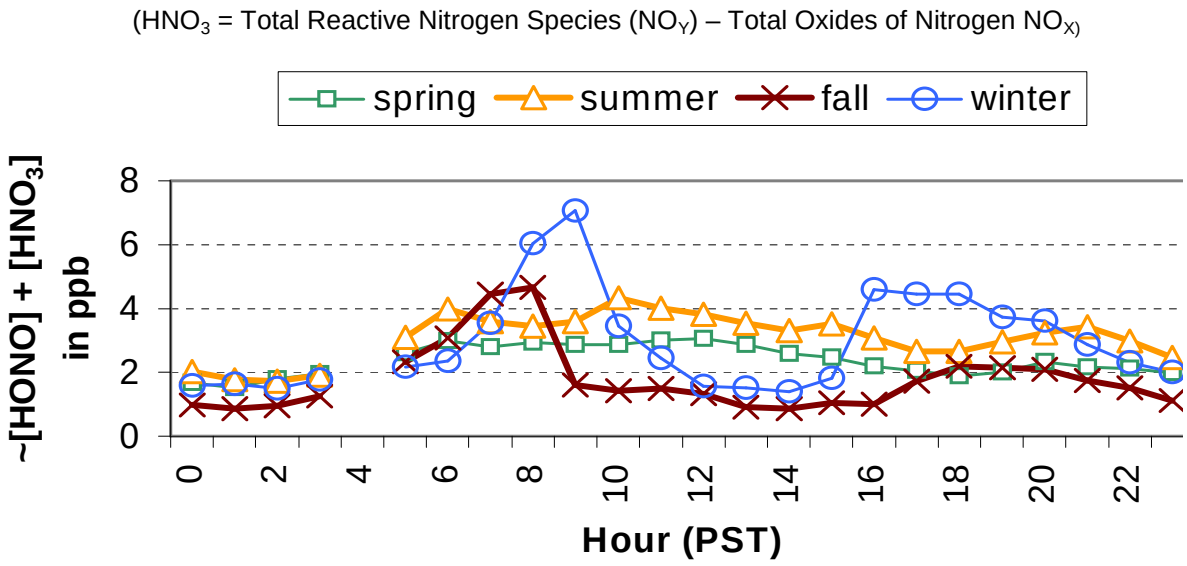

Table 3-14. Nitrogen-specie measurements as reported by Tarnay and LTADS.

Nitrogen Specie	Concentrations (ng N/m^3) observed by:				
	Tarnay during summers (2001 / 2002) in alpine forests near Bliss State Park & Incline Village			LTADS annual (2003)	
	Day	Night	Mean	Median	Maximun
HNO_3	364 / 238	154 / 182	234	127	651
NH_3	280 / 294	686 / 140	350	634	3,360
NH_4NO_3 @ Bliss	101*	101*	101*	49**	107**

* from IMPROVE PM2.5 during summer and fall of 1990-1996

** based on only 6 samples (collected between 9/18/03 – 12/16/03)

Carroll *et al*. (2003) performed detailed air and boat sampling over and on Lake Tahoe in coordination with LTADS. They noted high blank values and other analytical difficulties that the TWS also encountered. Nevertheless, using averages of the ensemble of denuder filter pack samples, it appears that ammonia increased slightly with height above the lake while nitric acid gas decreased slightly with height. The ammonium nitrate and gaseous nitrogen concentration range from Carroll *et al*. (2003) are between TWS reported median and maximum values. Please also note that ammonia fraction of nitrogen species from Carroll et al. (2003) and the TWS agree quite well.

Table 3-15. Aircraft measurements of nitrogen-species over Lake Tahoe during summer/fall seasons.

Nitrogen Specie	Concentrations (ng N/m^3) observed by:				
	Zhang (2001)[1]	Carroll (2002)[2]		LTADS (2003)	
	Mean	Minimum	Maximum	Median	Maximun
HNO_3 (g) + NO_3^- (p)	420	---	---	290	939
NH_3 (g) + NH_4^+ (p)	1330	---	---	1,015	3,492
ON (g) + ON (p)	210	---	---	---	---
TN (g)+(p)	1,960	---	---	1,278	3,843
NH_4NO_3	---	84	714	270	1,010
TN (g)	---	364	4,310	775	3,579
NH_3 fraction of TN	---	55%		51%	

[1] based on three samples from *Zhang et al.* (2002)

[2] based on *Carroll et al.* (2003)

3.2.2.3 Seasonal Concentration Profiles by Specie

Both the dry and wet LTADS deposition estimates were generated from ambient concentrations. The ambient concentrations used as the basis of the deposition estimates are presented in **Table 3-16**. Concentrations tend to be higher in the more urbanized locations with season of peak concentrations depending on the pollutant specie. Concentrations at Big Hill tend to be highest in summer and fall when upslope air flow transports pollutants into the Sierra Nevada. The northern portion of the Tahoe Basin also tends to have the highest concentrations during summer and fall when soils are drier and activities are greater. In the southern portion of the basin, concentrations tend to be higher in winter and fall when the air is more stable and the down slope flows that collect the urban emissions persist longer.

Table 3-16. Seasonal average concentrations (ng/m^3) of particulate matter, nitrogenous species, and phosphorus as observed during LTADS.

Site	Network	Parameter	Winter	Spring	Summer	Fall	Annual*
Big Hill	TWS	HNO_3	135	196	1009	816	*646*
Lake Forest	TWS	HNO_3	214	229	470	647	390
SLT-Sandy Way	TWS	HNO_3	1201	617	1075	1294	1047
SLT-SOLA	TWS	HNO_3	1136	548	940	1111	934
Thunderbird Lodge	TWS	HNO_3	227	228	525	379	340
Big Hill	TWS	NH_3	127	182	892	719	*574*
Lake Forest	TWS	NH_3	708	373	767	835	671
SLT-Sandy Way	TWS	NH_3	773	684	1060	1227	936
SLT-SOLA	TWS	NH_3	2286	868	1506	2029	1672
Thunderbird Lodge	TWS	NH_3	77	62	290	277	177
Big Hill	TWS	NH_4	50	428	789	552	*548*
Bliss SP	MVS	NH_4	56			144	*129*
Buoy TB1 (east)	MVS	NH_4	254	383	349	421	*329*
Buoy TB4 (west)	MVS	NH_4	233	367	313	364	*304*
Lake Forest	TWS	NH_4	210	260	377	297	286
LF_Coast Guard	MVS	NH_4	112	192	264	195	191
SLT-Sandy Way	TWS	NH_4	456	438	520	496	478
SLT-SOLA	TWS	NH_4	400	411	443	382	409
Thunderbird Lodge	TWS	NH_4	160	336	412	287	299
Timber Cove	MVS	NH_4	278	344	192		*298*
Wallis Pier	MVS	NH_4	57	190	259	184	173
Wallis Tower	MVS	NH_4	44	163	289	182	170
Zephyr Cove	MVS	NH_4	97	324	400	213	259
Big Hill	TWS	NO_3	192	936	1691	1394	*1254*
Bliss SP	MVS	NO_3	129			206	*193*
Buoy TB1 (east)	MVS	NO_3	607	617	286	427	*503*
Buoy TB4 (west)	MVS	NO_3	571	582	197	438	*450*
Lake Forest	TWS	NO_3	404	475	656	617	538
LF_Coast Guard	MVS	NO_3	253	192	96	173	179
SLT-Sandy Way	TWS	NO_3	934	894	1137	1155	1030
SLT-SOLA	TWS	NO_3	949	862	855	1012	920
Thunderbird Lodge	TWS	NO_3	342	471	729	577	530
Timber Cove	MVS	NO_3	418	317	275		*368*
Wallis Pier	MVS	NO_3	128	221	122	196	167
Wallis Tower	MVS	NO_3	112	215	129	161	154
Zephyr Cove	MVS	NO_3	286	437	185	277	296
Big Hill	TWS	P	40	40	40	40	40
Bliss SP	MVS	P	40	40	40	40	40
Buoy TB1 (east)	MVS	P	40	40	40	40	40
Buoy TB4 (west)	MVS	P	40	40	40	40	40
Lake Forest	TWS	P	40	40	40	40	40

Site	Network	Parameter	Winter	Spring	Summer	Fall	Annual
LF Coast Guard	MVS	P	40	40	40	40	40
SLT-Sandy Way	TWS	P	40	40	40	40	40
SLT-SOLA	TWS	P	40	40	40	40	40
Thunderbird Lodge	TWS	P	40	40	40	40	40
Timber Cove	MVS	P	40	40	40	40	40
Wallis Pier	MVS	P	40	40	40	40	40
Wallis Tower	MVS	P	40	40	40	40	40
Zephyr Cove	MVS	P	40	40	40	40	40
Big Hill	TWS	PM10	1810	5526	12142	9859	*8672*
Lake Forest	TWS	PM10	15835	11708	13852	13907	13826
SLT-Sandy Way	TWS	PM10	21829	12719	13324	17734	16402
SLT-SOLA	TWS	PM10	24424	13080	17460	17582	18137
Thunderbird Lodge	TWS	PM10	3311	4523	9120	6198	5788
Big Hill	TWS	PM2.5	1357	3735	6602	4962	*4821*
Lake Forest	TWS	PM2.5	5032	2981	6142	4789	4736
SLT-Sandy Way	TWS	PM2.5	10154	4889	7111	9772	7982
SLT-SOLA	TWS	PM2.5	8963	3982	7049	8238	7058
Thunderbird Lodge	TWS	PM2.5	2341	2446	5800	3745	3583
Big Hill	TWS	TSP	3163	6429	16120	13559	*11484*
Bliss SP	MVS	TSP	3600			6414	*5945*
Buoy TB1 (east)	MVS	TSP	4725	9866	7757	6389	7184
Buoy TB4 (west)	MVS	TSP	4909	9029	7871	8028	*7270*
Lake Forest	TWS	TSP	17574	16183	19562	18155	17869
LF_Coast Guard	MVS	TSP	8170	8914	15263	7760	10027
SLT-Sandy Way	TWS	TSP	29279	15779	18628	20770	21114
SLT-SOLA	TWS	TSP	29929	15148	17635	21971	21171
Thunderbird Lodge	TWS	TSP	3640	4738	9120	6528	6007
Timber Cove	MVS	TSP	9826	3840	10535		*8167*
Wallis Pier	MVS	TSP	19230	5422	14513	8579	11936
Wallis Tower	MVS	TSP	17666	10810	12469	12110	13264
Zephyr Cove	MVS	TSP	8575	10318	21602	14971	13867

* The annual mean is the average of the seasonal means. In cases when the seasonal mean is based on incomplete data (potentially non-representative mean), the cell has been highlighted in yellow. The annual mean for the pollutants with incomplete data is based on the median result of the 4-season mean, the mean of the representative seasons, and the average of all individual samples. The annual means not represented by the 4-season mean are presented in italicized blue font.

3.2.2.4 Temporal and Spatial Variations in Ozone

Ozone was not a primary pollutant of interest in LTADS. However, ozone is a pollutant of concern in many areas of California. Although the Tahoe Basin is currently in attainment of the national 1-hour and 8-hour and the California 1-hour ambient air quality standards, its air quality does exceed the TRPA threshold for forest health (1-hr

average, 0.070 ppm). In addition, ozone concentrations in the Tahoe Basin have historically exceeded the concentration level associated with the recently adopted California 8-hour health-based standard. During LTADS, ozone was monitored at two new locations (Big Hill and Lake Forest) and at four long term monitoring sites (Echo Summit and SLT – Sandy Way in California; Cave Rock and Incline Village in Nevada). The various ozone ambient air quality standards applicable in the Tahoe Basin and a summary of the ozone concentrations observed during 2003 are presented in this section.

Various governmental authorities have established ozone air quality standards/thresholds to protect health and welfare in the Lake Tahoe Air Basin. The averaging periods and concentration levels are illustrated in **Figure 3-29**. Note that the State of California recently adopted an 8-hour standard in addition to its current 1-hour standard. Both of the California standards are more stringent than the National standards. These standards are established to protect public health. The Tahoe Regional Planning Agency has adopted an environmental threshold to protect forest health. As shown in **Figure 3-29**, the TRPA ozone threshold (1-hour not to exceed 0.08 ppm) is the most restrictive standard applicable to the Tahoe Basin. Because 1-hour concentrations infrequently exceed the TRPA threshold (equivalent to 80 ppb), a 70 ppb cutpoint was used in several analyses to assess the frequency, timing, and spatial distribution of high ozone concentrations.

To provide a regional context of the ozone concentrations downwind of the Sacramento metropolitan area, the maximum 1-hour and 8-hour average ozone concentrations observed in the central Sierra Nevada are shown in **Figure 3-30**. The ozone plume downwind of Sacramento typically achieves its maximum concentrations in the foothills of the Sierra Nevada (e.g., Folsom, Placerville, Auburn). As illustrated in **Figure 3-30**, peak 1-hr ozone concentrations drop off significantly by the time the plume reaches the Sierra (Big Hill at 6155' elevation) and more by the crest of the Sierra (Echo Summit at 7382' elevation). The peak 1-hour concentrations in the Tahoe Basin were comparable to that observed at the crest (i.e., Echo Summit). The peak 8-hour concentrations decline most between Big Hill and Echo Summit. The maximum 8-hr ozone concentrations observed within the Basin were comparable and slightly lower than at Echo Summit, perhaps due in part to local emissions of nitric oxide (NO), which suppresses (initially) ozone concentrations.

The number of days when ozone concentrations at different sites exceeded the 1-hr California Ambient Air Quality Standard (CAAQS) (95 ppb) and the 8-hr National Ambient Air Quality Standard (NAAQS) for ozone during 2003 decreased even more dramatically than peak concentrations (**Figure 3-31**). Neither of the standards was exceeded at Echo Summit or within the Tahoe Basin. **Figure 3-31** illustrates that the Sacramento ozone plume does not transport intact high into the Sierra. In fact, the light winds associated with high ozone episodes in the Sacramento Valley seldom transport the polluted air in the surface layer far into the Sierra before the slopes cool in the evening and downslope airflow develops. The more likely scenario is that warm air

rising above the western slopes of the Sierra mixes the ozone into a deeper volume of air and increasing the regional background concentration of ozone.

Because the frequency of ozone concentrations exceeding the NAAQS or the CAAQS is so low in the LTADS study area, the counts of hours when 1-hr ozone concentrations exceeded 70 ppb, the TRPA threshold (80 ppb), and California standard (95 ppb) during 2003 are shown in **Figure 3-32** for the monitoring sites in the Sierra. The 1-hour CAAQS was not exceeded within the Tahoe Basin during 2003. In fact, the Lake Tahoe Air Basin is classified as attaining the CAAQS. However, the 1-hr CAAQS was exceeded on occasion at the Big Hill site, which is located ~20 miles upwind of the Tahoe Basin on the western slope of the Sierra Nevada. More significantly, the 70 ppb cutpoint and the TRPA threshold were exceeded during more than 400 and 125 hours, respectively, at the Big Hill site, which is primarily impacted by pollutants from the Central Valley. The 70 ppb cutpoint and the TRPA threshold were exceeded much less frequently (less than 100 and 10 hours, respectively) at the Echo Summit site located further east on the Sierra crest at the southwestern edge of the Tahoe Basin. Exceedances of the 70 ppb cutpoint on the floor of the Tahoe Basin declined another 70% from that at the Echo Summit site (i.e., to < 30 hours). Although South Lake Tahoe is the largest urbanized area, and presumably most polluted, in the Basin, the number of exceedances there is least because the fresh emissions of nitric oxide (NO) suppress the ozone levels.

The pattern of exceedances of the National and the new California 8-hour ozone standards (**Figure 3-33**) is similar to that of the 1-hour exceedances. The NAAQS is only exceeded at the Big Hill site upwind of the Tahoe Basin. Although the Lake Tahoe Air Basin currently attains the 1-hour CAAQS, the Basin will be designated as a non-attainment area because ozone concentrations within the Basin exceeded the new California 8-hour standard of 0.070 ppm on 7 days alone in 2003 at the Echo Summit site. As with the 1-hour exceedances, the 8-hour standard is exceeded about 10 times more often at Big Hill than at Echo Summit (62 vs. 7 days).

The number of hours when the 70 ppb cutpoint was exceeded is shown by hour of the day in **Figure 3-34** for the Big Hill and Echo Summit sites. Although ozone concentrations exceeding 70 ppb can occur essentially any hour of the day, the most prevalent period, at both sites, is in the late afternoon and early evening – past the time of peak local formation but consistent with potential transport up the Sierra slopes from the Central Valley. The much higher frequency of exceedances during these hours at Big Hill than at Echo Summit indicate that the polluted air mass once it passes Big Hill often does not arrive at Echo Summit or that the ozone concentrations are reduced below 70 ppb by the time the air arrives at Echo Summit. Both sites have minor local sources of NO, so any decrease in concentrations is due to some combination of dispersion, deposition, or advection out of the area. The high number of exceedances in the early morning hours at Big Hill is consistent with upslope air flow reversing to downslope flow and remaining on the western slope of the Sierra throughout the night. The only period of the day when the number of exceedances is comparable at the two

sites is during the late morning when both sites would experience increased vertical mixing of the atmosphere and downmixing of potentially polluted air aloft. The hourly distribution of exceedances of the 70 ppb cutpoint within the Tahoe Basin is shown in **Figure 3-35**. Most of the high ozone hours in the northern portion of the basin occur around midday when local formation would be greatest but also when vertical mixing of the air is greatest and could tap potentially high ozone concentrations transported aloft. Interestingly, the exceedances of the 70 ppb cutpoint are most frequent in the late afternoon at the Cave Rock site (east side of Lake), not unlike at the Echo Summit site in the late afternoon. High ozone concentrations during daylight hours, when photosynthesis is active and stomata are open, would have the most adverse impact on plants and trees.

The monthly distribution of ozone concentrations exceeding the 70 ppb cutpoint is shown in **Figure 3-36** for the two upwind sites and in **Figure 3-37** for the in-basin sites. Ozone concentrations can exceed the 70 ppb cutpoint during any month around summer (May – October) but are most likely during July and August at the Big Hill site. Concentrations exceeding 70 ppb at the Echo Summit site were most frequent in May and July (June to a lesser extent). In-basin exceedances of the 70 ppb cutpoint occurred between May and August with a greater tendency in May and June. It is interesting to note that the periods with the greatest frequency of exceedances of the 70 ppb cutpoint are in the late spring/early summer at the Tahoe sites; this is before the season of peak exceedances at the Big Hill site.

The diurnal variation in ozone concentrations at a trio of sites representing upwind (Big Hill), basin boundary/Sierra crest (Echo Summit), and in-basin lake level (Cave Rock) is shown by month in **Figures 3-38 through 3-41**. Unlike the two upwind sites, which are minimally impacted by local emissions, the ozone pattern at Cave Rock exhibits a dip around 7 am when fresh NO emissions associated with the morning commute drain from the highway toward the Lake and the monitor. A corresponding dip in ozone concentrations is typically not observed in the afternoon commute when winds are typically upslope (from the west) and thus the monitor “sees” the ozone before the air mass reaches the NO emissions along the highway and are depressed. Focusing on the Echo Summit data, which represent regional background ozone concentrations approaching the Tahoe Basin, the diurnal variation is very small. The ozone concentrations hover around 40 ppb during the winter and shift up to over 50 ppb during spring. The concentrations exhibit the greatest diurnal variation during summer when minimums are in the 40s and maximums approach 60 ppb. During July and August, the broad peak in concentrations reaches its maximum in the late afternoon. The ~4 ppb bump-up during these months, when the length of days and the duration of upslope air flow are longest, is consistent with the movement of polluted air into the Sierra Nevada. During fall, the diurnal range decreases and becomes stable in the low 40s by November.

Figure 3-29. Applicable ozone standards in the Lake Tahoe Air Basin.

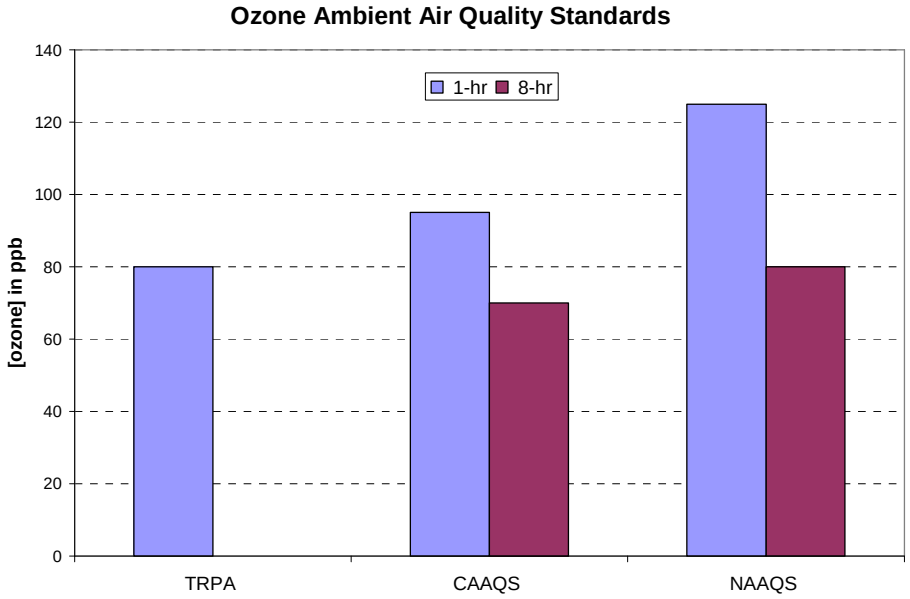

Notes:
TRPA – Tahoe Regional Planning Agency threshold to protect forest health (80 ppb for 1-hr mean)
CAAQS – California Ambient Air Quality Standards (≡95 ppb for 1-hr mean; 70 ppb for 8-hr mean)
NAAQS – National Ambient Air Quality Standard (≡125 ppb for 1-hr mean; 80 ppb for 8-hr mean)

Figure 3-30. Maximum 1-hour and 8-hour ozone concentrations observed in 2003 at locations west of and within the Lake Tahoe Air Basin.

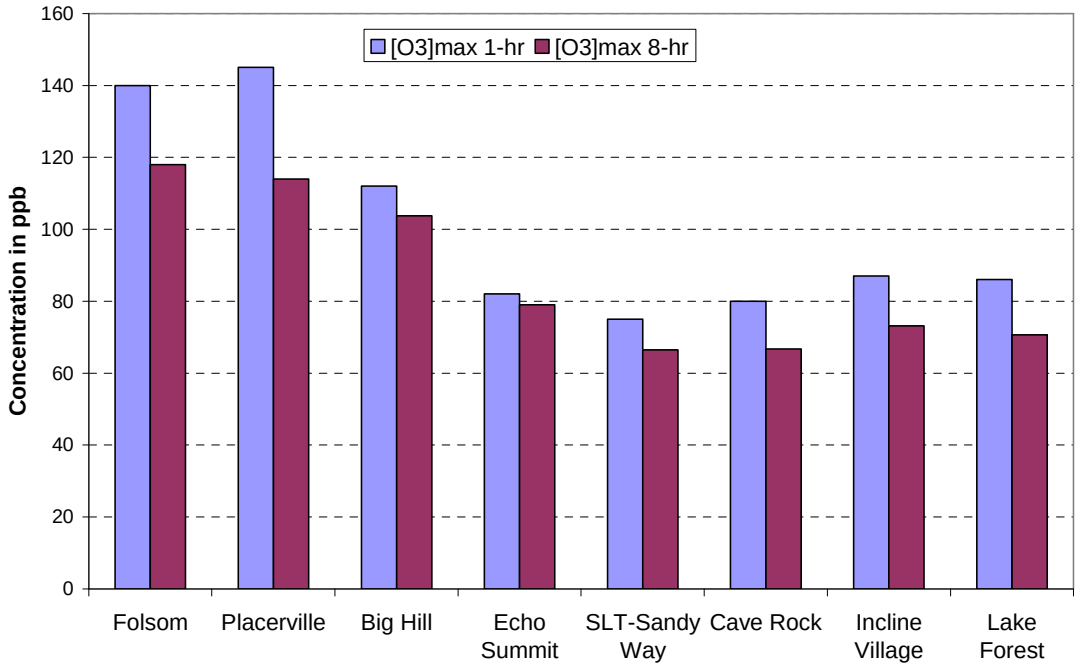

Figure 3-31. Number of days during 2003 when the California 1-hr and national 8-hr ambient air quality standards for ozone were exceeded at locations west of and within the Tahoe Air Basin.

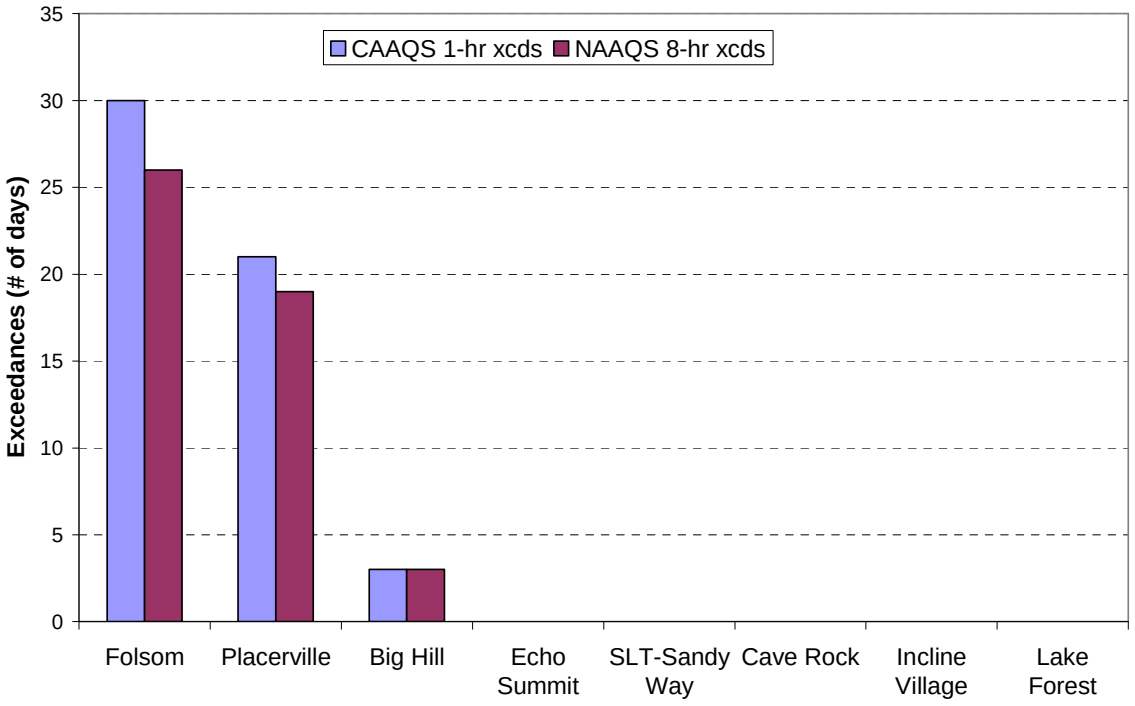

Figure 3-32. Annual total of hours during 2003 when 1-hour ozone concentrations exceeded selected cutpoints (70 ppb; TRPA threshold – 80 ppb; CAAQS – 95 ppb) at Big Hill and the five ozone monitoring sites located within the Tahoe Basin.

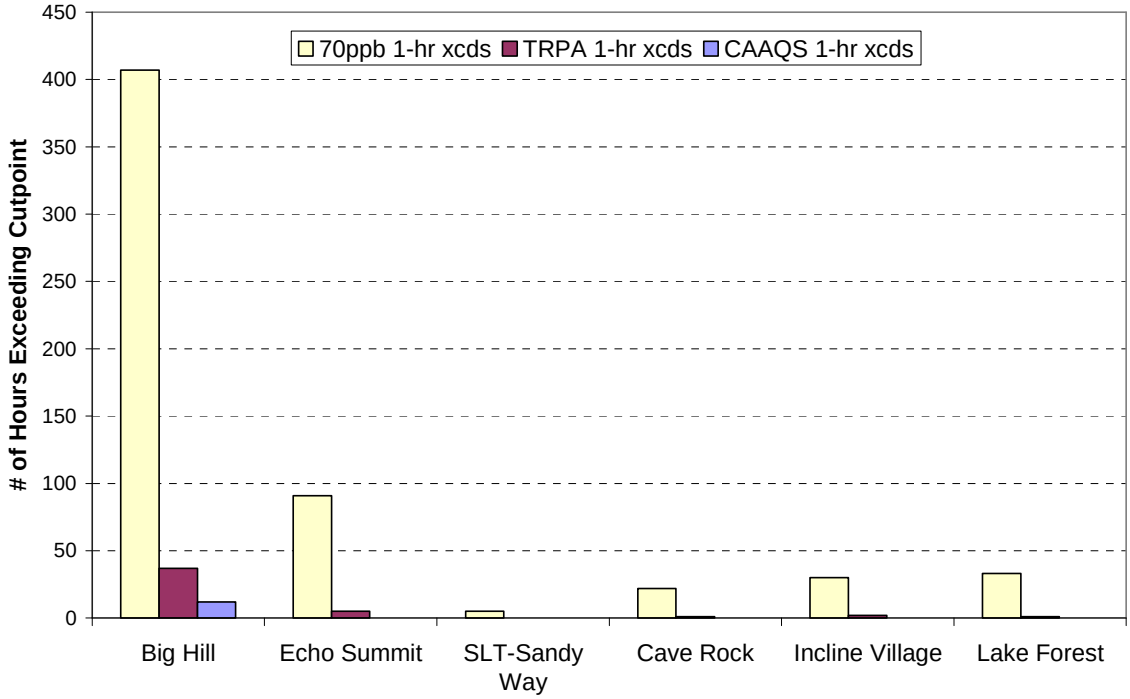

Figure 3-33. Annual number of days during 2003 when 8-hour ozone standards (CAAQS – 70 ppb; NAAQS – 85 ppb) were exceeded at Big Hill and the five ozone monitoring sites located within the Tahoe Basin.

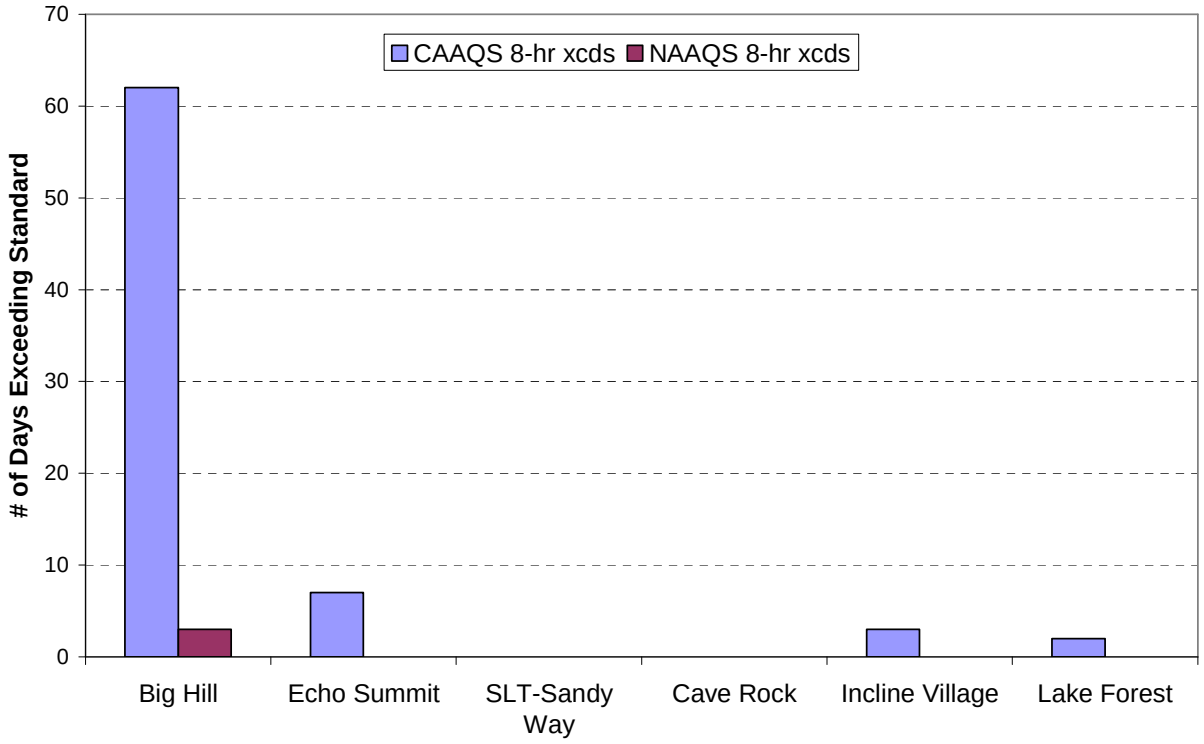

Figure 3-34. Frequency of hours during 2003 when 1-hour ozone concentrations exceeded 70 ppb at the Big Hill and Echo Summit sites.

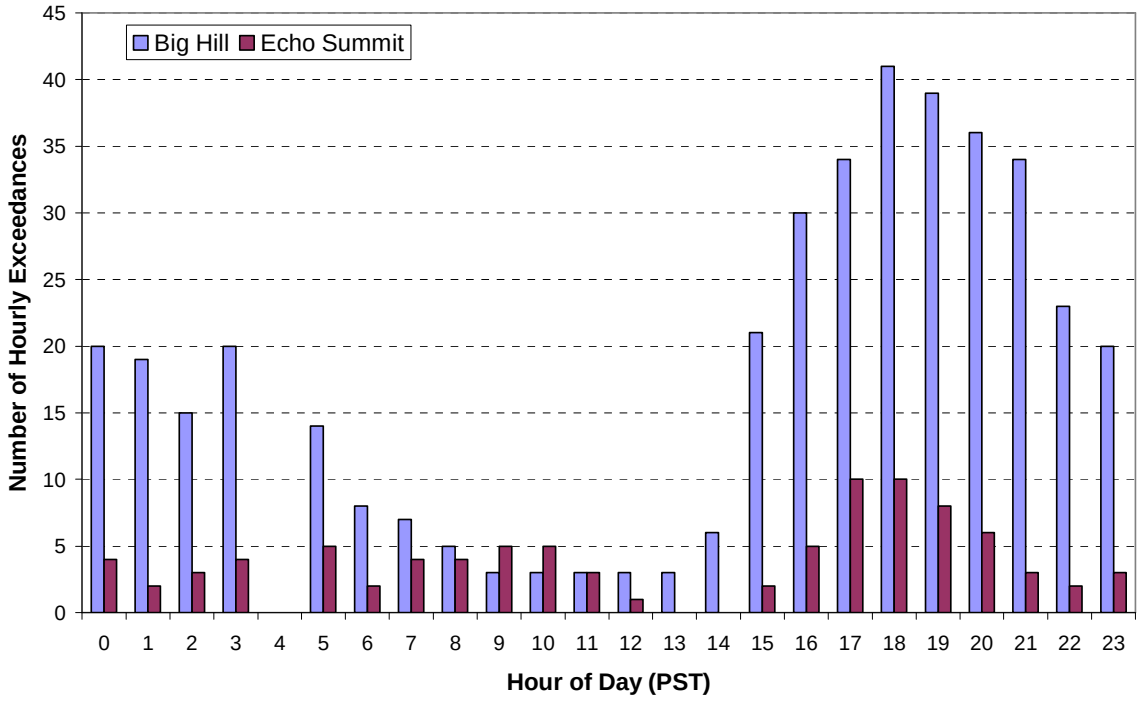

Figure 3-35. Frequency of hours during 2003 when 1-hour ozone concentrations exceeded 70 ppb at sites within the Lake Tahoe Air Basin.

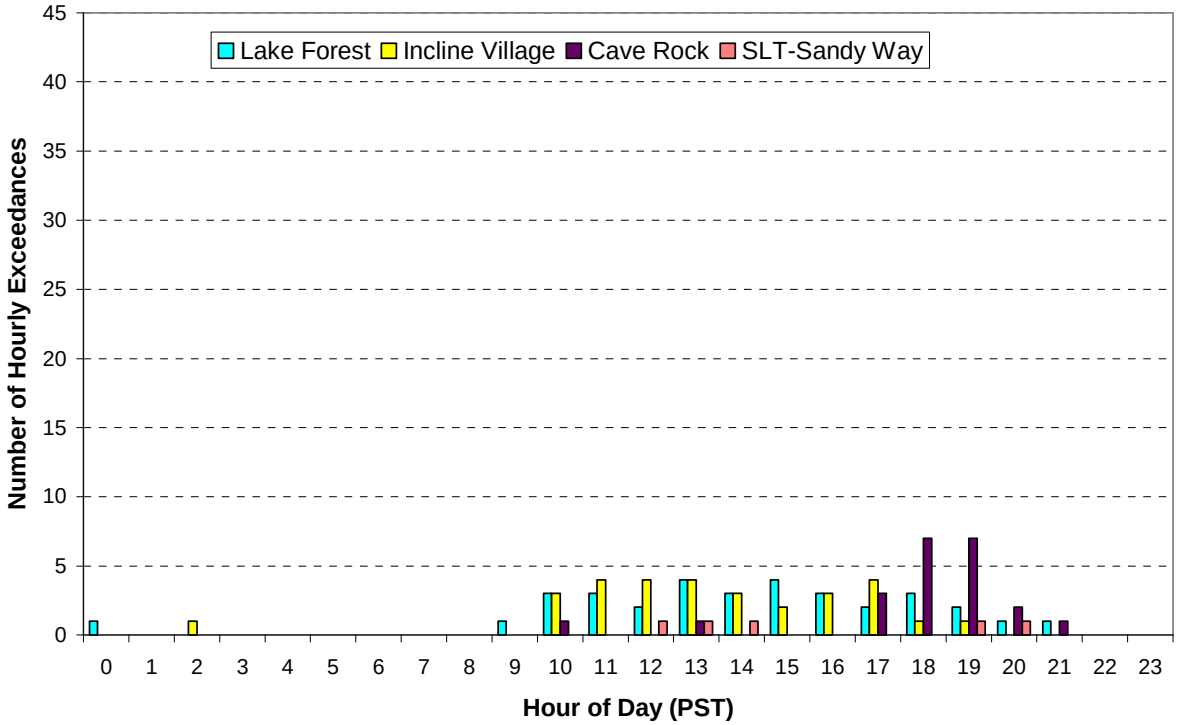

Figure 3-36. Frequency of hours by month during 2003 when 1-hour ozone concentrations exceeded 70 ppb the at Big Hill and Echo Summit sites.

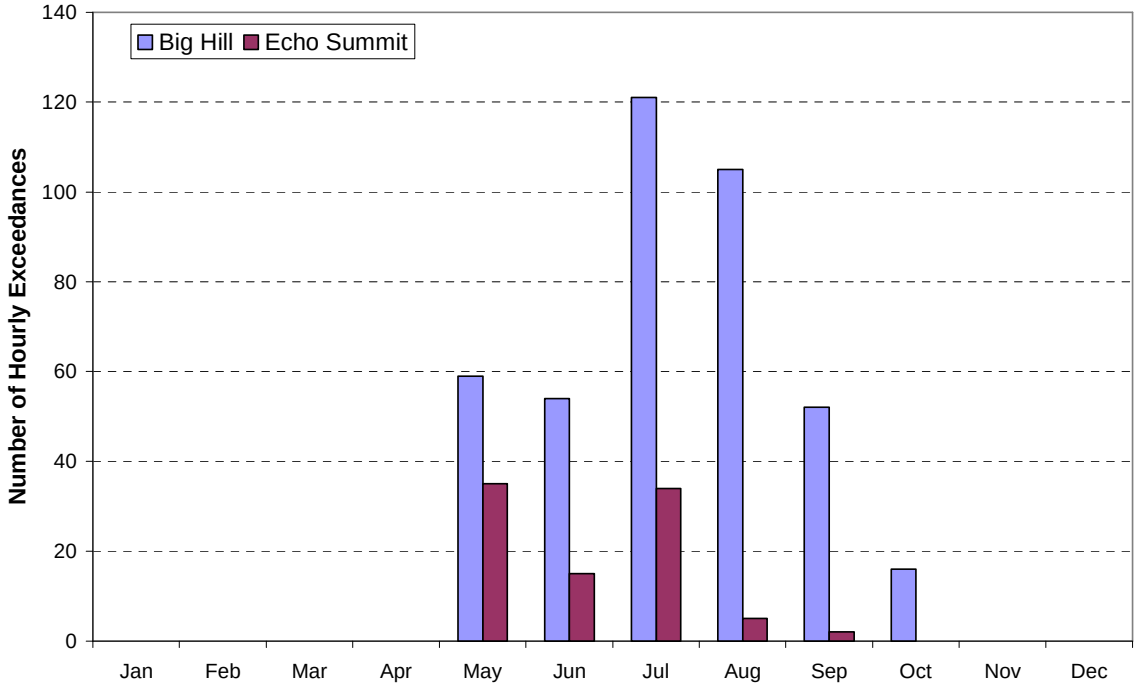

Figure 3-37. Frequency of hours by month during 2003 when 1-hour ozone concentrations exceeded 70 ppb at sites in the Tahoe Basin.

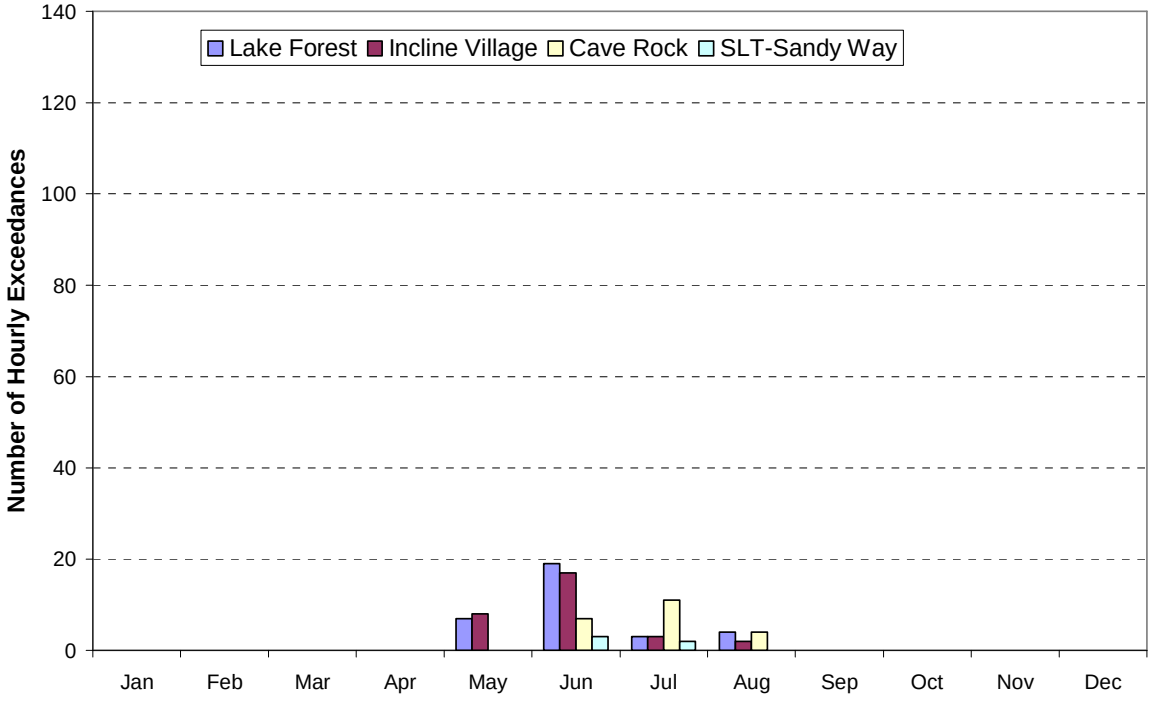

Figure 3-38. Diurnal variations in ozone concentrations during Dec, Jan, Feb (winter).

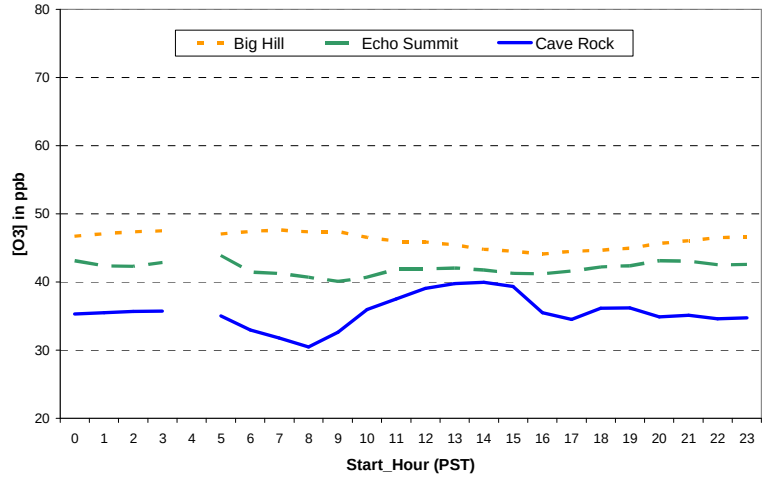

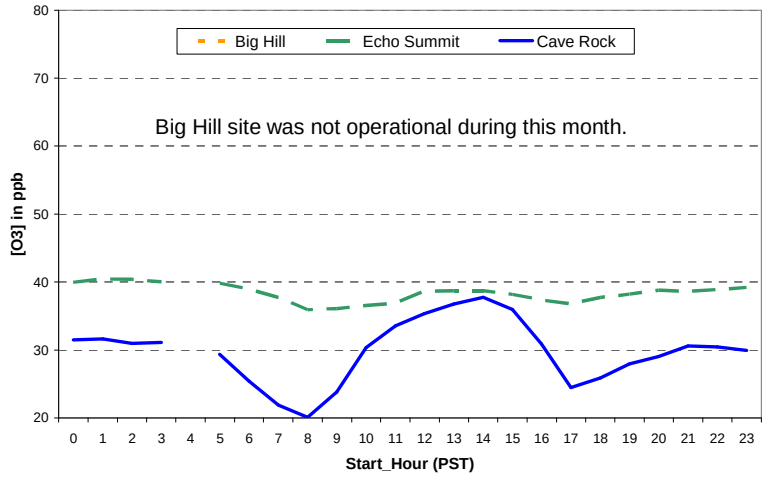

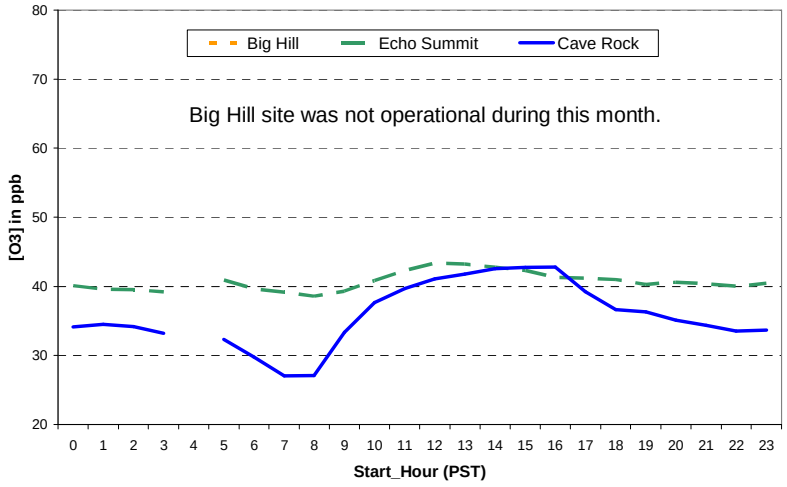

Figure 3-39. Diurnal variations in ozone concentrations during Mar, Apr, May (spring).

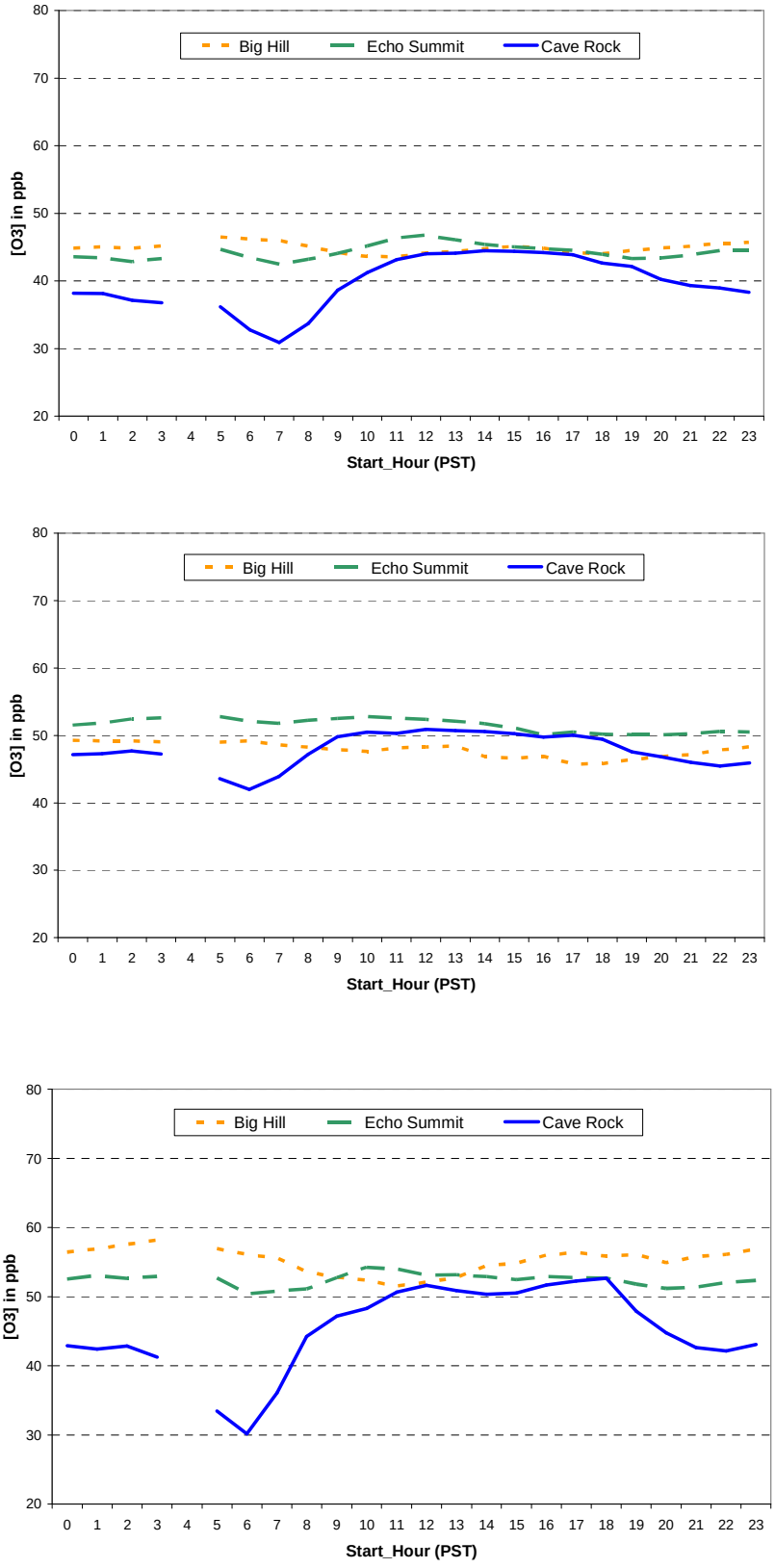

Figure 3-40. Diurnal variations in ozone concentrations during Jun, Jul, Aug (summer).

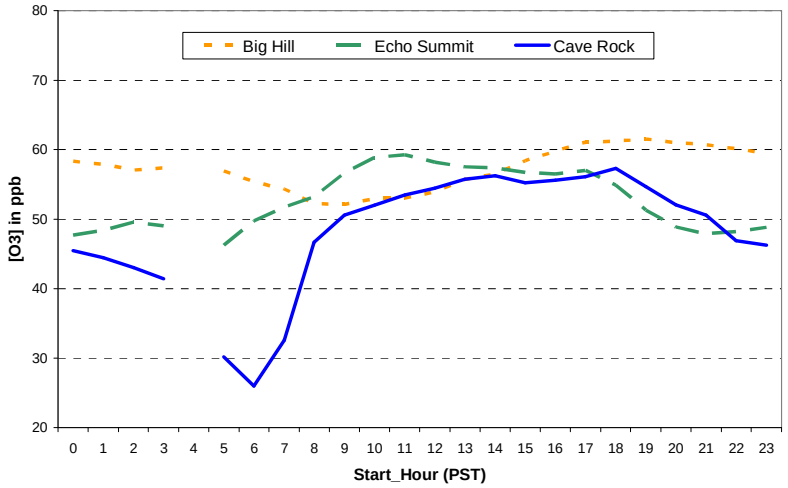

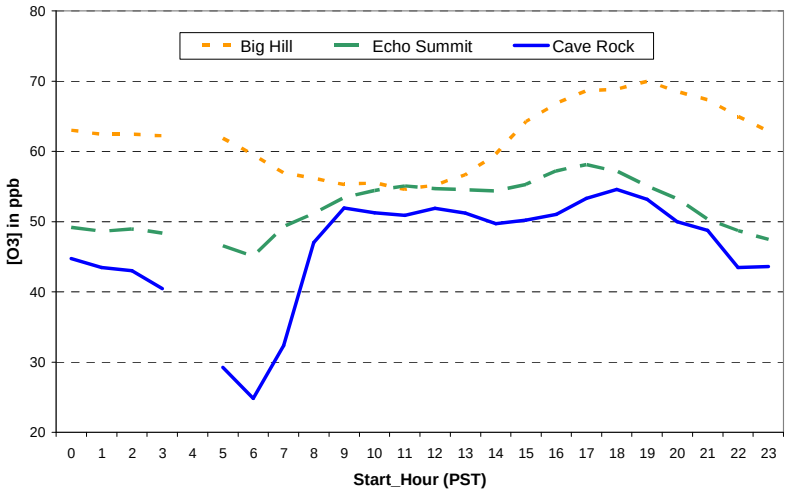

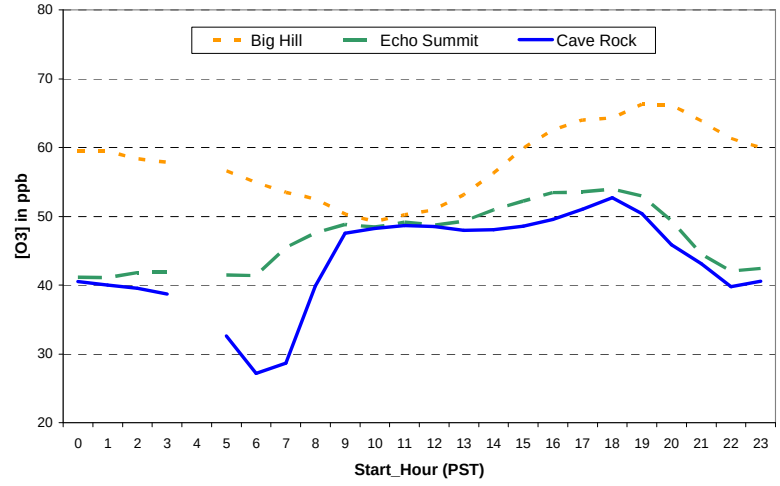

Figure 3-41. Diurnal variations in ozone concentrations during Sep, Oct, Nov (fall).

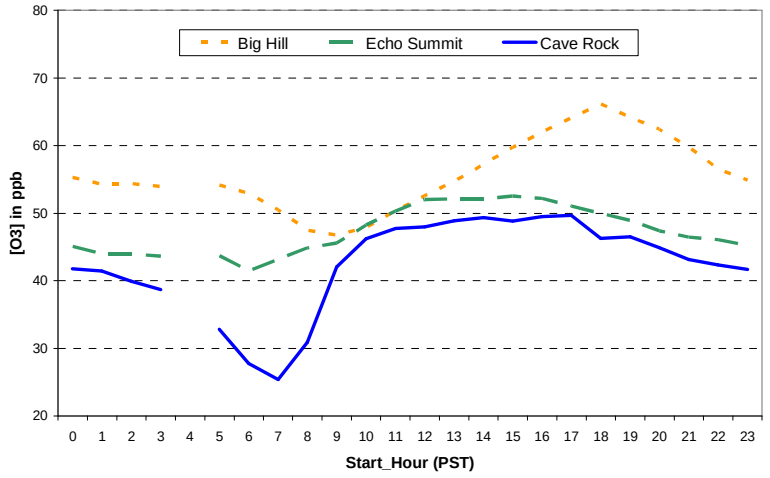

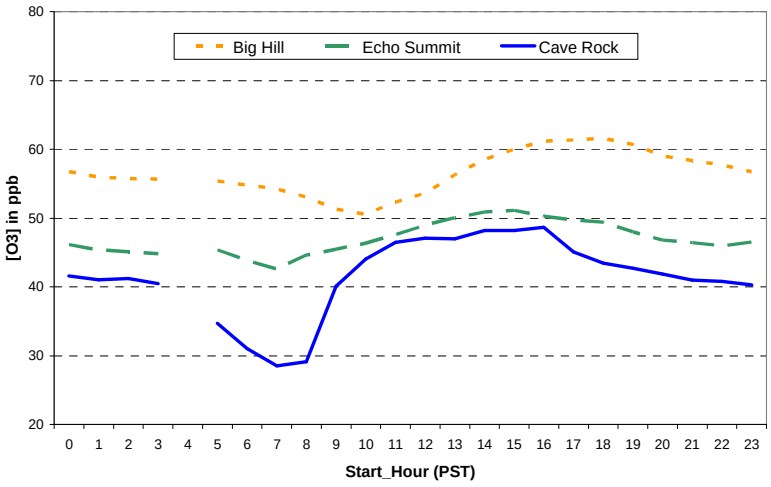

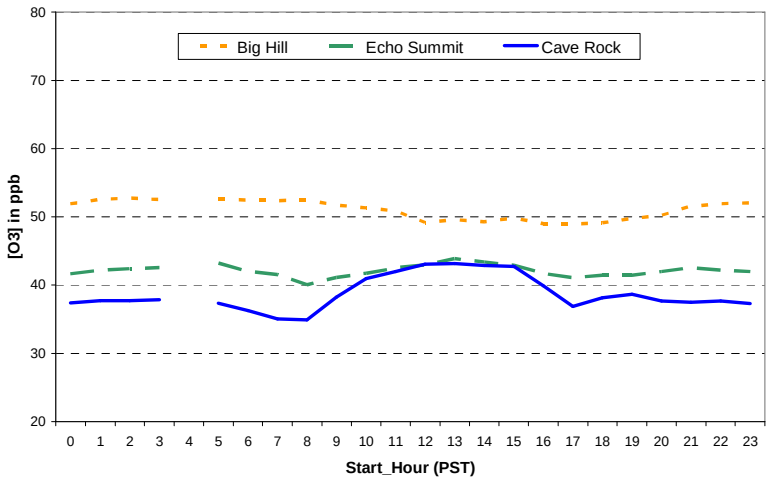

3.2.3 Total Nitrogen

Because a total nitrogen calculation is only possible for locations with both gas and particle phase concentrations, the data summaries of total nitrogen are confined to TWS sites (**Table 3-17**).

There is a wide seasonal variation across these sites. In winter, the populated sites in the basin are clearly highest, with the south shore sites (Sandy Way, SOLA) much higher than the other sites. In summer, the south shore still is high but the difference from winter is modest. At Big Hill total nitrogen is very low in the winter (the limited number of samples may have been a factor), rises in spring, and peaks in the summer to levels comparable to South Lake Tahoe. Lake Forest shows a pattern similar to south Lake Tahoe with the lowest levels in the spring and moderately high levels in the other seasons. The unpopulated east shore (Thunderbird) shows the least seasonal signal and is the lowest year-round.

The split among the gas and aerosol species is also highly variable across the network. Total nitrogen distributions (percent of N) are shown in **Table 3-18**. Approximately 70% of the dry N deposition comes from the deposition of NH_3 and NH_4^+, both being highly water soluble.

The aerosol fraction (nitrate + ammonium) is greatest at the less-populated sites (Thunderbird and Big Hill), while the ammonia gas fraction peaks in the populated areas (SOLA/Sandy Way and Lake Forest). Nitric acid, by contrast, is a relatively constant fraction at all sites. On average, 70% or more of total N is from ammonia plus ammonium, with over 50% of total N from ammonia alone. Thus, total atmospheric N is primarily determined by the supply of ammonia, regardless of its site-specific aerosol-gas partitioning.

Table 3-17. Total nitrogen from TWS aerosol and gas measurements.

Lake Tahoe Atmospheric Deposition Study Nitrogen Total, Nitrates, Ammonium Ion, Nitric Acid, Ammonia (ug/m3)									
	Nitrogen Particulate & Gas (N)					Nitrates	Ammonium	Nitric Acid	Ammonia
Site	Winter	Spring	Summer	Fall	Study Average	(Mass)	(Mass)	(Mass)	(Mass)
Big Hill	0.22	0.76	1.95	1.52	1.33	1.25	0.55	0.65	0.57
Lake Forest	0.93	0.67	1.17	1.20	0.97	0.48	0.26	0.47	0.67
Sandy Way	1.47	1.24	2.83	1.94	1.63	1.05	0.50	1.00	0.95
SOLA	2.73	1.38	1.88	2.30	2.13	0.81	0.39	0.96	1.73
Thunderbird	0.32	0.47	0.82	0.67	0.57	0.53	0.29	0.34	0.18
Maximum Basinwide (excludes Big Hill)					3.84	1.79	0.78	2.93	4.08
2nd Maximum Basinwide (excludes Big Hill)					3.84	1.73	0.71	1.91	3.59
Average Basinwide (excludes Big Hill)					1.35	0.47	0.27	0.69	0.85
Median Basinwide (excludes Big Hill)					1.28	0.38	0.25	0.57	0.77
Minimum Basinwide (excludes Big Hill)					0.15	0.02	0.01	0.08	0.04

Table 3-18. Contributions of nitrogen species from TWS measurements.

	Nitrates	Ammonium	Nitric Acid	Ammonia	$NH_4^+ + NH_3$	$HNO_3 + NO_3^-$	Total N (ng/m^3)
Site	**% of Total**	**% of Total**	**% of Total**	**% of Total**	**% of Total**	**% of Total**	**Study Average**
Big Hill	21	32	11	36	68	32	1,333
Lake Forest	11	21	11	57	78	22	973
Sandy Way	15	24	14	48	72	28	1,627
SOLA	9	14	10	67	81	19	2,125
Thunderbird	21	40	13	26	66	34	566

3.3 Summary

The CARB initiated the LTADS in 2002 to quantify the contribution of atmospheric deposition to the declining clarity of Lake Tahoe. The initial study design, which included routine monitoring supplemented by special studies to address pertinent atmospheric processes (e.g., emissions, chemistry, conditions aloft, particle deposition), was described in a June 10, 2002 draft work plan for LTADS. The monitoring network was designed to provide information on the spatial variations around the lake and upwind of the basin. A total of five sites were selected for a one-year monitoring program featuring the TWS. The fives sites selected were: South Lake Tahoe (SOLA and Sandy Way) representing the major urban environment in the basin; Lake Forest (near Tahoe City) representing a less urban environment; Thunderbird Lodge representing the background conditions in the basin; and Big Hill representing the environment upwind of the Tahoe basin. The TWS provided two-week integrated samples of ammonia, nitric acid, TPS, PM10, and PM2.5 and served as the backbone of the monitoring plan. The two week sampling duration avoided problems associated with episodic sampling and non-representative contributions from specific sources. Mini-Vol samplers were used to measure TSP at remotes sites and were deployed under two different monitoring schemes: buoy Mini-Vols for TSP (typically 24 hours) and non-buoy Mini-Vols for TSP (duration and frequency varied).

Field blanks were applied to subtract the background contribution from the sampling environment and field operation. TWS field blanks were collected only at a single site (SOLA) for 10% of the ambient sampling period. Three field blanks were collected for Mini-Vol TSP samples. The limited and site specific field blanks may affect the results of the ambient samples.

A total of 129 sets of TWS samples, including TSP, PM10, and PM2.5, 36 sets for buoy Mini-Vol TSP samples, and 129 sets for non-buoy Mini-Vol TSP samples were collected in LTADS. Replicate analyses were performed on 10% of the ambient samples. The chemical data were evaluated for internal consistency by examining the physical consistency and balance of reconstructed mass, based on chemical species versus measured mass. In general, the samples collected met the criteria of internal physical consistency. A few TWS samples were suspected to be outliers; however, no field flag was noted for these samples (with the exception of one laboratory flag).

The highest annual averages TSP (22 µg/m^3) and PM10 (19 µg/m^3) mass concentrations were observed at the SOLA site and the highest annual average PM2.5 mass concentration (9 µg/m^3) was observed at the SW site. The lowest TSP, PM10, and PM2.5 mass concentration were 6, 6, and 4 µg/m^3, respectively, and were observed at the TB site. PM10 mass comprised 80-90% of TSP mass and was approximately twice that of PM2.5 mass. The most abundant chemical species were OC (17-30%), silicon (11-16%), and aluminum (4-5%) for TSP; OC (16-28%), silicon (10-21%), and aluminum (4-7%) for PM10; and OC (42-52%), EC (5-16%), and ammonium (3-6%) for PM2.5. The lowest TWS TSP, PM10, and PM2.5 mass concentrations were observed from March to April 2003 at all five sites. TWS TSP, PM10, and PM2.5 mass concentrations observed at the BH, TB, and LF sites from May to October 2003 were twice as high as those observed from November 2002 to February 2003; however, TWS TSP, PM10, and PM2.5 mass concentrations were comparable during these two periods at the SOLA and SW sites. The elevated TWS TSP, PM10, and PM2.5 mass concentrations at the SOLA and SW sites from November 2002 to February 2003 were due to elevated OC and EC concentrations, which were likely the result of the increased traffic volumes and wood burning associated with winter activities.

The annual average mass concentrations and chemical species were the highest in TPS and the lowest in PM2.5 at the same site; however, such physical consistency was not necessarily observed for TWS samples at the same sampling period. For example, PM_{10} mass concentration higher than TSP mass concentration was occasionally observed. Such sampling bias can be attributed to the low TWS sampling flow rate of 1.67 liter per minute, low mass concentration of ambient particulate matters, long sampling duration, and sampling artifacts of semi-volatile species.

The annual average PM_{10} mass concentration comprised more than 80% of the TSP mass concentration. Bounces and penetration of particles larger than 10 µm through the impactor can increase the PM10 mass concentration. Particle bounce and penetration efficiency depends on the characteristics of 50% cutpoint curve and material of impaction substrate and particle bounce is more pronounced as the sampling time (i.e., particle loading on impaction substrate) increases (Chang, et al, 1999, Tsai, et al, 1995), as well as at low particle concentrations.

The sampling artifacts of semi-volatile species on sampling media can either introduce positive or negative sampling artifacts. The sampling artifacts of semi-volatile species depend on ambient sampling temperature, relative humidity, the species' disassociation constant, the ratio of species in particulate and gas phases, and the pressure drop through the sampling media (Chang et al 2000b, Stelson, and Seinfeld, 1982, Zhang and McMurry 1987, Zhang and McMurry 1992). Although negative sampling artifacts of nitrate losses can be quantified through the backup filter, it is not clear how absorption of OC onto the quartz filters might create positive sampling artifacts during analysis. As OC is the most abundant species in TWS TSP, PM10, and PM2.5, a denuder for volatile organic species and a backup filter should be used for better assessment of PM mass and chemical concentrations.

Except for a couple of sites in the winter period, staff has confidence in the LTADS seasonal particulate matter concentrations in TSP, PM10, and PM2.5. Staff believes the LTADS nitrogen specie concentrations (gas and particulate matter in all size fractions) are representative of Tahoe Basin atmospheric chemistry and processes. The LTADS phosphorus observations suffered from the difficulties all analyses of ambient P face. The dust experiments suggest that particulate concentrations at the shoreline are significantly higher than concentrations over the lake. The LTADS deposition estimates, because they are based on shoreline observations, are thus likely an overestimation as well. Staff did not study inert particles in detail. By using all PM data (i.e., all species), the staff's analysis presents a maximum bounding estimate for atmospheric deposition of PM to Lake Tahoe. A simple analysis of likely soluble materials (i.e., ion chromatography and automated colorimetry measurements) indicates that about 20-25% of the PM mass is soluble and would not remain as particles in the water. Other potentially soluble components would reduce the number and mass of inert particles further. Thus, a crude adjustment factor of 75% to the total PM deposition estimates presented in Chapters 4 and 5 may be needed to accurately represent the atmospheric PM that remains as PM once deposited to the Lake.

With respect to gaseous pollutants, concentrations are typically representative of clean conditions. Seasonal mean concentrations of nitric acid ranged from about 200 to 1300 ng/m^3 (0.1 to 0.5 ppb) and generally being lowest in the spring and highest in the fall. Seasonal mean concentrations of ammonia ranged from about 200 to 2300 ng/m^3 (0.3 to 3.3 ppb) and generally being lowest in the spring and highest in the summer and fall. The highest ammonia concentrations were observed at the SOLA site, which is strongly influenced by activity on Highway 50, during winter when the number of hours with downslope air flow across Highway 50 is greatest. The peak ozone concentration in the Tahoe Basin during 2003 was 87 ppb, below the California public health 1-hour standard but above the TRPA forest health 1-hour threshold. The number of hours during 2003 when ozone concentrations were greater than 70 ppb declined from 400+ hours at the Big Hill site (on the western slope of the Sierra Nevada) to 90+ hours at the Echo Summit site (on the Sierra crest and the southwestern boundary of the Tahoe Basin) to 30+ hours at Incline Village (near lake-level in the Tahoe Basin).

3.4 References

Bevington, P.R., (1969). Data Reduction and Error Analysis for the Physical Sciences. McGraw Hill, New York, NY.

Carroll, J.J., Anastasio, C., and Dixon, A.J., (2004). Keeping Tahoe Blue through Atmospheric Assessment: Aircraft and Boat Measurements of Air Quality and Meteorology near and on Lake Tahoe, report prepared for California Air Resources Board, Sacramento, CA, June.

Chang, M.C., Kim, S., and Sioutas, C., (1999). "Experimental studies on particle impaction and bounce; effects of substrate design and material." *Atmospheric Environment*, **15**: 2313-2323.

Chang, M.-C.; Sioutas, C.; Kim, S.; Gong, H. Jr.; and Linn, W.S., (2000a). Reduction of nitrate losses from filter and impactor samplers by means of concentration enrichment. *Atmos. Environ*. **34**, 85-98.

Chang, M.C**.**, Kim, S., Sioutas, C., Gong, H., Anderson, K., and Linn, W., (2000b) "The effect of concentration enrichment on losses of nitrate from filters and impactor samplers." *Atmospheric Environment*, **34** (1): 85-98.

Chow, J.C. and Watson, J.G., (1989). Summary of particulate data bases for receptor modeling in the United States. In Transactions, Receptor Models in Air Resources Management, Watson, J.G., editor. Air & Waste Management Association, Pittsburgh, PA, pp. 108-133.

Chow, J.C.; Watson, J.G.; Pritchett, L.C.; Pierson, W.R.; Frazier, C.A.; and Purcell, R.G., (1993). The DRI Thermal/Optical Reflectance carbon analysis system: Description, evaluation and applications in U.S. air quality studies. *Atmospheric Environment* **27A** (8), 1185-1201.

Chow, J.C. and Watson, J.G., (1994a). Guidelines for PM10 sampling and analysis applicable to receptor modeling. Report No. EPA-452/R-94-009. Prepared for U.S. EPA, Office of Air Quality Planning and Standards, Research Triangle Park, NC, by Desert Research Institute, Reno, NV.

Chow, J.C.; Watson, J.G.; Fujita, E.M.; Lu, Z.; Lawson, D.R.; and Ashbaugh, L.L., (1994b). Temporal and spatial variations of PM2.5 and PM10 aerosol in the Southern California Air Quality Study. *Atmospheric Environment* **28** (12), 2061-2080.

Chow, J.C. and Watson, J.G., (1999). Ion chromatography in elemental analysis of airborne particles. In Elemental Analysis of Airborne Particles, Vol. 1, Landsberger, S., Creatchman, M., editors. Gordon and Breach Science, Amsterdam, pp. 97-137.

Chow, J.C., Watson, J.G., and Wiener, R.W., (2005) Method No. 508: PM2.5 sampling and gravimetric analysis by Federal Reference Method. In Methods of Air Sampling

and Analysis, Lodge, J.P. Editor. Air and Waste Management Association, Pittsburgh, PA.

Cliff, S., (2005). Quality Assurance Analysis of Filter Samples Collected during the Lake Tahoe Atmospheric Deposition Study using Synchrotron X-Ray Fluorescence, report prepared for California Air Resources Board, Contract No. 03- 334. April 30, 2005.

DRI (2000). DRI Standard Operating Procedure #2-204.6 - Thermal/Optical Reflectance Carbon Analysis of Aerosol Filter Samples, Reno, NV, June.

Fitz, D. and Hering, S., (1996). Further Evaluation of a Two-Week Sampler for Acidic Gases and Fine Particulate, report prepared for California Air Resources Board, Contract No. 93-339, May.

Hidy, G.M., (1985). Jekyll Island meeting report: George Hidy reports on the acquisition of reliable atmospheric data. *Environmental Science & Technology* **19** (11), 1032-1033.

Lioy, P.J.; Mallon, R.P.; and Kneip, T.J., (1980). Long-term trends in total suspended particulates, vanadium, manganese, and lead at near street level and elevated sites in New York City. *Journal of the Air Pollution Control Association* **30** (2), 153-156.

Pathak, R.K.; Yao, Z.; and Chak, K.C., (2004). Sampling artifacts of acidity and ionic species in PM2.5, *Environ. Sci. Technol.* **38**, 254-259.

Stelson, A.W. and Seinfeld, J.H., (1982). Relative humidity and temperature dependence of the ammonium nitrate dissociation constant, *Atmos. Environ.* **16**:983-992.

Tarnay, L., Gertler, A.W., Blank, R.R., Taylor Jr., G.E., (2001). Preliminary measurements of summer nitric acid and ammonia concentrations in the Lake Tahoe Basin air-shed: implications for dry deposition of atmospheric nitrogen. *Environmental Pollution* **113**, 145-153.

Tarnay, L.W., Gertler, A.W., and Taylor Jr., G.E., (2002). An Inferential Model for HNO_3 Deposition to Semi-arid Coniferous Forests, *Atmos. Environ.*, **36**, 3277-3287.

Tsai, C.J. and Chen, Y.H., (1995). Solid particle collection characteristics on impaction surface of different design. *Aerosol Sci. Technol.* **23**: 96-106.

Watson, J.G.; Lioy, P.J.; and Mueller, P.K., (1989). The measurement process: Precision, accuracy, and validity. In Air Sampling Instruments for Evaluation of Atmospheric Contaminants, Seventh Edition, Hering, S.V., editor. American Conference of Governmental Industrial Hygienists, Cincinnati, OH, pp. 51-57.

Watson, J.G. and Chow, J.C., (1992). Data bases for PM10 and PM2.5 chemical compositions and source profiles. In Transactions, PM10 Standards and

Nontraditional Particulate Source Controls, Chow, J.C. and Ono, D.M., editors. Air & Waste Management Association, Pittsburgh, PA, pp. 61-91.

Watson, J.G.; Lioy, P.J.; and Mueller, P.K., (1995). The measurement process: Precision, accuracy, and validity. In Air Sampling Instruments for Evaluation of Atmospheric Contaminants, Cohen, B.S. and Hering, S.V., editors. American Conference of Governmental Industrial Hygienists, Cincinnati, OH, pp. 187-194.

Watson, J.G.; Chow, J.C.; and Frazier, C.A., (1999). X-ray fluorescence analysis of ambient air samples. In Elemental Analysis of Airborne Particles, Vol. 1, Landsberger, S. and Creatchman, M., editors. Gordon and Breach Science, Amsterdam, pp. 67-96.

Watson, J.G.; Turpin, B.J.; and Chow, J.C., (2001). The measurement process: Precision, accuracy, and validity. In Air Sampling Instruments for Evaluation of Atmospheric Contaminants, Ninth Edition, Cohen, B.S. and McCammon, C.S., Jr., editors. American Conference of Governmental Industrial Hygienists, Cincinnati, OH, pp. 201-216.

Zhang, X. and McMurry, P.H., (1987). Theoretical analysis of evaporative losses from impactor and filter deposits. *Atmos. Environ.* **21**: 1779-1789.

Zhang, X. and McMurry, P.H., (1992). Evaporation losses of fine particulate nitrates during sampling. *Atmos. Environ.* **26A**: 3305-3312.

Zhang, Q., Carroll, J.J., Dixon, A.J., and Anastasio, C. (2002). Aircraft Measurements of Nitrogen and Phosphorus in and around the Lake Tahoe Basin: Implications for Possible Sources of Atmospheric Pollutants to Lake Tahoe. *Environ. Sci. Technol.*, Vol. 36, 4981-4989.

This page blank intentionally.

4. Dry Atmospheric Deposition

The primary goal of the Lake Tahoe Atmospheric Deposition Study (LTADS) is to quantify the contribution of dry atmospheric deposition to Lake Tahoe as an input to modeling lake clarity and developing a Total Maximum Daily Load (TMDL) –based water quality management program for the lake. Wet deposition is also an important input to the Lake, but was not a major focus of the LTADS field study for a number of reasons. LTADS did not emphasize observations of wet deposition because, with proper siting and care in sampling, observed wet deposition to surrogate surfaces may be used to infer wet deposition to the Lake. To support existing wet deposition measurements, Chapter 5 presents estimated wet deposition onto Lake Tahoe during 2003 based on a first principles analysis of seasonal air quality concentrations and the number of hours when precipitation fell.

The LTADS estimate of dry deposition strives to include all optically and biologically significant materials in the air over the lake, including gas and particle phase nitrogen and particle phase phosphorus that fertilize phytoplankton, and non-soluble (“inert”) particulate matter that, once deposited in the lake, may scatter light or serve as growth sites for microscopic organisms. The calculation of dry deposition provided here assumes that dry deposition processes occur during every hour throughout the year, irrespective of whether or not there is any precipitation. This is one of several assumptions that are intended to provide a conservatively large estimate of dry deposition.

Secondary goals of LTADS include identification and ranking of emissions sources and consideration of the relative impacts of local emissions and those emissions transported into the basin upon ambient concentrations and deposition. These are addressed elsewhere in this report. However, for perspective while reading this chapter, it is worth noting that the relative contributions of emissions sources to the concentrations observed near the Lake are expected to provide a reasonable first-order estimate of the relative contributions of those sources to deposition to the Lake. As outlined later in this chapter, the dry deposition rates generally respond linearly to increase or decrease in ambient concentrations, although those rates also respond to wind direction and increase with wind speed. However, because of the daily variation in wind direction, reductions in ambient concentrations at different times of day will generally have different effects on the rate of dry deposition to the Lake. Reductions in emissions and ambient concentrations near the Lake during night and early morning hours (when wind direction is typically from land toward the Lake) would generally have the greatest effect in reducing dry deposition to the Lake.

Deposition to land surfaces and subsequent transport to the Lake is outside the scope of LTADS; however, it is included in the overall watershed analysis for the TMDL process. Materials deposited on land and subsequently transported to the Lake are not explicitely estimated, but will be included in the estimates of other nutrient and sediment inputs such as stream flow and direct runoff to the Lake. These estimates which include indirect atmospheric deposition are being developed under the auspices of the

Lahontan Regional Water Quality Control Board (RWQCB). Lahontan RWQCB is also estimating inputs from streambed erosion, shoreline erosion, and ground water exchange. However, the relative contribution of deposition to land areas with subsequent transport to the Lake is expected to be small relative to that in other watersheds. First, the ratio of Lake area (500 km^2) to land area (800 km^2) exceeds that of many watersheds. Second, the high proportion of natural surfaces at Tahoe increases percolation and decreases runoff of precipitation compared to more urbanized areas.

Sections 4.1 and 4.2 discuss the general methodology used to derive the estimates of dry deposition to the Lake surface and detail meteorological conditions relevant to variations in the concentrations and deposition velocities. Section 4.3 details the methods used for calculation of deposition velocities and dry deposition rates for gases and particles. Section 4.4 discusses the assumptions used in the deposition calculation and the potential for introduction of bias by those assumptions. The chapter concludes with estimates of the seasonal and annual dry deposition of nitrogen species, phosphorus and particulate matter to the Lake surface.

4.1 General Methodology

The general approach of estimating atmospheric dry deposition rates by using observed atmospheric concentrations in conjunction with theoretical deposition velocities is a well-established methodology (e.g., Brook et al. 1999; Smith et al. 2000, Wesely and Hicks, 2000; Lu et al. 2003). The deposition velocity for a particular substance or chemical species depends in large part on the meteorological conditions. Historical and LTADS observations show that air quality and meteorology in the Tahoe basin have strongly repetitive temporal patterns. Both concentrations and deposition velocities were characterized at time scales relevant to their intrinsic variations. Hourly observations of meteorological conditions provide sufficient temporal resolution of deposition velocities.

Chemical composition is largely driven by local and regional human activity patterns. These are cyclical and regularly repeated, but within the precision required for annual deposition estimation, the variation in chemical composition is largely seasonal. Chemical characterization of air pollutants for LTADS was thus simplified to two-week integrated sampling, which adequately reflected compositional variation due to changing emission patterns and seasonal meteorology.

Conversely, for many species, concentrations show large diurnal variation due to the varying rates of emission and dilution. This variation was captured by LTADS with hourly air pollutant concentrations monitored by relatively simple continuous instruments reporting time-resolved (and sometimes size-resolved) bulk aerosol data and a limited set of time-resolved gases.

As described in chapter 3, to generate an idealized diurnally and chemically resolved picture of air quality at a monitoring site, the two week sampler (TWS) data were used to construct a “conceptual model” that describes the mean air quality observed at representative sites during each season. The conceptual model was then merged with

the observed seasonal diurnal concentration patterns. Finally, the seasonal diurnally and chemically resolved air quality was combined with diurnal patterns of airflow and deposition velocity derived from the hourly meteorological data to generate a realistic chemically resolved dry deposition estimate.

Thus, to summarize the methods that are detailed in the following sections, deposition velocities representative of conditions at specific sites were estimated for each hour for which meteorological data were available. Each hourly deposition velocity was multiplied by a representative concentration for the same hour based on measurements at a nearby air quality site; their product is the estimated deposition rate for that hour. The seasonal averages of the hourly deposition rates were used to represent the deposition rate for each 3-month season. The seasonal average deposition rates are associated with a specific area of the Lake. Deposition rates are summed over four seasons to provide an annual estimate for each quadrant of the Lake and summed across all quadrants to provide rates of deposition to the Lake as a whole.

4.1.1 Atmospheric Deposition Model Used in LTADS

LTADS methodology estimates the dry deposition of a pollutant to the lake surface as the product of that pollutant's concentration and its deposition velocity. Ambient concentrations (C) and deposition velocities (V_d) vary temporally, spatially, and by pollutant. Due to cost, time, and physical constraints on the LTADS program, directly measuring every variable useful to refining an estimate of deposition to the lake was not possible. Instead, a tiered, climatological approach was used. Successive tiers indicate increasing data needs and analytical complexity to better resolve and define the deposition velocities and concentrations. At each level the same conceptual framework is applied, the rate of dry deposition of a species is the integral of the ambient concentration multiplied by its deposition velocity.

$$\text{Deposition Flux (F)} = C \times V_d.$$

These deposition flux estimates are integrated or summed over time and area to estimate the annual deposition to the Lake surface.

The pollutant concentrations are based on observations and were interpolated or extrapolated by various means to compensate for missing data. Physically reasonable deposition velocities were calculated from observed meteorological values (e.g., wind direction, wind speed, air temperature, and water temperature). For unknown or poorly known parameters associated with ambient concentrations or deposition velocities, upper and lower estimates of the parameters enable bounding limits of the deposition to the Lake to be provided.

As demonstrated in the figure below, this method can be represented by a tiered approach, with each succeeding level requiring more data and yielding improved flux estimates.

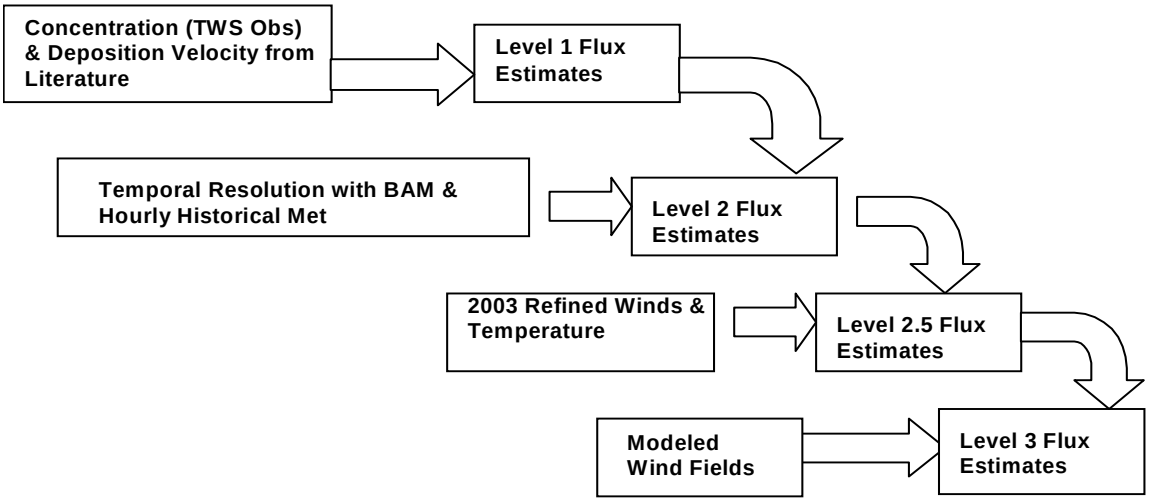

The deposition estimates presented in this document correspond to the Level 2.5 approach, where TWS and mini-vol concentration measurements were used to provide mean seasonal concentrations. These seasons were defined as winter (December, January, and February), spring (March, April, and May), summer (June, July, and August), and fall (September, October, and November). The mean seasonal concentrations were then refined to diurnal concentrations based on hourly data (e.g., BAM PM data, gaseous pollutant data). These hourly seasonally averaged concentration data were then merged with hourly deposition velocities to produce hourly deposition rates that were summed seasonally and annually. Assumptions associated with the calculation of deposition velocities (e.g., mean particle size within size fractions, limits on maximum deposition velocities) were varied over a range of feasible values to provide bounding estimates of the atmospheric deposition of N, P, and PM. A flow chart describes the input data steps used to calculate dry deposition for LTADS.

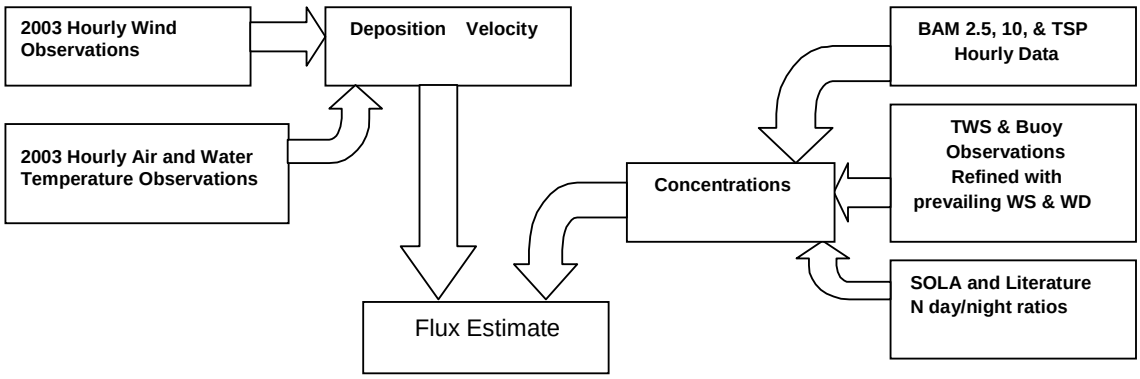

4.1.2 Spatial Resolution - Lake Quadrants

Deposition to the lake surface was calculated as an unweighted average of seasonal deposition rates within four sectors, representing roughly equal areas of the lake area (**Figure 4-1**). These quadrants were crudely defined based on air quality measurements and similar densities of population and activity.

Figure 4-1. Conceptual View of Lake Quadrants Used to Represent the Spatial Variations in Ambient Concentrations and Deposition Rates.

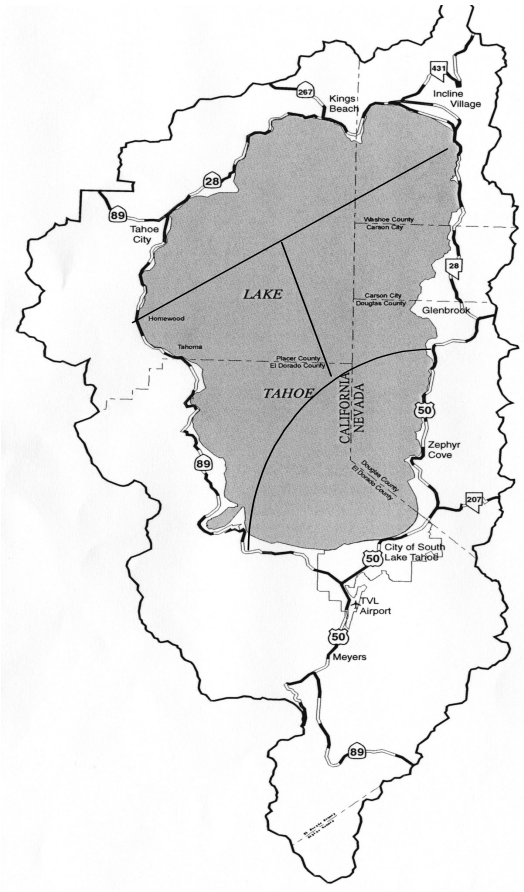

The sources of the meteorological and concentration data used to represent these quadrants were as follows:

- N & NW Lake –Meteorological data from the U.S. Coast Guard (USCG) Pier and concentrations from Lake Forest (LF) were used to calculate deposition for this area.
- S & SE Lake –Meteorological data from the Timber Cove pier were used to characterize the deposition velocities. Meteorological data from buoys TDR1 and TDR2 were also considered for comparison purposes but not used in the deposition estimates presented here. Seasonal average concentrations from Sandy Way in South Lake Tahoe were used to calculate deposition rates. Observations of the

diurnal variation in PM concentrations at Sandy Way and SOLA sites were combined as described later.

- E & NE Lake – Meteorological data from Cave Rock and concentrations observed at Thunderbird were used to calculate deposition rates. Meteorological data from Tahoe Vista pier were also used for comparison purposes.
- W & SW Lake – Meteorological data from Sunnyside Pier were used to calculate deposition velocities. Seasonal average concentrations were extrapolated from Thunderbird to the west shore based on comparison of two-week average observations at Thunderbird and shorter term measurements of TSP at Bliss during fall and winter. This data is limited but three similarities between the Bliss and Thunderbird sites suggest the extrapolation is a reasonable approach. First, emissions related activities (population density and traffic volume) are similarly low on the west and east shores compared to those within more urbanized areas. Second, regional wind flow tends to be from the SW so that Thunderbird and the east shore are frequently downwind of Bliss and the west shore. Third, average TSP mass concentrations observed at the two sites during limited periods of concurrent monitoring were similar.

Based on the similarities between Bliss and Thunderbird, the seasonal average concentration of each size category of PM (PM2.5, PM10, and TSP) was assumed equal to that measured with the TWS at Thunderbird. In addition the diurnal variations in concentrations of PM by size category at Bliss were also assumed to be equal to those observed with the BAM at Thunderbird. Although the PM masses at Thunderbird and Bliss are assumed to be equal, the seasonal average concentrations of nitrogen in aerosol form at Bliss (i.e., NH_4^+ and NO_3^-) were assumed to be one-half the concentrations observed at Thunderbird in the dry deposition calculations. This is a conservative assumption because the limited number of PM observations of nitrogen species at Bliss indicated they were lower than one-half of the concentrations at Thunderbird. Seasonal average concentrations of nitrogen in gaseous form (i.e., NH_3 and HNO_3) were assumed to be equal to concentrations observed with the TWS at Thunderbird. Aerosol nitrate and ammonium concentrations observed at Thunderbird were surprisingly high and may not be representative. At Bliss during the fall, aerosol nitrate (NO_3^-) concentrations averaged about 10%, and aerosol ammonium (NH_4^+) averaged about 20% of concentrations at Thunderbird. However, the treatment of aerosol concentrations has less influence on estimates of total nitrogen deposition because deposition of gaseous nitric acid and ammonia dominate.

For each of the four quadrants, seasonally averaged concentrations of particle masss and nitrogen contained in the various nitrogen species are shown in **Figures 4-2 and 4-3**, respectively. These figures are based on the seasonal measurements summarized in **Table 3-15**. For lower, central, and upper estimates of phosphorus deposition, an ambient concentration of 40 ng P/m^3 was assumed to be constant across all sites and seasons; thus, phosphorus concentrations are not illustrated seasonally. However, because deposition velocity is a function of particle size, the distribution of phosphorus between size fractions was varied. Additionally, the seasonally averaged concentrations contained diurnal variations as described in section 4.1.3. The resulting

estimates of seasonally averaged hourly concentrations were then paired with deposition velocities calculated from meteorological data representative of the same quadrants.

Figure 4-2. Seasonal average concentrations of PM, by Size, as observed with the TWS at Lake Forest, Sandy Way – South Lake Tahoe, and Thunderbird, and inferred for the West Shore as described in the text.

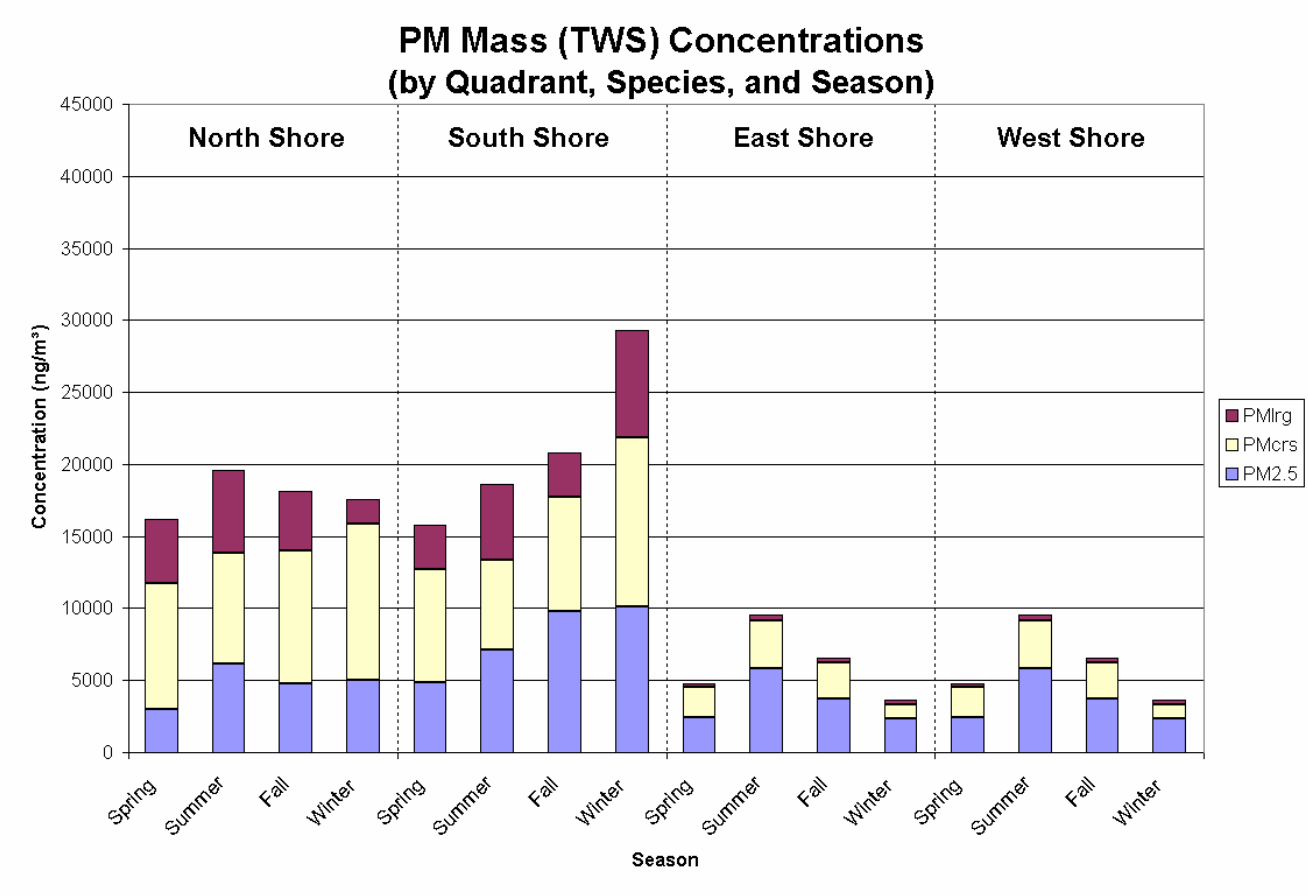

Figure 4-3. Seasonal average nitrogen concentrations, by chemical species and location, as observed at Lake Forest, Sandy Way - South Lake Tahoe, and Thunderbird, and inferred for the West Shore as described in the text.

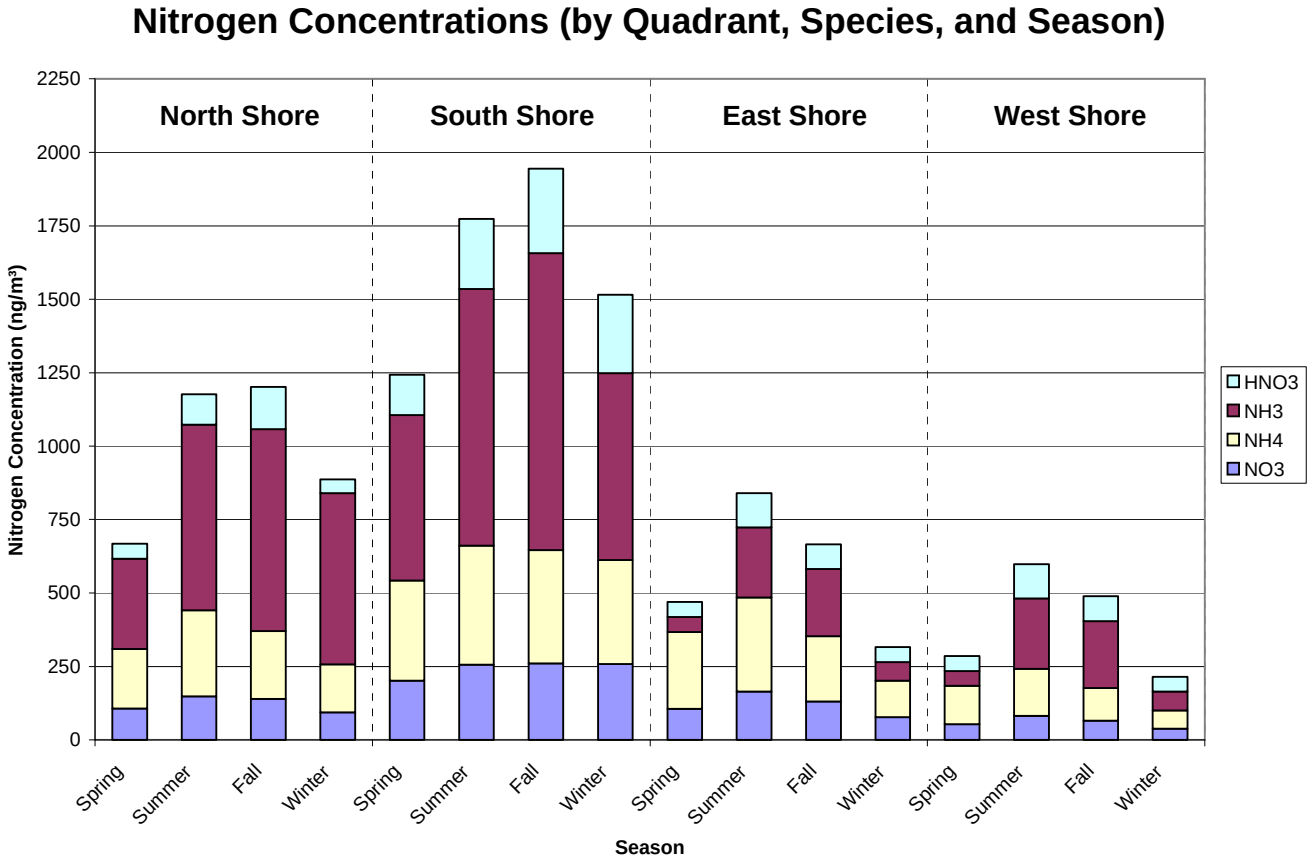

4.1.3 Temporal Resolution of Concentrations

Because meteorological conditions such as wind direction and speed change substantially throughout the day and both ambient concentrations and deposition velocities respond to those changes, the covariance of concentration and deposition velocity can be substantial. Thus, use of the product of seasonal average concentration and seasonal average deposition velocity generally would not represent average deposition rate. The covariance of ambient concentrations near the Lake and the meteorological factors controlling deposition velocities will generally be greatest for those species that are directly emitted by sources located near the Lake.

Representation of the temporal variation in deposition velocity is relatively straightforward because continuous meteorological measurements are generally available through the year. For calculation of deposition rates similar temporal resolution of concentrations would be ideal for species that are easily measured with continuous instruments. However, for the species of interest at Tahoe, such temporal

resolution was neither necessary nor possible (due to limitations of available measurement methods and logistical and funding constraints).

LTADS constructed a representation of the diurnal variations in concentrations for most species of interest. As suggested by the seasonally averaged hourly BAM observations presented in **Chapter 3**, the strong mesoscale meteorological influences in the Basin cause the diurnal variations in PM concentrations to be fairly regular within each season. This temporal regularity was exploited to develop a simple observation based model of diurnal variation of concentrations during each season.

Hourly concentrations were represented as the product of a seasonal average concentration (**Figures 4-2 and 4-3**) and an observationally based multiplier unique to each species, season, and hour of the day. The multipliers for Lake Forest, South Lake Tahoe and Thunderbird are listed in **Table 4-1**. The average of the ratios for any 24-hour period is unity. Thus, the hourly multipliers as applied in calculation of deposition rates do not alter a seasonal average PM mass concentration as observed with the TWS but merely apportion it by hour of day in a manner consistent with the seasonally averaged BAM observations.

The multipliers were derived from hourly concentrations of PM size fractions observed with BAMs at Sandy Way, Thunderbird, and Lake Forest. The BAM is a certified federal equivalent method for 24-hour average PM10 mass concentration (i.e., equivalent to the mass of PM10 traditionally collected as a 24-hour integrated filter sample). To provide a 24-hour average, the BAM measures and integrates 24 individual hourly observations of PM mass. In LTADS, individual hourly BAM observations were not used directly but instead were averaged to represent the diurnal variation in PM mass concentration. The BAM-measured hourly mass concentrations were averaged across each 3-month season for each hour of the day. Averaging across 90+ hours to represent concentrations at a specific time of day over a three-month season is expected to provide at least as reliable an observation as does averaging across a 24-hour day.

As discussed in Chapter 3 the BAMs were equipped with size selective inlets to measure PM2.5, PM10, and TSP allowing calculation of the concentrations of PM2.5, PM_coarse (PM10 - PM2.5), and PM_large (TSP - PM10). The diurnal variation in PM concentration for each size fraction is summarized by 24 hourly ratios for each season and site. These are the ratio of hourly concentration to seasonal average concentration. For each site and season the diurnal variation in PM2.5 was represented by the diurnal variation in PM2.5 as measured with the BAM. The diurnal variations in PM_coarse and PM_large were each assumed to be represented by the diurnal variation of the sum of PM_coarse and PM_large. This assumption is based on the fact that sources generally emit both PM_coarse and PM_large while different sources and atmospheric processes are generally responsible for PM2.5. This allowed use of a more stable metric (TSP minus PM2.5), instead of calculating both TSP minus PM10 and PM10 minus PM2.5. **Table 4-1** shows the ratios that were used. **Figures 4-4 through 4-7** illustrate those ratios observed at sites on the north, and south shores.

Diurnal variation in concentrations of the aerosol nitrogen species (NO_3^- and NH_4^+) were assumed, irrespective of the size fraction in which they were measured, to vary diurnally according to the variation in the PM2.5 mass as observed with the BAM at each site. The rationale for this assumption is that the processes forming aerosol nitrogen species are relatively disconnected from processes that form coarse and large particles. In any case, the estimates of total nitrogen deposition are dominated by the deposition of gaseous species and so are relatively insensitive to details of the aerosol concentrations or their diurnal variations.

For South Lake Tahoe a slightly modified approach was taken to utilize the available BAM observations from SOLA and Sandy Way. BAM TSP was measured at both sites; BAM PM2.5 and PM10 were measured at Sandy Way. There were significant differences in the diurnal patterns of BAM TSP concentrations at the two sites, due to their locations with respect to local sources. During downslope flow, SOLA is downwind of commercial and residential areas and nearby South Lake Tahoe Blvd, but during the same hours, Sandy Way was upwind of South Lake Tahoe Blvd and much of the commercial activity. To provide a reasonable approximation of the diurnal variation in concentrations advected to this quadrant of the Lake the diurnal variation in concentrations of PM_coarse and PM_large were represented as the diurnal variation in the average of BAM measured TSP at SOLA and Sandy Way. The diurnal variation in PM2.5 concentration was represented by BAM PM2.5 observations at Sandy Way.

For the gaseous species diurnal variations of concentrations were based upon limited observations compared to those available for PM. Continuous hourly observations of gaseous concentrations at Sandy Way were used to estimate the seasonal diurnal variations in nitric acid as discussed in **Chapter 3**. Those results are illustrated in **Figure 4-8** with seasonal ratios of hourly to average concentrations. In the absence of other information, this diurnal profile for nitric acid at Sandy Way was extrapolated to all quadrants. Although this extrapolation is somewhat tenuous its effect on deposition rates should be small because temporal variations of nitric acid concentrations will be less influenced by shifts in local winds compared to PM. That is because nitric acid, unlike PM is not directly emitted by very localized sources but instead takes some time to form in the atmosphere. Accordingly covariance of concentration and deposition velocity will be much less for nitric acid than for PM concentrations.

Because there were no data available to indicate diurnal variation in ammonia gas concentrations at Lake Tahoe its concentration was treated as constant within each season and quadrant. For possible future research, if measurement methods become available with better temporal resolution for nitric acid or ammonia, the cost, value and feasibility of obtaining such measurements should be considered.

Table 4-1. Diurnal variation of particle mass concentrations observed with BAMs (seasonal average of concentration by hour of day / seasonal average for all hours) at Lake Forest and Thunderbird. PM2.5, PM_coarse, and PM_large are indicated as 2.5, crs, and lrg.

	Lake Forest															
	Fall				Summer				Spring				Winter			
Hour	2.5	crs	lrg	crs+lrg	2.5	crs	lrg	crs+lrg	2.5	crs	lrg	crs+lrg	2.5	crs	lrg	crs+lrg
0	0.9	0.5	0.1	0.3	0.9	0.7	0.2	0.5	0.5	0.5	0.6	0.6	0.9	0.3	0.3	0.3
1	1.0	0.5	0.1	0.4	1.0	0.6	0.5	0.6	0.4	0.6	0.6	0.6	1.0	0.3	0.5	0.4
2	0.9	0.5	0.1	0.4	1.0	0.7	0.4	0.6	0.3	0.4	0.5	0.5	0.9	0.3	0.2	0.3
3	0.8	0.4	0.1	0.3	0.8	0.7	0.4	0.6	0.2	0.4	0.5	0.4	0.9	0.3	0.4	0.3
4	0.9	0.5	0.1	0.3	0.8	0.8	0.6	0.7	0.2	0.5	0.5	0.5	0.8	0.3	0.4	0.4
5	0.9	0.8	1.3	1.0	1.0	1.5	1.3	1.4	0.4	0.4	0.6	0.5	0.9	0.5	0.4	0.4
6	1.0	1.5	1.7	1.6	1.2	2.1	2.6	2.3	0.5	0.3	0.7	0.6	1.0	0.7	0.9	0.8
7	1.1	2.1	2.9	2.5	1.2	1.7	3.1	2.3	0.8	0.7	1.0	1.0	1.1	1.9	1.7	1.8
8	0.9	1.3	1.9	1.6	1.4	0.8	0.5	0.7	1.3	1.4	1.2	1.2	1.3	2.5	2.6	2.5
9	0.8	0.9	1.2	1.0	1.1	0.8	0.3	0.6	1.1	1.7	1.3	1.4	1.4	2.4	2.6	2.5
10	0.8	0.8	0.9	0.8	0.9	0.6	0.3	0.5	1.6	1.4	1.3	1.3	0.8	0.3	0.3	0.3
11	0.8	0.8	1.1	1.0	0.9	0.5	0.6	0.5	1.7	1.2	1.4	1.4	0.7	0.4	0.1	0.3
12	0.8	1.0	1.1	1.0	0.9	0.6	0.6	0.6	1.7	1.2	1.4	1.4	0.6	0.3	0.2	0.3
13	0.7	1.2	1.4	1.3	0.7	0.7	0.8	0.8	1.6	1.5	1.3	1.3	0.7	0.3	0.3	0.3
14	0.8	0.9	0.9	0.9	0.6	0.9	0.7	0.8	1.6	1.5	1.3	1.3	0.7	0.3	0.3	0.3
15	0.9	1.0	1.1	1.1	0.6	1.0	0.8	0.9	1.6	2.1	1.2	1.4	0.8	0.6	0.5	0.5
16	1.2	1.8	2.5	2.1	0.8	0.8	1.1	0.9	1.5	1.9	1.2	1.3	1.1	3.1	3.4	3.3
17	1.3	1.9	2.1	2.0	1.1	1.1	1.8	1.4	1.5	1.6	1.3	1.3	1.6	2.5	2.7	2.6
18	1.4	1.4	1.3	1.4	1.3	1.8	2.3	2.0	1.4	1.0	1.2	1.2	1.4	2.0	2.0	2.0
19	1.3	1.0	0.7	0.9	1.4	1.7	1.6	1.7	1.2	1.0	1.4	1.3	1.2	1.3	1.2	1.3
20	1.3	0.9	0.5	0.7	1.3	1.1	1.2	1.1	1.0	0.7	1.1	1.0	1.0	1.0	1.0	1.0
21	1.4	0.8	0.4	0.7	1.2	1.0	1.0	1.0	0.8	0.7	1.0	0.9	1.0	1.1	0.9	1.0
22	1.1	0.7	0.3	0.5	1.0	1.0	0.5	0.8	0.6	0.6	0.9	0.8	1.1	0.7	0.7	0.7
23	1.0	0.6	0.1	0.4	0.9	0.9	0.7	0.8	0.4	0.7	0.8	0.7	1.0	0.4	0.5	0.5

	Thunderbird Lodge															
	Fall				Summer				Spring				Winter			
Hour	2.5	crs	lrg	crs+lrg	2.5	crs	lrg	crs+lrg	2.5	crs	lrg	crs+lrg	2.5	crs	lrg	crs+lrg
0	1.1	0.8	0.5	0.7	1.0	0.9	0.7	0.8	1.2	1.0	0.7	0.9	1.2	0.9	1.0	0.9
1	1.2	0.7	0.1	0.5	0.9	0.8	0.4	0.6	1.3	0.9	0.7	0.8	1.2	0.8	2.2	1.2
2	1.3	0.5	0.3	0.4	1.0	0.7	0.5	0.6	1.1	0.8	0.8	0.8	1.0	1.0	0.8	0.9
3	1.1	0.7	0.0	0.4	1.0	0.8	0.6	0.7	0.9	0.9	1.0	1.0	0.8	1.2	0.8	1.1
4	0.9	0.9	0.2	0.6	1.0	1.0	0.4	0.6	0.9	1.0	0.9	0.9	0.9	0.9	0.9	0.9
5	0.8	0.9	0.2	0.7	1.2	0.5	0.8	0.6	0.9	0.9	1.1	0.9	1.0	1.0	0.9	1.0
6	0.8	1.1	0.6	0.9	1.2	0.7	0.7	0.7	0.9	0.9	1.0	0.9	1.0	1.2	0.5	0.9
7	0.9	1.3	1.7	1.5	1.0	1.1	0.6	0.8	1.0	0.9	0.7	0.8	1.0	0.9	1.2	1.0
8	0.7	1.1	0.8	1.0	1.2	0.6	0.8	0.7	1.4	0.6	0.9	0.7	1.0	0.9	0.9	0.9
9	0.8	1.2	1.9	1.5	1.2	0.6	1.6	1.1	1.2	0.7	1.0	0.8	1.0	1.1	1.0	1.1
10	0.9	1.0	1.1	1.1	1.1	0.3	1.2	0.8	1.1	1.0	0.7	0.8	0.9	1.2	1.2	1.2
11	0.8	1.2	1.4	1.3	1.1	0.6	1.5	1.1	0.9	1.0	0.9	1.0	1.1	0.7	1.4	0.9
12	0.8	1.3	1.2	1.2	0.8	1.1	1.8	1.4	0.8	1.2	1.0	1.1	1.0	0.7	1.6	1.0
13	0.9	1.3	1.9	1.5	0.7	1.2	1.5	1.4	0.8	1.0	1.5	1.2	1.1	0.8	1.2	0.9
14	0.9	1.0	1.6	1.2	0.9	1.3	1.8	1.6	0.8	1.0	1.3	1.1	1.1	1.4	1.1	1.3
15	1.1	1.4	1.7	1.5	1.0	1.4	1.2	1.3	0.9	1.0	1.4	1.2	0.9	1.4	0.8	1.2
16	1.2	1.3	1.0	1.1	0.9	1.4	1.4	1.4	1.0	1.0	1.4	1.2	1.0	0.9	0.7	0.9
17	1.1	1.1	1.4	1.2	0.9	1.4	1.3	1.4	1.0	1.2	1.1	1.2	1.0	1.2	0.6	1.0
18	1.2	0.9	0.8	0.9	0.9	1.9	1.4	1.6	1.0	1.2	1.2	1.2	0.8	1.3	0.9	1.2
19	1.1	1.1	0.8	1.0	0.9	1.7	0.9	1.3	1.0	1.4	1.0	1.2	1.1	1.2	0.5	1.0
20	1.1	0.9	1.1	1.0	0.8	1.3	0.7	1.0	1.0	1.2	1.1	1.1	1.0	0.9	1.0	0.9
21	1.0	0.9	0.7	0.8	0.9	1.3	0.8	1.0	0.9	1.0	1.2	1.1	1.0	0.9	0.8	0.9
22	1.0	0.8	1.4	1.0	1.1	0.8	0.8	0.8	0.9	1.0	0.9	1.0	1.0	0.9	0.9	0.9
23	1.2	0.6	1.4	0.9	1.1	0.7	0.7	0.7	1.0	1.1	0.7	0.9	1.0	0.7	1.0	0.8

Table 4-1 Continued. Diurnal variation of particle mass concentrations observed with BAMS at Sandy Way BAMs in South Lake Tahoe. Column labeled SLSW is the average of TSP observed at Sandy and SOLA.

	Sandy Way																			
	Fall					Summer					Spring					Winter				
Hour	2.5	crs	lrg	crs+lrg	SLSW	2.5	crs	lrg	crs+lrg	SLSW	2.5	crs	lrg	crs+lrg	SLSW	2.5	crs	lrg	crs+lrg	SLSW
0	1.3	0.6	0.3	0.5	0.7	0.9	0.7	0.4	0.6	1.0	1.3	0.4	0.3	0.4	1.1	1.3	0.5	0.4	0.5	0.8
1	0.9	0.5	0.3	0.4	0.7	0.8	0.7	0.2	0.5	0.8	1.1	0.5	0.3	0.4	0.9	1.1	0.3	0.5	0.4	1.0
2	0.6	0.5	0.2	0.4	0.6	0.8	0.5	0.3	0.4	0.7	0.8	0.5	0.2	0.3	0.8	0.7	0.2	0.3	0.3	0.8
3	0.5	0.4	0.2	0.3	0.5	0.8	0.5	0.4	0.4	0.6	0.8	0.4	0.3	0.3	0.5	0.6	0.2	0.3	0.2	0.6
4	0.4	0.5	0.4	0.4	0.5	0.7	0.6	0.3	0.5	0.7	0.8	0.4	0.4	0.4	0.7	0.5	0.2	0.3	0.2	0.5
5	0.5	0.4	0.4	0.4	0.5	0.7	0.7	0.6	0.7	0.8	0.7	0.5	0.5	0.5	0.8	0.4	0.3	0.3	0.3	0.5
6	0.6	0.8	0.6	0.7	0.9	0.7	0.8	1.1	1.0	1.2	0.7	0.6	0.7	0.7	1.1	0.5	0.5	0.2	0.4	0.6
7	0.6	1.3	1.5	1.4	1.4	0.8	0.9	1.2	1.1	1.0	0.8	0.9	1.3	1.1	1.2	0.6	0.8	0.6	0.7	0.9
8	1.0	1.2	1.6	1.4	1.4	0.9	1.1	1.0	1.1	0.9	0.8	1.1	1.4	1.3	1.1	0.8	1.3	1.4	1.3	1.5
9	0.6	1.1	0.7	0.9	0.9	1.0	1.0	1.1	1.1	0.9	0.7	1.5	1.5	1.5	1.0	0.7	1.1	1.8	1.4	1.7
10	0.6	1.2	1.1	1.1	0.9	1.2	1.1	1.1	1.1	0.9	0.7	1.6	1.2	1.4	1.0	0.5	1.6	1.5	1.6	0.8
11	0.5	1.1	1.1	1.1	0.8	1.2	1.1	1.3	1.2	1.0	0.7	1.5	1.7	1.6	1.0	0.4	1.7	1.3	1.6	0.7
12	0.5	1.1	1.3	1.2	0.8	1.1	1.1	1.3	1.2	0.9	0.8	1.7	1.6	1.6	1.0	0.4	1.8	1.3	1.6	0.7
13	0.5	1.2	1.2	1.2	0.9	1.1	1.1	1.3	1.2	0.9	0.7	1.5	1.4	1.4	1.0	0.5	1.6	1.6	1.6	0.7
14	0.5	1.2	1.4	1.3	0.9	0.9	1.1	1.5	1.3	1.1	0.6	1.6	1.4	1.5	1.0	0.4	1.7	1.6	1.6	0.7
15	0.6	1.2	1.5	1.3	1.0	0.8	1.2	1.4	1.3	1.1	0.8	1.4	1.3	1.4	1.0	0.4	1.7	2.3	1.9	0.8
16	0.7	1.3	1.8	1.5	1.2	0.7	1.2	1.2	1.2	1.1	0.8	1.3	1.3	1.3	1.0	0.6	1.5	2.0	1.7	1.2
17	1.3	1.8	2.2	2.0	1.8	0.8	1.3	1.0	1.2	1.0	0.8	1.3	1.5	1.4	1.0	1.2	1.6	1.8	1.6	1.9
18	1.9	1.8	2.0	1.9	1.8	1.0	1.4	1.3	1.4	1.2	1.1	1.2	1.4	1.3	1.2	1.9	1.4	0.9	1.3	1.8
19	2.4	1.4	1.3	1.4	1.5	1.3	1.6	1.6	1.6	1.6	1.7	1.1	1.5	1.3	1.5	2.1	1.3	1.0	1.2	1.5
20	2.2	1.1	1.1	1.1	1.3	1.6	1.4	1.4	1.4	1.5	1.8	1.0	1.0	1.0	1.3	2.4	1.0	0.6	0.8	1.4
21	2.2	0.9	0.7	0.8	1.1	1.7	1.2	1.1	1.1	1.2	1.9	0.8	0.8	0.8	1.1	2.3	0.8	0.6	0.8	1.2
22	1.5	0.8	0.5	0.7	0.9	1.3	0.9	1.0	1.0	1.0	1.6	0.7	0.6	0.7	0.9	1.9	0.6	0.6	0.6	1.0
23	1.5	0.7	0.4	0.6	0.8	1.2	0.8	0.5	0.7	0.8	1.5	0.6	0.4	0.5	0.8	1.6	0.4	0.6	0.5	0.8

Figure 4-4. Lake Forest, Winter and Spring, Diurnal Variation in Particle Mass Concentrations by Particle Size
(**Note:** Vertical axis is the ratio of hourly average to seasonal average.)

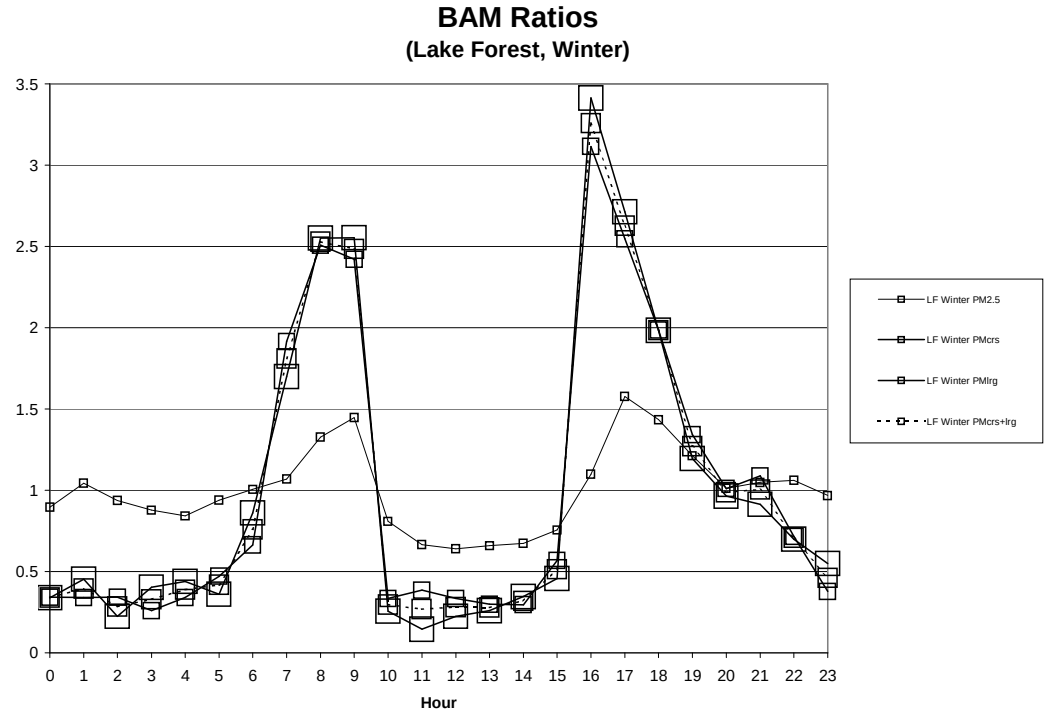

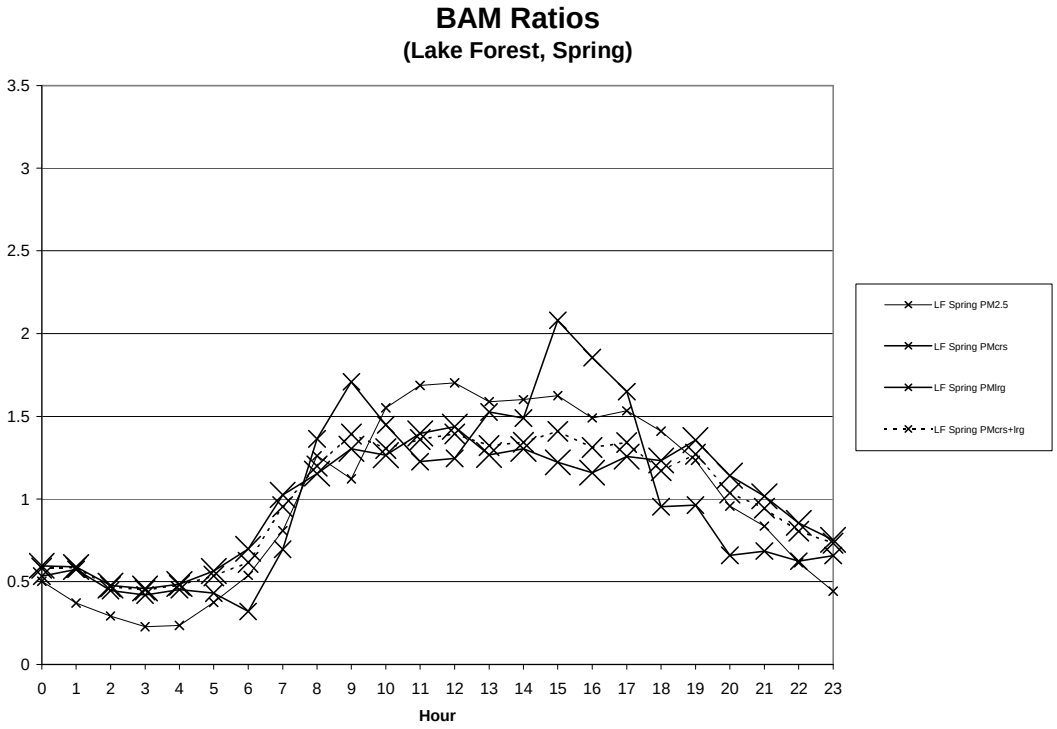

Figure 4-5. Lake Forest, Summer and Fall, Diurnal Variation in Particle Mass Concentrations by Particle Size.

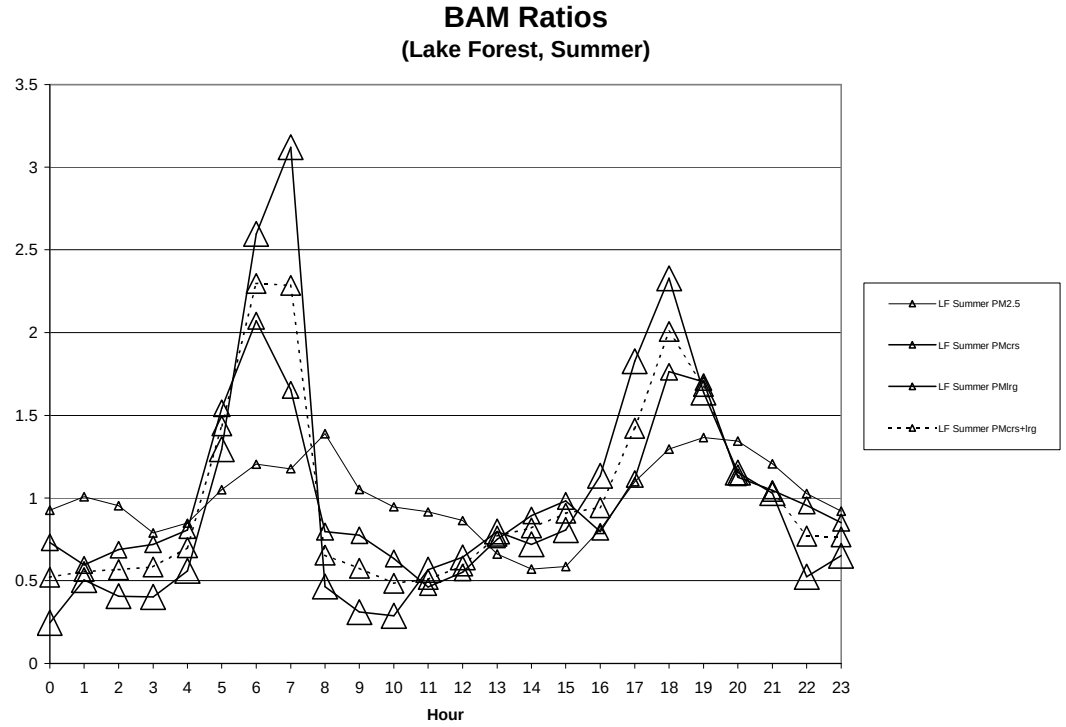

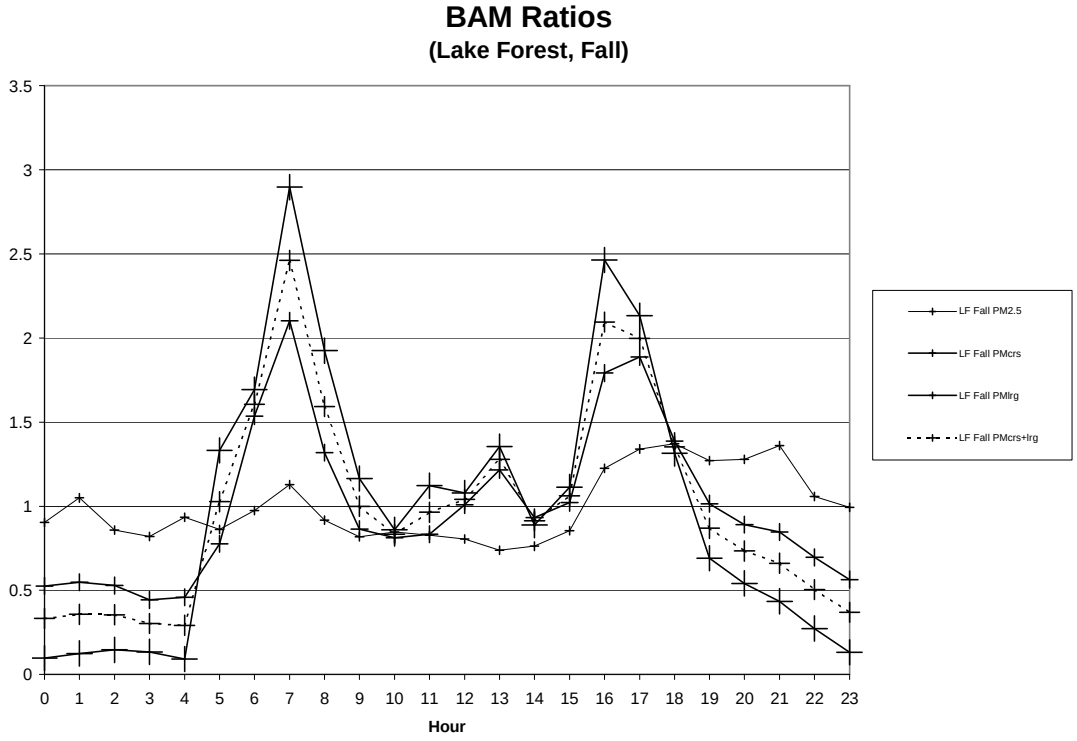

Figure 4-6. South Lake Tahoe, Winter and Spring, Diurnal Variation in Particle Mass Concentrations by Particle Size as in Table 4-1
(**Note:** SW indicates Sandy Way observations. SLSW is the average of SOLA and Sandy Way TSP)

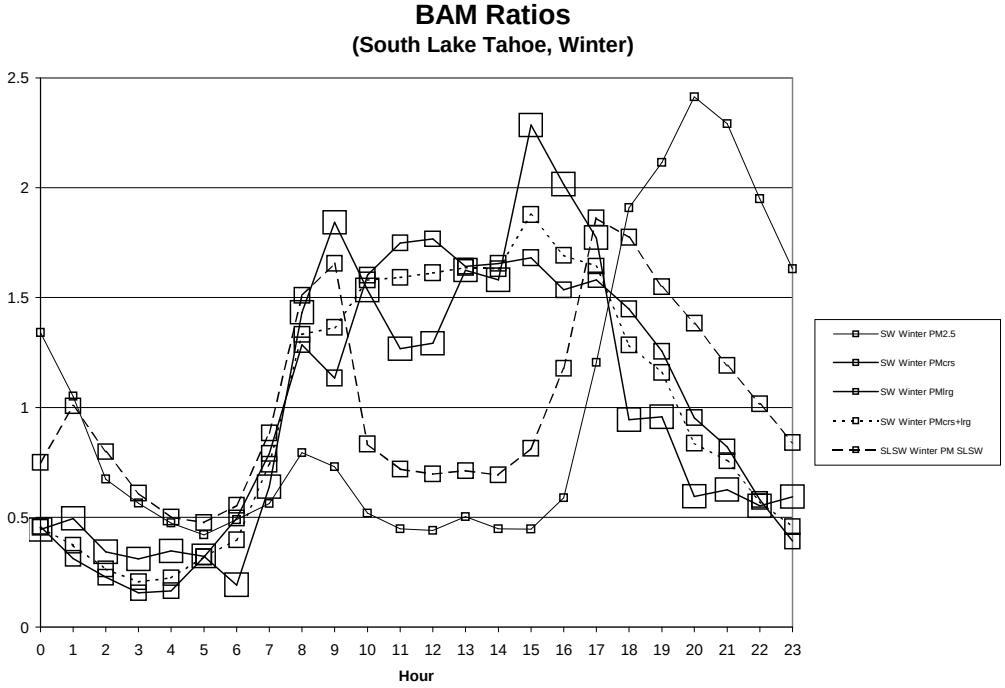

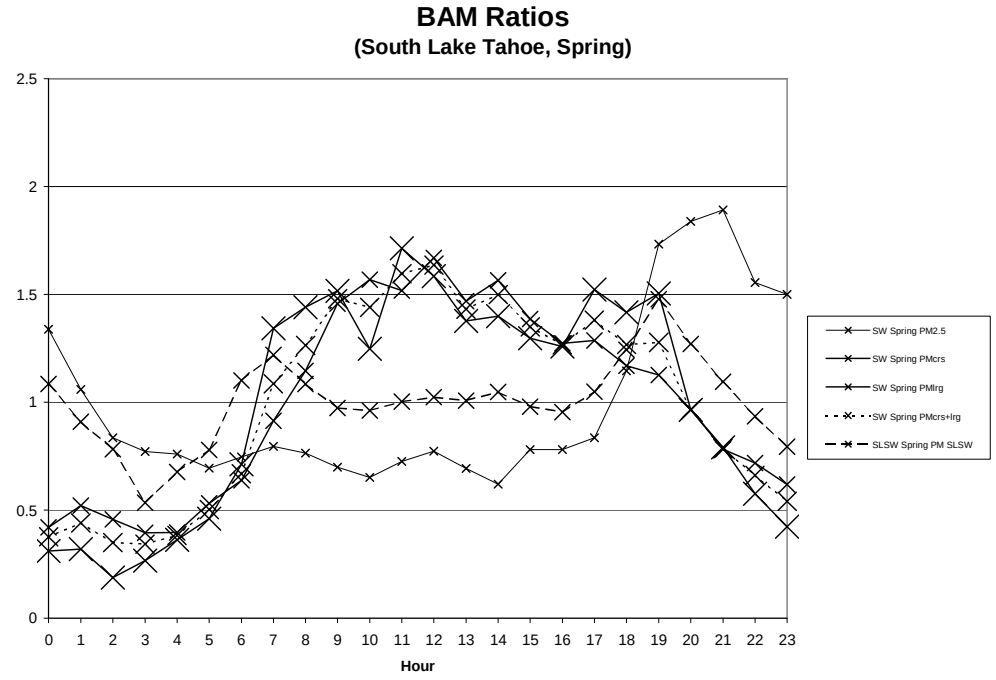

Figure 4-7. South Lake Tahoe, Summer and Fall, Diurnal Variation in Particle Mass Concentrations by Particle Size as in Table 4-1 (continued)
(**Note:** SW indicates Sandy Way observations. SLSW is the average of SOLA and Sandy Way TSP.

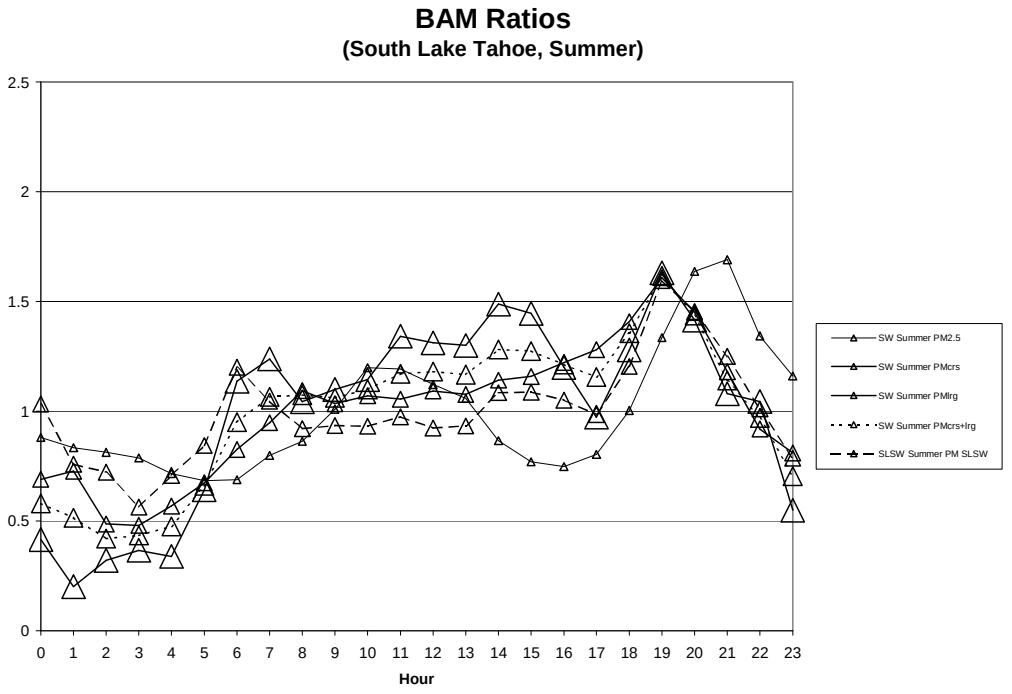

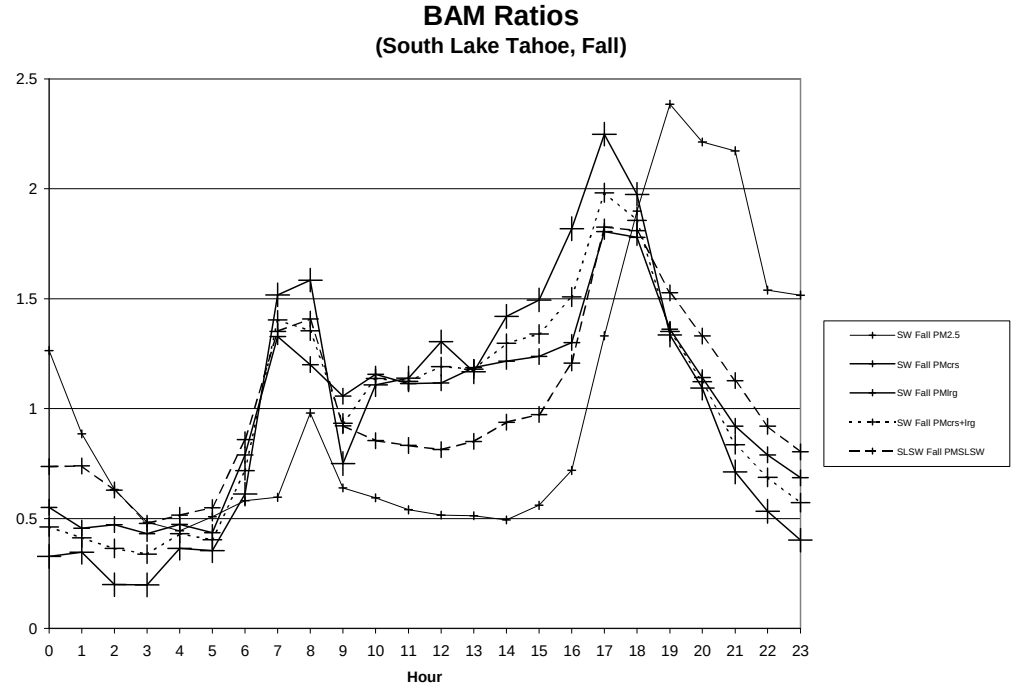

Figure 4-8. Estimated Diurnal Variation of Nitric Acid Concentration at Sandy Way by Season.
(**Note:** In the absence of observations of the diurnal variation of ammonia gas concentrations, seasonal average ammonia gas concentrations for each quadrant were assumed to be constant across the hours of the day.)

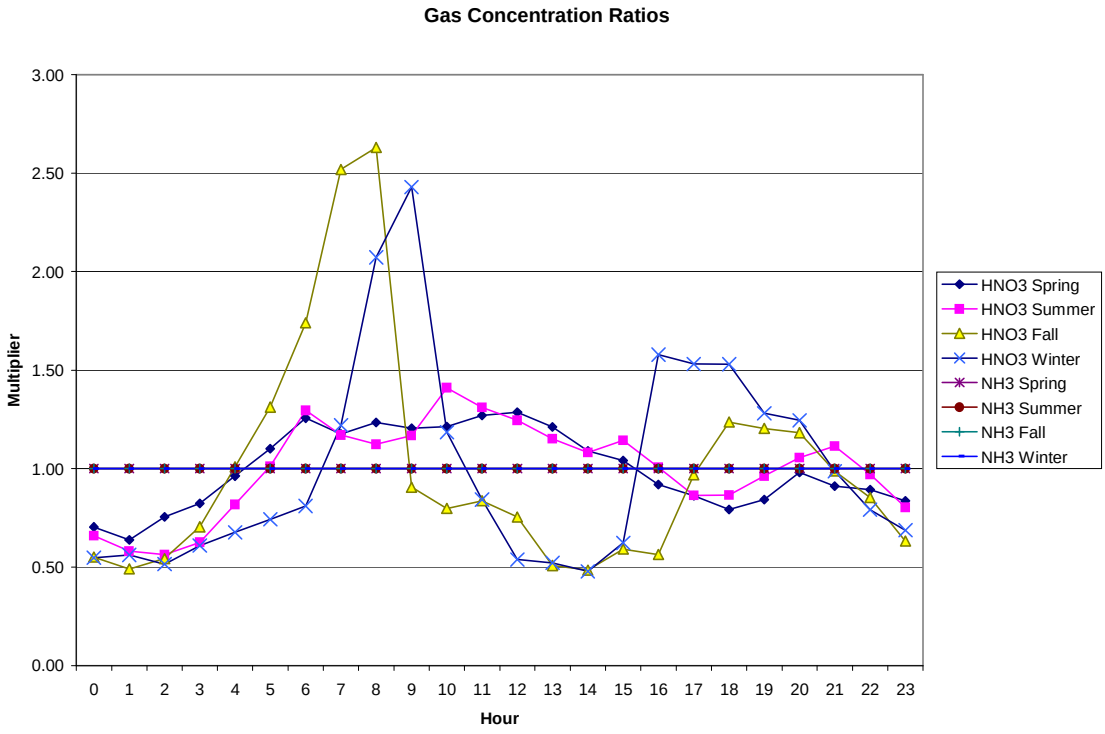

4.2 Meteorology and Context for Deposition Calculations

Because population, roads, and other activities that generate emissions in the Tahoe Basin are generally located near the shore of the Lake, the daily patterns of airflow are critically important to the impacts that pollutant concentrations have on the Lake. In addition, the deposition velocity over the near-shore waters depends on the wind direction because the roughness elements over land are much larger than over water and those roughness elements affect the amount of atmospheric turbulence for some distance over the Lake during periods of offshore wind direction. For these and other reasons the meteorological observations presented in Chapter 2 are of practical importance to calculation of rates of dry deposition.

The observed winds, which are understood as the sum of the interactions of synoptic scale, mountain-valley, and lake-land winds, were presented in detail in Chapter 2 and Appendix A. For insight specifically into the dynamics of lake-land breezes and their patterns the reader is referred to a detailed analysis by Sun, et al. (1997) of winds and meteorological fluxes over Candle Lake during the Boreal Ecosystem Atmosphere Study (BOREAS). Candle Lake is not entirely analogous to Lake Tahoe because it lacks the steepness of adjacent terrain. However, the analysis provides insight into the dynamics at Tahoe and is based on very extensive and specialized observations,

including direct measurements of meteorological fluxes at various altitudes over Candle Lake. For the reasons provided by Sun et al., lake-land breezes can affect circulations through relatively deep layers.

The importance of drainage flows to rates of dry deposition to the Lake is largely due to the proximity of steep terrain and concentration of population near the shoreline. The mountain-valley drainage flow that frequently occurs during late night and early morning hours increases in depth with distance downslope, but, even at the base of the slopes, is expected to be relatively shallow compared to the land-lake breeze. Never the less, the drainage flow is very important to the movement of pollutants toward the Lake because the local emissions are generally emitted and mixed into only a shallow layer. The thermal differences that drive shallow drainage flows also impose a thermal stratification that limits the vertical mixing. Thus, concentrations associated with emissions near the surface around the shoreline of Lake Tahoe are expected to be regularly transported onto the Lake in those drainage flows.

4.2.1 Winds

Wind speed is generally the most important meteorological determinant of deposition velocity over open waters at Lake Tahoe. Wind speed is also important in characterizing the roughness of the Lake surface and quantifying the turbulent kinetic energy (TKE) of the atmosphere and (vertical) fluxes of momentum, heat, and chemical species of interest. The Lake surface can be predicted to be either aerodynamically smooth or aerodynamically rough based upon the observed wind speeds. Giorgi (1986) indicated that open waters are aerodynamically smooth for wind speeds of less than 3 m/s, fully aerodynamically rough for wind speeds greater than 7 m/s, and in transition from fully smooth to fully rough for intermediate wind speeds.

The direction of the wind has a large effect on deposition velocity near the shoreline because of the sharp difference in the size of roughness elements on land (trees and buildings) versus on the water (ripples or waves). Wind direction also determines source-receptor relationships (e.g., during which hours the Lake is affected by advection of emissions from nearby traffic). Because the winds affect both ambient concentrations and deposition velocity, the covariance of the two cannot be ignored in the calculation of the deposition rates.

As an illustration of the importance of the mesoscale wind patterns, the diurnal variation in wind direction during the summer of 2003 is plotted for a north-shore and a south-shore surface location in **Figure 4-9**. The winds at any given time of day tend to be in opposing directions at the two locations. The direction (from which the wind comes) is shown in degrees. Either 0 or 360 degrees indicates wind from the north, 90 degrees indicates wind from the east, 180 degrees indicates wind from the south, and 270 degrees indicates wind from the west. Comparing the two plots, winds are down-slope during the night (from the NNW at the north-shore and SSE at the south-shore), shift to up-slope after sunrise (SE through SW at north-shore and NW at the south-shore), and transition back to down-slope flow after sunset. The up-slope/down-slope airflow is quite evident at all monitoring sites around the Lake during all seasons of the year,

although migrating storm/low pressure systems during the winter and spring disrupt the pattern.

Figures 4-10 and 4-11 show the distribution of wind directions and wind speeds by time of day at the South Lake Tahoe Airport and Tahoe City in midsummer (July and August). Note that an offshore wind direction at South Lake Tahoe is from the SSW (190–200 degrees) and at Tahoe City is from the west (about 270 degrees). The wind speed bins (in m/s) are 0.5-1.5 (black), 1.5-3 (yellow), 3-5 (red), 5-7 (blue), 7-10 (green), and >10 (light blue). Note that winds above 7 m/s are so infrequent as to not be detectable on this graph of the observations. For reference, 5 m/s is about 10 knots or 11 miles per hour.

Offshore or drainage winds dominate during the late night and early morning hours at both sites. Note also that (as expected with steeper terrain) the drainage flows at South Lake Tahoe Airport are of higher speed than at Tahoe City. However, the wind speeds at both sites are less than 5 m/s for nearly all hours. Even during the late morning and afternoon periods at South Lake Tahoe, when the wind speeds are highest, the wind speed exceeds 5 m/s for only about 25 percent of the time and does not exceed 7 m/s for any appreciable number of hours. The infrequency of winds greater than 5 m/s and rarity of winds above 7 m/s suggests that breaking waves and spray are not important during most hours of the year and will not appreciably affect estimates of annual average deposition rates.

Table 4-2 shows the frequency distributions of observed wind speeds by season at five sites around and on the Lake. The monitoring sites were located on piers and a buoy and, in the case of Cave Rock, at the edge of Lake Tahoe. Observations differed in height but were extrapolated to a common reference height of 10 m. The wind speeds were generally less than 3 m/s. We concluded from the observed wind speeds and the work of Georgi (1986) that the Lake surface was aerodynamically smooth for over two thirds of the hours, in transition from smooth to rough for about one fourth of the hours, and fully rough for less than 6 percent of the hours. At all sites, the frequency of winds greater than 7 m/s was greatest in the spring and least in the summer. Wind speeds greater than 7 m/s were observed the most frequently (12 percent of hours) at buoy TDR2 during spring.

Differences in frequency distributions of wind speed may be due to general location, local site characteristics, and differences in seasons of operation. Key differences in location include relative position around the lake, proximity to steep terrain, and local exposure to sunlight. Terrain near the Coast Guard pier is gentle compared to many other areas of the shoreline. Buoy TDR1 and the Coast Guard pier are both well exposed to winds from the south and southwest and they have very similar frequencies of wind speeds especially for speeds above 3 m/s. Wind speeds are lower at Sunnyside on the west shore where a daytime onshore Lake breeze direction is counter to regional flow. In contrast, on the north and especially the east shores, the direction of daytime upslope or lake-breeze air flow will tend to reinforce regional air flows.

Differences between sites in the frequency distribution of wind speeds may also be caused by the blocking effects of terrain.

Low wind speeds at Cave Rock might be due in part to a blocking effect of steep terrain immediately to the east which could decrease the horizontal wind speed in the immediate area during flow from the west or east. Cave Rock differed from the pier and buoy meteorological sites in that it was land-based and also operated as an air quality site, not a purely meteorological site. In comparing the observed wind speed frequencies, note also that the rates of data recovery and seasons of operations differ. Three sites, the U.S. Coast Guard pier, Sunnyside pier, and the TDR1 buoy operated in all four seasons and had considerably more hours of observations than the other sites. These sites with more complete seasonal representation were used for calculation of deposition velocities and rates.

Table 4-3 shows the frequencies of onshore, sideshore, and offshore wind directions observed at Timber Cove pier in South Lake Tahoe and at the U.S. Coast Guard pier located in the Lake Forest area on the north shore of Lake Tahoe.

The regional flow from the south or southwest is generally most consistent in the spring, moderate in the summer, and light in the fall. The wind direction during winter varies with the passage of low pressure storm systems, being generally from the southwest before, south during, and northwest after storms. Local flows are important during all seasons and vary in direction and speed with hour of day, with the land-lake temperature difference, and radiative heating and cooling of the surrounding slopes. As the number of hours of darkness increase from summer to winter, the frequency of downslope and offshore flow tends to increase at all sites, but especially below steeper terrain. During winter months, the greater frequency of offshore winds at USCG and onshore winds at Timber Cove is partly due to regional winds from the north and northwest after passage of storms.

Table 4-2. Frequency distribution of observed wind speeds by site and season. Wind speeds are extrapolated from instrument height to a common reference height of 10 meters. N is the number of hours of observations during each season.

Wind Speed Frequency

Wind (m/s)	U.S. Coast Guard Pier				
	Annual	Spring	Summer	Fall	Winter
0 - 0.5	0.03	0.02	0.02	0.02	0.06
0.5 - 1.5	0.19	0.18	0.20	0.17	0.20
1.5 - 3	0.48	0.42	0.51	0.50	0.50
3 - 5	0.16	0.18	0.15	0.18	0.14
5 - 7	0.09	0.14	0.09	0.08	0.07
7 - 10	0.04	0.05	0.03	0.05	0.03
10 - 12	0.00	0.01	0.00	0.01	0.00
12 - 999	0.00	0.00	0.00	0.00	0.00
N =	8356	2206	1882	2126	2142

Wind (m/s)	TDR1 Buoy				
	Annual	Spring	Summer	Fall	December
0 - 0.5	0.03	0.02	0.02	0.02	0.11
0.5 - 1.5	0.20	0.18	0.17	0.17	0.33
1.5 - 3	0.51	0.42	0.44	0.50	0.81
3 - 5	0.17	0.18	0.12	0.18	0.23
5 - 7	0.10	0.14	0.08	0.08	0.11
7 - 10	0.04	0.05	0.03	0.05	0.04
10 - 12	0.00	0.01	0.00	0.01	0.00
12 - 999	0.00	0.00	0.00	0.00	0.00
N =	8354	2205	1882	2125	2142

Wind (m/s)	Timber Cove Pier				
	3-Season	Spring	Summer	Fall	Winter
0 - 0.5	0.03	N/A	0.02	0.03	0.08
0.5 - 1.5	0.13		0.14	0.11	0.15
1.5 - 3	0.46		0.50	0.46	0.35
3 - 5	0.21		0.19	0.22	0.24
5 - 7	0.11		0.11	0.10	0.13
7 - 10	0.06		0.05	0.07	0.05
10 - 12	0.00		0.00	0.00	0.00
12 - 999	0.00		0.00	0.00	0.00
N =	4389	0	1708	1949	732

Wind (m/s)	Cave Rock Air Quality Site				
	3-Season	Spring	Summer	Fall	December
0 - 0.5	0.18	N/A	0.20	0.17	0.15
0.5 - 1.5	0.31		0.31	0.32	0.28
1.5 - 3	0.25		0.28	0.26	0.15
3 - 5	0.20		0.19	0.19	0.24
5 - 7	0.05		0.02	0.05	0.14
7 - 10	0.01		0.00	0.01	0.04
10 - 12	0.00		0.00	0.00	0.00
12 - 999	0.00		0.00	0.00	0.00
N =	4787	0	1967	2085	735

Wind (m/s)	Sunnyside Pier				
	Annual	Spring	Summer	Fall	December
0 - 0.5	0.08	0.09	0.05	0.05	0.17
0.5 - 1.5	0.55	0.51	0.65	0.51	0.50
1.5 - 3	0.31	0.31	0.28	0.37	0.25
3 - 5	0.05	0.07	0.02	0.06	0.06
5 - 7	0.01	0.01	0.00	0.01	0.02
7 - 10	0.00	0.00	0.00	0.00	0.01
10 - 12	0.00	0.00	0.00	0.00	0.00
12 - 999	0.00	0.00	0.00	0.00	0.00
N =	7849	2207	2207	2134	1301

Table 4-3. Frequency distribution of onshore, sideshore, and offshore wind directions observed at Timber Cove pier in the City of South Lake Tahoe and the US Coast Guard pier in Lake Forest on the north shore.

Season	Spring		Summer		Fall		Dec Only	Dec Only	Jan-Feb
Site	Timber Cove	USCG	Timber Cove	USCG	Timber Cove	USCG	Timber Cove	USCG	USCG
Wind Direction									
Onshore	N/A	0.30	0.30	0.37	0.21	0.30	0.09	0.36	0.30
Sideshore	N/A	0.11	0.12	0.15	0.07	0.15	0.03	0.17	0.11
Offshore	N/A	0.60	0.58	0.48	0.72	0.56	0.88	0.46	0.60

Figure 4-9. Diurnal Profiles of Wind Directions during summer 2003 at North Shore and South Shore Locations on Lake Tahoe.

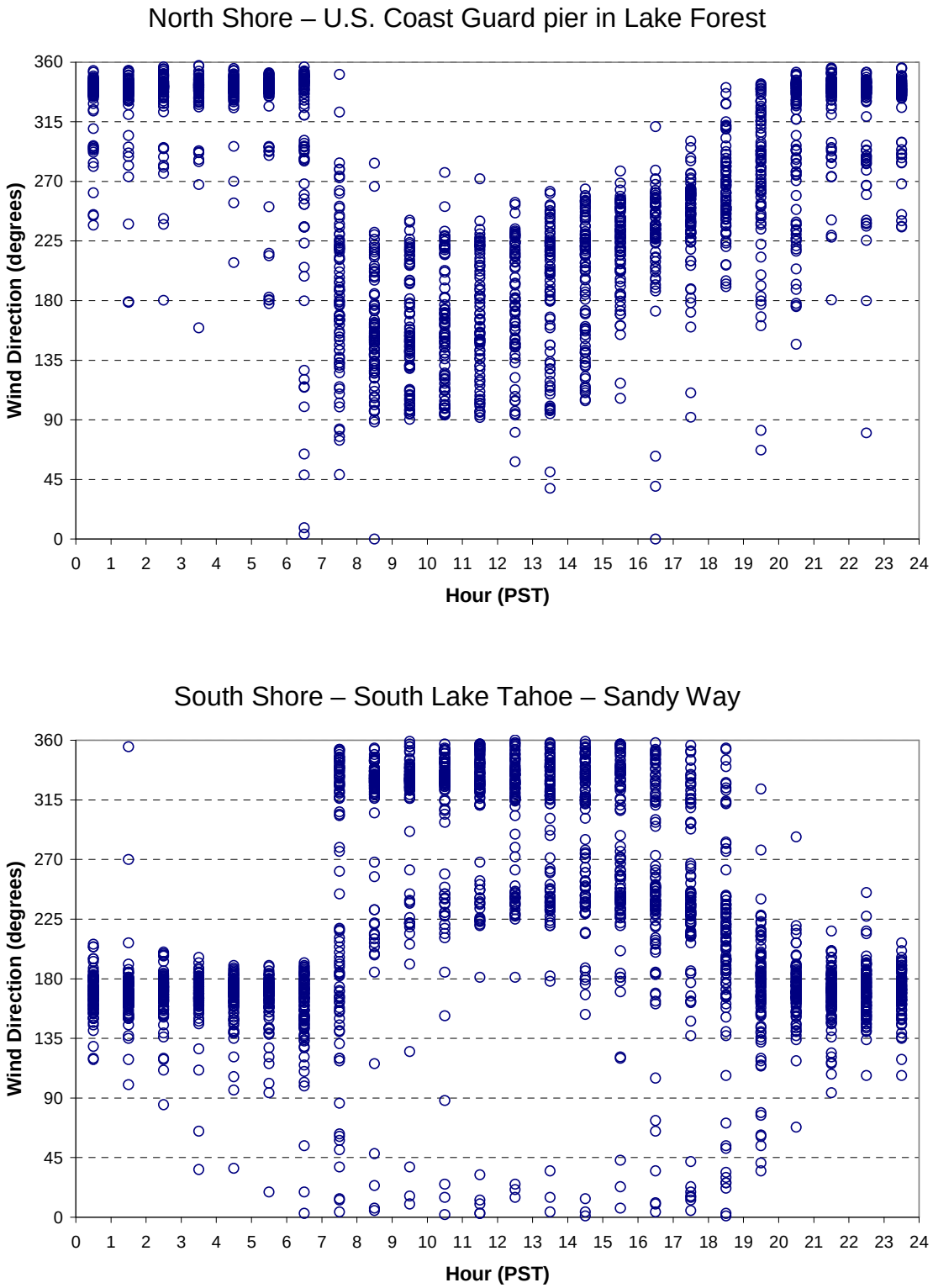

Figure 4-10. Distribution of Wind Speed and Wind Direction at South Lake Tahoe Airport during July and August by hour of day.

Hour labels indicate the beginning of the hour (i.e., 00-03 indicates 0000-0359). Colors indicate wind speed categories in m/s. Length of bars indicates the percent of hours of wind from a particular direction and within a speed category. The interval between rings is 10 percent.

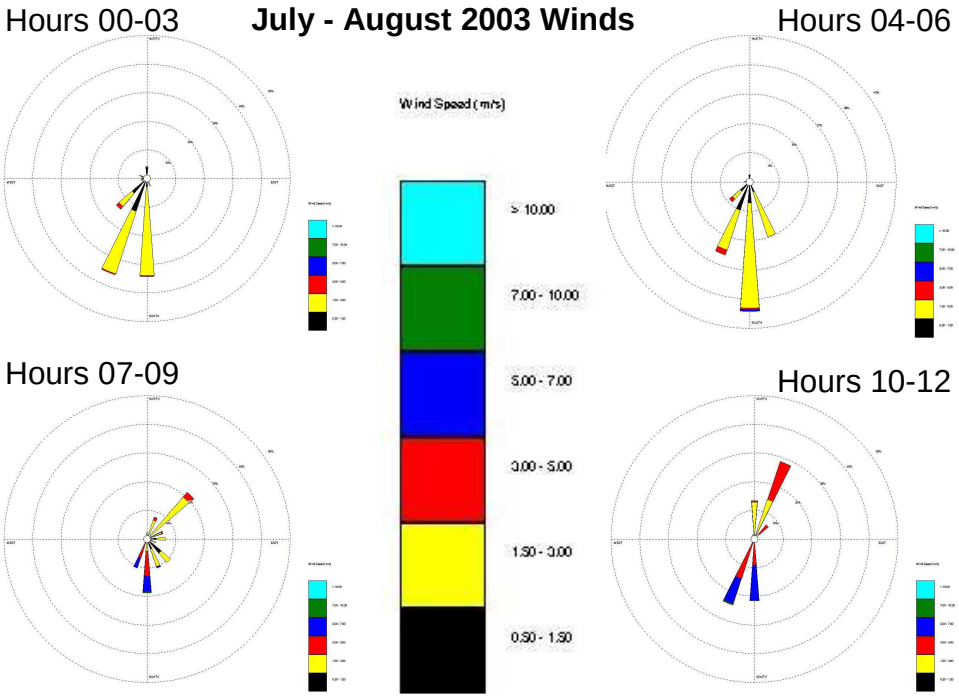

Figure 4-11. Distribution of Wind Speed and Wind Direction at Tahoe City during July and August by Hour of Day.

Hour labels indicate the beginning of the hour (i.e., 00-03 indicates 0000-0359). Colors indicate wind speed categories in m/s. Length of the bars indicates the percent of hours of wind from a particular direction and within a speed category. Except for hours 22-23 (not shown) the interval between rings is 10 percent.

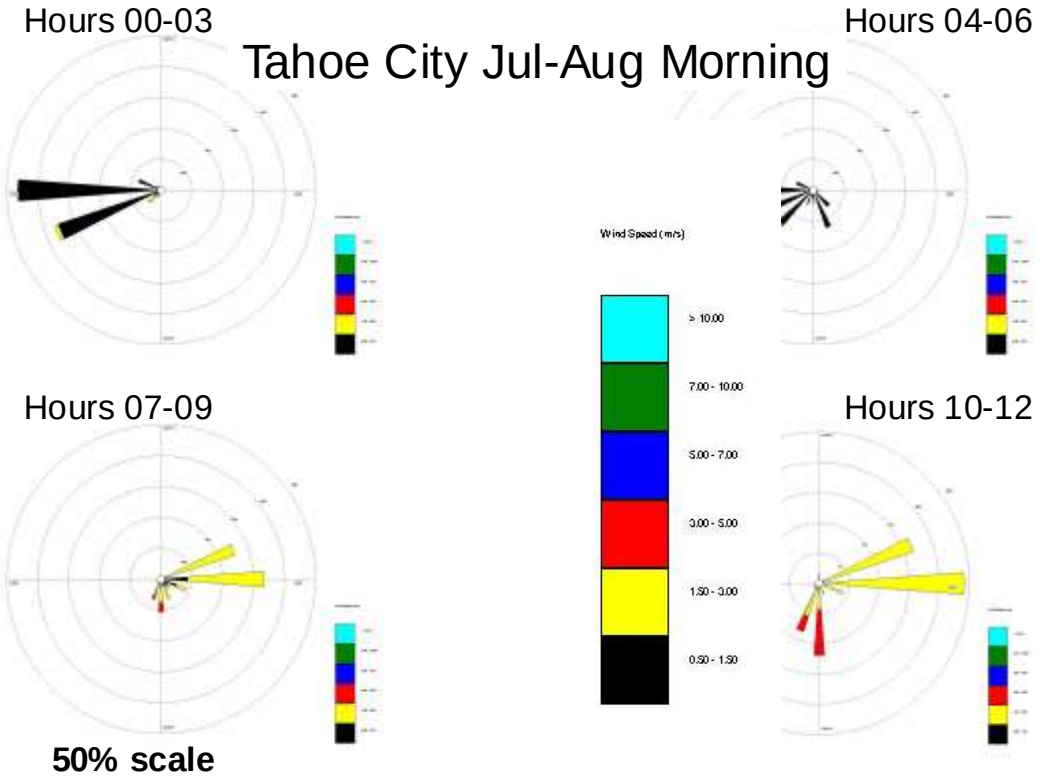

4.3 Deposition Velocity

Deposition velocities for gases and particles were modeled for each hour of 2003 for which meteorological data (wind direction, wind speed, air temperature, and water temperature) were available at a representative site. Ambient concentrations, which were paired with the calculated deposition velocities, were measured at the land-based monitoring sites, which were generally located near the shoreline. Sampling inlets for the TWS were 2.1 m above ground level, except at Sandy Way where the inlet was 2.1 m above the flat roof of the one-story building. The methods of calculating deposition velocity are explained in the following sections along with assumptions and caveats. The code used to calculate the deposition velocities and combine those deposition velocities with ambient concentrations to calculate deposition rates for each quadrant is provided in Appendix B.

4.3.1 Calculation of Deposition Velocities and Resistances of Gases

The dry deposition rate is modeled as the product of concentration and deposition velocity, integrated over a variety of gaseous species and spectrum of particle sizes, over time, and across the area of the Lake surface.

The "deposition velocity" (V_d) is the rate of deposition or flux (F), with units of mass/area/time) divided by the difference in concentrations in the well-mixed atmosphere (C) versus air at the surface where removal takes place (C_0).

$$V_d = F / (C - C_0) \quad (4.1)$$

In many cases C_0 equals or approaches zero so that the deposition rates, or flux (F), of a compound equals or can be approximated by:

$$F = V_d * C \quad (4.2)$$

Thus, the deposition velocity is the deposition rate normalized for concentration, providing a measure of the environmental propensity for atmospheric deposition independent of ambient concentration. Although it has units of velocity (distance/time, usually expressed in cm/sec), it does not describe a physical process or velocity.

Estimation of V_d requires consideration of the controlling processes that comprise it. V_d is commonly estimated using a model of resistances or conductances analogous to electrical circuitry. For gases, the total resistance to transfer (R_{total}) is the sum of three basic resistances acting in series (see **Figure 4-12**). These are the aerodynamic resistance (R_a), the "quasi-laminar" boundary layer (or viscous sub-layer) resistance (R_b), and the surface (or vegetation canopy) resistance (R_c).

R_a is the resistance to mixing through the boundary layer toward the surface by means of the dominant process, turbulent transport. A large value of R_a would indicate a relative lack of turbulence.

The quasi-laminar layer resistance, R_b, is resistance to movement across the thin layer (0.1 – 1 mm) of air that is in direct contact with a surface and not moving with the mean flow of the wind. Through this thin layer, in the absence of turbulence, the primary transport process for gases is molecular diffusion. For gases the quasi-laminar layer resistance is designated as R_b. For particles the important transport processes in this layer are Brownian motion and inertial impaction). To differentiate from gases, the quasi-laminar layer resistance for particles is designated as R_d. R_c, the resistance of a compound to uptake by a surface, varies both with the surface and the chemical species or physical state (gas or particle). For gases the deposition velocity can be expressed as:

$$V_d = 1/(R_a + R_b + R_c) \quad (4.3)$$

Highly reactive and highly soluble gases, such as nitric acid and ammonia are readily deposited to water surfaces and so their values of R_c (and C_o) over water are essentially zero. For gases in general we have also assumed that $R_a >> R_b$. Thus, for the gases of interest for nitrogen deposition to the waters of Lake Tahoe, **equation 4.3** is simplified as:

$$V_d = 1/R_a \quad (4.4)$$

Figure 4-12. Resistance Model for Dry Deposition of Gas.
(Source: http://www.atmosp.physics.utoronto.ca/people/ulrike/lecture-notes/Lecture3.ppt)

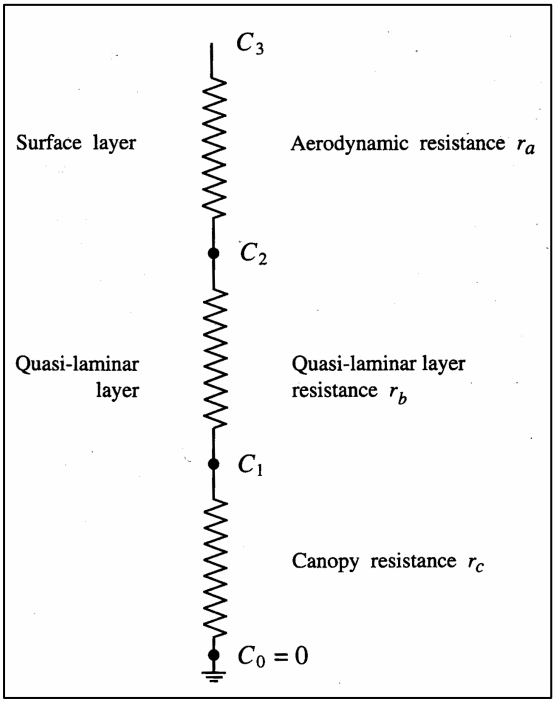

For deposition of particles, it is also necessary to consider a gravitational settling which is a parallel path for deposition that is not shown in **Figure 4-12**. Gravitational settling is generally important for larger particles, i.e., with particle diameter (Dp) >> 1 µm. When estimating deposition of particles, it is also necessary to calculate a quasi-laminar layer resistance, which, in the case of particle deposition, is designated as R_d. Before any further discussion of the quasi-laminar layer resistance for particles, R_d, and the gravitational settling of particles, the calculation of the aerodynamic resistance, R_a, which is the same for both gases and particles, will be detailed.

4.3.1.1 Primary Calculation of Aerodynamic Resistance

The aerodynamic resistance, R_a, is controlled by the level of atmospheric turbulence available to transport gases and particles in the air into close proximity to the surface. The subsections that follow describe methods for calculation, including for completeness, one that was not applied in these calculations. All require estimation of the Monin-Obhukov Length (L) scale, which is a stability parameter. Also discussed, in the final subsection, are caveats regarding estimation of R_a for the near shore zone during offshore flow. Common assumptions about the variation in wind speed with height through the surface layer may not hold at the measurement heights due to larger values of the aerodynamic roughness length (Z_0) over land.

A commonly used formulation for aerodynamic resistance assumes similarity between turbulent transport of chemical species and turbulent transport of momentum. That formulation is:

$$R_a = U / (U_*)^2, \quad (4.5)$$

where U is the wind speed and U_* (pronounced Ustar) is the friction velocity. The friction velocity is a measure of the shearing stress of the wind on the surface below. It is defined as the square root of the surface shear stress divided by the density of air. Methods used to estimate U_* are provided in the following sections. The wind speed is usually directly measured. Although friction velocity may be determined by direct measurement of momentum flux by the eddy covariance (EC) method, friction velocity is less exactly but commonly estimated from more routine meteorological measurements of wind speed and temperature at multiple heights.

LTADS calculated the friction velocity and aerodynamic resistance using the formulation of Byun and Dennis (1995) adapted for use over water. The relationship of wind speed (U_z) to height above the surface (z) is the logarithmic profile adjusted for stability of the atmosphere as described by the Monin Obhukov Length scale (L). Their formulation depends on whether the atmosphere is stable or unstable, as indicated by the sign of L.

For the stable atmosphere case, where $L > 0$ (based on $T_{air} > T_{water}$),

$$U_z = [(U_*)/(k)] * [\ln((z)/ Z_0) + 4.7 * (z - Z_0/L)], \quad (4.6)$$

where:

k = Von Karmen constant = 0.4

Z_0 = aerodynamic roughness length

U_* = friction velocity. The square of the friction velocity equals the wind-induced shear stress at the surface divided by density of air.

For the unstable atmosphere case, where $L < 0$ (based on $T_{air} < T_{water}$),

$$U_z = [(U_*)/(k)] * [\ln(\text{numerator}/\text{denominator})], \quad (4.7)$$

where:

$$\text{numerator} = [(1 + 16 * z / |L|) - 1]^{½} * [(1 + 16 * Z_0 / |L|) + 1]^{½}$$

$$\text{denominator} = [(1 + 16 * z / |L|) + 1]^{½} * [(1 + 16 * Z_0 / |L|) - 1]^{½}$$

Thus, with thermally neutral atmospheric conditions, the wind speed is logarithmic with height and the terms that involve the Monin-Obhukov Length scale (L) modify the wind profile in response to the influences of non-neutral thermal stratification.

A physical meaning for the Monin-Obhukov Length scale (L) is that it is proportional to the height in the surface layer at which the shear forces are first dominated by the buoyant forces. Shear forces generally produce turbulent kinetic energy (TKE) near the surface whereas buoyancy forces generally increase with height through the surface layer and commonly produce TKE due to convection or suppress TKE under stable conditions. Under convective conditions buoyant and shear production of TKE are approximately equal at a height of z = -0.5 L. The Monin-Obhukov length scale is defined in terms of the vertical fluxes of momentum and heat evaluated near the surface and is derived from a non-dimensional form of the turbulent kinetic energy equation. Appendix F and Stull (1988) among others discuss how L represents the relative importance of sources of TKE based on terms in the TKE equation.

LTADS did not directly measure fluxes of momentum and heat flux; thus, to determine hourly values of L, a simple parameterization provided by Hanna et al. (1985) and used in the CALMET meteorological model (Scire et al., 2000a) for calculation of momentum flux over water, was employed.

$$L = (T_a + 273.16)\,[((0.75 + (0.067)(U_{10}))/1000]^{3/2} / [(E2)(T_a - T_w)] \quad (4.8)$$

where:

T_a is the observed air temperature
U_{10} is the wind speed extrapolated to 10 meters
T_w is the observed water temperature
E2 = 0.0051

Because the observed water temperature may be sensitive to the wind speed during that hour and to the depth of the observation, the sensitivity of the deposition estimates to an arbitrary bias in water temperature was investigated. With an arbitrary bias of 3 ºC (5.4 ºF) added to the observed water temperature for all hours, estimated annual dry deposition increased by about 7 to 16 percent. The increases varied between the pairs of air quality and meteorological monitoring sites used and differences in the estimates were generally largest for gases and fine particles. The sign of any actual bias in observed water temperature due to the effects of wind speed or measurement depth would depend largely on the sign of the net radiation at the water surface. Thus, the effects would tend to average out over diurnal cycles and across seasons and the net effect of bias in observed water temperatures should have minimal effect on the annual deposition estimates.

The formulation of aerodynamic roughness length (Z_0) over water is from Hosker, (1974) and takes the following form.

$$Z_0 = (0.000002)(U_{10})^{5/2} \quad (4.9)$$

As discussed in Section 4.3.1.5, near the shoreline the value of Z_0 also depends strongly upon wind direction and this was taken into account in the iterative solution.

In the absence of resource intensive direct measurements of the friction velocity (U_*), the value of U_* can be calculated from the wind speeds and temperatures observed at two or more heights. By using an iterative method it is also possible, based on water temperature and meteorological observations at a single height, to calculate the values of friction velocity (U_*), aerodynamic roughness length (Z_0), and Monin-Obhukov Length scale (L). Multiple iterations are needed because of the interdependence of these variables.

LTADS used an iterative solution in which Z_0 and L were estimated using formulations that require input of an estimated wind speed at 10 meters (U_{10}). For initial estimates of Z_0 and L the wind speed at the instrument height was substituted for wind speed U_{10} in **equations 4.8 and 4.9**. Successive estimates of U_{10} were made with **equations 4.6 and 4.7** and Z_0 and L were recalculated upon each new estimate of U_{10}. Note that the equations 4.8 and 4.9 are specific to applications over water.

From **equations 4.5 and 4.6-4.7** the aerodynamic resistance, R_a, takes the following forms. For the stable atmosphere case, where $L > 0$ (based on $T_{air} > T_{water}$),

$$R_a = [1/(k * (U_*))] * [\ln(z/ Z_0) + 4.7 * (z/L)], \quad (4.10)$$

For the unstable atmosphere case, $L < 0$ (based on $T_{air} < T_{water}$),

$$R_a = [1/(k * (U_*))] * [\ln(\text{numerator/denominator})], \quad (4.11)$$

where:

$$\text{numerator} = [(1 + 16 * z / |L|) - 1]^{½} * [(1 + 16 * Z_0 / |L|) + 1]^{½}$$

$$\text{denominator} = [(1 + 16 * z / |L|) + 1]^{½} * [(1 + 16 * Z_0 / |L|) - 1]^{½}$$

4.3.1.2 Aerodynamic Resistance from Bulk Estimate of Momentum Flux

For comparison purposes, LTADS also estimated the aerodynamic resistance by applying a bulk coefficient method to calculate momentum flux and friction velocity and using the results in **equation 4.5**. The CALMET model (Scire, et al., 2000) uses the same bulk coefficient method for calculating momentum flux over water. The friction velocity, U_*, was calculated in m/s as by Garratt, et al. (1977):

$$U_* = U_{10} (C_{UN})^{½}, \quad (4.12)$$

where the bulk coefficient, C_{UN} is given by:

$$C_{UN} = (0.75 + 0.67 * U_{10}) / 1000, \quad (4.13)$$

R_a is then calculated from equation 4.5 in units of s/m or in units of s/cm as

$$R_a = [(U_{10}) / (U_*)^2] /100, \quad (4.14)$$

The simple formulations for the aerodynamic resistance and the friction velocity provided by **equations 4.12 – 4.14** do not address the effects of thermal stability or convection and, thus, the estimates they provide only reflect the effects of wind speed.

Estimates of $1/ R_a$, provided by the formulation of Byun and Dennis (described in the previous section), were compared the estimates provided by the bulk coefficient calculation. The comparison was restricted to estimates for the open water areas (more than 1 km offshore) because the bulk coefficient method in the form shown in equations 4.13 and 4.14 is only applicable to open water areas. The estimates from the formulation of Byun and Dennis averaged about one third higher with some variation due to differences in the wind speeds and stability between sites and seasons. Recall from **equation 4.4** that for the gases of interest, the deposition velocity is predicted as $1/ R_a$.

The values for $1/R_a$ provided by the bulk coefficient method were merely used as a gross check on the estimates provided by the formulation of Byun and Dennis. They were not otherwise utilized in the estimates of annual deposition which are presented later in this chapter. Those estimates of dry deposition are based on the formulation of Byun and Dennis.

In previously reported comparisons (ARB, January 2005), due to time constraints, the observed wind speeds were used directly in **equations 4.13 and 4.14** without having been extrapolated to 10 meters. Since then, staff compared the results of the bulk calculation of aerodynamic resistance (**equation 4.14**) using the wind speed at the measurement height and also at the reference height of 10 meters and found that the change in results was minimal.

4.3.1.3 Potential Alternative Calculation of Aerodynamic Resistance

Valigura (1995) modeled deposition of HNO_3, making the common assumption that $R_a >> R_b$. He assumed similarity between turbulent transport of heat and chemical species for calculation of R_a. Heat flux was modeled by iterative solution of a surface energy balance. To verify the model, Valigura compared measured and modeled values of skin temperature and heat flux. The results were reported to be inconclusive and differences, between measured and modeled values, were attributed to a possible mismatch in scales of observations obtained with aircraft-based and boat-based instruments.

For completeness and comparison with the current results, it may be possible to make calculations by an adaptation of Valigura's method. That would require information on the balance of net radiation based upon measurements or parameterizations suitable for the altitude of Lake Tahoe and availability of supporting meteorological data (e.g., cloud type and height). However, adequate data for verification of the modeling may not be available and this investigation could not be attempted within the timeframe available for releasing this final report. However, if this type of analysis were attempted in the future, observations of water skin temperature and incoming short- and long-wave radiation would be very useful for verification.

4.3.1.4 Potential for Independent Validation of Aerodynamic Resistance Estimates

Because the aerodynamic resistance is defined by fluxes of heat and momentum, there is a potential for independent validation of estimates of aerodynamic resistance by comparing modeled fluxes with observed fluxes. Although not collected as part of LTADS, some eddy covariance measurements of momentum flux, heat flux, sensible heat flux, and friction velocity are available from experiments at Lake Tahoe and elsewhere. Use of these data would require quality assurance analyses first, but they could be used for an independent estimate of the uncertainty in the values of aerodynamic resistance that are predicted using the methods discussed above.

4.3.1.5 Caveats Regarding Roughness Length and Aerodynamic Resistance

The formulations used here to estimate R_a assume a logarithmic wind profile (modified for the effects of stability). But the assumed form of the wind profile is not valid at heights of less than 50 times the aerodynamic roughness length (Brutsaert, W., 1982). The following paragraphs define the aerodynamic roughness length and describe its treatment in the calculations of aerodynamic resistance, particularly for situations with measurement heights or reference heights less than 50 times Z_0.

The aerodynamic roughness length scale, Z_0, represents the effects of surface roughness on the wind flow as that roughness affects the generation of shear induced turbulence. The aerodynamic roughness length is not equal to the height of individual roughness elements, but there is a one-to-one correspondence between these roughness elements and the aerodynamic roughness length. The amount of downwind turbulence generated by wind flow over a rough surface is a factor in determining the vertical profile of wind speed and the aerodynamic resistance, R_a. Z_0 is used to represent this effect in the equations of the vertical profile of wind speed, momentum flux, and aerodynamic resistance. Particularly for larger values of Z_0, the aerodynamic resistance and the deposition velocity are sensitive to Z_0. (The zero plane displacement height, defined as the height at which the horizontal wind speed goes to zero, has been ignored in these calculations, but does not significantly affect the calculations.)

Over open water, the shear force of the wind causes waves to develop and Z_0 is commonly estimated as a function of either friction velocity or wind speed. Various formulations are available dating from the classical formulation by Charnock (1955) to the formulation used here (Hosker, 1974) that was presented as equation 4.9. This calculation of Z_0 also applies near shore when the wind direction is onshore (from Lake toward land).

When the wind direction is offshore (from land to water), there is advection of greater turbulence associated with greater surface roughness elements over land as was observed by Sun (2001) in coastal environments. The effect is to decrease aerodynamic resistance and increase deposition velocity in the near-shore zone when the wind is offshore. This effect is implemented by making separate calculations for offshore wind direction and onshore wind direction. During offshore flow, to represent

conditions at the shoreline (and at the piers where the meteorological measurements were made) the aerodynamic resistance is calculated using an aerodynamic roughness length of 1 meter to characterize the effects of the land area immediately upwind. This value of Z_0, for offshore wind direction, in turn affects the calculation of the friction velocity and extrapolation of the wind speed to 10-meters above the surface. The result is to decrease R_a and increase deposition velocity. The advection of turbulence from over land is assumed to affect the aerodynamic resistance from the shoreline to a distance of 1 km offshore. The computations assume a linear decay of the near-shore R_a to the open-water R_a at a distance of 1 km offshore.

Over open water and in the near-shore zone with onshore flow, the Z_0 is sufficiently small, on the order of 0.0001 m, that the assumed form of the wind profile is reasonable at heights well below the heights of wind observations. However, with offshore winds, the larger surface roughness elements over land affect the flow over the near-shore waters increasing the aerodynamic roughness length to 1 or 2 meters, so that the assumption of a log wind profile is not satisfied near the surface. Even with a moderate assumption of Z_0 = 1 m in the vicinity of the pier mounted meteorological instruments, the assumed form of a basically logarithmic wind profile is thus not theoretically valid at the measurement heights which are less than 10 meters. This constraint is widely ignored in the literature, largely because little error is introduced for most uses of the logarithmic profile. But this turns out not to be the case for the calculation of the aerodynamic resistance.

The calculated values of R_a are inordinately sensitive to Z_0 when Z_0 is of the same order of magnitude as the observation height Z. For this situation the calculated values of R_a were unreasonably small and the resulting estimates of deposition velocity were unrealistically large. This was remedied by setting a lower limit of 1/6 s/cm for R_a for the “best” estimate of deposition rates which results in and upper limit of 6 cm/s for deposition velocity of gases. For the lower and upper limit estimates the limitations on $1/R_a$ were set at 3 and 10 cm/s respectively. Selection of these values were based on literature indicating the maximum observed deposition rates over water for a reactive soluble gas (SO_2) were in the range of 3 to 4.5 cm/s and a desire, consistent with the LTADS purpose, to ensure that for the upper-limit estimate the deposition velocities and deposition rates would be sufficiently inclusive. Sehmel (1980), citing Whelpdale and Shaw (1974) and others, reports observed deposition velocities for SO_2 to water surface ranging from 0.16 to 4 cm/s, with the range of values dependent on atmospheric stability. In the near-shore zone at Lake Tahoe offshore flow frequently consists of down-slope cold air drainage over a warmer water surface. Thus, near shore during nocturnal and early morning offshore flow periods in most seasons, thermal instability is the norm. Thus, buoyant forces are expected to generate turbulence in addition to any shear induced turbulence. However, with typically low wind speeds production of turbulence due to wind shear should be weak. Thus, the assumptions for aerodynamic resistance in the near-shore zone during offshore flow periods are expected to provide conservatively large deposition velocities. The lower limit of 1/6 s/cm for R_a and resulting upper limit deposition velocity of 6 cm/s for gases was invoked in the near-shore areas for most hours of offshore flow but was not invoked for mid-Lake areas or

near-shore areas during onshore flow. Thus, this limit is only applied in the near-shore region when larger values of Z_0 were used during hours of offshore flow. The near-shore region affected by the upper limit on deposition velocity was estimated to extend 1 km from shore and to comprise 20 percent of the surface area of the Lake.

4.3.1.6 Quasi-laminar Layer Resistances (R_b) for Gases and (R_d) for particles

Resistances R_b for gases and R_d for particles are their resistances to transport through the very thin (0.1 – 1 mm) viscous sub-layer at the surface. This layer is also referred to as the quasi-laminar layer (Hicks, 1982) or the laminar deposition layer (Scire et al., 2000a). Others have used the term viscous layer. The quasi-laminar resistance (R_b) for gases is differentiated from the quasi-laminar resistance for particles (R_d). Use of the term "quasi" can serve as a reminder that for rough surfaces a laminar layer may only be intermittently present and that the formulations for smooth surfaces and rough surfaces differ.

Transport through this thin layer is by molecular diffusion for gases and by Brownian motion and impaction for particles. For gases, R_b is generally considered to be very small compared to R_a. However for estimating the deposition velocity of particles, R_d must be explicitly calculated. Because the quasi-laminar layer resistance for particles (R_d) and the particle gravitational settling velocity (V_g) require some of the same variables, the formulas for their calculation are grouped in Section 4.3.2.

4.3.1.7 Surface Resistance (R_c)

The surface resistance of water is very small (effectively 0) for both particles and highly reactive or soluble gases such as nitric acid or ammonia. The relative contribution of nitrogen to the Lake by deposition of other non-soluble, non-reactive gaseous N species, such as NO_2, is very small because R_c is a large limiting resistance and the deposition velocity is very small. Although LTADS is not estimating deposition over land surfaces, it may be of interest that for moderately reactive chemical species, such as ozone or NO_2, the surface resistance, R_c, over land varies spatially with differences in land use and vegetation type and temporally with biophysical responses of vegetation to light, moisture, etc.

4.3.2 Deposition of Particles

The equations for deposition of particles are similar in form to the equation for deposition of gases but differ in several particulars. For estimating deposition velocities for particles, gravitational settling velocity, V_g, must be considered in addition to the resistances discussed above and shown in **Figure 4-12** for gases. Note that gravitational settling is an alternative and competing pathway. However, it is primarily important for deposition of larger (> 10 µm) particles. Although the quasi-laminar layer resistance for particles is analogous to that for gases, its formulation must differ to represent the different processes (Brownian motion and impaction) acting to transport particles (rather than gas molecules) across that layer. The primary mechanism is Brownian motion for fine particles, and impaction for larger particles (of D_p >>1 µm). The quasi-laminar layer resistance for particles, R_d, is greatest for particles in the size

range of D_p ~0.3-0.5 µm because the rates of Brownian diffusion and impaction for these particle sizes are both low. For this size range, R_d over water can be a primary constraint to deposition causing a minimum in V_d for accumulation mode particles. A representation of the effects of particle size on deposition velocity is shown in **Figure 4-13**.

4.3.2.1 Traditional Formulation of Particle Deposition Velocity

In **equations 4.1 - 4.4** and **Figure 4-12**, we presented the general model for deposition of gases. The equations for deposition of particles are similar in form but add the effects of settling velocity of large particles as a competing pathway taking the form of either the commonly used **equation 4.15** or the corrected **equation 4.18**. The formulation of particle deposition given in **equation 4.15** is common to many current air quality models (e.g., CALPUFF and ISCST3) was initially used by LTADS. Many authors, e.g., Slinn and Slinn (1980), Pleim et al. (1984), and Seinfeld and Pandis (1998) have presented this general form shown below.

$$V_d = V_g + [1/(R_a + R_d + R_a * R_d * V_g)] \quad (4.15)$$

The gravitational settling velocity, V_g, is not simply additive because it is a parallel path in competition with the path shown in **Figure 4-12**. The equations for the gravitational settling velocity, V_g, and quasi-laminar layer resistance, R_d, are given below along with additional variables used in their calculation. Note that the formulation for the aerodynamic resistance, R_a, is that of Byun and Dennis, which was presented previously and is applicable to either particles or gases.

Figure 4-13. Deposition Velocity is a Non-Linear Function of Particle Size.
Source: http://www.atmosp.physics.utoronto.ca/people/ulrike/lecture-notes/Lecture3.ppt

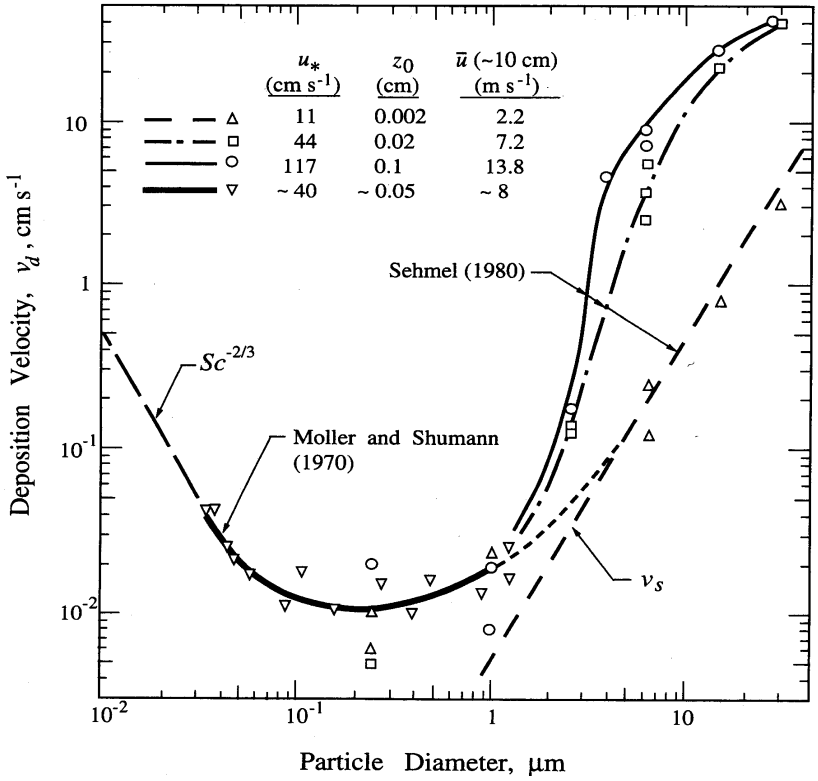

Resistance is the inverse of conductance and is a means to quantify limitations of a particular conductance mode. Movement of particles across the quasi-laminar layer is by Brownian motion and inertial impaction. Thus, the quasi-laminar layer resistance describes to what extent transfer of particles across the layer by Brownian motion and inertial impaction limits the rate of deposition. The quasi-laminar resistance for particles (R_d) is analogous to but differentiated from the quasi-laminar layer resistance for gases (R_b) which expresses the extent to which conductance of gas molecules across the quasi-laminar layer by molecular diffusion is a rate limiting step for deposition of gases.

$$R_d = (1/(U_*)) / (Sc)^{-2/3} + 10^{-3/St}, \quad (4.16)$$

where:

Sc = Schmidt number = Va / Db, where:

Va = viscosity of air = 0.15 cm^2/s

Db = Brownian diffusivity (cm/s) = 8.09 * (Ta + 273.16) * 10^{-10} * Scf/diam_pm, where:

Scf = Cunningham slip correction factor

= 1 + (2 * (x2) * (a1 + a2 * exp$^{(-a3 * diam_pm/x2)}$) / (diam_pm * 0.0001),

where:

x2 = 0.0000065

$a_1 = 1.257$
$a_2 = 0.4$
$a_3 = 0.000055$
diam_pm = measured, or assumed, diameter of particle

St = Stokes number = $(V_g/a_g) * (U_*)^2 / Va$, where:
a_g = acceleration due to gravity (981 cm/s^2)

The formulation presented here for quasi-laminar boundary layer resistance is strictly speaking only applicable to aerodynamically smooth surfaces, although this distinction is frequently ignored in the literature. However, the distinction between smooth and rough formulations is not critical to the LTADS estimates of deposition. The differences in resistance are significant only for fine particles which make up a minor fraction of the deposited particle mass. Also, for most hours over Lake Tahoe, the wind speeds are sufficiently low that the water surface is aerodynamically smooth. The frequency distribution of wind speeds presented in **Table 4-2** and discussed in Section 4.2.1 suggests that the lake surface is aerodynamically rough for only a few percent of the hours, in transition from smooth to rough for about one-fourth of the hours, and aerodynamically smooth for over two-thirds of the hours.

The gravitational settling velocity, Vg, was introduced previously. It is primarily dependent of particle size and density. In units of (cm/s) it is calculated as:

$$V_g = [(\rho_p - \rho_a) * a_g * [diam\_pm]^2 c_2] * Scf / (18* Va), \quad (4.17)$$

where:
ρ_p = density of particle; value input (~1-3 g/cm^3)
ρ_a = density of air (g/cm^3)
= 0.012 *[(Ta + 273.16)/273.16] * (Pa / 1000),
where:
Pa = atmospheric pressure (mb)
$c_2 = 0.00000001$ cm^2/mm^2

4.3.2.2 Corrected Formulation of Particle Deposition Velocity

Although **equation 4.15** is still very widely applied, Venkatram and Pleim (1999) showed that it violates the fundamental physical constraint of mass conservation and derived a corrected formulation that satisfies that constraint.

$$V_d = V_g/[1-e^{-Vg(Ra +Rd +Rc)}] \quad (4.18)$$

Substitution of **equation 4.18** for **equation 4.15** brings a small reduction in estimated deposition velocities. The reductions in annual deposition velocity vary mainly with particle size and also vary slightly with the seasonal and site specific meteorological conditions. Annual deposition velocities for fine (<2.5 µm) and large (>10 µm) particles were only reduced by about 1 to 6 percent. Predicted deposition velocities for coarse particles ($2.5 < d_p < 10$ µm) generally decreased by between 10 and 15 percent with

use of **equation 4.13**. The percent reduction in estimated deposition velocity as a function of particle size is shown in **Figure 4-14**.

In contrast to previous reports and memos, the deposition rates for particles reported here are based upon **equation 4.18**. By use of the corrected formula (equation 4.18 in place of 4.15) estimates of deposition velocity for coarse particles are reduced by about 10 to 15 percent, and estimates of the deposition of fine and large particles are reduced by less than 10 percent. This caused a modest reduction in estimates of deposition amounts of phosphorus and particles. However, there was little effect on the estimates of nitrogen deposition because the deposition of aerosol nitrogen (nitrate and ammonium) is dwarfed by deposition of gaseous ammonia and nitric acid.

Figure 4-14. Percent change in annual average deposition velocity by particle size for mid-Lake areas in response to substitution of **equation 4.18** (Venkatram and Pleim, 1999) for equation 4.15 (Pliem, et al., 1984; Seinfeld and Pandis, 1998).

Changes in calculated deposition velocity varied slightly due to differences in meteorological conditions at U.S. Coast Guard Pier, TDR1 buoy, and Tahoe Vista pier.

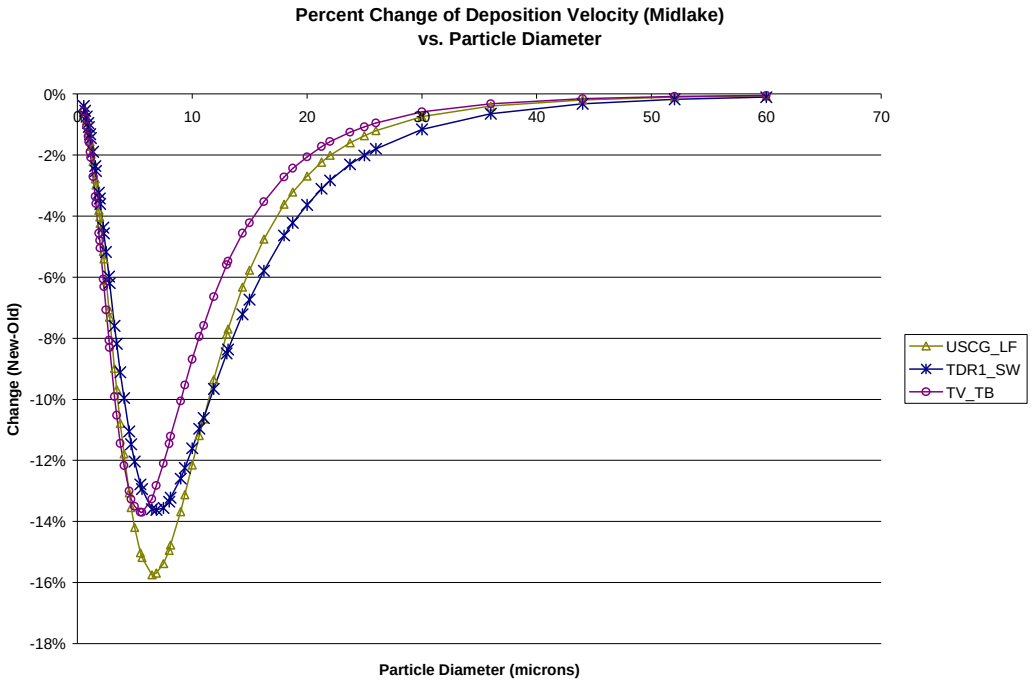

4.3.2.3 Effects of Hygroscopic Particle Growth

The potential effects of growth of particle size by uptake of water vapor are not quantified in the deposition rates presented here. The deposition of particles in general, and phosphorus-containing particles in particular, could be increased somewhat by hygroscopic growth but that effect is not expected to be large. First, the particles that

contain phosphorus are not necessarily hygroscopic. Second, the amount of growth before deposition occurs may be minimal. Early modeling of particle growth (Williams, 1982) assumed equilibrium between water vapor and aerosols. However, Zufall et al. (1998) concluded that particles larger than 0.1 µm do not reach equilibrium before depositing and showed that models assuming equilibrium can overestimate the effects of hygroscopic growth on deposition by as much as a factor of 5. Hygroscopic particle growth may affect deposition rates positively or negatively in amounts that depend on the environmental conditions and the chemical composition and initial size of the particles. Using alternative models that do not assume equilibrium, Pryor, et al. (2000) indicated hygroscopic growth may increase the deposition rate significantly for highly hygroscopic particles in the size range of Dp ~ 0.3-10 µm, but the particles observed in LTADS are primarily comprised of less hygroscopic constituents.. The size of NH_4NO_3 aerosol is likely Dp ~ 0.3-6 µm but NH_4NO_3 is only expected to contribute a very minor amount of the N load compared to gaseous HNO_3 and NH_3. For Dp < 0.3 µm and moderate wind speeds (U<10 m/s), particle growth is expected to decrease Brownian diffusion, thus increasing R_d and thereby decreasing V_d. For Dp > 10 µm the effect of hygroscopic growth is to increase impaction and V_g but the relative change in deposition velocity is less. At higher wind speeds, the viscous layer is thinner and inertial impaction acts more effectively so that particles deposit more quickly and the effects of particle growth are minimal.

4.3.2.4 Effects of Spray

The estimated annual deposition rates presented in this report are based upon hourly concentrations and deposition velocities calculated without explicit consideration of the effects of spray. The discussion which follows illustrates that the effects of spray on the annual deposition rates at Tahoe must be minor. The main points that are pertinent and developed below are: 1) dry deposition over water is enhanced for specific particle sizes when strong winds generate breaking waves and spray, 2) wind speeds sufficient to substantially affect deposition rates through the generation of breaking waves and spray occur less than six percent of hours on an annual basis at Lake Tahoe, 3) a substantial portion of modeled increases in deposition velocity were associated with hygroscopic growth, 4) the presence of spray did not appreciably increase the modeled deposition velocity of particles larger than 3 or 4 microns, and 5) during high winds atmospheric concentrations will generally be at a minimum, due to enhanced mixing and dilution.

Pryor and Barthelmie (2000) indicate that wind blown spray associated with breaking waves and bubble bursting have the potential to increase particle deposition by three processes. Firstly, ejection and deposition of droplets may induce turbulence in the laminar surface layer. Secondly, as they fall, droplets may sweep in-situ gases and particles towards the surface. Finally, as particles are transported through the near-surface layer they will encounter higher humidity levels when spray is present and if the particles are hygroscopic they will absorb water and grow in size (affecting their diffusivity). Pryor and Bartholemie explicitly modeled these three processes and their predicted effects on deposition velocities for hygroscopic particles (NO_4NO_3) of various sizes and with various wind speeds.

They reported that with wind speeds of 5 m/s bubble bursting and spray increased modeled deposition rates by up to ten percent for small (< 3 or 4 μm) particles but deposition rates of larger (> 4 μm) particles were not appreciably affected by spray. They report that these modeling results were consistent with results of wind tunnel studies of deposition over water (Larsen et al., 1995) which showed that increasing simulated area of white cap cover from 0 to 25 percent increased average deposition velocities by less than 30 percent. With higher (10 and 15 m/s) wind speeds, the deposition velocities modeled by Pryor and Barthelmie for small (< 4 μm) hygroscopic particles increased by factors of 1.5 and 2 respectively but did not appreciably increase deposition rates for larger (> 4 μm) particles. Although deposition velocities for particles smaller than 4 μm could be significantly increased (e.g., by a factor of two) during hours with such high winds this is only a very small fraction of the total hours and about one half or less of the total particle mass. Frequency distributions of wind speed and direction were reported in **Tables 4-2 and 4-3** as meteorological context for understanding patterns of deposition at Lake Tahoe. Note that wind speeds of 7-10 (and > 10 m/s) were only observed during 4 (and 2) percent of hours at the windiest site, buoy TDR2. Thus, the effect of spray on annual deposition rates is probably less than 2 percent even if there were no correlation between wind speed and concentrations. However, we know that higher wind speeds will generally result in significantly increased mixing and substantially lower concentrations compared to the annual average. Thus, although the effect of spray on deposition rates for small particles during specific hours can be significant, the effects of spray are expected to increase estimated annual deposition rates at Lake Tahoe by less than one percent. Thus, mechanistic modeling or explicit calculations of the effects of spray on deposition rates for individual hours would be an inappropriate use of resources within the goals and framework of LTADS.

4.4 Short- term Targeted Studies of PM Distribution

The discussion in section 4.3 explains how particle size influences deposition. Because the LTADS baseline monitoring was limited in spatial resolution and was limited to three gross size ranges (<2. 5 μm, 2.5-10 μm, >10 μm), additional information on size distributions and their spatial variations is desirable to confirm that deposition calculations based on the simplified LTADS size data would reasonably represent the deposition environment at Lake Tahoe. This section describes the salient findings of a series of experiments conducted during LTADS using optical particle counters to characterize the temporal and spatial variation of particle size distributions.

4.4.1 Overview of Particle Count Experiments

The overall goal was to understand how concentrations and particle size distributions might differ with location and time (compared to measurements at the LTADS sites) and to better understand how those gradients might affect the deposition estimates.

4.4.1.1 Program Goals

The particle count experiments addressed these areas of concern:

- Spatial variation among monitoring environments (*e.g.* urban vs. rural).
- Spatial variation between lakeshore and mid-lake areas
- Spatial variation near roadways and monitoring sites due to dilution and deposition of roadway emissions
- Temporal variation due to shifts in wind direction.

Due to limitations of time and funding, these experiments were largely exploratory, with only enough data collected in each experiment to permit evaluation of general structure and trends. The data presented here are strongest when viewed qualitatively, showing how particle concentrations and size distributions vary at Lake Tahoe. Although the sampling periods were chosen to represent conditions "typical" of the Tahoe basin, the actual particle concentrations measured in these experiments may not be representative of long term conditions.

The particle size count "bins" (0.5-1, 1 - 2.5, 2.5 – 5, 5 - 10, 10 - 25, and 25+ μm) span the ranges of interest for lake clarity, from the particles that scatter light in the lake (0.5 - 2.5 μm) to large soil particles which can deliver significant amounts of mineral nutrients and support algal growth. Particles less than 0.5 μm were not counted, but these particles do not effectively scatter light and do not contribute significant mass. The LTADS filter-based measurements do include the fraction of combustion-derived and secondary particles smaller than 0.5 μm; since the deposition calculations are based on the filter data, their absence in the count data is not carried over to the deposition estimates.

4.4.1.2 Particle Counter Calibration and Validation of Data

The principal instrumentation used in the dust experiments was a set of Climet CI-500 optical particle counters. These counters draw a stream of air through an optical chamber where, one-at-a-time, particles in the air stream pass through the beam of a solid-state laser. Light scattered by a particle is sensed photoelectrically, with the strength of the scattering converted into particle size based on scattering cross-section, and the number of particles in each size "bin" is recorded over a standard sampling period (for LTADS, typically one or twenty minutes). There is a maximum count rate, beyond which multiple particles are sensed together (causing mis-sizing), but concentrations observed in the Tahoe region never exceeded the count-rate capability of the instruments.

These instruments are calibrated at the factory, and cannot be adjusted by the user. Validation of calibration was determined by side-by-side testing of multiple instruments before and after each field experiment. An example is shown as **Figure 4-15**. Repeated intercomparisons showed minimal drift over the life of the LTADS field program. After each experiment, counts from instruments showing statistically significant bias in any size bin relative to CI-500 #105 were adjusted to eliminate that bias in final particle counter data.

The relationship between counts and mass was investigated by comparing count-estimated hourly aerosol mass with hourly BAM data for a week at the SOLA monitoring site (**Figure 4-16**). Aerosol volume was estimated by assuming that all particles in each size bin were spheres with a diameter equal to the geometric mean of the maximum and minimum size for the bin. Volume was converted to mass by assuming a particle density of 1 for all particles less than 2.5 μm, 2.5 for all particles over 10 μm, and intermediate values for particles between these two ranges (**Table 4-4**). These densities imply an increasing geological contribution for larger particle size, with the density of quartz (2.5) representing geological materials. Fine organic particles from combustion are assumed to be dominated by organics with a density near 1 and nitrates and sulfates are assumed to have a similar density due to their association with water. Although the BAM derived mass values were not expected to be reliable for individual hours the time series of mass from the two methods are similar and the scatter plot shows an r^2 of 0.4. Thus it appears that the particle counts can provide a useful semi-quantitative indication of particle mass. The count-based mass estimates do not include any particles smaller than .5 μm but this mass is not significant.

Figure 4-15. Comparison of data from between two collocated CI-500 samplers.

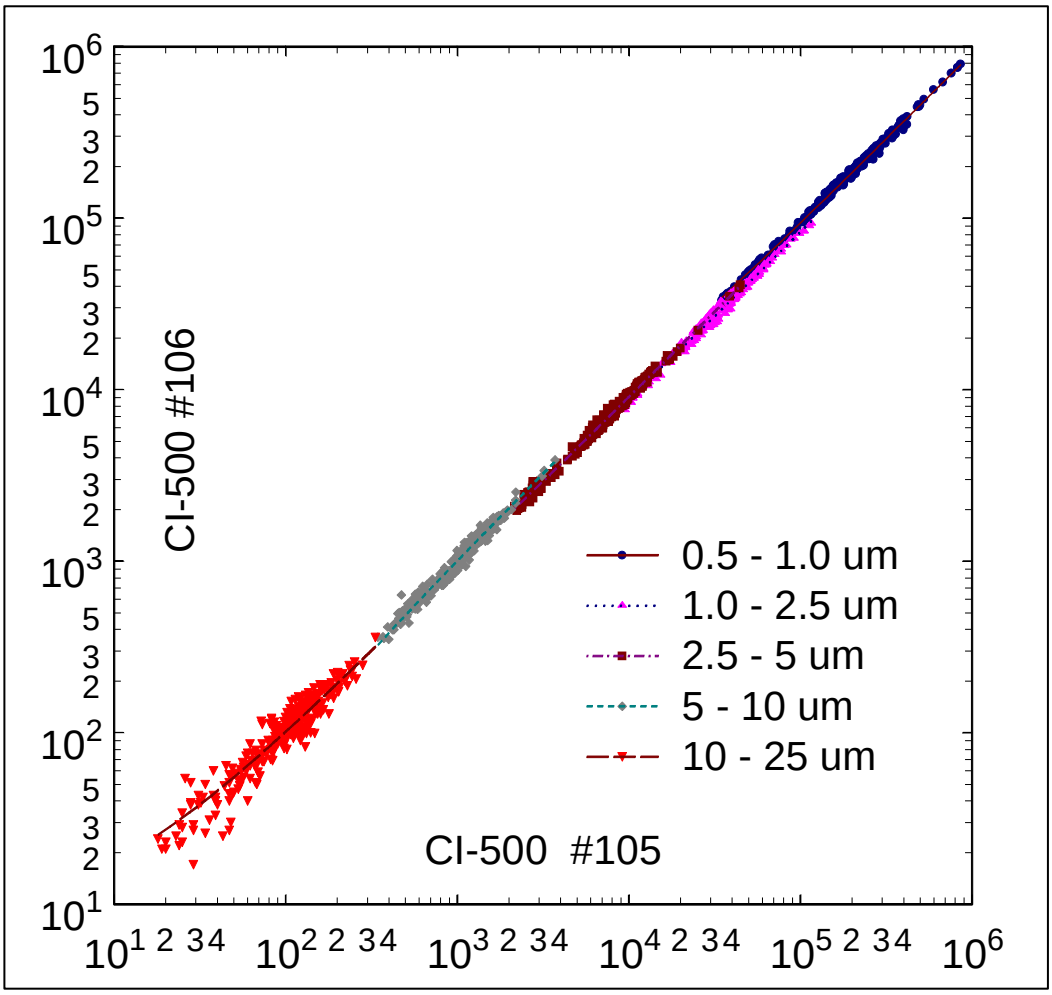

Table 4-4. Assumed densities of particles by size bin. These densities were utilized to generate count-based estimates of mass, for comparison with BAM TSP observations of mass (see Figure 4-16).

Particle Size (µm)	Assumed Density (g/cc)
0.5 - 1	1
1 - 2.5	1
2.5 - 5	1.5
5 - 10	2
10 - 25	2.5
> 25	2.5

Figure 4-16. Comparison of Size-Resolved CI-500 (#105) Interpreted Aerosol Mass with Hourly TSP BAM Data at SOLA.

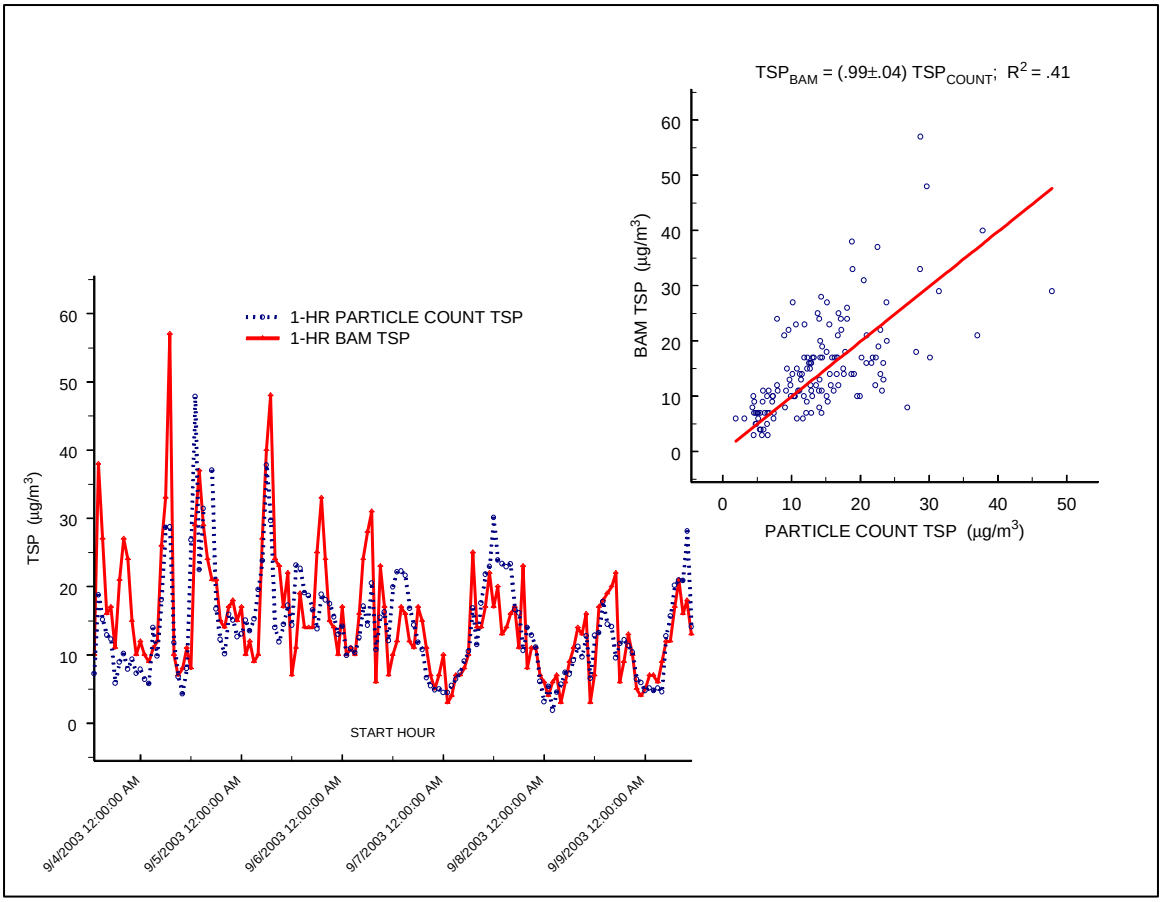

4.4.2 Spatial Variation among Terrestrial Monitoring Environments

Since land use in the LTADS study area ranges from urban to wilderness, comparisons were run among three sites - the urban SOLA site, the upland BLIS IMPROVE site, and a remote, unpopulated site at about the same elevation but outside the Tahoe Basin (Burnside Lake in the Hope Valley region, 24 km south of SOLA).

4.4.2.1 Remote Rural Sites

The Hope Valley area has minimal population, and Burnside Lake site is about 6 km from the nearest settlement or paved road. The nearest particle source was a small campground about 0.25 km from the measurement site. The rural sample within the Tahoe Basin was taken at the BLIS IMPROVE site, an unpopulated area on the west side of the basin about 200 m above the lake. The particle size distributions obtained were taken the morning after a rain event and are generally representative of "clean" conditions in the region (**Figure 4-17**). The vertical scale dM/dD is the change in particle mass per change in particle diameter, thus it is a measure of relative mass within size fractions.

Figure 4-17. Particle size distributions at remote rural sites in Hope Valley (Burnside Lake) and Tahoe Basin (BLIS) on morning of June 26, 2003.

Vertical bars are 1-σ range for each size bin. Steps in cumulative mass plots denote widths of size bins.

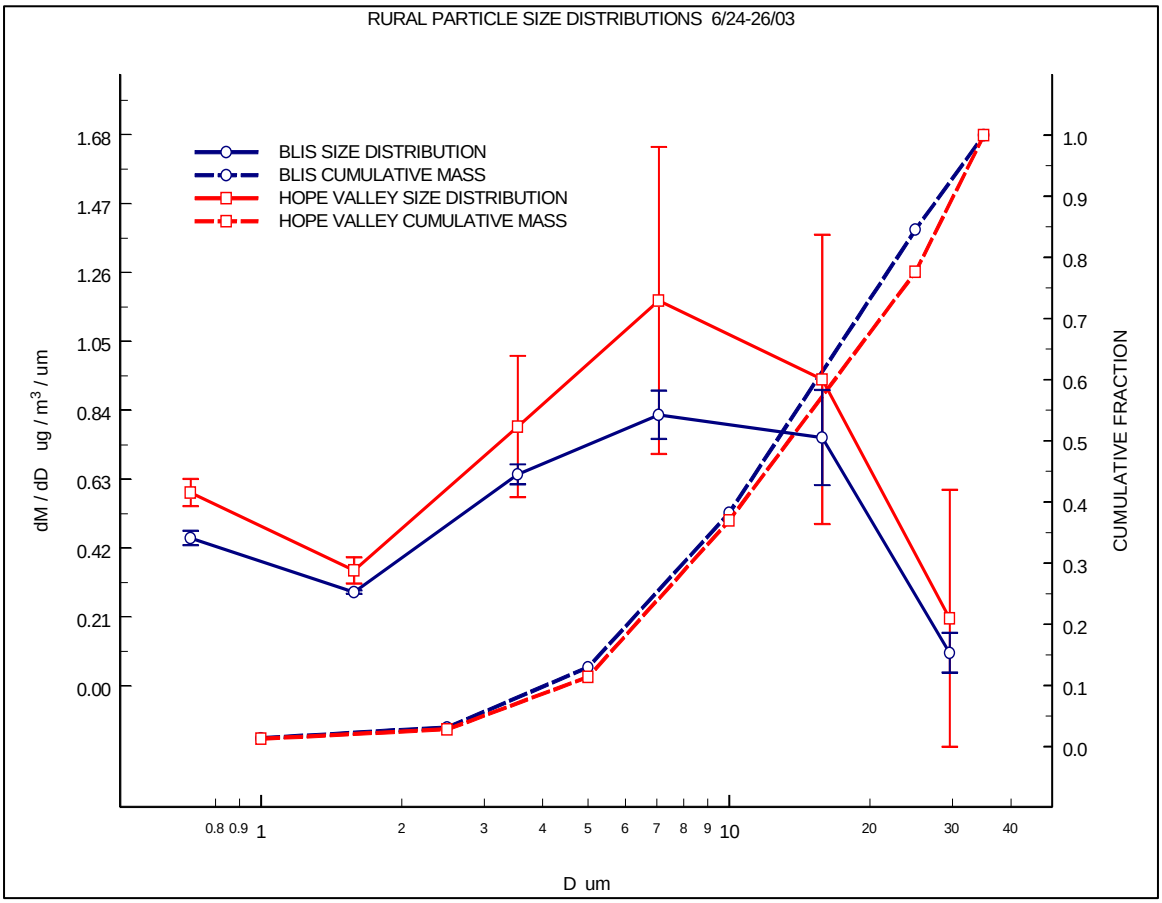

The mean (±1σ) TSP (Total Suspended Particulate) concentration at Burnside Lake was 23±12 μg/m^3 (the large variability suggests possible influence by our vehicle travel to the site); TSP at BLIS for the same period was 16±3 μg/m^3. The cumulative mass curves show that both sites were dominated by larger particles; fines (<2.5 μm) were less than 5 percent of the estimated mass, while large particles (>10 μm) were nearly 2/3 of the total. Given the wide variability (denoted by the vertical bars) and the overall low aerosol loading, these sites can be considered comparable.

The shapes of these particle size distributions show the multi-modal nature of particles. The larger sizes (>2.5 μm) are composed of mechanically generated material (primarily soil "dust"), while the fines (<2.5 μm) are dominated by chemically generated materials (combustion products and secondary aerosols formed in the atmosphere from gaseous precursors).

4.4.2.2 Populated Areas in the Tahoe Basin

The populated sites in the Tahoe Basin exhibit a wide range of particle concentrations due to effects of location, season, and proximity of human activity. The SOLA monitoring site was located on an undeveloped lakefront lot in the City of South Lake Tahoe, with US Hwy 50 (Lake Tahoe Blvd.) about 50 m south, and the lakeshore about 50 m north of the instrument platform.

The SOLA site provided a unique opportunity to examine the variation of aerosol burden on the populated shoreline. During night and morning hours cold air drainage causes air to flow from the urban area, across the highway, and out over the lake; during midday, solar heating of the land induces a lake breeze that brings air from the lake onshore. Thus SOLA experiences diurnal oscillation between the high urban aerosol concentrations associated with a population center and heavily traveled arterial highway (land breeze) and very clean air drawn off the lake (lake breeze). The contrast in particle size distributions for these two extremes is shown in **Figure 4-18**. Note that the concentrations at SOLA during onshore and offshore flow bracket the concentrations observed at the rural sites (**Figure 4-17**, dM/dD / $\mu g/m^3$ / µm).

The combination of urban emissions (smoke, dust, etc.) and roadway emissions from Hwy 50 drove the TSP (mean ± 1σ) to 274±51 $\mu g/m^3$. This high concentration measured directly downwind of the roadway during the evening commute is not representative of the general area. The midday onshore flow was much lower, with TSP at 9.6±2.7 $\mu g/m^3$. **Table 4-5** shows the ratios of observed concentrations for periods of offshore versus onshore flow, by size fraction. During offshore flow there is no minimum of concentration in the 1 – 2.5 µm size bin, presumably because the local dust emissions from the roadway overwhelm the fine combustion fraction even below 2.5 µm. However, during onshore flow a minimum of concentration for the 1 – 2.5 µm size bin is visible, although it is less distinct than in the distributions at the rural sites.

The enhanced ratios for the >2.5 µm size cuts suggest that the major effect of proximity to the highway is road dust (exhaust particles are smaller than 2.5 µm). Like the rural size curves, the SOLA onshore flow size curve has a local minimum in the 1-2.5 µm size range. Conversely, the offshore flow curve does not share the local minimum. The data in **Table 4-5** show the strong bias in the large particle sizes. The elevated particle loading in the 1-2.5 µm size range during offshore flow is probably the lower end of the coarse particle mode size distribution.

The observed monotonic increase with particle size for the ratios of concentration during offshore versus onshore is consistent with our understanding of the effects of deposition and dispersion. Two processes may explain this pattern. First, we expect to see relatively more large particles directly downwind of roadways because the regional emissions are less rich in large particles compared to emissions from the roads. Second, because larger particles tend to deposit more quickly, the fraction of large particles in the onshore flow is lower because the air trajectory has had a long

residence time over the lake, and is not dominated by the very local emissions, and thus contains a lower fraction of short-lived (larger) particles. Data discussed in the next section indicate that both processes contribute to the observed difference.

4.4.3 Spatial Variation between Lakeshore and mid-lake Areas

The strong difference between the composition of air under different flow regimes observed at SOLA (see previous section) suggests that air flowing from land out onto the lake is not simply diluted, but undergoes transformation by selective deposition of terrestrial pollutants and mixing with regional "background" air. This pattern suggests that there is a zone of terrestrial influence near shore, which grades outward to a well-mixed mid-lake environment.

In order to evaluate the extent of land-lake interaction a series of experiments were conducted using instruments mounted on the U.C. Davis research vessel RV Frantz. The basic experimental design was to sample mid-lake air and shore-zone air by running in open water and cruising the shoreline during evening and morning hours when downslope air drainage drives offshore flow. The pollutant measurements taken on the boat included NOy recorded continuously (a few seconds time resolution) and a CI-500 particle counter collecting particle size data with a resolution of 1 minute. The NOy is interpreted as a tracer for NOx-producing combustion (primarily motor vehicles), fine particles are interpreted as combustion (i.e. " smoke"), and coarse particles are interpreted as road dust. Cruising at about 4 knots (0.5 m / sec) produced transect data with spatial resolution on the order of 120 m.

Sampling under stable meteorological conditions during downslope flow, the RV Frantz night-morning data focus on the strong downslope flow regimes, and represent the peak conditions for terrestrial effects on the lake. Limited data taken during well mixed periods show that the shore - mid-lake contrast is much weaker at midday or when regional winds mix air throughout the Tahoe Basin.

The evening and morning courses were very similar, with each consisting of an outbound leg from Tahoe City crossing open waters toward the north east shore near Incline Village and a return leg following close to the north shore. The morning outbound leg differed from the evening outbound leg in that it passed farther south of Stateline Point, and ended a little farther south near the east shore.

Figure 4-18. Extreme results in the diurnal aerosol cycle at SOLA. The difference in TSP concentration is a factor approximately 30:1, necessitating the logarithmic scale in the plot. The shapes of the distributions indicate a bias toward large particles during offshore flow (see Table 4-5).

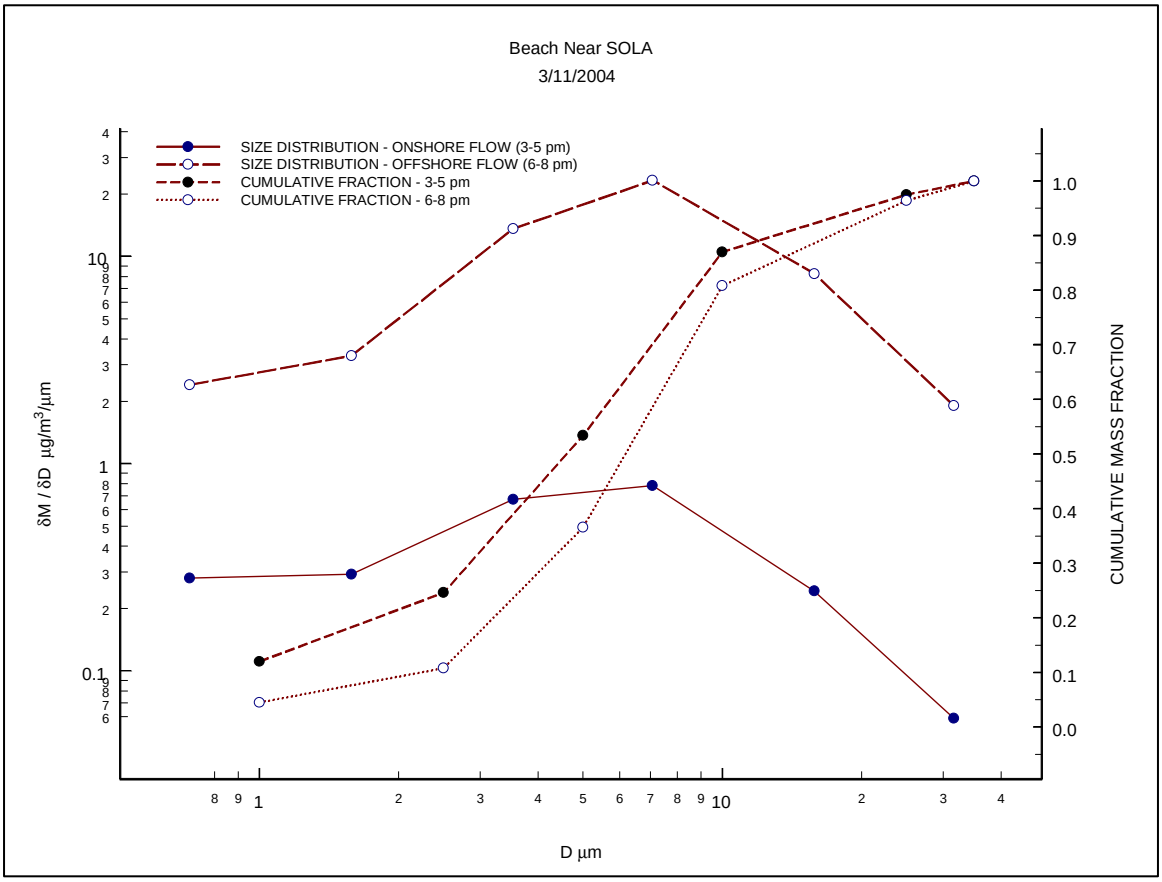

Table 4-5. Ratio of mean offshore to mean onshore size-resolved and total aerosol concentrations for the data from Figure 4-18.

SIZE_BIN	OFFSHORE / ONSHORE
0.5 - 1 um	8.2
1 - 2.5 um	11.3
2.5 - 5 um	20.2
5 - 10 um	29.8
10 - 25 um	33.9
>25 um	31.9
PM25	10.8
PM10	26.7
TSP	25.2
COARSE	29.7
LARGE PM	27.0

The time series of observed NO_y concentration and PM2.5 counts are plotted (**Figure 4-19**) on the chart along the boat track as circles with diameter proportional to concentration or count. (If viewed in black and white the red circles (NO_y) appear light grey and the green (PM2.5 counts) are darker. The evening measurements (**Figure 4-19**, top) show relatively low pollutant levels over open water (the straight transect from Tahoe City to the east shore) and higher concentrations near the shoreline on the return leg as downslope flow carried both NOy and particles onto the lake in the near shore zone.

Morning conditions were quite different. Because the morning cruise (**Figure 4-19**, bottom) measured much lower pollutant levels over open water, the course from Tahoe City (3:20 am) to the northeast shore (4:15 am) is barely discernable. Concentrations were also very low along the shoreline until after 5 am off Stateline and Kings beach. The downslope air flow was strong throughout during the morning cruise, but, prior to 5 am PST, showed no pollutant flux from the urbanized shoreline. Later, as human activity picked up, first NOy concentration increased (motor vehicles) and later fine particle counts (possibly chimney smoke or road dust) showed a similar pattern to that observed the previous evening. Repeated cruises on both the north and south ends of the lake showed a similar dependence of concentrations on diurnal activity levels and wind direction.

Figure 4-19. Night and morning patterns of pollution, on north end of Lake Tahoe.

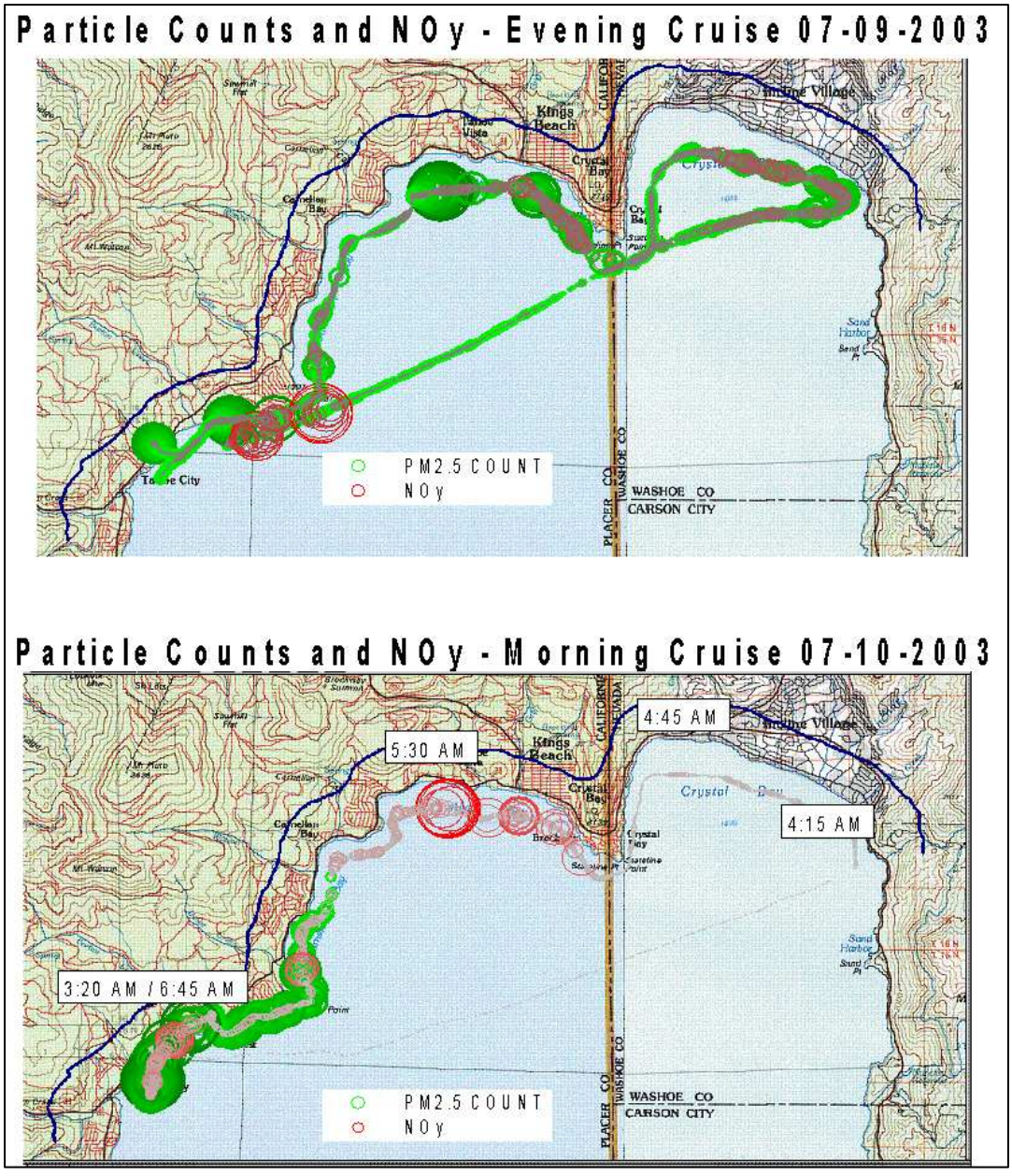

Figure 4-20 shows particle size data from a morning cruise on the south end of Lake Tahoe. In that cruise three distinct regimes were observed: air drainage from the SE shore (Zephyr Cove to Tahoe Keys) showed strong pollutant flux; air drainage from the largely unpopulated shoreline between Camp Richardson and Emerald Bay lacked strong pollutant signatures; and air encountered traversing the lake from Emerald Bay back to Zephyr Cove showed evidence of dilute accumulated pollution.

Figure 4-20. Particle size distributions observed during a morning cruise on the south end of Lake Tahoe. Strong pollutant flux was observed from the South Lake Tahoe area, while drainage air along the unpopulated shoreline was cleaner than that at mid-lake.

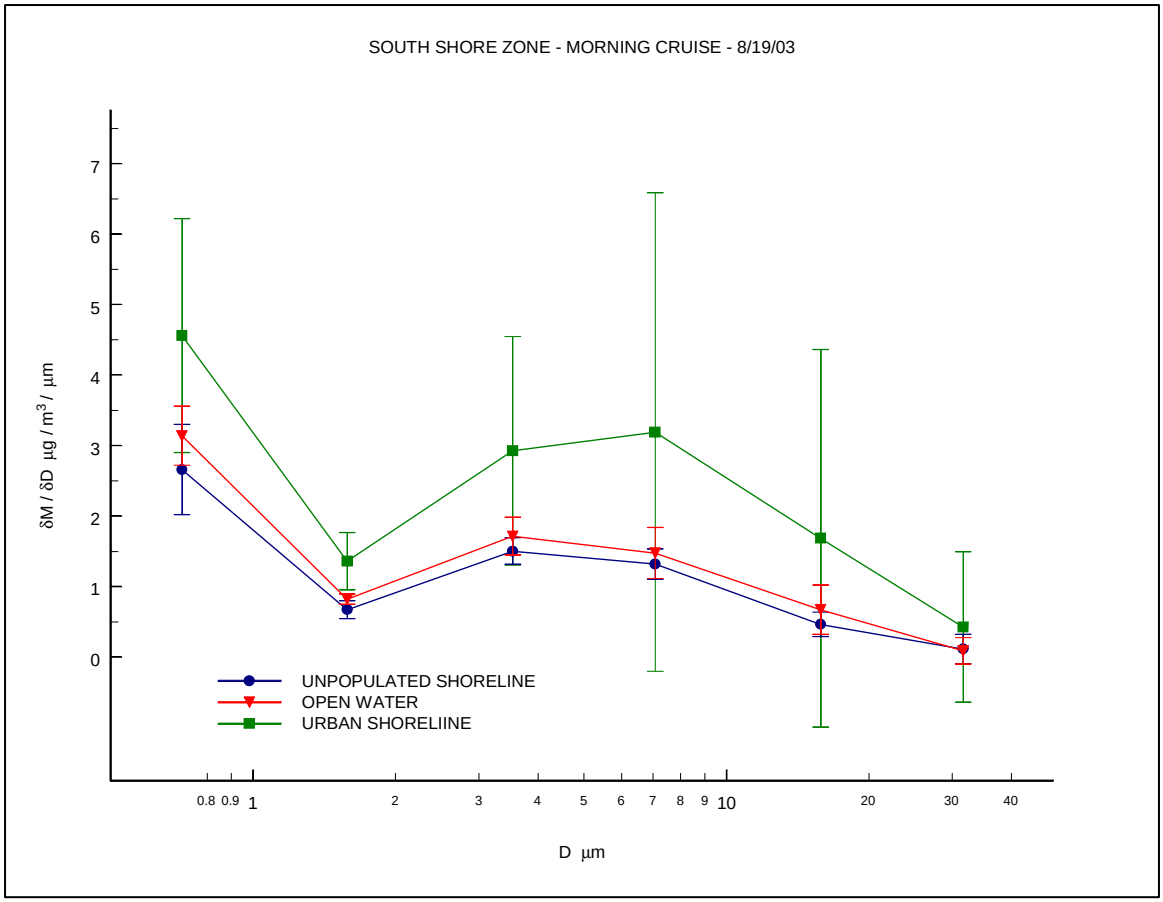

The particle size distribution from the "clean" shoreline approximates the "background" as measured at the remote sites (**Figure 4-17**), but the urban shore zone concentrations are much lower than the offshore flow observed at SOLA. This discrepancy suggests that there is strong dilution from shoreline to our monitoring path (approximately 0.3 km from the shoreline along most of the developed shoreline). The next section addresses this question.

4.4.4 Dilution and Deposition of Roadway Emissions

Because the SOLA site data represents both the well-mixed lake environment (during onshore flow) and the strong local effect of Hwy 50 traffic and other urban emissions (during offshore flow) it is desirable to understand the local particle concentration gradients. Because human activity and development is generally near the shoreline and emissions from roadways may impact several of the LTADS monitoring sites we

made measurements to better understand the gradients between the roads and the shoreline. The roads appeared to be a major source of particles in the Tahoe Basin, but, as expected, within a short distance downwind the observed concentrations decreased and size distributions changed significantly compared to those measured near the roadside.

During downslope flow on the evening of March 11, 2004, three optical particle counters were operated near the SOLA site at distances of 6, 16, and 100 m from the nearest traffic lane of Highway 50. Estimated mass concentrations, calculated from the particle counts, declined significantly with downwind distance (**Figure 4-21**). The observed decrease of concentration with downwind distance is further characterized by fitting power functions of the form $C=C_0\ e^{-K(x)}$ to the data, where C is concentration at distance x downwind, C_0 is concentration (extrapolated) at the nearest traffic lane, and K is the "depletion coefficient" for the selected particle size class. A constant depletion coefficient implies an equal fractional decline in concentration per unit distance of transit downwind from the road. However, the observed decline is due to the combined effects of deposition and dispersion and their relative influences will change with distance.

For the purpose of the following analysis we assumed the particle dispersion is effectively size-independent over the horizontal scale of this experiment (about 100 m). In general, for the different size fractions any differences in upwind concentration or vertical profiles of concentration would cause the ground level concentrations to decline at different rates with downwind distance (because the same vertical mixing would incorporate different aloft concentrations into the plume). However, to the contrary, we assumed that over this distance the local emissions of particles from the roadway overwhelmed the background particle concentrations in all size fractions.

To investigate the roles of dispersion and deposition we compared the depletion coefficients for the different size fractions as calculated from the observed particle counts. Our general understanding of deposition (see **Fig. 4-13**) suggests that the loss of fine particles (~1 μm) over such a short transit should be negligible. The smallest depletion coefficient (for particles of 0.5-1 or 1-2.5 μm diameter) was attributed entirely to dispersion and was assumed to represent the rate of dispersion for all size fractions. Thus, for each size fraction, subtracting this dispersion coefficient from the depletion coefficient provided a "deposition" coefficient. For each size fraction this deposition coefficient was used to calculate the fraction of particles that would remain in the atmosphere at the SOLA site and at the beach (50 and 100 m from the road).

Table 4-6 shows the results of such a treatment for morning and evening experiments near SOLA. Although the conditions (traffic, temperature, humidity and wind speeds) differed between the two experiments, both were under down-slope flow conditions and the patterns of concentration were similar. Similar fractions of particles were predicted to remain in the atmosphere and the variation in ratios of predicted atmospheric survival of PM at the beach compared to at SOLA ("beach/SOLA ratio") differed between size fractions in a similar manner. The 0.5 – 1 and 1 – 2.5 μm fractions appear to have

similar rates of depletion, the depletion is greater for the coarse particles (2.5 – 5 and 5 -10 µm), and depletion is much greater for particles larger than 10 µm.

We expect that the local roadway emissions of both coarse and large particles dominate concentrations downwind and that for these size fractions any effects of possible differences in upwind concentrations or vertical profiles would be minimal. Thus, the difference in depletion for coarse and large particles should be a measure of their loss by deposition over this short distance. On the other hand, there is a greater potential for upwind particle concentrations to influence the apparent rate of depletion for the fine particles, so conclusions about the relative losses for fine versus coarse particles are less certain.

Figure 4-21. Change in particle concentrations observed at, and fitted power functions for, the area downwind of Highway 50 at SOLA on the evening of March 11, 2004. Dotted lines are 95% confidence bounds for the fits.

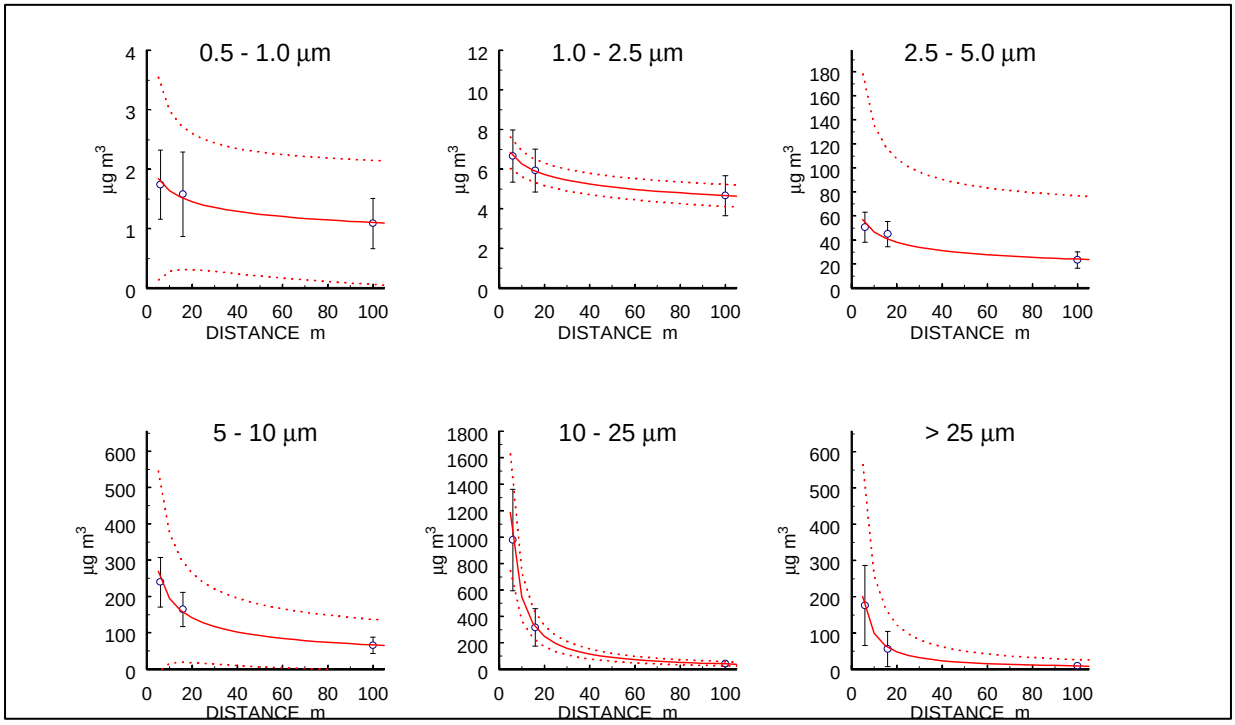

Table 4-6. Computation of size-resolved particle loss between SOLA and the lakeshore for dispersion experiments on afternoon of March 11 and morning of March 12, 2004.

STAGE	TOTAL REDUCTION COEFF	DISPERSION COEFF	DEPOSITION COEFF	SURVIVING FRACTION AT SOLA (50 m)	SURVIVING FRACTION AT BEACH (100 m)	BEACH / SOLA RATIO	UNCERTAINTY
	MAR 11 - PM						
0.5 - 1 um	-0.171	-0.127	-0.044	0.843	0.818	0.97	3%
1 - 2.5 um	-0.127	-0.127	0.000	1.000	1.000	1.00	1%
2.5 - 5 um	-0.286	-0.127	-0.158	0.538	0.482	0.90	7%
5 - 10 um	-0.464	-0.127	-0.337	0.268	0.212	0.79	3%
10 - 25 um	-1.122	-0.127	-0.995	0.020	0.010	0.50	1%
>25 um	-1.027	-0.127	-0.900	0.030	0.016	0.54	6%
	MAR 12 - AM						
0.5 - 1 um	-0.124	-0.124	0.000	1.000	1.000	1.00	2%
1 - 2.5 um	-0.165	-0.124	-0.042	0.850	0.826	0.97	0%
2.5 - 5 um	-0.269	-0.124	-0.145	0.567	0.513	0.90	6%
5 - 10 um	-0.416	-0.124	-0.292	0.318	0.260	0.82	3%
10 - 25 um	-0.916	-0.124	-0.792	0.045	0.026	0.58	1%
>25 um	-0.916	-0.124	-0.792	0.045	0.026	0.58	5%

These data, taken together with the findings of the near-shore boat sampling discussed in Section 4.5.3 indicate that downslope winds deliver concentrated particle plumes to the lake from the heavily developed urban and residential portions of the lake shore, and that these plumes diminish in intensity fairly quickly with increasing distance from the source. Although there are no simultaneous off-shore size-resolved data to compare with these experiments, a rough sense of the scale of off-shore transport can be found by applying the concentrations and apparent rate of reduction from these experiments to the concentrations observed on the lake under similar meteorological conditions (**Figures 4-19 and 4-20**). Concentrations observed in the urban shore zone would be reached about 250 m offshore, and concentrations near those measured in open water would be reached about 500 m from shore. Although highly uncertain due to the mismatched data, this calculation suggests that the shore zone effect is limited to a few hundred meters to 1 km, and shows consistency between the roadside and on-lake results.

4.4.5 Estimated Particle Number and Deposited Fraction

In addition to providing nutrients for algae that reduce lake clarity, atmospheric deposition also adds inert (non-soluble) particles to the lake. These inert particles scatter light within the water column with an optical efficiency that is strongly dependent on their size and chemical composition. The numbers of these inert particles within the aerosol mass is not well known, but LTADS obtained some particle count data during short-term monitoring. The particle count information, when combined with particle chemical data from the LTADS and IMPROVE filter records, can be used to generate a rough estimate of the optical efficiency characteristics of deposited particles. Count and

mass data averaged over a week at SOLA are shown in **Figure 4-22**. The left vertical scale, dN/dD, describes the change in particle number (N) per change in particle diameter (D), indicating relative numbers of particles by size bins of particle diameter. In this example, near and downwind of highway 50 at the SOLA site in South Lake Tahoe the fine fraction (D < 2.5 µm) contained over 95% of the particle numbers but less than 10% of the mass. The coarse fraction contained a few percent of the particle count and about 45% of the mass. Large particles (> 10 µm) comprised about one percent of the particle number and about 50% of the total mass.

Figure 4-22. Mean particle number and cumulative mass and number distributions at SOLA 9/2-9/2003. Arrows denote filter sample size ranges in the LTADS measurements. Fines dominate in numbers; large particles dominate in mass.

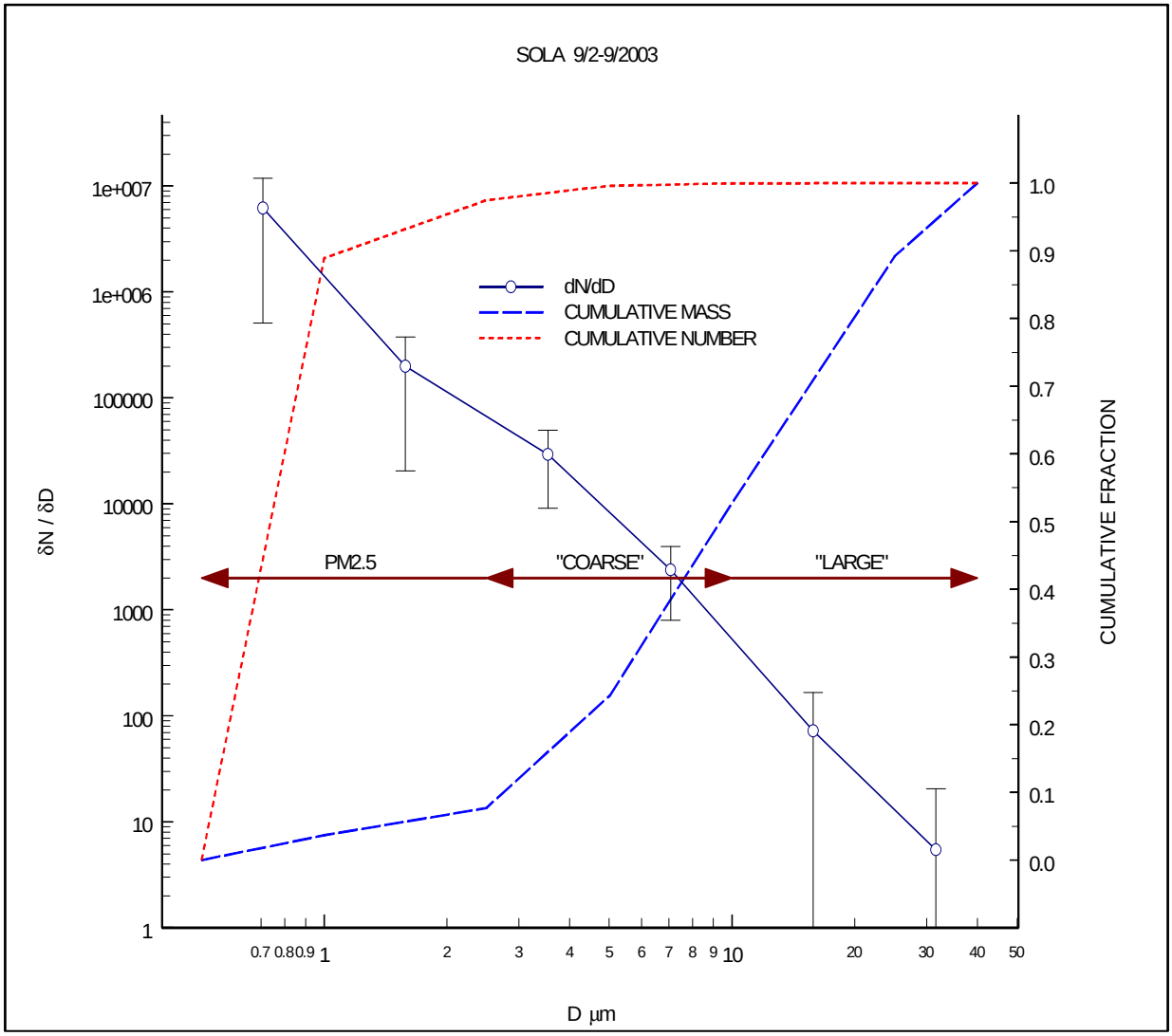

The size ranges of concern for light scattering by inert particles in the lake fall in the PM2.5 fraction. Within that fraction, there are three general classes of chemical materials based on their effect on lake turbidity:

1. soluble species (*e.g.* sulfates and nitrates) that dissolve into the lake water and have no residual optical effect;
2. organic materials which, although largely insoluble, have refractive indices near that of water, and thus are optically unimportant; and
3. inert materials (*e.g.* soot and soil minerals) that persist within the water column after deposition and contribute to the turbidity of the lake.

Computing the inert fraction of deposited particle numbers requires first converting particle mass as measured with the filters to estimated particle numbers, then allocating the numbers to the three particle types listed above.

The first five panels of **Figure 4-23** illustrate the relationship between observed particle counts and particle mass estimated from those count observations. For the particle size categories spanning a relatively small range of particle diameters, mass and particle counts are closely related. For fine or large particles, or even for coarse particles the observed particle mass appears to provide a reasonably consistent estimate of particle numbers. However, if fine and coarse are combined and examined together as PM10, or, especially if large particles are also included (as in the definition of TSP), then there is very little relationship between particle mass and numbers. The final panel in **Figure 4-23** compares the scatter of 1-hour BAM TSP measured mass ($\mu g/m^3$) versus total particle counts.

Because there is such a large range of counts between the 0.5-1 µm and 1-2.5 µm size bins, the chemical allocation of PM2.5 is subdivided based on size distributions for "typical" aerosols to estimate where each chemical type lies in the size-number distribution. The allocation of chemical species for LTADS is based in part on limited size-resolved chemical data available from Mt. Lassen (**Figure 4-24**). Although Lassen is a more remote site it provides size resolved and chemically speciated data not otherwise available in the Sierra Nevada at a similar elevation and distance from the Pacific. Based on location Lassen is subject to similar meteorological regimes and potential transport from populated areas in coastal and valley areas to the west and from Asia. By that reasoning we expect a similar chemical speciation at Lassen despite a somewhat more aged air mass, less urban influence, and lower concentrations at Lassen. An observed strong similarity between Lassen air quality and that in less-developed areas of the Tahoe basin (e.g. Bliss State Park) means that, lacking Tahoe specific data, Lassen is a reasonable analog for typical, basin-wide conditions. Moreover, size distributions by species should be similar because the origins of the materials play a large role in their particle sizes - soil dust is dominated by mechanically produced particles, thus it will tend to large particle sizes; combustion products are produced chemically and tend to smaller sizes.

Figure 4-23. Particle count - mass regressions from experiments at SOLA.

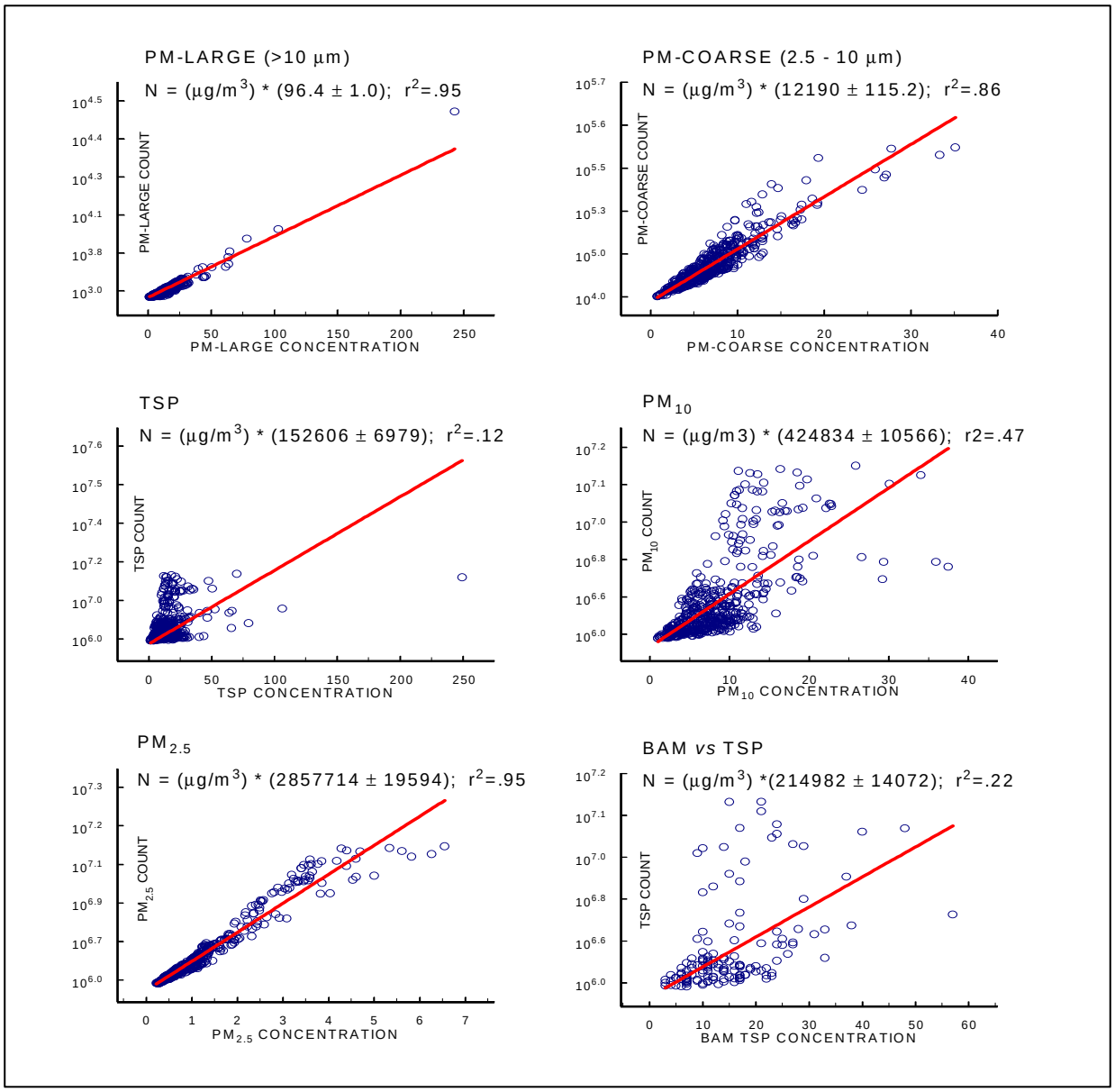

Figure 4-24. Size distributions and mass fractions of various elements at Mt. Lassen.

Solid line = mass fraction, dashed line = cumulative fraction. S represents soluble species; Zn and K inert combustion products; Si, Al, and Fe represent inert soil components. Vertical lines mark limits of the 0.5 -1 µm and 1 - 2.5 µm size ranges.

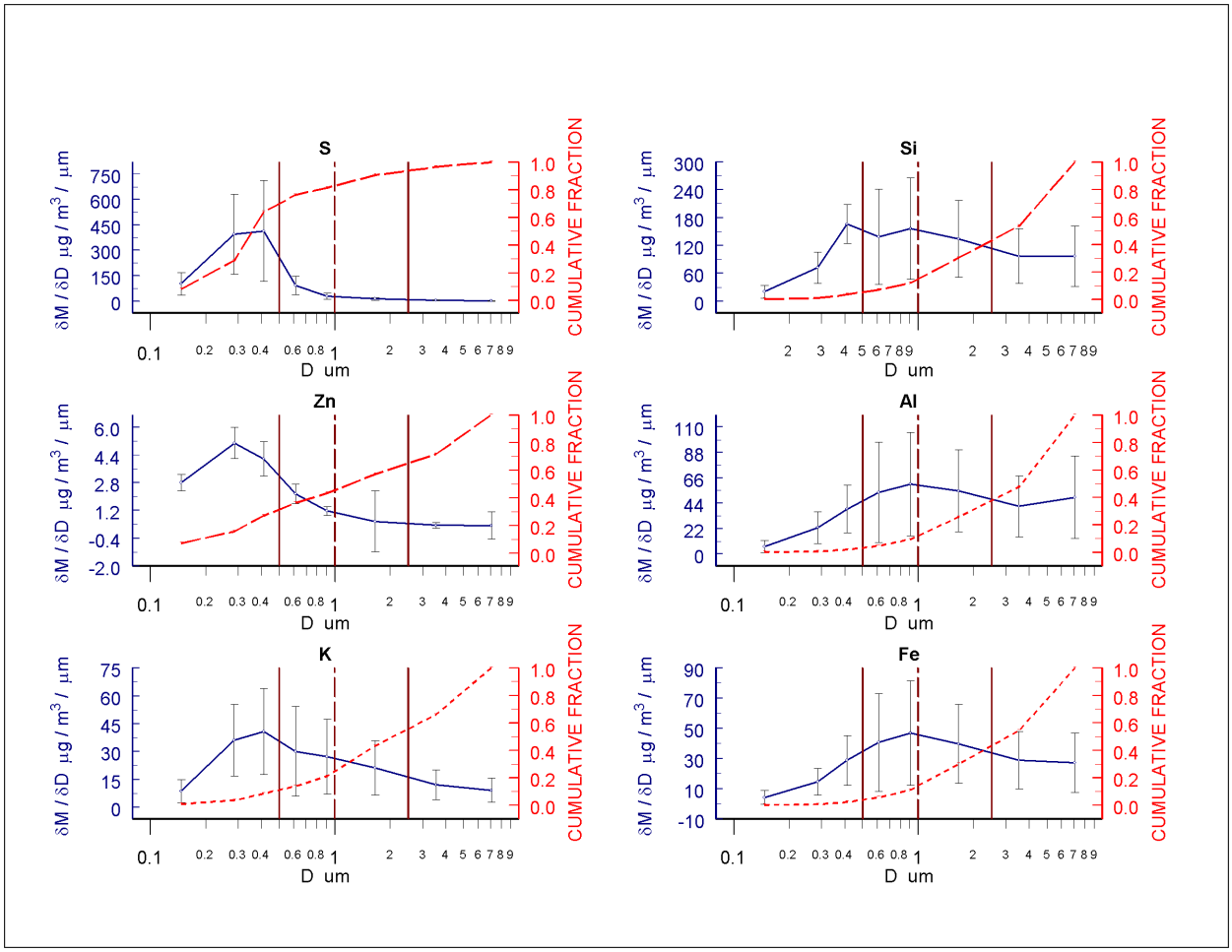

Using a combination of the regressions of PM2.5 particle counts versus mass (**Figure 4-23**) and inferences drawn from the Mt. Lassen data (**Figure 4-24**) a species allocation scheme was developed for the LTADS PM2.5 data. The results of applying this scheme to SOLA data are shown in **Table 4-7**.

Table 4-7. Allocation of particle types to seasonal data from SOLA.

	PM2.5 ng/m3		FRACTION OF PM2.5			TYPICAL COUNT % 91.2%	8.8%	COUNT
SOLA ANNUAL	MEAN	TYPE	0.5 - 1.0 um	1.0 - 2.5 um	all PM2.5	0.5-1 um COUNT	1 - 2.5 um COUNT	FRACTION
SOIL	1122	INERT	10.2%	26.1%	36.4%	2360787	581300	31%
EC	1726	SOLUBLE	9.2%	7.3%	16.5%	2126856	161464	24%
OC	2955	OM	15.6%	31.6%	47.2%	3585128	703299	45%
SO4	574							
NO3_	389							
MF	8841	PERCENT	35.0%	65.0%	100.0%	8072770	1446063	
SOLA APR-OCT								
SOIL	1166	INERT	10.0%	29.0%	39.0%	1861900	523776	31%
EC	1258	SOLUBLE	12.2%	9.6%	21.8%	2283354	173345	32%
OC	1952	OM	12.9%	26.3%	39.2%	2419717	474679	37%
SO4	711							
NO3_	294							
MF	7173		35.1%	64.9%	100.0%	6564971	1171800	
SOLA MAY-SEP								
SOIL	1120	INERT	9.7%	28.9%	38.7%	1735421	499949	30%
EC	1138	SOLUBLE	13.4%	10.5%	23.9%	2392770	181652	35%
OC	1749	OM	12.4%	25.1%	37.4%	2208371	433219	35%
SO4	754							
NO3_	279							
MF	6859		35.5%	64.5%	100.0%	6336562	1114819	
SOLA NOV-MAR								
SOIL	1040	INERT	10.6%	23.0%	33.6%	3345836	705868	31%
EC	2594	SOLUBLE	6.1%	4.8%	10.8%	1919790	145745	16%
OC	4812	OM	18.3%	37.3%	55.6%	5817624	1141250	53%
SO4	321							
NO3_	565							
MF	12168		35.0%	65.0%	100.0%	11083250	1992863	

The table shows that the particles greater than 1 μm constitute less than 10 percent of the PM2.5 count, with over 90 percent below that size. The table also shows that the relative composition of PM2.5 varies, with inert particles a fairly constant fraction (33-39 percent), while solubles vary seasonally, from a low near 10 percent in winter to more than double (24 percent) in summer. Organic particles also show significant seasonality, varying between a winter peak of over half (56 percent) to a summer minimum (37 percent).

The last columns in **Table 4-7** show the concentration model converted into particle counts. The optical implications of these calculations are that strongly scattering fine inert particles constitute about 30 percent of PM2.5 particles, regardless of season, while most of the seasonal variation is in the optically weak organic and soluble particles. These calculations suggest that rough estimation of the inert particle deposition load can be done by simple linear adjustment of the estimated particle number based on the PM2.5 regression in **Figure 4-24**.

4.5 Key Assumptions and Resultant Bias

Identified in this section are key assumptions used in the estimation of deposition velocities and, subsequently, pollutant deposition. They are approximately ordered by the magnitude of the bias they may introduce into the estimates of deposition. Some assumptions clearly will introduce a positive bias. This was intentional so that the contribution of atmospheric deposition in the TMDL would not be underestimated.

4.5.1 Assumptions Likely to Introduce the Largest Bias

The assumption that concentrations of PM measured over land (at Sandy Way in SLT, Lake Forest on the northwest shore, and Thunderbird on the east shore) are also representative of concentrations over mid-Lake areas would likely introduce a very significant positive bias in estimated deposition rates for PM because the urban measurement sites are significantly impacted by local PM emission sources. Based on the brief experiments described in Section 4.4 and expectations regarding patterns of deposition and dispersion, significant decreases in downwind PM concentrations are likely over some areas of the Lake. Nevertheless, such estimates are useful because they provide a reference and upper bound on the annual dry deposition. Thus they are presented for reference in Appendix L.

Peer reviewers commented that this conservative assumption reduced the utility of the estimates. We agree and in particular were concerned that comparisons of estimates of dry deposition and estimates of other inputs to the Lake would be difficult because of the bias included in that previous estimate.

To provide a more realistic estimate of deposition, the measured concentrations of PM in the urban areas were assumed to be depleted by a modest amount over the Lake. For several reasons the nitrogen concentrations were not assumed to be depleted. Compared to PM, nitrogen species (dominated by ammonia and nitric acid) are more regionally mixed and the nitric acid is formed in the atmosphere rather than directly emitted. Because the ammonia gas and nitric acid gas appear to be mixed through deeper layers, it is expected that vertical mixing over the Lake will tend to refresh surface concentrations of those species over the Lake. The vertical mixing is generally enhanced during hours of offshore flow because at those times the Lake is usually warmer than the air flowing onto it. Similarly, because ammonia and nitric acid are more regionally dispersed than the PM, horizontal dispersion downwind of the urban area monitoring sites is much less of an issue. Thus, nitrogen species concentrations measured at the urban sites are expected to be relatively similar to those on the Lake.

The deposition estimates provided here assume a modest depletion in concentrations of PM and phosphorus over the Lake compared to concentrations observed at the urban monitoring sites (Sandy Way and Lake Forest). For estimating the depletion of concentration the observations at Thunderbird were utilized as an indicator of concentrations on the Lake. The Thunderbird site is located far from busy local roadways and experiences onshore flow for many hours of the day. In contrast the

urban sites (Sandy Way and Lake Forest) are relatively close to emission sources and are subject to some urban influences regardless of wind direction.

Depletion of PM concentrations was assumed for the north and south Lake quadrants only. For the north quadrant the concentration of each size fraction was reduced from the Lake Forest concentration by 25% of the difference between the Lake Forest and Thunderbird concentrations. The calculation of concentration for the south quadrant was analogous, but used PM concentrations from Sandy Way instead of from Lake Forest. The reduction in PM concentration was calculated independently for each of the three size fractions. As a result, the reductions in concentration were greatest for the large particles and least for the fine particles, reflecting the fact that the observed PM_large concentrations were much lower at the Thunderbird site compared to the urban sites. Differences were much less for the PM2.5 concentrations.

The validity of these assumptions concerning spatial and temporal variations in particle mass concentrations and particle size distributions over the Lake can be partially evaluated against the particle counts obtained during the short term targeted studies (Section 4.4). Although those are of limited duration and based upon particle counts instead of measured mass, those studies do support the expected decrease in concentration out over the Lake. However, more quantitative extrapolations from this data are not warranted because those studies are temporally and spatially limited, and represent only snap shots of conditions during a few seasons.

4.5.2 Assumptions Likely to Introduce Moderate Positive Bias

The assumptions concerning the spatial variations of concentration are thought to be the largest source of uncertainty in the deposition estimates. Relatively modest bias may be introduced by the additional assumptions listed below.

- A modest overestimation of dry deposition may result from calculating dry deposition as occurring during all periods, including those with precipitation. Thus, a potential positive bias is included in the estimates of dry deposition by over-counting hours of dry deposition. During 2003, trace (or more) precipitation was measured at Incline Creek for 6% of hours (503) and 25% of days (92). However, this overestimation is moderated by the manner concentrations were treated. Average concentrations reported for each season were based upon all available two-week data, including periods of precipitation with presumably lower concentrations.

- The distributions of particle sizes within each of the three measured PM size categories (or bins) were not known. Assumed characteristic particle diameters were utilized for calculation of lower, central, and upper bound estimates of deposition velocity. For this purpose, the assumed particle diameter used to represent the rate of mass deposition for a size bin should be skewed toward the upper bound of the bin; first, because the larger particles contain a disproportionately large fraction of that bin's mass and, second, because the deposition velocity generally increases with particle size (especially within the coarse and large particles categories). For the lower and upper bound estimates, extreme

particle diameters were chosen to ensure the appropriate bias in the calculated mass deposition rates for each bin. For the central estimates the assumed particle diameter for PM_large is expected to provide a substantial positive bias and the assumed diameter for PM_coarse is expected to be approximately neutral with respect to any bias. The assumed particle diameters for each size fraction are listed in **Table 4-8** for the lower, central, and upper estimates.

The characteristic diameters assumed for the upper estimate very obviously overstate the size of PM_fine and PM_coarse and based on the particle count observations also overstate the size of PM_large. Clearly, PM-fine must include particles smaller than 2.5 µm and the assumption of 2.5 µm as the characteristic size must overestimate the size. Similarly for PM_coarse (2.5 µm < PM diameter < 10 µm) an assumed diameter of 10 µm must overestimate the characteristic size and thus the deposition velocity of PM-coarse. For PM_large (TSP – PM10), a characteristic diameter of 25 µm was assumed for the upper estimate. While there is no upper limit defined on the diameter of TSP or PM_large, the available data suggests that 25 µm is an overestimate of the characteristic particle size of PM_large, and thus will overestimate the deposition velocity for PM-large. Although larger particle sizes have been observed in urban areas of southern California by Lu, et al. (2003), the available LTADS data suggest that particles larger than 25 µm contribute a very small fraction of the mass of PM_large over Lake Tahoe. This conclusion is based both on the size resolved optical particle counts and on comparison of mass in PM_coarse versus PM_large from the TWS data. Thus, there is reasonable certainty that the assignment of 25 µm as the characteristic size for large particles is sufficiently conservative to represent the worst case condition at the shoreline of the Lake. Applying these same particle sizes for calculations at mid-Lake should be yet more conservative as an upper bound of deposition to the Lake.

Table 4-8. Assumptions regarding characteristic particle sizes and maximum allowable aerodynamic conductance.

Type of Estimate	Assumed Diameter for Particle Size Fraction (µm)			"Cap" on 1/Ra (cm/s) (max aerodynamic conductance)
	Fine (PM2.5)	Coarse (PM10 – PM2.5)	Large (TSP – PM10)	
Lower	1	2.5	10	3
Central	2	8	20	6
Upper	2.5	10	25	10

4.5.3 Assumptions Expected to Introduce a Smaller Positive Bias

Several assumptions are expected to cause a small positive bias in the estimated deposition rates. These biases are thought to be insignificant compared to other uncertainties.

- Deposition velocities of the gases HNO_3 and NH_3 were approximated as the inverse of the aerodynamic resistance R_a (assumed $R_a >> R_b$ and $R_c \sim 0$). This is a standard assumption for deposition of very reactive or soluble gases over water (e.g., Valigura, 1995) but may produce a small positive bias in deposition velocity when R_a is very small.
- As discussed previously, small values of aerodynamic resistance calculated in the near-shore zone during offshore flow are known to be unrealistic and thus were not used in calculation of the deposition estimates. The assumption of a logarithmic wind profile (modified by stability effects) is valid at heights above 50 times the aerodynamic roughness length scale (Z_0) but not for heights that are of the same order as Z_0. Thus, for the near-shore zone during offshore winds it was necessary to set a maximum value for the inverse of aerodynamic resistance. Maximum values were assigned as 3, 6, and 10 cm/s for the lower bound, central, and upper bound estimates. These were used as the maximum deposition velocity for the gases (ammonia and nitric acid) and were also used in calculation of the deposition velocity for particles. The assumption of a 6 cm/s cap on $1/R_a$ for the central estimate case is rather generous maximum and is likely to result in a positive bias in deposition velocities of gases and particles for some periods in the near-shore zone. But note that it is only applied to a limited area of the Lake, and only during offshore winds, so the effect on average deposition rates to the Lake is expected to be small. The cap on $1/R_a$ (10 cm/s) used for the upper limit estimate was chosen as the largest value found in the literature for any modeling of gaseous deposition and it is likely more than double the actual maximum deposition based on observed rates for SO_2 to water surfaces (Whelpdale and Shaw, 1974; Sehmel, 1980). The cap of 10 cm/s is expected to cause a positive bias in the estimates of deposition velocity for gaseous species, PM2.5 and to a lesser extent for PM_coarse but will have little effect on deposition estimates for PM_large.

- Increased turbulence due to roughness over land (assumed to be 1 m) was assumed to be advected to 1 kilometer offshore. The deposition velocity in this near-shore zone was calculated as the average of the over-water and near-shore deposition velocities. Calculation of deposition velocity assumed Z_0 of 1 m at the shoreline and Z_0 as a function of wind speed over open water. This is the arithmetic equivalent of a linear decay of the shoreline deposition velocity to the lower open water deposition velocity at a distance of 1 km offshore. Thus, for estimation of R_a near the shoreline during periods of offshore winds, an appropriately higher estimate of deposition velocity (than would be provided by the standard over-water formulations) was provided by adjusting Z_0 to appropriate values for forested areas. However, the use a Z_0 of 1 m caused the maximum deposition velocity to be invoked for the near-shore zone. This may result in some over estimation of deposition in this limited area.

- The calculated effects of atmospheric stability on turbulence and deposition velocity were based on the observed hourly air and water temperatures. Implicit is an assumption that the temperature at the air-water interface equals the measured water temperature (at 2 cm depth). If winds are calm this assumption is likely to overestimate the temperature at the water interface at night and underestimate it during the day. Because calms are more frequent at night the overall bias would be a small overestimation of surface temperature and a bias toward overstating instability. This very small effect would cause a very slight overstating of the deposition velocities.

4.5.4 Assumptions Presumed to be Approximately Bias Neutral

The following assumptions were made as part of the analysis and are intended to support reasonable estimates of the rate of deposition. Though they may introduce a bias, the direction (sign) is not readily apparent.

- Neglecting the effects of particle growth may introduce a small negative bias in total particle mass deposition. For large and very small particles (< 0.5 µm), hygroscopic increase in particle size over the Lake would increase deposition velocities, so neglect of this particle growth may under estimate deposition rates. However, for the minor fraction of particles in the 0.5 – 1 µm size range, deposition velocity would be decreased with an increase in particle size. For LTADS, a small negative bias is expected because most of the observed mass is in the size ranges for which deposition velocities are increased with particle diameter.

- Neglecting the effects of breaking waves and spray underestimates annual deposition rates for particles at Lake Tahoe by less than one percent. See Section 4.3.2.4 for the background information and observations that support this quantification.

- Aerodynamic roughness length, Z_0, over open water was calculated based upon wind speed as shown in **equation 4.9**. This is expected to be bias neutral.

4.6 Variations in Deposition Velocity

The deposition velocities calculated from the meteorological data in this analysis exhibited significant temporal variation as well as spatial variation between near-shore and open-water areas. The significant temporal variation in calculated deposition velocities was associated mainly with the daily variation in wind speed and direction. In contrast, relatively small differences were found between the averaged deposition velocities calculated from the meteorological data of the different sites.

4.6.1 Temporal Variations in Deposition Velocity

Figures 4-25 through 4-27 illustrate the diurnal variations in deposition velocities based on the meteorological data from specific sites. The deposition velocities are averaged by hour of day across a seasonal period to provide a 24-hour representation of the diurnal course of deposition velocity. The averaging masks day-to-day differences in meteorology, highlighting the effects of the slope flows and land-Lake breezes that tend to repeat at similar times each day. Deposition velocities shown are examples based on meteorological data from a few specific sites. The complete list of sites included the U.S. Coast Guard pier on the northwest shore (about 3 km northeast of Tahoe City), Tahoe Vista pier on the north shore west of Incline Village, Cave Rock boat launch on the east shore, Timber Cove pier in the City of South Lake Tahoe, Sunnyside pier on the west shore (about 3 km south of Tahoe City), and TDR1 and TDR2 buoys (respectively located approximately about 3 km east of Meeks and Emerald Bays).

The estimates of deposition velocity for soluble and reactive gases (shown in **Figures 4-25 and 4-26**) are directly dependent on meteorological conditions because they are estimated as the inverse of the aerodynamic resistance. Deposition velocities for open water areas (and for the near-shore zone during onshore flow) are shown in **Figure 4-25** and are based on meteorological data from the Coast Guard and Timber Cove piers. The estimates for the mid-Lake open water areas are independent of wind direction. Their daily variation is due primarily to changes in wind speed and secondarily to changes in the air-water temperature difference. The summer average of hourly deposition velocity for gases at the U.S. Coast Guard pier is less than 0.2 cm/s for two hours between sunrise and mid morning. In the spring the hourly average peaks at about 0.7 cm/s in late afternoon when the wind speed typically is highest. The range of variation can be much greater on a daily basis than is apparent in the averages.

Deposition velocities predicted for the shore zone, seasonally averaged by hour of day, are illustrated in **Figure 4-26** along with the same mid-lake deposition velocities as were shown in **Figure 4-25**. The large variations in the shoreline deposition velocities are the result of the changes in wind direction and associated assignments of Z_0. The diurnal variation in the seasonally averaged near-shore deposition velocity mainly reflects the relative frequency of onshore versus offshore flow by hour of day. The upper curves (near-shore deposition velocity) dip toward the lower curves (mid-lake deposition velocity) for hours with offshore flow. Recall that for individual hours of onshore flow the shoreline and mid-lake deposition velocities are equal by definition. In contrast, for

hours of offshore flow, due to sensitivity of the aerodynamic resistance to the larger roughness length assumed over land, the deposition velocity at the shoreline is generally set to the maximum allowed value (which was a cap of 6 cm/s for the central estimate shown here). Thus the seasonally averaged deposition velocity at the shoreline approaches 6 cm/s during hours that wind direction is generally offshore and approaches the smaller mid-Lake value during hours that the wind is generally onshore.

These figures illustrate that the deposition velocities of gases for the near shore zone are sensitive to both the cap that is assumed for the maximum deposition velocity and the fraction of time when the wind direction is offshore. However these values are applied over a relatively small fraction of the Lake. For the calculation of deposition rates, the average of the shoreline and mid-lake deposition velocities is applied to the near-shore zone defined as the waters within 1 km of shore and constituting 20 percent of the area of the Lake. This is the arithmetic equivalent of assuming a linear decay of the deposition velocity, from the shoreline value to mid-Lake value at a distance of 1 km from the shore.

Deposition velocities for particles, estimated for the near shore and mid-lake areas, are shown in **Figures 4-27**. For estimation of the particle deposition, seasonal deposition velocities were calculated for each hour of the day just as was done for the gases (shown in **Figures 4-25 and 4-26**). However, to simplify **Figure 4-27**, to highlight the dependence of deposition velocity on particle size, and to illustrate the differences between near-shore and mid-lake deposition velocities, seasonal values are not plotted. Instead, the plotted values for each site are the average by hour of day for the entire year. For these plots, a maximum value of 6 cm/s was assumed for $1/R_a$ and particle diameters were assumed to be 2, 8, and 20 µm, corresponding to the central estimate assumptions.

With the scale necessary to accommodate the larger shoreline deposition velocities, the diurnal variation in mid-lake deposition velocities is less noticeable. However, the annual average of the mid-lake deposition velocity varies by about a factor of 3 with time of day for 2 µm particles. For the mid-lake area, the estimated deposition velocity of an 8 µm particle is several times greater than that of a 2 µm particle, and similarly the deposition velocity of a 20 µm particle is about 5 times larger than that of an 8 µm particle.

The annual curves are smoothed by the seasonal progression in the times of sun rise and sun set and the changes in sun angle that power the upslope-downslope and lake-land breezes. However, the daily and seasonal changes in air-water temperature difference have sufficient effect on the local winds that the patterns of their influence are apparent in the diurnal variation of the estimated deposition velocities even after averaging on an annual basis.

It is clear that the estimate of deposition velocity at the shoreline for each particle size is driven mainly by the wind direction and the assumed capping value for $1/R_a$. Note that the upper limit of the seasonally averaged estimates of deposition velocity at the

shoreline is set by the particle size and the assumed capping value of 6 cm/s for $1/R_a$, which is typically invoked during offshore flow. The lower limit of deposition velocity in the near shore area occurs during hours of onshore flow when it is equal to the deposition velocity calculated for open water areas. The seasonally averaged shoreline deposition velocity approaches these limits during hours of the day when the wind direction is fairly consistently either offshore or onshore.

The similarity in daily patterns of deposition velocities calculated from meteorological observations at the U. S. Coast Guard and Sunnyside piers on the north and west shores is striking (**Figure 4-27**). These similarities evidence the significant influence of the locally generated upslope/downslope and onshore/offshore wind patterns. The small differences between the two sites in estimates of near shore deposition velocities are mainly due to differences in the persistence of offshore flow.

It is apparent that for the near shore zone during hours with offshore winds the relative change in estimated deposition velocity with increasing particle size is smaller than for open water areas. This shows the influence of the large value assumed for $1/R_a$ (6 cm/s) compared to a much smaller value calculated for open water areas. The sensitivity of the aerodynamic resistance and deposition velocity to the aerodynamic roughness length is quite evident.

Figure 4-25. Seasonally averaged hourly deposition velocities for soluble or reactive gases by hour of day over open waters of the mid Lake.

Station name is source of meteorological observations.

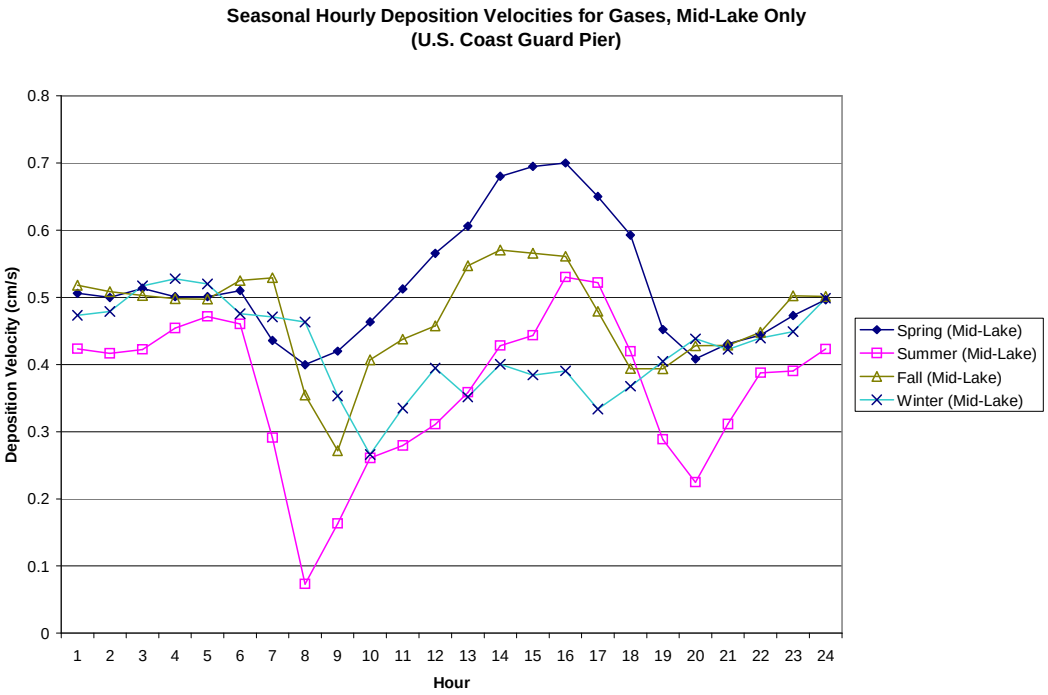

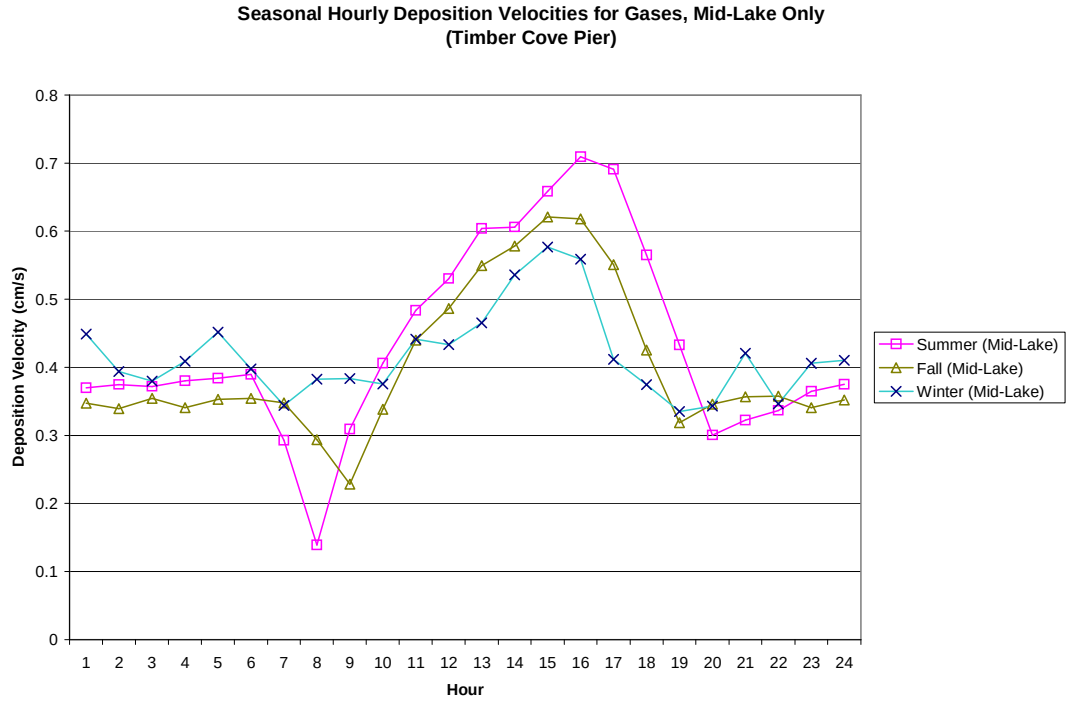

Figure 4-26. Seasonally averaged hourly deposition velocities for soluble or reactive gases by hour of day near the shoreline (upper curves) and over open mid-lake waters (lower curves).

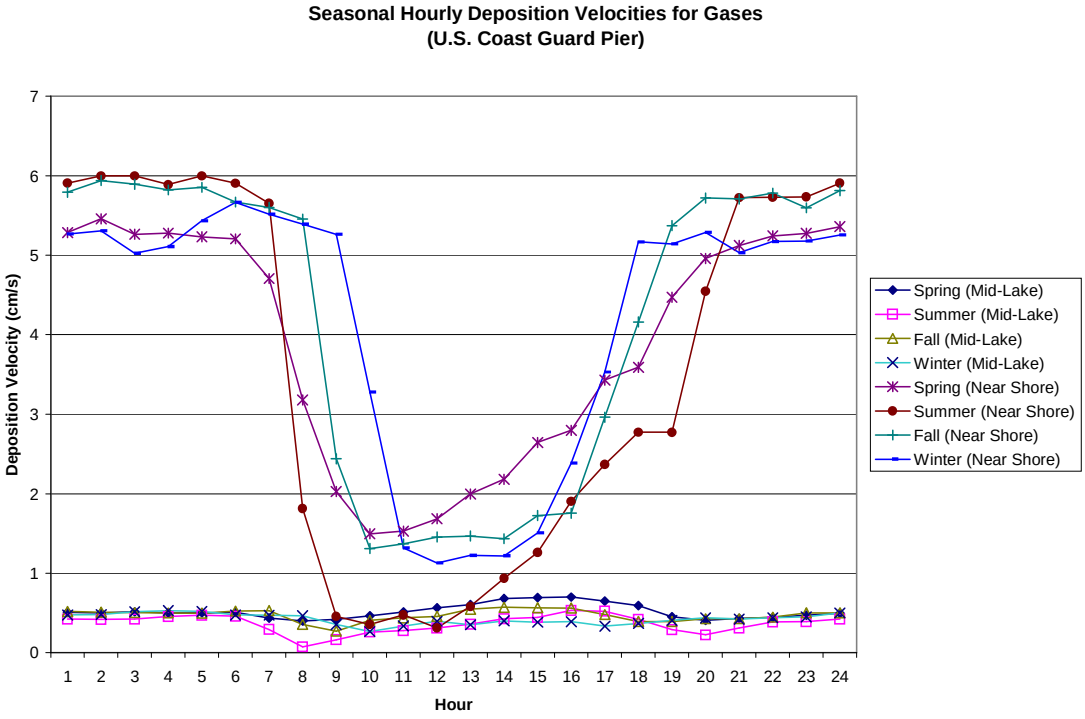

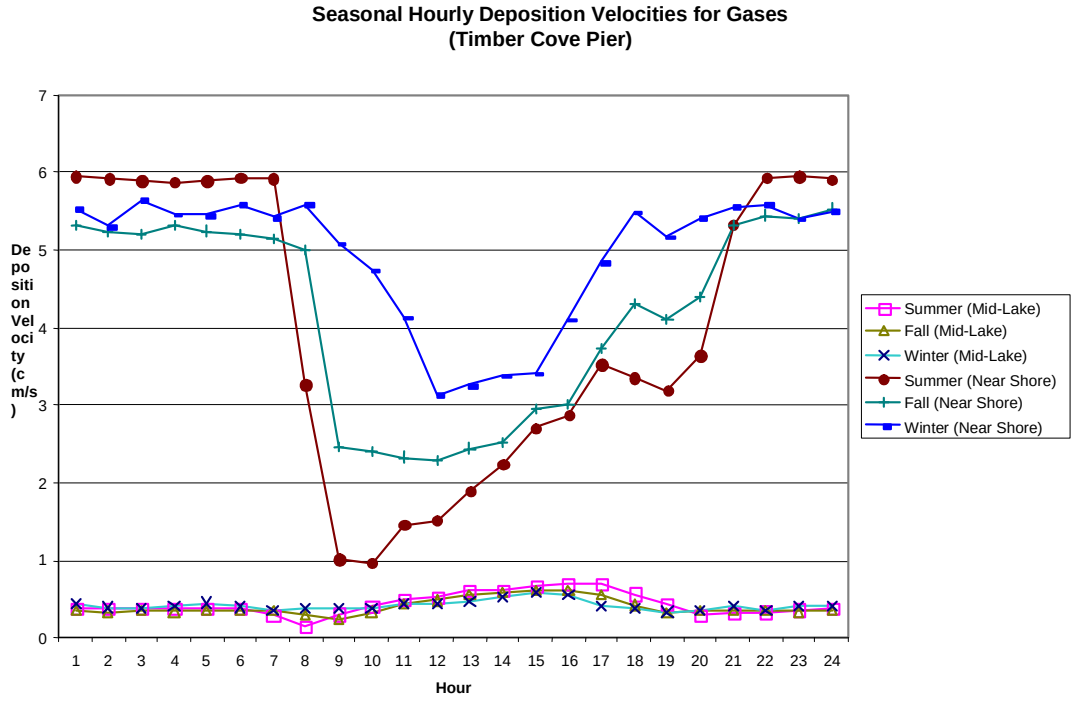

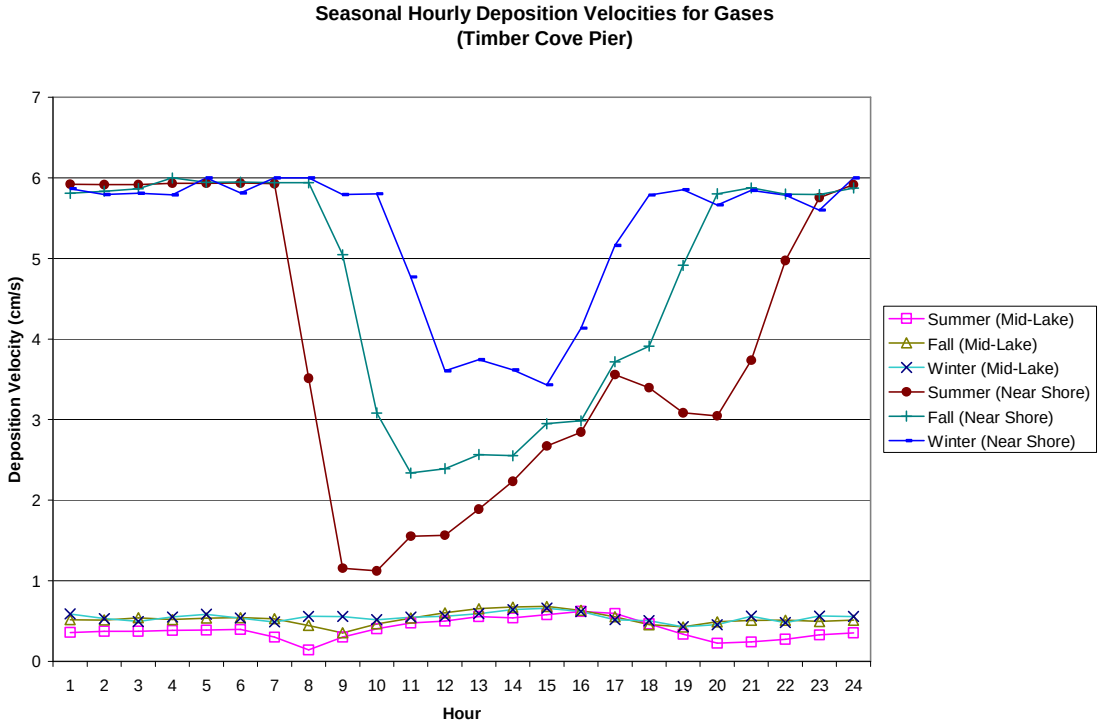
Seasonal Hourly Deposition Velocities for Gases
(Timber Cove Pier)
Deposition Velocity (cm/s)
0
1
2
3
4
5
6
7
1 2 3 4 5 6 7 8 9 10 11 12 13 14 15 16 17 18 19 20 21 22 23 24
Hour
Summer (Mid-Lake)
Fall (Mid-Lake)
Winter (Mid-Lake)
Summer (Near Shore)
Fall (Near Shore)
Winter (Near Shore)

Figure 4-27. Annual averages of estimated hourly deposition velocities by hour of day, for particles of diameter 2, 8, and 20 µm on based on meteorology from U.S. Coast Guard and Sunnyside piers.

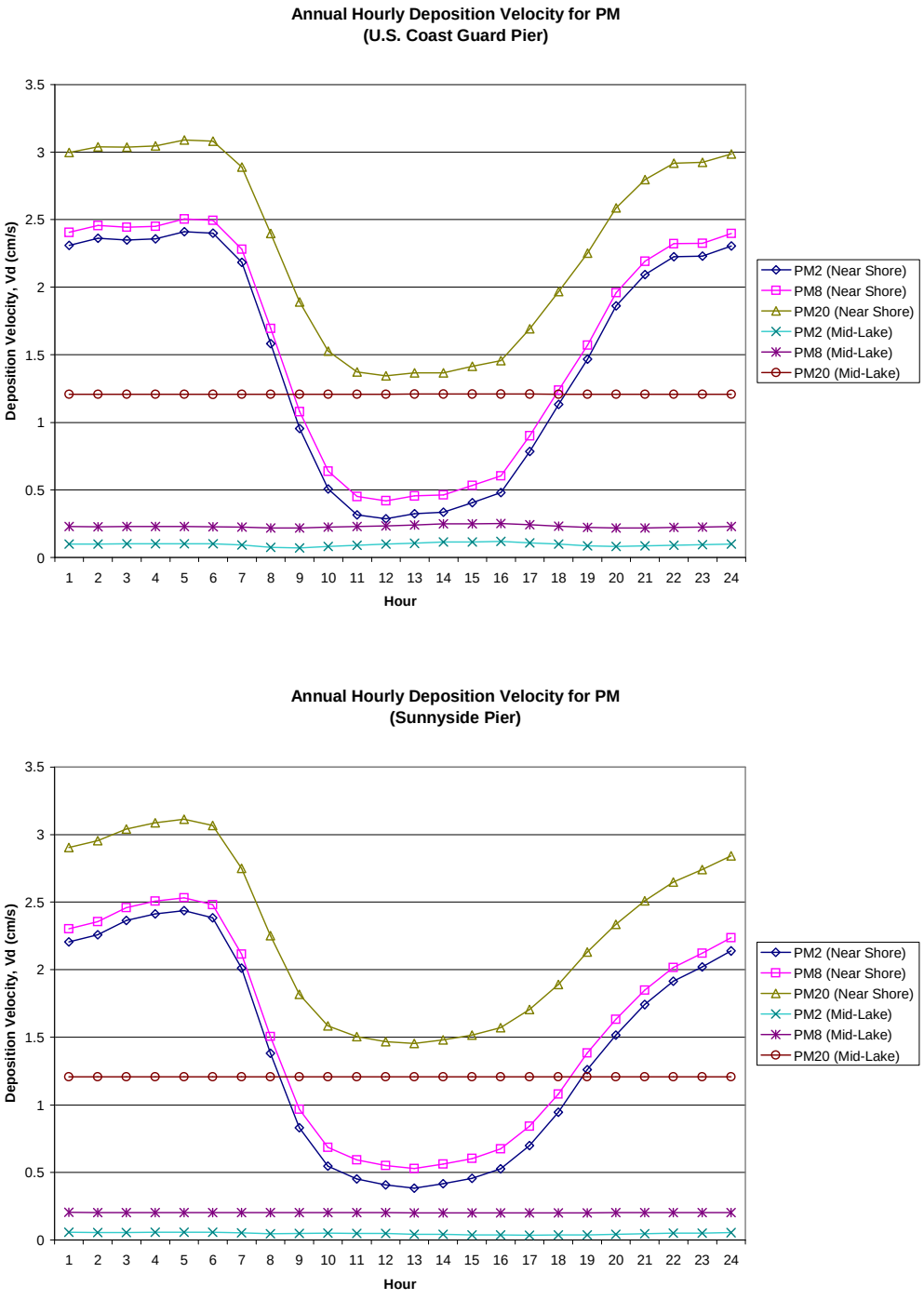

Table 4-9 displays estimates of the annual averaged deposition velocities for three sites. Deposition velocities for gases are followed by deposition velocities for characteristic particle sizes grouped according to the assumptions for the lower bound (1, 5, 15 μm), best (2, 8, 20 μm), and upper bound (2.5, 10, 25 μm) estimates. Estimates are shown for the weighted average of near-shore and mid-lake areas, "composite", and for these areas individually. The composite deposition velocity for the Lake as a whole is simply the weighted average of the near-shore and mid-lake areas (20 and 80 percent respectively). The lower deposition velocities for mid-lake areas are presumed to be the more reliable numbers. The larger deposition velocities for the near-shore zone are a consequence of the conservative capping values (of 3, 6, and 10 cm/s for $1/R_a$). Notice that the relative differences in deposition velocity, between near-shore and mid-lake zones, are greater for the gases and fine particles than for large particles.

Seasonal averages are calculated based upon the hours in each three month season for which data is reported. The U.S. Coast Guard pier site operated in all four seasons, however, Buoy TDR2 did not report data for any of the winter months and Timber Cove reported no data for the spring months. Thus differences in wind speeds and estimated deposition velocities between SE Buoy TDR2 and Timber Cove may be due in part to seasonal differences in data recovery.

Table 4-9. Comparison of annual average deposition velocities estimated based upon meteorological observations from three sites (with the assumption that $1/R_a$ is capped at a maximum of 6 cm/s).

Differences in wind speeds and estimated deposition velocities between SE Buoy TDR2 and Timber Cove may be due in part to seasonal differences in data recovery at these sites.

Sites		US Coast Guard Pier				SE Buoy, TDR2				Timber Cove			
Gas or PM-size	Characteristic Particle Diameter	Wind Speed (m/s)	**Deposition Velocities (cm/s)** Composite	Near-shore	Mid-Lake	Wind Speed (m/s)	**Deposition Velocities (cm/s)** Composite	Near-shore	Mid-Lake	Wind Speed (m/s)	**Deposition Velocities (cm/s)** Composite	Near-shore	Mid-Lake
Gases	N/A	2.9	0.8	2.1	0.5	2.9	0.8	1.9	0.5	3.1	0.8	2.2	0.4
PM-Fine	1.0		0.3	1.1	0.1		0.2	0.8	0.1		0.2	0.8	0.1
PM-Coarse	5.0		0.3	1.1	0.2		0.3	0.9	0.2		0.3	0.9	0.2
PM-Large	15.0		0.9	1.6	0.7		0.9	1.4	0.7		0.9	1.4	0.7
PM-Fine	2.0		0.3	1.1	0.1		0.3	0.9	0.1		0.2	0.8	0.1
PM-Coarse	8.0		0.5	1.2	0.3		0.4	1.0	0.3		0.4	1.0	0.3
PM-Large	20.0		1.4	2.1	1.2		1.4	1.9	1.3		1.4	1.8	1.2
PM-Fine	2.5		0.3	1.1	0.1		0.3	0.9	0.1		0.2	0.8	0.1
PM-Coarse	10.0		0.6	1.3	0.4		0.5	1.1	0.4		0.5	1.0	0.4
PM-Large	25.0		2.1	2.7	1.9		2.0	2.5	1.9		2.0	2.5	1.9

4.7 Calculated Dry Deposition

The deposition rates, calculated as described in the previous sections, are presented and examined in this section. To summarize, the Lake was modeled as having four quadrants. Seasonal average concentrations of nitrogen species, phosphorus and PM mass were constructed from the TWS observations at representative sites in three quadrants and were estimated for a fourth quadrant based upon ratios of concentrations observed with shorter duration samples and at monitoring sites with the TWS. Diurnal variation in particle concentrations as averaged on a seasonal basis were inferred from observations of three particle size fractions obtained from BAMs collocated with the TWS. The seasonal diurnal concentrations were multiplied by a seasonally averaged diurnal deposition velocity based on data from a nearby meteorological site.

For more conservative estimates of dry deposition (in the previous draft report and Appendix L), concentrations measured on land were assumed to be representative of both the near shore and open water areas of the Lake. Although this is a conservative approximation, recall that the TWS integrates over periods of both offshore flow when concentrations were relatively high and onshore flow when the concentrations were typically lower.

The estimates of deposition presented here are less conservative but more realistic. We agreed with reviewer comments that the assumption of no depletion for PM and phosphorus would make those estimates overly conservative and reduce their utility for comparison with estimates of other types of inputs to the Lake. Thus we have assumed modest decreases in concentrations of PM and phosphorus (but not nitrogen) over the Lake compared to the concentrations measured on land. The assumed reductions were selected based on the results of the short term monitoring (Section 4.4) and the factors discussed in Section 4.5.1.

On the other hand, nitrogen concentrations were assumed not to decrease over the Lake. The nitric acid and ammonia which dominate the total nitrogen deposition appear to be relatively well distributed vertically so that vertical mixing over the Lake would refresh surface concentrations. This is the case for several reasons. The time scales necessary for chemical conversion of the directly emitted NO and NO_2 into nitric acid would allow extensive mixing and thereby cause local horizontal and vertical gradients in concentrations to be relatively small. Ammonia gas also appears to be well distributed in the vertical.

4.7.1 Estimates of Annual Dry Deposition to the Lake

Lower, central, and upper estimates of dry deposition provided here all assume the same modest reduction in PM and phosphorus concentrations on the urban zones of the Lake relative to the measured concentrations at the urban monitoring sites. The differences between the lower, central, and upper estimates are based on the following factors.

For estimates of dry deposition of gases (nitric acid and ammonia) only the assumed caps on 1/Ra cause variation between the lower, central and upper estimates. The assumptions influencing deposition of particles include the assumed cap for $1/R_a$ and the assumed particle sizes for calculation of deposition velocities for each of the three measured particle size fractions. The range of assumed maximum values capping $1/R_a$ primarily affects the estimates of dry deposition of the gases nitric acid and ammonia, and to a lesser extent the deposition velocity for fine particles. The assumed cap values have relatively little effect on deposition velocity for large particles. The estimates for deposition of phosphorus are influenced by the assumptions that influence the PM deposition estimates and also by assumptions about the distribution of phosphorus between size fractions. However, the assumed total concentration of phosphorus (40 ng/m^3) was the same for the lower, central, and upper estimates.

Although the same total concentration of phosphorus (40 ng/m^3) was assumed for the lower, central, and upper estimates, differences were assumed in how the phosphorus was apportioned between particle size fractions and in the characteristic diameters for those size fractions). For the lower estimate, the phosphorus was assumed to be mainly in the fine fraction, with 32 ng P/m^3 in PM2.5 and 8 ng P/m^3 in PM_coarse, This distribution is unlikely because phosphorus appears to be mainly of geological origin, not combustion, and thus it is more probably mainly in the coarse and large fractions. Accordingly, for the central estimate the phosphorus was assumed to be distributed 20, 60, and 20 percent between the three size fractions, i.e., with 8, 24 and 8 ng of P/m^3 in PM2.5, PM_coarse, and PM_large. For the upper limit estimate the same distribution between size fractions was assumed as for the central estimate, but with larger characteristic diameters. As it was assumed that PM concentrations in each size fraction were decreased in the north and south urban quadrants, by a modest percent compared to the observed concentrations at Lake Forest and Sandy Way, so also were phosphorus concentrations assigned to each of the same size fractions assumed to be reduced by the same factors in those two quadrants.

Tables 4-10, 4-11, and 4-12 show the lower, central, and upper estimates of seasonal and annual dry deposition in metric tons. The three estimates assume the same modest decrease in PM and phosphorus concentrations for the urban zones of the Lake. The nitrogen deposition estimates assume no decrease over the Lake relative to concentrations at the monitoring sites. Note that the expected accuracy of the estimates is not supportive of more than one significant figure; non-significant figures are included to allow the reader to compare the effects of the underlying assumptions (lower, central, and upper) upon the resulting estimates of dry deposition.

The estimates of annual dry deposition for total nitrogen range from 70 to 170 metric tons, with a central estimate of about 120 metric tons (MT). Estimates of annual PM mass deposition range from less than 400 to 900 MT, with a central estimate of 600 MT. The lower estimate of annual phosphorus deposition (less than 1 metric ton) assumes a phosphorus concentration of 40 $nanograms/m^3$ for all quadrants and hours but assigns it (80%) to fine particles with a characteristic diameter of 1 μm and 20% to particles with a characteristic diameter of 5 μm. The decrease in phosphorus concentration in each

size fraction is the same relative change as assumed for the PM fractions (for the urban quadrants). The central and upper bound estimates for dry deposition of phosphorus range from 2 to 3.6 metric tons. Both assumed phosphorus concentrations of 40 ng/m^3 assigned 80% and 20% to the coarse and large fractions. For the central estimate reasonable values of characteristic diameters were assumed for each PM size fraction. For the upper estimate larger characteristic diameters were assumed. Similarly, for the upper bound estimate an extreme value was assumed for the cap on $1/R_a$. Although **Tables 4-10, 4-11, and 4-12** present useful estimates for deposition of PM for the Lake a whole, the assumption that phosphorus concentrations remain constant at 40 ng P/m^3 in the east and west quadrants but decrease offshore in the north and south quadrants is not as satisfactory.

On the other hand, a lower but still reasonable alternative estimate of phosphorus deposition is also possible (but not included in the tables and not carried forward as an official estimate). The alternative assumption is that the phosphorus concentrations are best scaled directly from the PM concentrations in each size fraction. From the mix of emission sources at Tahoe, the estimated phosphorus contents of PM2.5, PM_coarse, and PM_large were estimated to be 0.07, 0.17, and 0.19 percent respectively. Applying these values for phosphorus content and the estimated PM deposition in each size fraction lowers estimates of phosphorus deposition by a factor of two and provides a closer link to the PM mass observations. This calculation provides a central estimate of annual dry deposition of phosphorus in the amount of 1 metric ton and an upper estimate of 1.5 metric ton. Thus, it is our expectation that the true value for annual phosphorus deposition is less than 2 metric tons.

Table 4-10. Lower bound estimates with modest depletion of mid-lake phosphorus and PM concentrations. Gaseous nitrogen (GN), aerosol nitrogen (AN), total nitrogen (TN = GN +AN), aerosol phosphorus (AP), and mass from all sizes of PM. N species concentrations were assumed to be depleted at mid Lake relative to land observations. Assumes CAP on $1/R_a$ is 3 cm/s, particle deposition velocities are based on assumed diameters of 1, 5 and 15 microns for PM2.5, PM_coarse, and PM_large. Assumes a phosphorus concentration of 40 ng/m^3 (mostly in the fine fraction, with 32 ng/m^3 in PM2.5, 8 ng/m^3 in PM_coarse, and none in PM_large). Concentrations of phosphorus, PM2.5, PM_coarse and PM_large in the north (and south) quadrants were assumed to be equal to the concentrations observed at LF (or SW for the south quadrant) less 25 percent of the difference between LF and TB (or SW and TB) concentrations.

1_5_15	Season	HNO3	NH3	GN	NH4	NO3	AN	TN	AP	PM2.5	PMcrs	PMlrg	Mass
USCG-LF	Spring	0.4	2.5	2.9	0.2	0.3	0.5	3.4	0.05	3	11	24	37
	Summer	0.7	4.2	4.9	0.0	0.4	0.4	5.3	0.04	4	8	30	42
	Fall	1.1	5.5	6.7	0.2	0.2	0.4	7.1	0.04	4	10	22	36
	Winter	0.4	4.4	4.8	0.1	0.0	0.2	5.0	0.04	4	11	9	24
	Annual	2.6	17	19	0.6	0.9	1.5	21	0.16	15	39	85	140
TC-SW	Spring	1.3	5.3	6.6	0.3	0.3	0.6	7.2	0.05	5	10	16	31
	Summer	1.7	6.3	7.9	0.4	0.6	1.0	8.9	0.04	5	7	28	40
	Fall	2.6	9.0	11.6	0.3	0.4	0.6	12.3	0.05	8	10	16	34
	Winter	2.6	6.1	8.7	0.2	0.2	0.4	9.1	0.04	9	14	39	61
	Annual	8.1	27	35	1.1	1.5	2.6	37	0.18	26	40	100	170
CR-TB	Spring	0.3	0.6	0.8	1.0	0.5	1.4	2.3	0.05	2	3	3	7
	Summer	0.5	1.1	1.7	0.9	0.5	1.5	3.2	0.04	2	3	3	9
	Fall	0.5	1.4	1.9	0.7	0.4	1.1	3.0	0.04	2	3	2	7
	Winter	0.4	0.5	1.0	0.3	0.2	0.5	1.4	0.05	2	1	2	6
	Annual	1.8	3.6	5.4	2.8	1.6	4.5	9.9	0.18	9	10	10	29
SS-BL	Spring	0.3	0.3	0.5	0.3	0.1	0.5	1.0	0.03	1	2	1	5
	Summer	0.4	0.9	1.3	0.5	0.3	0.7	2.0	0.03	2	3	3	7
	Fall	0.5	1.4	1.9	0.3	0.2	0.5	2.4	0.04	2	2	2	7
	Winter	0.3	0.4	0.7	0.1	0.1	0.2	1.0	0.04	1	1	2	5
	Annual	1.5	3.0	4.5	1.2	0.7	1.9	6.4	0.14	6	8	9	23
All Lake	Spring	2.2	8.7	11	1.8	1.2	2.9	14	0.18	10	25	45	80
	Summer	3.3	13	16	1.8	1.7	3.6	19	0.14	13	21	64	98
	Fall	4.8	17	22	1.5	1.2	2.7	25	0.16	16	25	43	84
	Winter	3.7	12	15	0.7	0.6	1.3	16	0.17	16	26	53	95
	Annual	14	50	64	6	5	10	74	0.66	56	100	200	360

Table 4-11. Central estimates of seasonal and annual dry deposition to Lake Tahoe (metric tons/year) with modest depletion of concentrations of PM and phosphorus over the Lake.

Gaseous nitrogen (GN), aerosol nitrogen (AN), total nitrogen (TN = GN + AN), aerosol phosphorus (AP), and mass of all sizes of PM. Assumes CAP on $1/R_a$ is 6 cm/s, particle deposition velocities are based on assumed diameters of 2, 8, and 20 microns for PM2.5, PM_coarse, and PM_large. Assumes a phosphorus concentration of 40 ng/m^3, distributed between PM2.5, PM_coarse, and PM_large with 8, 24, and 8 ng of P/m^3 respectively.

2_8_20	Season	HNO3	NH3	GN	NH4	NO3	AN	TN	AP	PM2.5	PMcrs	PMlrg	Mass
USCG-LF	Spring	0.6	3.7	4.2	0.3	0.4	0.7	5.0	0.13	3	17	42	62
	Summer	1.0	6.4	7.4	0.1	0.6	0.7	8.1	0.12	4	14	53	72
	Fall	1.7	8.3	10	0.3	0.4	0.7	11	0.13	4	17	39	60
	Winter	0.6	6.8	7.3	0.2	0.1	0.3	7.6	0.12	4	18	17	39
	Annual	3.9	25	29	1.0	1.5	2.5	31	0.50	16	67	150	230
TC-SW	Spring	1.9	7.8	9.7	0.5	0.5	1.0	11	0.13	5	16	29	49
	Summer	2.5	9.5	12	0.6	1.0	1.6	14	0.13	6	12	49	67
	Fall	4.0	14	18	0.5	0.6	1.1	19	0.13	9	16	28	52
	Winter	4.0	9.4	13	0.3	0.4	0.6	14	0.12	9	21	68	98
	Annual	12.3	40	53	1.8	2.5	4.3	57	0.51	28	65	170	270
CR-TB	Spring	0.4	0.8	1.3	1.6	0.8	2.4	3.7	0.16	2	5	5	12
	Summer	0.9	1.9	2.7	1.7	0.9	2.6	5.3	0.15	3	7	5	15
	Fall	0.9	2.2	3.1	1.1	0.8	1.9	5.0	0.15	3	5	4	12
	Winter	0.7	0.8	1.5	0	0.4	0.8	2.3	0.16	2	2	4	9
	Annual	2.8	5.8	8.6	4.9	2.8	7.7	16	0.62	9	19	18	47
SS-BL	Spring	0.4	0.5	0.9	0.6	0.2	0.8	1.7	0.15	1	4	3	8
	Summer	0.7	1.6	2.3	0.8	0.5	1.3	3.6	0.15	2	6	5	14
	Fall	0.9	2.3	3.1	0.6	0.4	0.9	4.1	0.15	2	5	4	11
	Winter	0.5	0.7	1.2	0.2	0.2	0.4	1.6	0.15	1	2	4	7
	Annual	2.5	5.0	7.5	2.2	1.2	3.4	11	0.59	7	18	16	40
All Lake	Spring	3.3	13	16	3.0	2.0	5.0	21	0.57	11	42	78	130
	Summer	5.0	19	24	3.2	3.0	6.2	31	0.55	15	40	110	170
	Fall	7.4	26	34	2.5	2.1	4.6	38	0.56	17	43	75	140
	Winter	5.8	18	23	1.1	1.0	2.1	26	0.56	17	44	92	150
	Annual	22	76	98	10	8	18	116	2.2	60	170	360	590

Table 4-12. Upper bound estimates, with modest depletion of phosphorus and PM concentrations over the Lake.

2.5_10_25	Season	HNO3	NH3	GN	NH4	NO3	AN	TN	AP	PM2.5	PMcrs	PMlrg	Mass
USCG-LF	Spring	0.8	5.1	6.0	0.5	0.6	1.1	7.1	0.19	3	24	65	91
	Summer	1.4	9.3	11	0.1	1.0	1.1	12	0.19	5	21	82	110
	Fall	2.5	12	14	0.5	0.5	1.0	15	0.19	4	24	60	89
	Winter	0.8	9.9	11	0.4	0.1	0.5	11	0.18	4	27	26	57
	Annual	5.6	36	42	1.5	2.2	3.7	45	0.74	16	95	230	340
TC-SW	Spring	2.6	11	14	0.7	0.7	1.5	15	0.19	5	22	45	71
	Summer	3.5	14	17	0.9	1.5	2.5	20	0.19	6	18	76	100
	Fall	5.8	20	25	0.7	0.9	1.6	27	0.19	9	22	44	75
	Winter	5.9	14	20	0.4	0.5	1.0	21	0.18	9	30	110	140
	Annual	18	58	76	2.7	3.7	6.5	82	0.75	29	91	270	390
CR-TB	Spring	0.6	1.2	1.8	2.5	1.2	3.7	5.5	0.24	2	7	8	17
	Summer	1.3	2.8	4.1	2.6	1.4	4.0	8.1	0.23	3	10	8	21
	Fall	1.3	3.3	4.6	1.7	1.1	2.9	7.5	0.23	3	8	6	17
	Winter	1.0	1.2	2.2	0.6	0.6	1.2	3.4	0.18	2	3	6	12
	Annual	4.2	8.6	13	7.4	4.3	11.7	25	0.87	10	28	28	67
SS-BL	Spring	0.7	0.7	1.4	0.9	0.4	1.3	2.6	0.23	1	6	4	12
	Summer	1.1	2.5	3.6	1.3	0.7	2.0	5.6	0.22	2	10	8	21
	Fall	1.3	3.5	4.8	0.9	0.6	1.4	6.2	0.23	2	8	6	16
	Winter	0.8	1.0	1.9	0.3	0.3	0.6	2.4	0.17	2	3	6	11
	Annual	3.9	7.7	12	3.3	1.9	5.3	17	0.85	7	27	25	59
All Lake	Spring	4.7	18	23	4.6	3.0	7.5	30	0.84	11	58	120	190
	Summer	7.3	28	35	4.9	4.6	9.5	45	0.83	16	59	180	250
	Fall	11	38	49	3.8	3.2	6.9	56	0.83	18	61	120	200
	Winter	8.5	26	34	1.7	1.5	3.2	38	0.72	17	63	140	220
	Annual	31	110	140	15	12	27	170	3.2	63	240	560	860

4.7.2 Seasonal and Spatial Variations in Deposition Rates

Figure 4-28 illustrates the seasonal estimates for dry deposition of total nitrogen by Lake quadrant and chemical species, for the central estimate case (as in **Table 4-11**). It is clear that the estimate of total nitrogen deposition is dominated contributions from the south and north shores, primarily in the form of ammonia gas and secondarily in the form of nitric acid.

Similarly, **Figure 4-29** illustrates the fraction of particle mass estimated to be deposited in each of the size fractions, for the central estimate assumptions. The deposition of large particles dominates the estimate of total dry deposition of PM. The differences in observed concentrations used to represent the different quadrants were related to the densities of population and human activity in those regions but were also modified by relative proximity of activity to the sampling site. In particular, recall that Thunderbird was much farther from roadways than were the north and south quadrant sites.

The amount by which concentrations differ between the lakeshore and mid-lake and the uncertainty that difference introduces into the deposition estimates have not been quantified. The methods used are expected to provide conservative results. Decay in concentration with distance downwind is greater when the observed concentration is near a source, usually a heavily travel road, as was the case for Lake Forest, SOLA, and Sandy Way (but not Thunderbird). In the case of a line source such as a highway with steady winds, horizontal dispersion may be unimportant. However, the effect of vertical dispersion in decreasing surface concentrations with increasing distance immediately downwind from the road may be very large (because the initial vertical dispersion by mechanical mixing at the road is typically relatively shallow). Thus, small differences in conditions during an observation period would result in quite different results. The actual decay in concentration with distance from shore will depend on the deposition velocity, depth of mixing, and concentrations in and above the mixed depth and will also be affected by any change in depth of vertical mixing on land or with increasing distance downwind over the Lake.

Clearly, the number of variables involved and the difficulty of resolving spatial variations in mixing depth over the water provide challenges to predicting the variation in concentration with distance from shore. Some understanding of spatial variations in ambient particle concentrations was obtained from examination of spatial and temporal variations in observed particle counts in Section 4.4. Examining these limited observations of particle count may be more instructive than inferring possible spatial variation of concentrations from a first principles analysis or modeling without sufficient input data to adequately constrain the results. However, care must be taken in the interpretation of the observations because the processes involved in creating spatial variations in concentration over the Lake include the combined effects of source strength, deposition, horizontal and vertical dispersion, and growth of the mixing depth, with none fully quantified. Thus, the observed concentrations at a point in time should not be over-interpreted, particularly in the absence of ancillary measurements to describe the processes at work in modifying the concentrations.

The vertical extent of mixing will generally differ greatly over the Lake from that over land and those differences will vary with season and time of day. It is possible to make bounding calculations regarding differences between mid-lake and shoreline mass concentrations and deposition rates, but consulting the observed spatial and temporal variations in particle counts and associated estimates of mass concentrations are likely more useful to understanding and refining estimates of deposition.

4.7.3 Diurnal Variation in Deposition Rates

Diurnal variation in annual deposition rates for gaseous ammonia and nitric acid and PM2.5 mass are illustrated in **Figures 4-30 and 4-31**. Clearly differences are associated with choice of a site to provide meteorological data for calculation of deposition velocity. However, these differences are illustrative both of the temporal variations in deposition rates and of uncertainty contained in the estimates. The sites chosen to supply the meteorological data for calculation of the deposition velocity for each quadrant were those thought to provide the most representative observations for the quadrant and the most complete data recovery. The estimated deposition velocities and deposition rates were compared using alternative choices of sites, and estimated deposition rates were similar, except for the cases of sites with limited sampling duration or data recovery.

Figure 4-28. Contributions to total nitrogen deposition by quadrant, chemical species, and season.

Uses central estimate assumptions: maximum value of $1/R_a$ is 6 cm/s, characteristic particle diameters of PM2.5, PM_coarse, and PM_large are 2, 8, and 20 microns.

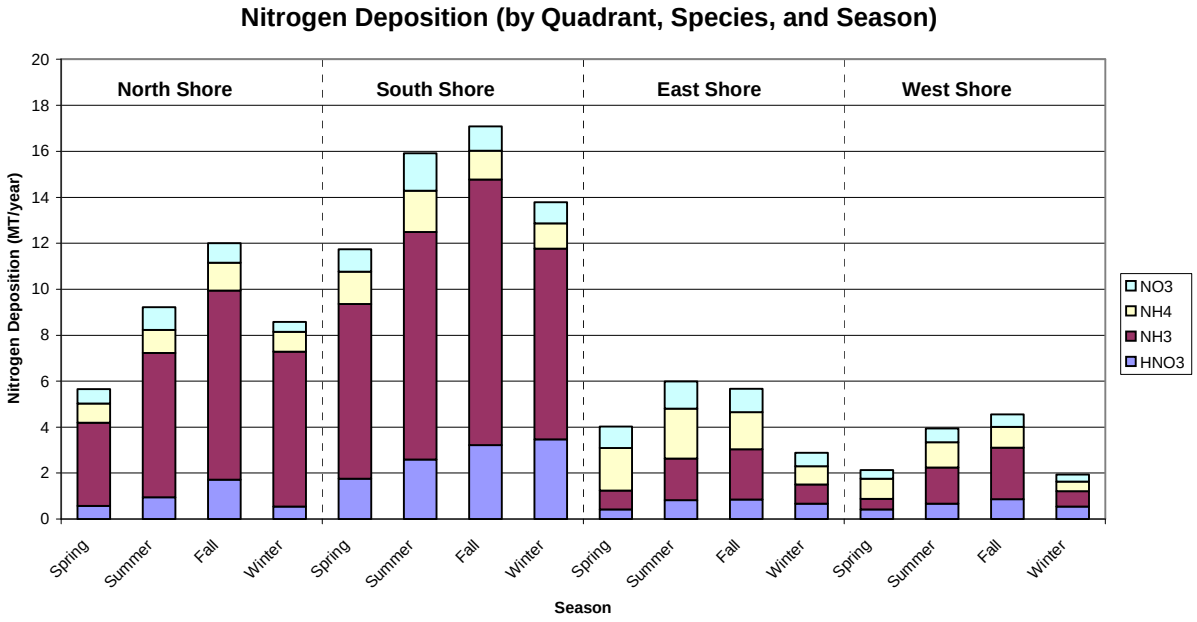

Figure 4-29. Contributions to dry deposition of particle mass, by quadrant, season, and particle size.

Uses central estimate assumptions regarding aerodynamic resistance and particle diameter corresponding to **Table 4-11**.

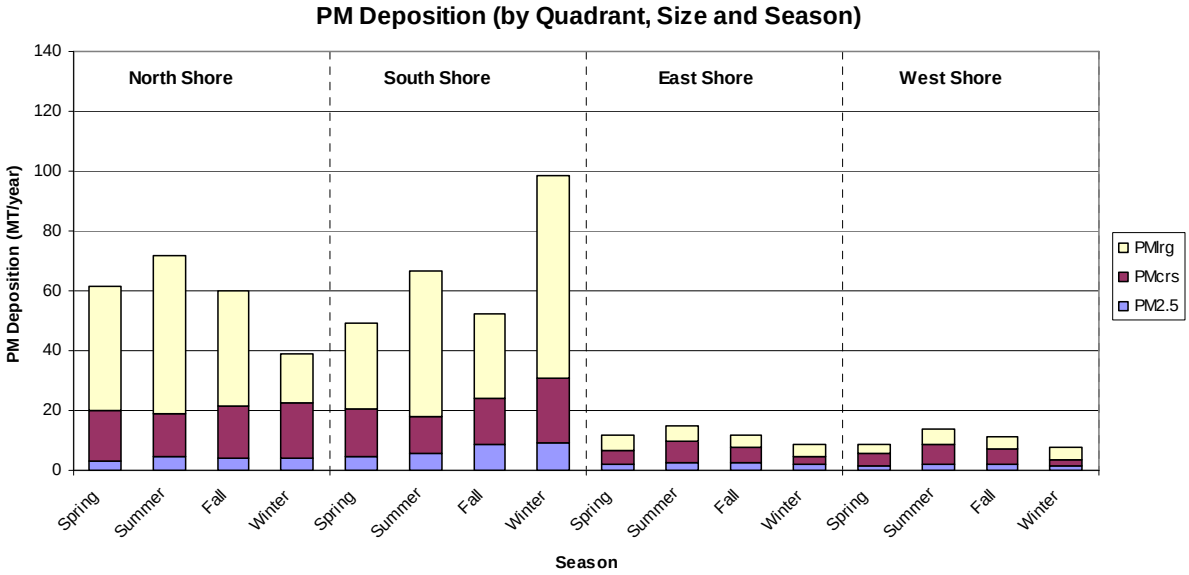

Figure 4-30. Diurnal variation in relative deposition rates of ammonia and nitric acid gas.

Time series are labeled as paired air quality and meteorological monitoring sites. All values are based upon the central estimate assumptions. Units are (ng-N/ m^3)x(cm/s).

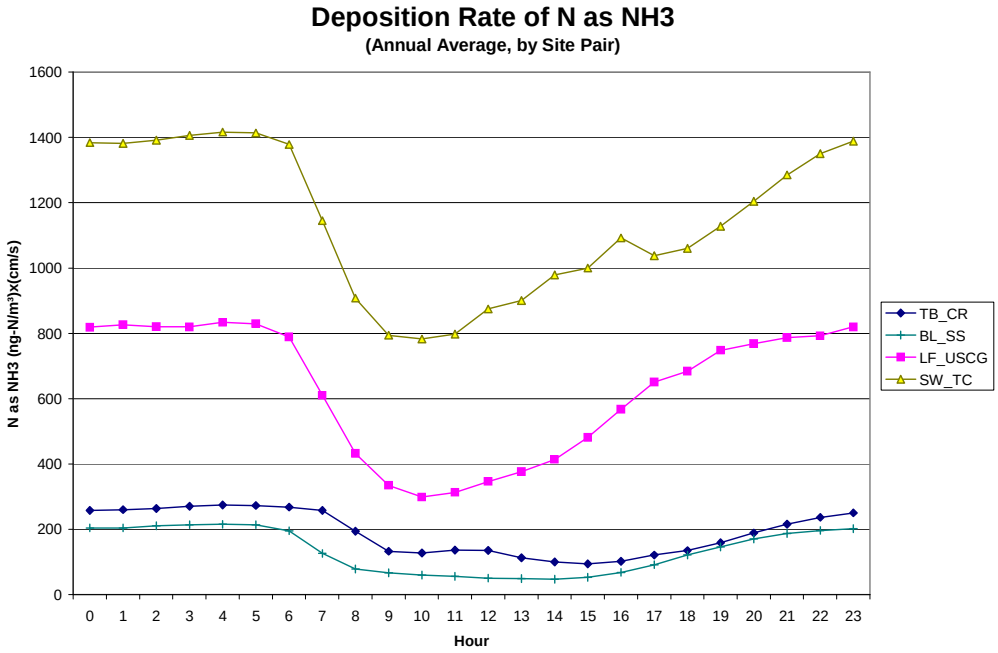

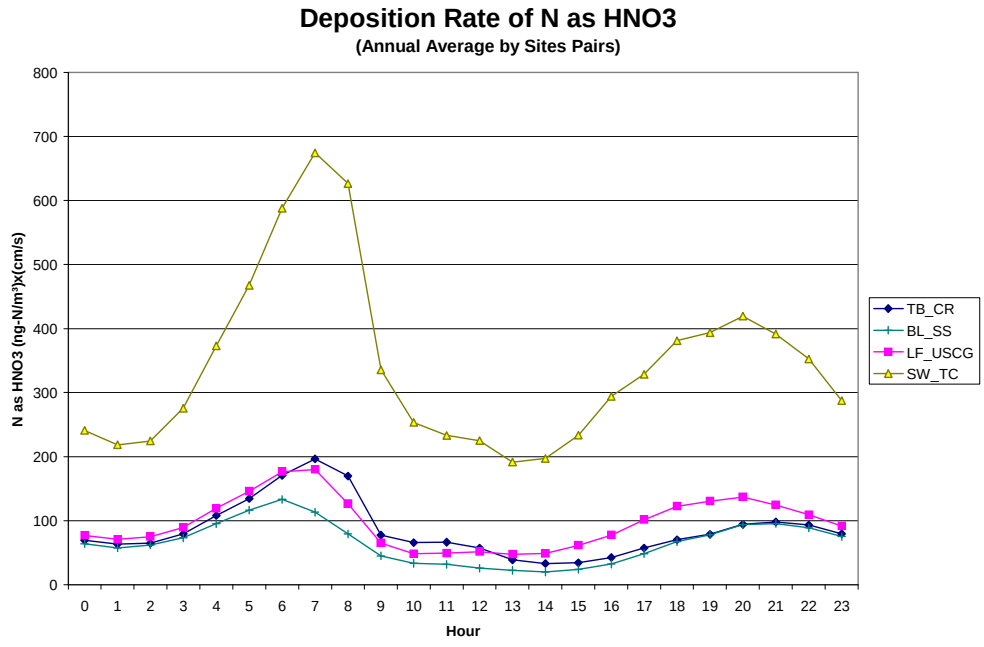

Figure 4-31. Comparison of diurnal variation in estimated mass deposition of PM2.5, PM_coarse, and PM_large for various pairs of air quality and meteorological monitoring sites.

All values are based on the central estimate assumptions. Units are [(ng/m3)x(cm/s)]. Note, vertical scale is expanded for coarse and large fractions compared to fine fraction.

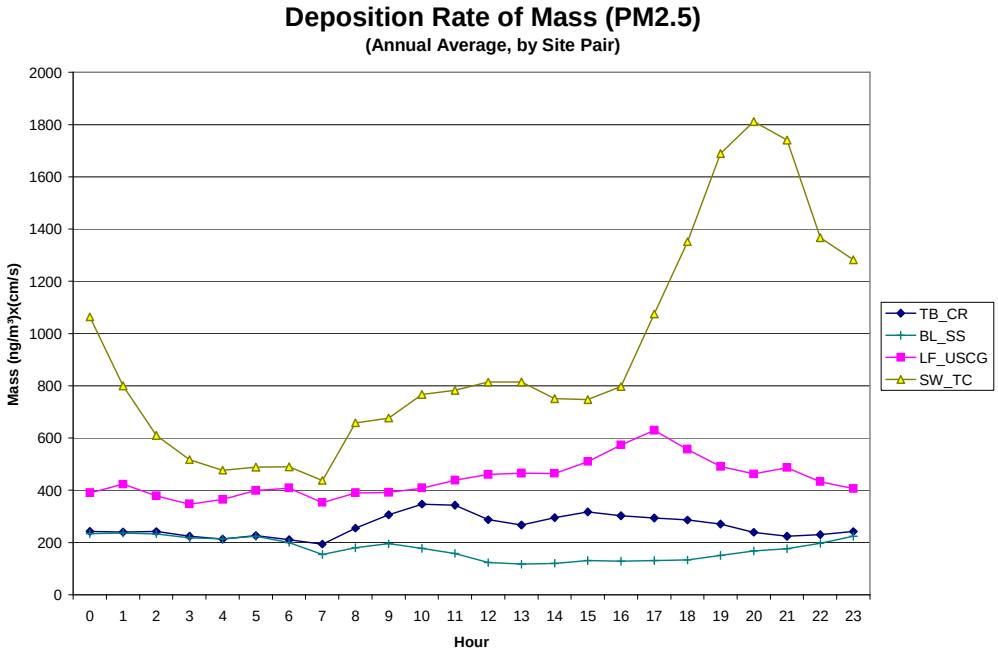

Figure 4-31 continued.

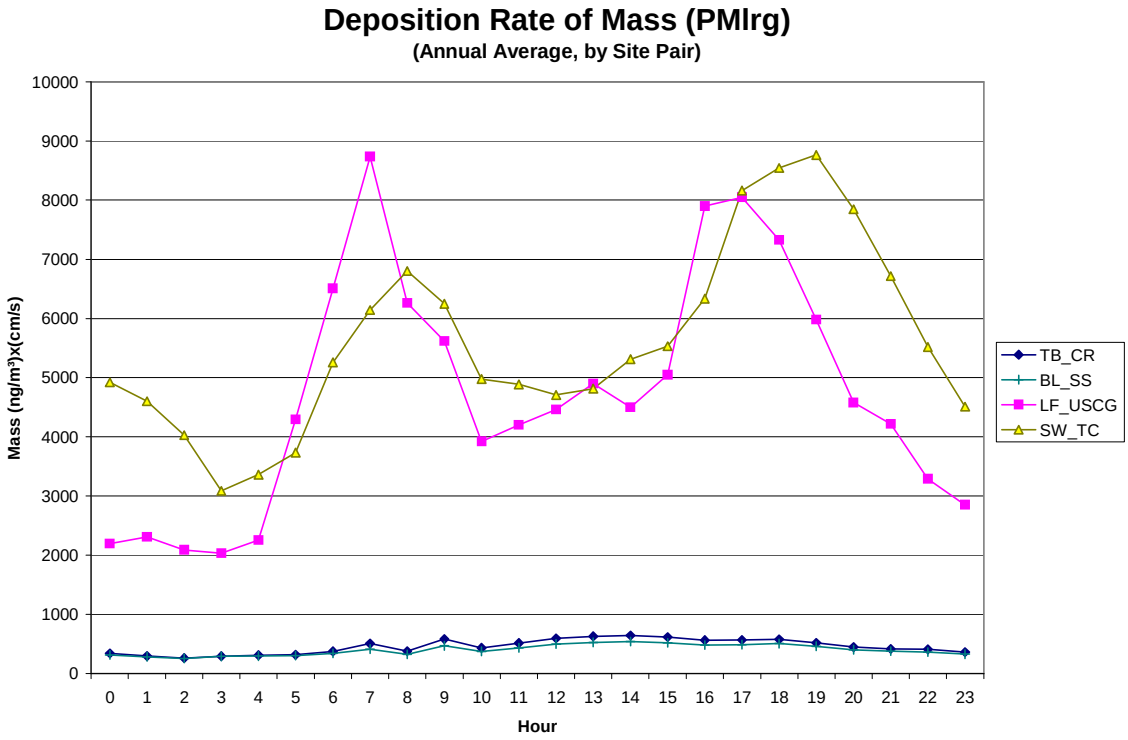

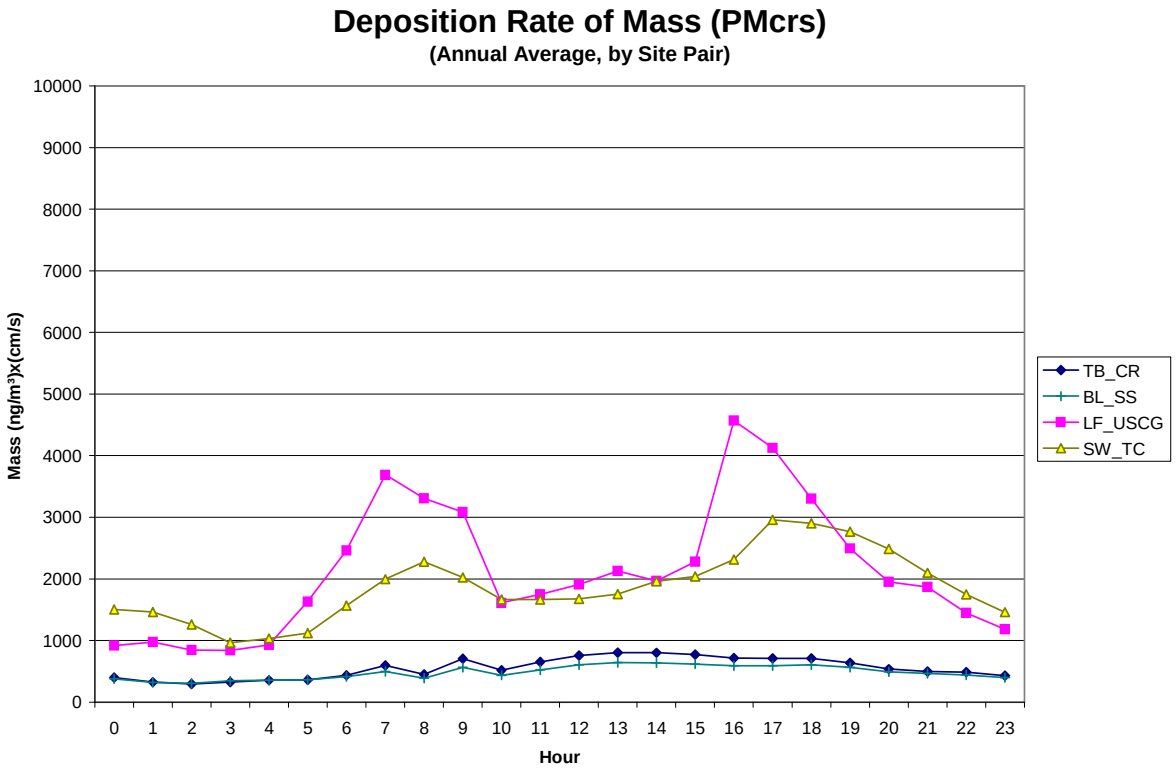

4.8 Summary

This chapter has presented the methodology used to calculate seasonal and annual dry deposition to Lake Tahoe, the assumptions used, and ranges of estimated annual dry deposition of nitrogen, phosphorus, and PM mass to the surface of Lake Tahoe. Estimates were based on the ambient concentrations and meteorology observed during LTADS. Due to difficulties in monitoring low concentrations of phosphorus, a representative concentration was assumed to be 40 ng P/m^3 for shore and near-shore areas. We assumed a modest decrease of phosphorus and PM (but not nitrogen) concentrations over the Lake for the north and south quadrants.

Annual dry deposition of nitrogenous species was estimated to be between 70 and 170 metric tons, with a central estimate of 120 metric tons assuming no decrease in concentrations of nitrogen species on the Lake compared to the monitoring sites.

Assuming modest depletion of phosphorus concentrations analogous to those reductions assumed for PM provided estimates for annual dry deposition that ranged from 0.6 to 3 metric tons, with a central estimate of 2.2 metric tons of phosphorus.

The estimates of annual PM deposition ranged from 360 to 900 metric tons, with a central estimate of 600 metric tons.

An alternative estimate of phosphorus deposition, lower by a factor of two, would be predicted by scaling phosphorus deposition to the estimates for dry deposition of PM using a predicted percent phosphorus in each size fraction of PM. Emission inventory information for the types of sources at Lake Tahoe predicts phosphorus concentrations of 0.07, 0.17, and 0.19 percent in PM2.5, PM_coarse, and PM_large. Using this scaling strategy and the same modest depletion of PM concentrations in the south and north quadrants (as were used for the estimates in **Tables 4-10, 4-11, and 4-12**), results in annual estimates of phosphorus deposition of 0.6 to 1.5 metric tons, with a central estimate of 1 metric ton.

This report assumes the values provided in **Tables 4-10, 4-11, and 4-12** as the lower bound, central, and upper bound estimates of dry deposition. The next chapter will use a conceptual model, seasonal air quality concentrations from the TWS network and the number of hours when precipitation fell to develop physically reasonable wet deposition estimates. Those estimates of wet deposition will then be combined with the estimates of dry deposition found in **Tables 4-10, 4-11, and 4-12** to estimate total atmospheric deposition loads to Lake Tahoe during LTADS.

4.9 References

Air Resources Board (2005), “Lake Tahoe Atmospheric Deposition Study Interim Report,” ARB Research Division Reports, Cal/EPA 1001 I Street, Sacramento, California 95814.

Barthelmie R.J. and S.C. Pryor (2003), “Can satellite sampling of offshore wind speeds realistically represent wind speed distributions?” *Journal of Applied Meteorology,* **42**, 83-94.

Brook, J.R., L. Zhang, F. Di-Giovanni, and J. Padro (1999), “Description and evaluation of a model of deposition velocities for routine estimates of air pollutant dry deposition: I Model development,” *Atmospheric Environment*. **33**: 5037-5051.

Brook, J.R., L. Zhang, Y.F. Li, and D. Johnson (1999) “Description and evaluation of a model of deposition velocities for routine estimates of air pollutant dry deposition: II Review of past measurements and model results.” *Atmospheric Environment.* **33**: 5053-5070.

Brutsaert, W. (1982) "Evaporation into the Atmosphere: Theory, History and Applications " Boston: D. Reidel. (Russian translation: Ispareniye v atmosferu. Leningrad, U.S.S.R.: Gidrometeoizdat. 1985).

Byun, D.W. and Dennis (1995), “Design artifacts in Eulerian air quality models: Evaluation of the effects of layer thickness and vertical profile correction on surface ozone concentrations.” *Atmospheric Environment*, **29**, No. 1, 105-126.

Charnock, H. (1955), “Wind stress on a water surface,” *Quart. J. Roy. Meteor. Soc.*, **81**, 639–640.

Garratt, J.R. (1977), “Review of drag coefficients over oceans and continents,” *Mon. Weather Rev.*, **105**, 915–929.

Giorgi, F. (1986) “A particle dry-deposition parameterization scheme for use in tracer transport models.” *J. Geophys. Res.*, **91**, 9794–9806.

Giorgi, F. and Chameides, W.L. (2003), *Journal of Geophysical Research Atmosphere*, **91**, 14367+.

Hanna, S.R., L.L. Schulman, R.J. Paine, J.E. Pleim, and M. Baer (1985), “Development and evaluation of the offshore and coastal dispersion model” *J. Air Poll. Contr. Assoc.*, **35**, 1039-1047.

Hicks, B.B. (1982), “Critical assessment document on acid deposition,” ATDL Contrib. File No. 81/24, Atmospheric Turbulence and Diffusion Laboratory, Oak Ridge, TN.

Hosker, R.P., Jr., (1974) “A comparison of estimation procedures for over-water plume dispersion.” Presented at the Symposium of Atmospheric Diffusion and Air Pollution, Santa Barbara, California, September 9-13, 1974. Conference Proceedings, 281-288.

Larsen, S.E., J.B. Edson, P. Hummelshøj, N.O. Jensen, G. de Leeuw, and P.G. Mestayer (1995), “Dry deposition of particles to ocean surfaces, “ *Ophelia*, **42**, 193–204.

Lu R., R.P. Turco, K. Stolzenbach, et al. (2003), “Dry deposition of airborne trace metals on the Los Angeles Basin and adjacent coastal waters,” *Journal of Geophysical Research Atmosphere*, **108** (D2): 4074-4074.

Pleim, J., A. Venkatram and R. Yamartino (1984), “ADOM/TADAP model development program. Volume 4. The dry deposition module,” Ontario Ministry of the Environment, Rexdale, Ontario.

Pryor S.C. and Sorensen L.L. (2000), “Nitric acid-sea salt reactions: Implications for nitrogen deposition to water surfaces,” *Journal of Applied Meteorology*, **39** No. 5, 725-731.

Pryor S.C. and Barthelmie R.J. (2003), “Long term variability of flow over the Baltic,” *International Journal of Climatology*, **23**, 271-289.

Scire, J.S., F.R. Robe, M.E. Fernau, R.J. Yamartino, (2000), “A User’s Guide for the CALMET Meteorological Model,Version 5,” Earth Tech, Inc., Concord, MA. pp. 332.

Scire, J., D.G. Strimaitis, R.J. Yamartino (2000a), ”A User’s Guide for the CALPUFF Dispersion Model (Version 5),“ Earth Tech, Inc., Concord, Massachusetts. pp. 521.

Sehmel, G.A., (1980) “Particle and Gas Dry Deposition: A Review” *Atmospheric Environment*, **14**, 983-1011.

Seinfeld, J.H., and S.N. Pandis, (1998), “Atmospheric Chemistry and Physics: From Air Pollution to Climate Change”, John Wiley & Sons, Inc., NY.

Slinn, S.A. and W.G.N. Slinn (1980), “Predictions for particle deposition and natural waters,“ *Atmospheric Environment*, **14**, 1013-1016.

Smith R.I., D. Fowler, M.A. Sutton, C. Flechard, and M. Coyle (2000), “Regional estimation of pollutant gas deposition in the UK: model description, sensitivity analyses and outputs,” *Atmospheric Environment,* **34**, 3757-3777.

Stull, R.B. (1988), “An Introduction to Boundary Layer Meteorology”, Kluwer Academic Publishers, Dordrecht, Boston, London.

Sun, J. and co-authors (1997), “Lake induced atmospheric circulation (s) during BOREAS,” *Journal of Geophysical Research Atmosphere* **102**, 29, 155-166.

Sun JL, D. Vandemark, L. Mahrt, et al. (2001), “Momentum transfer over the coastal zone,” *Journal of Geophysical Research Atmosphere*, **106** (D12): 12437-12448.

Venkatram, A. and J. Pleim (1999), “The electrical analogy does not apply to modeling dry deposition of particles,” *Atmospheric Environment*, **33**, 3075-3076.

Valigura, R.A. (1995), “Iterative bulk exchange model for estimating air-water transfer of HNO_3” *Journal of Geophysical Research Atmosphere*, **100**, 26045-26050.

Wesley M.L. and B.B. Hicks (2000), “A review of the current status of knowledge on dry deposition,” *Atmospheric Environment*, **34**, 2261-2282.

Whelpdale, D.M. and R.W. Shaw (1974), Sulfur dioxide removal by turbulent transfer over grass, snow, and water surfaces. *Tellus*, **26**, 1(2), 196-204.

Williams, R.M. (1982), “A Model for Dry Deposition of Particles to Natural Water Surfaces,” *Atmospheric Environment*, **16**, No. 8, 1933-1938.

Zufall, M.J., C.I. Davidson, P.F. Caffrey, et al. (1998), “Airborne concentrations and dry deposition fluxes of particulate species to surrogate surfaces deployed in Southern Lake Michigan,“ *Environmental Science and Technology*, **32** (11), 1623-1628.

5. Wet Atmospheric Deposition

5.1 Introduction

Historical wet/dry deposition measurements with bucket samplers indicate that wet deposition is a major component of the total annual atmospheric deposition to Lake Tahoe (Jassby, et al., 1994). Wet deposition removes nitrogen, phosphorus, and particulate matter from the air via two main processes: nucleation scavenging and impaction scavenging. Nucleation scavenging occurs when particles act as cloud condensation nuclei. As water accumulates on the particle, the aerosol may increase in size until the cloud (fog) droplets deposit on surfaces or fall out of the air as precipitation. Impaction scavenging occurs when precipitation removes aerosols by physical contact (or absorption in the case of water-soluble gases such as ammonia and nitric acid) with the much larger water droplet or snowflake. Because snowflakes have a much larger surface area than a raindrop and more than half of the annual precipitation hours in the Tahoe Basin occurs as snow (**Figure 5-1**), wet deposition by snowfall is a significant component of the total atmospheric deposition in the Tahoe Basin. Most of the total annual precipitation in the Tahoe Basin occurs during the winter and spring (see **Figure 2-3**).

Wet deposition measurements (besides those routinely collected by the Tahoe Research Group) were not a component of the LTADS field study. However, CARB staff estimated wet deposition onto Lake Tahoe during 2003 based on a simple analysis of seasonal air quality concentrations from the TWS network and the associated seasonal number of hours when precipitation fell. This analysis was necessary to develop total annual PM deposition estimates as the conventional wet deposition measurements with a surrogate surface do not make particulate matter (PM) measurements. The assumption is that, if the simple wet deposition model applied here reasonably reproduces the wet deposition estimates of N and P with the surrogate surfaces (deemed to be accurate), then the wet deposition estimate for PM is more likely to be reasonably accurate.

Precipitation amounts in the northern Sierra Nevada during 2003 were less than normal with only the months of April, August, and December being wetter than normal (**Figure 5-2a**). On a seasonal basis (i.e., winter – January, February, and December; spring – March through May; summer – June through August; and fall – September through November) and focusing on the long-term monitoring site in Meyers, CA (located near to and southwest of South Lake Tahoe), precipitation amounts in the Tahoe Basin in 2003 was about 25% below normal in winter, 25% above normal in spring, slightly above normal in summer, and about 50% below normal in fall (**Figure 5-2b**).

Figure 5-1. Estimated proportion of rain and snow observed in precipitation at Incline Creek, 2003.

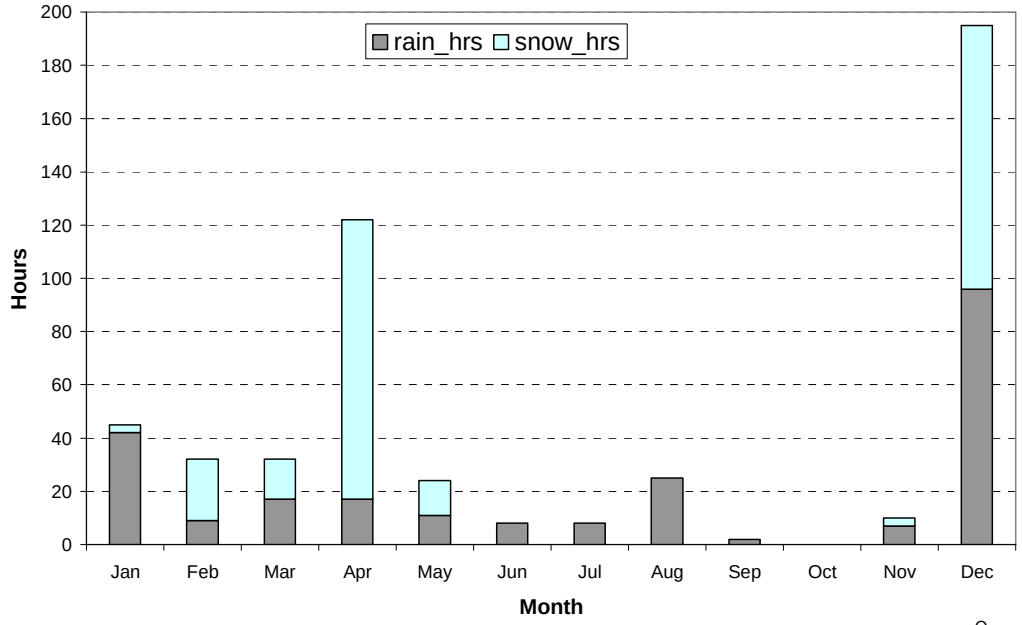

Note: the number of snow and rain hours is based on the air temperature at ground level relative to 0 ^{O}C when precipitation was reported; actual snow hours would be greater because cloud temperatures are colder than the ground-level temperature.

Figure 5-2a. Monthly precipitation in 2003 (bars) compared to long-term means (lines).

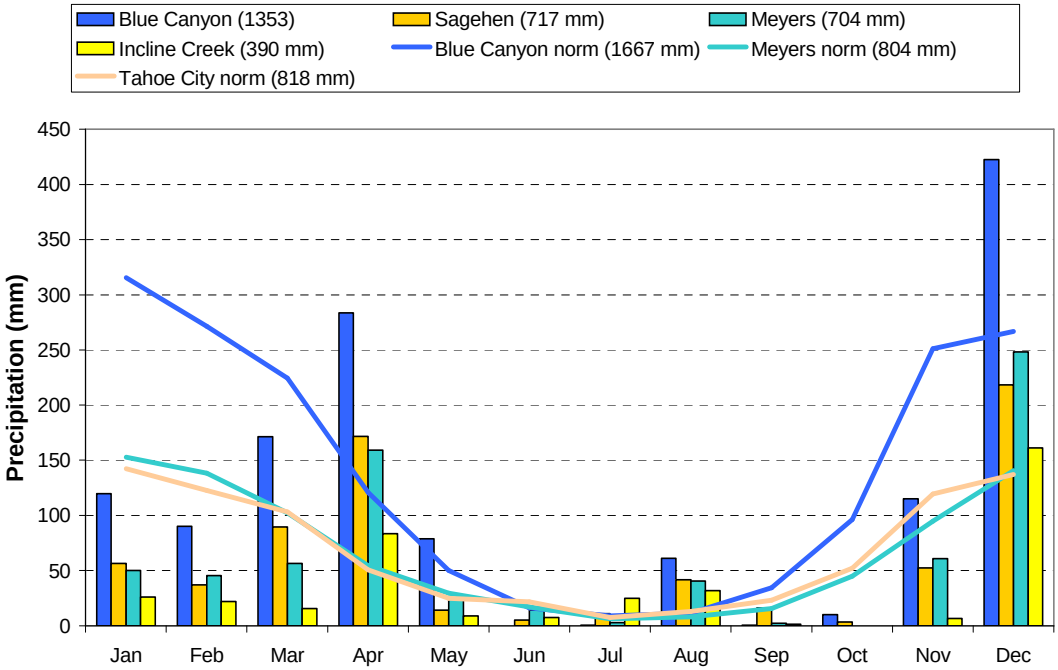

Note: Blue Canyon is located west of the Sierra Nevada crest; Sagehen is located east of the Sierra crest but northwest of the Tahoe Basin; Meyers is located in the southern Tahoe Basin; Incline Creek is located in the northeastern Tahoe Basin; and Tahoe city is located on the northwestern shore of Lake Tahoe.

Figure 5-2b. Seasonal precipitation in 2003 (bars) compared to long-term means (lines). The annual precipitation totals for 2003 and long-term means are shown in the legend box.

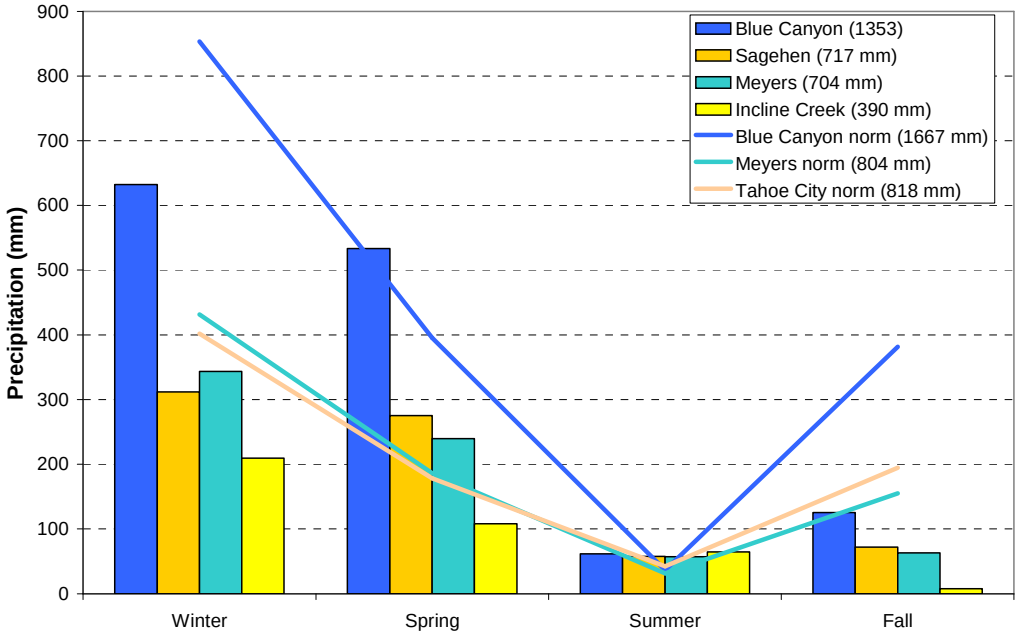

5.2 Conceptual Model of Wet Deposition

The wet deposition loading of a pollutant is estimated from the mass of that pollutant in a "cylinder" above the Lake, and the frequency and efficiency with which that air volume is cleansed by precipitation. The mass of a pollutant in the air above the Lake in each season is estimated by multiplying the seasonally and spatially representative ambient concentration of each pollutant by the volume of air (surface area of Lake Tahoe times the depth of the cylinder being cleansed by precipitation). The annual wet deposition loading is then the sum of these seasonal masses times the number of precipitation events during each associated season.

The wet deposition analysis was divided into two components addressing locally-generated pollutants and transported (regional background) pollutants (**Figure 5-3**). Conceptually, the local component is represented by the removal of pollutants over Lake Tahoe (based on measurements near the shoreline) and extending 700 meters from the Lake's surface up to a representative altitude of the crest of the surrounding mountains (i.e., local pollutants are trapped in the Tahoe Basin by the mountains surrounding the Lake or are advected out of the Basin if they rise higher). In a similar manner, the transport component of the wet deposition is represented by the washout of regional pollutants in a layer of air extending 3000 meters above the mountain crests (i.e., the air of regional origin that passes over the Tahoe Basin).

Figure 5-3. Conceptual model of regional and local components of wet deposition estimate to Lake Tahoe. (BH – Big Hill, LF – Lake Forest, BL – Bliss State Park, SW – SLT-Sandy Way, TB – Thunderbird Lodge)

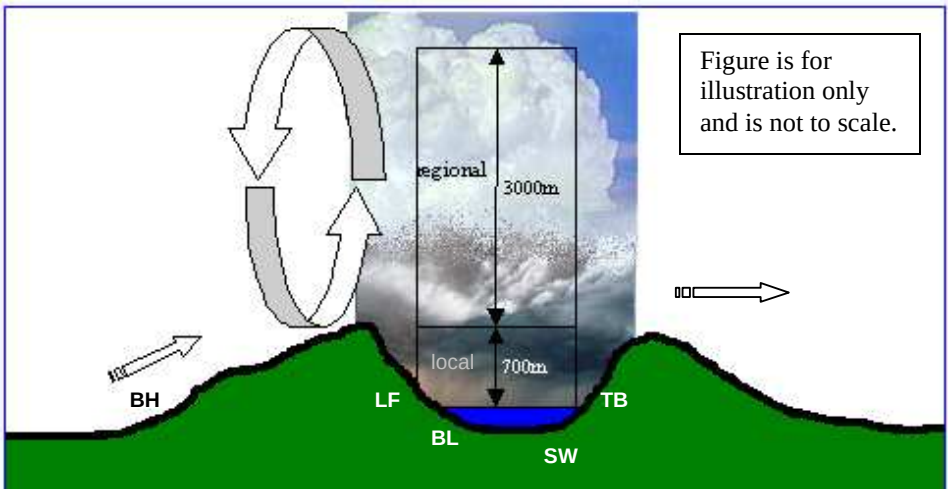

As regional airflow carries pollutants up the western slope of the Sierra, they are mixed through a deep layer during precipitation periods. Although thunderstorm tops in northern California typically reach 9000 m to 12,000 m (30,000 to 40,000 feet) MSL, the depths of the storms are generally about 6000 m to 9000 m (20,000 to 30,000 feet), with even shallower storms common during the winter (NWS, 2003). Vertical mixing in the atmosphere is not as deep during non-storm conditions as indicated in **Figure 5-4**, which shows summer pollutant profiles above Big Hill as measured by an airplane. Even so, most of the pollutant emissions, although originating near ground level, mix upward (more than 1000 m) due to solar heating on the western slope of the Sierra. This mixing of pollutants may extend up to the base of the subsidence inversion frequently observed during summer around 3,000 m MSL (10,000 – 11,000 feet) or 300 – 600 m above the crest of the Sierra Nevada. The atmospheric mixing associated with storms (instability) would mix these pollutants up through a deeper layer (i.e., the depth of the storm cloud or about 6000 m). Thus, the surface-based pollutant concentration measurements at Big Hill are representative of the average pollutant concentrations in a relatively deep layer of air (1000 – 1500 m during stable periods and 6000 m or more during storms. Staff assumed that the average pollutant concentration throughout the storm layer would be about ½ of the measurement at ground level at Big Hill. The equivalent formulation in the wet deposition model is to represent the mass of material available for removal as wet deposition as $[AQ]_{BH}$ x 3000m, rather than ½ x $[AQ]_{BH}$ x 6000 m. Thus, the transport (regional) component of wet deposition is represented by the washout of the regional pollutant concentrations characterized by conditions at Big Hill in a 3000 m layer of air above the crest of the Sierra Nevada.

The local component is represented by local pollutant concentrations (i.e., the Tahoe 4-quadrant average) in a 700 m layer of air extending from the Lake's surface to the height of the Sierra crest. These regional and local concentrations in the upper and

lower sections of a cylinder above the Lake (separated at the height of the Sierra Nevada) were characterized seasonally and represent the pollutant loadings potentially available for wet deposition to the Lake. The actual amount of wet deposition is determined by the seasonal frequency of precipitation removing the pollution.

The wet deposition calculations used ground level, ambient pollutant concentrations observed by the TWS network during the cleanest (representative) 2-week measurement period during winter and spring to represent the cleaner air quality associated with organized (frontal) precipitation periods. Because precipitation does not constantly occur during a 2-week period, the use of the minimum 2-week concentrations likely overestimates the actual concentrations during storms. For summer and fall when precipitation events consist of scattered showers, seasonal mean ambient concentrations were used. Under typical dry conditions, pollutant concentrations begin to decline with increasing altitude due to dispersion of primarily ground-based emissions and mixing with typically cleaner air found aloft. However, during a thunderstorm, deep vertical mixing occurs and the ambient pollutant concentrations are smaller and not likely to decline as rapidly with altitude (i.e., similar amount of total pollutant mass but distributed through a deeper layer of air than what occurs under dry conditions). Thus, the seasonal mean is the best estimate of the air quality in the column of air when isolated showers develop.

Figure 5-4a. Data from a morning aircraft spiral above Big Hill on August 22, 2002, 0814-0830 PST.

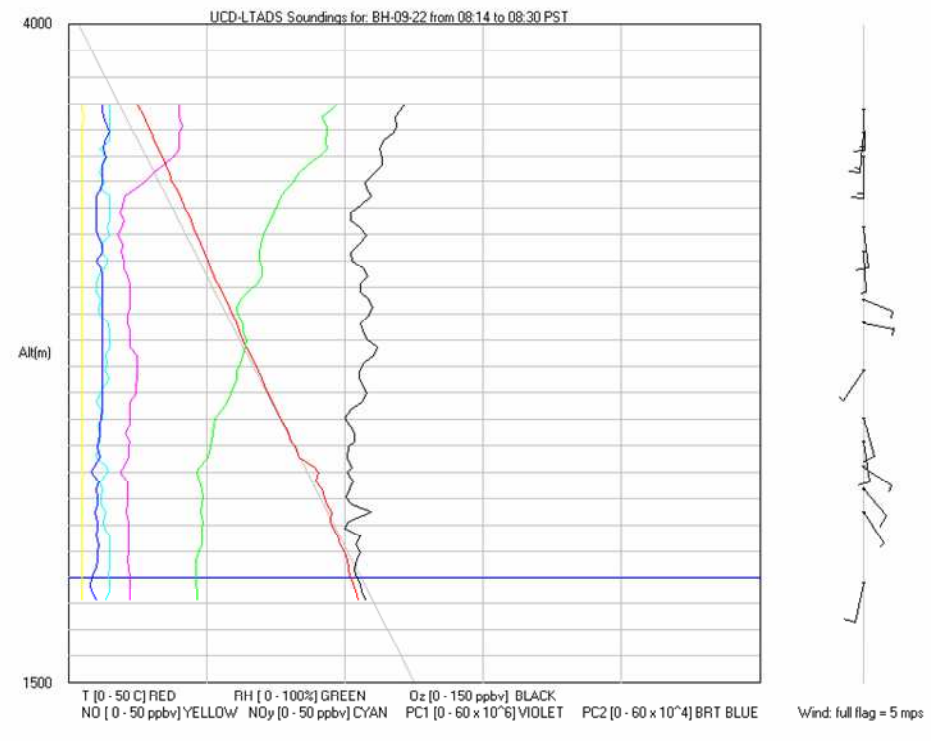

Figure 5-4b. Data from an afternoon aircraft spiral above Big Hill on July 31, 2002, 1738-1751 PST.

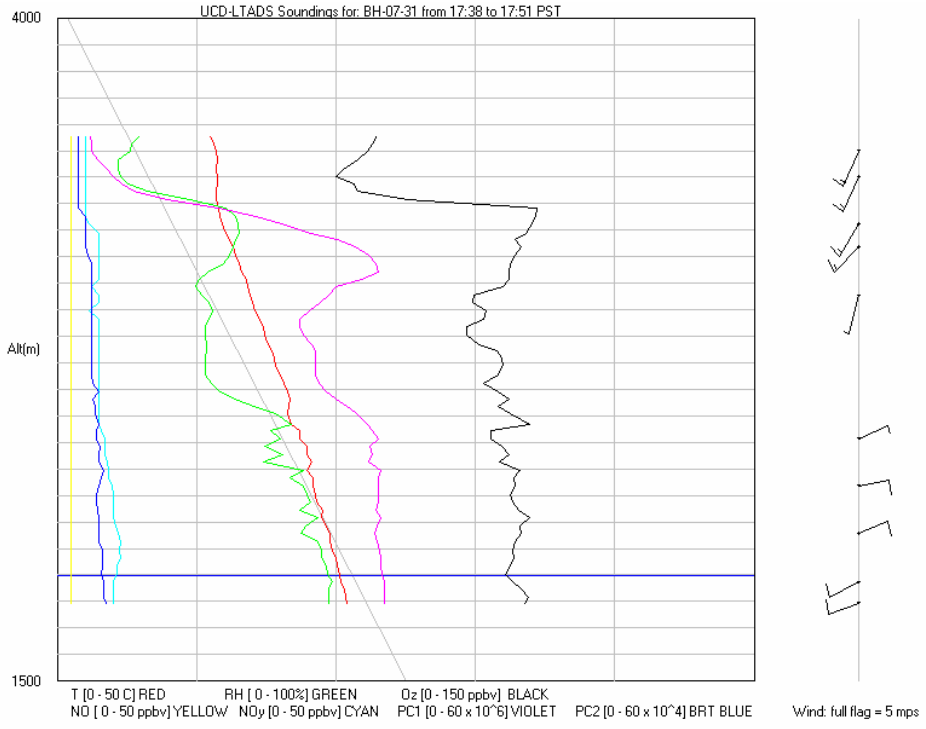

This wet deposition analysis uses precipitation data collected during 2003 at Incline Creek located near the northeast shore of Lake Tahoe. Precipitation in this portion of the Tahoe Basin is comparable to other monitoring sites in the region for frequency (**Figures 5-5a, c**) but below average for quantity (**Figures 5-5b, d**). Schumann et al. (1988) suggest that the bulk of the air pollution is removed during the beginning of the storm (precipitation) and Zinder et al. (1988) suggest that below-cloud removal can be efficient. Consequently, CARB staff believes that the frequency of precipitation events is a better indicator of the wet deposition of atmospheric pollutants than is the amount of precipitation. Thus, this analysis is based on the assumption that any precipitation, whether light or intense, will cleanse the air of pollutants. Byers (1965) suggests that an hundredth of an inch of rain in one hour will remove about 75% of the aerosol pollutants in the air.

Staff's analysis assumed that ambient pollutant concentrations were replenished every hour. This may be reasonable for regional transport and local gaseous and PM2.5 emissions but might not be for larger particles. Thus, the wet deposition analysis likely overestimates the actual deposition of PM. An alternative assumption might be that large particles of local origin are only regenerated on a daily basis rather than an hourly basis due to the time needed for generation (e.g., diurnal emission cycles, drier roads) and for particle growth. Based on the average precipitation frequency in 2003, which indicated about 5 hours of precipitation per day when precipitation occurred) and assuming that PM2.5 comprises ~50% of the total PM mass during the primary wet deposition seasons of winter and spring, this assumption (daily rather than hourly

replenishment of PM_coarse and PM_large) would reduce the wet deposition estimates of PM to 60% of the deposition estimated on an hourly replenishment basis.

Figure 5-5a. Number of days with precipitation during 2003, by month.

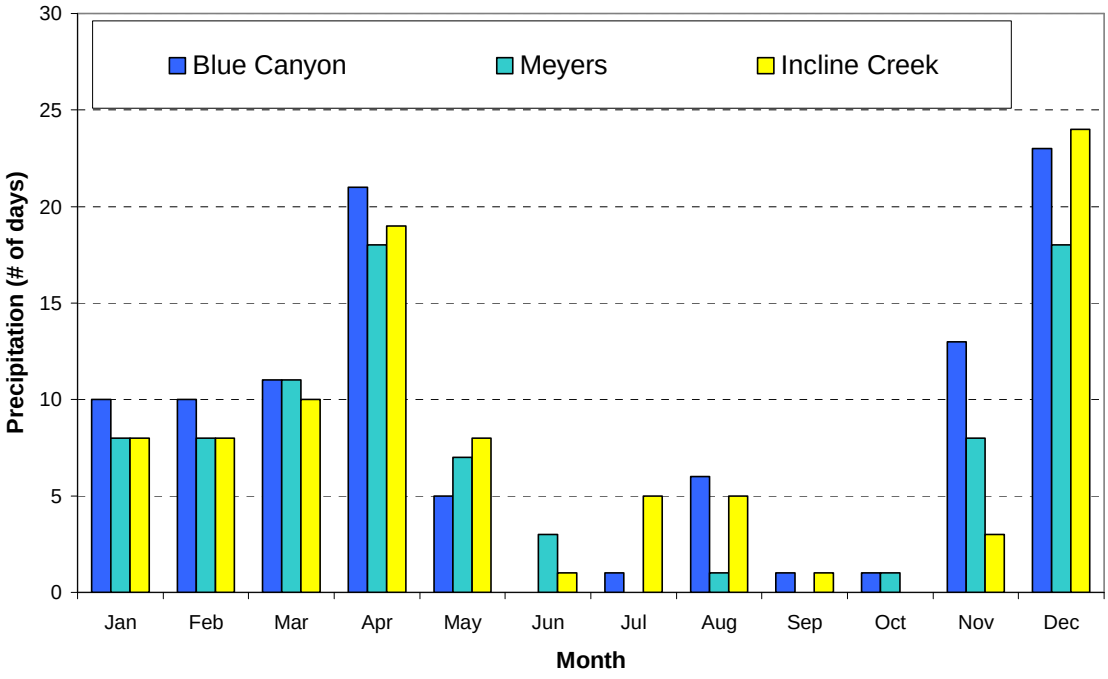

Figure 5-5b. Precipitation amounts during 2003, by month. Long-term normal annual precipitation totals are shown in parentheses.

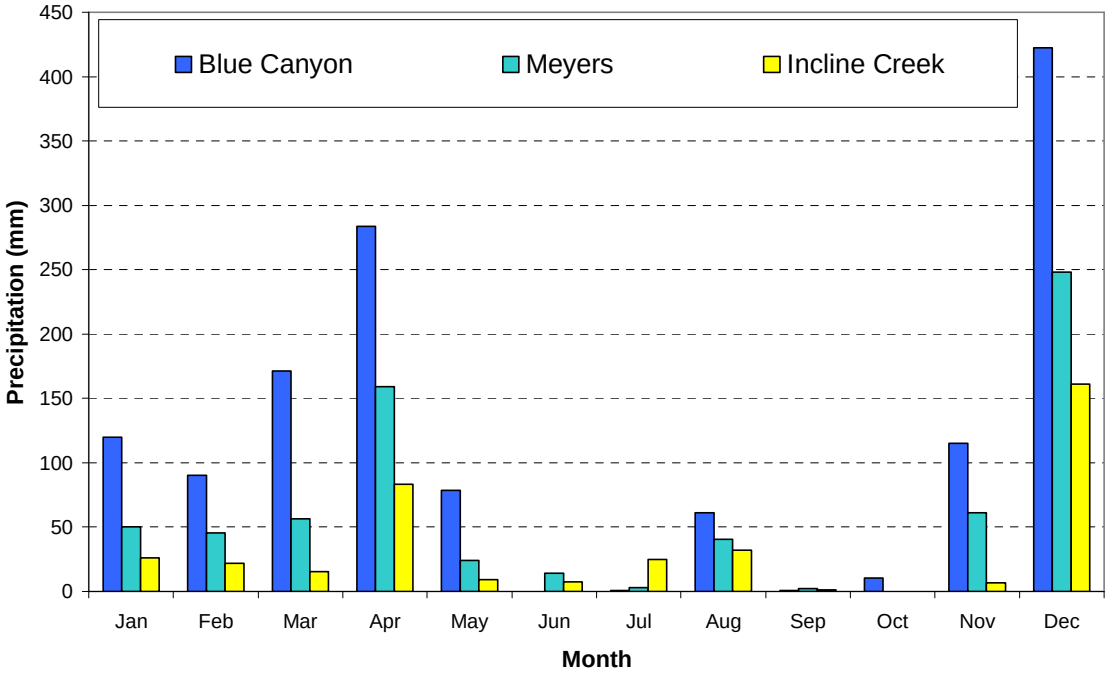

Figure 5-5c. Number of days with precipitation during 2003, by season.

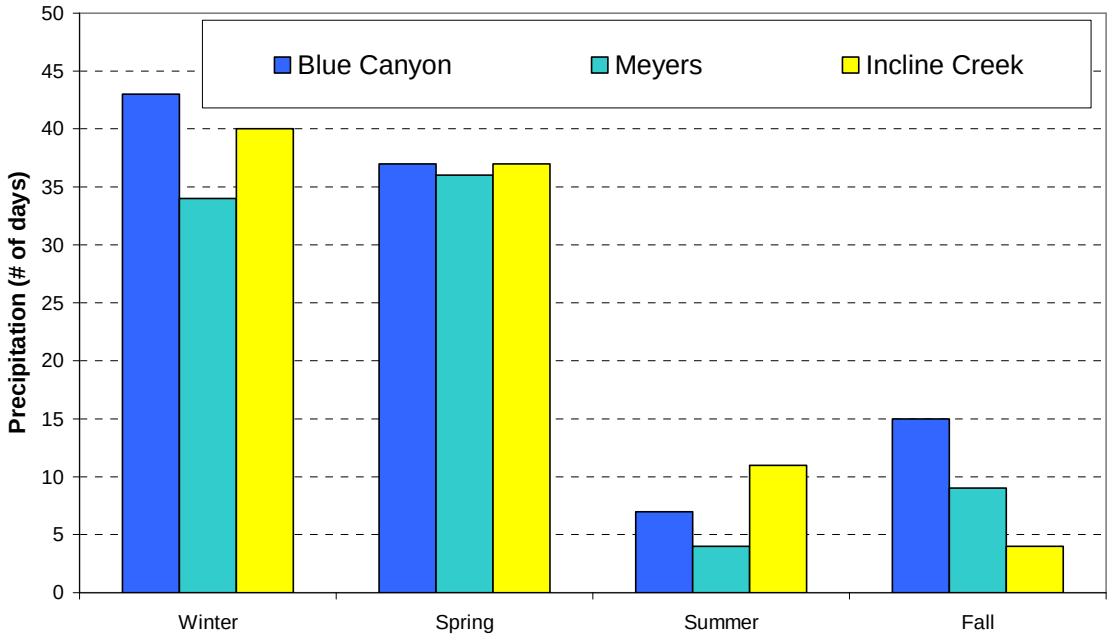

Figure 5-5d. Precipitation amounts during 2003, by season.

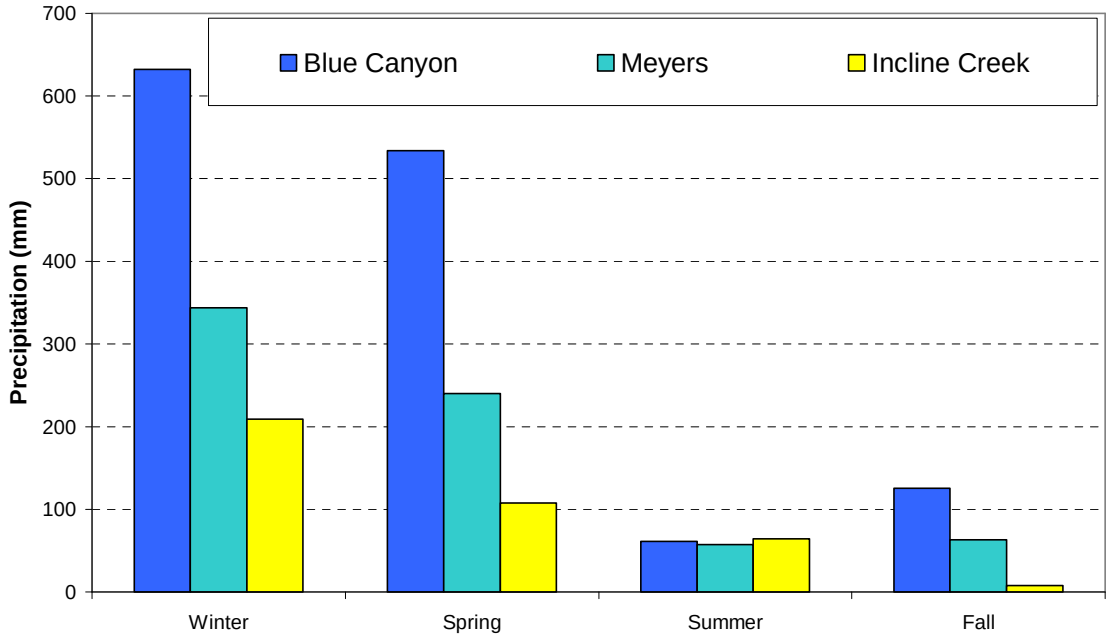

5.2.1 Wet Deposition from Regional Pollution Sources

The concentration of each pollutant in the transport layer is based on measurements during each season at Big Hill, the upwind regional air quality site (see Regional Source listing in **Table 5-1**). Because precipitation occurs differently in summer and fall (isolated showers) as compared to winter and spring (frontal systems), seasonal mean specie concentrations were used for summer and fall wet deposition estimates and the minimum 2-week average specie concentration observed during winter and spring were used for the winter and spring wet deposition estimates. Gaseous and aerosol pollutants are included in the conceptual wet deposition model. TSP and the associated species (NH_4^+ and NO_3^-) were used because: a) the enhanced vertical and horizontal air motion during storms could permit some large particles to traverse the Sierra Nevada and arrive at Lake Tahoe before depositing, and b) the PM method comparison indicated the TSP concentrations by the TWS may be biased low ~5 ug/m^3 (15-20%) compared to the other PM measurement methods. The following wet deposition calculations assume that the pollutant concentrations at Big Hill are well-mixed in a 3000 meter thick air layer above the crest of the Sierra Nevada due to the vigorous mixing during storms. Given that the typical thickness of a storm cloud in this region is about 6000 meters (NWSFO, 2003), this assumption is equivalent to saying that the average pollutant concentration throughout the 6000 m storm cloud is one-half the pollutant concentration at ground-level (i.e., the total mass available for deposition is the same).

As the air mass is transported over the Tahoe Basin, precipitation washes the regional pollutants out of the air. The Sierra Nevada enhances precipitation on its western slope and crest but the mountain range also creates a rain shadow downwind (east) of the crest. Considering long-term precipitation averages (along a line segment from Big Hill to Lake Tahoe) indicates that about 10 percent of a storm band's total precipitation (and presumably pollutant load), on average, falls onto Lake Tahoe as it travels from Big Hill, over the Sierra Nevada, and to Lake Tahoe (**Figure 5-5**). Given the limited air pollution sources between Big Hill and Lake Tahoe, about 10% of the pollutants embedded in the original air mass can actually fall onto Lake Tahoe. Furthermore, all of the pollutants that actually survive the trip to Tahoe are not necessarily washed out of the air by precipitation and various assumptions about pollutant wash-out efficiency must be made. The meteorological assumptions in the wet deposition estimates are summarized in **Table 5-2** and are described in more detail below.

Table 5-1. Seasonal air quality concentrations (from TWS network) used in estimating wet deposition to Lake Tahoe during 2003. Representative minimum 2-week pollutant concentrations were used for winter and spring while seasonal means were used for summer and fall.

Pollutant	Pollution Source	TWS Site	Seasonal Concentrations (ng/m^3)			
			winter	spring	summer	fall
Ammonia (NH_3)	regional	Big Hill	65	89	984	719
	local	SLT – Sandy Way	469	480	1043	1227
	local	Lake Forest	513	229	861	835
	local	Thunderbird Lodge*	11	40	298	277
Nitric Acid (HNO_3)	regional	Big Hill	87	99	1127	816
	local	SLT – Sandy Way	719	405	772	1294
	local	Lake Forest	111	140	564	647
	local	Thunderbird Lodge*	145	80	530	379
NO_3 (in TSP)	regional	Big Hill	177	617	1763	1394
	local	SLT – Sandy Way	774	629	1210	1155
	local	Lake Forest	279	341	657	617
	local	Thunderbird Lodge*	124	278	1014	577
NH_4 (in TSP)	regional	Big Hill	30	208	430	552
	local	SLT – Sandy Way	191	244	336	496
	local	Lake Forest	54	139	301	297
	local	Thunderbird Lodge*	65	127	289	287
P^+	regional	Big Hill	27	26	30**	31**
	local	SLT – Sandy Way	17	28	40	40
	local	Lake Forest	9	32	40	40
	local	Thunderbird Lodge*	20	27	40	40
PM	regional	Big Hill	1586	3984	15,165	12,797
	local	SLT – Sandy Way	9274	10,674	14,654	21,339
	local	Lake Forest	5222	9277	14,756	15,138
	local	Thunderbird Lodge*	1650	2957	10,116	7760

* DL Bliss SP was not part of the TWS network but was the sampling site used to represent air quality in the SW quadrant of the basin. Limited LTADS sampling and long-term IMPROVE sampling at DL Bliss indicated low concentrations and similarity with TWS measurements at Thunderbird Lodge. For the purpose of estimating the mean concentrations of pollutants within the basin, staff assumed concentrations at Bliss were the same as at Thunderbird Lodge.

\+ [Phosphorus]s in winter and spring are 40 ng/m^3 times the seasonal ratios of $[TSP]_{2\text{-wk minimum}}/[TSP]_{mean}$.

** [P]s at Big Hill in summer and fall are 40 ng/m^3 times the seasonal ratios of [PM10]/[TSP] (assumes P in PM with diameter > 10 um does not transport over the ~25 miles to Lake Tahoe).

Table 5-1a. Size breakdown of seasonal particulate matter concentrations (from TWS network) used in estimating wet deposition to Lake Tahoe during 2003. Representative minimum 2-week pollutant concentrations were used for winter and spring while seasonal means were used for summer and fall.

Pollutant	Pollution Source	TWS Site	Seasonal Concentrations (ng/m^3)			
			winter	spring	summer	fall
PM_fine	regional	Big Hill	563	1905	6887	4962
	local	SLT – Sandy Way	6333	3771	5922	9772
	local	Lake Forest	1576	2016	6286	4506
	local	Thunderbird Lodge	1307	1786	5723	3745
PM_coarse	regional	Big Hill	344	1795	4855	4898
	local	SLT – Sandy Way	1837	4483	7000	7961
	local	Lake Forest	3640	7204	7761	9402
	local	Thunderbird Lodge	197	1111	3859	2575
PM_large	regional	Big Hill	678	284	3423	2938
	local	SLT – Sandy Way	1104	2420	1732	3606
	local	Lake Forest	8	57	719	1230
	local	Thunderbird Lodge	146	60	534	1440

Table 5-2. Meteorological assumptions for estimating wet deposition to Lake Tahoe in 2003.

Parameter (units) \ Season:	Estimate Range	winter	spring	summer	fall
MD - atmospheric mixing depth (meters)[1]	regional pollution	3000	3000	3000	3000
	local pollution	700	700	700	700
PF - precipitation frequency (hours/days)	lower bound[2]	184/30	120/28	28/8	8/3
	central estimate[3]	272/40	178/37	41/11	12/4
	upper bound[4]	374/50	245/46	56/14	17/5
(transport / local) fraction of precipitation that falls onto Lake Tahoe (%)[5]	lower bound	5 / 100	5 / 100	5 / 5	5 / 5
	central estimate	10 / 100	10 / 100	10 / 10	10 / 10
	upper bound	15 / 100	15 / 100	15 / 15	15 / 15
washout efficiency (%)	lower bound	50	50	50	50
	central estimate	75	75	75	75
	upper bound	100	100	100	100

[1] mixing depth layers are stacked with the "local" contribution on bottom (extending from the Lake surface at ~1900 m MSL to Basin ridgeline at ~2600 m MSL) and with the "regional" or "transport" contribution on the top (extending 6000 m from the Basin ridgeline at ~2600 m MSL to ~8600 m MSL). Because pollutant concentrations at Big Hill are well-mixed (at least through 1000 m during stable periods and 6000 m or more during unstable periods), concentrations at Big Hill were assumed to be representative of a well-mixed air layer 3000 m thick (i.e., ~2x the minimum mixing depth and ~½x the mixing depth during precipitation events). Any greater mixing would likely entrain "clean" air aloft. Because storms would increase mixing through a depth of 6000 m or more but not the mass of pollutants, the total transport mass available for wet deposition would remain the concentration at Big Hill times the area of Lake Tahoe times 3000 m. Similarly, the total local mass available for wet deposition is the 4-quadrant average local concentration times the area of Lake Tahoe times 700 m. Thus, the total depth of the cylinder above the Lake from which wet deposition was estimated is 3700 m.

[2] lower bound = includes 0.75 x central estimate of precipitation days and 0.90 x central estimate of hours of precipitation/day (i.e., 68% of number of precipitation hours in central estimate)

[3] central estimate = actual observation at Incline Creek during 2003

[4] upper bound = includes 1.25 x central estimate of precipitation days and 1.10 x central estimate of hours of precipitation/day (i.e., 138% of precipitation hours in central estimate)

[5] winter & spring feature organized storm systems while summer & fall feature scattered showers; winter & spring transport fraction based on west-to-east fraction of total precipitation between Big Hill and eastern shoreline of Lake Tahoe; summer & fall fractions based on fraction of lake surface experiencing shower (showers more likely to occur over land than lake).

The regional (transport) component of wet deposition is represented by:

WetDep_regional (metric tons) = $[pollutant]_{Big\ Hill}$ * MD * CF * PF * HW * VW, where:

$[pollutant]_{Big\ Hill}$ = the seasonal representative concentration of a particulate or gaseous pollutant at Big Hill in ng/m^3. With limited emission sources between Big Hill and Lake Tahoe, and assuming good atmospheric mixing by the time the polluted air mass arrives at Big Hill, concentrations at Big Hill are assumed to be reasonably representative of concentrations along Sierra Nevada west of Lake Tahoe and transported over Tahoe Basin). In the calculations for summer and fall when precipitation falls as scattered showers, the seasonal mean concentrations are used; for the winter and spring calculations when widespread precipitation is associated with frontal passages, the observed seasonal minimum 2-week-average concentrations are used.

MD = mixing depth (transportable pollutants measured at Big Hill were assumed to be mixed throughout 3000 meters above the crest of the Sierra Nevada),

CF = conversion factor of 5.01×10^{-7} (converts concentration units (ng/m^3) and surface area of Lake Tahoe to metric tons of pollutant per meter of altitude (i.e., mixing depth) available for wet deposition,

PF = precipitation frequency (varies with type of pollutant); specifically, the number of *hours* during each season with measurable precipitation for gases and secondary particulate matter; the number of *days* during each season with measurable precipitation for primary particulate matter, which includes phosphorus. This construct applies an assumption of rapid (hourly) replenishment of atmospheric concentrations for gases and secondary particles but slower (daily) replenishment of primary particles,

HW = horizontal washout or fraction of total precipitation falling on Lake Tahoe (i.e., during winter and spring when storm systems occur, the fraction of total precipitation falling between Big Hill and Lake Tahoe that falls onto Lake Tahoe; during summer and fall when precipitation occurs as scattered showers, the areal fraction of the Lake impacted by showers),

VW = vertical washout efficiency (i.e., fraction of total transported pollutant mass actually washed out of air column by precipitation)

The annual wet deposition due to regional sources of pollution is simply the sum of the seasonal, regional wet deposition estimates.

5.2.2 Wet Deposition from Local Pollution Sources

The local component of wet deposition is estimated in a manner similar to the regional component. Instead of a layer of air above the height of the Sierra Nevada, this layer of air with local pollutants extends from the Lake surface up to 700 meters (the base of the “transport” layer). Because the pollutants in this surface layer of air are close to their sources and are not mixed as well as in the transport layer, the average pollutant

concentration in the local layer of air was estimated as the mean of the pollutant concentrations in four quadrants around the Lake. Thus, a regional mean of the seasonal minimum 2-week average pollutant concentrations measured near the shoreline in four quadrants of the Lake was assumed to extend from the Lake's surface up to 700 meters (approximate height of mountain ridgeline above the Lake) during winter and spring. For summer and fall wet deposition estimates, the seasonal mean concentrations were used. The basic equation representing wet deposition of local air pollution is:

WetDep_local (metric tons) = $[pollutant]_{4\text{-quad mean}}$ ***** MD ***** CF ***** PF ***** HW * VW, where:

- [pollutant] = the regional concentrations of a particulate or gaseous pollutant in ng/m^3 (average pollutant concentrations from four sites characterizing four quadrants around the Lake); seasonal concentration means were used for summer and fall when scattered showers occur; seasonal minimum 2-week average concentrations were used during winter and spring when frontal storms occur,
- MD = mixing depth (local pollutants were assumed to be mixed through 700 meters),
- CF = conversion factor of 5.01×10^{-7} (converts concentration units (ng/m^3) and surface area of Lake Tahoe to metric tons of pollutant per meter of altitude (i.e., mixing depth) available for deposition,
- PF = precipitation frequency (definition varies with pollutant type for the purpose of applying different rates of replenishment of atmospheric concentrations) i.e., the number of hours during season with measurable precipitation for gases and secondary particulate matter; the number of days during each season with measurable precipitation for primary particulate matter, which includes phosphorus,
- HW = horizontal washout of fraction of Lake Tahoe impacted by precipitation (i.e., during winter and spring when storm systems occur, precipitation falls over the whole Lake and the HW=1; during summer and fall when precipitation occurs as scattered showers, the HW (areal fraction of Lake Tahoe Impacted by showers) varied among 0.05 for the Lower Bound, 0.10 for the Central Estimate, and 0.15 for the Upper Bound),
- VW = vertical washout efficiency (i.e., fraction of local pollutants washed out of the local air layer by precipitation)

The annual wet deposition due to local sources of pollution is simply the sum of the seasonal, local wet deposition estimates.

5.2.3 Wet Deposition Assumptions

Many of the assumptions used in this analysis could be refined with additional review of meteorological data collected during LTADS or previously. A synopsis of the model parameters and the associated assumptions is presented below.

Pollutant Concentrations – To generate seasonal estimates of wet deposition, seasonal pollutant concentrations were input. Except for the DL Bliss State Park data, which were estimated and not directly measured, the lowest representative 2-week mean concentration for each pollutant (based on data from the TWS network) were input for each site for the winter and spring seasons and seasonal mean concentrations were input for the summer and fall seasons. Because precipitation does not occur continuously during the summer and fall or even for two weeks during the winter and spring seasons, these concentrations (and the subsequent wet deposition estimates) may be biased high to some extent. Because the air quality in the Bliss quadrant of the basin is normally good, the effect of the assumptions for the Bliss site is generally minor. In addition, P concentrations were only infrequently quantifiable during LTADS. In the dry deposition estimates, staff assumed [P]s of 40 ng/m^3 based on the limited number of phosphorus detections during LTADS, measurement uncertainties, and assumed corrections. To characterize phosphorus concentrations during the frontal storm precipitation periods (i.e., winter and spring), the [P]s (fixed at 40 ng/m^3) during winter and spring were multiplied by the seasonal ratios of $[TSP]_{2\text{-week minimum}}/[TSP]_{\text{seasonal mean}}$. The 40 ng/$m^3$ [P]s during summer and fall at the regional transport site (Big Hill) were multiplied by the ratios of [PM10]seasonal mean/[TSP]seasonal mean to account for much of the P being in large particles that do not transport well over the ~25 miles to Lake Tahoe and the likely greater PM exposure at Big Hill compared to forested areas of the western Sierra slope (Cleveland Fire previously burned most of the trees in the area and the site is on an exposed hilltop with some vehicular activity in the vicinity with road access to a microwave tower, heliport, and forest fire lookout).

Mixing Depth – total of 3700 m divided into an upper regional component of 3000 m and a lower local component of 700 m. The mixing depth was not varied by deposition estimate level but was segregated for characterizing the vertical distribution of regional and local pollutants. Essentially all pollutant sources in the Tahoe Basin are near ground level. The rationale for using a 3 km mixing depth for regional pollutants is that vertical air motion during storms and the transport of material over the western slope of the Sierra would entail mixing of the air as it moves up the slopes of the Sierra. Storm clouds lift and mix the air several kilometers above the ridge crest and have an average thickness of about 6000 meters (NWSFO, 2003). Ground-level concentrations of N, P, and PM would be diluted with “cleaner air” aloft. The wet deposition model assumes that the ground-level concentrations are twice the average concentration throughout the 6000-meter mixed layer. In addition, local pollutants were assumed to be uniformly mixed up to 700 meters (the approximate height of Sierra Nevada crest). The model presumes that deeper mixing would allow the locally-generated pollutants to blow out of the Tahoe Basin.

Precipitation Hours – To facilitate the estimation of wet deposition, the seasonal number of precipitation hours was determined by multiplying the number of seasonal days by the seasonal average number of precipitation hours during a day with precipitation. Because the amount and frequency of precipitation can vary dramatically from year to year, this estimate was allowed to vary and to contribute to the range in wet deposition estimates. The number of hours when precipitation occurred during 2003 at Incline

Creek is shown in **Figure 5-6**. The summer precipitation was showery and not likely to be uniform over the Basin on any given day but, on average, the seasonal precipitation frequencies are comparable throughout the basin (**Figure 5-5c**). As shown in **Figure 5-6**, there is a correlation between the number of hours and the amounts of precipitation, with the summer showers being more intense (more water per hour of precipitation). The 2003 precipitation data at Incline Creek and other locations in/near the Tahoe Basin are contrasted in **Figure 5-5**.

Hours of Precipitation per Day – Precipitation during storm passage does not typically occur continuously for 24 hours. During 2003 at Incline Creek, the average number of hours with rain or snow per precipitation day was 6.8, 4.8, 3.7, and 3.0 hours during winter, spring, summer, and fall, respectively. The values used in the bounding analyses ranged from a minimum of 2.7 to a maximum of 7.5 hours per day. The assumption in the wet deposition model is that the each air mass represented by an hour of time (whether in the regional air layer aloft or the local air layer below the Sierra Crest) contains the materials represented by the respective sources (Big Hill for regional) and (mean of SLT-Sandy Way, Thunderbird Lodge, Lake Forest, and DL Bliss SP for local). With each hour, new air masses with similar ambient concentrations enter the Tahoe Basin (i.e., there is no temporal variation in the concentrations of material being advected to the Tahoe Basin and local sources within the Basin rapidly replenish the local material being lost). This assumption will overestimate the actual wet deposition if pollutant concentrations are not rapidly regenerated after wet deposition has occurred. The hourly regeneration assumption is not likely to be valid for the regeneration of primary PM concentrations due to wet surfaces. The lower and upper bound estimates assume a ±10% variation in the number of hours per day of seasonal precipitation. If the variations in the number of days with precipitation and the duration of precipitation are taken together, the lower and upper bound estimates represent a ±38% variation in the number of precipitation hours during any year.

Precipitation Days – The number of days per year with measurable precipitation in the Tahoe Basin was based on 2003 data from Incline Creek, located on the NE side of Lake Tahoe. The number of days with measurable precipitation by season in 2003 was 40, 37, 11, and 4 for winter, spring, summer, and fall respectively. Typically, precipitation during the summer and early fall months is associated with isolated thunderstorms and the precipitation frequencies and amounts on average are roughly similar around the Basin. However, during the passage of synoptic storm systems (generally occurring from November through April), the precipitation amounts on the eastern side of the Lake are about ½ the amount on the western side of the Lake. The frequency of days with precipitation does not vary as much from west to east in the Basin based on the 2003 data; however, analysis of precipitation during additional years is needed to confirm the relatively spatially-uniform frequency. The number of days with precipitation also varies from year to year. Precipitation amounts around the Tahoe Basin during 2003 were generally below normal with an atypical seasonality. Additional analysis is warranted to better quantify the potential variation in wet deposition due to inter-annual variations in the number of precipitation hours. The lower and upper bound

estimates assumed a ±25% variation in the number of precipitation days. On an annual basis, this equates to a lower bound of 69 precipitation days, a central estimate of 92 precipitation days, and an upper bound of 115 of precipitation days per year.

Fraction of precipitation to Lake Tahoe – The fraction of the precipitation, cleansing the transported (regional background) pollution that falls directly on Lake Tahoe was assumed to be 5, 10, and 15% respectively for the lower, central, and upper estimates. This parameter for the transported portion of the wet deposition assumes that most of the precipitation and washout of the transported material will occur over the Sierra Nevada due to orographic lifting. As indicated by contours of annual precipitation amounts, only a relatively small portion of the transport washout actually falls directly on Lake Tahoe (**Figure 5-7**). These percentages were applied to the winter and spring seasons when synoptic-scale storms move through the region. During summer and fall when precipitation is more showery, the areal coverage of the scattered showers was assumed to be 5, 10, and 15% respectively for the lower, central, and upper estimates. These are crude estimates based on a thunderstorm being 6-10 km in diameter (Byers, 1965). Compared to the surface area of Lake Tahoe (500 km^2), the area impacted by a thunderstorm (30-80 km^2) represents 6-16% of the Lake's surface. Of course, more than one thunderstorm may develop but they are also more likely to develop over land than the lake itself. Similarly for wet deposition of locally generated pollutants, the fraction of precipitation falling on the Lake was assumed to be 100% during the winter and spring, and to be 5, 10, and 15% respectively for the lower, central, and upper estimates of the areal coverage of scattered showers in summer and fall.

Washout Efficiency – 50, 75, and 100%. Another major assumption in the wet deposition analysis is the efficiency with which the precipitation washes the pollutants out of the atmosphere. This parameter applies a factor to the total mass of material in the volume of air above the Lake to estimate the amount of wet deposition to the lake surface. It quantifies the amount of material actually "washed" out of the air. For this analysis, 50, 75, and 100 percent washout efficiencies were assumed for the bounding estimates. The central estimate is based on Byers (1965) who notes that a modest precipitation rate removes 75% of the aerosols in the column within the first hour of precipitation. Obviously, the upper estimate is the most extreme option possible. The lower bound was set to maintain a comparable deviation from the central estimate.

The detailed results of the CARB wet deposition analysis are presented below and have been divided into "transport" and "local" components to provide a "guestimate" of the relative contributions of regional and local pollution sources to total wet deposition onto Lake Tahoe.

5.3 Estimates of Wet Deposition Associated with Transport

Reiterating, the estimated transport component of the wet deposition to Lake Tahoe assumes that storm systems carry pollutants from the coast and Central Valley of California up the Sierra Nevada slope. Some of the transported pollution, whether initially as condensation nuclei or absorbed on the precipitation, falls directly onto Lake Tahoe. The transport component is based on air quality concentrations measured at

the Big Hill site, located about 30 miles upwind of the center of Lake Tahoe and about the same elevation as Lake Tahoe. This site was operated with a comprehensive suite of measurements during LTADS to characterize the regional air pollution (not influenced by local sources) available for potential transport into the Tahoe Basin. No significant anthropogenic emission sources exist between Big Hill and Lake Tahoe. The air quality at Big Hill thus serves as an upper estimate of the concentrations of pollutants actually available for transport to Lake Tahoe because additional dispersion, diffusion, and deposition would occur during any potential air parcel's horizontal and vertical (over the Sierra Nevada) transport to Lake Tahoe. The nitrogenous compounds considered in this deposition assessment were the soluble gases, ammonia (NH_3) and nitric acid (HNO_3), and the soluble ammonium (NH_4^+) and nitrate (NO_3^-) ions found in particles of all sizes (i.e., TSP). Wet deposition estimates are also provided for phosphorus (P) and particulate matter (PM) of all sizes: PM_fine (i.e., PM2.5), PM_coarse (i.e., 2.5 µ < PM_diameter < 10 µ), PM_large (i.e., PM_diameter > 10 µ), which are summed together to represent wet deposition of total PM.

Figure 5-6. Monthly distribution of precipitation at Incline Creek, 2003.

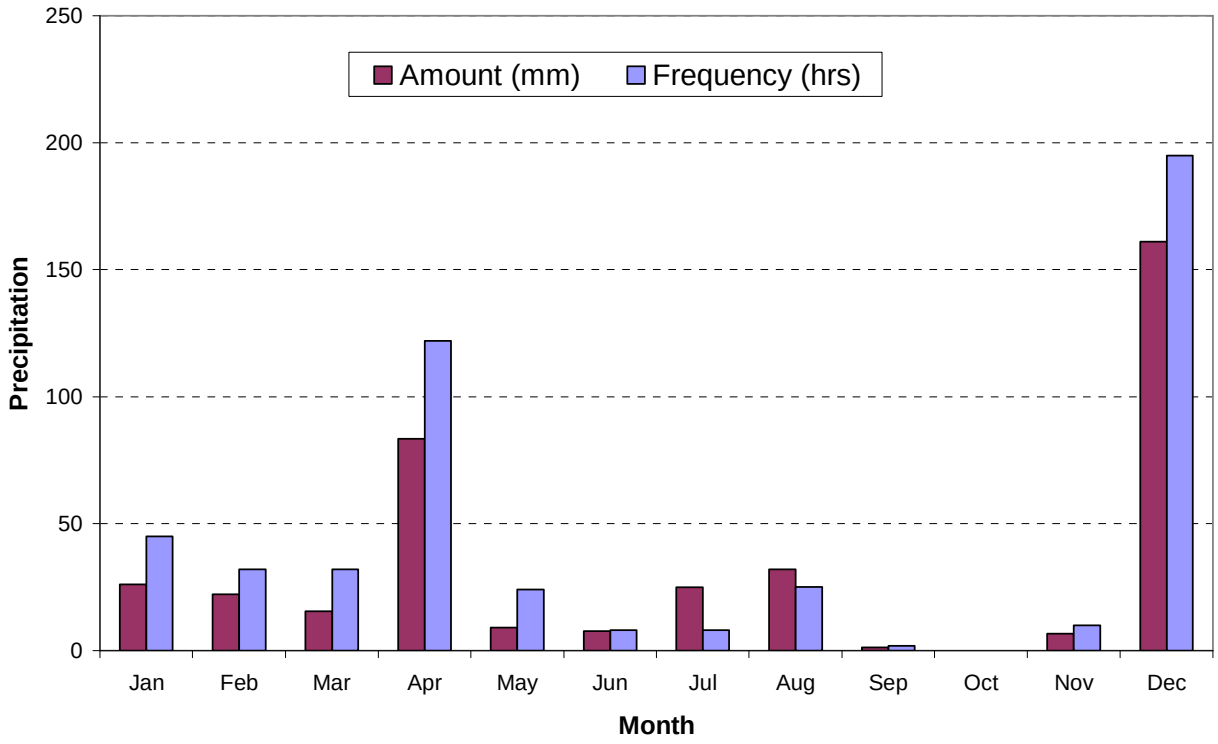

Storms associated with frontal passages (primarily winter and spring) carrying pollutants from the west toward the Tahoe Basin do not drop all of their precipitation directly on Lake Tahoe. Assuming that the air quality at Big Hill is representative of the concentrations along the western slopes of the Sierra Nevada west of Lake Tahoe, an assumption must be made about the proportion of precipitation that occurs along the west-to-east passage of the storms. Because the Sierra Nevada force the air to rise as

it crosses them, most of the storm precipitation occurs on the western slopes and crest of the Sierra Nevada, with the Tahoe Basin being somewhat in the rain shadow of the mountain range (**Figure 5-7**). For this analysis, 5, 10, and 15 percent of the total pollutant load in the storm precipitation (along a line from Big Hill to Lake Tahoe) is estimated to fall directly onto Lake Tahoe under the low, central, and upper estimate scenarios. In other words, most of the precipitation and pollutant load falls out before they reach the Tahoe Basin.

Because the pollutant concentrations from the TWS network are 2-week averages and precipitation does not fall constantly for two weeks, the wet deposition analysis matched the minimum 2-week concentrations in the winter and spring seasons with the respective seasonal occurrence (# of hours) of precipitation in the Tahoe Basin (represented by Incline Creek). Because the isolated thunderstorms of summer and fall occur in air with typical seasonal concentrations, seasonal mean pollutant concentrations were used in the wet deposition analysis of the summer and fall seasons. Thus, the transport component of the wet deposition analysis assumes that the concentrations measured at Big Hill are available for potential transport to Lake Tahoe and are represented by the seasonal mean concentrations during summer and fall but by the 2-week minimum seasonal concentrations during winter and spring. These "transportable" concentration estimates (ng/m^3) at Big Hill are shown in **Table 5-3** for TSP_NH_4, TSP_NO_3, P, PM, HNO_3, and NH_3. Considering only the nitrogen component of each compound (shown in parentheses as ng N/m^3), the bulk of the N available for transport is in NH_3, particularly in summer. As might be expected based on emission sources and meteorological processes, the potential for transport of nitrogen, as well as P and PM, to the Tahoe Basin is greatest in the summer and fall when the ground is driest, forest and camping fires are most common, and the long hours of daylight favor more air flow up the western slopes of the Sierra Nevada.

The seasonal transportable concentrations of pollutants in the atmosphere at Big Hill were then multiplied by the seasonal frequency of precipitation events in the Tahoe Basin. Washout of the pollutants was assumed to occur for each hour of precipitation (i.e., new air being advected into Basin had background levels of materials). A cleansing efficiency factor was applied to account for the proportion of material theoretically washed out (i.e., a portion of the pollution load remains in the air). The lower, central, and upper estimates of transported wet deposition assumed 50, 75, and 100 percent vertical washout, respectively, of the pollutant materials in the transport portion of the cylinder of air above Lake Tahoe (i.e., 700 – 3700 m AGL layer).

The direct atmospheric loading of transported (regional background) N, P, and PM to Lake Tahoe was estimated in metric tons as the seasonal representative (N,P,PM) concentrations times the mixing depth (MD, altitude to which material is uniformly mixed and represented by surface concentrations; assumed constant in this analysis but varies diurnally and seasonally) times 5.01×10^{-7} (to convert ng/m^3 to metric tons, assuming surface area of Lake Tahoe = 501 km^2) times the number of precipitation hours (PF) during each season times the horizontal fraction of precipitation downwind of Big Hill that falls directly on Lake Tahoe (HW) times the vertical washout efficiency

Figure 5-7. Annual average precipitation (inches) in Northern California – 1961-90 mean.

(Note the enhanced precipitation along the western slope of the Sierra Nevada due to orographic lifting of the air. Storm systems typically move from the west southwest toward the east northeast. The Tahoe Basin is on the lee side of the Sierra where annual precipitation amounts decline. Integrating along the line from Big Hill upwind air quality site to Lake Tahoe (solid line), the precipitation amount over Lake Tahoe is about 10% of the total precipitation falling along the potential transport route of pollutants from Big Hill to Lake Tahoe. Considering a line from Sacramento (dashed line), the precipitation amount over Lake Tahoe is about 3% of the total precipitation falling along the potential transport route of pollutants from the Central Valley to Tahoe.)

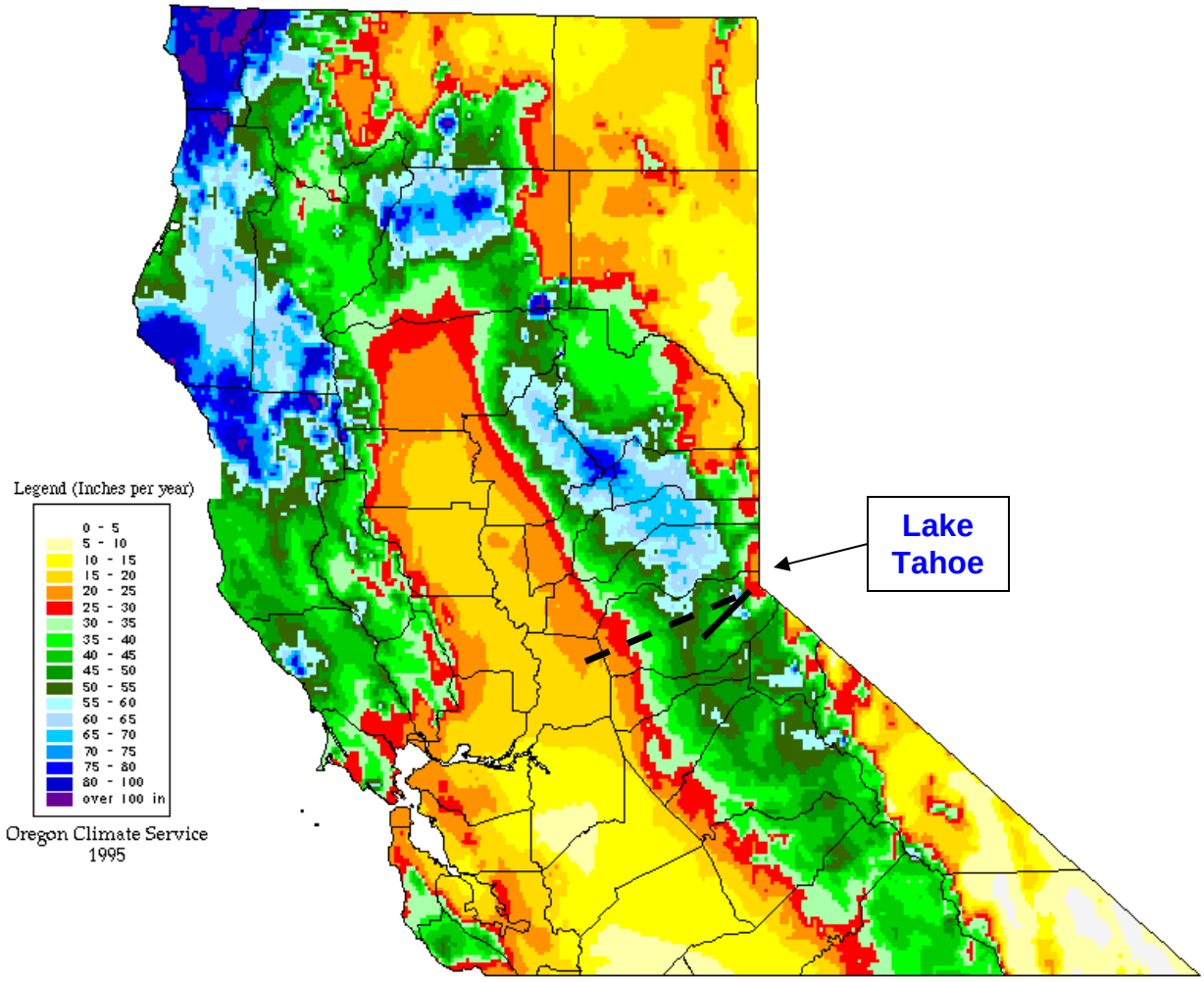

(VW) of the precipitation. In equation form with the subscript "s" representing each season, the seasonal wet deposition due to transport is estimated as:

$$\mathbf{WetDep\_transport_{(N,P,PM)} = ([N,P,PM]_s * MD * PF_s) * 5.01x10^{-7} * HW * VW}.$$

The annual wet deposition is estimated by summing the seasonal values. The lower, central, and upper wet deposition estimates are determined from ranges in values for PF, HW, and VW.

Table 5-3. Concentrations (ng/m^3) observed in each season at Big Hill and used in the LTADS estimation of direct atmospheric wet deposition to Lake Tahoe due to transport (regional background). (Note: Minimum representative 2-week concentrations are shown for winter and spring while seasonal mean concentrations are shown for summer and fall. For P, a base concentration of 40 ng/m^3 was assumed. For the winter and spring seasons when synoptic storms occur, the base concentration was multiplied by the seasonal ratios of the $[TSP]_{2\text{-week minimum}}/[TSP]_{mean}$ at Big Hill. Because most of the P mass is in larger particles (which are not likely to transport the full distance to Tahoe during dry stable conditions), the base [P] was multiplied by the seasonal ratio of [PM10]/[TSP] at Big Hill. Nitrogenous specie concentrations are also shown in parentheses as ng N/m^3.)

[Pollutant] (ng/m^3) **\ Season:**	**Estimate Range**	**winter**	**spring**	**summer**	**fall**
TSP_NH_4	Central	30 (23)	208 (162)	430 (335)	303 (236)
TSP_NO_3	Central	177 (40)	617 (139)	1763 (398)	1394 (315)
HNO_3	Central	87 (19)	99 (22)	1127 (250)	816 (181)
NH_3	Central	65 (53)	89 (73)	984 (810)	719 (592)
TN	Central	(135)	(396)	(1793)	(1324)
P	Central	27	26	30	31
PM	Central	1586	3984	15,165	12,797
PM_fine	Central	563	1905	6887	4962
PM_coarse	Central	344	1795	4855	4898
PM_large	Central	678	284	3423	2938

The estimated transport contributions to the wet atmospheric deposition to Lake Tahoe are presented by pollutant and season in **Table 5-4**. Annually, ammonia is the predominant nitrogen specie being transported and deposited (~8 metric tons N) but ammonium and nitrate particles are slightly lower (~6 metric tons N each). Nitric acid is the least common nitrogen specie being deposited at ~2 metric tons N). Transported phosphorus deposition is less than 2 metric tons per year and PM deposition is a little over 200 metric tons per year. Spring dominates the transported PM deposition with summer a close second, and winter third. The amount of PM deposition transported in fall is small compared to the other seasons. The summer concentrations are greater than in spring but the precipitation frequency is much greater during spring than summer.

Table 5-4. Seasonal estimates of direct atmospheric wet deposition to Lake Tahoe due to transport (regional background) in 2003 (metric tons; N species as N).

Parameter	Estimate \ Season:	winter	spring	summer	fall	Annual
TSP_NH_4	lower bound	0.2	0.7	0.4	0.1	1.3
	central estimate	**0.7**	**3.3**	**1.6**	**0.3**	**5.8**
	upper bound	2.0	8.9	4.3	0.9	16.0
TSP_NO_3	lower bound	0.3	0.6	0.4	0.1	1.4
	central estimate	**1.2**	**2.8**	**1.8**	**0.4**	**6.3**
	upper bound	3.4	7.7	5.1	1.2	17.3
NH_3	lower bound	0.4	0.3	0.8	0.2	1.6
	central estimate	**1.6**	**1.5**	**3.7**	**0.8**	**7.6**
	upper bound	4.5	4.0	10.3	2.2	21.0
HNO_3	lower bound	0.1	0.1	0.3	0.1	0.5
	central estimate	**0.6**	**0.4**	**1.2**	**0.3**	**2.4**
	upper bound	1.6	1.2	3.2	0.7	6.7
Total N	lower bound	0.9	1.8	1.9	0.4	5.0
	central estimate	**4.2**	**7.9**	**8.3**	**1.8**	**22.2**
	upper bound	11.4	21.9	22.8	4.9	61.0
Phosphorus	lower bound	0.0	0.0	0.0	0.0	0.1
	central estimate	**0.1**	**0.1**	**0.0**	**0.0**	**0.3**
	upper bound	0.3	0.3	0.1	0.0	0.7
Particulate Matter	lower bound	2	4	5	1	12
	central estimate	**7**	**17**	**19**	**6**	**48**
	upper bound	18	42	47	14	121
PM_fine	lower bound	0.6	2.0	2.1	0.6	5.3
	central estimate	**2.5**	**7.9**	**8.5**	**2.2**	**21.3**
	upper bound	6.4	19.9	21.4	5.6	53.2
PM_coarse	lower bound	0.4	1.9	1.5	0.6	4.3
	central estimate	**1.6**	**7.5**	**6.0**	**2.2**	**17.3**
	upper bound	3.9	18.7	15.1	5.5	43.2
PM_large	lower bound	0.8	0.3	1.1	0.3	2.5
	central estimate	**3.1**	**1.2**	**4.2**	**1.3**	**9.8**
	upper bound	7.6	3.0	10.6	3.3	24.5

5.4 Estimates of Wet Deposition Associated with Local Pollutant Sources

The calculation of wet deposition due to local sources of nutrients and particulate matter has assumptions similar to those in the transport component. In the case of wet deposition of materials of local origin, it is assumed that precipitation is equally likely to fall on the Lake as on land (where measurements were made) and that the pollutant concentrations are equally high over the Lake as near the shoreline.

The local component assumes that the air pollutants available for removal/washout to the Lake are represented by the seasonal shoreline averages of N, P, and PM concentrations in 4 quadrants (S-SE quadrant represented by South Lake Tahoe-Sandy Way, N-NW quadrant represented by Lake Forest, E-NE quadrant represented by Thunderbird Lodge, and W-SW quadrant represented by Bliss State Park). The lowest representative 2-week pollutant concentrations in winter and spring and seasonal mean concentrations for summer and fall are shown by site and season in **Table 5-1**. The seasonal basin mean concentrations (estimated by the 4-quadrant mean) are shown in **Table 5-5**. Because the number of phosphorus analytical detections was low, the TSP_P concentration for each season was set at 40 ng/m^3. For the local wet deposition estimates, the estimated 40 ng/m^3 [P] at each site was multiplied by the ratios of the seasonal $[TSP]_{2\text{-week minimum}}/[TSP]_{mean}$ during the organized storms of winter and spring. The estimated 40 ng/m^3 P concentration was used directly for the summer and fall calculations (i.e., no depletion in local ambient concentrations when only scattered showers involved).

Given the enhanced wind speeds and vertical air motions during precipitation events and the proximity of local sources to the Lake, TSP was assumed to be transportable to the Lake. The PM_nitrogen species (i.e., NH_4^+ and NO_3^-) being transported to the shoreline were also estimated from the TSP measurements.

The total average N concentrations in the Tahoe Basin were lower than at the upwind Big Hill site during summer and fall when the winds carry pollutants from the Central Valley into the Sierra Nevada. Total N concentrations are comparable at Big Hill and within the Tahoe Basin during the spring when atmospheric mixing is generally good. During the winter however, the Tahoe Total N values are higher than at the Big Hill site due to poorer dispersion of emissions between storms in the Tahoe Basin and weaker advection of pollutants from the Central Valley toward the Sierra Nevada. When storms do transport pollutants, the unstable conditions and wet deposition result in low ambient concentrations at the Big Hill site. At both the upwind site (Big Hill) and the Tahoe sites, NH_3 comprised the bulk of the total N concentrations during summer and fall while particulate NH_4 can also be a significant component in spring.

As was the case for the regional source analysis, the estimate of wet deposition from local sources also assumed a range of meteorological variables, which are listed in **Table 5-2**. Because the number of samples when P was detectable in the Tahoe Basin was low, the analysis assumed a seasonally and spatially constant P concentration. Using an average Tahoe P value of 40 ng/m^3 during LTADS is consistent with ambient

measurement techniques, with emission inventory estimates, and with values observed in other sampling programs in the Sierra (dichotomous and toxic measurements).

The range of wet deposition estimates from local sources was created from a range of meteorological estimates. For lower bound, central, and upper bound estimates, many of the meteorological parameter values are naturally the same as those assumed for wet deposition of transported materials. One significant difference in the meteorological assumptions for regional and local sources is the fraction of precipitation washing out directly on the Lake (HW). Because the analysis estimates the amount of pollution in the volume of air directly above the Lake (501 km^2), no fractional correction is needed for the local wet deposition during the winter and spring when widespread storms occur. In the summer and fall when precipitation occurs as scattered rain showers, the areal precipitation fractions used were 5, 10, and 15% for the range of estimates.

The estimated local component of the wet atmospheric deposition to Lake Tahoe is presented by season in **Table 5-6**. As might be expected from the seasonal precipitation distribution, local wet deposition estimates are much higher in winter and spring than during summer and fall. The dominant nitrogen specie in the local deposition component was NH_3. The annual local wet deposition is dominated by the winter and spring seasons.

Table 5-5. Seasonal air quality concentrations (ng/m^3) estimated over Lake Tahoe (i.e., the 4-quadrant mean) and used in the estimation of direct atmospheric wet deposition to Lake Tahoe due to local pollutant sources in 2003. (Note: The 4-quadrant means of the seasonal minimum representative 2-week concentrations are shown for winter and spring while the 4-quadrant mean concentrations are shown for summer and fall. Nitrogenous specie concentrations are also shown in parentheses as ng N/m^3. [P]s in winter and spring are from the baseline [P] (i.e., 40 ng/m^3) multiplied by the seasonal ratios of $[TSP]_{2\text{-week minimum}} / [TSP]_{mean}$.)

[Parameter] (ng/m^3) \ Season:	Estimate Range	winter	spring	summer	fall
TSP_NH_4	fixed	74 (58)	159 (124)	304 (236)	231 (180)
TSP_NO_3	fixed	293 (66)	382 (86)	974 (220)	732 (165)
HNO_3	fixed	280 (62)	177 (39)	599 (133)	675 (150)
NH_3	fixed	251 (207)	197 (162)	625 (515)	654 (539)
TN	fixed	(393)	(412)	(1104)	(1034)
P	fixed	17	29	40	40
PM	fixed	4450	6466	12,413	12,999
PM_fine	fixed	2631	2340	5913	5442
PM_coarse	fixed	1468	3477	5620	5628
PM_large	fixed	351	649	880	1929

Table 5-6. Seasonal estimates* of direct atmospheric wet deposition to Lake Tahoe due to local sources in 2003.

Parameter	Estimate \ Season:	winter	spring	summer	fall	Annual
TSP_NH_4	lower bound	1.9	2.6	0.1	0.0	4.5
	central estimate	**4.1**	**5.8**	**0.3**	**0.1**	**10.2**
	upper bound	7.6	10.6	0.7	0.2	19.1
TSP_NO_3	lower bound	2.1	1.8	0.1	0.0	4.0
	central estimate	**4.7**	**4.0**	**0.2**	**0.1**	**9.1**
	upper bound	8.7	7.4	0.7	0.1	16.9
NH_3	lower bound	6.7	3.4	0.1	0.0	10.2
	central estimate	**14.8**	**7.6**	**0.6**	**0.2**	**23.1**
	upper bound	27.1	13.9	1.5	0.5	43.1
HNO_3	lower bound	2.0	0.8	0.0	0.0	2.9
	central estimate	**4.5**	**1.8**	**0.1**	**0.0**	**6.5**
	upper bound	8.2	3.4	0.4	0.1	12.1
Total N	lower bound	12.7	8.7	0.3	0.1	21.7
	central estimate	**28.1**	**19.3**	**1.2**	**0.3**	**48.9**
	upper bound	51.6	35.3	3.3	0.9	91.0
Phosphorus	lower bound	0.1	0.1	0.0	0.0	0.2
	central estimate	**0.2**	**0.3**	**0.0**	**0.0**	**0.5**
	upper bound	0.3	0.5	0.0	0.0	0.8
Particulate Matter	lower bound	23	32	1	0	56
	central estimate	**47**	**63**	**4**	**1**	**115**
	upper bound	78	105	9	3	195
PM_fine	lower bound	13.8	11.4	0.4	0.1	25.8
	central estimate	**27.7**	**22.8**	**1.7**	**0.6**	**52.7**
	upper bound	46.1	37.9	4.3	1.4	89.8
PM_coarse	lower bound	7.7	16.9	0.4	0.1	25.2
	central estimate	**15.4**	**33.8**	**1.6**	**0.6**	**51.5**
	upper bound	25.7	56.4	4.1	1.5	87.7
PM_large	lower bound	1.8	3.2	0.1	0.1	5.1
	central estimate	**3.7**	**6.3**	**0.3**	**0.2**	**10.5**
	upper bound	6.2	10.5	0.6	0.5	17.8

* units are metric tons except that the nitrogen compounds are presented as metric tons of N.

5.5 Summary of Wet Deposition Estimates for 2003

The results of these wet deposition estimates are presented in one seasonal summary by pollutant (**Table 5-7**) and three seasonal summary tables quantifying regional, local, and total wet deposition of total nitrogen, phosphorus, and particulate matter to Lake Tahoe (**Tables 5-8 through 5-10**).

The analysis indicates that the bulk of the N, P, and PM wet deposition originates from local pollution sources (**Figure 5-8**). The bulk of the wet deposition occurs during winter and spring. The greatest transport contribution occurs for PM_NH_4 and PM_NO_3 during the spring and summer. The bulk of the total annual wet deposition occurs during the winter and spring is from local emissions.

The seasonal variations in the relative contribution of each pollutant by source area ought to guide potential emission control decisions to ensure that control efforts will be optimized for effectiveness. It should also be noted for planning purposes that the wet deposition estimates are for 2003 and are based on the precipitation frequency in 2003. Based on the precipitation frequency in 2003 compared to the climatological norm, wet deposition in a normal year would be about 70% of the 2003 estimate that is presented in this report.

Table 5-7. Seasonal estimates of total direct atmospheric wet deposition to Lake Tahoe in 2003 (metric tons*).

Parameter	Estimate \ Season:	winter	spring	summer	fall	annual
TSP_NH_4	lower bound	2.1	3.3	0.5	0.1	5.8
	central estimate	**4.8**	**9.1**	**1.9**	**0.4**	**16.0**
	upper bound	9.6	19.5	5.0	1.1	35.1
TSP_NO_3	lower bound	2.4	2.4	0.5	0.1	5.4
	central estimate	**5.9**	**6.8**	**2.0**	**0.5**	**15.4**
	upper bound	12.1	15.1	5.8	1.3	34.2
NH_3	lower bound	7.1	3.7	0.9	0.2	11.8
	central estimate	**16.4**	**9.1**	**4.3**	**1.0**	**30.7**
	upper bound	31.6	17.9	11.8	2.7	64.1
HNO_3	lower bound	2.1	0.9	0.3	0.1	3.4
	central estimate	**5.1**	**2.2**	**1.3**	**0.3**	**8.9**
	upper bound	9.8	4.6	3.6	0.8	18.8
Total N	lower bound	13.6	10.5	2.2	0.5	26.7
	central estimate	**32.3**	**27.2**	**9.5**	**2.1**	**71.1**
	upper bound	63.1	57.2	26.1	5.8	152.0
Phosphorus	lower bound	0.1	0.1	0.0	0.0	0.3
	central estimate	**0.3**	**0.4**	**0.1**	**0.0**	**0.7**
	upper bound	0.6	0.7	0.1	0.0	1.5
Particulate Matter	lower bound	25	36	6	2	68
	central estimate	**54**	**80**	**22**	**7**	**163**
	upper bound	96	147	56	18	316
PM_fine	lower bound	14.4	13.4	2.5	0.7	31.1
	central estimate	**30.2**	**30.7**	**10.2**	**2.8**	**74.0**
	upper bound	52.4	57.8	25.7	7.0	142.9
PM_coarse	lower bound	8.1	18.8	1.9	0.7	29.5
	central estimate	**17.0**	**41.3**	**7.6**	**2.8**	**68.8**
	upper bound	30.6	75.1	19.2	7.0	130.9
PM_large	lower bound	2.6	3.5	1.2	0.4	7.6
	central estimate	**6.8**	**7.5**	**4.5**	**1.5**	**20.3**
	upper bound	13.8	13.5	11.2	3.8	42.4

* units are metric tons except that the nitrogen compounds are presented as metric tons of N.

Table 5-8. Estimated Wet Deposition of Nitrogen to Lake Tahoe in 2003 (metric tons N).

Estimate	winter	spring	summer	fall	Annual
CARB Lower Bound					
Regional background	0.9	1.8	1.9	0.4	5.0
Local	12.7	8.7	0.3	0.1	21.7
TOTAL	**13.6**	**10.5**	**2.2**	**0.5**	**26.7**
CARB Central Estimate					
Regional background	4.2	7.9	8.3	1.8	22.2
Local	28.1	19.3	1.2	0.3	48.9
TOTAL	**32.3**	**27.2**	**9.5**	**2.1**	**71.1**
CARB Upper Bound					
Regional background	11.4	21.9	22.8	4.9	61.0
Local	51.6	35.3	3.3	0.9	91.0
TOTAL	**63.0**	**57.2**	**26.1**	**5.8**	**152.0**

Table 5-9. Estimated Wet Deposition of Phosphorus to Lake Tahoe in 2003 (metric tons).

Estimate	winter	spring	summer	fall	Annual
CARB Lower Bound					
Regional background	0.0	0.0	0.0	0.0	0.1
Local	0.1	0.1	0.0	0.0	0.2
TOTAL	**0.1**	**0.1**	**0.0**	**0.0**	**0.3**
CARB Central Estimate					
Regional background	0.1	0.1	0.0	0.0	0.3
Local	0.2	0.3	0.0	0.0	0.5
TOTAL	**0.3**	**0.4**	**0.0**	**0.0**	**0.7**
CARB Upper Bound					
Regional background	0.3	0.3	0.1	0.0	0.7
Local	0.3	0.5	0.0	0.0	0.8
TOTAL	**0.6**	**0.8**	**0.1**	**0.0**	**1.5**

Table 5-10. Estimated Wet Deposition of PM to Lake Tahoe in 2003 (metric tons).

Estimate	winter	spring	summer	fall	Annual
CARB Lower Bound					
Regional background	2	4	5	1	12
Local	23	32	1	0	56
TOTAL	**25**	**36**	**6**	**1**	**68**
CARB Central Estimate					
Regional background	7	17	19	6	48
Local	47	63	4	1	115
TOTAL	**54**	**80**	**23**	**7**	**163**
CARB Upper Bound					
Regional background	18	42	47	14	121
Local	78	147	9	3	195
TOTAL	**96**	**189**	**56**	**17**	**316**

Table 5-10a. Estimated Wet Deposition of PM_fine to Lake Tahoe in 2003 (metric tons).

Estimate	winter	spring	summer	fall	Annual
CARB Lower Bound					
Regional background	0.6	2.0	2.1	0.6	5.3
Local	13.8	11.4	0.4	0.1	25.8
TOTAL	**14.4**	**13.4**	**2.5**	**0.7**	**31.1**
CARB Central Estimate					
Regional background	2.5	7.9	8.5	2.2	21.3
Local	27.7	22.8	1.7	0.6	52.7
TOTAL	**30.2**	**30.7**	**10.2**	**2.8**	**74.0**
CARB Upper Bound					
Regional background	6.4	19.9	21.4	5.6	53.2
Local	46.1	37.9	4.3	1.4	89.8
TOTAL	**52.5**	**57.8**	**25.7**	**7.0**	**142.9**

Table 5-10b. Estimated Wet Deposition of PM_coarse to Lake Tahoe in 2003 (metric tons).

Estimate	winter	spring	summer	fall	Annual
CARB Lower Bound					
Regional background	0.4	1.9	1.5	0.6	4.3
Local	7.7	16.9	0.4	0.1	25.2
TOTAL	**8.1**	**18.8**	**1.9**	**0.7**	**29.5**
CARB Central Estimate					
Regional background	1.6	7.5	6.0	2.2	17.3
Local	15.4	33.8	1.6	0.6	51.5
TOTAL	**17.0**	**41.3**	**7.6**	**2.8**	**68.8**
CARB Upper Bound					
Regional background	3.9	18.7	15.1	5.5	43.2
Local	25.7	56.4	4.1	1.5	87.7
TOTAL	**29.6**	**75.1**	**19.2**	**7.0**	**130.9**

Table 5-10c. Estimated Wet Deposition of PM_large to Lake Tahoe in 2003 (metric tons).

Estimate	winter	spring	summer	fall	Annual
CARB Lower Bound					
Regional background	0.8	0.3	1.1	0.3	2.5
Local	1.8	3.2	0.1	0.1	5.1
TOTAL	**2.6**	**3.5**	**1.2**	**0.4**	**7.6**
CARB Central Estimate					
Regional background	3.1	1.2	4.2	1.3	9.8
Local	3.7	6.3	0.3	0.2	10.5
TOTAL	**6.8**	**7.5**	**4.5**	**1.5**	**20.3**
CARB Upper Bound					
Regional background	7.6	3.0	10.6	3.3	24.5
Local	6.2	10.5	0.6	0.5	17.8
TOTAL	**13.8**	**13.5**	**11.2**	**3.8**	**42.4**

Figure 5-8. Seasonal estimates of wet deposition to Lake Tahoe during 2003 due to local and regional sources.

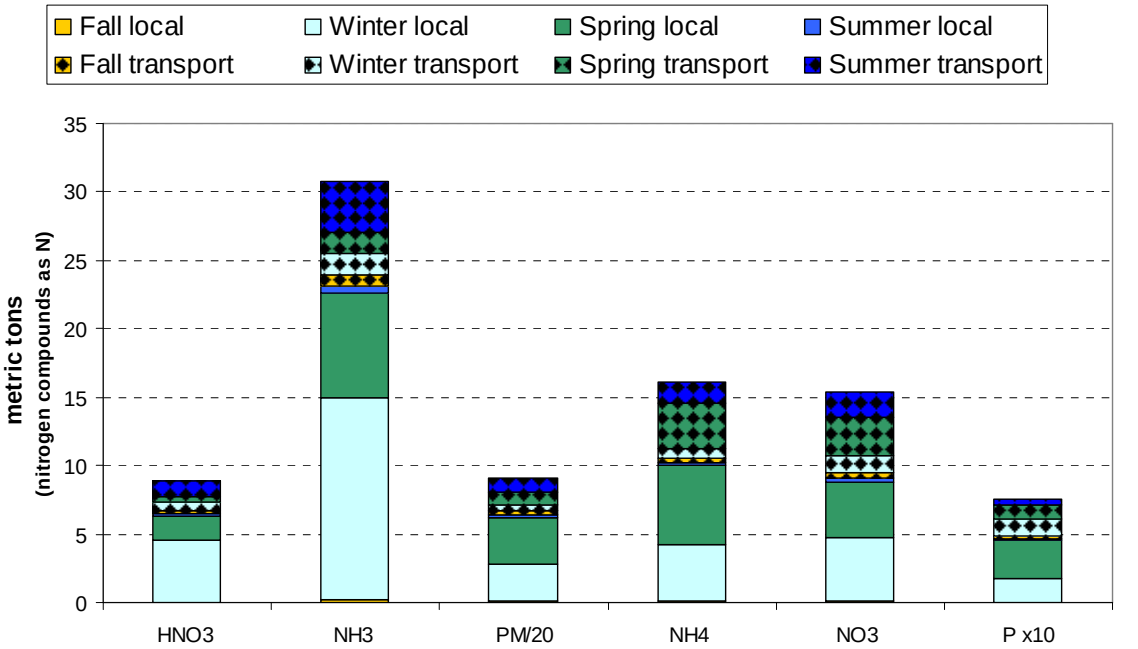

Note adjustment to PM and P values. Actual PM dep is 20 times greater and actual P dep is 10 times less than indicated on Y-axis.

5.6 Comparison with Measurements from Surrogate Surfaces

The Tahoe Research Group (TRG) has collected deposition data for a number of years with a variety of surrogate surface samplers at a limited number of locations. These deposition samplers are briefly described in Appendix A. Only the Wallis Residence (tower) site in Tahoe City (aka Ward Lake Level) has a long-term data record for deposition. CARB staff has reservations about the representativeness of this sampling site because trees have grown around the sampling tower (**Figure 5-9**). In particular, deciduous trees have grown immediately adjacent to the tower, have been cut back, and have re-grown to a height exceeding that of the deposition samplers. These trees likely have an irregular impact on deposition at this site as the impact likely depends on wind direction, wind speed, and season (e.g., leaves, pollen, insects, birds). Wet deposition estimates from surrogate surfaces presumably would have fewer variables affecting the deposition amounts than the dry deposition estimates because the falling precipitation would not be as impacted by sampler- or tree-induced turbulence. The TRG dry deposition bucket sampler was modified in 1989 to include distilled de-ionized water to better represent dry deposition to a water surface. This modification was a particularly significant improvement in N deposition estimates to Lake Tahoe because the measurements then included the contribution of water-soluble gases such as ammonia and nitric acid.

These surrogate surface deposition samplers also receive particulate matter of all sizes (e.g., dust, detritus, pollen, insects, bird droppings) in contrast to the LTADS samplers

(TWS and MVS) which did not collect particles greater than 25 – 30 µm in aerodynamic diameter. As an anecdotal illustration, pine pollen in the spring and early summer is known to cover surfaces and to cover Lake Tahoe and is also captured in the surrogate surface samplers; it is noteworthy that the deposition samples with operator notes indicating the presence of pollen in the sample also tended to have higher phosphorus and ammonium loadings than other samples. Removal of these "pollen-contaminated" samples helped to create the large difference between the "raw" and "edited" wet deposition results shown for the Ward Lake Level site in **Table 5-11**. In late 2001, a National Acid Deposition Program (NADP) site (Sagehen Creek) was established northwest of the Tahoe Basin. Measurements for this site in the NDAP program are also included in **Table 5-11** to provide an additional context of the wet deposition data collected in the Sierra Nevada near Lake Tahoe. Of additional interest is the apparent potentially large year-to-year variation in wet deposition exhibited at the Sagehen site.

The CARB annual wet deposition estimates (i.e., 31 metric tons as N of NH_4^+ and NO_3^-, 71 metric tons of TN, and 1 metric ton of P) are about 30% lower for total nitrogen and 20% lower for nitrogen (ammonium plus nitrates) but about 75% lower for total phosphorus than with the edited data from the surrogate surface (bucket) method (**Table 5-11**). The lower LTADS estimates are not unexpected because the Ward LL site is more heavily impacted than other deposition sampling sites near and on Lake Tahoe. A wet deposition comparison for PM cannot be made because no PM measurements are being made with the current surrogate sampler methods.

Another factor in the comparison of P wet deposition estimates by CARB and TRG is that the CARB P assumes total P. However, the wet/dry deposition bucket measurements have indicated that approximately 50% of the total P is biologically active and available. Thus, CARB's Central Estimate of P wet deposition to Lake Tahoe from the atmosphere likely overestimates the amount of biologically available P being deposited to the Lake from the atmosphere by up to a factor of two.

A seasonal comparison of the LTADS wet deposition estimates with the TRG measurements during 2003 (and with the National Acid Deposition Monitoring Program measurements during 2003 and 2004 of HN_4^+ and NO_3^- at Sagehen northwest of the Tahoe Basin) is provided in **Figures 5-10a-d**. The central LTADS estimate is indicated by the circle with the upper and lower extremes (representing minimum and maximum conceivable estimates, very low probability of being beyond the bounds). The TRG measurement results indicate the range of the original (raw) measurements and the results after editing suspect samples. Except for NO_3^-, the LTADS wet deposition estimates for 2003 are in rough agreement with the TRG measurements. Most of the LTADS estimates are lower than the TRG measurements, especially during summer and fall. The primary reason for this is likely that the LTADS estimate is based on the frequency of precipitation while the TRG measurements are pro-rated to the total amounts of precipitation. Thus, the TRG measurement procedure may be biased high if pollutant washout occurs primarily during the beginning of storms and deposition is not constant throughout the precipitation event. Also of interest is the magnitude of the inter-annual variation in deposition results for Sagehen.

Table 5-11. Wet Deposition Rate Measurements Extrapolated to Lake Tahoe (metric tons/year; nitrogen data are in metric tons N per year).
(Note: Measurements of PM deposition are not made with the surrogate surface samplers used by TRG or NADP. The NADP analysis does not include TKN or P.)

Estimate	Nitrogen+	Phosphorus	PM
TRG Wet			
3-site (WY82)[1]	36.3	2.3	---
3-site (5/83-6/84)[2]	44.2	2.4	---
Ward LL (1989-91)[3]	29.0	5.0	---
Ward LL (1989-91)[4]	40.2	5.1	---
Ward LL raw / edited (2003)	70.2 / 52.3	4.6 / 3.8	---
Ward LL raw / edited (2003)*	103.9* / 109.8*		---
NADP Wet		---	
Sagehen Creek (2003)	38.2	---	---
Sagehen Creek (2004)	16.2	---	---

+ – Nitrogen measurement only includes NH_4^+ and NO_3^- except when marked with an asterisk
* – Nitrogen includes total kinetic nitrogen (TKN, primarily NH_3), in addition to NH_4^+ and NO_3^-
[1] – sites: Incline Village, Glenbrook, & Meyers
[2] – sites: Tahoe Vista & SLT-Bijou
[3] – Jassby (1994); assuming 90 days with precipitation
[4] – Reuter and Tarney (2004)

Figure 5-9. TRG Ward Lake Level (aka Wallis Tower) deposition sampling site.

5.7 Wet and Dry Deposition

The estimates of wet deposition summarized in Section 5.5 derive from an analysis based upon basic principles and a wide range of assumptions. The estimates of dry deposition provided in Chapter 4 were based upon established modeling methods but also required some assumptions to deal with uncertainty in variables that were not quantified through observations. Because the dry deposition estimates are derived through established modeling methods and required fewer assumptions, they are expected to be more reliable than the estimates of wet deposition. Recall too from previous chapters the various assumptions that would affect the deposition estimates. For example, the PM deposition estimates assume that all particles are insoluble. In reality, the TWS sampling results indicate that 20-25% of the particle mass is soluble. Thus, the actual PM deposition affecting water clarity is about 75-80% of the amounts reported in this chapter. Also, as noted in Chapter 2, the wet deposition estimates for a year with a "normal" precipitation frequency could be decreased from the 2003 estimate by, at most, another 30% for both particulate and gaseous pollutants.

Bearing in mind that a lower level of confidence is associated with the estimates of wet deposition compared to those for dry, the two are nonetheless combined in the tables that follow in this section for the convenience of those persons primarily interested in obtaining estimates of the approximate total atmospheric deposition to the Lake. Note too that these atmospheric deposition estimates are for 2003. Central, lower, and upper bound estimates of wet and dry deposition are combined in **Tables 5-12, 5-13, and 5-14** to provide central, lower, and upper bound estimates of total atmospheric deposition. It is also important to remember the different caveats and uncertainties associated with the total deposition estimates by LTADS and total deposition measurements by TRG. As shown in **Figures 5-11a) and b)**, significant differences exist between the two approaches for ammonium (TRG ~2x LTADS) and nitrates (TRG ~3x LTADS). Because the TRG dry deposition method is water-based, ammonia and nitric acid, both of which are water soluble, may be included in the ammonium and nitrates measurements. This possibility is reinforced by the fact that the two methods are in approximate agreement for the estimates of Total Nitrogen (**Figure 5-11c)**). The total phosphorus deposition estimates by LTADS are 50-70% lower than the TRG estimates, which is not unreasonable given the biases in the two methods (**Figure 5-11d)**). As indicated by the range between the bounding estimates, the uncertainty of the LTADS central estimate cannot be considered to be less than ±50%.

Figure 5-10a. Seasonal comparison of LTADS estimate with TRG measurement of ammonium (NH_4^+) wet deposition at Lake Tahoe during 2003.

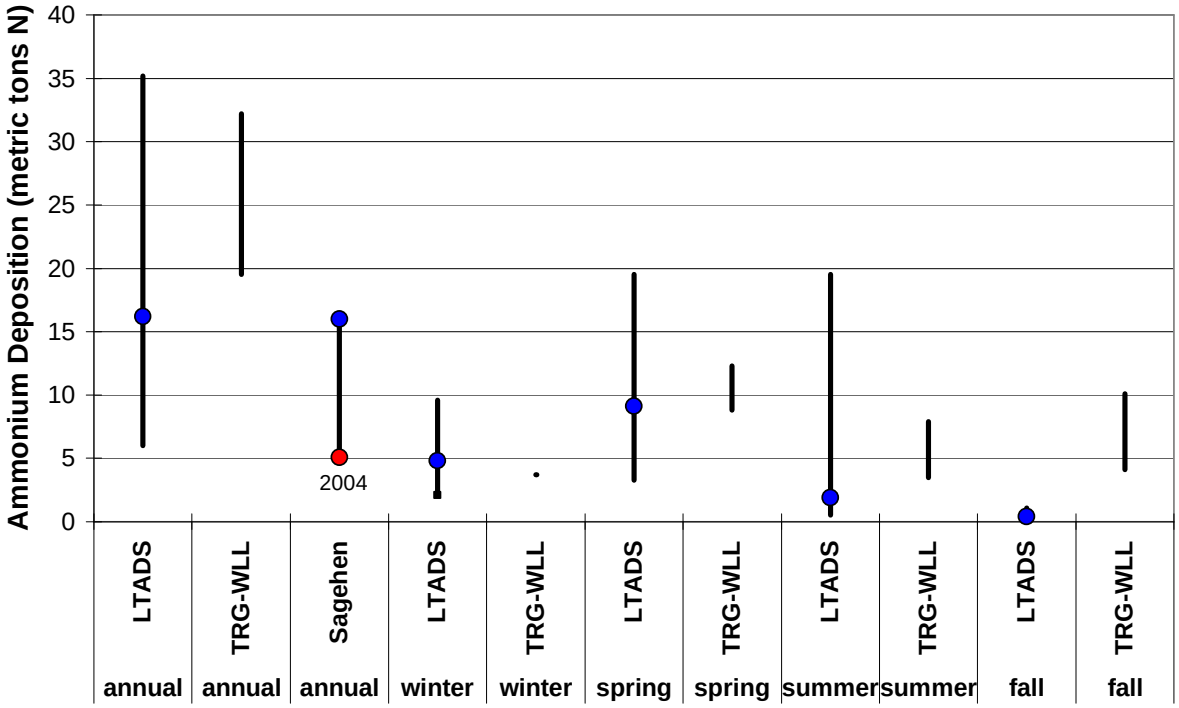

Figure 5-10b. Seasonal comparison of LTADS estimate with TRG measurement of nitrate (NO_3^-) wet deposition at Lake Tahoe during 2003.

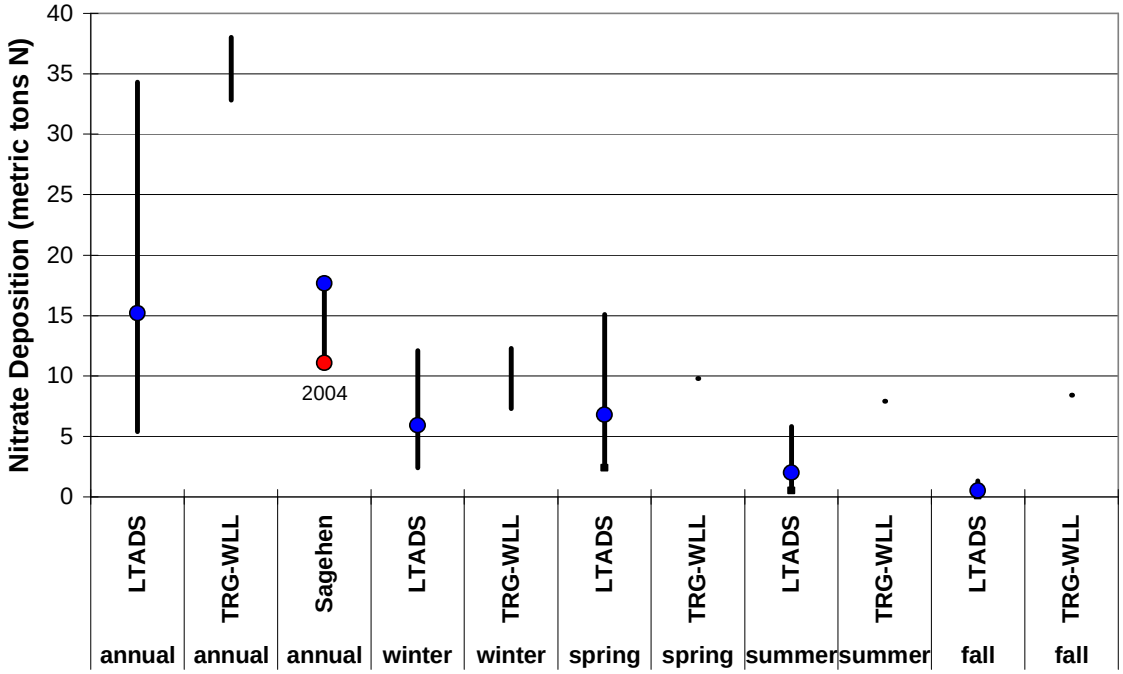

Figure 5-10c. Seasonal comparison of LTADS estimate with TRG measurement of total nitrogen wet deposition at Lake Tahoe during 2003. LTADS data include NH_4^+, NO_3^-, NH_3, and HNO_3 while TRG data include NH_4^+, NO_3^-, and TKN.

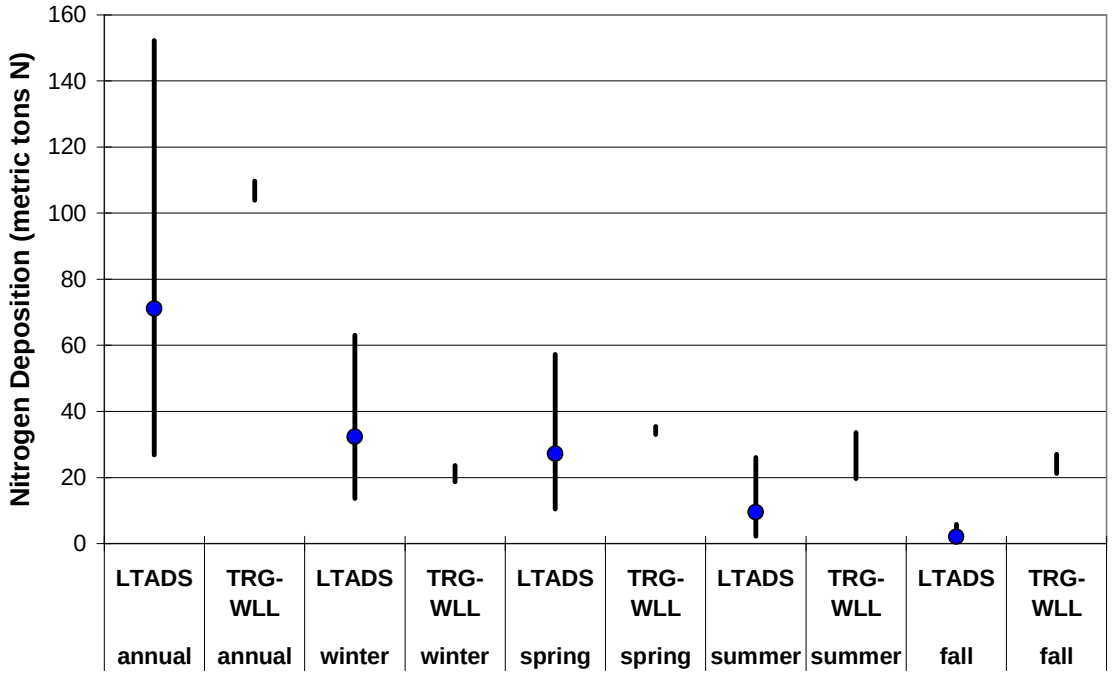

Figure 5-10d. Seasonal comparison of LTADS estimate with TRG measurement of total phosphorus wet deposition at Lake Tahoe during 2003.

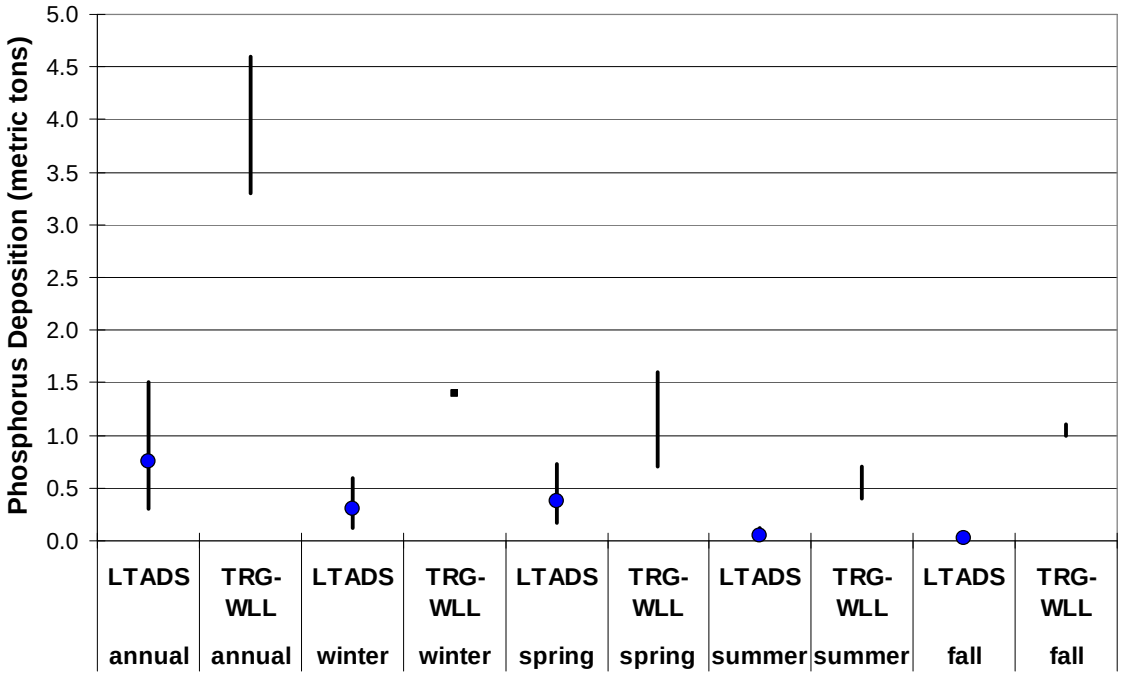

Table 5-12. Central estimates of dry and wet deposition to Lake Tahoe in 2003 combined to provide a central estimate of total deposition (metric tons; nitrogenous compounds as metric tons N).

Parameter	Estimate \ Season:	winter	spring	summer	fall	Annual
TSP_NH4	Central dry	1.1	3.0	3.2	2.5	10
	Central wet	4.8	9.1	1.9	0.4	16
	Total	**5.9**	**12.1**	**5.1**	**2.9**	**26**
TSP_NO3	Central dry	1.0	2.0	3.0	2.1	8
	Central wet	5.9	6.8	2.0	0.5	15
	Total	**6.9**	**8.8**	**5.0**	**2.6**	**23**
NH3	Central dry	17.7	12.8	19.4	26.4	76
	Central wet	16.4	9.1	4.3	1.0	31
	Total	**34.1**	**21.9**	**23.7**	**27.4**	**107**
HNO3	Central dry	5.8	3.3	5.0	7.4	22
	Central wet	5.1	2.2	1.3	0.3	9
	Total	**10.9**	**5.5**	**6.3**	**7.7**	**31**
Total N	Central dry	25.6	21.1	30.6	38.4	116
	Central wet	32.3	27.2	9.5	2.1	71
	Total	**57.9**	**48.3**	**40.1**	**40.5**	**187**
Phosphorus	Central dry	0.6	0.6	0.6	0.6	2.2
	Central wet	0.3	0.4	0.0	0.0	0.7
	Total	**0.9**	**1.0**	**0.6**	**0.6**	**2.9**
Particulate Matter	Central dry	153	131	167	135	590
	Central wet	54	80	23	7	163
	Total	**207**	**211**	**190**	**142**	**753**

Table 5-13. Lower bound estimates of dry and wet deposition to Lake Tahoe in 2003 combined to provide a lower bound estimate of total deposition (metric tons; nitrogenous compounds as metric tons N)**.**

Parameter	Estimate \ Season:	winter	spring	summer	fall	Annual
TSP_NH4	low dry	0.7	1.8	1.8	1.5	6
	low wet	2.1	3.3	0.5	0.1	6
	Total	**2.8**	**5.1**	**2.3**	**1.6**	**12**
TSP_NO3	low dry	0.6	1.2	1.7	1.2	5
	low wet	2.4	2.4	0.5	0.1	5
	Total	**3.0**	**3.6**	**2.2**	**1.3**	**10**
NH3	low dry	11.5	8.7	12.6	17.3	50
	low wet	7.1	3.7	0.9	0.2	12
	Total	**18.6**	**12.4**	**13.5**	**17.5**	**62**
HNO3	low dry	3.7	2.2	3.3	4.8	14
	low wet	2.1	0.9	0.3	0.1	3
	Total	**4.3**	**4.2**	**5.1**	**3.8**	**17**
Total N	low dry	16.5	13.8	19.4	24.8	74
	low wet	13.6	10.5	2.2	0.5	27
	Total	**30.1**	**24.3**	**21.6**	**25.3**	**101**
Phosphorus	low dry	0.2	0.2	0.1	0.2	0.7
	low wet	0.1	0.1	0.0	0.0	0.3
	Total	**0.3**	**0.3**	**0.1**	**0.2**	**1.0**
Particulate Matter (TSP)	low dry	95	80	98	84	360
	low wet	25	36	6	1	68
	Total	**120**	**116**	**104**	**85**	**428**

Table 5-14. Upper bound estimates of dry and wet deposition to Lake Tahoe in 2003 combined to provide an upper bound estimate of total deposition (metric tons; nitrogenous compounds as metric tons N).

Parameter	Estimate \ Season:	winter	spring	summer	fall	Annual
TSP_NH4	high dry	1.7	4.6	4.9	3.8	15
	high wet	9.6	19.5	5.0	1.1	35
	Total	**11.3**	**24.1**	**9.9**	**4.9**	**50**
TSP_NO3	high dry	1.5	3.0	4.6	3.2	12
	high wet	12.1	15.1	5.8	1.3	34
	Total	**13.6**	**18.1**	**10.4**	**4.5**	**46**
NH3	high dry	26.0	18.1	28.2	38.4	110
	high wet	31.6	17.9	11.8	2.7	64
	Total	**57.6**	**36.0**	**40.0**	**41.1**	**174**
HNO3	high dry	8.5	4.7	7.3	11.0	31
	high wet	9.8	4.6	3.6	0.8	19
	Total	**18.3**	**9.3**	**10.9**	**11.8**	**50**
Total N	high dry	37.7	30.3	45.0	56.3	170
	high wet	63.1	57.2	26.1	5.8	152
	Total	**100.8**	**87.5**	**71.1**	**62.1**	**322**
Phosphorus	high dry	0.7	0.8	0.8	0.8	3.2
	high wet	0.6	0.8	0.1	0.0	1.5
	Total	**1.3**	**1.6**	**0.9**	**0.8**	**4.7**
Particulate Matter	high dry	224	191	250	196	900
	high wet	96	147	56	17	316
	Total	**320**	**338**	**306**	**213**	**1216**

Figure 5-11a. Total (wet + dry) ammonium (NH_4^+) deposition estimates for 2003.

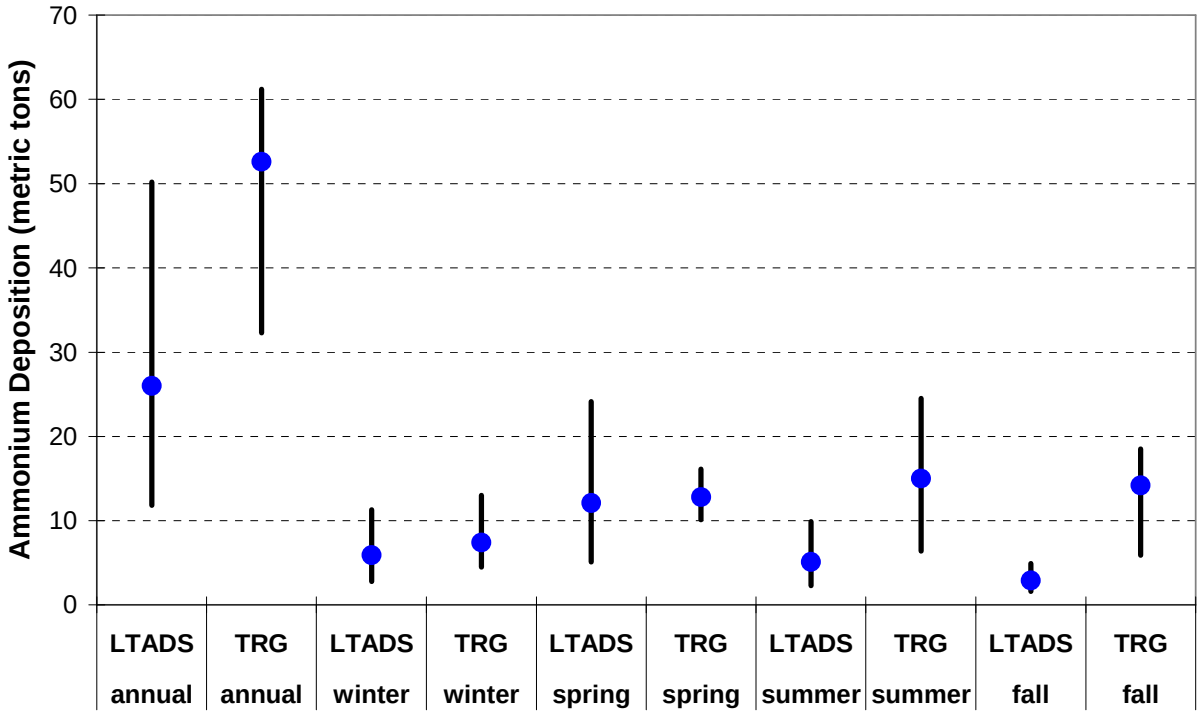

Figure 5-11b. Total (wet + dry) nitrates (NO_3^-) deposition estimates for 2003.

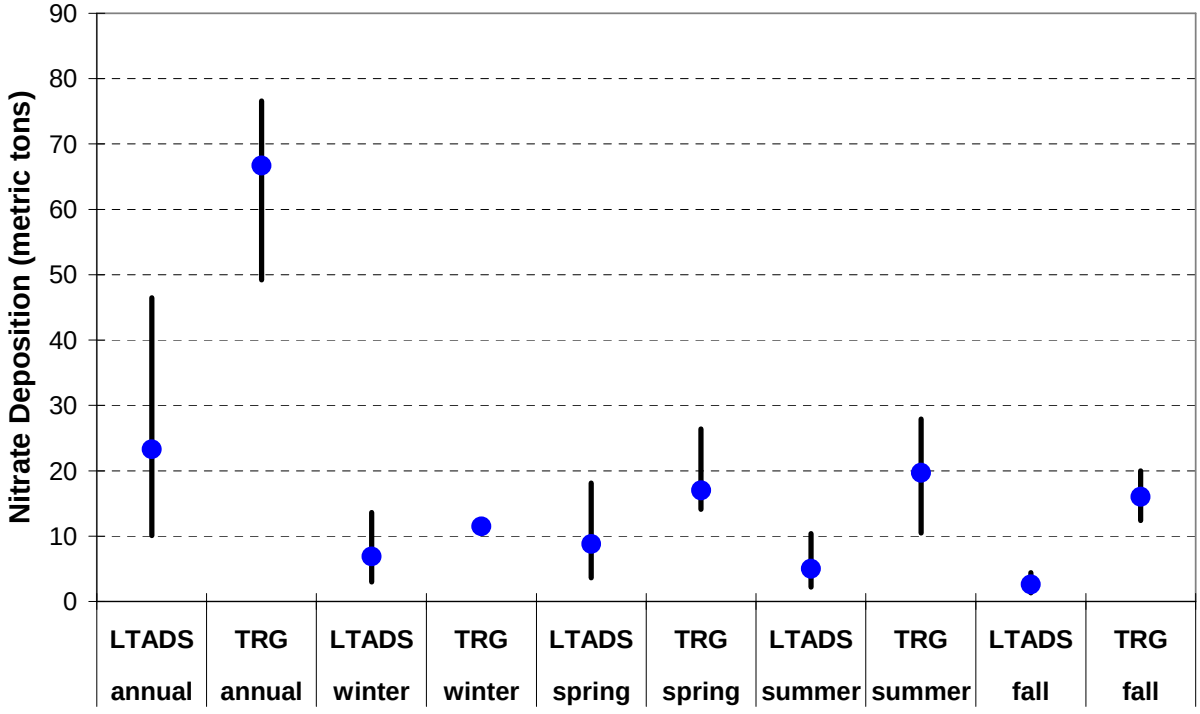

Figure 5-11c. Total (wet + dry) total nitrogen (TN) deposition estimates for 2003.

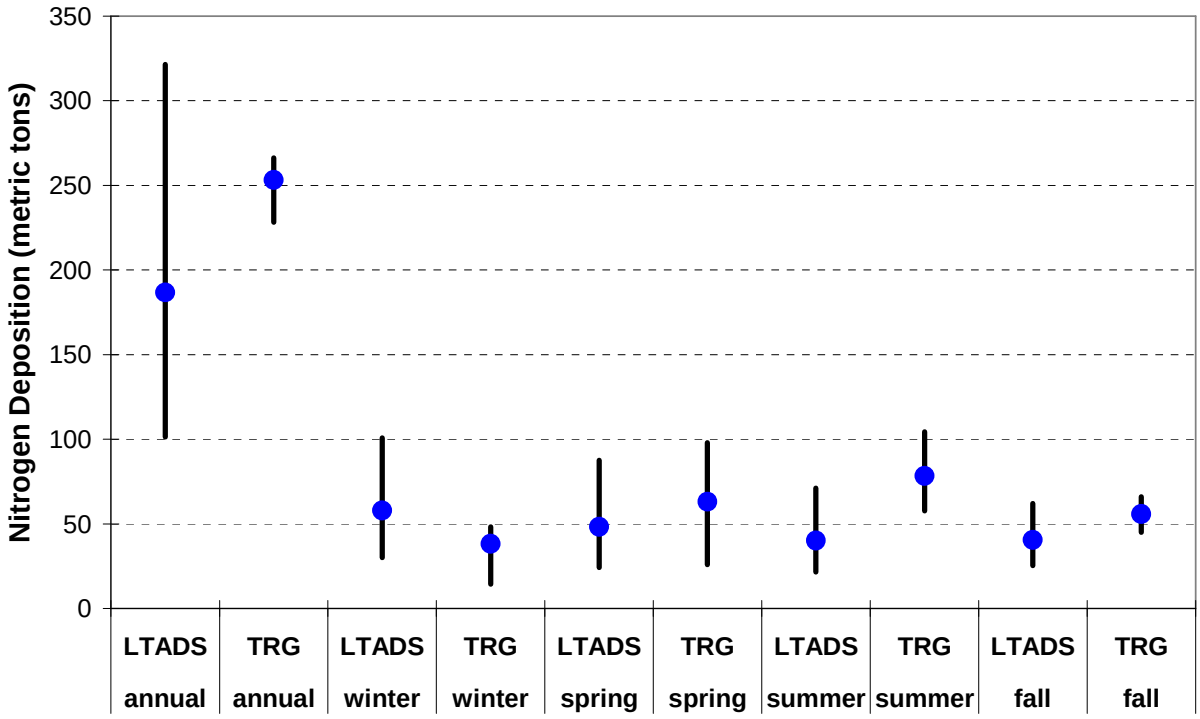

Figure 5-11d. Total (wet + dry) phosphorus (P) deposition estimates for 2003.

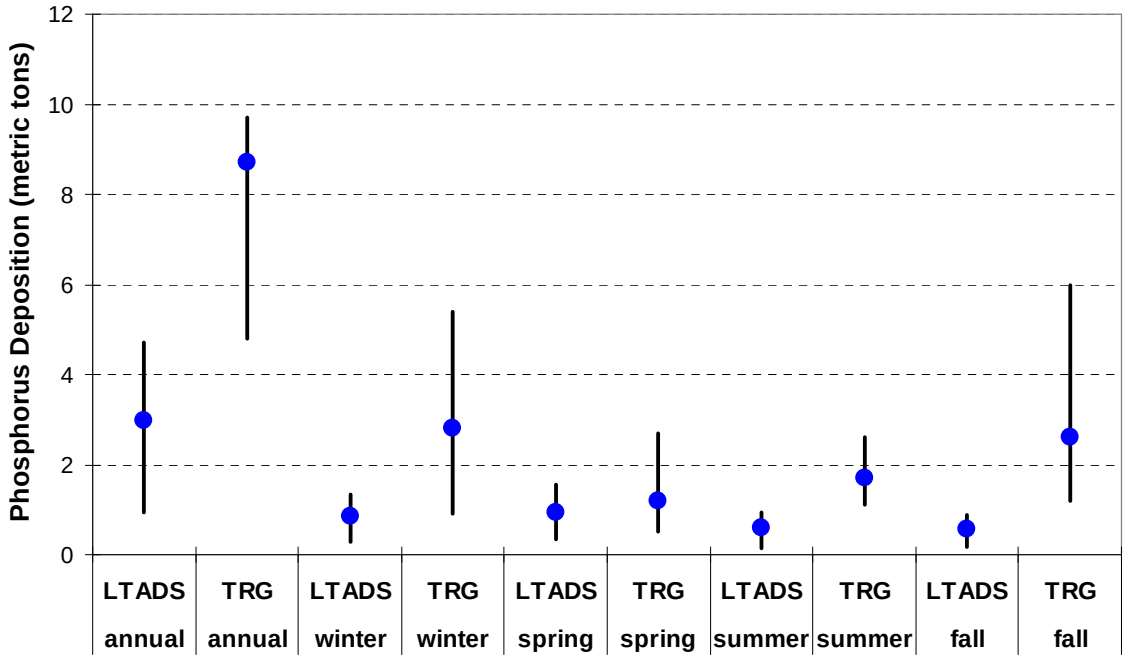

5.8 References

Byers, H.R. (1965). In *Elements of Cloud Physics*, University of Chicago Press, Chicago, p. 28.

Hales, J.M. (1991). "Atmospheric process research and process model development", in *Acidic Deposition: State of Science and Technology, Vol. I: Emissions, Atmospheric Processes, and Deposition*. U.S. National Acid Precipitation Program, Washington, DC.

Hales, J.M. (1995). "Acidic Precipitation", Ch. 12 in H.B. Singh, ed., *Composition, Chemistry, and Climate of the Atmosphere*, Van Nostrand Reinhold, New York, pp. 443-479.

Jassby, A. D., Reuter, J. E., Axler, R. P., Goldman, C. R., and S. H. Hackley (1994). "Atmospheric deposition of nitrogen and phosphorus in the annual nutrient load of Lake Tahoe", *Water Resources Research*, **30**, 7, 2207-2216, July.

National Weather Service Forecast Office (2003). "WFO Sacramento County Warning Area Meteorology" (http://www.wrh.noaa.gov/sto/CWA.php).

Reuter, J.E. and L.W. Tarnay. (2004). "Analytical review of nutrient deposition to Lake Tahoe. I. Nitrogen." Tahoe Research Group, John Muir Institute for the Environment, University of California, Davis. 13 p.

Schumann, T., Zinder, B., Waldvogel, A. (1988). "Aerosol and hydrometeor concentrations and their chemical composition during winter precipitation along a mountain slope -- I. Temporal evolution of the aerosol, microphysical and meteorological conditions." *Atmospheric Environment* **22**(7), pp. 1443-1459.

Zinder B., Schumann T., and Waldvogel A. (1988) "Aerosol and hydrometer concentrations and their chemical composition during winter precipitation along a mountain slope -- II. Enhancement of below-cloud scavenging in a stably stratified atmosphere." *Atmospheric Environment* **22**(12), pp. 2741-2750.

This page blank intentionally.

6. Air Pollution Transport

6.1 Background

Air parcels containing pollutants move through the atmosphere as winds and general weather patterns distribute them. The pollutants may detectably persist a short distance or, given certain meteorological regimes, occasionally cross continents and oceans. The impact of the pollutant transport depends on the magnitude and rate of emissions from sources (i.e., source strength) and any additional pollutant input during transport. The impact of the pollutant transport also depends on the meteorological variables that control deposition, transformation, and dissipation within the air parcel, the movement to other locations, and, in the case of transport above the surface layer, the downward mixing to the earth's surface at the receptor location.

Transported air parcels that encounter clouds have their pollutant load subject to additional chemical transformations interacting with droplets within clouds and physical transformation as soluble gases dissolve in the droplet or particles absorb water to create larger particles. Air pollution transport is a most complex phenomenon.

The focus of LTADS was primarily on quantifying direct dry deposition of nitrogenous compounds, phosphorus, and particulate matter to Lake Tahoe and on better characterizing the pollutant sources. As part of that characterization, the transport of nitrogen oxides into the Sierra Nevada, which serves as an upper limit of transport to the Tahoe Basin, received the greatest attention. Potential particulate matter transport to the Tahoe Basin is addressed tangentially in this report via discussion of atmospheric processes as they constrain PM transport and related PM studies. For example, the transport of Asian dust is discussed in Appendix B (Analysis of Historical Aerosol Data). This chapter attempts to characterize the various atmospheric processes influencing the potential transport of pollutants, such as reactive oxides of nitrogen, particulate matter, and ozone, to the Tahoe Basin. A formal, quantitative analysis of the transport of air pollutants to the Tahoe Basin is beyond the purview of LTADS personnel and is left to future investigators.

As noted earlier, phosphorus is found in the atmosphere in very low concentrations and measurements of phosphorus usually encounter analytical difficulties. The phosphorus data collected in LTADS did not provide the measurement sensitivity (low concentrations and short measurement period) sufficient to address potential phosphorus transport to the Tahoe Basin. The study of phosphorus transport to the Tahoe Basin will remain in the theoretical arena until better measurement methodologies are developed and self absorption correction factors are refined for XRF analysis of PM larger than 2.5µm. These are fundamental challenges that will limit any analyses of phosphorus transport in the near future.

Reactive nitrogen species, such as nitric acid and organic nitrates, potentially part of the Sacramento plume that may reach the Tahoe Basin, were targeted for study (Cohen and Murphy, 2005). Although ammonia measurements were made with the network of Two-Week-Samplers and with an annular denuder on the aircraft, the results were less

definitive than desired because of high blank values. Although natural sources of ammonia exist (e.g., animals, soil microbes), it is likely that the prodigious emissions of ammonia from agricultural and livestock operations in the Central Valley overwhelm other sources. However, a study of potential ammonia transport (particularly aloft as transformation and deposition likely significant in surface layer) to the Tahoe Basin is left to future investigators due to the limited measurements of ammonia aloft and characterization of natural and anthropogenic sources. The bulk of this chapter investigates potential reactive nitrogen species transport to the Tahoe Basin and is primarily excerpts from the Cohen and Murphy final report.

The Tahoe Basin is located to the east-northeast of the San Francisco Bay Area and the Sacramento metropolitan region. Because the synoptic winds at this latitude are typically westerly (i.e., from the west), there is the potential for polluted air to be transported from these areas to the Tahoe Basin. However, the impact of transported pollutants is not solely a function of the amount of emissions from upwind areas. Emissions undergo chemical reactions, diffusion, dispersion, and deposition after being released. Thus, ambient concentrations of primary (directly emitted) pollutants generally decline with time and distance transported from the source. Furthermore, the concentrations of secondary pollutants also eventually decrease due to dispersion, deposition, and chemical reaction.

Meteorological conditions strongly influence the ambient concentrations of pollutants resulting from their emission, transformation, advection, and deposition. Ambient temperatures influence emission rates (biogenic and evaporation), chemical reaction rates, winds, and vertical mixing of the atmosphere. Wind direction and speed, as well as vertical mixing, primarily determine the dispersion and ultimately the ambient concentrations resulting from the emissions. Lastly, the Sierra Nevada mountain range acts as a barrier to reduce the potential impact of transported emissions and reaction products from the Central Valley. Emissions from upwind areas such as San Francisco and Sacramento are diluted during transport, which takes many hours. For example, pollutants emitted in Sacramento into a 10 mph surface wind would take about 10 hours to traverse the distance to Lake Tahoe. However, wind speeds of this magnitude and faster typically cause low pollutant concentrations.

The scenarios potentially transporting pollutants from the Central Valley to Lake Tahoe involve one-day surface transport during summer, multi-day surface transport, and pollutants transported in winds above the surface layer. Most commonly, the pollutants from the upwind regions act to raise regional background concentrations entering the Tahoe Basin rather than directly causing exceedances (e.g., of the State 1-hour ozone air quality standard - not to exceed 0.09 ppm) in the Tahoe Basin (Carroll et al., 1998; Carroll et al., 2000). The relatively low ambient pollutant concentrations, combined with the complex topography and low spatial density of meteorological and air quality monitoring locations in the Tahoe region, make evaluations of transport difficult. Data from infrequent aircraft flights to sample air quality aloft in the Sierra Nevada and Tahoe Basin (Carroll et al., 1998) do not support the transport of an “intact” polluted air mass to the Tahoe Basin. However, ozone measurements at ground-level and aloft in many

largely rural areas of California that are located downwind of major urban centers frequently have elevated regional background ozone concentrations of about 50 ppb (Carroll et al., 1998; CARB, 1997). Another factor that must be considered to properly assess the impact of transport on air quality in the Tahoe Basin is the semi-permanent thermal inversion layer located about 10-11,000 feet MSL over the Basin. When present, this inversion would inhibit the mixing of air above it into the air below it. Because transport of pollutants in the surface layer is limited by diurnal variations in upslope and downslope airflows, the most effective altitude for potential transport to the Tahoe Basin would be about 8-10,000 feet MSL (i.e., above the Sierra Nevada but below the elevated inversion). Furthermore, pollutant concentrations transported into the Basin in that layer of air would undergo some dilution when mixed with the cleaner air below (i.e., between 6-8,000 feet MSL).

6.2 Reactive Nitrogen Species

Nitrogen oxide and ammonia deposition to the Lake Tahoe basin and more broadly throughout the Sierra Nevada may have negative consequences associated with changing the nutrient balance and pH of lakes and streams. It may also alter ecosystem function by changing nitrogen-limited systems to ones that are saturated with available nitrogen. One study (Korontzi, Macko, et al. 2000) showed that nitrogen deposition to the forests of the San Bernardino Mountains, west of the Los Angeles Basin, has shifted the ecology in low lying regions from nitrogen limited to nearly nitrogen saturated conditions. They also report a correlation between nitrogen deposition and increased NO_3^- in the region's watersheds.

Species-specific effects on California's ecology have also been the subject of discussion. For example, Keeley and Fotheringham (1997) argue that NO or NO_2 may be a signaling agent for seed germination in fire sensitive species. Downwind of urban areas, the implication is that many species may be perpetually germinating instead of germinating only after the clearing effects of fire. Nasholm, Ekblad, et al. (1998) report direct uptake of artificially deposited organic nitrogen compounds (amino acids) and this raises the question of whether atmospheric organic nitrates might be directly assimilated, either as nutrients or with toxic consequences. Recent work at the plant and leaf scale show that the mechanisms for nitrogen oxide exchange are complex and that there may be a compensation point controlling biosphere-atmosphere fluxes of some nitrogen oxides (Lerdau, Munger et al. 2000; Sparks, Monson et al. 2001). A compensation point is an atmospheric concentration below which nitrogen oxides are in the net emitted and above which they are, in the net, deposited to an ecosystem.

A large fraction of the input of nitrogen to Lake Tahoe is thought to occur by wet and dry deposition of atmospheric reactive nitrogen (both nitrogen oxides, collectively known as NO_Y, and ammonia) to surfaces (water, leaves, soils, etc.) within the Tahoe Basin. Atmospheric NO_Y in the form of the chemical species NO and NO_2 (collectively known as NO_X), gas and particle phase nitric acid, and organic nitrates (in gas and particle phases) deposit to the materials on the Earth's surface at different rates because each pollutant has a different solubility and reactivity. Further complicating the situation, it is

known that NO and NO_2 are both deposited to and emitted from snow, soils and terrestrial plants depending on chemical and meteorological conditions at the surface and in the surrounding atmosphere. Emissions of species other than these three are possible. For example, HONO emissions from surfaces are thought to be important to the OH chemistry of urban areas--but little is known about emission rates of other reactive nitrogen species. In the Lake Tahoe region, significant deposition of nitrogen oxides is thought to be occurring both directly to the lake surface and to the surrounding basin followed by runoff into the lake. Understanding the sources and the chemical speciation of nitrogen oxides in the atmosphere upwind of the Tahoe Basin is essential for evaluating models used to design control strategies aimed at reducing the nitrogen inputs to the Lake. Sources of atmospheric nitrogen oxides may include 1) emissions from the Central Valley (specifically, the southern Sacramento Valley and northern San Joaquin Valley) and the San Francisco Bay Area (e.g., combustion, bacterial modification of fertilizers, and natural bacterial emissions) that are then transported to the Tahoe Basin, 2) anthropogenic emissions within the Tahoe Basin (e.g., motor vehicles and wood burning), and 3) emissions from bacterial sources in the soils and forests surrounding the lake.

Despite this wide range of policy relevant and scientifically interesting issues, the difficulty of accurately measuring nitrogen oxides and their deposition rates has prevented the development of an accurate, complete and detailed mechanistic understanding of nitrogen oxide deposition from emerging. The work by Cohen and Murphy was aimed at understanding the contribution of atmospheric nitrogen from west of the Tahoe Basin to the nitrogen oxide burden within the basin. The goals were to provide a detailed baseline of high time resolution observations of the annual cycle of four different types of reactive nitrogen oxides just to the west of the Tahoe Basin, to make those observations available to other investigators within ARB or elsewhere and to develop analyses using this data set. Further, the Big Hill observations were combined with data from separately funded work at UC Blodgett Forest and with data sets from other ARB investigators to provide a more quantitative understanding of the mechanisms and processes that establish the amount of each different nitrogen oxide species in the air to the west of the Tahoe Basin. The location at Big Hill permitted only characterization of air outside the basin. Nonetheless, the constraints developed from the Big Hill data set provide a maximum estimate of the contributions of transport from the west to the composition of air at the peak of the Sierra Nevada and the western edge of the Tahoe Basin.

6.3 Chemistry of Nitrogen Oxides

Nitric oxide (NO) is the primary reactive nitrogen compound emitted by biological activity and as a byproduct of combustion. Once emitted NO rapidly (~100 seconds) interconverts with NO_2

$$NO + O_3 \rightarrow NO_2 + O_2 \qquad R_1$$

$$NO_2 + \text{light} + O_2 \rightarrow NO + O_3 \qquad R_2$$

Collectively NO and NO_2 are referred to as NO_X and the sum of NO_X and all higher oxides of nitrogen is referred to as NO_Y. Higher oxides of nitrogen are formed in reactions of the radicals OH, HO_2 and RO_2 with NO and NO_2.

$$NO_2 + OH \rightarrow HNO_3 \qquad R_3$$

$$NO_2 + R'(O)O_2 \rightarrow R'(O)O_2NO_2 \qquad R_4$$

$$NO + R''O_2 \rightarrow R''ONO_2 \qquad R_5$$

These reaction products have very different properties. Peroxynitrates are thermally unstable and form a reservoir for NO_X, in which the partitioning depends on the ambient temperature. HNO_3 and hydroxyalkyl nitrates (R" = ROH) are very water soluble while the peroxy nitrate and alkyl nitrate products of R_4 and R_5 are only weakly water soluble. As a result of its solubility, HNO_3 is rapidly (on a time scale of hours within the planetary boundary layer) removed from the atmosphere by deposition to the Earth's surface and/or rapidly scavenged in water rich aerosol, which then deposit to the Earth's surface. Less is known about the deposition rates of hydroxyalkyl nitrates but measurements of their Henry's law solubilities strongly suggest that their deposition rates should be similar to that of HNO_3. Deposition of NO_2, alkyl nitrates, and peroxynitrates are a factor of 10 slower than deposition of HNO_3 (Wesely and Hicks 2000). The most abundant peroxynitrate, PAN, is a known phytotoxin at the concentrations (~5 ppb) encountered immediately downwind of Sacramento (Cape 2003). HNO_3 also reacts with NH_3 in the gas phase or within particles to produce an ammonium nitrate salt: NH_4NO_3. The equilibrium is shifted toward ammonium nitrate aerosol at low temperature and high relative humidity, and the particles may have different atmospheric lifetimes than gas phase HNO_3 (Seinfeld and Pandis 1998).

$$NH_3(g) + HNO_3(g) \rightarrow NH_4NO_3\,(s) \qquad R_6$$

The nitrate radical, NO_3, is formed from the oxidation of NO_2 by O_3 (R_7). At night, when the very rapid photolysis of NO_3 (R_8) is not occurring, NO_3 accumulates:

$$NO_2 + O_3 \rightarrow NO_3 + O_2 \qquad R_7$$

$$NO_3 + light + O_2 \rightarrow NO_2 + O_3 \qquad R_8$$

and then reacts to form N_2O_5 via R_9:

$$NO_2 + NO_3 \rightarrow N_2O_5 \qquad R_9$$

HONO is also rapidly photolyzed during the day and accumulates at night as a result of mechanisms that are poorly understood, but appear to be equivalent to:

$$2NO_2 + H_2O \rightarrow HONO + HNO_3 \qquad R_{10}$$

N_2O_5 and HONO are highly reactive with and soluble in water and are likely removed from the atmosphere on contact with most surfaces. The role of these important nighttime compounds in redistributing reactive nitrogen is not well understood. It is likely that some of the N_2O_5 hydrolyzes (reacts with water vapor) to form nitric acid, particularly during winter,

$$H_2O + N_2O_5 \rightarrow 2HNO_3 \qquad R_{11}$$

6.4 Transport Concepts

Transport of nitrogen oxides from the Central Valley and the western slopes of the Sierra Nevada to the Tahoe Basin can result from processes that include: a) direct transport within the planetary boundary layer (PBL), b) direct transport above the PBL, and c) accumulation of pollutants in a regional background (**Figure 6-1**). The first two of these mechanisms operate on a daily timescale. Accumulation of pollutants in a regional background and subsequent transport to the Tahoe Basin operates on a longer timescale (i.e., multiple days). All three of these mechanisms are expected to operate, though to differing extents, every day. Research also suggests that biomass burning may be a significant source of atmospheric nitrogen and phosphorus in the Tahoe Basin (Zhang et al. 2002) and it is well known that biomass fires can be significant sources of longer lived pollutants such as CO on a continental scale (Novelli et al. 2003). Fires are episodic in nature, the extent to which their emissions will impact the Basin rests on their frequency, intensity, and proximity to Tahoe.

Figure 6-1 depicts the possible pathways of pollutants originating in the Central Valley that are transported toward the Tahoe Basin. The dotted line is used to suggest the mixing height or upper edge of the planetary boundary layer (PBL). Urban emissions may be transported within the PBL along path 1 or lofted above and transported in the free troposphere by a combined path involving arrows 2 and 3. Emissions in the Sacramento urban area that are advected eastward undergo dilution and chemical reactions as well as receiving additional emissions (anthropogenic and biogenic) and depositing on surfaces. If the westerly air flow (i.e., from the west) is sufficiently strong or persistent during a given day, it may reach the Tahoe Basin. Arrow 4 is dashed to emphasize the uncertainty regarding the duration and strength of conditions that directly transport an air parcel originating in the valley to the east before the winds reverse to downslope at night. While pollutants may not be directly transported to Tahoe within the mixed layer, emissions into an air mass that washes up and down the slope of the Sierra every day may increase the regional background over time, eventually contributing to elevated reactive nitrogen in the air that reaches the Tahoe Basin.

Alternately, some air masses may be lofted high above the floor of the Central Valley and move eastward over the western Sierra disconnected from interactions with the surface (arrows 2 and 3). Air masses that pass over the roughly 3000 m peaks to the west of the Lake Tahoe Basin or flow through canyons may subsequently be mixed

downward and be exposed to the lake surface (arrow 5). The downward mixing of material transported over the Sierra Nevada will be limited by the presence of a semi-permanent temperature inversion above Lake Tahoe between 3,000 and 3,400 meters MSL (indicated by a heavy dashed line). Additionally, the routine presence of surface inversions and seasonal differences in the relative air-water temperatures over the lake can dramatically affect atmospheric mixing and deposition to the Lake. Thus, a detailed understanding of how air mixes vertically within the Tahoe Basin (arrow 5) is necessary to assess the influence of remote nitrogen sources. Pollutants transported aloft via arrows 2 and 3 will have no effect on Lake Tahoe unless they enter the mixed layer above the lake, which would permit their eventual deposition. An assessment of the probability of such events is beyond the scope of this chapter.

The overall impact of remote sources of atmospheric reactive nitrogen on Lake Tahoe depends on the appropriately weighted combination of all the transport pathways noted above. In the summer, the prevailing wind flow is from the west at all altitudes more than 2000 m above the surface. During the day, heating of the western Sierra generates upslope winds that transport air from the valley floor into the mountains, regardless of the dominant flow regime within the Central Valley itself (Zaremba and Carroll 1999). In the winter, significant periods of high pressure in the region cause inland valleys and basins to fill with cold air leading to low mixing heights and weak winds. Local pollutants tend to accumulate and long-range transport of emissions is less likely. While the pattern of upslope/downslope flow is observed on some winter days, the shorter periods of daylight mean that upslope flow persists for a much smaller fraction of the day. **Figure 6-2** shows the summer and winter patterns of upslope/downslope flow at the University of California's Blodgett Forest Research Station (UC-BFRS, 1400 m ASL).

Figure 6-1. Topographical diagram of airflow along the western slope of the Sierra Nevada and potential surface and aloft inversions over Lake Tahoe that inhibit mixing.

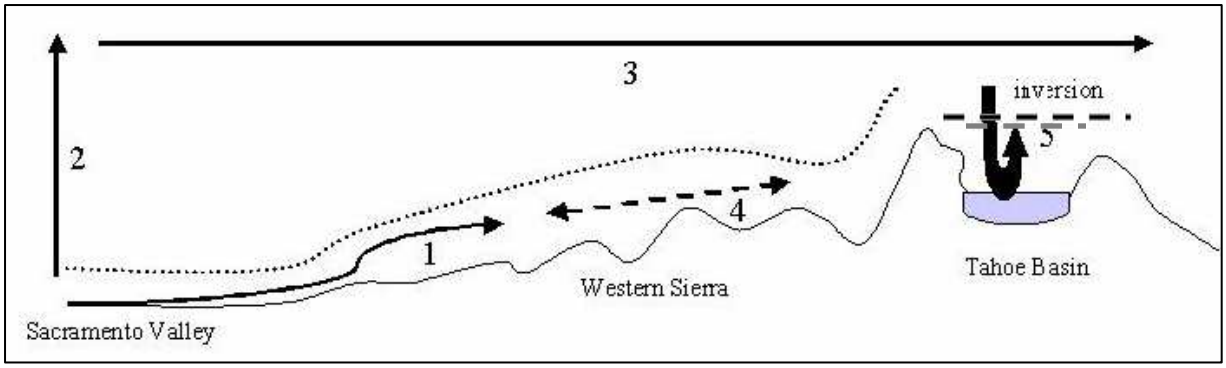

Figure 6-2. Half-hour averages of wind direction observations at Blodgett Forest during 2001. Summer refers to data between day 155 and 255 (June 5- Sep 12) and winter refers to data before day 50 (Feb 20) and after day 300 (Nov 2).

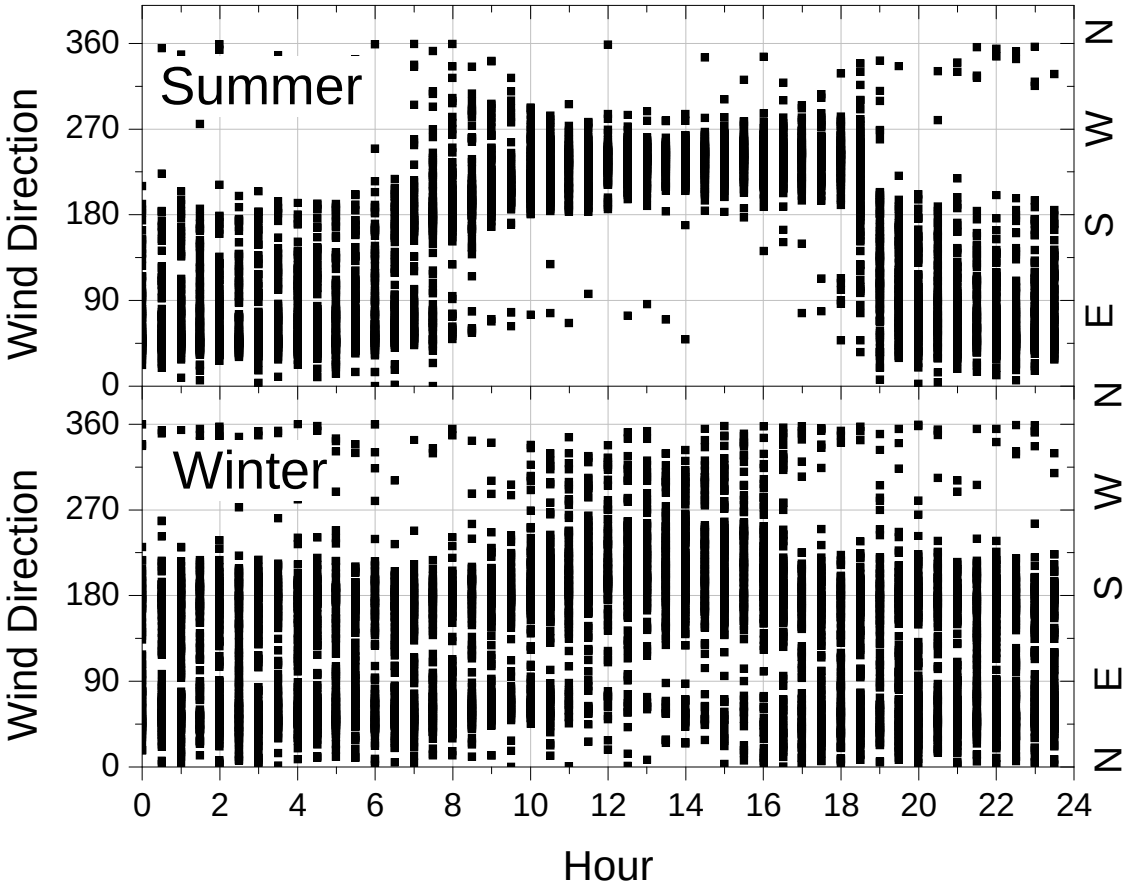

6.5 The Urban Plume

The daily evolution of the Sacramento urban plume during the summer is remarkably consistent. During the day, terrain driven winds blow steadily from Sacramento into the Sierra Nevada foothills – drawing air into the sparsely populated mountains. During the night, the wind reverses and clears out the mountains replacing the urban plume with the regional background. Observations of atmospheric composition and meteorology show this pattern persists to at least 1200 m elevation (Carroll and Dixon 2000). Transport of anthropogenic emissions from the Sacramento metropolitan area as a result of this meteorological flow pattern is evident in observations of anthropogenic hydrocarbon, ozone, and nitrogen oxide concentrations at the University of California Blodgett Forest Research Station, which peak in the late afternoon/evening and decrease steadily with the downslope flow during the night. *Van Ooy and Carroll* (1995) measured ozone and local meteorological variables (temperature, wind speed, wind direction, relative humidity, and solar radiation) at six sites along a 400 km north-south transect of the Sierra Nevada foothills (1100 – 1200 m elevation) during the summer of 1992. At the three sites where east-west wind patterns are predominant, as they also

are at UC-BFRS, there was a strong correlation between wind direction and ozone concentrations. At these sites, there was a regular diurnal pattern with ozone concentrations peaking at 15:00 to 17:00 PST (Pacific Standard Time) and reaching a minimum at 7:00 PST. At the other three sites where north-south winds were predominant, the diurnal variation in ozone was small. The sites with east-west wind patterns had higher peak ozone abundances and violated the one-hour state ozone standard of 0.90 ppm up to 40% more often than the sites with predominantly north-south winds indicating sites with east-west wind patterns such as UC-BFRS represent a maximum effect of transport. The major climate variables controlling transport in the region (temperature, sunlight, precipitation, relative humidity, and wind) as measured in Sacramento have been nearly constant for 20 years (1980 to 1999) (**Figure 6-3**). Thus emissions in the Central Valley should have been transported with equal efficiency throughout this 20-year period.

These analyses suggest the plume traveling into the foothills of the Sierra from the valley serves as a mesoscale (100 km), daytime flow reactor that can be characterized as a Lagrangian air parcel transported from the valley into the Sierra Nevada. *Dillon et al.* (2002) used comprehensive (ozone, speciated nitrogen oxides, speciated anthropogenic and biogenic hydrocarbons, and meteorology) and extensive (spanning the years 1997 to 2002) observations at Folsom, California and five hours downwind at the University of California – Blodgett Forest Research Station to evaluate transport from Sacramento into the mid-Sierra during the summer (**Figure 6-4**). The observations at Folsom effectively integrate all of the emissions to the west. Dillon (2002) established that a Lagrangian analysis captures the essential features of the chemistry and transport and fit the parameters of a Lagrangian model to the observations. Comparison of ozone and meteorological observations to the north of UC-BFRS at Blue Canyon and to the south at Sly Park support the suggestion that the observations and the model analysis are regionally representative.

Measurements of speciated NO_X and individual NO_Y species at UC-BFRS (1998-present) demonstrate pronounced seasonal variability (Day et al. 2002) (**Figure 6-5**). The Lagrangian model has only been applied to summer time conditions when upslope transport is expected to be at a maximum. To obtain an annually complete picture, other approaches are required to interpret the reactive nitrogen measurements because of different source distributions, and more importantly, very different meteorological conditions.

Figure 6-3. Monthly averaged observations at the Sacramento Executive Airport (WBAN 23232) demonstrate the inter- and intra-annual variance of climatological variables in the region from 1980 through 1999. The line with solid squares is the median of monthly means while the gray swath denotes the 1σ variance. a) maximum daily temperature; b) percent of total possible hours of direct sunlight (no observations were available in 1998 and 1999); c) sum of monthly rainfall; d) the lowest relative humidity recorded each day (typically a late afternoon observation); e) daily origin direction of 24 hour average of recorded winds (also called resultant wind direction); f) 24 hour average of recorded wind speeds.

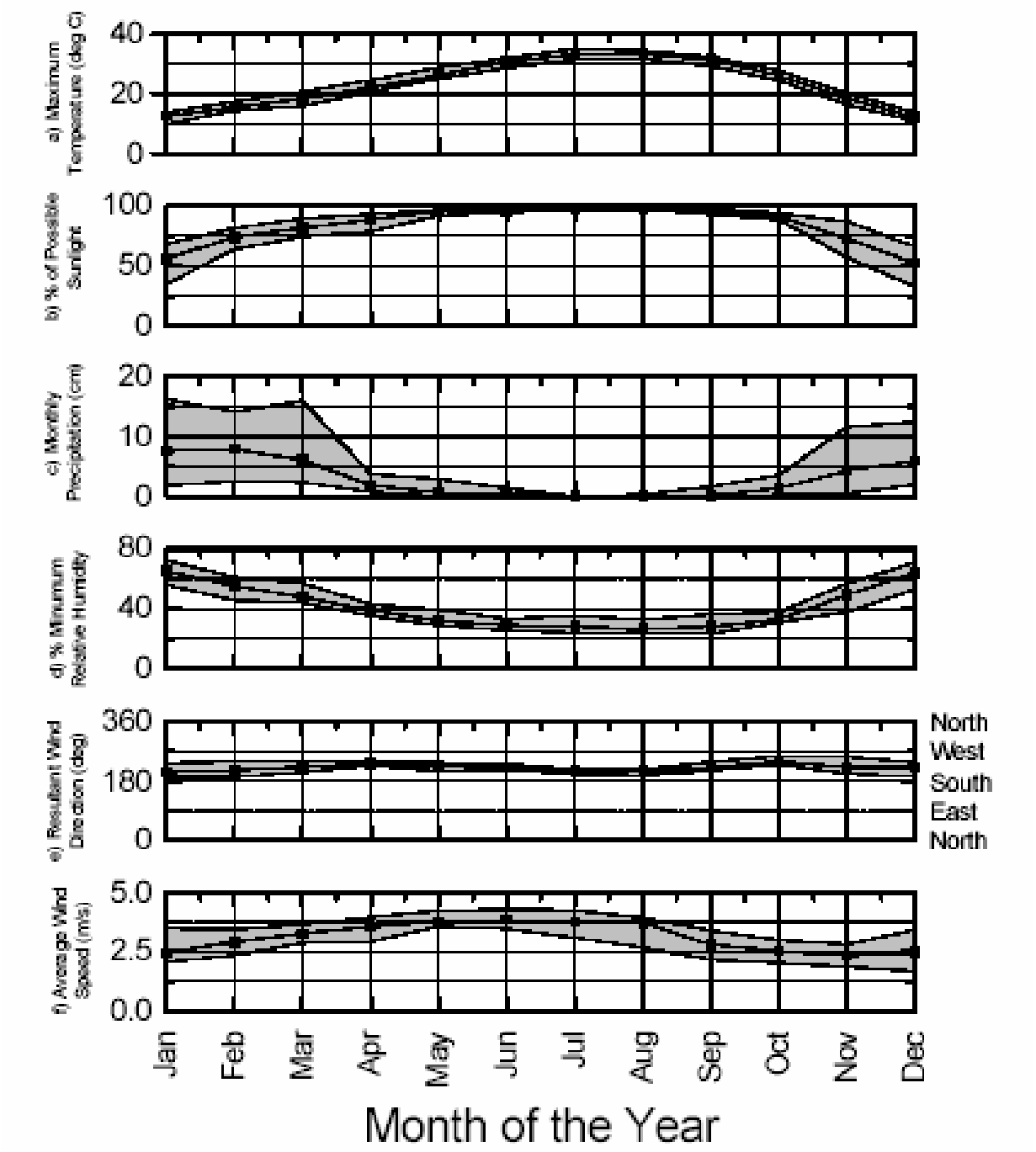

Figure 6-4. Major roads and 1998 California Air Resources Board atmospheric sampling sites upwind of the Blodgett Forest Research Station: Photochemical Assessment Monitoring Station sites (circled P), co-located ozone, nitrogen oxide and non-methane hydrocarbon monitors (+), co-located ozone and nitrogen oxide monitors (star), and ozone monitors (diamond). Most observations used in this study were taken from the Blodgett Forest Research Station, Del Paso Manor, and the Folsom sampling sites.

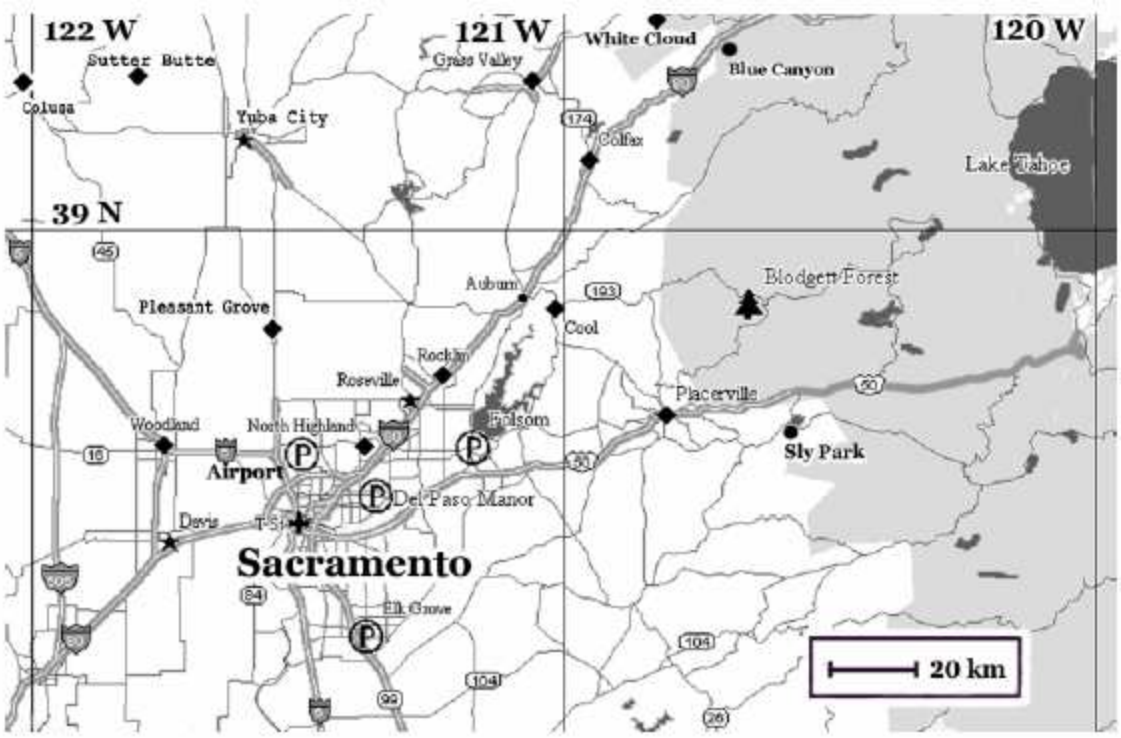

Figure 6-5. Concentrations (ppb) of nitrogenous air pollutants at UC-BFRS 2000-2002 (30 minute averages and 7-day running medians).

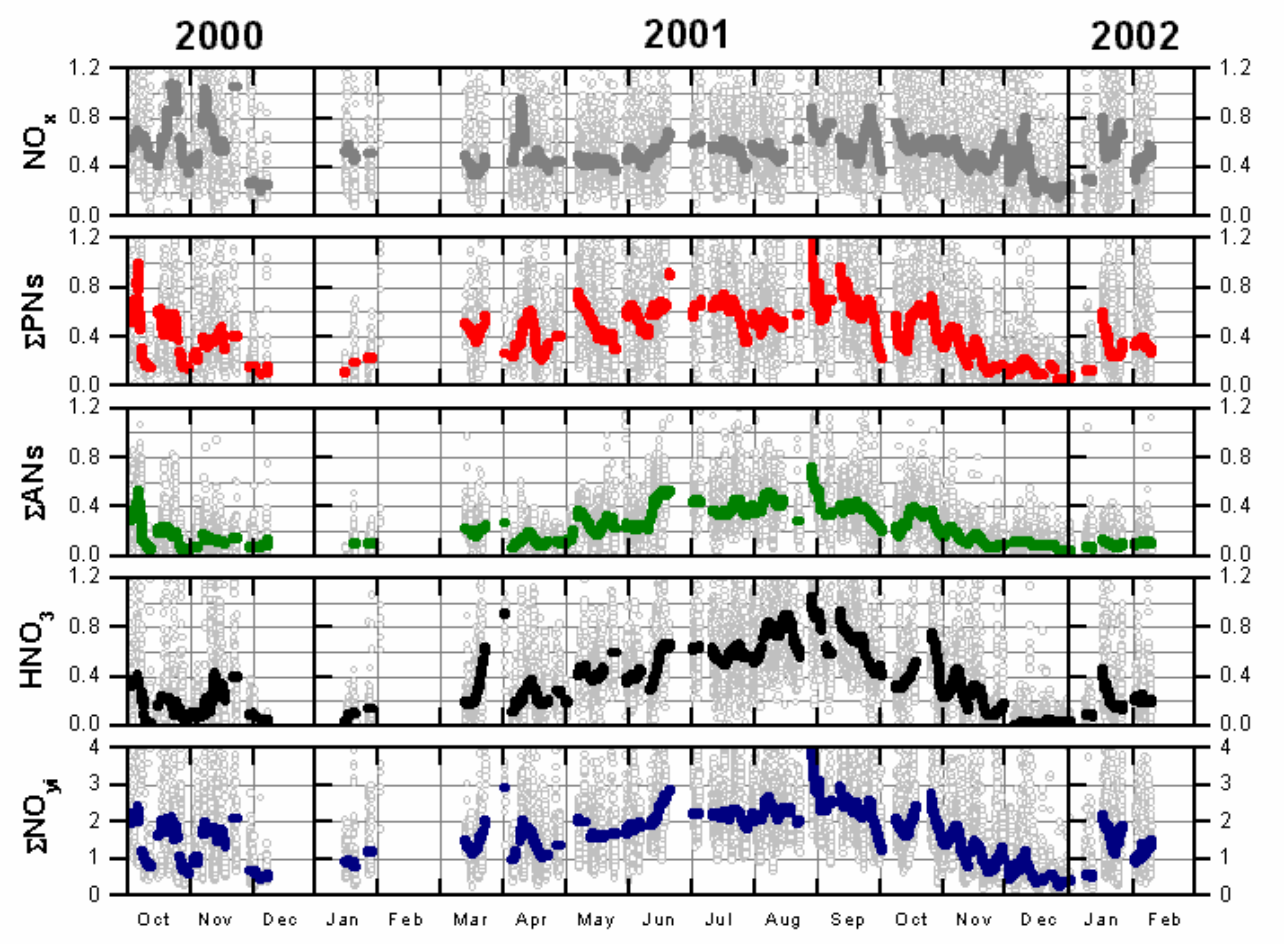

6.5.1 Mixing

Parameters in the model described by Dillon (2002) include mixing of the urban plume with the regional background, chemical processing, emission and deposition. By treating NO_Y as a conserved quantity, the calculations represent an upper limit to the contribution of urban NO_X in the Sierra because chemical factors also act to reduce NO_Y. Assuming approximately a 25% per hour reduction in concentrations due to mixing with cleaner background air during daytime upslope flow (Dillon, 2002), emissions in the Sacramento area would have been diluted to 28% of their initial concentrations by the time the plume arrived at UC-BFRS (5 hours downwind from the suburbs of Sacramento). If we extrapolate these results to Tahoe, which is another 4 hours downwind, the urban portion of the concentrations would be 10% of their initial values. In summer, the regional background in the area is estimated to be 1.9 ppb and daytime NO_Y mixing ratios in the downwind suburbs of Sacramento are 7 ppb; thus, about 5.1 ppb is the direct result of emissions in the Sacramento source area. Based on mixing alone and after five hours of transit, the concentration of NO_Y at UC-BFRS

would be 3.4 ppb (1.5 ppb from the plume, and 1.9 from the regional background). Extrapolating another 4 hours to the Tahoe Basin, the concentration of NO_Y would be 2.4 (0.5 ppb from the plume, and 1.9 from the regional background). Observations by *Carroll et al.* (2002) along a transect at 2000 m suggest that the urban plume usually stops before the crest and does not progress across the mountains into the Tahoe Basin, indicating that direct transport of inorganic nitrogen from the Central Valley is likely smaller than this estimate.

6.5.2 HNO_3 Formation and Deposition

Chemical production of HNO_3 followed by rapid deposition removes NO_Y, reducing the urban contribution below the estimate given above for mixing alone. Dillon (2002) determined that the effective OH mixing ratio that acts over the 5 hour transport time to Blodgett Forest is about 1.4×10^7 molecules/cm^3 or (0.6 ppt). NO_2 reacts rapidly with OH to form HNO_3 ($k \sim 9 \times 10^{-12}$ s^{-1} cm^3/molec) and in the absence of other reactions of NO_2, approximately 90% of the suburban NO_2 would be converted to HNO_3 prior to reaching UC-BFRS. HNO_3 is deposited on a time scale set by the ratio of the deposition velocity to the boundary layer height. Using literature estimates for the deposition velocity (0.035 m/s) (Hanson and Lindberg 1991) and the boundary layer height (800 m) (Seaman et al. 1995), results in a lifetime of 6.3 hours. Thus about 50% of the HNO_3 formed during the transit to UC-BFRS is deposited along the way and about 85% is deposited before it gets to the Tahoe Basin. *Day et al*. (2002) provide analysis of the daily cycle of HNO_3 that suggests this estimate of the HNO_3 lifetime is too long (perhaps because the deposition velocity is closer to 0.05 m/s). During the daytime, the HNO_3 concentration is observed to be nearly in a chemical stationary state with a production term characterized by R_3 and loss to deposition. This would not be the case if the time scale for production and deposition were much longer than 3 hours. This result implies that more than 70% of the HNO_3 formed during transit from Sacramento to Tahoe is deposited along the western slope of the Sierra Nevada. This short lifetime suggests that attention be focused on the controls over NO_2 mixing ratios in the Tahoe Basin (or anywhere else where dry HNO_3 deposition is a potential problem).

6.5.3 Organic Nitrate (RO_XNO_2) Formation

Other photochemical byproducts that act as a sink or reservoir for NO_Y include peroxy nitrates and alkyl nitrates formed by the reaction of RO_2 with NO_2 and NO respectively. In the concentration range of NO_Y encountered outside urban areas, organic nitrates can be the major sink of NO_Y radicals. While HNO_3 forms efficiently under high NO_Y conditions, RO_xNO_2 formation becomes more favorable as the NO_Y to hydrocarbon ratio decreases. The lower deposition velocity of organic nitrates lengthens their lifetime in the plume but also makes them less efficient as a source of atmospheric nitrogen to the surface. Hydroxy alkyl nitrates are expected to have comparable deposition velocities to HNO_3, but it is unclear what fraction of organic nitrates these comprise. Peroxy nitrates are thermally unstable and therefore capable of sequestering NO_Y under cold conditions and releasing it once temperatures rise. This can be an effective mechanism for transporting reactive nitrogen to distant places. Observations by *Day et al.* (Day et

al. 2003) at UC-BFRS show that for many parts of the year, the sum of all organic nitrate species is often the most significant fraction of NO_Y in the plume by the time it reaches the site. More needs to be known about the behavior of these species to assess their potential to deliver reactive nitrogen to Lake Tahoe. Note that atmospheric chemists refer to $RONO_2$ and RO_2NO_2 collectively as 'organic nitrates'; a term that should not be confused with 'organic nitrogen', which is used to refer to compounds with a C-N bond. Little is known about the aqueous decomposition of peroxy and alkyl nitrates, and whether their NO_3 group would contribute to nitrate measurements in analysis of lake water or precipitation.

6.5.4 Downwind Emissions

The observations and analyses of nitrogen oxides at UC-BFRS indicate that emissions into the urban plume continue after it passes over Folsom. These emissions are large ~0.44 ppb/hr. After the five hours of travel on the way to UC-BFRS the total emissions are 2.2 ppb, an amount in excess of the background concentration observed at the site and fully 2/3 of the amount observed at the peak of the urban plume. This result strongly implies that transportation along the 50 and 80 highway corridors, contribution from housing beyond the edge of the Sacramento suburbs and direct emissions from the local ecosystems are significant contributors to NO_Y in the Sierra. Further research is required to quantify the amount contributed by each of these distinct sources.

6.5.5 Summary of Plume Transport and Chemistry

This analysis makes use of a continuous long term dataset that allows for the evaluation of statistics. This comprehensive record of meteorology and chemical composition at UC-BFRS is consistent with other observations from the western slope of the Sierras including aircraft measurements, data from Big Hill (1850 m), and short term ozone studies. Using a model that accounts for the combined effects of emissions, chemistry, deposition and dilution which can be tested against an inclusive set of observations allows us to develop a representation of the mean behavior of NO_Y species in the region. The influence of the urban plume causes an increase in the typical daytime peak mixing ratio of NO_Y at UC-BFRS, which occurs just prior to sunset, to near 3.3 ppb, an amount that is 1.4 ppb above the regional background of 1.9 ppb. For most of the day, the observed mixing ratios are much less than this peak value with a daytime average concentration of about 2.5 ppb (0.6 ppb above the regional background). Thus on an average day at UC-BFRS, the contribution of the urban plume raises the diurnally averaged NO_Y by 32% over the background. Assuming the Lagrangian parameters represent transport beyond UC-BFRS then further dilution and deposition of HNO_3 along the plume's trajectory to the Lake will mean an even lower contribution of NO_Y from the urban plume to the Tahoe Basin.

At least as important as the total amount of NO_Y transported within the plume, is the change in species distribution as the plume evolves. HNO_3 dominates the higher oxides of nitrogen (NO_Z) near emission sources of NO_X but is rapidly lost if the air mass remains in contact with the surface. On the other hand, the plume becomes relatively enriched in organic nitrates as it progresses through the day with the sunlight driving

hydrocarbon oxidation, creating RO_2 radicals to combine with the NO_X in the plume. These hydrocarbons have both anthropogenic and biogenic sources. If nitrogen oxides emitted in the Central Valley do reach the Tahoe Basin it is likely they will make it there in the form of organic nitrates. Production of fine particles (<2.5 μm aerodynamic diameter) containing nitrate may be another mechanism for transporting reactive nitrogen, as this size of aerosol has a substantial lifetime (hours-days) in an air mass.

The direct extrapolation of the plume analysis presented above in order to understand inputs to Lake Tahoe is only accurate if the upslope flow is strong enough and persistent enough to deliver air from the Central Valley to the Tahoe Basin in one day. If an average daytime wind speed of 3.5 m/s is used, it would be possible for an air mass to leave Sacramento at 10 am and travel 130 km east to the Tahoe Basin by 8 pm that night. Using appropriately timed NO_2, NO_X, and NO_Y observations from monitoring sites along the Sacramento-Tahoe transect in July enables us to examine the evolution of reactive nitrogen in the plume (**Figure 6-6**). As described above, as the plume moves away from Sacramento and ages, the abundance of reactive nitrogen decreases as the result of dilution, processing and deposition. However, NO_X observations at South Lake Tahoe are substantially higher than one would expect from an extension of the values at UC-BFRS and Big Hill, suggesting a substantial contribution from local in-basin emission sources.

Limited aircraft measurements of HNO_3/NO_3^-, NH_3/NH_4^+, and organic nitrogen in the gas and particle phase have been made in the Tahoe Basin and at low and mid-elevation sites along the western slope of the Sierra Nevada (Zhang et al. 2002). While the abundance of these species is significantly lower in the Tahoe Basin than on the western slope of the Sierra Nevada, the distribution between the species was found to be similar in all locations. The authors infer from these observations that under summertime meteorological conditions, Central Valley emissions can be a significant source of nitrogen to the basin. However, because the timescale of photochemistry and deposition of the nitrogen oxides is short, we expect the distribution among different classes of NO_Y to have strong variations depending on the time of day and proximity to the source. Further, if the Central Valley were the main source of HNO_3 and NH_3 for all the sites, one might actually expect a very different distribution of nitrogen because the Tahoe Basin is further along (spatially and temporally) the generally west to east air flow transect than are the lower elevation sites. Additionally, there may be some bias resulting from the timing of the measurements: all the western slope measurements occur between noon and 4 pm while half of the Tahoe Basin measurements are in the morning. These intermittent observations are not sufficient to address the issue of transport from the western slope of the Sierra Nevada into the Tahoe Basin.

6.6 Key Research Issues

Measurements made upwind of the basin can be used as a boundary condition on the total amount of reactive nitrogen available in upwind air masses before they enter the Lake Tahoe basin. Data collected at sites on the western slope of the Sierra suggest that the transit time of a boundary layer air mass from Sacramento to Lake Tahoe exceeds the period of upslope flow during a summer day. This implies that if upwind

reactive nitrogen emissions from urban areas have any impact over Lake Tahoe, then it is through an increase in the regional background. The lifetime of reactive nitrogen is largely determined by the deposition rates of its constituent members. Organic nitrates and NH_4NO_3 aerosol (PM 2.5) are longest-lived and therefore most likely to persist in the background, but by this logic they are also the least likely to deposit to the lake surface. Thus it is easy to imagine a scenario in which the majority of reactive nitrogen in an air mass over Lake Tahoe has its origin in aged Sacramento emissions but the recent in-basin emissions of NO_X, quickly oxidized to HNO_3, are what actually deposits to the lake surface.

Figure 6-6. Reactive nitrogen observations along the Sacramento-Tahoe transect. The distance from Sacramento was multiplied by an average wind speed of 3.5 m/s to estimate the time the air mass would arrive at each site after leaving Del Paso at 10 am. Observations at each site were averaged for an hour around the estimated time. For example, UC-BFRS lies 80 km downwind of Del Paso, and NO_2 and air mass observations between 3 pm and 5 pm were averaged to produce the points reported at 4 pm. The error bars represent the standard deviation of the average.

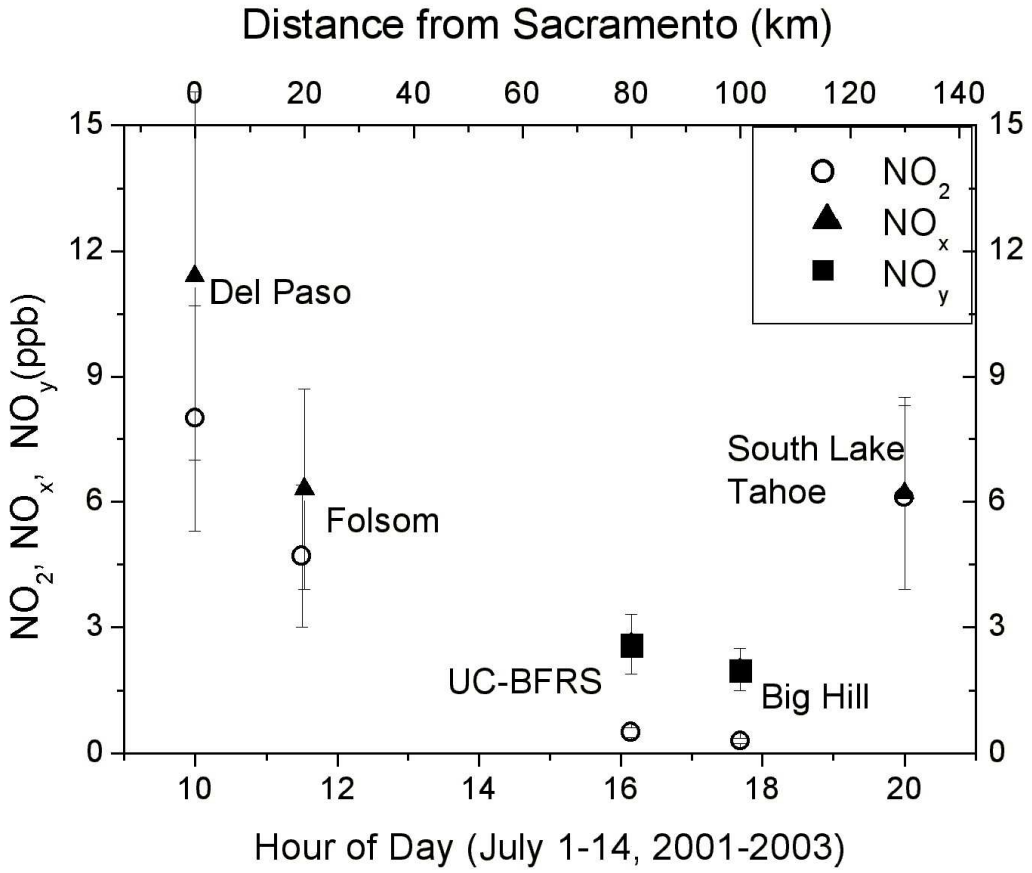

6.7 Results and Analyses of Big Hill Measurements

Tunable Diode Laser Induced Fluorescence (TDLIF) has a history of successfully providing measurements of NO_Y species, NO_2, peroxy nitrates, alkyl nitrates, and HNO_3 (Cohen and Murphy 2005). Big Hill is located at ~6200' MSL on the western slope of the Sierra to the southwest of the Tahoe Basin. Big Hill is a well-exposed peak on the western slope of the Sierra and perfectly situated to observe air parcel transport above terrain-induced influences (**Figure 6-7**). The orientation of the valleys and river canyons around Big Hill also indicates potential surface layer transport paths roughly parallel to Highway 50 (**Figure 6-8**). Further focusing on the topography, it is clear that Big Hill lookout and helipad are a significant distance from Ice House campgrounds and any potential local source impacts (**Figure 6-9**). The experimental sites and instruments used are described in further detail in *Cohen and Murphy* (2005).

Figure 6-7. View of Big Hill site from the west.

Measurements of the NO_Y species NO_2, peroxy nitrates, alkyl nitrates and HNO_3 were made between March 2003 and February 2004 at Big Hill, whenever electricity was available to power the instrument. Despite being located in close proximity to the Sacramento Municipal Utilities District tower, power at the site failed frequently during the study, often during times of bad weather. Meteorological variables, ozone, and PM were also measured and are incorporated into the analysis. The corresponding measurements made at Blodgett Forest were included to develop a more complete picture of the factors controlling the distribution of reactive nitrogen within the region.

The annual cycle of measurements will be discussed with reference to seasonal differences and their causes. Then the summertime data (June through October) will be analyzed more fully to examine correlations between trace gas constituents and climate variables.

Figure 6-8. Map of Crystal Springs area showing Union Valley reservoir just to the north of the Big Hill lookout site and Highway 50 at the bottom of the map.

6.7.1 Regional Transport

Due to its position on the western slope of the Sierra Nevada, Big Hill is subjected to regular wind patterns, especially during the summer. Daytime heating causes upslope flow, which draws air from California's Central Valley eastward into the higher elevations

of the Sierra Nevada range. When the sun sets, the flow reverses and the air drains from higher elevations back toward the valley floor. This flow regime persists along much of the western slope of the Sierra Nevada and strongly influences the seasonal and diurnal patterns observed in primary and secondary pollutants seen in the region.

Figure 6-9. Higher resolution map of topographical features and roads in proximity to the Big Hill monitoring site.

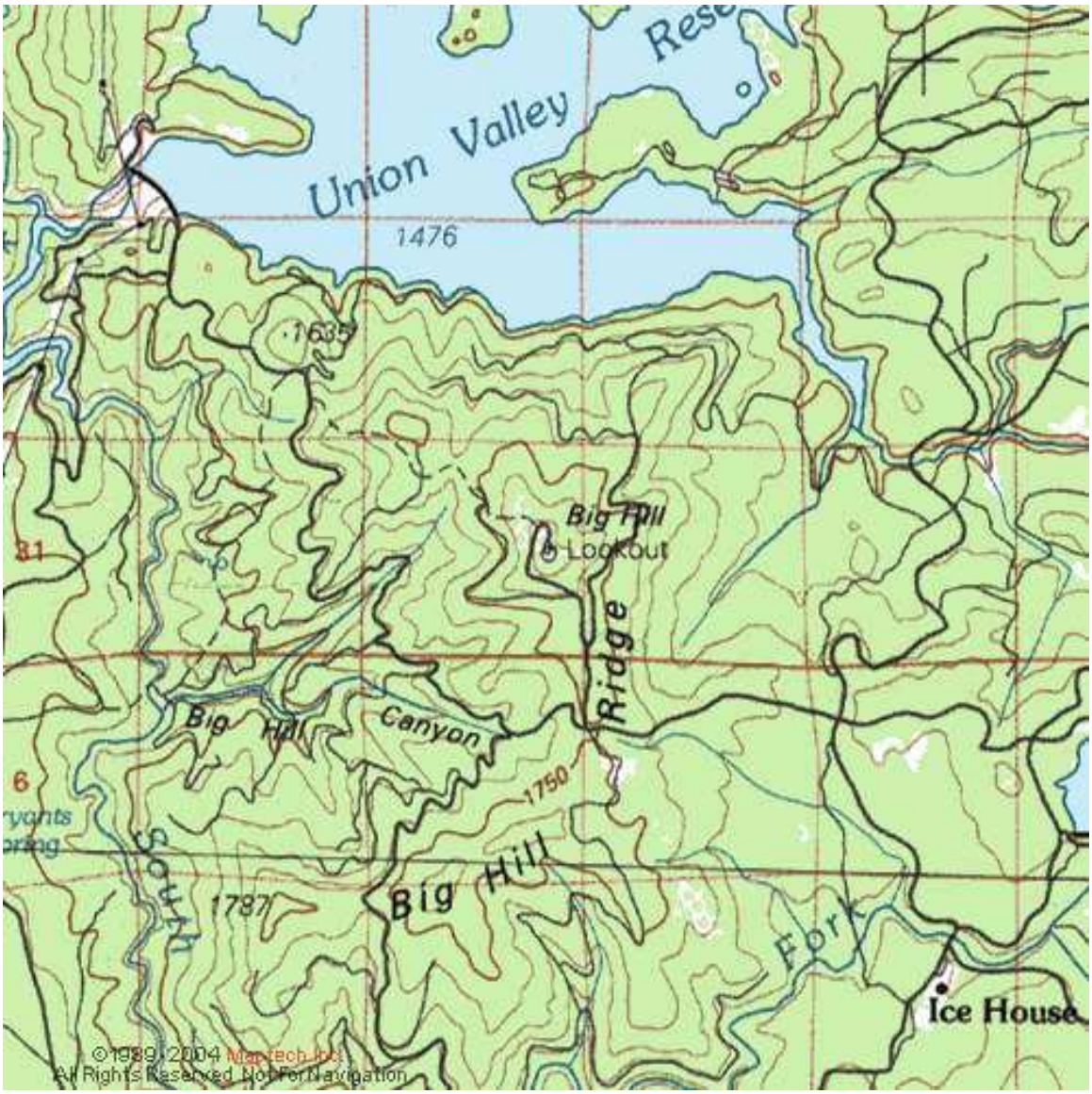

Figure 6-10 shows the location of Big Hill with respect to the nearby city of Sacramento and identifies many other air quality monitoring sites in the region that sample air from the Sacramento urban plume. Wind speed and direction measurements made at Blodgett Forest, Big Hill, and other Air Resources Board sites show that the general

wind direction in the region is from the WSW during the day and the east at night. Blodgett Forest tends to experience winds from the NE at night while flow at Big Hill is from the SE, likely due to topographical differences between the two sites. Big Hill lies roughly 80 km from the eastern edge of the Sacramento suburbs, thus with an average wind speed of 15 km/h, it takes an air mass over 5 hours to reach the monitoring site. During the five hour transit time, the concentration of constituents within the urban plume may be altered by dilution, deposition, photochemical transformations and further emissions. A simple Lagrangian model using measurements made at sites along the Sacramento – Lake Tahoe transect allows us to separate out these parameters and identify the variables constraining nitrogen oxide concentrations in the Sierra Nevada foothills downwind of Sacramento.

As we noted before, observations made at these ground sites reflect the processing of boundary layer air masses during the daytime. Evidence that will be described later shows that at 1850 m elevation, Big Hill frequently experiences nighttime downslope flow, possibly from the free troposphere. **Figure 6-1** is a depiction of the region with the topographical features highlighted. The boundary layer, shown as the dotted line, is expected to be surface-tracking, at least to altitudes of 2000 m in the daytime, and is significantly shallower at night. Flow near the surface follows arrows 1 and 4 with the second arrow dotted and bi-directional to represent the fact that once the sun sets, the flow reverses. Air that is lofted above the Central Valley (arrow 2) will likely be carried eastward with the prevailing winds (arrow 3). Both of these trajectories can bring air masses that have received urban emissions of NO_X toward the Lake Tahoe Air Basin. In the case of surface flow, observations suggests that the wind rarely blows upslope hard enough and for a sufficient number of hours to deliver a species emitted in Sacramento to the Lake Tahoe Air Basin in the same day. Air masses following higher altitude paths may move further to the east in a given day but there must subsequently be a mechanism for that air to mix downwards in order for it to interact with the lake surface.

Figure 6-11 shows calculations of the net weekly east-west airflow for a full year at Camino, based on wind speed and direction measurements at a California Irrigation Management Information Systems (CIMIS) site. Camino is close to Highway 50 between Blodgett Forest and Big Hill. The data suggests the while net airflow between March and October is from west to east, during the winter months long periods of downslope flow result in the net direction of flow at the surface being from Lake Tahoe toward Sacramento. During the winter, daytime upslope flow is generally too short-lived to transport anthropogenic pollutants from the Central Valley significantly further east than Big Hill. This analysis does not take into account the effect of transport aloft or the inclusion of pollutants into storm systems, which tend to move rapidly from west to east during the winter months.

On an average mid-summer day, an air mass originating in the Sacramento area moves roughly 100 km up the western slope of the Sierra Nevada (i.e., west to east) while the sun is up, and then may backtrack 40 km toward the west overnight when the flow is reversed (i.e., east to west). This pattern results in air sloshing back and forth along the

western slopes of the Sierra Nevada and significantly increases the regional background of reactive nitrogen. At lower elevation sites, like Blodgett Forest, air masses measured at night were likely also sampled several hours earlier when they passed by in the opposite direction. At Big Hill, after midnight the lower abundance of H_2O and NO_Y in the air suggests that the site is experiencing descending air.

Figure 6-10. Map of Central California including air quality monitoring sites in portions of the Sacramento Valley and Mountain Counties air basins. Sites marked with stars are State or local monitoring sites, while sites marked with circles are sites where the UC Berkeley TD-LIF instrument has been deployed to make measurements of nitrogen oxide species. The dominant daytime and nighttime wind directions are depicted by the arrows and the inset shows the location of the region within the state of California.

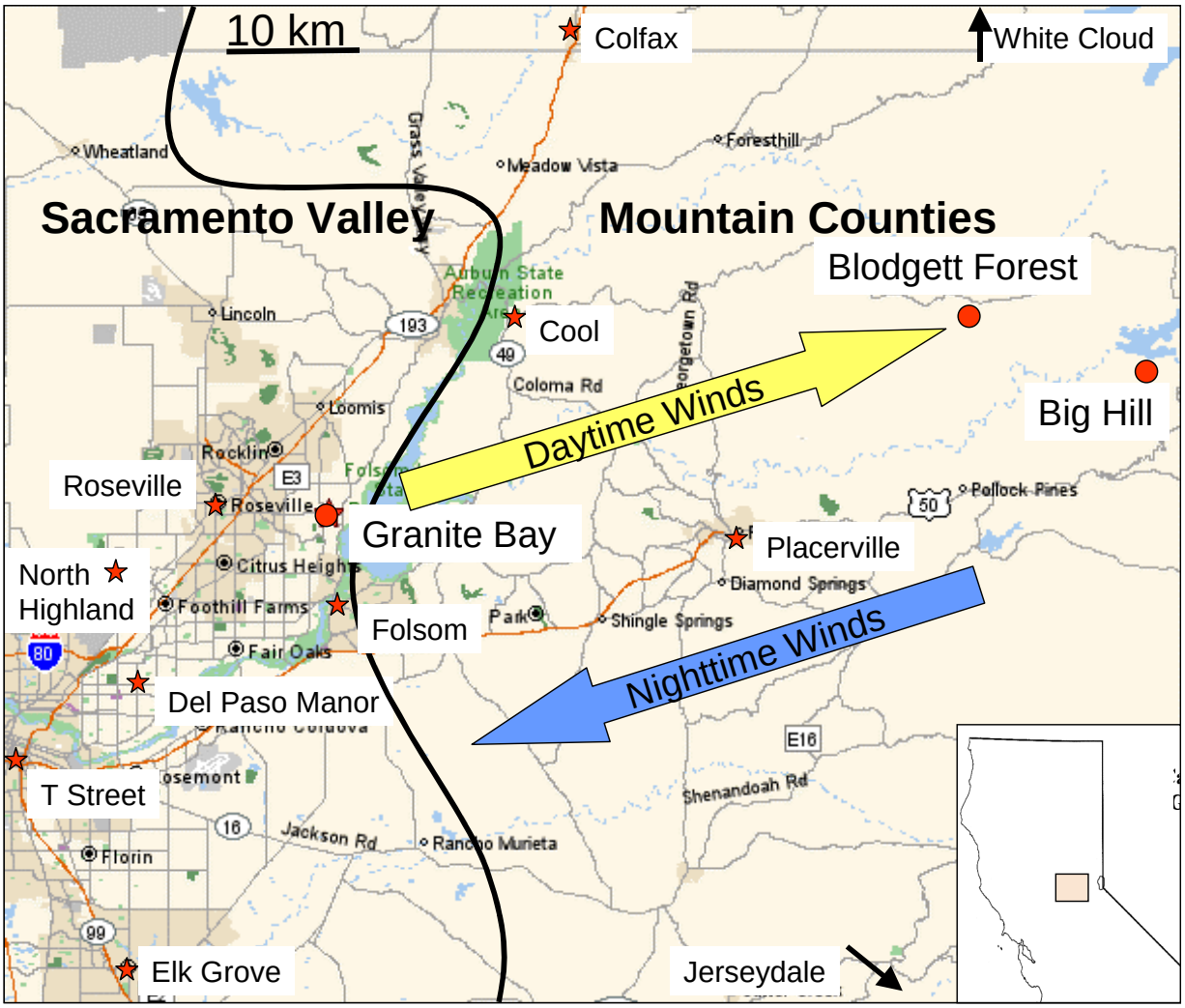

Figure 6-11. Depiction of regional weekly net airflow using meteorological data from the Camino CIMIS site close to Pollock Pines near Highway 50. Between March and October, net flow in the region is from west to east; however, this trend is reversed during the winter months.

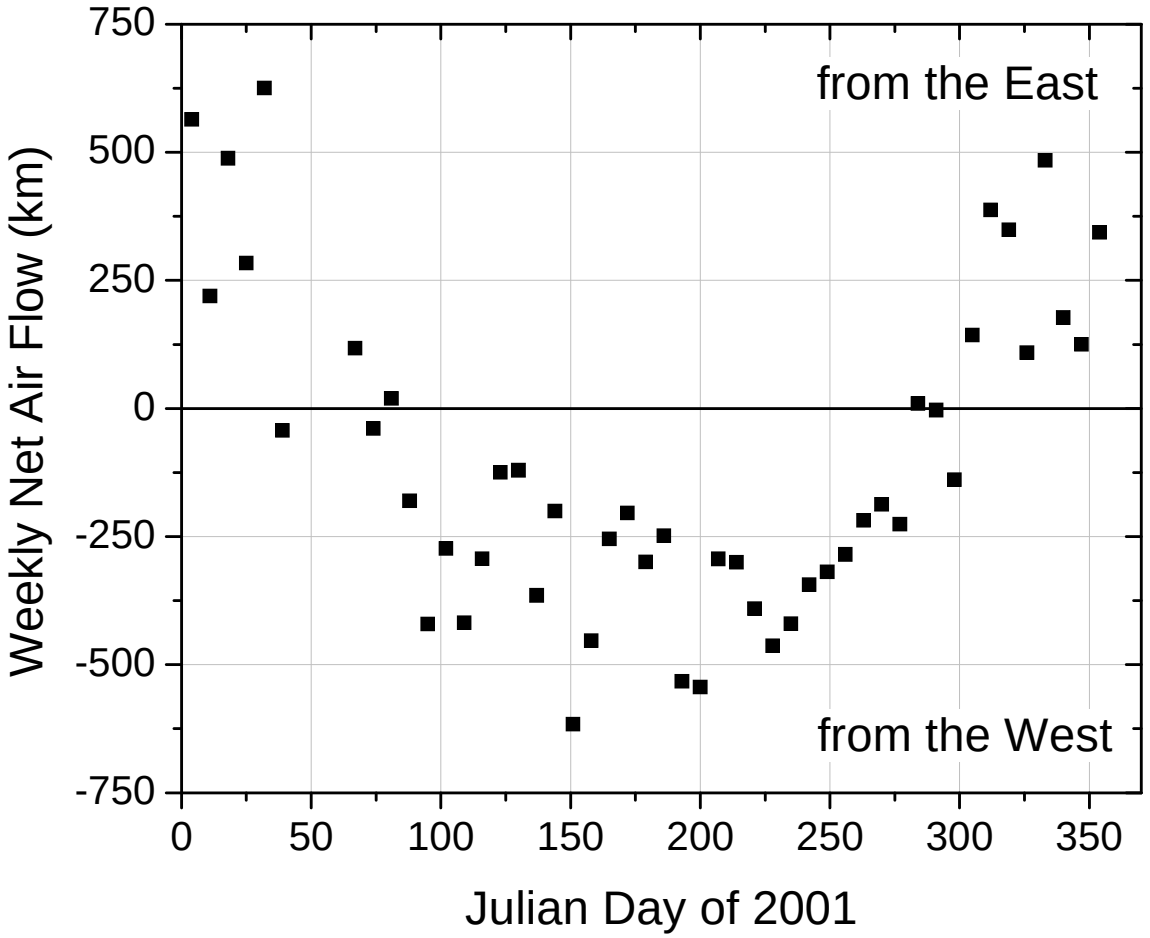

6.7.2 Seasonal Cycles in Nitrogen Oxide Species

Data was obtained at Big Hill for a full annual cycle from March 2003 – February 2004, allowing comparison of meteorology and reactive nitrogen for all the seasons. **Figure 6-12** presents observations of temperature, absolute water vapor (calculated as a mole fraction in parts per thousand), and total reactive nitrogen NO_Y (i.e., NO_2 + ΣPN + ΣAN + HNO_3). From the temperature data, it seems reasonable to consider two different sets of conditions: summer (June through October) and winter (November through April). ΣPN are formed through the association of a peroxy radical and nitrogen dioxide, but only those derived from acyl peroxy radicals are stable enough to survive in the atmosphere. The most common peroxyacyl nitrate is peroxy acetyl nitrate (PAN). ΣAN or alkyl nitrates are formed photochemically through the association of peroxy radicals with nitric oxide. The RO_2 + NO reaction can also form ozone; hence, the alkyl nitrate concentrations are generally a good indication of ozone production.

Because of power delivery problems virtually no data were collected during May 2003. While the relative humidity was quite low during the summer months, the water vapor mole fraction is actually higher on average during summer compared to winter. Reactive nitrogen is higher during the summer months at the site though there is substantial day-to-day variability. Most notable perhaps is that the lower values, generally measured during the early morning, reach down almost to zero during the winter but generally not below 0.5 ppb in the summer. This seasonal cycle is consistent with corresponding measurements carried out at Blodgett Forest from 2001-2003. While emissions of precursor NO_X are not known to change substantially in the region by season, what does change is the extent to which these urban emissions are processed and transported to the western slope of the Sierra. As discussed above, net surface flow during the winter months is actually from east to west, so reactive nitrogen does not have the same opportunity to build up in the region that it does in the summer. The seasonal cycle in NO_Y at Big Hill and Blodgett Forest is very different than that observed at sites that do not have a seasonal cycle in transport patterns. For example, Harvard Forest (a rural setting in north-central Massachusetts) continues to sample air from urban sources to a similar extent throughout the year. During winter, lower rates of oxidation reduce the conversion of NO_2 to HNO_3, the ultimate sink of NO_Y, and therefore maximum NO_Y values are measured during the winter months (Munger, Wofsy et al. 1996; Moody, Munger et al. 1998).

Figure 6-13 displays the full annual record for all the individual NO_Y compounds measured. The organic nitrate species, $RONO_2$ and RO_2NO_2 clearly maximize during the summer months, when higher temperatures and photochemical activity result in increased precursor VOC emissions, more rapid photochemistry and more persistent transport. HNO_3 is also generally higher during the summer months, averaging around 0.5 ppb, but higher excursions tend to occur during the winter months. NO_2 has the least clear seasonal cycle, likely because of compensatory effects between transport and chemistry. During the hot summer months, strong transport of urban emissions to remote high-elevation sites is offset by rapid photochemical oxidation of NO_X to NO_Y. In the winter, the plume will have barely reached the site before downslope flow will carry the urban influence away but a much greater fraction of the total NO_Y will remain as NO_2 due to reduced photochemistry.

Many of the winter season high NO_Y events, especially in November 2003, occurred during prescribed burning events carried out by the US Forest Service or Sierra Pacific Industries, who own much of the nearby forests. Smoke plumes could also be seen from apple orchards and vineyards near Pollock Pines. During these nearby burning events, NO_2 and HNO_3 were the most substantial contributions to NO_Y and particulate nitrate was likely an important constituent based on data from the BAM and two week samplers. Some of the low values measured during the winter are the result of precipitation events that scrub soluble forms of NO_Y, such as HNO_3, from the atmosphere.

Figure 6-12. Full dataset obtained at the Big Hill monitoring site for NO_Y (ppb), absolute water (parts per thousand, ‰), and temperature (^{O}C). Data acquisition began March 5, 2003 (day 64) and ended on Feb 23, 2004 (day 54); however, data are plotted on a calendar year basis to aid the interpretation of seasonal patterns.

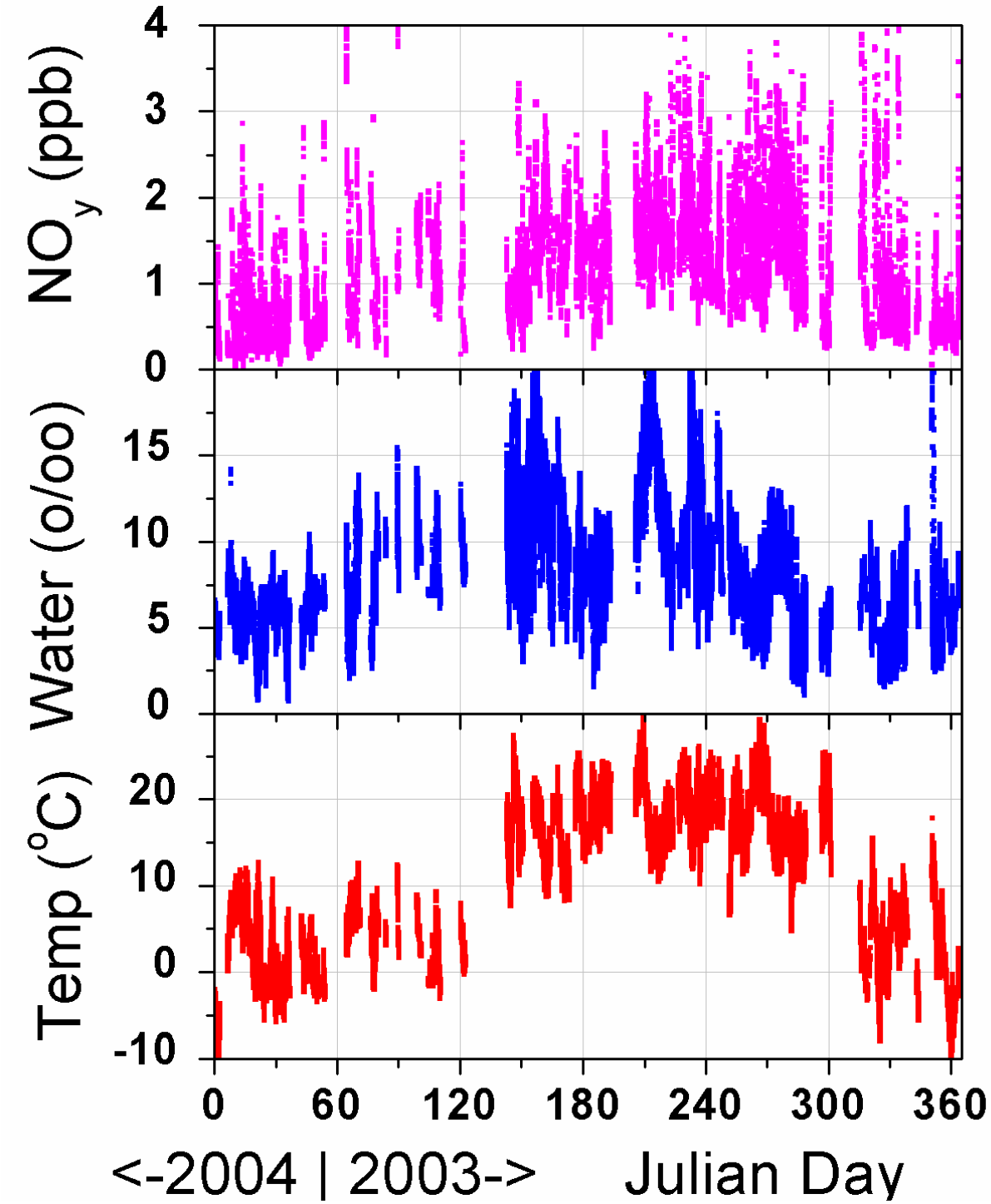

Figure 6-13. Annual record of individual NO_{yi} species, NO_2, ΣPNs, ΣANs and HNO_3, measured at Big Hill. Data points represent a 3-minute average and all concentrations are reported in parts per billion by volume. Data acquisition began March 5, 2003 (day 64) and ended on Feb 23, 2004 (day 54); however, data are plotted on a calendar year basis to aid the interpretation of seasonal patterns.

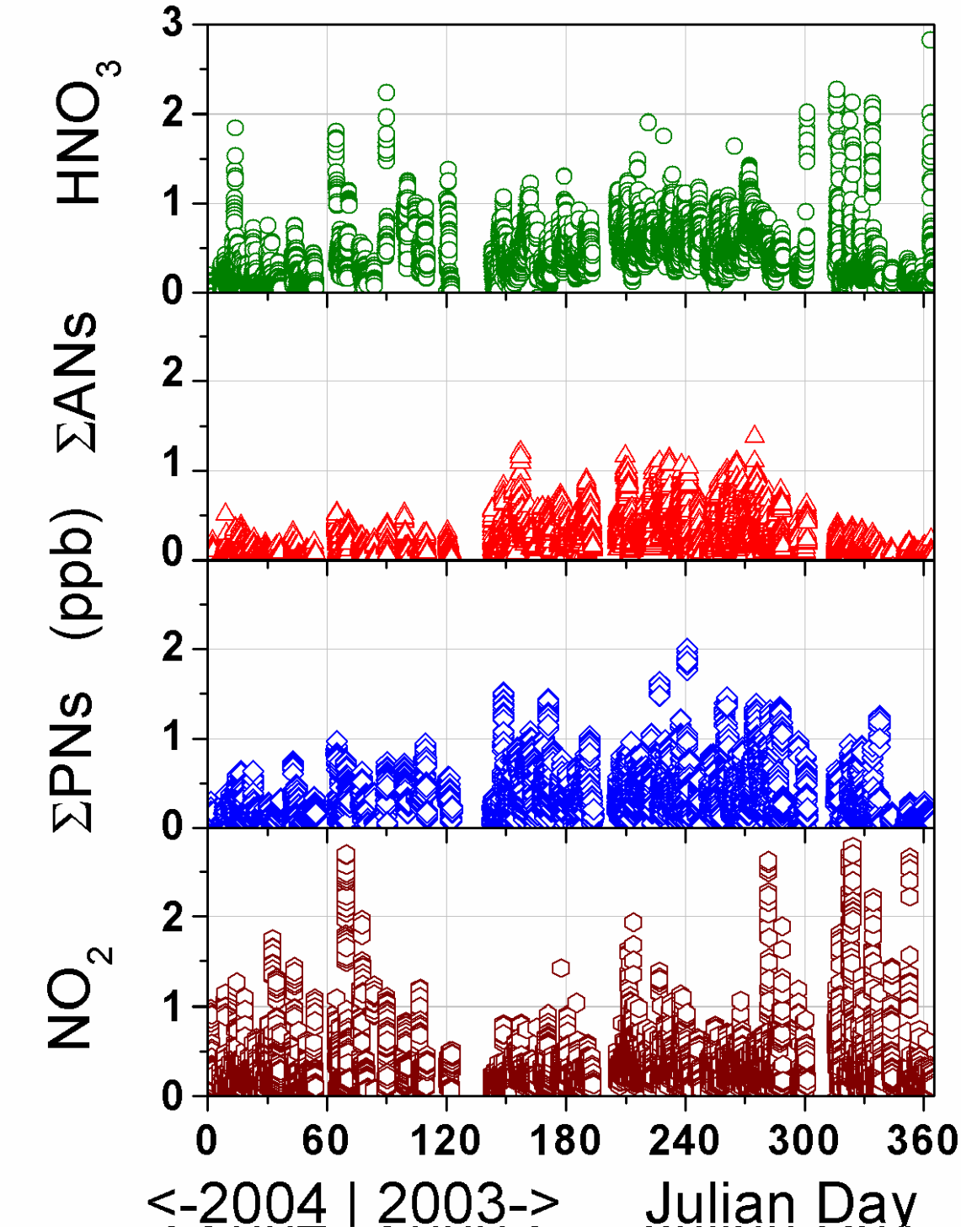

6.7.3 Summer and Winter Timelines

In this section a summer week and a winter week will be examined in more detail to look at the variability in meteorological conditions and reactive nitrogen and ozone concentrations observed at Big Hill. **Figure 6-14** shows meteorological data from a typical summer week that starts with hot dry conditions, with a cooler wetter weather pattern moving in on day 232. The pattern of upslope – downslope flow is dominant on all days except the day of the weather shift. Daytime winds are close to 4 m/s, while at night wind speeds average around 1 m/s and are more variable in direction.

Figures 6-15 and 6-16 show the observations of ozone, total NO_Y and the individual NO_Y species for the same time period. The late afternoon maximum is consistent with transport of urban pollutants by daytime upslope flow along the western Sierra slopes. Interestingly, while NO_2 and ΣPN exhibit the characteristic afternoon peak on day 230, it is noticeably absent in both O_3 and ΣAN, a co-product of ozone. In general, the patterns of NO_Y and O_3 track each other during the summer months. HNO_3 is the only NO_Y compound which remains as abundant during the cooler, wetter conditions at the end of the week. While total NO_Y values do not decrease significantly at the end of the week, ozone is close to 30 ppb, and there is little apparent photochemical production.

Figure 6-17 shows the same meteorological variables as **Figure 6-14**, but for a week in late November. Winter conditions are less consistent than during the summer, but this data does demonstrate some widespread features in the data collected during the winter at Big Hill. The weather is cooler and the relative humidity is higher during this time period. Several days of strong flow from the southwest are interrupted on day 324 with a return to the more common upslope – downslope pattern but with weaker winds. **Figure 6-18** shows that the diurnal variability in ozone has diminished significantly and values for the week all lie between 45 and 65 ppb. Ozone is no longer correlated with NO_Y, which is likely influenced by burning events during days 322-324. **Figure 6-19** shows that strong flow from the west delivered high concentrations of NO_2, HNO_3 (and likely particulate nitrate) to the Big Hill site, which is likely due to plumes from upwind burning events. At the end of the weeklong period a diurnal cycle in NO_2, and especially ΣPN can be seen with the return to the usual flow pattern. Just as ozone concentrations have ceased to rise significantly above background values in the region, ΣAN remains very low throughout most of the winter.

Figure 6-14. Observations of relative humidity (%), temperature (°C), wind direction, and wind speed (m/s) from a typical summer week at Big Hill.

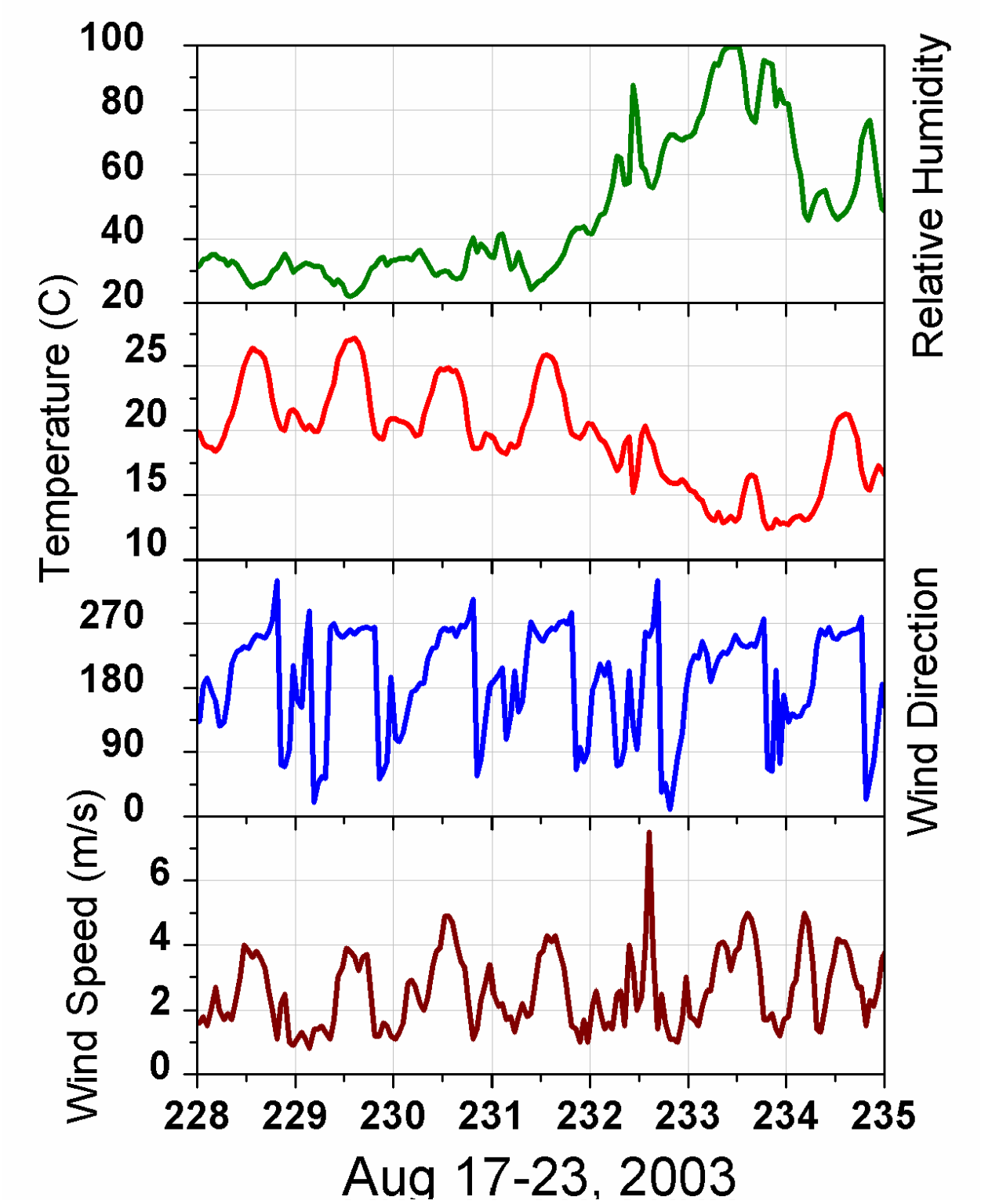

Figure 6-15. Concentrations of NO_y and O_3 (ppb) and PM10 (µg/m^3) from a typical summer week at Big Hill.

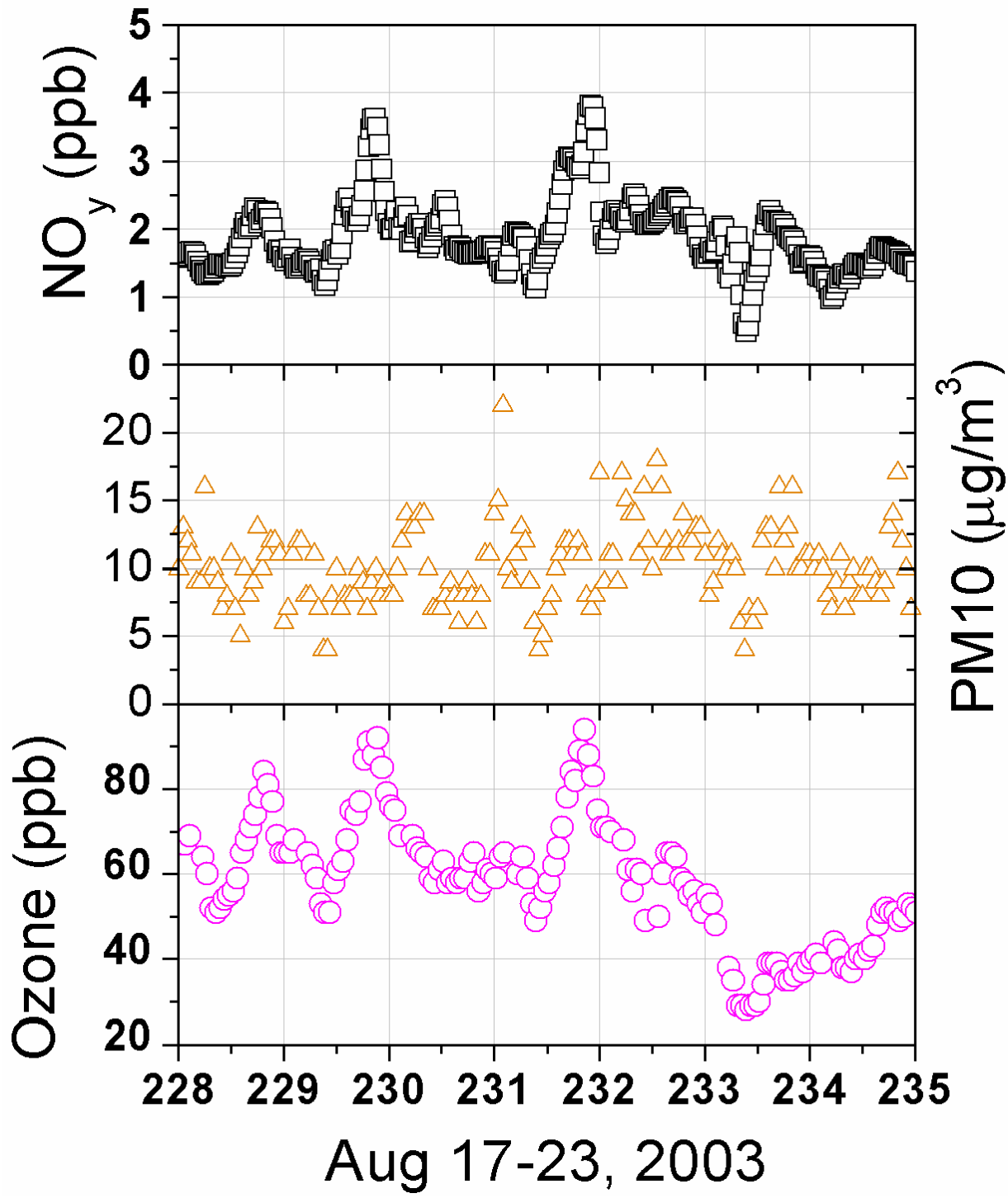

Figure 6-16. Concentrations (ppb) of NO_2, ΣPNs, ΣANs and HNO_3 from a typical summer week at Big Hill.

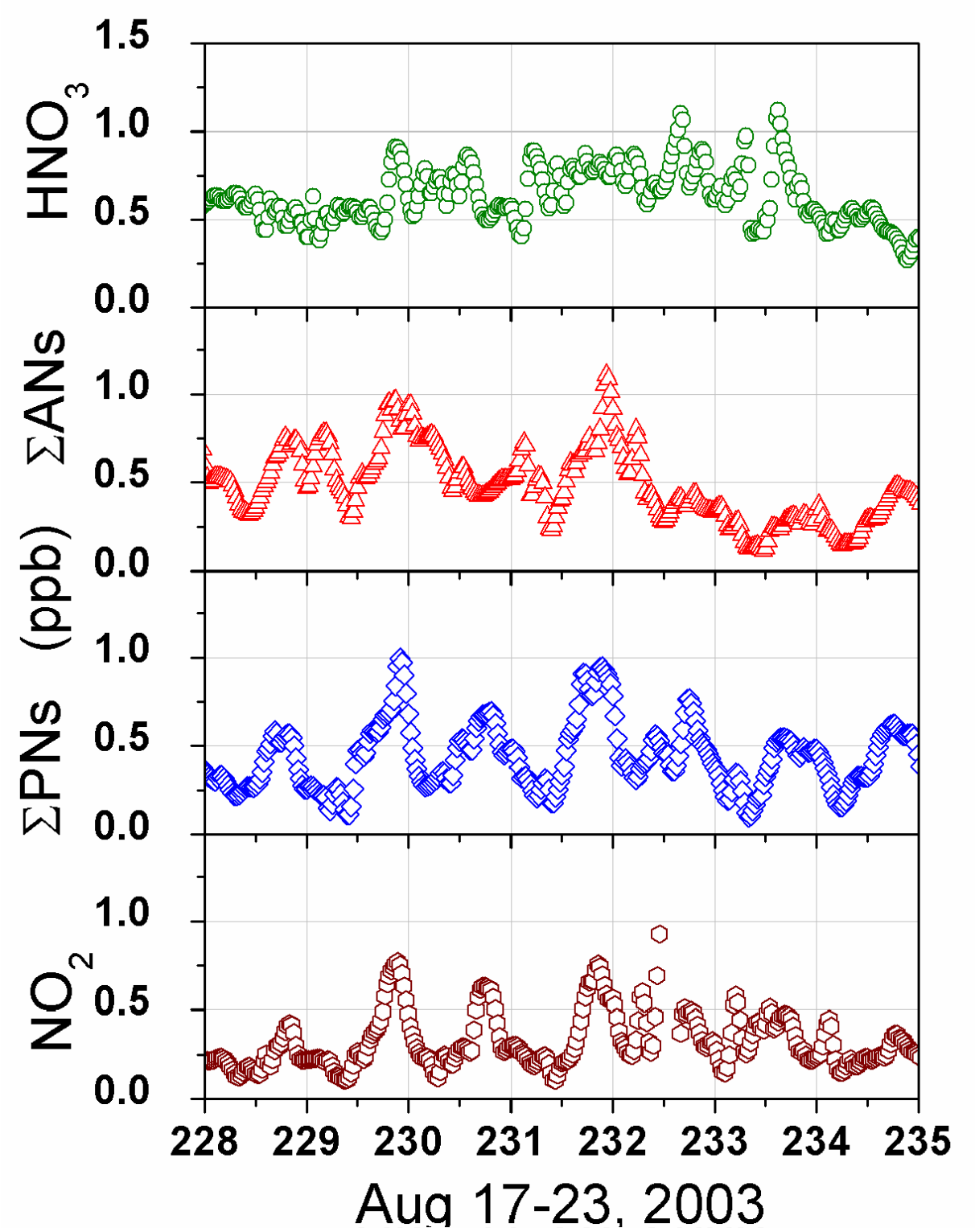

Figure 6-17. Observations of relative humidity (%), temperature (°C), wind direction, and wind speed (m/s) from a typical winter week at Big Hill.

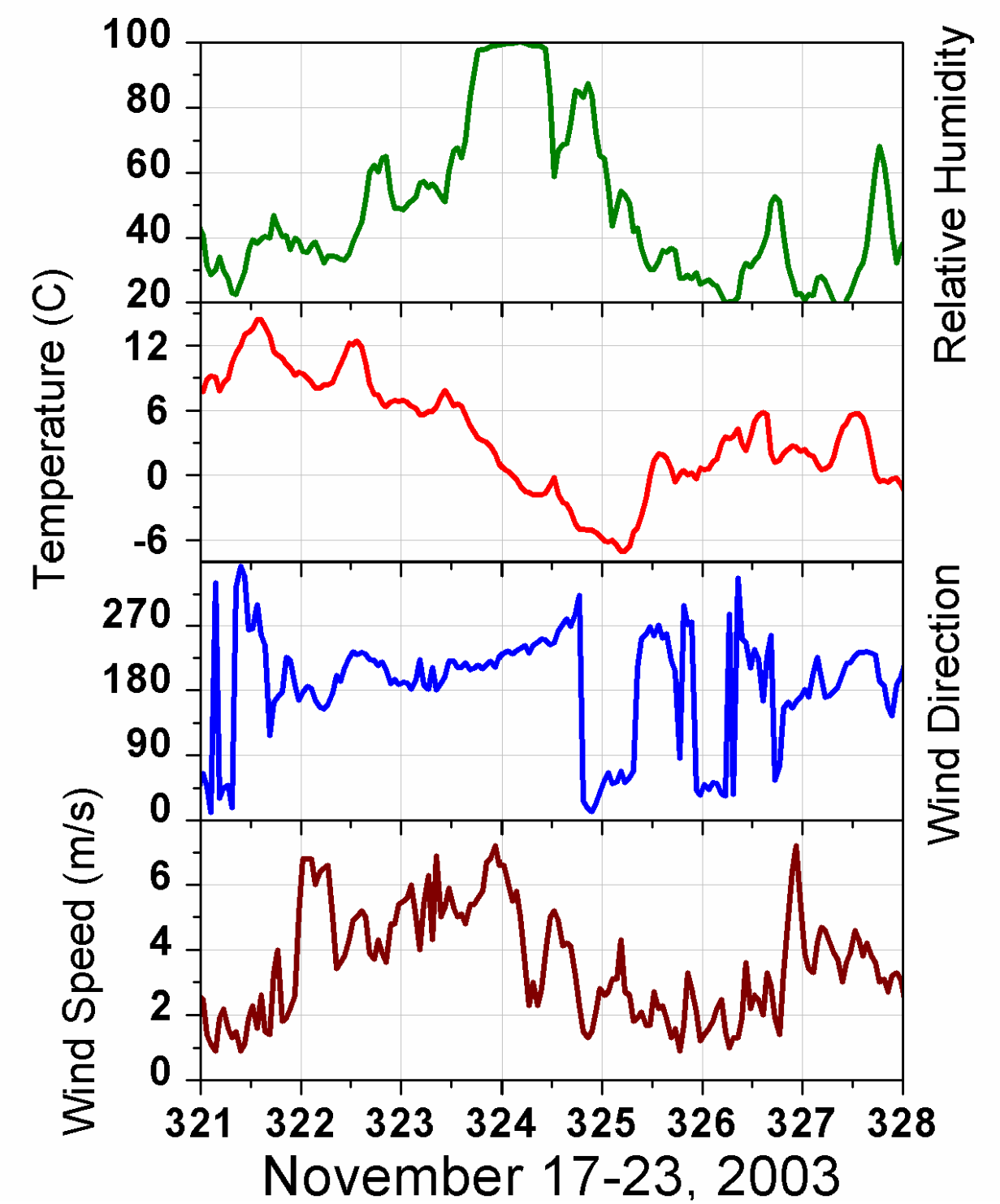

Figure 6-18. Concentrations of NO_y and O_3 (ppb), and PM10 ($\mu g/m^3$) from a typical winter week at Big Hill.

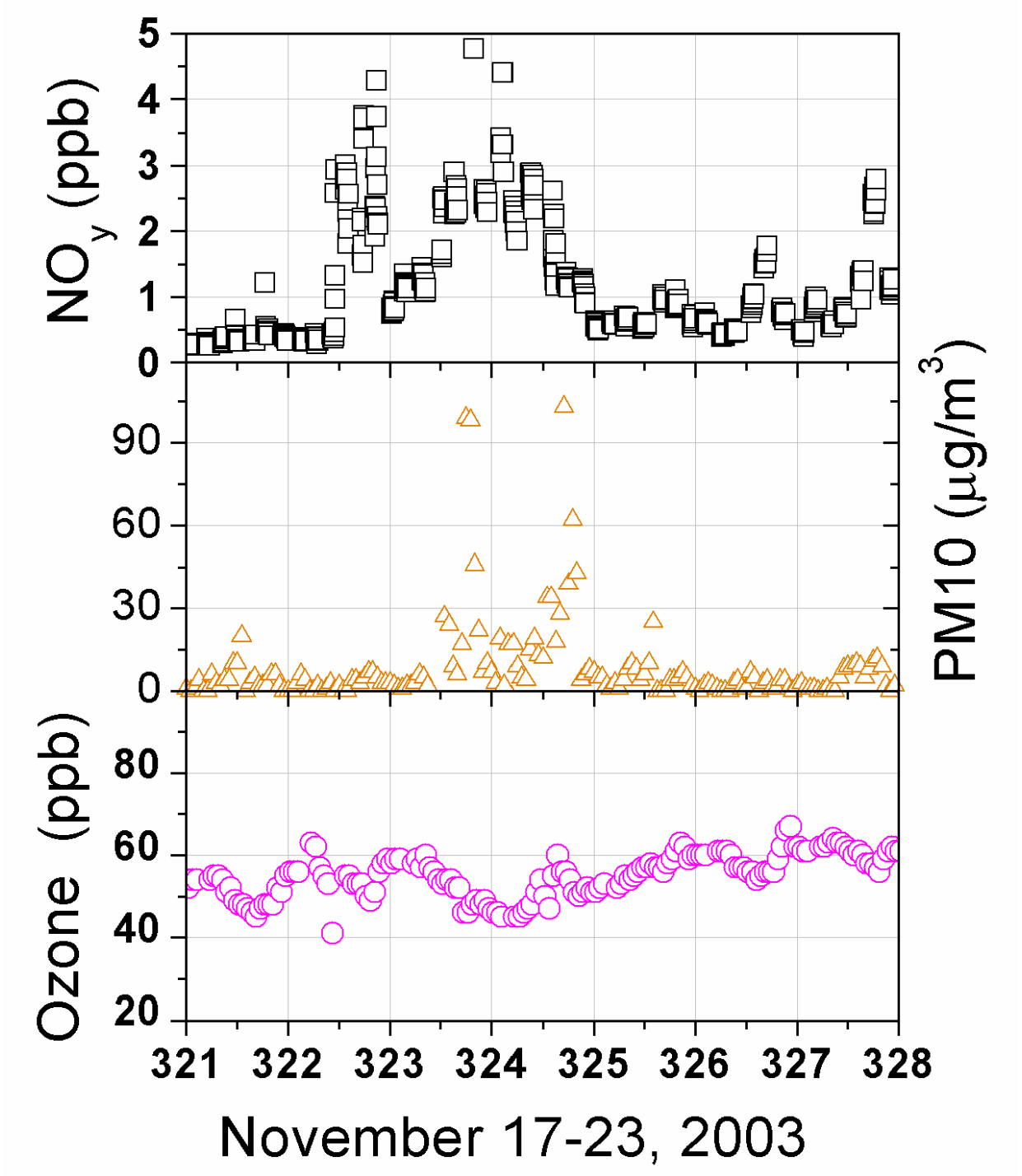

Figure 6-19. Concentrations (ppb) of NO_2, ΣPNs, ΣANs and HNO_3 from a typical winter week at Big Hill. Note different axes on NO_2 panel.

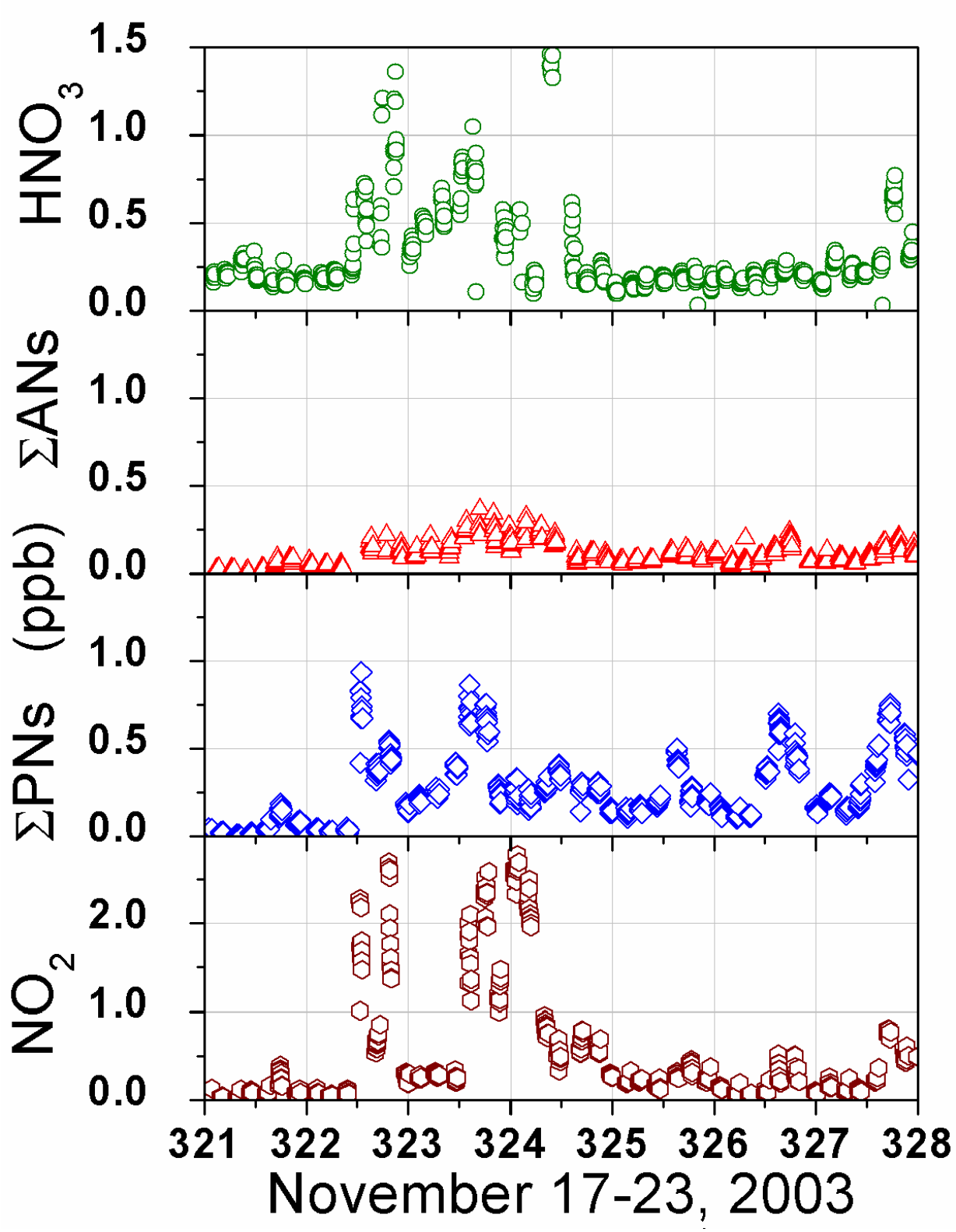

6.7.4 Summertime Diurnal Profiles of Meteorology, Trace Gases and Particles

Figure 6-20 demonstrates the remarkably consistent meteorology experienced by the Big Hill site during the summer months (June through October in the following analysis). Temperatures were between 10 and 30 °C, with an average swing of approximately 7 °C between night and day. Rain was extremely rare and the relative humidity was generally between 25 and 50 %. With the exception of very few days, between roughly 9 am and 8 pm, the wind blows from the west. Wind direction during the night is more variable but is generally from the east or southeast. Wind speed maximizes during the afternoon at about 4 m/s, and is slowest in the early evening when the predominant flow is changing direction from upslope to downslope. Wind speeds during the night are more variable but are generally slower than during the day. The regularity of transport and climate variables is exploited to analyze the data statistically and increase our understanding of the important parameters involved in determining NO_Y distribution in the region.

The summertime diurnal cycles in the individual reactive nitrogen species are shown in **Figure 6-22**. HNO_3 has a remarkably flat diurnal profile at the Big Hill site, in contrast to measurements made by TD-LIF at both Blodgett Forest and Granite Bay, a Sacramento suburb. At those sites, the profile of HNO_3 followed that of the sun, peaking in the middle of the day and decreasing to close to zero at night. The rationale behind the different pattern at Big Hill is two-fold: during the day HNO_3 at Big Hill is lower because the site is further from the NO_X source and the HNO_3 made along the way has had more time to deposit, while at night HNO_3 is higher than other surface sites because it is sampling descending air characteristic of the free troposphere, in which the HNO_3 formed has not had the opportunity to deposit.

Peroxy nitrates have a substantial diurnal profile at Big Hill, peaking between 2 pm and 6 pm at values more than double those observed during early morning hours. As we noted before ΣPN are formed through the association of a peroxy radical and nitrogen dioxide, but only those derived from acyl peroxy radicals are stable enough to survive in the atmosphere. The most common peroxy nitrate, peroxy acetyl nitrate (PAN), is the result of the photochemical oxidation of acetaldehyde in the presence of NO_X. Acyl peroxy nitrates act as a thermally labile reservoir for both RO_2 and NO_2 radicals and therefore on cooler days can sequester these radicals and reduce photochemical ozone production. Peroxy nitrates can also be responsible for transporting reactive nitrogen far from its original source, and act as a radical source upon subsequent decomposition. PAN is known to be acutely toxic to plants at high concentrations, but not much is known about the effects of chronic exposure at the ppb-level. Organic nitrates have relatively low water solubility and their contribution to reactive nitrogen deposition is not well understood.

Figure 6-20. Observations of relative humidity (%), temperature (°C), wind direction, and wind speed (m/s) by hour of day for the entire summer (June through October) at Big Hill. Individual half-hour data points for each day (open symbols) are overlaid by the averages for each half-hour observation (solid symbols).

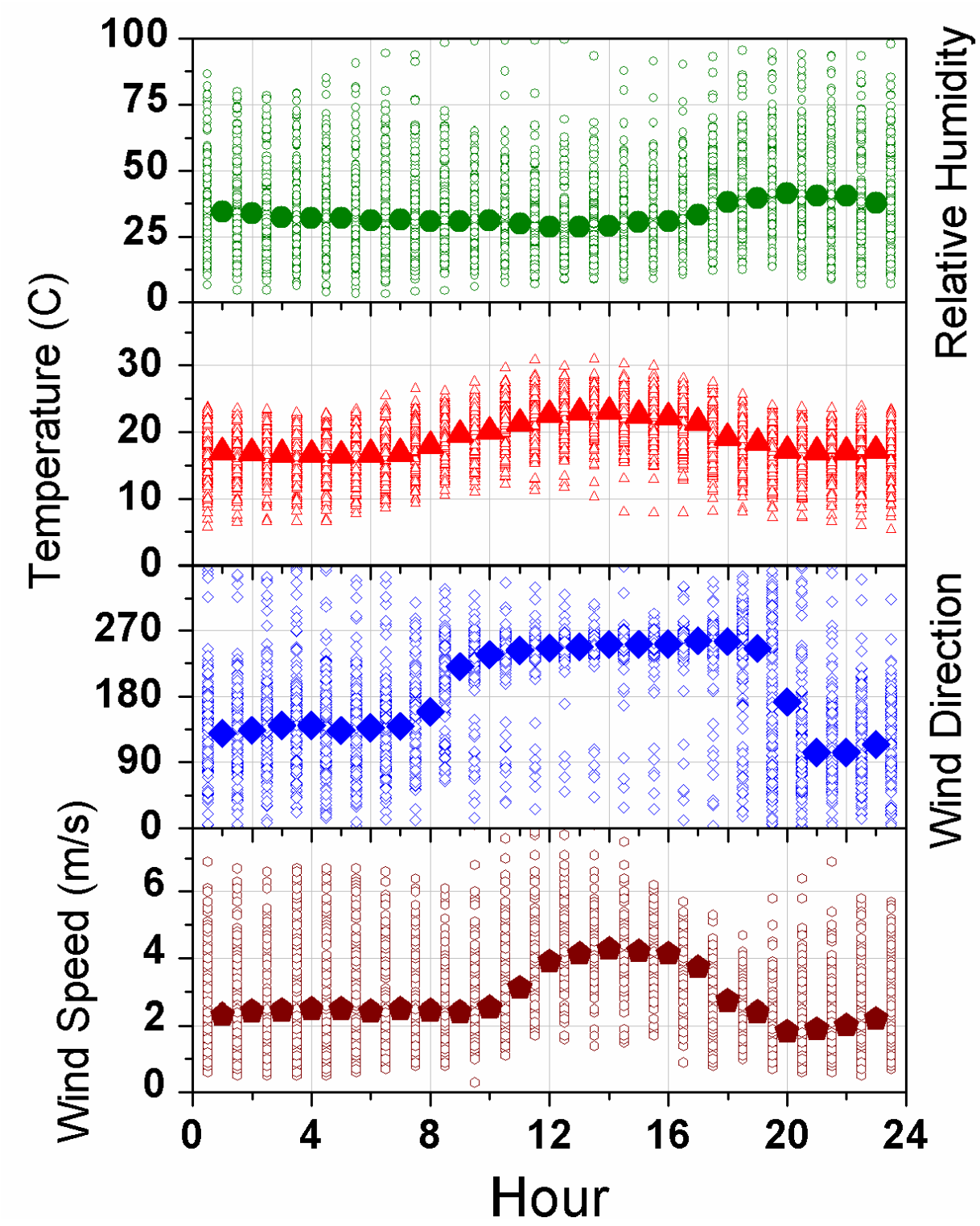

Figure 6-21. Diurnal profile of summertime concentrations of NO_y and O_3 (ppb), and PM10 ($\mu g/m^3$) at Big Hill. Individual measurements (open shapes) of O_3 and PM10 were made every hour at Big Hill, and the NO_y data has been averaged to half-hour points. The average value for every hour or half-hour is overlaid in the solid points.

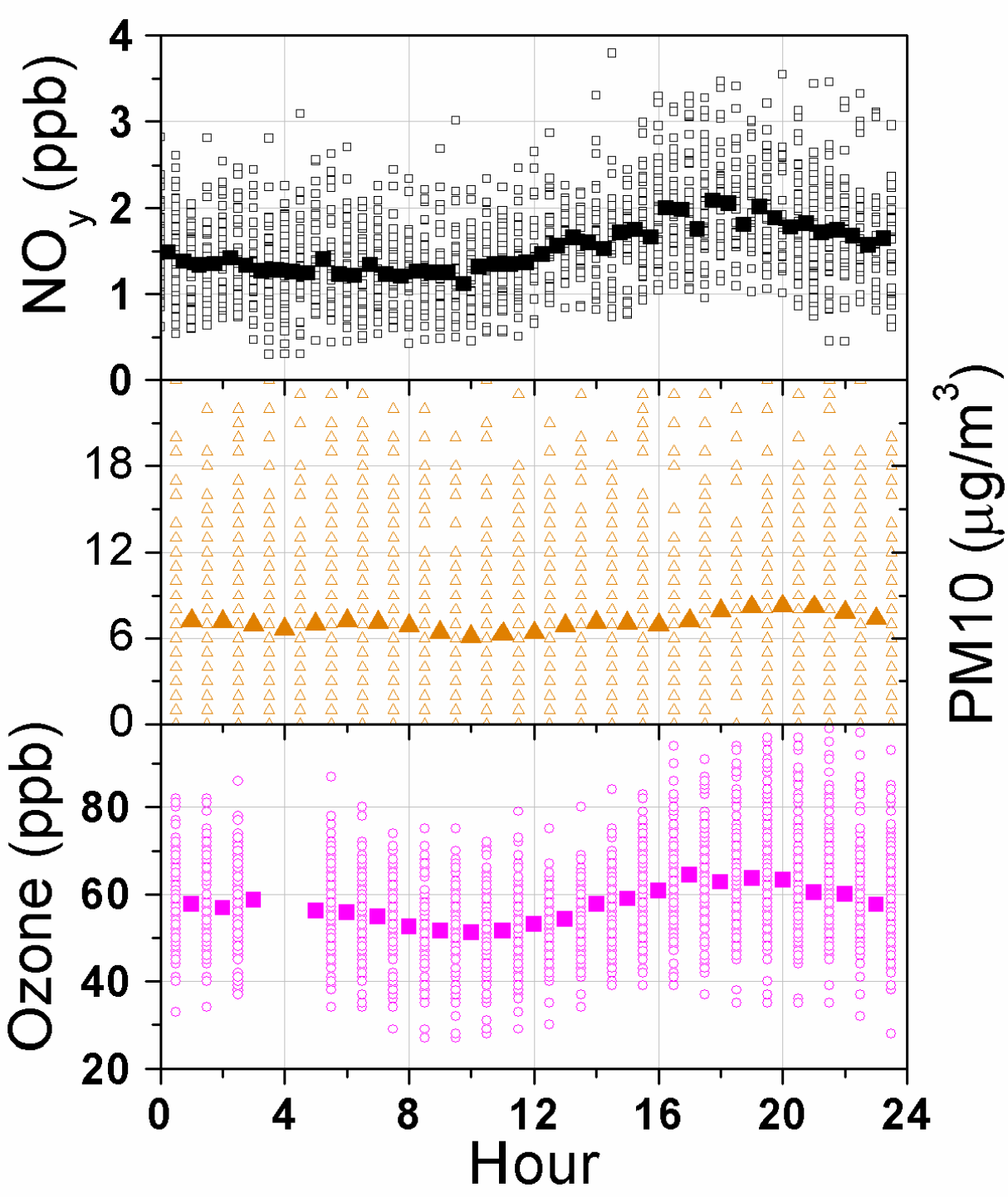

Figure 6-22. Diurnal profile of summertime concentrations (ppb) of NO_2, ΣPNs, ΣANs and HNO_3 at Big Hill. Individual half-hour data points for each day (open symbols) are overlaid by the averages for each half-hour concentration (solid symbols).

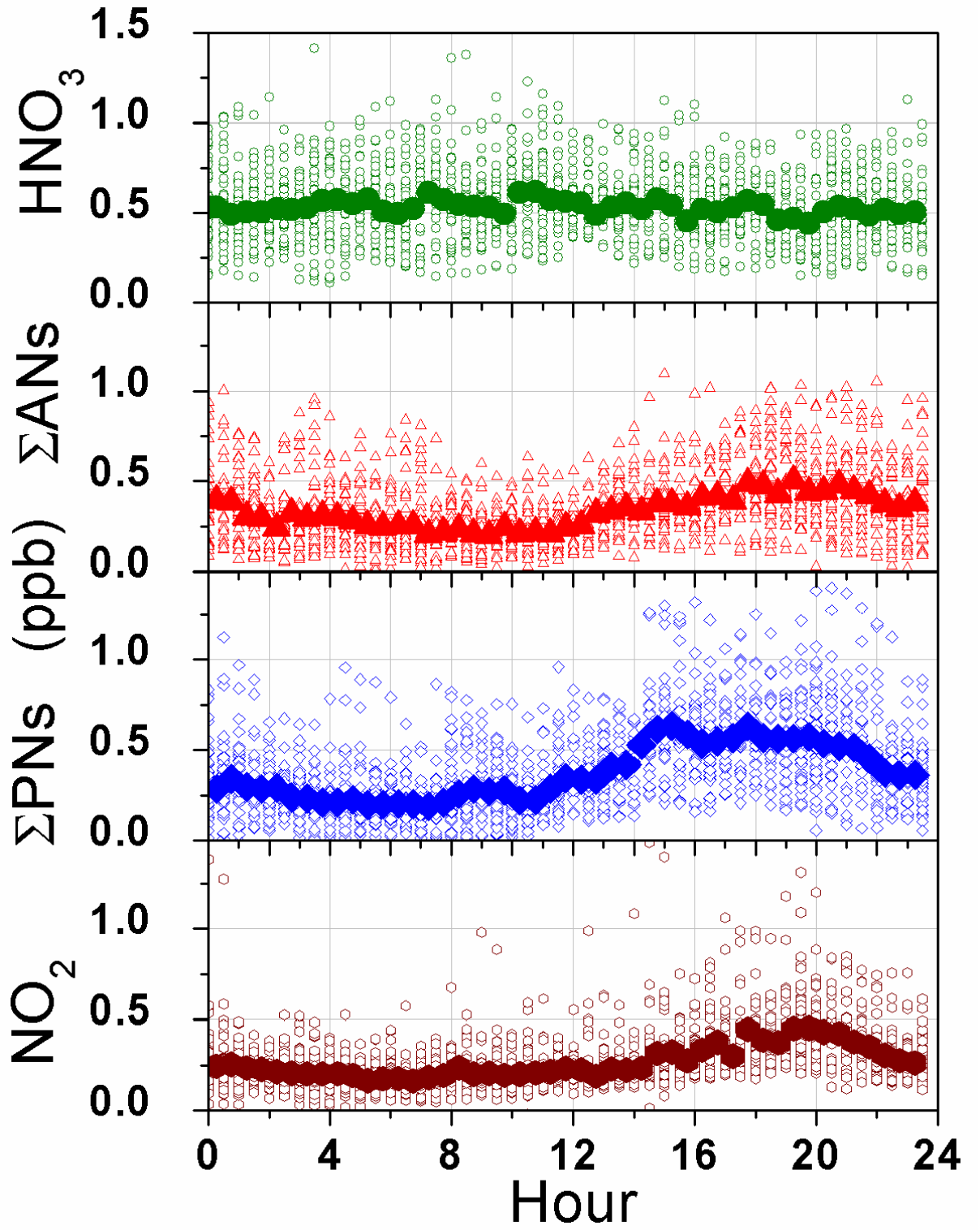

Nitrogen dioxide also has a strong diurnal cycle and has the latest peak of all of the reactive nitrogen compounds at Big Hill. The delayed timing of the peak concentrations can be explained by a combination of transport and photochemistry. The NO_2 emitted into the plume takes around six hours to arrive at the Big Hill site. The air mass containing emissions from the Sacramento area often begin in the late morning to move up the slopes of the Sierra Nevada just when photochemical activity is peaking and the conversion of NO_X to higher NO_Y species is maximizing. Air masses leaving Sacramento in the afternoon and arriving at Big Hill in the early evening experience lower levels of actinic radiation and therefore the latter part of the urban plume has a larger fraction of NO_2 remaining. Peak concentrations in this "tail" portion of the plume are roughly double the early morning minimum values.

Figure 6-23 shows the partitioning of the NO_Y budget at Big Hill by time of day. During the early morning hours, when the site experiences dry, clean air almost 40% of the NO_Y is HNO_3, with the other three classes of compounds contributing about 20% each. At the height of the plume in the late afternoon, the contribution of HNO_3 has shrunk to 25% and ΣPN have become more important. NO_2 never accounts for more than 25% of the NO_Y measured at the site and is most important near sun set. The contribution of ΣAN varies from 15% of NO_Y during the early morning hours to about 25% in the evening. Peroxy nitrates are most important at the site during mid-afternoon, when they make up almost one third of the reactive nitrogen.

6.7.5 Summertime Distribution of Reactive Nitrogen and Correlation with Other Variables

Changes in climate can be expected to drive differences in both transport and chemistry, affecting the geographical and temporal extent to which the urban plume affects remote sites, and the chemical partitioning with the plume. One of the most important climate variables that govern the distribution of reactive nitrogen oxides is the temperature. The summertime data was divided into two sets of days, half of which had a maximum daytime temperature above 20 °C and half of which did not. The average amount of NO_Y in the plume was 1.9 ppb on both of the two sets of days, suggesting that local temperature is not a good indicator of the transport efficiency of the plume. However, the partitioning of reactive nitrogen among its constituent species is strongly influenced by temperature as shown in **Figure 6-24**. The top panel shows the partitioning among NO_Y species arriving at the site between 1 pm and 8 pm on days when the maximum temperature exceeded 20 °C. Comparison with cooler temperature data displayed in the bottom panel shows that while NO_2 has undergone similar amounts of photochemical processing under both sets of conditions, lower temperatures favor the accumulation of peroxy nitrates over the production of alkyl nitrates and nitric acid. Peroxy nitrates account for over one third of the reactive nitrogen under the cooler temperatures, sequestering a substantial amount of reactive nitrogen in this reservoir. The reduced contribution of alkyl nitrates at lower temperatures is consistent with fewer RO_2 and NO_X radicals being available to react to form ozone. Indeed, the mean ozone concentration in the plume is 64 ppb on the hot days and 58 ppb on cool days, suggesting that temperature plays a crucial role in determining the availability of alkyl nitrates for ozone production. Another facet of the temperature effect may be the

increased emissions of many biogenic VOC at higher temperatures. A shift in the hydrocarbon composition toward longer chain compounds as opposed to carbonyl compounds could favor the production of alkyl nitrates over peroxy nitrates.

Figure 6-23. Fractional NO_y speciation by time of day during summer months at Big Hill.

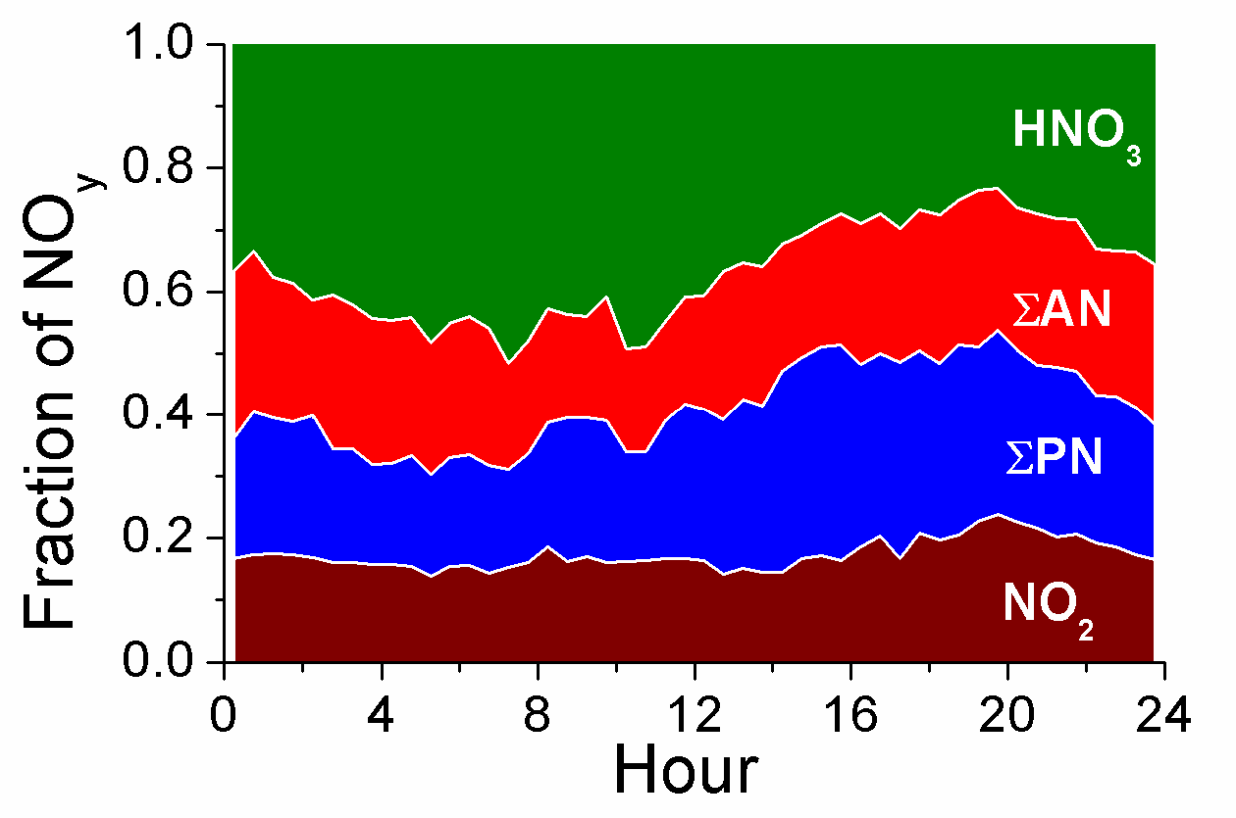

In **Figure 6-25**, the correlation between total reactive nitrogen and the mole fraction of water is shown. This relationship is not as clear at Blodgett Forest, where it is likely that the transpiration of nearby vegetation has a strong influence on the water budget at the site. In contrast, water vapor appears to be a good indicator of transport of polluted air masses at a high elevation site such as Big Hill. Observations during the night indicate that the descending air, whether from aloft or mountain slope drainage, tends to be much drier and have reduced total reactive nitrogen. The absolute humidity of the air mass records the degree of mixing that the relatively moist, polluted urban plume has undergone in transit to the high elevation site.

Figure 6-26 depicts the remarkable correlation between reactive nitrogen and ozone at the Big Hill monitoring site throughout the summer. Observations made during afternoon upslope flow are highlighted in orange and show that higher values for ozone and NO_Y occur when the urban plume is influencing the site. Other high values are measured shortly after the wind has shifted direction and the air passing back by the site is still characteristic of plume air.

Figure 6-24. Distribution of NO_Y during daytime upslope airflow at Big Hill. The data were separated by temperature such that the top chart includes data from days on which the daytime maximum temperature at the site exceeds 20 °C, while the bottom chart shows data from cooler days on which the temperature was never higher than 20 °C.

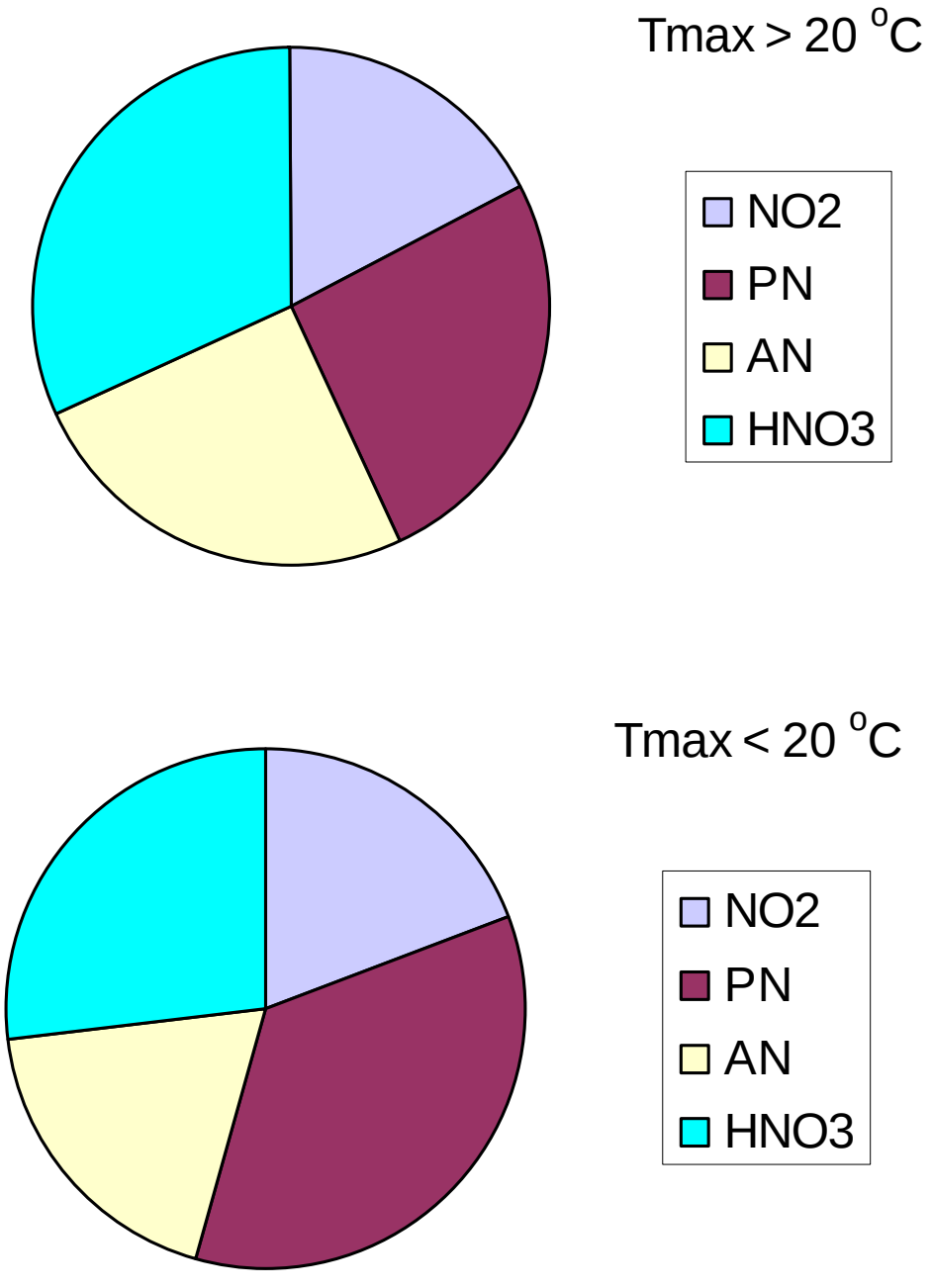

Figure 6-25. Relationship between reactive nitrogen (ppb) and mole fraction water vapor (parts per thousand; ‰) during summer months at Big Hill.

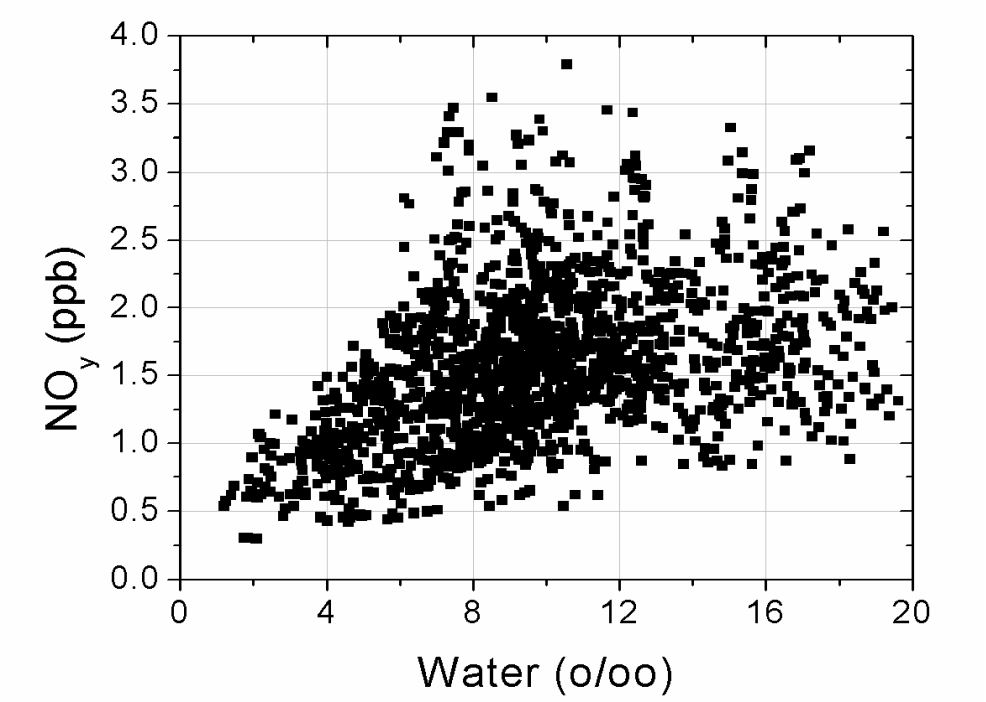

The relationship between NO_Y and ozone is expected because both are derived from precursor emissions of nitrogen oxides. While ozone can be anti-correlated with NO_X in urban areas with high NO concentrations, we expect ozone production to be limited by the availability of nitrogen oxides in remote areas like Big Hill. Minimum values of NO_Y (< 1 ppb), which occur in the early morning hours, are associated with ozone levels between 35 and 60 ppb, while maximum values of NO_Y (> 2.5 ppb) are associated with ozone between 65 and 95 ppb. Clearly, the chemistry and transport patterns responsible for transforming and transporting nitrogen oxides to the western slope of the Sierra Nevada also have similar effects for the reaction products, including ozone and total reactive nitrogen.

A great deal of insight can be gained by comparing observations made at Big Hill to corresponding measurements at the Blodgett Forest site. As mentioned above, both sites lie along the Sacramento – Lake Tahoe transect, but Big Hill is at a higher elevation, a greater distance from the city, and has less vegetation and cooler temperatures. Our analyses of the diurnal cycles at the two sites suggest that they sample similar air masses during upslope flow and we restrict the comparison to the times between 1 pm and 8 pm when both sites are strongly influenced by the Sacramento urban plume. **Figures 6-27 a-f** show the frequency distributions for the individual reactive nitrogen species, total NO_Y and O_3 for both the Big Hill and Blodgett Forest sites. In the case of NO_2, Big Hill values (median 0.25 ppb) are on average less that half those of Blodgett Forest with significantly fewer half-hour periods with more than 1 ppb. This means that the dilution and photo-oxidation of NO_2 in the plume is

quickly reducing its concentration several hours downwind of Sacramento. In this region, ozone production is expected to be NO_X-limited so it can also be inferred that instantaneous ozone production rates drop off quickly between Blodgett Forest and Big Hill.

Figure 6-26. Relationship between ozone (ppb) and reactive nitrogen (ppb) during summer months at Big Hill. Observations made during upslope flow in the plume are in orange.

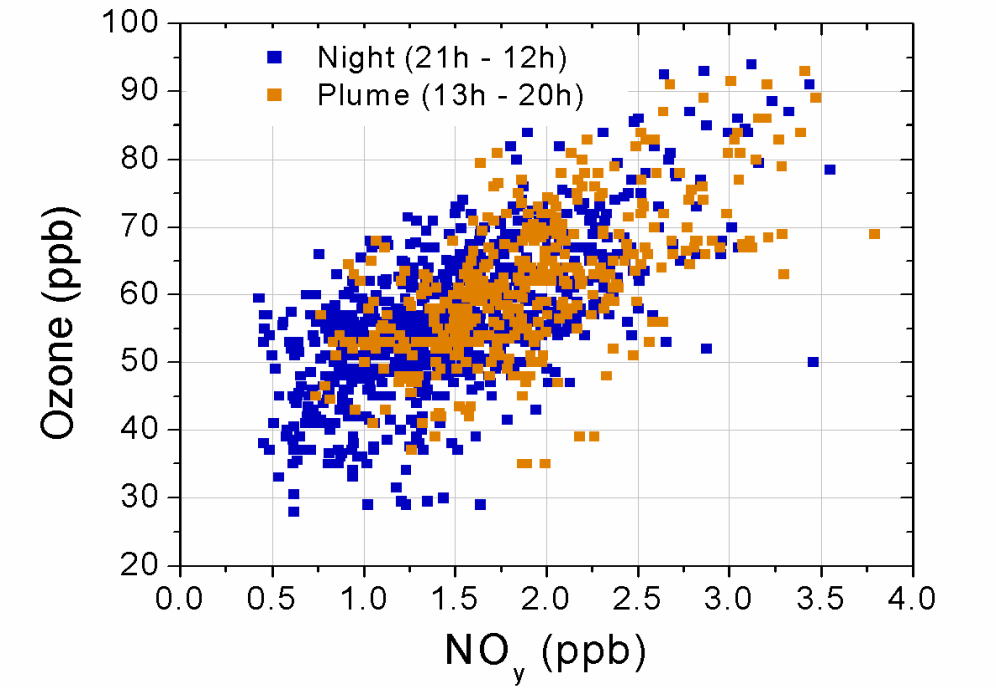

Peroxy nitrates have a wider probability distribution at Blodgett Forest than at Big Hill and higher median observations. While absolute ΣPN concentrations are higher on average at UC-BFRS, the ratio of peroxy nitrates to NO_2 is actually higher at Big Hill, likely due to the lower temperatures, stabilizing the reservoir species. This confirms that, as the plume is advected, it is being significantly diluted with air that has less NO_2 and ΣPN, and that the photochemical oxidation of NO_2 to peroxy nitrates acts as a permanent sink of NO_X when temperatures are cool. The probability distributions of alkyl nitrates are extremely similar at the two sites, but for different reasons. The breadth in the distribution at Big Hill derives from a stronger diurnal cycle than at Blodgett Forest, where it appears to result from more day-to-day variability.

Nevertheless, detailed comparison of the observations of alkyl nitrates at the two sites suggests that as a group these compounds are lost very slowly to deposition but are diluted when mixed with air from the free troposphere. Correlations between alkyl nitrates and CO and O_3 show that they are associated with polluted, upslope air and are formed in conjunction with ozone during photochemical activity. The deposition of most

alkyl nitrates appears to be slow enough that a substantial fraction of what is produced in the plume stays in the atmosphere. From the perspective of nitrogen deposition, not enough is known about the behavior of these compounds at the surface.

The fact that HNO_3 concentrations are similar, regardless of the wind direction at Big Hill suggests that there is no significant advection of HNO_3 from Sacramento to the Lake Tahoe Air Basin. HNO_3 concentrations are lower and less variable at Big Hill compared to Blodgett Forest. However, similar to the peroxy nitrates, considered in a relative sense, HNO_3/NO_2 in the plume is higher at Big Hill. The flat diurnal profile for HNO_3 at Big Hill suggests that this site is far enough from fresh NO_X sources that much of the HNO_3 produced during oxidation has already had the chance to deposit before reaching high elevation sites at the surface. Blodgett Forest has high daytime NO_2 concentrations capable of generating strong local production of HNO_3, but HNO_3 production at Big Hill is less efficient both because the plume is more dilute and because lower temperatures lead to the sequestration of NO_2 by peroxy nitrate formation.

The distribution of total NO_Y at the two sites reflects the proximity of Blodgett Forest to Sacramento in both the higher average and the greater variability in concentrations. At Blodgett Forest, the total NO_Y in the plume varies between 1-5 ppb, whereas at Big Hill it ranges from 0.5-3.5 ppb. The data used in this analysis was not limited to days on which there was persistent upslope flow, thus some of the lower numbers likely result from days on which the urban plume did not influence the site. The greater variability in total NO_Y compared to any of its constituent species shows that the variability in NO_{Yi} is not driven by differences in partitioning among the available reactive nitrogen, but more importantly in the extent to which the total urban emissions are influencing these remote sites. It is not clear from the meteorological observations, aside from wind direction, which conditions result in higher concentrations of reactive nitrogen being transported in the boundary layer along the western slope of the Sierra.

Finally, the distribution of ozone with the urban plume is shown for each site in **Figure 6-27f**. Remarkably, the median ozone concentration at each site is very similar, but Blodgett Forest shows both more low values and more high values. The similarity between the two sites results partly from the fact that daytime ozone values are generally not more than a factor of two higher than the regional background, so mixing with the background drives concentrations toward a common value. From a regulatory standpoint, the Blodgett Forest site is much more likely to exceed the federal 8 hour ozone standard because of the significantly higher number of observations above 85 ppb. Comparison of ozone at the two sites suggests that the efficiency of ozone production has slowed considerably by the time the plume has reached Blodgett Forest, and it can no longer match the decreases in ozone due to dilution and deposition as the air moves toward Big Hill. This information can be used to ascertain the extent of influence of the urban plume on ozone in the region.

Figure 6-27 a-f. Frequency distributions of half-hour average NO_{yi} and O_3 concentrations during summer in the urban plume at Blodgett (red) and Big Hill (black).

a) nitrogen dioxide

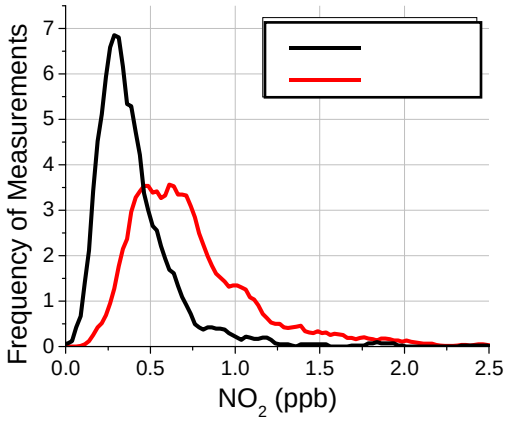

b) peroxy nitrates

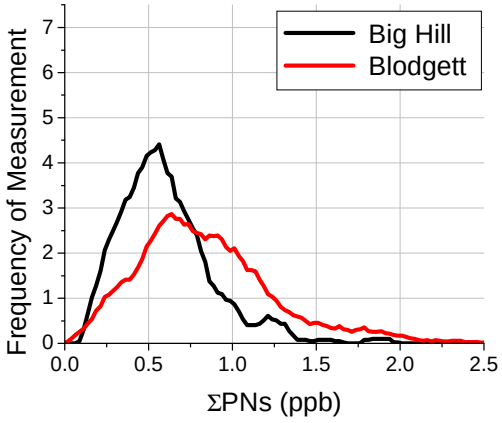

c) alkyl nitrates

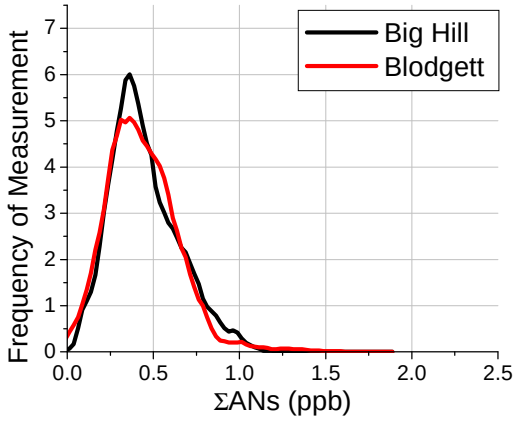

d) nitric acid

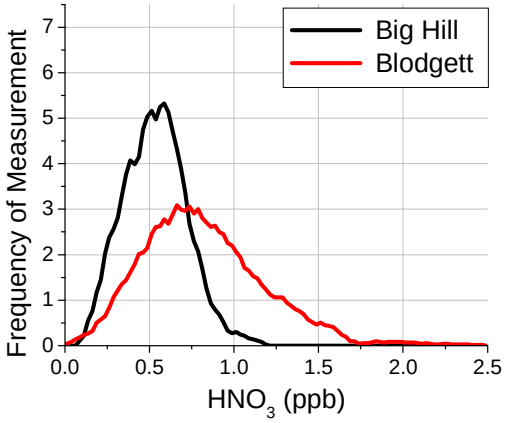

e) total reactive oxides of nitrogen

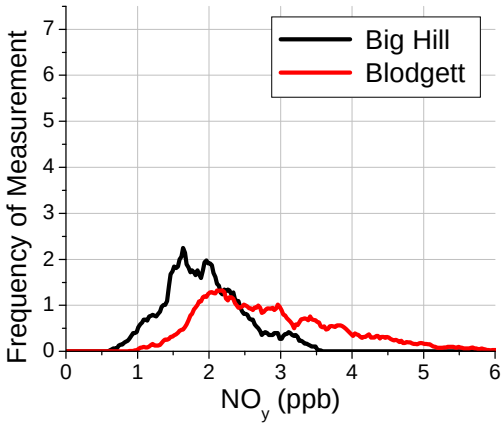

f) ozone

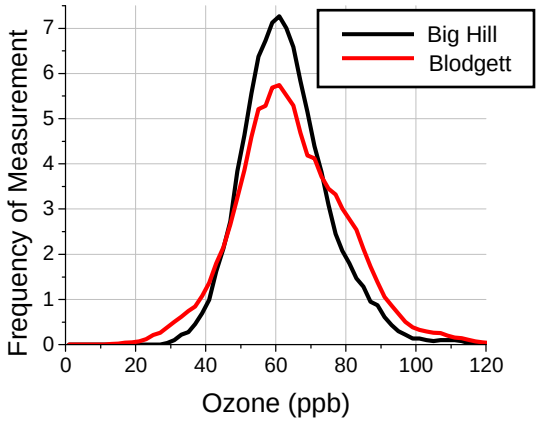

6.7.6 Observational Constraints on the Transport of Nitrogen Oxides

Table 6-1 compiles data from the frequency distributions shown in **Figure 6-27** for the Blodgett Forest and Big Hill sites. Because the data sets are comprehensive and the meteorological conditions have predictable recurring patterns, it is possible to treat the data statistically. We have combined these data sets, along with observations made in the summer of 2001 at Granite Bay, a suburb of Sacramento near Folsom, to constrain a Lagrangian model of the plume that includes photochemistry, deposition, dilution, and emissions as it is advected eastward from the urban area over the western slopes of the Sierra. **Figure 6-28** shows the concentrations of NO_2 and NO_X (NO_Y, which would be ≥ NOx, was monitored at the special study sites) as the air moves along the Sacramento – Tahoe transect. Concentrations were averaged for different time periods depending on the location, reflecting the Lagrangian nature of the analysis, and using observed wind speeds to establish the transit time of the plume.

Table 6-1. Concentration statistics for 1 pm – 8 pm, June-October, at Blodgett Forest and Big Hill. For each pollutant listed, the median, 5th and 95th percentile values have been calculated in ppb.

	Blodgett Forest			Big Hill		
Species	Median (ppb)	5th percentile	95th percentile	Median (ppb)	5th percentile	95th percentile
NO_2	0.63	0.30	1.70	0.33	0.16	0.78
ΣPN	0.79	0.27	1.75	0.55	0.21	1.07
ΣAN	0.41	0.15	0.77	0.39	0.16	0.78
HNO_3	0.79	0.33	1.48	0.53	0.25	0.85
NO_y	2.68	1.57	4.92	1.84	1.05	2.99
O_3	61.5	40.7	88.4	60	45	82

Using observations of anthropogenic VOC from Granite Bay and Blodgett Forest in 2001, we have confirmed the estimate for a dilution rate of approximately 0.25/hour found by Dillon (2002). Analysis of the NO_2, ΣPN, ΣAN, HNO_3 and O_3 measurements provides constraints on the rates of further NO_X emissions, photochemical oxidation, and deposition within the urban plume as it moves up the western slope of the Sierra Nevada. HNO_3 production is most efficient at the high NO_X concentrations of Sacramento, but as the plume moves eastward and biogenic emissions of VOC are added, the production of organic nitrates begins to compete for NO_X. Between Folsom and Blodgett Forest, there are relatively high production levels of all forms of NO_Z (≡ ΣPN + ΣAN + HNO_3) because of the optimal balance between NO_X and RO_X precursors. Comparison of Blodgett and Big Hill data suggest that the fate of ΣPN depends on the temperature, that ΣAN are well-conserved within the plume, and that deposition of HNO_3 is the most important sink of total reactive nitrogen. The lifetime to

deposition of HNO_3 in the plume is estimated at less than five hours and since most of the production occurs close to the city, a considerable amount of the HNO_3 present in the plume has been lost before it arrives at Big Hill. Our observations suggest that a substantial amount of mixing occurs across the boundary between the surface layer and the free troposphere, which implies that the plume is responsible for exporting substantial amounts of reactive nitrogen that can be transported above the continent at high altitudes. Clearly, local emissions from South Lake Tahoe dominate over the contribution of the processed and diluted reactive nitrogen present in any air masses that may reach the Tahoe Basin. To quantitatively assess the relative importance of upwind transport and local emissions in the Tahoe Basin as a whole would require analysis of measurements from other Tahoe sites further from roads and other intense NO_X sources.

Figure 6-28. Reactive nitrogen observations along the Sacramento-Tahoe transect. The distance from Sacramento was multiplied by an average wind speed of 3.5 m/s to estimate the time the air mass would arrive at each site after leaving Del Paso at 10 am. Observations at each site were averaged for an hour around the estimated time. For example, UC-BFRS lies 80 km downwind of Del Paso, and NO_2 and NO_Y observations between 3 pm and 5 pm were averaged to produce the points reported at 4 pm. The error bars represent the standard deviation of the average.

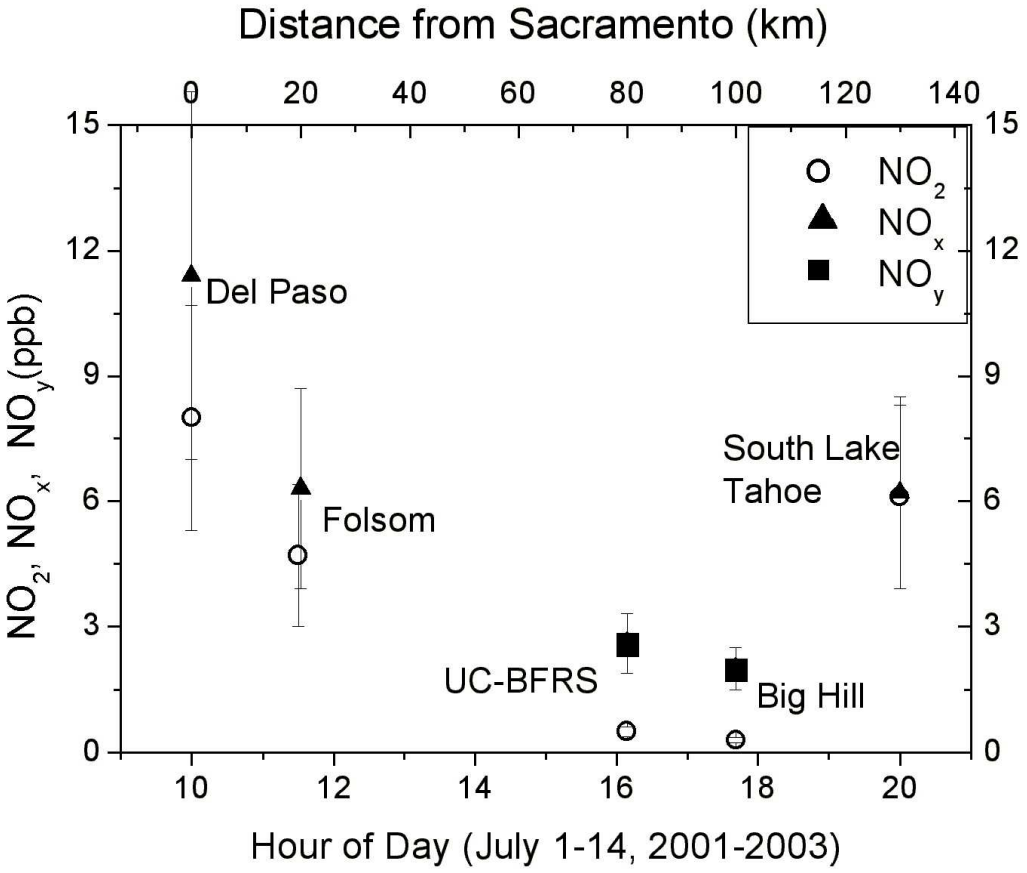

6.8 Ozone

State law (H&SC 39610) directs ARB to assess the role that pollution transport has on violations of the State ozone standard, namely, the contribution of ozone and ozone precursors in upwind regions to the ozone concentrations in downwind regions. Over the last decade, ARB has published a number of assessments describing the transport relationships among California regions. The last such assessment was published in 2001. Past ARB transport assessments have found the Broader Sacramento Area to have an overwhelming transport impact on several counties located within the Mountain County Air Basin, including two that border the Lake Tahoe Air Basin (Nevada County and the eastern portion of Placer County). No assessment has been made of ozone transport into the Tahoe Basin because the 1-hour California Ambient Air Quality Standard for ozone is not being violated. However, with the recent adoption of an 8-hour California Ambient Air Quality Standard (0.070 ppm), ambient data show that ozone concentrations in the Tahoe Basin exceeded this standard multiple times in the last three years. As a result, we expect the Lake Tahoe Air Basin will be designated as non-attainment for ozone when State area designations are reviewed in fall 2006. The designation of the Lake Tahoe Air Basin as non-attainment with respect to the State 8-hour ozone standard will then trigger a formal assessment of the relative contribution of upwind emissions to ozone concentrations in the Lake Tahoe Air Basin that violate State ozone standards.

Historical (Duckworth et al., 1979), routine (Echo Summit), and LTADS (Big Hill) data for ozone in the Sierra Nevada west of Tahoe indicate infrequent ozone concentrations approaching ambient air quality standards and even less evidence of the one-day transport of such concentrations into the Tahoe Basin. Furthermore, the duration of upslope winds when ozone concentrations are high is generally too short to affect the transport of pollutants from the Central Valley to the Tahoe Basin in one day (Duckworth, 1979; Carroll, 1998). This is because high ozone concentrations occur downwind of Sacramento under light wind conditions and the mesoscale meteorological pattern of upslope winds during the afternoon would reverse to downslope winds in the evening before the high concentrations could transport the full distance to Tahoe. The LTADS (2003) ozone data summaries (frequency, timing, and spatial distribution of moderate to high concentrations) presented in Chapter 3 indicate that the transport of ozone concentrations greater than 70 ppb to the Tahoe Basin is likely limited.

6.9 Conclusions and Implications

The motivation for collecting data at Big Hill and the focus for this analysis has been to quantify the distribution of reactive nitrogen oxides at a site upwind of Lake Tahoe and use those measurements to assess the role of transport along the western slope of the Sierra in contributing to nitrogen deposition in Lake Tahoe. By combining the data we obtained at Big Hill with corresponding measurements at Blodgett Forest, we have developed a highly constrained model of the processes that govern reactive nitrogen distribution during the summer months in the region. Data collected during winter months shows that the meteorology does not favor net transport of pollutants from west

to east in the surface layer. Plumes from several prescribed burns were measured, often containing higher concentrations of reactive nitrogen than the urban plume, but likely having significantly reduced geographical influence. Total reactive nitrogen in the region is likely at a maximum during the summer when better upslope transport occurs. Observations from more sites are necessary to quantify the importance of fire events as a source of reactive nitrogen to Lake Tahoe. Based on our analyses of the observations made, we can draw the following conclusions:

- During summer months, the Sacramento region is the dominant source of reactive nitrogen in the urban plume on the western slope of the Sierra Nevada
- HNO_3 deposition is sufficiently fast that very little remains in the urban plume by the time it reaches high elevation sites near the western rim of the Tahoe Basin
- At Big Hill, similar concentrations of HNO_3 are found in air masses coming from the west and the east, suggesting that urban areas to the west of Lake Tahoe cannot be identified as important sources
- Organic nitrates are significantly elevated in the urban plume compared to background conditions but their contribution to nitrogen deposition is poorly understood
- During winter months, total reactive nitrogen is lower, net flow at the surface is downhill, and the Sacramento urban plume rarely reaches the western rim of the Tahoe Basin
- Individual winter episodes of high NO_2 and inorganic nitrates associated with small-scale burning events along the western slope of the Sierra Nevada may generate HNO_3 that can reach Tahoe.

6.10 References

Cape, J.N. (2003). “Effects of airborne volatile organic compounds on plants [Review].” Environmental Pollution, **122**(1), 145-157.

CARB (1997). "Monitoring in Ozone Transport Corridors." ARB Contract No. 94-316. Final report prepared for California Air Resources Board by Technical & Business Systems, Inc. July.

Carroll, J.J., Dixon, A.J. (1998), “Tracking the Sacramento Pollutant Plume over he Western Sierra Nevada.” Final Report prepared for the California Air Resources Board, Interagency Agreement No. 94-334, March.

Carroll, J.J., and Dixon, A.J. (2000). “Meteorological and Air Pollution Profiles in the Lake Tahoe Basin.” UC Davis.

Carroll, J.J., and Dixon, A.J. (2002). “Regional scale transport over complex terrain, a case study: tracing the Sacramento plume in the Sierra Nevada of California.” *Atmospheric Environment*, 36(23), 3745-3758.

Cohen, R. and Murphy, J. (2005), “Keeping Tahoe Blue: Quantifying Atmospheric Nitrogen Oxides in the Lake Tahoe Basin,” Final Report prepared for the California Air Resources Board, Interagency Agreement No. 01-327, January.

Day, D.A., P.J. Wooldridge, et al. (2002). "A Thermal Dissociation-Laser Induced Fluorescence instrument for in situ detection of NO_2, Peroxy(acyl)nitrates, Alkylnitrates and HNO_3." *J. Geophys. Res.* **107**(D6): 10.1029/2001JD000779.

Day, D.A., M.B. Dillon, et al. (2003). "On alkyl nitrates, O3 and the "missing Air mass"." *J. Geophys. Res.* **108** (D16).

Dillon, M.B. (2002). The chemical evolution of the Sacramento urban plume. *Chemistry*. Berkeley, University of California, Berkeley**:** 206.

Duckworth, S. and Crowe D. (1979). "Ozone Patterns on the Western Sierra Slope -- Downwind of Sacramento during the Summer of 1978." *ARB Technical Report*. Technical Services Division. Sacramento. March.

Flocke, F., A. Volzthomas, et al. (1991). "Measurements of Alkyl Nitrates in Rural and Polluted Air Masses." *Atmospheric Environment Part a-General Topics* **25**(9): 1951-1960.

Garcia, C., Gouze, S., Wright, J., and Hackney, R. (2001), "Assessment of the Impacts of Transported Pollutants on Ozone Concentrations in California," *ARB Staff Report: Initial Statement of Reasons*, March.

Hanson, P.J., and Lindberg, S.E. (1991). “Dry deposition of reactive nitrogen compounds: a review of leaf, canopy, and non-foliar measurements.” *Atmospheric Environment*, 25A(8), 1615-1634.

Keeley, J.E. and C.J. Fotheringham (1997). "Trace gas emissions and smoke-induced seed germination." *Science* **276**(5316): 1248-1250.

Korontzi, S., S.A. Macko, et al. (2000). "A stable isotopic study to determine carbon and nitrogen cycling in a disturbed southern Californian forest ecosystem." *Global Biogeochemical Cycles* **14**(1): 177-188.

Lerdau, M.T., L.J. Munger, et al. (2000). "Atmospheric chemistry - The NO_2 flux conundrum." *Science* **289**(5488): 2291-2293.

Moody, J.L., J.W. Munger, et al. (1998). "Harvard forest regional-scale air mass composition by Patterns in Atmospheric Transport History (PATH)." *Journal of Geophysical Research-Atmospheres* **103**(D11): 13181-13194.

Munger, J.W., S.C. Wofsy, et al. (1996). "Atmospheric deposition of reactive nitrogen oxides and ozone in a temperate deciduous forest and a subarctic woodland. 1. Measurements and mechanisms." *Journal of Geophysical Research* **101**(D7): 12639-12657.

Nasholm, T., A. Ekblad, et al. (1998). "Boreal forest plants take up organic nitrogen." *Nature* **392**(6679): 914-916.

Novelli, P.C., Masarie, K.A., Lang, P.M., Hall, B.D., Myers, R.C., and Elkins, J.W. (2003). “Reanalysis of tropospheric CO trends: Effects of the 1997-1998 wildfires - art. no. 4464.” *Journal of Geophysical Research-Atmospheres*, 108(D15), 4464.

Seaman, N.L., Stauffer, D.R., and Lariogibbs, A.M. (1995). “A Multiscale Four-Dimensional Data Assimilation System Applied in the San Joaquin Valley During Sarmap .1. Modeling Design and Basic Performance Characteristics.” *Journal of Applied Meteorology*, 34(8), 1739-1761.

Seinfeld, J.H., and Pandis, S.N. (1998). *Atmospheric Chemistry and Physics*, John Wiley & Sons, New York.

Shepson, P.B., K.G. Anlauf, et al. (1993). "Alkyl Nitrates and Their Contribution to Reactive Nitrogen at a Rural Site in Ontario (Vol 27a, Pg 749, 1993)." *Atmospheric Environment Part a - General Topics* **27**(14): 2251-2251.

Sparks, J.P., R.K. Monson, et al. (2001). "Leaf uptake of nitrogen dioxide (NO_2) in a tropical wet forest: implications for tropospheric chemistry." *Oecologia* **127**(2): 214-221.

Van Ooy, D.J., and Carroll, J J. (1995). “The Spatial Variation of Ozone Climatology On the Western Slope of the Sierra Nevada.” *Atmospheric Environment*, 29(11), 1319-1330.

Wesely, M.L., and Hicks, B.B. (2000). “A review of the current status of knowledge on dry deposition [Review].” *Atmospheric Environment*, 34(12-14), 2261-2282.

Zaremba, L.L., and Carroll, J.J. (1999). “Summer wind flow regimes over the Sacramento Valley.” *Journal of Applied Meteorology*, 38(10), 1463-1473.

Zhang, Q., Carroll, J.J., Dixon, A.J., and Anastasio, C. (2002). “Aircraft measurements of nitrogen and phosphorus in and around the Lake Tahoe Basin: Implications for possible sources of atmospheric pollutants to Lake Tahoe.” *Environmental Science & Technology*, 36(23), 4981-4989.

THIS PAGE BLANK INTENTIONALLY

7. Characterization of PM and Nutrient (N & P) Sources

In addition to estimating the mass of nutrients and PM being deposited from the atmosphere to the surface of Lake Tahoe, staff investigated sources of air pollutant emissions in the Lake Tahoe Air Basin. Three approaches to source characterization are utilized and described in this chapter. The first is review of the existing emissions inventory for the California portion of the Lake Tahoe Air Basin to provide a broad overview of the sources in the Basin. The second is a summary of observations from limited, focused special studies undertaken in the context of LTADS to better characterize road dust emissions and wood smoke from fireplaces and stoves used for residential heating. The third is a review and analyses of the historical record of pollutant concentrations and meteorological conditions. Although inferential, we consider this to be the primary source of information about the relative impacts of sources on ambient concentrations and deposition.

Diverse types of data and analyses have the potential to improve understanding of the emissions sources that contribute to ambient atmospheric concentrations in the Tahoe Basin and deposition to the Lake surface. Those utilized include the current emissions inventory, the LTADS network observations, limited source-oriented monitoring, and focused studies designed specifically to improve the Tahoe inventory of motor vehicle and wood combustion emissions, and an extensive historical record of concentrations and meteorological observations. Although considered initially as a means to identify the relative contribution of various source types to ambient concentrations, application of a Chemical Mass Balance (CMB) was not pursued due to the limited resources available and the complexity of the analysis (e.g., variable source speciation profiles, measurement uncertainties associated with low ambient concentrations, and concentration measurement periods varying from one day to three weeks).

Although the LTADS monitoring network was designed mainly to support the primary study goal, that of quantification of atmospheric deposition of nitrogen, phosphorus, and particles to the Lake, it also provides information useful for understanding source-receptor relationships. The historical record of ambient concentrations was also supplemented with several short term local “dust experiments” (described in Chapter 4). Although these were designed to provide insights regarding temporal and spatial gradients in particle concentrations in between the monitoring sites, roads, shoreline, and offshore locations, they are also useful for inferring relative contributions from specific source types to deposition to Lake Tahoe. To improve specific aspects of the Tahoe emission inventory, focused limited field studies were conducted to better quantify emissions from wood combustion and motor vehicle operation. All of these observations, when examined in the light of temporal patterns of local emissions activity data and concurrent meteorological observations, provide inferential evidence about the relative impacts attributable to a specific emissions sources (e.g., nearest roadway) as compared to the cumulative impacts from other sources. The historical record of observed ambient concentrations provides some insights as to the relative importance

of emissions sources. Extensive analyses and conclusions drawn from these data form the final section of this chapter.

Staff consulted the current emission inventories for California and the Lake Tahoe Basin and used simple data analyses based on observed concentrations and meteorological conditions to identify the most pertinent pollutant source categories. The conclusions and results indicate the nature of the atmospheric deposition problem and suggest where control efforts could be directed to reduce the atmospheric loading to Lake Tahoe.

7.1 Existing Emission Inventory

Emission inventories quantify all known emission source types within the boundaries of a defined region. However, without air quality or dispersion modeling, they are not directly applicable for apportioning source contributions to ambient concentrations and neither are they applicable for apportioning deposition. The emissions are not directly related to observed concentrations because they do not include consideration of source-receptor relationships controlled by winds and mixing. Neither do they account for chemical transformations. Nevertheless, they do provide a great deal of perspective on the types of sources that may be important to both concentrations and deposition.

The emission inventory for the Lake Tahoe Air Basin has not been refined to support regulatory activity because the Basin currently meets the federal air quality standards. The inventory utilizes methodologies that are applicable statewide and thus it is not as closely linked to local information and conditions as it would be if it were required to support current regulatory actions. An additional limitation is that an emissions inventory for the Nevada portion of the Basin is not included in the CARB estimate, which is limited to the California portion of the Basin (~two-thirds of the total). To provide context, this review includes comparisons with inventories of emissions in surrounding areas.

For inventory purposes, emissions are quantified from emissions “activity” data, emission factors (profiles), and emission rates derived from results of representative source testing (e.g., grams of NO emitted per mile traveled by a particular vehicle type and model year operated in a specified manner to represent typical real world operation). Activity data for motor vehicle emissions could be hourly estimates of vehicle miles traveled by vehicle type, model and year, and road type. Similarly, activity data for a manufacturing or distribution facility might be the hours of operation and a throughput number (e.g., units manufactured per month, or gallons of fuel sold per month.) Other types of activity data (e.g., wood combustion per hour or month) might be estimated from a combination of population, percentage of dwelling units with fireplaces or wood stoves, and air temperature. The linkages between activity data, emission factors (profiles), and emission rates are based upon established procedures that are grounded in surveys and historical source test data from representative examples of the same source type.

Inventories for different pollutants vary in their level of accuracy with the information available for a particular region or source type. Evaporative emissions from individual vehicles are measured by enclosure of those vehicles in a chamber subjected to a prescribed range of temperatures. Tail pipe emissions (e.g., NO and NO_2) from individual vehicles are measured while the vehicles are operated under prescribed speeds and loads on a dynamometer. Information from testing of individual vehicles is extrapolated through the use of various models to quantify the emissions of an entire fleet of vehicles. Models incorporate information and assumptions about the representativeness of vehicle models and age, mechanical condition, and their operating conditions (e.g., driving speeds and distances, and environmental temperatures).

The mass of road dust lofted by passage of motor vehicles is much more difficult to estimate than motor vehicle tail pipe or evaporative emissions. First, not being confined within a well defined space, indirect emissions of road dust from motor vehicle activity are far more difficult to source test. Second, defining representative conditions for testing is complicated because the emission rates are highly dependent on highly variable environmental factors (e.g., amount and type of dust on the roadway) and vehicle characteristics (e.g., vehicle speed, aerodynamics, tire size).

Thus, assembling a complete inventory that quantifies all known sources of emissions requires extrapolation from available information. The accuracy of the inventory is related to the linkages assumed, the degree of representativeness of source test conditions and activity data, and the amount of extrapolation required. For example, motor vehicle emission estimates may be based upon source testing conducted near sea level extrapolated to another altitude. Estimates of road dust emissions made based on tests in one area with a particular soil type will likely differ from those actually occurring in another region. Wood use for home heating in one area may be estimated based upon surveys of wood use in another area.

7.1.1 Lake Tahoe Emission Inventory

A summary overview of the Lake Tahoe Basin emission inventory is provided in **Figure 7-1**. For each of eight pollutant species, **Figure 7-1** lists the total emissions (tons/day) from sources within the Basin and breaks out the percentage of those emissions from each of 10 source categories. As in many other air basins, mobile sources are a major source category for reactive organic gases (ROG), carbon monoxide (CO), and oxides of nitrogen (NO_X), NH_3, and PM. Wood smoke from residential fuels combustion comprises the bulk of the PM_fine emissions.

As discussed in Chapters 3 and 4, NH_3 was found to be the primary component of N deposition to Lake Tahoe. Source categories that emit a significant percentage of the NH_3 include farming operations (that would include golf courses), on-road motor vehicles, waste burning (e.g., prescribed burns), and to a lesser extent residential wood burning. Nitric acid, which is a product of photochemical reactions that start with NO_x is another important chemical species with respect to nitrogen deposition. The main sources of NO_x are on-road motor vehicles and other mobile sources.

Direct emissions from on-road motor vehicles are indicated in yellow while direct emissions from other mobile sources are indicated in gold. Paved and unpaved road dust emissions, shown in orange and red respectively, are the major source categories for PM_coarse and PM_large.

Figure 7-1. Estimated emissions in the Lake Tahoe Air Basin for 2004 by source category. (CARB, 2005)

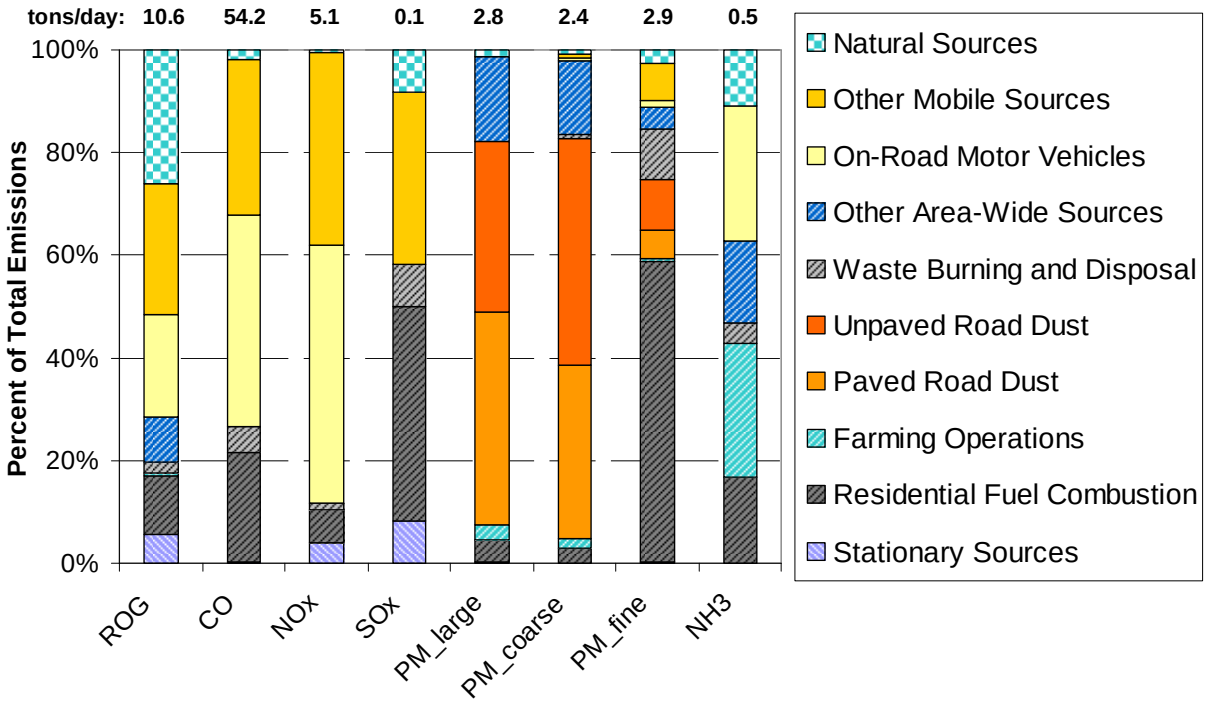

7.1.2 Comparison of Inventories in Neighboring Air Basins

A comparison between emissions from Lake Tahoe Air Basin and other air basins could be made with either the basin-wide mass emissions rates (mass/time) or the emissions densities (mass/time/area) for each of the air basins. In **Figure 7-2**, the graphical comparison of the mass emissions rates (mass/time) provided in the upper panel visually exaggerates the impacts from those air basins with larger areas. The emissions densities (mass/time/area) shown in the lower panel are more closely related to impacts on ambient concentrations and thus they provide a more meaningful basis for comparison of emissions between regions. When examined on the basis of their density, the Tahoe Basin's emissions for ROG, CO, and NO_X exceed those of Mountain Counties Air Basin but are much lower than those of the other neighboring air basins or regions.

Figure 7-3 shows the relative contributions of various source categories to the emissions of specific pollutants within central California that potentially affect the air

quality in the Tahoe basin (i.e., the region upwind and including the Lake Tahoe Air Basin). Contrasting with **Figure 7-1**, which shows the source contributions only within the Tahoe Air Basin, residential fuel combustion is a major source of fine particulate matter within the Tahoe basin.

Ammonia emissions (mass per time) by source category are contrasted for several air basins in **Figure 7-4**, but note that, for the reasons discussed below, the relative emissions do not indicate relative impacts. Clearly the ammonia emissions in the San Joaquin Valley (SJV) are substantial, but most of the area of the SJV is far south of Lake Tahoe. Similarly most of the Sacramento Valley is well north of Lake Tahoe. In addition, marine air that enters the central valleys through the Bay Area and delta and other gaps and lower passes in the coast range generally splits to follow the regional terrain. Typical flow is from north to south in the SJV and from south to north up the Sacramento Valley. Impacts affecting Lake Tahoe from emissions in upwind areas would also be limited to periods with sufficient vertical mixing as was discussed in Chapter 2. Thus, although **Figure 7-4** compares the mass of ammonia emissions estimated for 2004 in the Lake Tahoe Air Basin and nearby air basins, for the reasons discussed above, the amounts do not necessarily imply relative impacts on Lake Tahoe. Finally, the use here of emissions mass (tons/day) data instead of emissions density (tons/day/area) data for comparison purposes overstates the relative emissions due to the larger area of the SJV Air Basin.

The air basins differ substantially in their relative contributions of ammonia emissions from the various source types, as shown in **Figure 7-5**. Note that in the Lake Tahoe Air Basin the three largest source categories for ammonia emissions are motor vehicles, “farming” operations, and residential fuel combustion. These three source categories are estimated to account for 70 percent of the local ammonia emissions. These estimates of the contributions to total local ammonia emissions are consistent with the observed spatial variations in concentrations. Note that the greatest ammonia concentrations were observed in the more densely populated areas and at sites closest to roadways. Conversely, more spatially uniform ammonia concentrations than were observed during LTADS might be expected if there were substantial transport from other regions,

7.1.3 Historical Trends in Emission Rates at Tahoe

The estimated historical and forecasted future air pollution emissions for the California portion of the Lake Tahoe Air Basin are shown in **Figure 7-6**. From a long term perspective, emissions of both CO and ROG have declined substantially. Estimated emissions of NO_X have also declined but more slowly. Emissions of PM10 are estimated to be increasing. LTADS occurred during a projected stable period with respect to variations in emission amounts, with only CO and NO_X emissions declining.

Simple analyses relating concentrations and meteorology have the potential to provide strong corroborative information regarding the relative importance of different source types, both to the basin as a whole and to specific receptor locations. In an area as geographically unique as the Lake Tahoe Basin and having significant gradients in

emissions densities and spatially variable meteorology due to complex terrain, such corroborative analyses are an important means of confirming the relative impacts of source types. Such studies generally include spatially and temporally resolved emissions activity data, and observations of both ambient concentrations and meteorology.

7.2 Summary of Prior Analysis of Historical Aerosol Data

The data presented In Appendix B (Analysis of Historical Aerosol Data) show that the Lake Tahoe Basin is somewhat cleaner than the upwind lowland areas of California, but that it has considerably higher aerosol loading than non-urban sites in the Sierra-Cascade mountain chain.

Analysis of the data collected in the Tahoe Basin shows that local sources dominate for smoke and road dust, but are less significant for typical secondary urban/industrial pollutants such as sulfate.

Transport into the Tahoe Basin comes primarily from the tropospheric “background”, which consists of continental aerosols derived from Asia. This source is ubiquitous in the higher elevations of Sierra-Cascade range, and provides a small (on average 4½ $\mu g/m^3$) baseline aerosol concentration wholly outside the influence of activities anywhere in California (VanCuren, 2003). Transported aerosols originating within California appear to contribute, on average, about 2½ $\mu g/m^3$ (VanCuren, 2003). Fires outside the Tahoe Basin occasionally deliver large amounts of smoke to the basin, but they appear to have minimal impact on average aerosol loading.

Further study is needed to determine the spatial distribution of pollutants within the basin; the data from the Bliss and South Lake Tahoe monitoring sites probably represent the extremes of pollutant concentrations in the basin.

Figure 7-2. Comparison of total emissions (upper panel) and emissions densities (lower panel) for the San Francisco Bay Area Air Basin, the Greater Sacramento Area, and the counties of the Mountain Counties Air Basin located to the west of Lake Tahoe, and for the Tahoe Basin, estimated for 2004. (CARB, 2005)

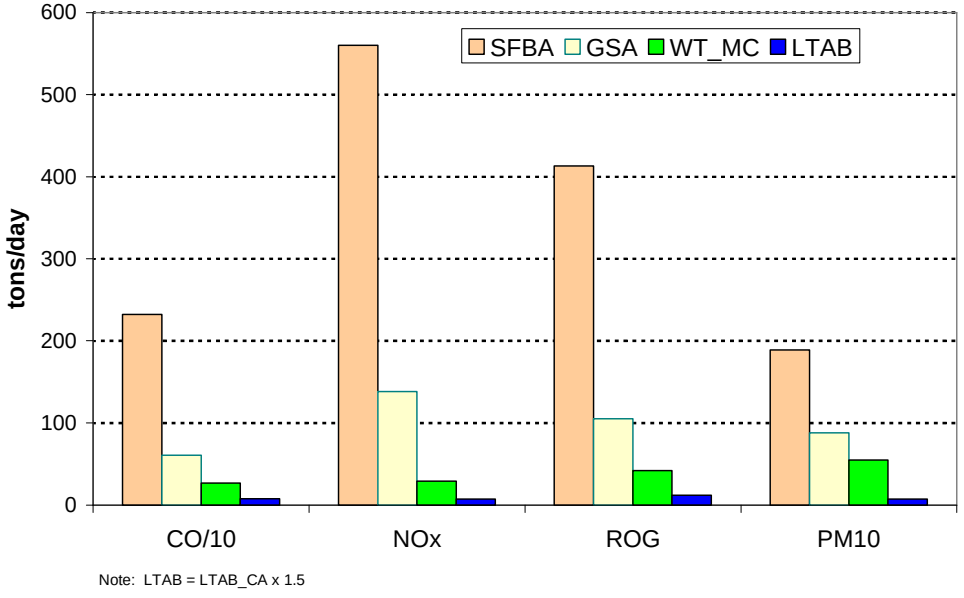

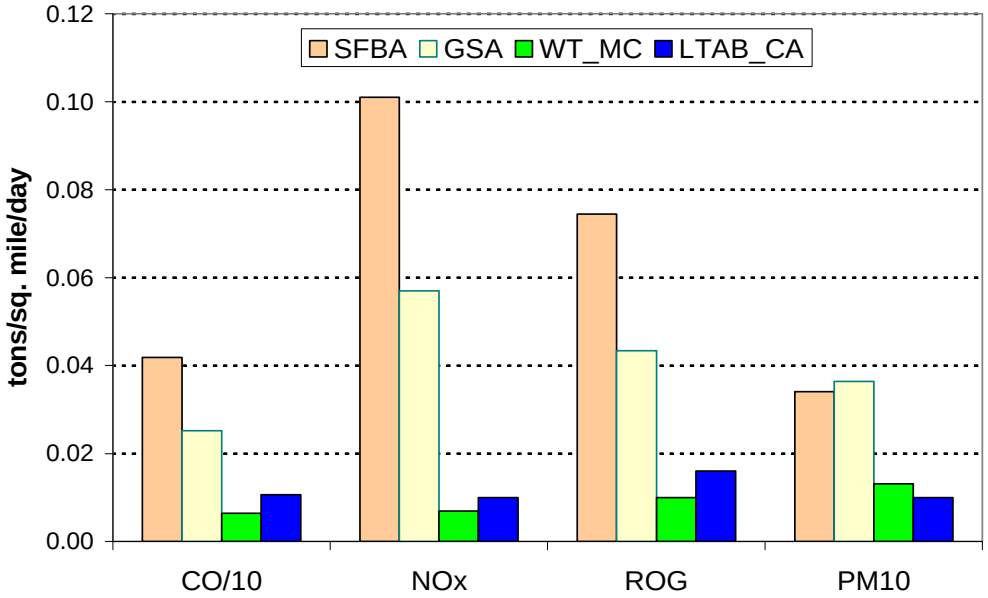

Notes: LTAB – Lake Tahoe Air Basin; analysis assumed that total emissions in LTAB = LTAB_CA times 1.5 to account for emissions in Nevada portion of the air basin.

SFBA – San Francisco Bay Area Air Basin.

GSA – Greater Sacramento Area (portions of Placer, Sacramento, and Yolo Counties in the Sacramento Valley Air Basin).

WT_MC – counties in Mountain Counties Air Basin that are located west of Lake Tahoe (Amador, El Dorado, Nevada, and Placer Counties).

CO/10 – the CO emission estimates have been divided by 10 to facilitate plotting on the same figure as the other emission types.

Figure 7-3. Estimated 2004 emissions by source category for combined area of SFBA, GSA, WT_MC, and LTAB. Contrast with Figure 7-1 for the LTAB only. (CARB, 2005)

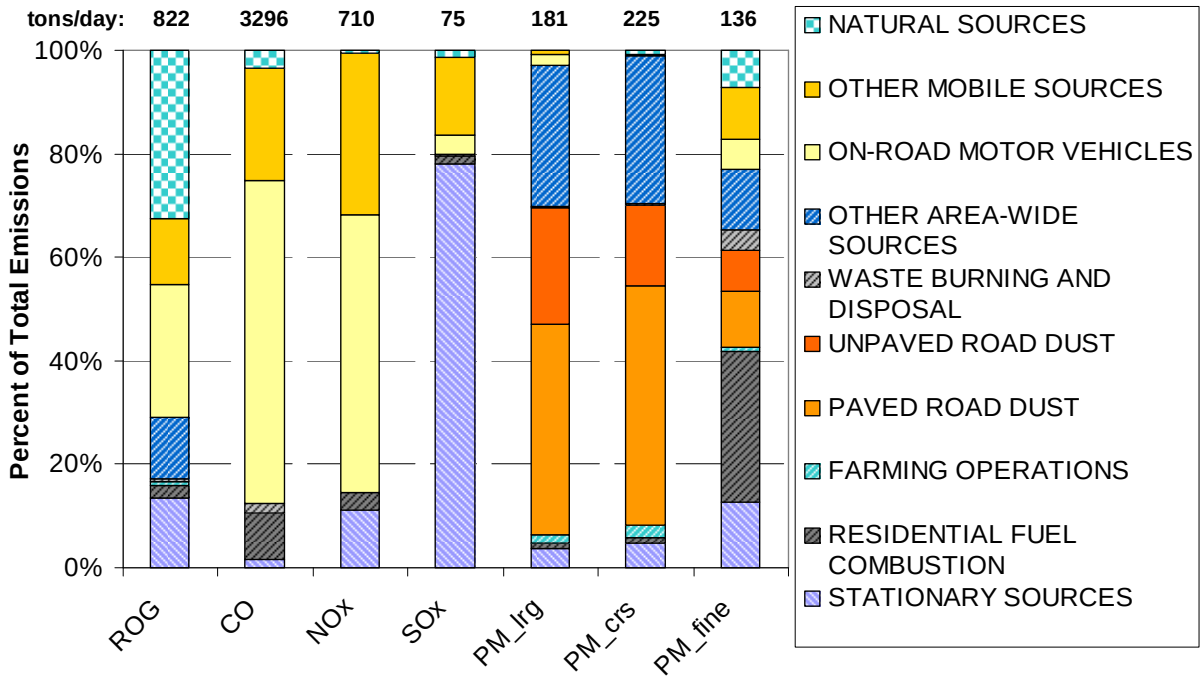

Figure 7-4. Comparison of ammonia emissions in Lake Tahoe, Mountain Counties, Sacramento Valley, and San Joaquin Valley Air Basins, for 2004. (Gaffney, 2004**)**

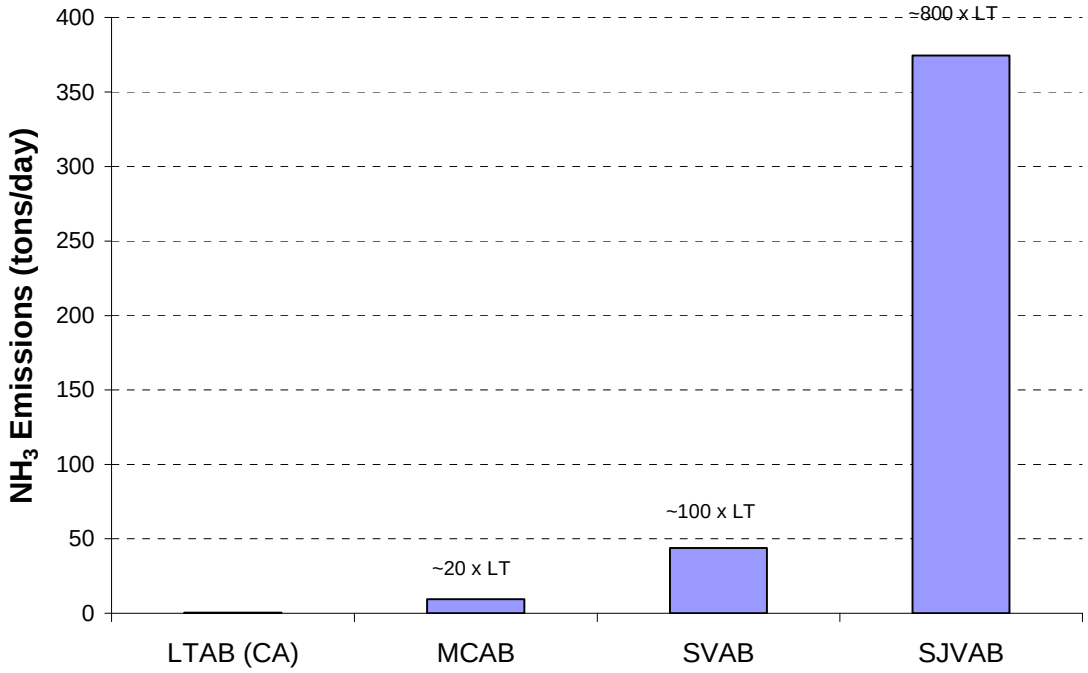

Figure 7-5. Percent of ammonia emissions by source category in the Lake Tahoe, Mountain Counties, Sacramento Valley, and San Joaquin Valley Air Basins as estimated for 2004. (Gaffney, 2004)

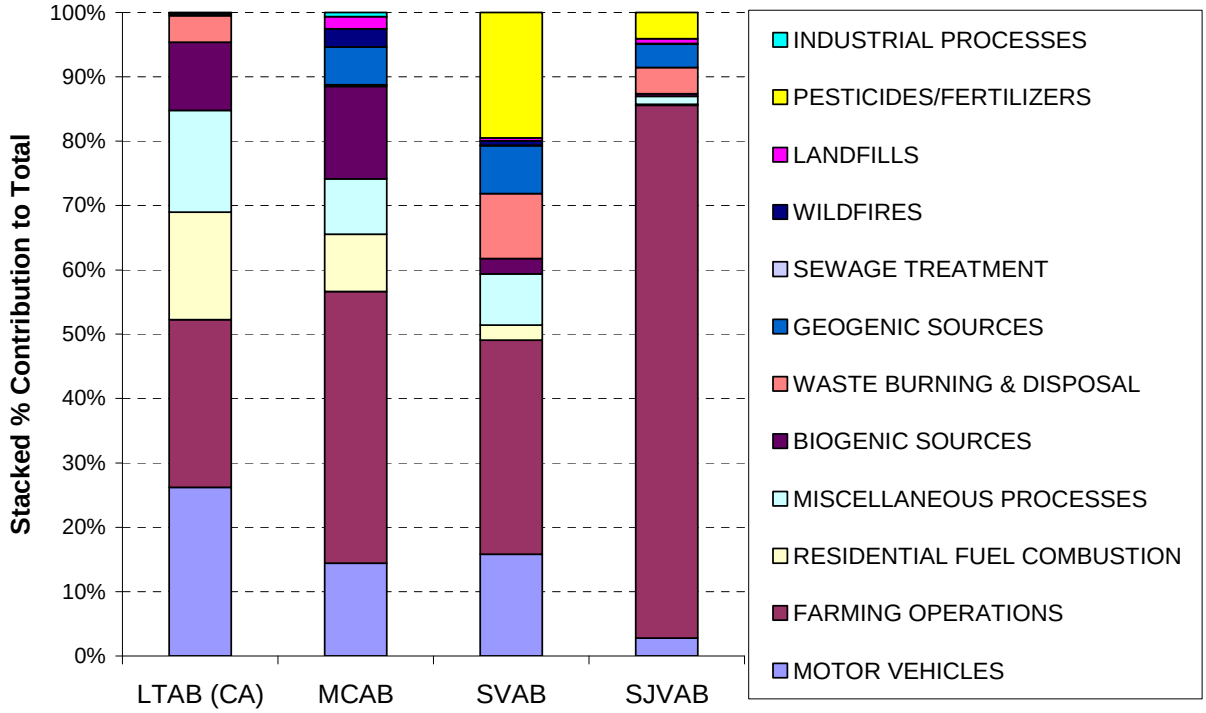

Figure 7-6. Historical and forecasted air pollution emission estimates for the California portion of the Lake Tahoe Air Basin. (CARB, 2005)

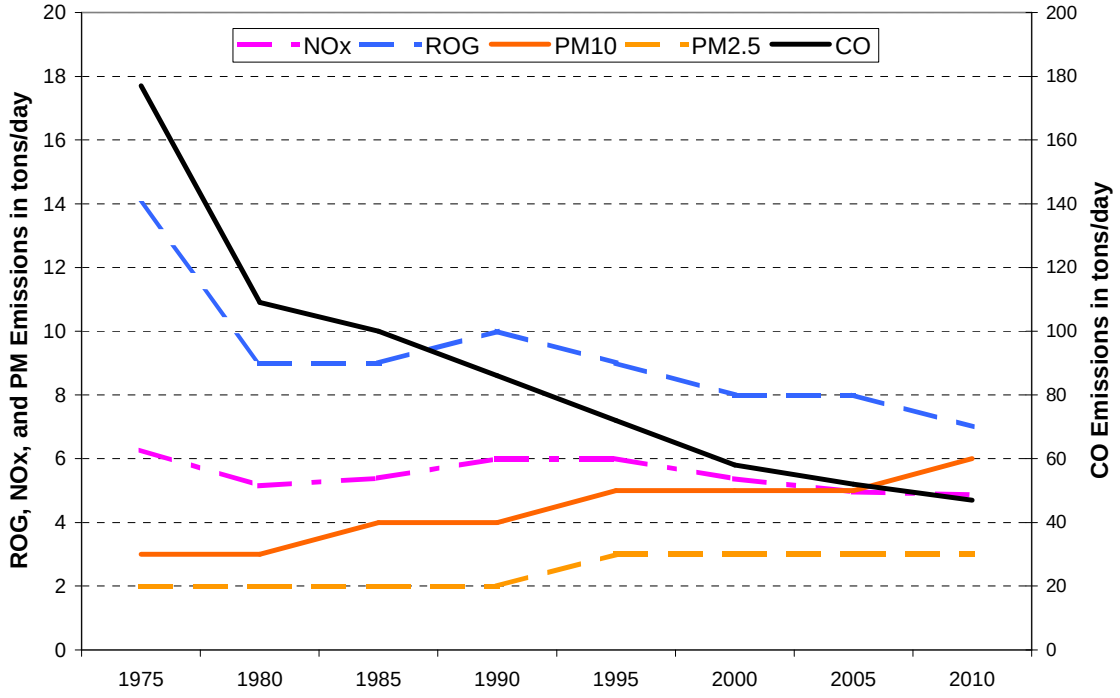

7.3 LTADS Studies to Improve the Tahoe Emissions Inventory

Unique challenges to constructing an emission inventory for the Lake Tahoe Air Basin include such things as differences between California and Nevada vehicle requirements, fuels, and air quality regulations, seasonally variable populations of residents and visitors, and alpine conditions not generally addressed in a statewide emissions estimation methodologies. The efforts undertaken were limited and narrowly focused to provide information that could be applied to improve the inventory with respect to estimates of emissions of road dust from motor vehicle operations and smoke from wood combustion.

The study approaches and results are summarized in this section. Insights from these special studies are also leveraged with results from the dust experiments (described in Chapter 3) that were designed to provide insights as to temporal and spatial variations in PM concentrations.

The unique situation at Lake Tahoe makes extrapolation of emissions activity data and emission factors developed in other areas problematic. Within an alpine environment there is a substantial population of permanent residents and a highly variable number of visitors. For estimation of motor vehicle emissions this presents several challenges. Nearly all CA vehicle source testing is conducted near sea level where oxygen vapor pressure is higher and ambient temperatures are constrained within a much smaller daily range than at Tahoe. Additionally, fleet characteristics are more difficult to specify with certainty due to differences between California and Nevada requirements for vehicles, registration, smog inspection requirements, and fuels. Additionally, fleet characteristics may change significantly with season or day of week due to the large visitor population and any weather related choices in vehicles or driving habits.

This section describes findings from the source characterization studies conducted for LTADS and also describes some limited analyses that aid in understanding the connections between emission activity patterns and ambient concentrations. The source types addressed here are road dust, motor vehicle emissions, and wood smoke.

7.3.1 Road Dust Observations

Road dust is a combination of traction control material, brake and tire wear, vegetative debris, deposited exhaust, and track out soil from unpaved roads (Kuhns, et al. 2004). Re-suspended road dust is associated with traction control material applied to the streets during winter. Wind blown dust occurs primarily in late summer during high-wind events when the soil moisture is at a minimum. Chemical analyses of road surface material indicate that most of the particulate matter is composed of crustal species (e.g., oxides of Al, Si, Ca, Fe, and Ti) (Watson et al, 1998; Chow et al., 2004). Connections between vehicle traffic activity and downwind PM ambient concentrations, nitrogen and phosphorus species concentrations within the activity-related plumes, and the content of fine (PM2.5) particles were the key areas of inquiry for the road dust part of the Desert Research Institute project (Kuhns, et al. 2004).

Connections between vehicle traffic activity and downwind PM ambient concentrations were investigated by DRI staff at a site near Sand Harbor. Sand Harbor is a park and beach area south of LTADS Thunderbird site. Sand Harbor is to the west of Highway 28 and the downwind site was to the east of the highway. The flux tower measurements were based on an up-wind/down-wind technique that has been often used by other investigators (Gillies et al., 1999). The DustTraks instrument and associated interpretive techniques are developing staples of motor vehicle source characterization studies (Kuhns et al., 2004).

Dust experiments provided evidence of the connection between vehicle activity and particle counts and also showed that particle counts and concentrations declined rapidly with distance from the roadway. Observed concentrations immediately downwind of the roadway also decreased rapidly with height above ground level (agl). As shown in the upper panel of **Figure 7-7**, concentrations decreased by over 50 % at 3 meters agl as compared to 1 meter agl. Although it was not feasible to make concentration measurements above the plume, the available measurements suggest that the plume height is likely no more than 4 to 6 meters. Because the depth of the plume is so limited, concentrations will decline rapidly with distance downwind due to dispersion and deposition.

In the lower panel of **Figure 7-7** the flux of PM10 is clearly seen to respond to wind direction, illustrating the strong effect of motor vehicle activity on the nearby PM10 concentrations as expected due to lofting of road dust. This is consistent with the observed downwind decay of particle counts obtained with OPCs, as reported in Chapter 4. Recall that as roadway emissions moved downwind toward the Lake under off-shore winds, particle counts obtained with the OPCs declined quickly. Similarly, particle counts were lower over the Lake than on shore. Thus, PM mass concentrations must also decline with increasing distance from the roads and distance from the shoreline.

The LTADS monitoring sites were necessarily located in the vicinity of roadways because the purpose of the LTADS (quantification of deposition to the Lake surface) required observation of concentrations near the Lake shore and that is also where population and human activity are greatest. Thus, the role of road dust in deposition to the surface of the Lake may be accentuated by the proximity to the shoreline of roads with high traffic volume. In fact, some of the roads with highest activity levels are on the immediate periphery of the lake. Thus, it appears that road dust is a major source of PM concentrations near the Lake shore and a major source of PM deposition to the Lake surface.

However, the distance of sources from the Lake is an important factor and measurements near sources will provide a conservatively large estimate of concentrations at the shoreline of the Lake and an even more conservative estimate of concentrations over the Lake. If refinement of the current estimates of PM deposition is a priority, then additional characterization of offshore gradients in concentration would be recommended as the first improvement upon the current estimates.

In order to better understand the composition of road dust, as differentiated from the combination of road dust and direct emissions from motor vehicles, additional measurements were made. DRI staff vacuumed road dust from sites around Incline Village, Village Lakeshore, and Mays/Southwood and proceeded to re-suspend the dust in a small chamber. DRI staff then sampled the "re-suspended road dust" for LTADS standard chemical analyses. Although the resulting filter samples contained substantial mass of vacuumed road dust, the laboratory results showed non-detects and low concentrations for nitrate, ammonium, and phosphorus. Concentrations of ammonium ion are at best 0.2% of the road dust mass.

The analyses of these samples of road dust provided a basis for relating observed concentrations of coarse and large PM adjacent to roadways to estimated concentrations of fine (PM2.5) particles and concentrations of nitrogen and phosphorus species in the same plumes. The fine fraction of road dust made up roughly 20% of the total mass and concentrations of nitrogen species and P were low. Although a substantial portion of the sampled road dust mass was not identified, the analyses nevertheless suggested that road dust did not contribute significantly to nitrogen concentrations in PM samples at LTADS ambient air quality stations.
Specifically, the laboratory analyses of the samples collected at Incline Village showed no nitrates above uncertainties, less than 0.2% ammonium ion barely above uncertainties, and no phosphorus above uncertainties. Incline Village can be considered a low density urban site. Sand Harbor can be considered typical of many road sections surrounding areas of the Lake with lower population density. The road dust samples from Sand Harbor had reported composition of less than 2.5% nitrates, less than 4% ammonium ion, and contained no detected phosphorus above uncertainties. The highest PM2.5 mass concentrations observed was in the dust samples from Incline Village. In this sample the PM2.5 mass comprised slightly more than half of the corresponding PM10 mass concentration. Chemical speciation of size resolved particles was based upon laboratory analysis of the TSP, PM10, and PM2.5 filter samples. Collection of filter samples limited to finer particles (e.g., submicron particles) within the PM2.5 fraction was not feasible logistically and funding for additional laboratory analyses was beyond the resources of the project.

Limited observations were also made of the effects on local ambient concentrations associated with application of traction control material to roads (Kuhns, et al., 2004). PM concentrations were measured before and after application sand or brine to a road in Sand Harbor area. Observed concentrations likely responded not only to changes in traffic volume and application of traction control materials but also to changes in wind speed and vertical mixing.

7.3.2 Motor Vehicle Emissions

To better understand the role of motor vehicle emissions and their impact on ambient concentrations, there were four areas of study. It was first necessary to characterize traffic volumes on various road types. Second the actual fleet composition was needed to compare with defaults in California's EMFAC. Because California registered vehicles

have a distinct emission profile as contrasted with the "50 state" vehicles, it was also necessary to identify the fraction of California registered vehicles in the Tahoe Basin. Finally, the connection between motor vehicle emissions and ambient concentrations required investigation. The UC Riverside College of Engineering Center for Environmental Research and Technology (CE-CERT) used survey techniques and observational data to address these areas of study (Fitz et al., 2004).

7.3.2.1 Motor Vehicle Activity Data

Motor vehicle activity data includes vehicle traffic volumes and fleet composition which are summarized in **Figures 7-8 through 7-11**. **Figure 7-8** illustrates the relative levels of activity on three types of roads in Tahoe Basin. This limited data suggests residential vehicle miles traveled (VMT) are limited to 15% of all VMT and that arterial and major arterial traffic exceeded residential traffic by a substantial margin. The fleet composition by vehicle type during winter and summer is contrasted in **Figure 7-9** with the assumptions from California's EMFAC motor vehicle emissions platform. From a quick review, it seems that EMFAC fleet population data fall between winter and summer profile at Tahoe and are thus fairly reasonable. However, it also appears that trucks observed at Tahoe are heavier. A comparison of fleet data collected at Tahoe City spring winter and summer with the default fleet composition in EMFAC indicates that EMFAC may over-estimate VMT for light duty vehicles and underestimated it for medium duty vehicles (**Figure 7-10**).

As expected, and confirmed in **Figure 7-11**, the fraction of California registered vehicles in Tahoe Basin decreases significantly on the Nevada side of the basin. The on-road mobile source emission inventory for the LTAB ideally should reflect Tahoe specific data such as was collected in these studies.

7.3.2.2 Observed Relationships Between Activity Levels and Near Source Concentrations

DustTraks (Kuhns, et al. 2004) and ELPI instruments (van Gulijk, et al. 2001 &2003) provided data to understand the connections between road activity patterns and ambient gas and particle concentrations. **Figure 7-12** provides evidence for the connection between road traffic and ambient concentrations. Ammonia, PM, CO_2, and CO concentration peaks were, in particular, related to traffic patterns.

The ambient samples obtained at road side obviously included motor vehicle emissions in addition to road dust. Accordingly, they contained a higher fraction of fine particles and organic materials than did the samples of resuspended road dust. On the other hand, phosphorus concentrations were so low as to be below the limits of detection.

Referring back to **Figure 7-5** and the DustTrak measurements in **Figure 7-12**, note that motor vehicle emissions are a substantial portion of the ammonia inventory in the Lake Tahoe Air Basin and that the observed ammonia concentrations are correlated with vehicle traffic. Reflecting on measurements taken at Incline Village, the DustTrak measurements match well with published data (Kuhns et al., 2004).

Figure 7-7. Vertical profile of PM concentration 1 m from paved road (upper panel) and time series of PM10 flux perpendicular to road from DustTraks and wind vane (lower panel). The shaded band represents the range of wind directions that are within 45 degrees of perpendicular to the road. (Kuhns et al, 2004)

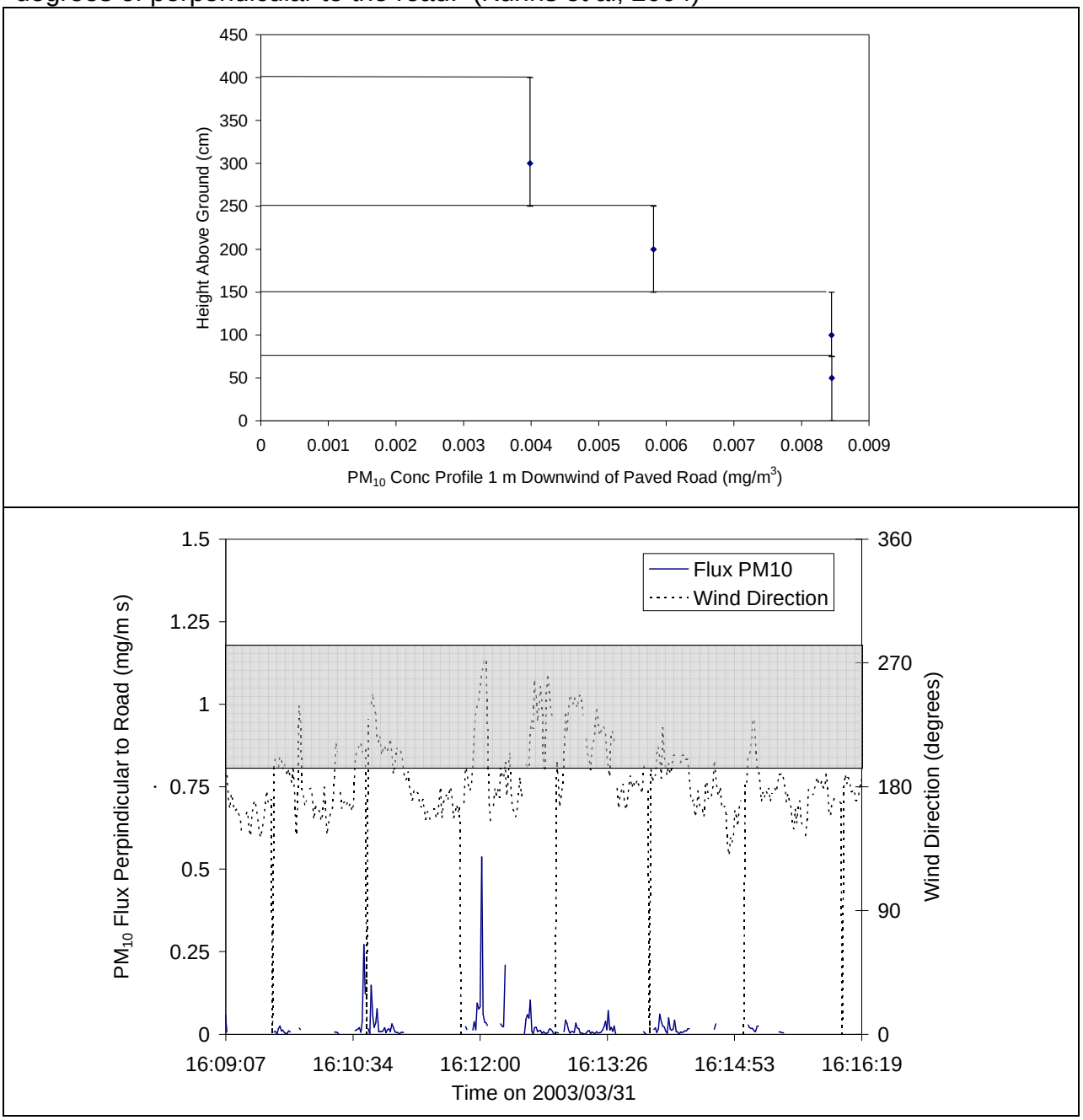

Compared to ozone precursors there has been comparatively little study of ammonia emissions from mobile sources until recently. Ozone precursors, NOx and ROG, both must be well characterized when considering strategies to meet the federal ozone standard. Ammonia has been of interest from a regulatory perspective less frequently

and in far more limited geographic areas (primarily where ammonium nitrate aerosol was a significant fraction of PM2.5 concentrations during winter exceedances of the federal PM2.5 standard).

It appears that ammonia emitted from motor vehicles is an important contributor to ammonia concentrations and nitrogen deposition at Lake Tahoe. This conclusion is based on the observed spatial patterns in ambient concentrations and the emission inventory. LTADS ambient monitoring sites at the north and south shores were generally located near major roads and as noted previously, concentrations of gas phase nitrogen species were significantly higher at these sites compared to sites farther from traffic. In addition, the inventory identified motor vehicles as one of the largest sources of ammonia emissions in the basin. The emission inventory information and the location of roads near the Lake indicate the importance of motor vehicle emissions.

Figure 7-8. Motor vehicle traffic volumes on three types of Tahoe Basin roads. (Fitz et al, 2004)

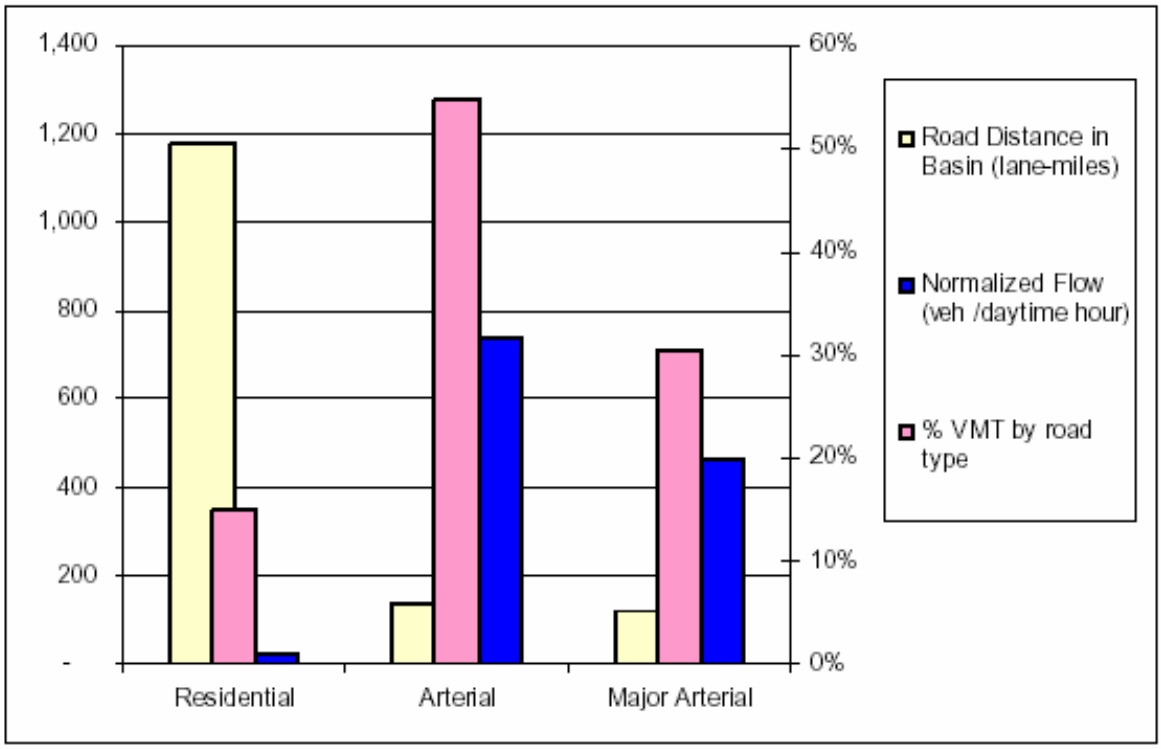

Figure 7-9. Fleet distribution at Tahoe City in comparison with current emissions model. (Fitz et al, 2004)

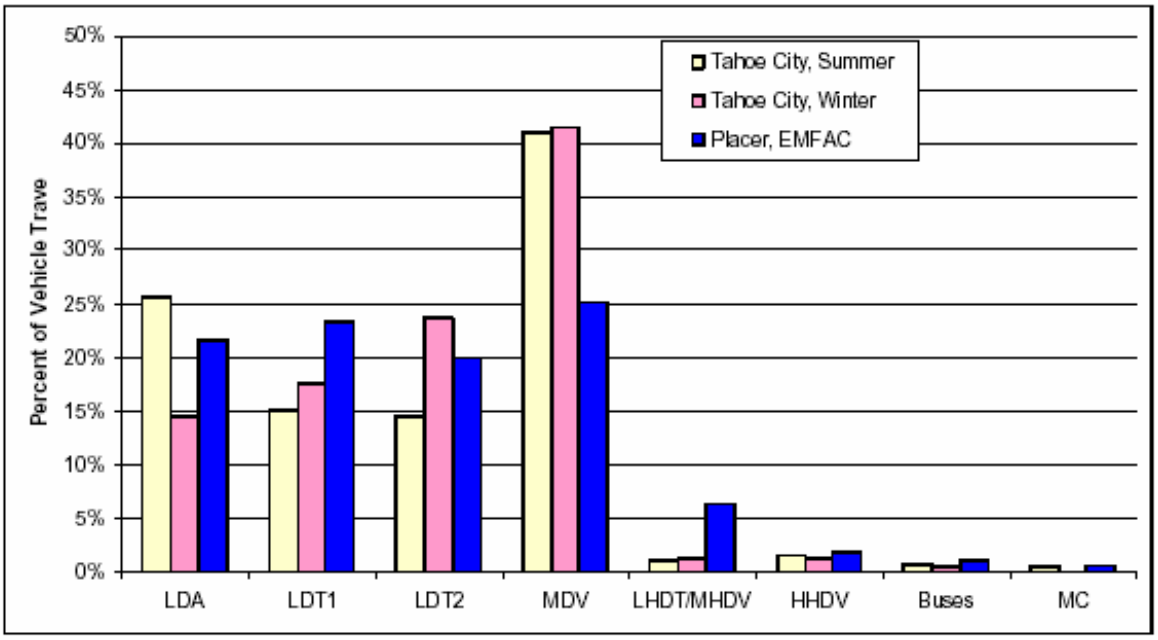

Figure 7-10. Fleet distribution in Tahoe Valley in comparison with current emissions model. (Fitz et al, 2004)

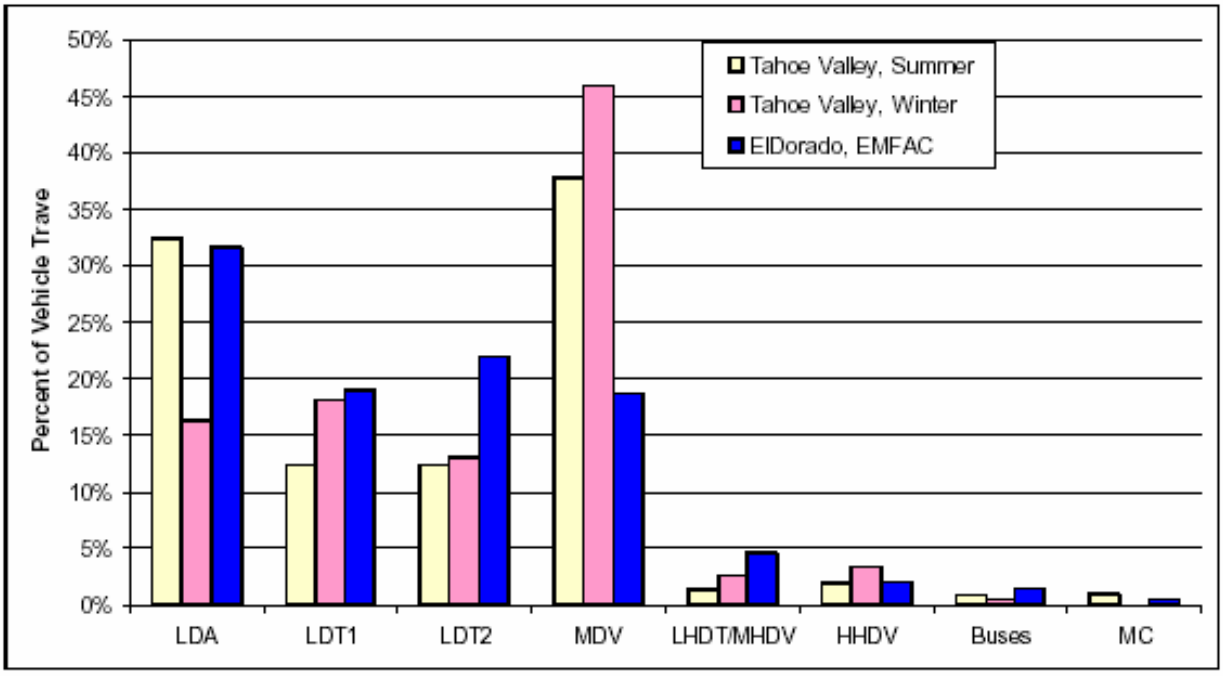

Figure 7-11. Fraction of California-registered vehicles in Tahoe Basin. (Fitz et al, 2004)

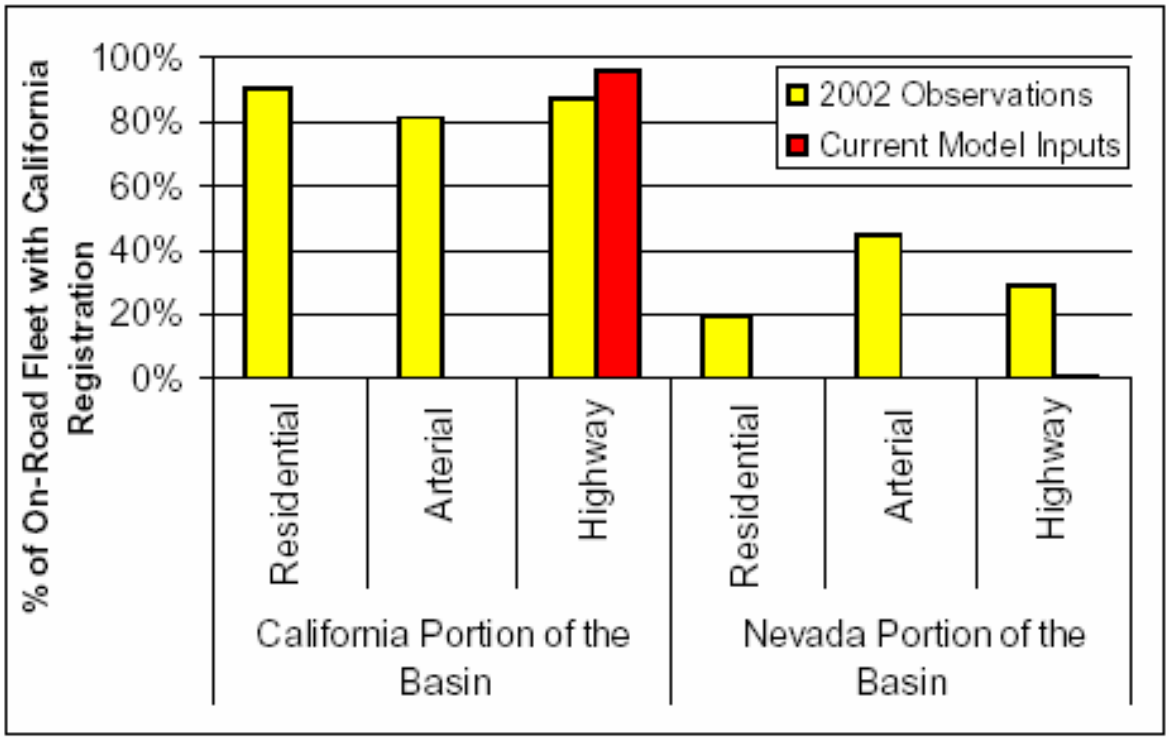

Figure 7-12. Time series of CO_2, CO, NO, NO_2, N_2O, NH_3, H_2O, and PM measured by ELPI and DustTracks. Shading indicates periods when measured concentrations are linked to passage of vehicles. Dashed black line represents the analytical uncertainty of gas phase measurements. (Kuhns et al, 2004)

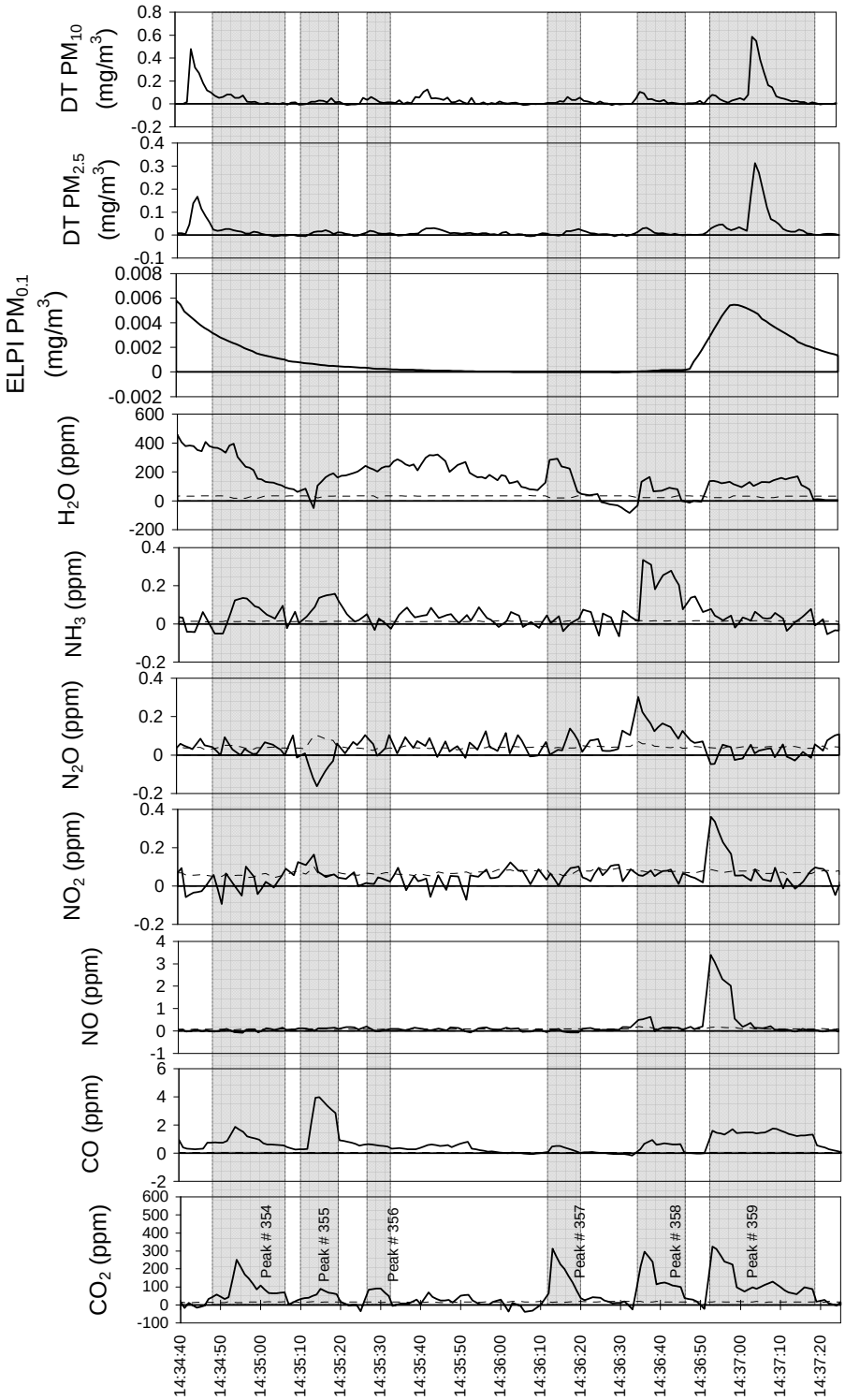

7.3.2.3 Connections between Motor Vehicle Activity & Ambient Concentrations

Beta Attenuation Monitors (BAM) were deployed during LTADS to provide hourly PM concentrations. Summaries of the hourly PM data and integration with meteorological data (e.g., wind directions) were used to provide a better understanding of the PM sources. The influence of motor vehicle emissions on PM concentrations at the Lake Forest Station is evident in **Figure 7-13**. PM concentrations observed at Lake Forest Station peak when traffic counts are high and the station is downwind of the roadway. A rapid decrease in concentrations occurred when the wind direction shifted to onshore in midmorning. Similarly a rapid increase in concentrations occurred in late afternoon when the wind direction began switching to downslope and offshore and the monitoring site was once again downwind of the roadway emissions. Winds blowing with a northerly component brought fresh motor vehicle and road dust emissions to the monitoring location while winds blowing from the south were onshore winds that blew roadway emissions away from the site. Traffic volumes increased rapidly after 5 a.m., remained high throughout the day, and tapered off during the evening. Even fine PM concentrations indicate some peaking during traditional traffic commute hours only to fall in mid-morning when the wind direction became onshore.

Similar observations of PM were made with BAMs at the Sandy Way and SOLA sites in South Lake Tahoe. At those sites located on either side of Highway 50, the PM concentrations were also observed to respond to emissions of road dust according to the diurnal shifts in wind direction (in the morning from downslope flow to upslope flow and in the late afternoon from onshore upslope flow to offshore downslope flow).

Figure 7-13. Lake Forest Mean PM by size, Wind Direction, & Traffic Counts in Winter.

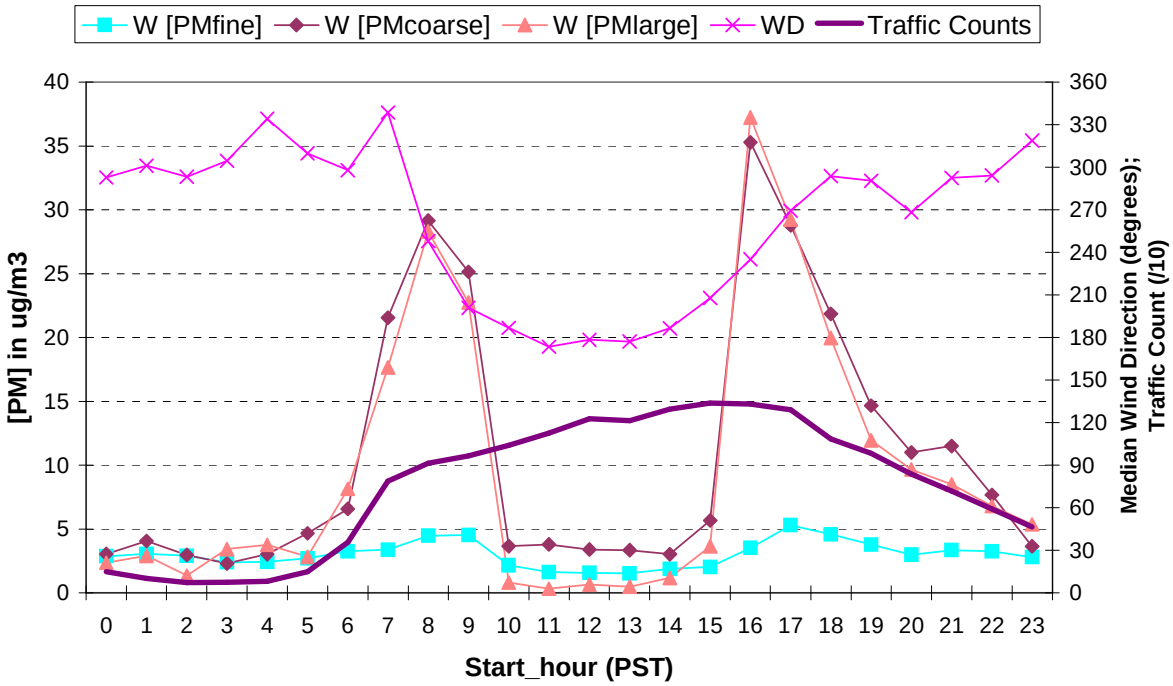

As illustrated in **Figure 7-14**, PM concentrations tended to peak around typical commute periods and thus are indicative of the large role road dust plays in determining ambient air quality. The effect is particularly enhanced during winter when road sanding material is applied and swept up. In reality, the sanding material effect is stronger than shown because the winter has periods of precipitation and storms that reduce the seasonal average of ambient concentrations. Thus, during post-storm periods when winds are light, PM concentrations can be very high. Conditions on a sample day (January 3, 2003) are presented in **Figure 7-15**. Winds were light (3-4 knots during the early morning hours, 1-2 knots during most of the day, and calm at 23:00) but exhibited typical diurnal variations in direction (i.e., upslope/onshore during the daylight hours and downslope/offshore during darkness); winds from the north, east, south, and west respectively correspond to 360^{O}, 90^{O}, 180^{O}, and 270^{O}. Note the large increase in TSP concentration at the SOLA site during the morning commute. The SOLA site is located north of Highway 50 and less than 50 yards from the roadway. The increase in TSP concentrations is not as large at the Sandy Way site because it is located a block south of Highway 50 and its measurements are from the top of a 1-story building. When the airflow reverses to onshore/upslope later in the morning, concentrations decline at the SOLA site but now increase at the Sandy Way site which is now downwind of Highway 50. Note that most of the TSP at Sandy Way at this time is from aerosols in the PM_coarse (2.5 µm < PM_diameter < 10 µm) and PM_large (10 µm < PM_diameter) sizes, which is consistent with road dust as the principle source of the material. Later in the afternoon when the airflow reverses direction again, TSP concentrations at SOLA increase while TSP at Sandy Way declines but does not become clean. Note in the evening that the PM2.5 concentrations increase dramatically and provide the bulk of the TSP concentration at that site. As indicated by the emissions figure (**Figure 7-1**) and the timing of the emissions, the PM2.5 is likely wood smoke from residential fuel combustion.

On numerous occasions during LTADS, TSP concentrations at the SOLA site would change by more than 99 $\mu g/m^3$. A summary of these instances, after screening for potentially spurious single hour events, is presented in **Figure 7-16** by season and hour of the day. Note that the majority of events occur during the winter and spring when road-sanding material is likely present. Also note that the times of the occurrences are consistent with a combination of increased motor vehicle activity (**Figure 7-17**) and stable atmospheric periods (e.g., low wind speeds during the transitions between downslope and upslope air flow, strong ground-level temperature inversions during the night). The occurrence of early morning PM spikes is rather unique to the SOLA monitoring site and not fully understood. However, a potential cause may be early morning traffic associated with the casinos in nearby Stateline. The traffic-counting site at Rufus Avenue is near the SOLA air quality site. When normalized to mid-week traffic volumes, the late night and early morning traffic volumes are 2-3 times higher on weekends and holidays (**Figure 7-18**). Thus, traffic associated with early morning gaming and entertainment activities on weekends may account for the bulk of the early morning spikes in PM concentrations.

The morning and evening commute periods also happen to occur near the times of transition between up-slope and down-slope airflows. Mean TSP concentrations associated with 1-hour reversals of wind direction (i.e., from offshore to onshore, typically in mid-morning, and from onshore to offshore, typically in evening) are plotted in **Figure 7-19** for the Cave Rock site, which is primarily impacted by motor vehicles. The site is located on the east side of Lake Tahoe (Nevada) and situated between Highway 50 and the Lake. Note that, except for winter mornings, the TSP concentrations are appreciably higher during offshore flow than during onshore flow. The change in TSP concentrations with change in wind direction is greatest during the morning in spring and summer and is greatest during the evening in fall and winter. This pattern is primarily due to days being shorter during fall and winter than during spring and summer and temporally matching the evening traffic period better.

The two TSP BAM monitoring sites in South Lake Tahoe, SOLA and Sandy Way, were located near each other with the SOLA site being north of Highway 50 and the Sandy Way site being 1 block south of Highway 50. Thus, the sites alternately detect the effects of traffic on Highway 50 during downslope and upslope airflow. The difference in TSP concentrations between the two sites (SOLA minus Sandy Way) is plotted by hour and season in **Figures 7-20 through 7-23**. When the difference is positive, TSP concentrations were higher at SOLA than at Sandy Way; when the difference is negative, TSP concentrations were lower at SOLA than at Sandy Way. Although there is some “noise” around the zero line due to “sloshing” of the air mass during shifts in wind direction, the plots obviously indicate influence of Highway 50 on TSP concentrations – TSP concentrations are higher at SOLA when the wind is offshore and higher at Sandy Way when winds are onshore.

Denuder measurements of ammonia and nitric acid at the nearby TWS sites in South Lake Tahoe (SOLA and Sandy Way) are plotted by TWS sampling period in **Figure 7-24**. **Figure 7-24** indicates better atmospheric mixing in the spring and early summer as concentrations are lower and more similar between the two sites. Because HNO_3 is a secondary (formed from chemical reactions in the atmosphere) pollutant, its concentrations tend to be more similar at the two nearby sites and exhibits less seasonal variation than the NH_3, which is a primary (directly emitted) pollutant, does. The differences in concentrations at the two sites (SW minus SOLA) are shown for each 2-week period in **Figure 7-25**. Negative values indicate that concentrations are higher at the SOLA site than the Sandy Way site. Although the nitric acid difference shows some variation, the ammonia concentrations are consistently higher at SOLA than at SW, although the difference is smaller during spring. The higher NH_3 at SOLA than at SW could be due to a couple of factors: its closer proximity to motor vehicle and biogenic emissions (SOLA site on open ground and near Highway 50 while SW site is on a roof in a paved area with little ground exposure). Because the [NH_3]s are highest in winter and the snow cover would absorb the NH_3 emissions from the ground and because [NH_3]s at SOLA are 2 times those at SW and 8 times those at Thunderbird, which has good biogenic exposure but not motor vehicle exposure, motor vehicles would seem to be a primary source of ammonia emissions at the SOLA site.

Figure 7-14. Seasonal mean diurnal TSP concentrations at SOLA in ug/m^3.

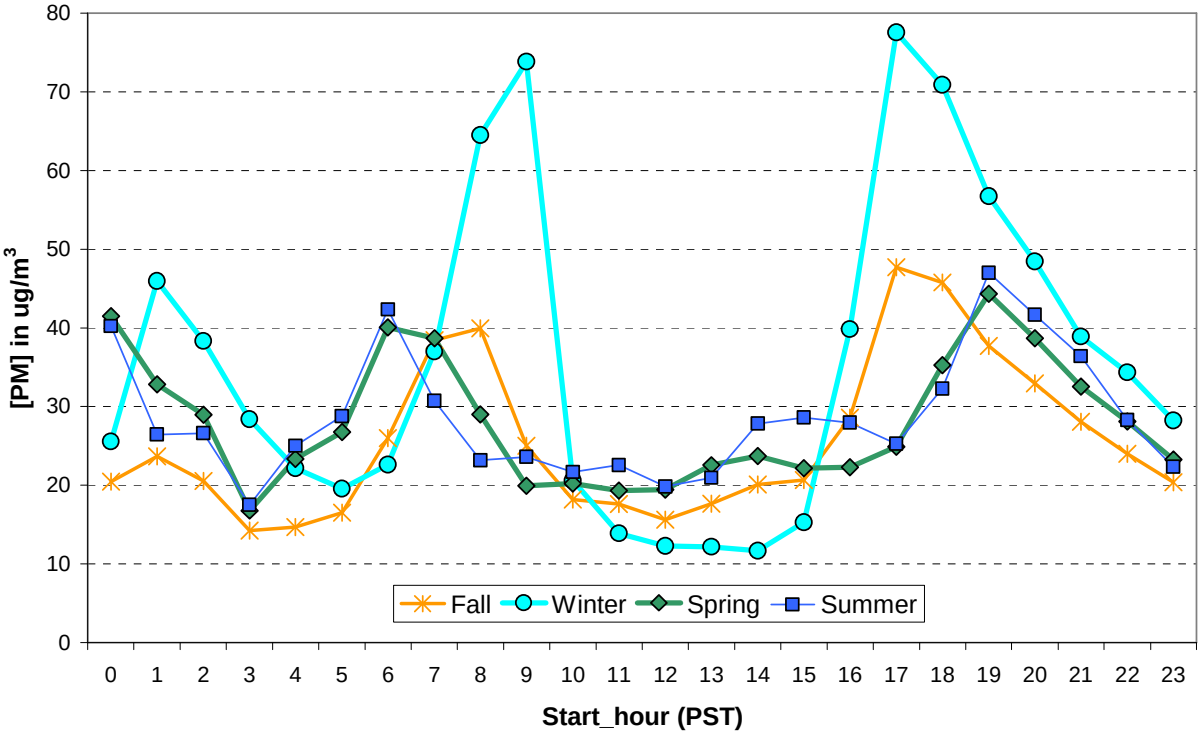

Figure 7-15. Observations reported for January 3, 2003.

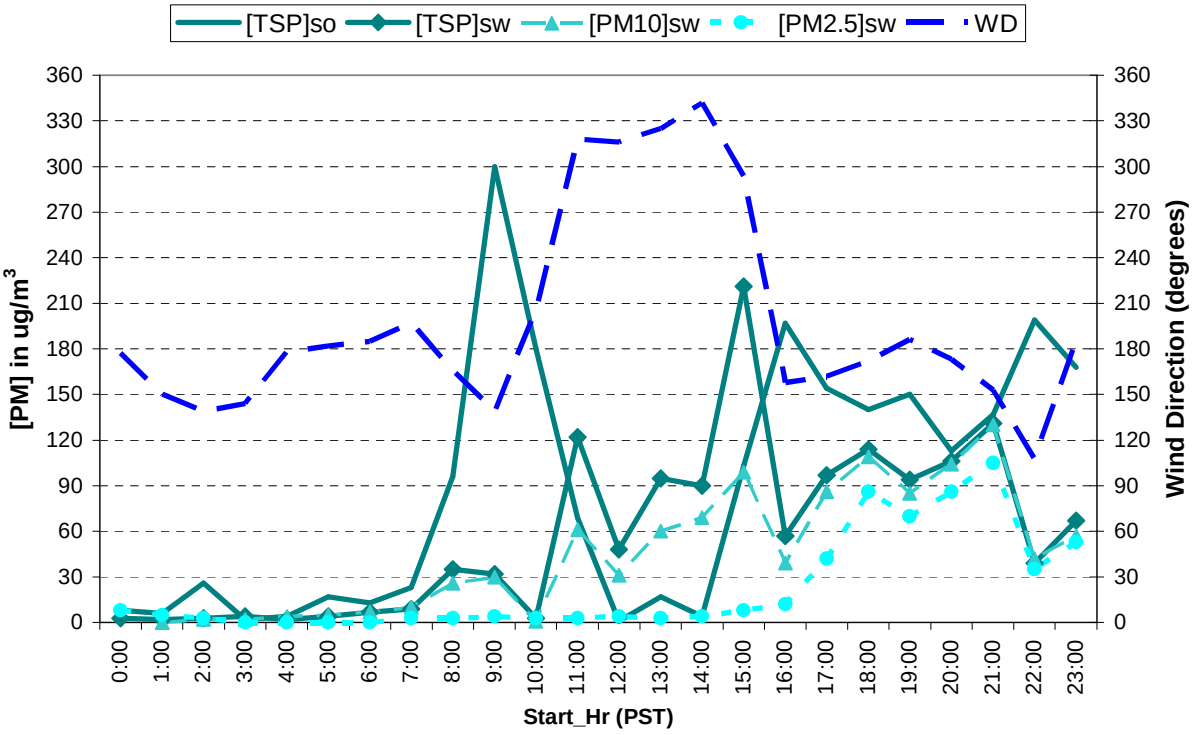

Figure 7-16. Count of instances when edited [TSP] at SOLA changed more than 99 ug/m^3 in one hour.

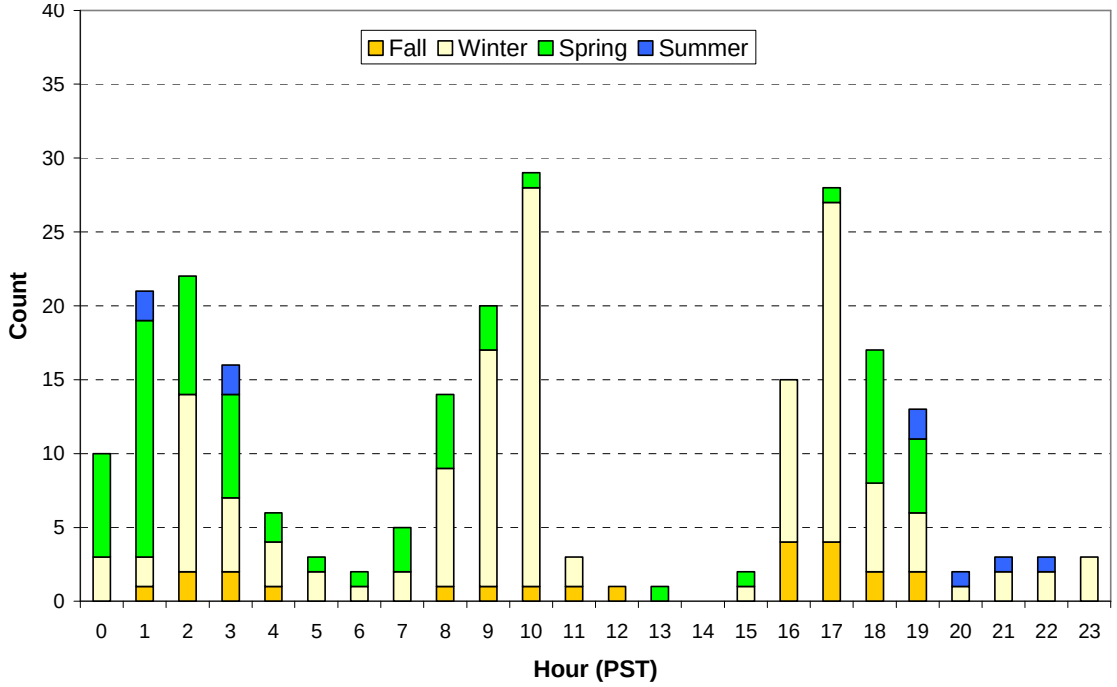

Figure 7-17. Traffic volumes based on measurements on Highway 50 near Rufus Avenue.

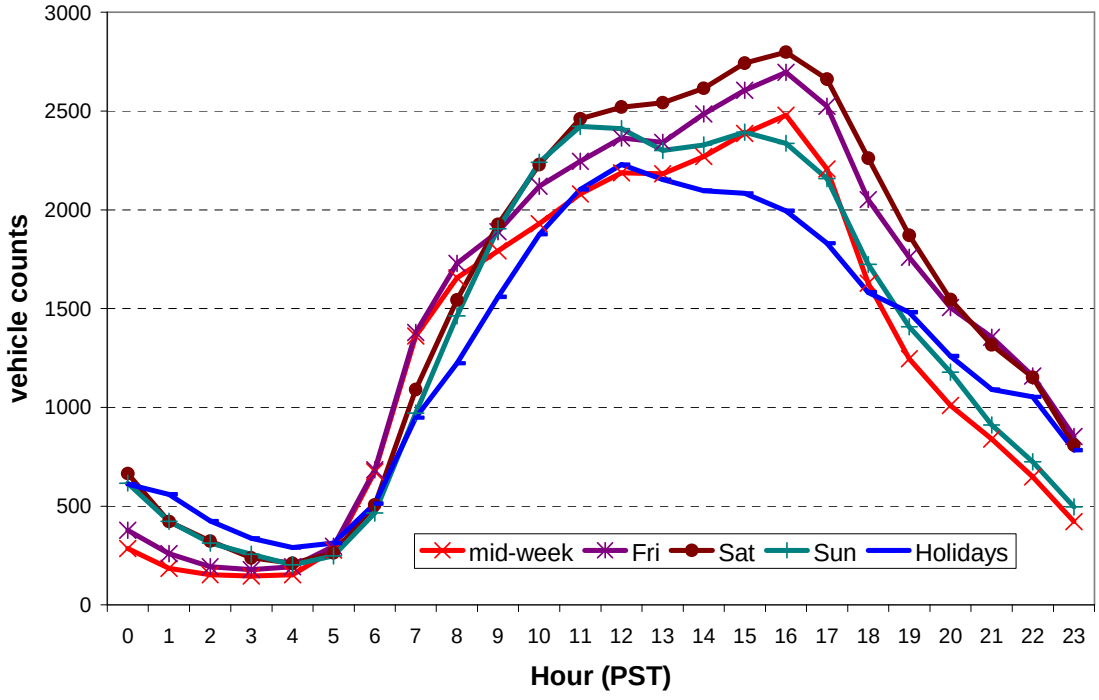

Figure 7-18. Traffic volumes on Highway 50 near Rufus Avenue normalized to mid-week traffic volumes.

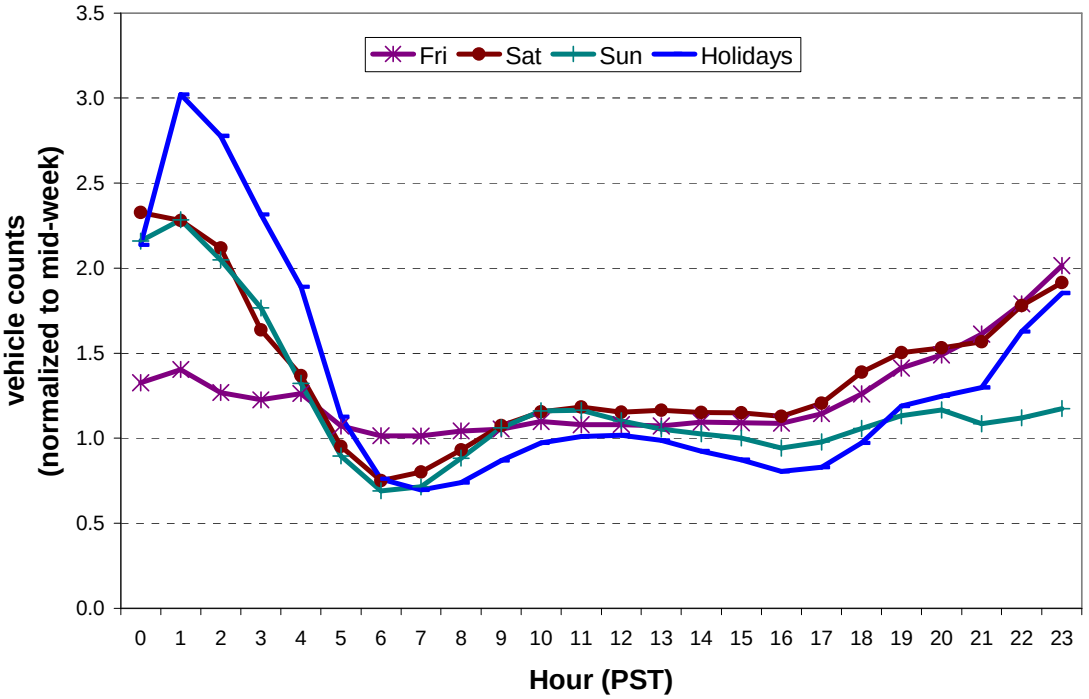

Figure 7-19. Mean TSP concentrations at Cave Rock associated with 1-hour reversals in wind direction during 2003. (Note: The orange plots represent the TSP during the wind reversal from offshore to onshore in the morning while the turquoise plots represent the TSP during the wind reversal from onshore to offshore in the evening. The darker shading represents the concentrations during offshore airflow while the lighter shading represents concentrations during onshore airflow.)

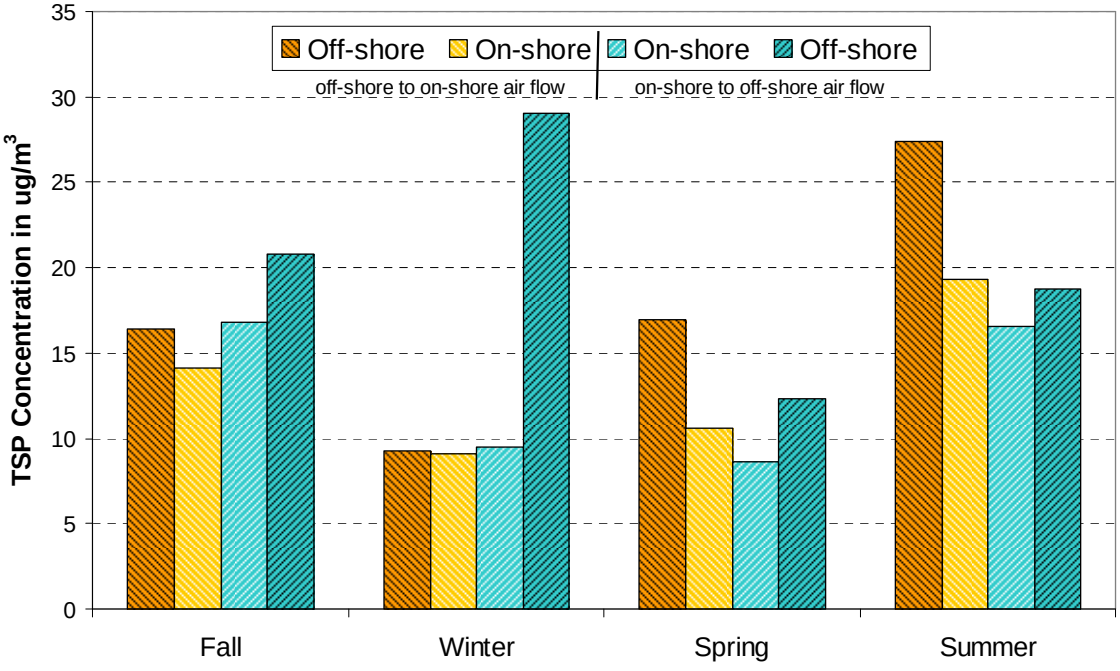

Figure 7-20. Difference in TSP concentrations at SOLA and Sandy Way (SOLA – SW) associated with offshore and onshore wind directions during winter months of 2003.

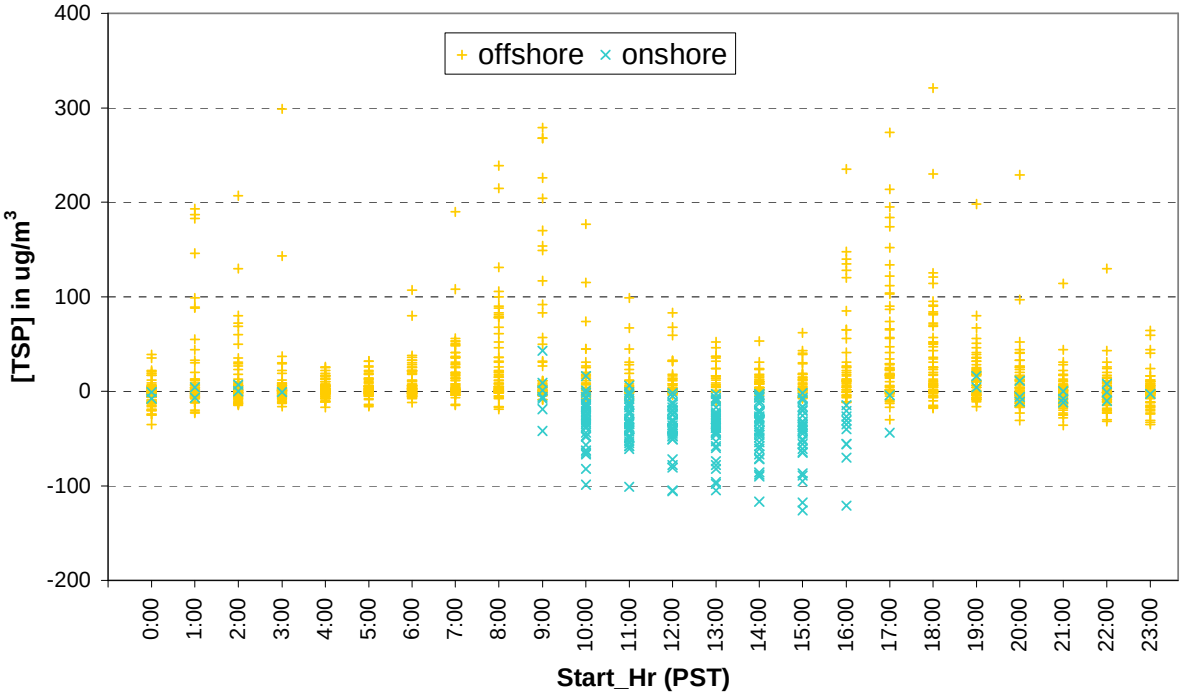

Figure 7-21. Difference in TSP concentrations at SOLA and Sandy Way (SOLA – SW) associated with offshore and onshore wind directions during spring months of 2003.

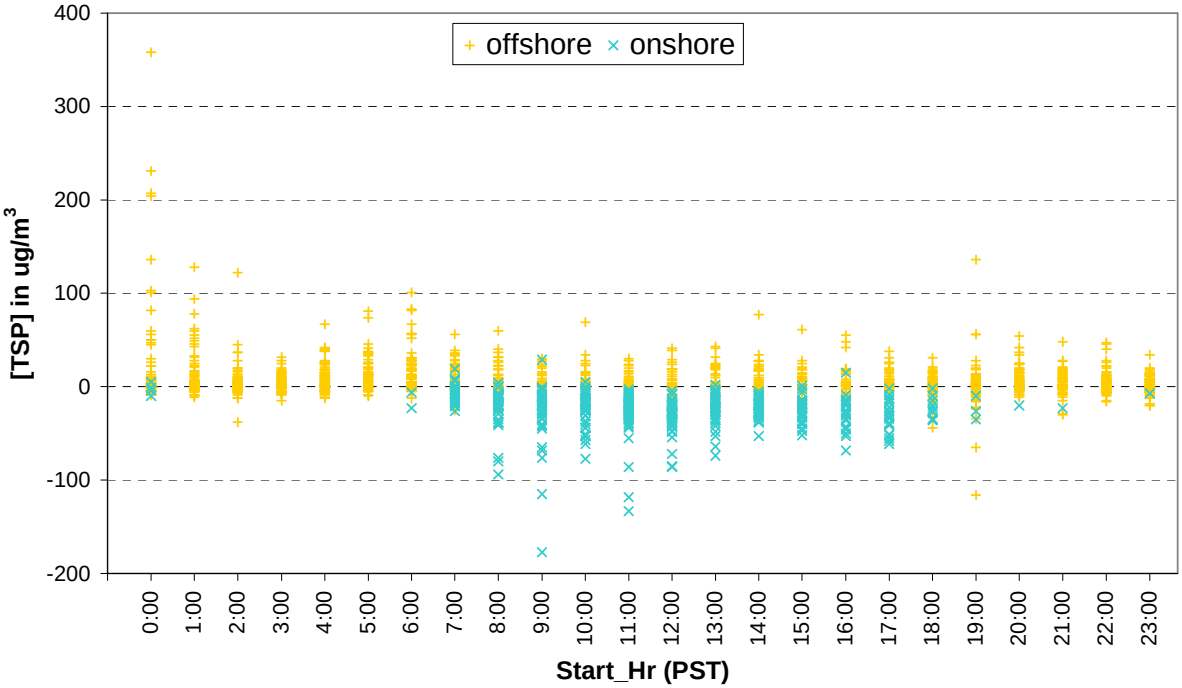

Figure 7-22. Difference in TSP concentrations at SOLA and Sandy Way (SOLA – SW) associated with offshore and onshore wind directions during summer months of 2003.

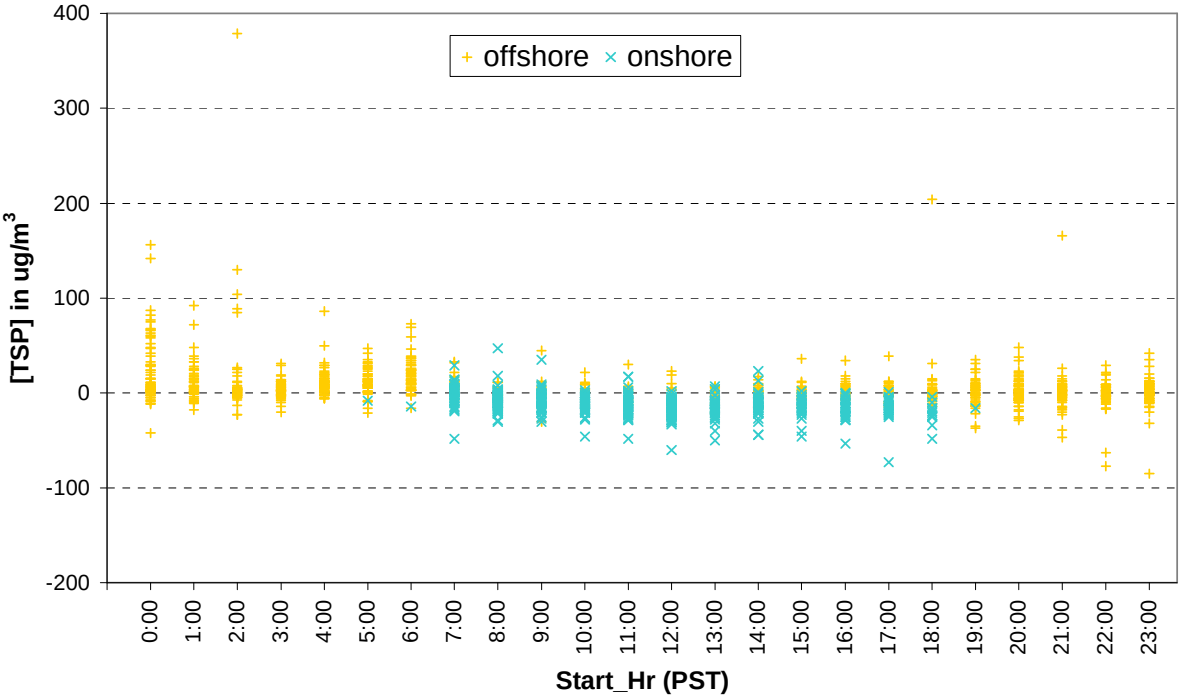

Figure 7-23. Difference in TSP concentrations at SOLA and Sandy Way (SOLA – SW) associated with offshore and onshore wind directions during fall months of 2003.

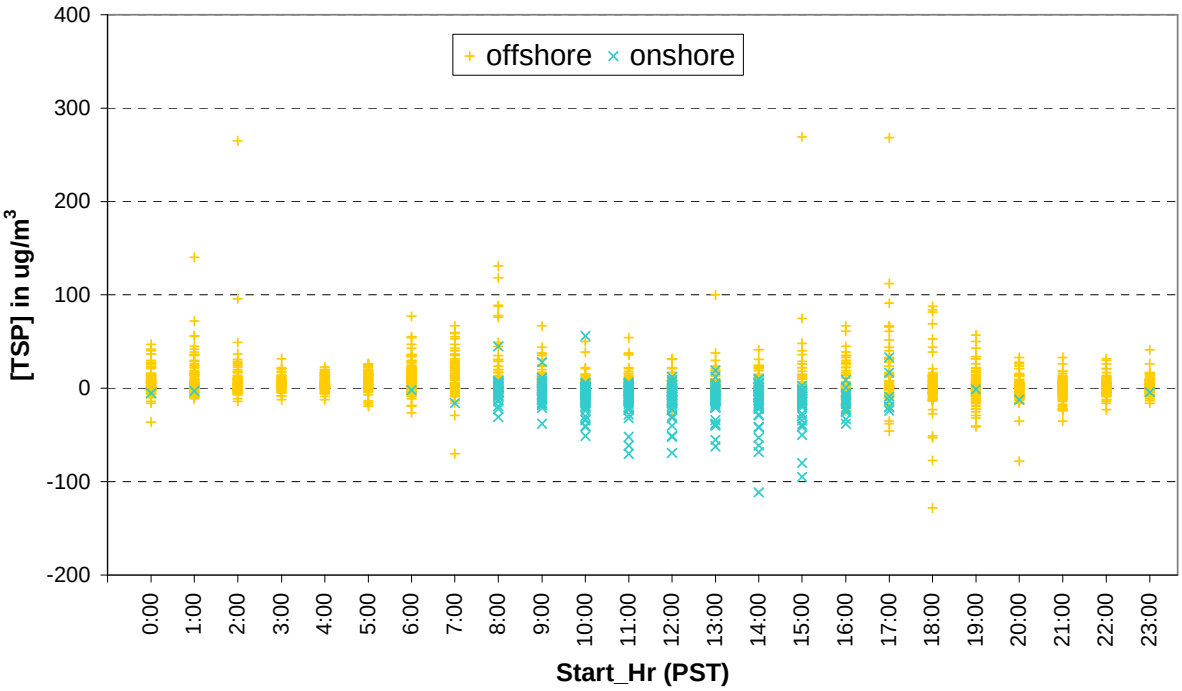

Figure 7-24. Temporal variation in ammonia and nitric acid concentrations at South Lake Tahoe sites (Sandy Way and SOLA) based on TWS program.

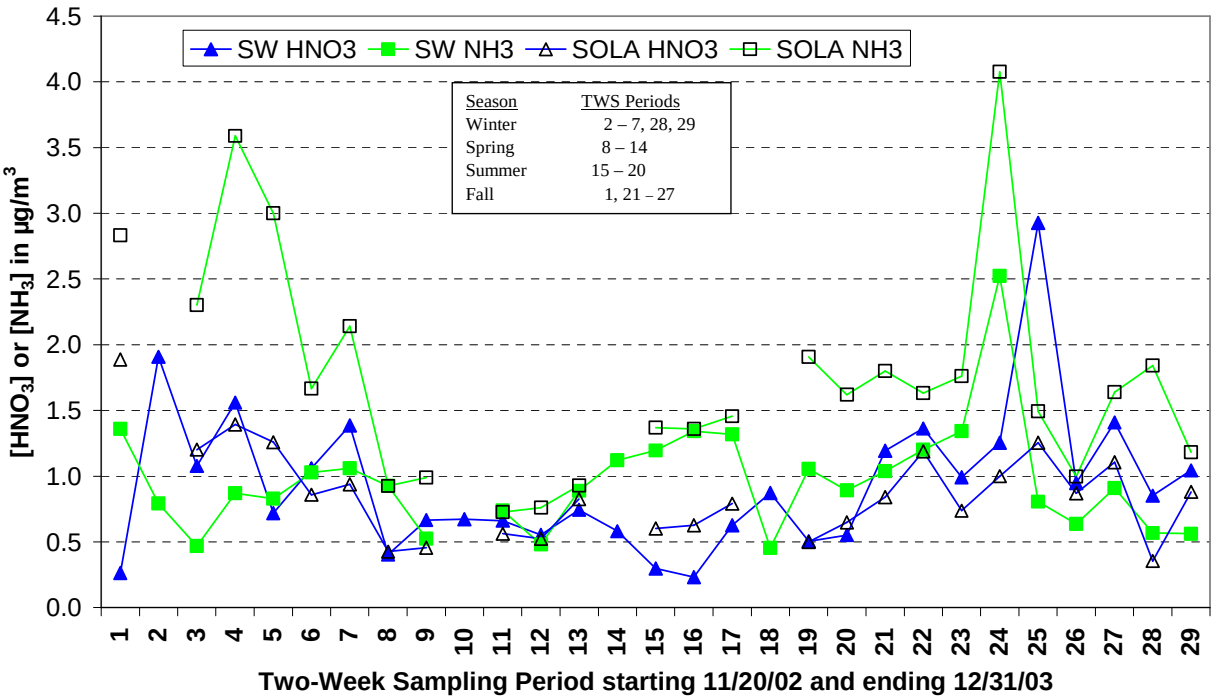

Figure 7-25. Sandy Way minus SOLA differences in ammonia and nitric acid concentrations in South Lake Tahoe.

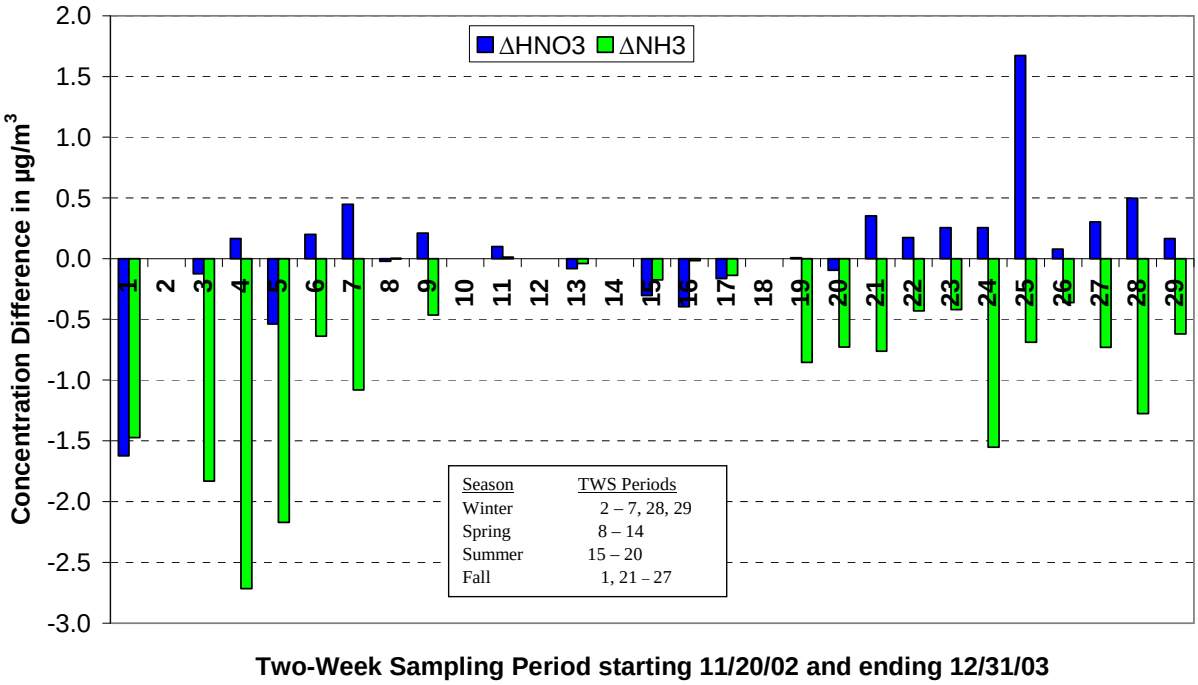

7.3.3 Residential Wood Smoke Emissions

LTADS approached residential wood smoke source characterization through residential chimney sampling (Kuhns et al., 2004) and neighborhood sampling (Fitz et al., 2004). We expected that fire place and wood stove plumes would enter the larger neighborhood volume of air and chimney emission concentrations would quickly disperse and deposit leading to lower concentrations for neighborhood samples. These lower concentrations would then better represent ambient air concentrations.

Using EPA Method 28 source testing, DRI analyses showed that substantial mass of particulate matter, nitrates, ammonium, and organic matter were emitted in the chimney smoke. Source profiles are generally used to provide pollutant emission factors, the ratios of the emitted constituents to the total mass of particulate matter sampled (Kuhns et al., 2004). Phosphorus was not observed in the chimney smoke at concentrations greater than the measurement uncertainty. This result is not unexpected as previous measurements characterizing P in firewood also report very little P. In fact, based on these earlier studies, the official P emission factor for firewood in ARB's emission inventory is zero. Official P emission factors are higher however for other types of fires because they contain live or recently alive vegetation which contains much more phosphorus. Official P emission factors are much higher than smoke for other common PM sources in the Tahoe Basin as indicated by **Table 7-1** and **Figure 7-26**. The ARB emission inventory also indicates that only about 5% of the total P atoms in road dust is found in soluble form, i.e., phosphates ($PO_4^{=}$).

As a result of limited surveys conducted during LTADS, a few generalizations can be made. The proportion of wood burning appliances was 59% wood stove, 25% fireplace without insert, 10% fireplace with insert, and 6% pellet stove. The average camper burned four logs per evening during the summer months and the average resident burned 7.4 logs over six hours during winter months.

As noted before, the neighborhood wood smoke profiles, collected by CE-CERT in the ambient air, are highly diluted compared to the concentrations measured in the source testing (Fitz et al., 2004). They reported filter sample mass and the results of elemental analysis with XRF. As the stack plume is dispersed and as heavier particles likely deposit out of the plume, concentrations are substantially reduced. As these source concentrations disperse and deposit to reach ambient air concentrations, PM10 mass is reduced by over 400 times and PM2.5 mass is reduced by over 800 times.

Figures 7-27a and 7-27b show the relative abundance of chemical species in the emissions from combustion of a hardwood (almond) and a soft wood (pine). After carbon and potassium, gas phase ammonia appears to be next highest species emitted from residential wood smoke.

Major chemical components of wood burning particulate matter emissions were organic carbon (OC) and elemental carbon (EC). Total Carbon (TC) accounted for 15% to 74%

of PM2.5 mass and TC fraction of PM2.5 mass from hardwood were generally higher than from softwood and higher from fireplaces than from wood stoves. Crustal elements were found with high variability, probably contributed from ambient background during sample collection.

Table 7-1. Phosphorus PM source profiles in CARB emission inventory. (CARB, 2002)

WEIGHT % of TSP	***WEIGHT % of PM 10***	***WEIGHT % of PM 2.5***	***PM PROFILE NAME***
0.7532	1.0695	0.8142	livestock operations dust
0.2723	0.2723	0.2723	PAVED ROAD DUST*
0.1602	0.1944	0.1997	windblown dust-unpaved rd/area
0.1499	0.1979	0.2273	CONSTRUCTION DUST
0.1499	0.1979	0.2273	landfill dust
0.1250	0.1250	0.1250	tire wear
0.1249	0.1679	0.1975	agricultural tilling dust
0.1249	0.1679	0.1975	windblown dust-agricultural lands
0.1096	0.1096	0.1096	UNPAVED ROAD DUST
0.0301	0.0301	0.0215	agricultural burning - field crops
0.0301	0.0301	0.0215	weed abatement burning
0.0295	0.0295	0.0205	grass/woodland fires
0.0295	0.0295	0.0205	open burning
0.0295	0.0295	0.0205	range improvement burning
0.0295	0.0295	0.0205	WASTE BURNING
0.0288	0.0288	0.0196	orchard prunings burning
0.0199	0.0199	0.0098	forest management burning
0.0199	0.0199	0.0098	timber and brush fires
0.0123	0.0127	0.0056	diesel vehicle exhaust
0.0000	0.0000	0.0000	brake wear
0.0000	0.0000	0.0000	FIREPLACES AND WOODSTOVES

* Official paved road dust factor. However, removal of an outlier data point, results in a P emission factor of 0.1372 for Paved Road Dust.

Note #1: These factors (dated 9/27/02) do not include newly discovered, potentially large self absorption correction factors for PM > 2.5 µm.

Note #2: Data from Turn et al. (1997), indicate comparable P fractions with pine slash burn (n=4 and 2 samples (Doug fir for PM2.5 & PM10) > uncertainty) P2.5 ~0.0097 and P10 ~0.0200 and fruit tree prunings (n=4 & none > uncertainty) P2.5 ~0.0200 and P10 ~0.0290).

Note #3: The PM sources shown in capital letters are the major PM sources in the Lake Tahoe Air Basin.

Figure 7-26. Ranking of phosphorus abundance in particulate matter sources (P as % of PM by weight) based on source profiles in CARB emission inventory. PM emission categories shown in capital letters are the main PM sources in the Tahoe Basin.

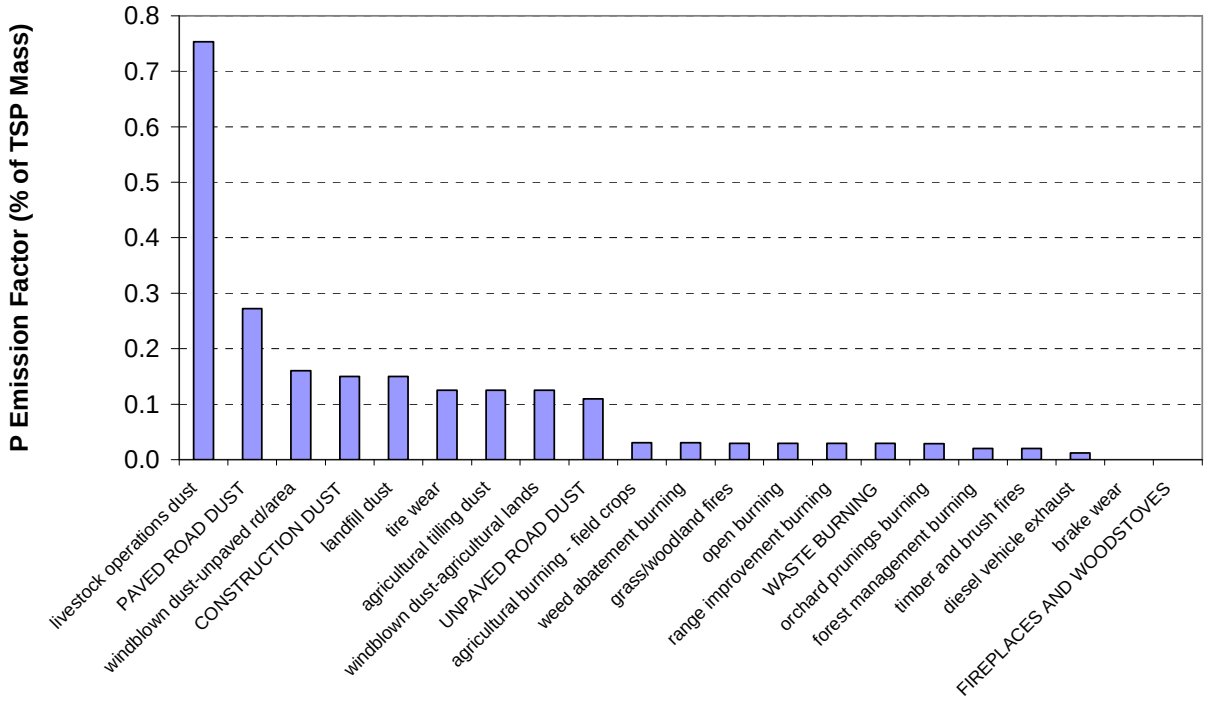

Figure 7-27. Comparison of the relative abundance of chemical species in wood stove emissions from combustion of a soft wood (pine) and a hard wood (almond) based on DRI analyses. (Kuhns et al, 2004)

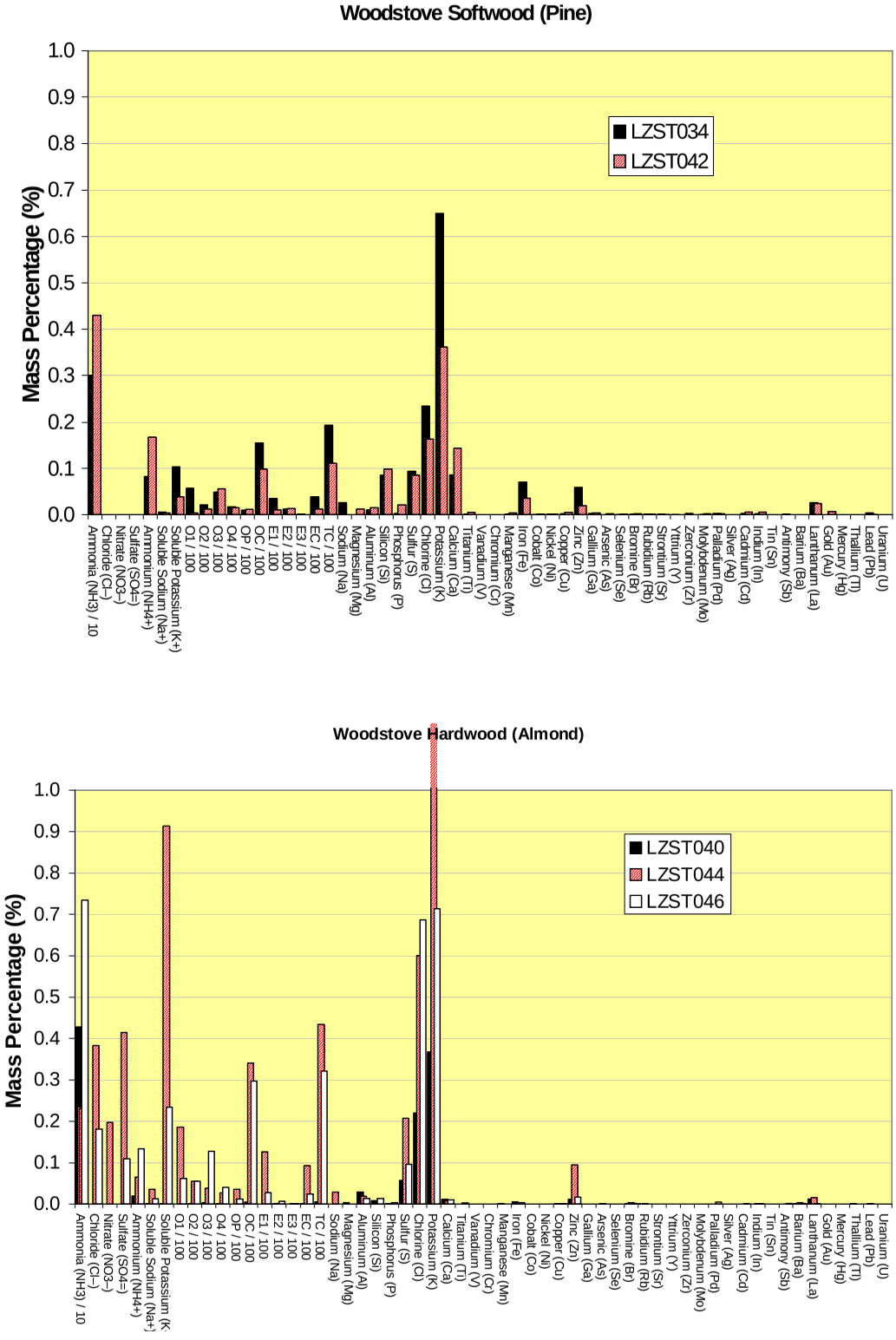

7.4 Natural Nutrient and Particulate Sources

As alluded to earlier in the emission source profiles, natural processes contribute to the emissions of ammonia, phosphorus, and particulate matter. If particular significance, related to comparison of LTADS results with TRG surrogate surface results, which can collect larger particles than the LTADS samplers, is the apparent influence of natural sources, particularly pollen. The extensive forest of pine trees in the Basin generate a large quantity of pollen, particularly in the late spring and early summer when anecdotal reports indicate extensive pollen covering surfaces, including the lake's surface. The results of the laboratory analyses conducted on the surrogate surface dry deposition samples collected by the TRG indicate that pollen and smoke can significantly increase the amount of nutrients to Lake Tahoe. Analytical results of dry deposition samples collected at TRG's Ward Lake Level (aka Wallis Tower) sampling site are plotted in **Figures 7-28 and 7-29** for the samples collected between May 1, 2002 and March 31, 2004. The estimated dry deposition rates (grams per hectare; g/ha) of nitrates and total Kjeldahl nitrogen (primarily ammonia) associated with each sample are plotted in **Figure 7-28**. Similarly, the estimated dry deposition rates of dissolved phosphorus and total phosphorus associated with each sample are plotted in **Figure 7-29**. The samples for which the sampler operator noted pollen or biological material (e.g., leaves, insects) in the sample are indicated by a yellow-colored bar. The samples for which the sampler operator noted smoke on the sample log are indicated by a rose-colored bar. Because the samples are collected over several days (7-10 days typically) and the operator is not always present, the notation of smoke being observed in the basin on the sample log report does not necessarily mean that the smoke physically impacted the sample nor that smoke did not impact the sample when the observer was not present. Thus, any conclusions regarding the impact of smoke on dry deposition samples are very tentative while the impact of pollen and other biological material actually observed in the sample are quite definitive.

The analytical results in **Figure 7-28** indicate the possibility of occasional smoke impacts and the high likelihood of biological impacts. Both of the very high nitrate results were associated with biologically impacted samples and the most of the high TKN results were also associated with biologically impacted samples. Similarly, the highest phosphorus results shown in **Figure 7-29** are almost always associated with biologically impacted samples. The biologically impacted samples are often several times greater than the temporally neighboring samples.

In addition, the year-round population of Canada geese in the Tahoe Basin has reportedly increased over the years. This increase has generated more complaints by property owners about the fouling of their property and increased speculation that these waterfowl could be an increasingly significant contributor to the nutrient load of the lake.

These natural sources of nutrients to the lake are not represented in the LTADS deposition estimates. Although these natural sources probably play a minor role in the annual deposition of nitrogen species because of other, more prodigious, sources, these natural sources could play a more significant role in the annual deposition of phosphorus due to the more limited input of P from other sources.

Figure 7-28. Nitrates and Total Kjeldahl Nitrogen Measurements associated with TRG's surrogate surface dry deposition sampler at the Ward Lake Level (Wallis Tower) site from May 1, 2002 through March 31, 2004.

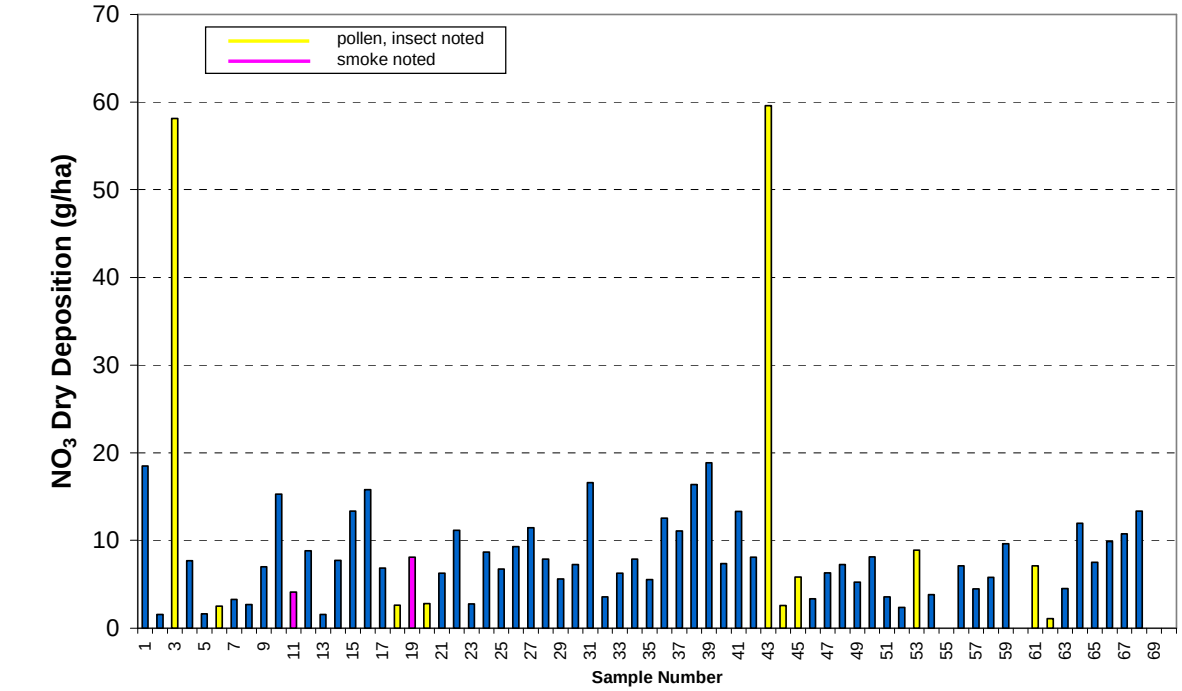

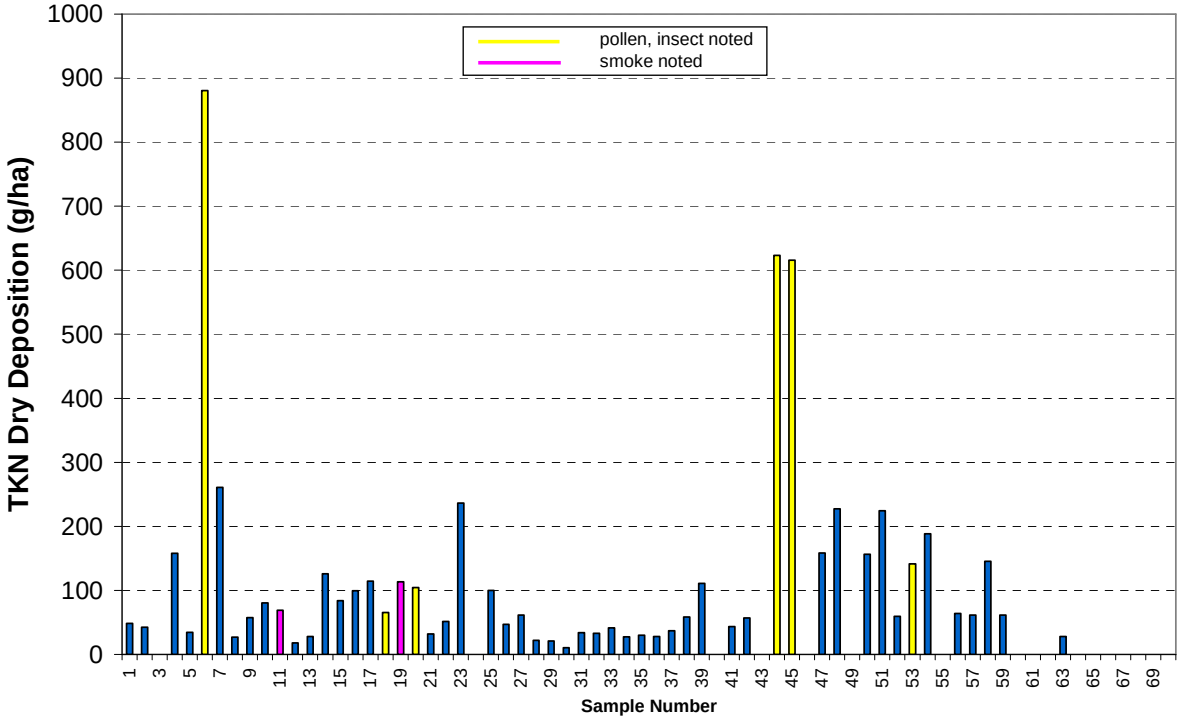

Figure 7-29. Dissolved Phosphorus and Total Phosphorus Measurements associated with TRG's surrogate surface dry deposition sampler at the Ward Lake Level (Wallis Tower) site from May 1, 2002 through March 31, 2004.

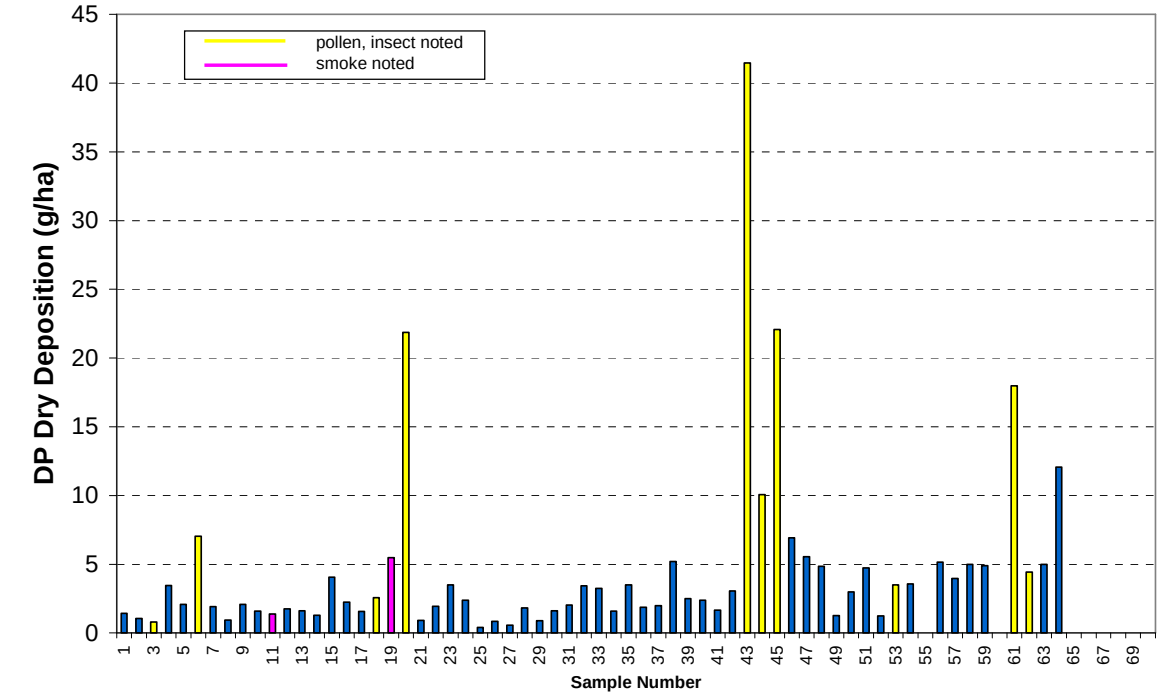

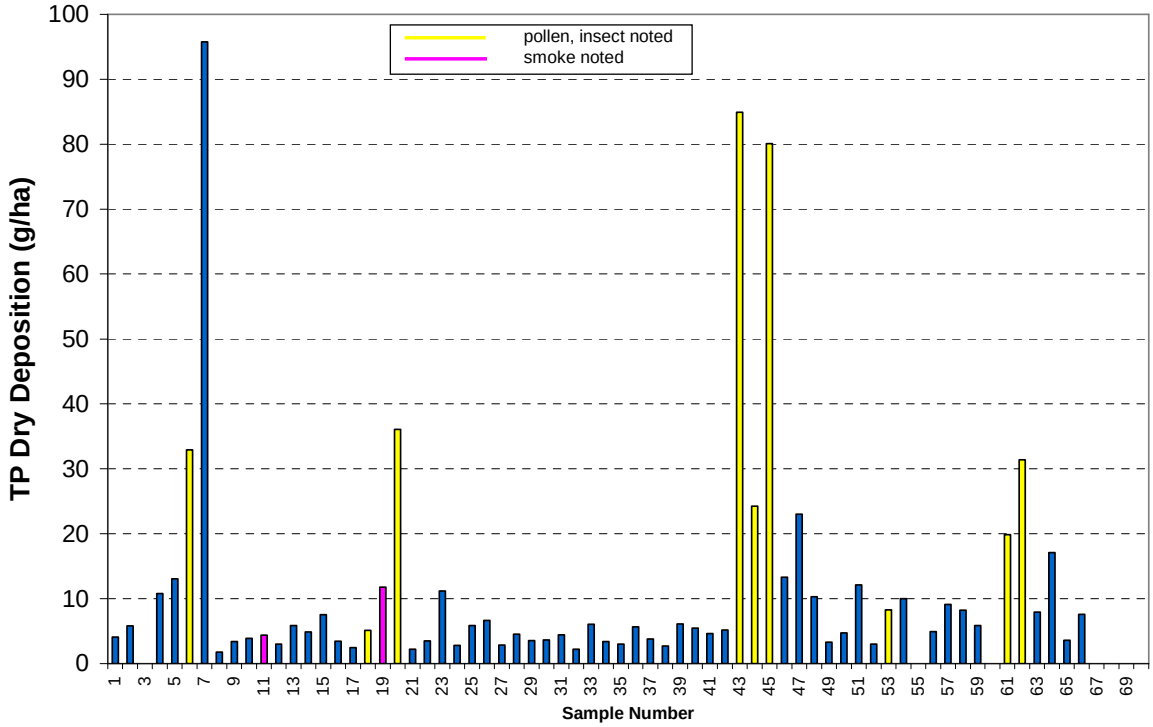

7.5 Conclusions

Multiple previous chapters in this report indicate that nitrogen is deposited to Lake Tahoe primarily in the form of ammonia gas and secondarily in the form of nitric acid. Aerosol species of nitrogen (ammonium and nitrate ions) are smaller contributors to atmospheric deposition of total nitrogen in the Tahoe Basin.

Both ambient measurements and the emission inventory suggest that local motor vehicle emissions are a source of ammonia. The inventory also indicates farming operations and residential fuel combustion as significant sources of ammonia. There is insufficient information to apportion with any certainty the ammonia between local and regional sources.

Based on observed concentrations, atmospheric lifetimes, and transport patterns we conclude that nitric acid deposited to the Lake must be primarily of local origin.

No conclusions are drawn from the LTADS ambient data about sources of phosphorus. However, the source samples collected prior to and during LTADS indicate that road dust may be the primary source with contributions from the burning of live vegetative material and lubricating oils. Surrogate surface (bucket) deposition samplers indicate that pollen may be a significant source of nutrients during the late spring and summer. Additional efforts to improve the quantification of natural sources of phosphorus, especially vegetative material and waterfowl, are warranted.

Road dust is the dominant source of PM concentrations at LTADS monitoring sites and in the immediate vicinity of the Lake, as inferred both from ambient concentrations and special source-oriented monitoring results. Road dust as the dominant source of PM is consistent with the inventory estimates of PM_coarse and PM_large provided in the current Lake Tahoe Air Basin emission inventory.

Road dust and wood smoke both appear to be important sources of fine particles. However, fine particles from these two sources likely differ in solubility and this fact may be important to consideration of their potential to impact water clarity. Insoluble particles would obviously have the potential to scatter light and to serve as a substrate for algal growth while soluble particles would not. The constituents of road dust are generally less soluble than fine particles from wood smoke or other combustion sources.

The location and timing of emissions is important to determining their potential for deposition to the Lake. Sources located near the Lake and at low altitude have much greater potential for deposition to the Lake than more distant sources. In general, emissions released during nighttime or early morning hours will have much greater potential for impacting the Lake than emissions occurring during morning through afternoon.

Thus the greatest potential for reducing deposition to the Lake would be through reducing emissions released near and immediately upwind of the Lake. Due to the

typical daily cycle of wind directions, reductions in emissions during late afternoon through mid morning would have more benefit than reducing emissions at mid-day or early afternoon. Similarly, reducing emissions that are released near ground level would be relatively more effective than reducing emissions released at altitude.

Emission inventories provide general information about the strengths of sources, but do not include source-receptor information necessary to apportion concentrations or deposition to source categories. For example, the emission inventory indicates that waste combustion is a larger source of fine particles than residential fuel combustion. However, the effective release height of these emissions (and thus their potential for contact with the lake surface) depends on the volume and temperature of the smoke. Similarly the location and timing of emissions relative to upslope and downslope winds is an important factor in determining whether there is potential for impact to the Lake.

In summary, motor vehicles exert a large influence on NOx, NH_3, PM_coarse, and PM_large concentrations in the Tahoe Basin while wood burning exerts the dominant influence on PM_fine concentrations.

7.6 References

Andronache, C, Kiang, C., Chameides, W., D. Davis, D., Anderson, B., Pueschel, R., Bandy, A., Thornton, D., Talbot, R., Kasibhatla, P. (1997) “Gas-to-particle conversion of tropospheric sulfur as estimated from observations in the western North Pacific during PEM-West B”, *J. Geophys. Res.*, **102**(D23), pp. 28511-28538.

Austin, J., and Gouze, S. (2001) *Ozone Transport: 2001 Review*, CARB Planning and Technical Support Div., Sacramento, CA, April, 2001.

Cadle, S., Mulawa, P., Hunsanger, E., Nelson, K., Rafazzi, R., Barrett, R., Gallagher, G., Lawson, D., Knapp, K., Snow, R. (1999) “Light-Duty Motor Vehicle Exhaust Particulate Matter Measurement in the Denver, Colorado, Area”, *J. Air & Waste Manage. Assoc.* **49**:PM, pp. 164-174.

Cahill, T. A. and Wakabayashi, P. (1993) “Compositional analysis of size-segregated aerosol samples”. Chapter 7 in *Measurement Challenges in Atmospheric Chemistry*. Leonard Newman, Ed., American Chemical Soc., pp. 211-228.

California Air Resources Board (CARB) (2002), Emissions Inventory CEIDARS, webpage (http://www.arb.ca.gov/ei/speciate/speciate.htm).

California Air Resources Board (CARB) (2003), *California Ambient Air Quality Data 1980-2001*, [CD-ROM PTSD-02-017-CD], http://www.arb.ca.gov/aqd/aqdcd/aqdcd.htm, CARB Planning and Technical Support Div., Sacramento, CA, December.

California Air Resources Board (CARB) (2004), Emissions Inventory Almanac, webpage (http://www.arb.ca.gov/app/emsinv/emseic1_query.php?F_DIV=-4&F_YR=2004&F_SEASON=A&SP=2005&F_AREA=AB&F_AB=LT&F_DD=Y).

California Air Resources Board (CARB) (2005), Emissions Inventory Almanac, webpage (http://www.arb.ca.gov/app/emsinv/fcemssumcat2005.php).

Chow, J.C., Watson, J.G., Kuhns, H.D., Eyemezian, V., Lownthal ,D.H., Crow, D.J., Kohl, S.D., Enelbrecht, J.P., and Green, M.C. (2004), "Source profiles for industrial, mobile, and area sources in the Big Bend Regional Aerosol Visibility and Observational (BRAVO) Study." *Chemosphere* Vol. **54**(2), pp. 185-208.

Coburn, T. (1998) "Statistical Analysis of Particulate Matter Emissions from Light-Duty and Heavy-Duty Diesel Vehicles", Final Report to The Northern Front Range Air Quality Study, U.S. Department of Energy, National Renewable Energy Laboratory, Denver.

Core, J.E., et al. (1989) "Receptor Modeling Source Profile Development for the Pacific Northwest States"; The Pacific Northwest Source Profile Library, Volume 2 - Project Final Report. State of Oregon Department of Environmental Quality, Portland, Oregon, September.

Elford, C.R. (1974) "The climate of California" in van der Leeden, F., and Troise, F.L. (Eds.), *Climates of the States*, Water Information Center, Port Washington, NY, pp. 538-594.

Fitz, D., Lents, J. (2004), "Improvement of the PM Emission Inventory for the Lake Tahoe Region." Final Report to Air Resources Board, UC Riverside College of Engineering Center for Environmental Research and Technology, April 15.

Gaffney, P. (2004), personal communication June 23, 2004, "Tahoe Ammonia for RD6_04.xls".

Gillies, J.A. Watson, J.G., Rogers, C.F., DuBois, D.W., Chow, J.C., Langston, R., and Sweet, J. (1999). "Long term efficiencies of dust suppressants to reduce PM10 emissions from unpaved roads." *Journal of the Air & Waste Management Association*, Vol. **49**(1), pp. 3-16.

Kuhns, H, Chang, M-C. O., Chow, J.C., Etyemezian, V., Chen, L-W. A. Nussbaum, N., Nathagoundenpalayam, S.K.K., Trimble, D., Kohl, S., MacLaren, M., Abu-Aliban, M., Gillies, J., and Gertler, A. (2004), "DRI Lake Tahoe Sources Characterization Study." Desert Research Institute, Final Report to Air Resources Board, October 22.

Malm, W., Sisler, J., Huffman, D., Eldred, R. and Cahill, T. (1994) "Spatial and seasonal trends in particle concentration and optical extinction in the United States", *J. Geophys. Res.* **99**(D), pp. 1,347-1,370.

Nevada Department of Environmental Protection (NDEP) Air Quality Data (http://ndep.nv.gov/baqp/trend01.htm), 2003.

Pollisar, A.V., Hopke, P.K., Malm, W.C., and Sisler, J.F. (1996) "The Ratio of Aerosol Absorption Coefficients to Sulfur Concentrations as an Indicator of Smoke from Forest Fires when Sampling in Polar Regions", *Atmos. Env*. **30**,1pp. 147-1157.

Seinfeld, J.H. (1986), *Atmospheric Chemistry and Physics of Air Pollution,* J. Wiley & Sons, p. 738.

Sisler, *et al.* (1996) *Spatial And Seasonal Patterns And Long Term Variability Of The Composition Of The Haze In The United States: An Analysis Of Data From The*

IMPROVE Network, Cooperative Institute for Research in the Atmosphere (CIRA), Colorado State University, Fort Collins, CO, ISSN: 0737-5352-32.

Turn, S., B. Jenkins, J. Chow, L. Pritchett, D. Campbell, T. Cahill, and S. Whalen, (1997) "*Elemental characterization of particulate matter emitted from biomass burning: Wind tunnel derived source profiles for herbaceous and wood fuels*", *J. Geophys. Res.*, **102**(D3), pp. 3633-3699.

van Gulijk, C., Marijnissen, J.C.M., Makkee, M. and Moulijn, J.A. (2003) "Oil-soaked sintered impactors for the ELPLI in diesel particulate measurements*." Journal of Aerosol Science*, Vol. **34**, pp. 635-640.

van Gulijk, C., Shouten, J.M., Marijnissen, J.C.M., Makkee, M. and Moulijn, J.A. (2001) "Restriction for the ELPI in diesel particulate measurements." *Journal of Aerosol Science*, Vol. **32**(9), pp. 1117-1130.

VanCuren, R., (2003) "Asian Aerosols in North America: Extracting the Chemical Composition and Mass Concentration of the Asian Continental Aerosol Plume from Long Term Aerosol Records in the Western United States", *J. Geophys. Res.*, **108**(D20), 4623, doi:10.1029/2003JD003459.

VanCuren, R., and T. Cahill (2002) "Asian aerosols in North America: Frequency and concentration of fine dust", *J. Geophys. Res.*, **107**(D24), doi:10.1029/2002JD002204, 28 December.

Watson, J.G., Fujita, E.M., Chow, J.C., Zielinska, B., Richards, L.W., Neff, W.D., and Dietrich, D. (1998), "Northern Front Range Air Quality Study." Final Report. Reno, NV, Desert Research Institute.

8. Findings, Insights, and Recommendations

LTADS stakeholders asked ARB staff to develop atmospheric deposition estimates for nitrogen (N), phosphorus (P), and particulate matter (PM). Stakeholders and the TMDL regulatory program needed an improved understanding of the atmospheric sources of N, P, and PM. Finally, stakeholders also desired to know the contribution of air pollution transport, from the Sacramento Valley and the San Francisco Bay Area air basins, to the pollutant burden in Lake Tahoe Air Basin. In response, ARB staff conducted a year-long field study and analyzed the resultant LTADS database. PM was monitored in three aerodynamic size ranges, <2.5 μm diameter (PM2.5), <10 μm diameter (PM10), and total suspended particulate matter (TSP). Concentrations were defined and deposition estimates were prepared for PM2.5, PM_coarse (2.5 – 10 μm diameter), and PM_large (>10μm) because the types of sources, chemical composition, solubility, and optical properties may differ markedly with size. Findings and insights gained are summarized by pollutant in this chapter. The potential value of additional research may be considered in the context of the information needs for regulatory decision-making and can be weighed against the resources required and any limitations in feasibility of current or foreseeable methods.

8.1 Deposition Estimates

The LTADS approach for estimating dry atmospheric deposition to Lake Tahoe is based on seasonal-average N, P, and PM mass concentrations being apportioned to seasonal hourly concentrations, based on continuous PM, NOx, and NOy measurements. These seasonally-averaged hourly concentrations were then merged with the hour by hour deposition velocities calculated from meteorological variables for each hour of every day to provide hourly dry deposition estimates, which were summed into seasonal estimates. In a less rigorous manner, the wet deposition estimates are based on seasonal air quality concentrations and precipitation frequency but also include an analysis involving basic physical principles and various assumptions regarding mixing heights, washout efficiency, etc.

The estimates from LTADS of the annual atmospheric deposition (dry and wet) of N, P, and PM to Lake Tahoe are presented, with upper and lower bounds, in **Tables 8-1 and 8-2**. CARB staff prepared these final estimates of direct atmospheric deposition to Lake Tahoe based on comments from peer reviewers and additional analyses. The updated analyses include improved formulation of the deposition velocity equations, improved characterization of seasonal ambient concentrations in the four quadrants of the Lake, etc. The seasonal deposition estimates (summarized in **Figure 8-1**) and the characterization of the emission sources and atmospheric processes at work in the Tahoe Basin will be used to guide the development of potential control measures to halt the declining clarity of Lake Tahoe and to restore the water clarity for which the Lake is famous. Background information, approaches, assumptions, and analyses leading to these atmospheric deposition estimates are presented in Chapters 4 and 5 of this report.

The LTADS annual atmospheric deposition estimate for nitrogen is dominated by gaseous N, primarily NH_3 and secondarily HNO_3, and is consistent with previous deposition estimates based on surrogate surface deposition samplers operated by TRG. However, previous TRG estimates of annual phosphorus deposition to the Lake are almost twice the central estimate for total annual phosphorus deposition from LTADS. Due to difficulties associated with the measurement of phosphorus in particulate matter, the CARB phosphorus deposition estimates use an assumed phosphorus concentration based on the range of P concentrations measured during LTADS and the operational limit of detection for phosphorus in ambient particulate matter samples. It should be noted that the Upper Estimate of P dry deposition to Lake Tahoe assumes the same P concentrations but assumes the maximum, or near maximum, particle size possible for the distribution of P within the particle size categories used for calculation of deposition velocities (i.e., the assumed particle sizes in the deposition velocity calculations were 2.5 µm, 10 µm, and 25 µm for PM_fine, PM-coarse, and PM_large). Thus, the Upper Estimate essentially maximizes the calculated deposition rate and dry deposition of P. Even the combined Upper Estimates of dry and wet deposition of P are less than half of the historical estimate of P from the TRG surrogate surface samplers. A potential cause of difference between the CARB and TRG P deposition estimates could be a difference in the size of particles collected. CARB's air quality measurements do not include very large particles, such as those associated with plant detritus and pollen, which the TRG surrogate surface deposition samplers, particularly at the tree-impacted site at Ward Lake Level, would include. Because these large particles would not transport long distances, deposition measurements on the shoreline and near trees would not be representative of deposition rates over the whole lake. The P results from the TRG's dry bucket sampler for periods when field notes indicate pollen was present in the sample suggest that natural sources could be a significant source of P input to the Lake.

Table 8-1. LTADS Estimates of Annual Dry Atmospheric Deposition to Lake Tahoe
(metric tons/year)

Pollutant	Lower Estimate	Central Estimate	Upper Estimate
N (NH_3, NH_4^+, HNO_3, NO_3^-)	70	120	170
P (P, PO_4^{-3})	1	2	3
PM_fine (<2.5 µ)	50	60	62
PM_coarse (>2.5µ and <10µ)	100	170	240
PM_large (>10 µ)	210	360	560
PM	360	590	860

Table 8-2. LTADS Estimates of Annual Wet Atmospheric Deposition to Lake Tahoe*
(metric tons/year)

Pollutant	Lower Estimate	Central Estimate	Upper Estimate
N (NH_3, NH_4^+, HNO_3, NO_3^-)	30	70	150
P (P, PO_4^{-3})	0	1	2
PM_fine (<2.5 µ)	30	75	145
PM_coarse (>2.5µ and <10µ)	30	70	130
PM_large (>10 µ)	10	20	40
PM	70	165	315

* The wet deposition estimates are based on a basic principles analysis with un-validated assumptions.

Figure 8-1. LTADS Central Estimate of Seasonal Total Atmospheric Deposition to Lake Tahoe.
(metric tons/year)*

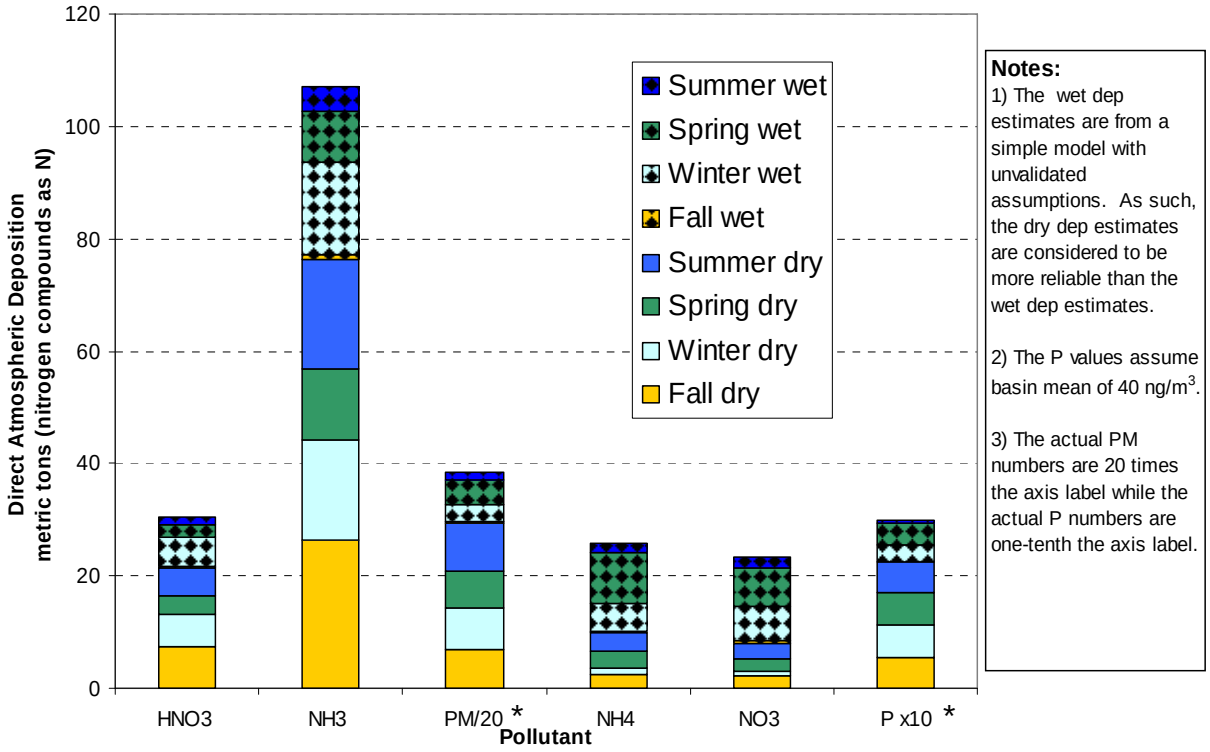

* Note adjustment to PM and P values. Actual PM dep is 20 times greater and actual P dep is 10 times less than indicated on Y-axis.

8.2 Particulate Matter

8.2.1 Findings

Measurements of particulate matter (PM) were made in three sizes (TSP, PM10, and PM2.5) with the Two-Week Sampler from late 2002 through 2003 at four locations in the Tahoe Basin. These data from the TWS network provide spatial, temporal, physical, and chemical insights into the nature of PM in the Tahoe Basin. Conclusions about the mass and speciation of TSP and PM10 are similar because coarse and large particles are generally emitted by the same sources and only a small portion of the TSP was present in sizes greater than 10 microns. The highest concentrations of atmospheric PM were found in places with the largest population and greatest vehicular traffic. Geographically, the highest levels of PM were observed during LTADS, in order of magnitude, at South Lake Tahoe (SOLA & Sandy Way sites), Tahoe City (Lake Forest), and Thunderbird Lodge. At the high PM locations, seasonal concentrations, in decreasing order, tended to be highest during winter, lower during summer and fall, and lowest during spring. At the low PM sites, concentrations, in decreasing order, tended to be highest during summer, lower in fall and spring, and lowest in winter. Thus, the high PM concentrations were coincident with proximity to vehicular traffic and with high

traffic seasons. These observations support the hypothesis that roadways and vehicular traffic are a major source of the atmospheric TSP in the Tahoe Basin.

For the locations with higher PM concentrations (Lake Forest, Sandy Way, & SOLA), the PM10 mass comprises between 75% and 85% of the TSP mass. At the location with the lowest PM concentrations (Thunderbird), PM10 and TSP concentrations were roughly equal and thus indicating that particles larger than 10 µm were generally not significant contributors to the TSP concentrations at locations isolated from local influences. This pattern is consistent with expectations that the relative concentrations of TSP, PM10, and PM2.5 mainly reflect their relative emission fraction close to a PM source and that the relative contribution of the larger, heavier particles would decline significantly with distance from a source.

Due to deposition and dispersion, atmospheric TSP concentrations decline substantially from the populated areas and roadways (Lake Forest – north, SOLA – south) to piers (Coast Guard pier – north, Timber Cove pier – south). Low population and low vehicular traffic areas (Bliss – west shore & Thunderbird – east shore) have dramatically lower TSP concentrations (1/5 of the high population, high vehicular traffic locales). Mid-lake TSP concentrations (buoys west & east) were similar to areas with minimal local emissions. Depending on wind direction, the closer a sampler was to vehicular traffic, the higher the TSP concentrations tended to be. Furthermore, the use of continuous monitors (BAM) rather than filter samples, frequently documented large temporal changes in PM concentrations when wind directions changed as well as documenting that the highest TSP and PM10 concentrations occur during the morning and evening commute periods, especially when winds were light and temperature inversions were present near ground level. These observations strongly support the hypothesis that roadways and vehicular traffic are a major source of atmospheric TSP and PM10 in the Tahoe Basin.

The majority of the PM mass is composed of (in order of total mass) soils, organic materials, particulate nitrogen, and elemental carbon. The composition of the PM also supports the hypothesis that roadway traffic is a major source of TSP emissions in the Tahoe Basin.

The observations and conclusions for PM_fine (i.e., PM2.5) have some similarities with and differences from those of the larger particles. First, the highest concentrations of atmospheric PM2.5 were also observed in places with the highest population and greatest vehicular traffic while the lowest PM2.5 concentrations were observed at the more remote Thunderbird site. At the locations with high PM concentrations (i.e., Lake Forest, Sandy Way, & SOLA), the PM2.5 mass was 30% to 40% of the TSP mass. At the location with low PM concentrations (Thunderbird), PM2.5 comprised 60% of the TSP mass. Seasonal PM2.5 at high concentration locations was much more variable than observed for the larger PM particles, with the only common feature being that the lowest PM2.5 concentrations occurred during spring. PM2.5 concentrations at the low concentration location (Thunderbird) varied seasonally, being highest during summer, lower in fall, lower still in spring, and lowest during winter.

Likewise, particles collected close to a source of gaseous or fine particle emissions are expected to contain more of the volatile chemical species such as nitrates and ammonium ion in the fine fraction. Far from a source, atmospheric processes are likely to allow accumulation of some of these volatile species onto larger particles. At locations with high PM2.5 concentrations (Lake Forest, Sandy Way, & SOLA), nearly all ammonium ions and 70% to 85% of the nitrate ions were in the PM2.5 fraction. At the location with lowest PM concentrations (Thunderbird), more than 35% of the ammonium ion and 55% of nitrate ions are in the PM_fine size fraction. The nighttime increase in PM2.5 observed at SLT-Sandy Way during the winter indicates that wood smoke is a contributor to PM2.5 concentrations.

8.2.2 Insights

The historical dry deposition measurements by the TRG rely on surrogate surface samplers, which can potentially capture any size of particle, including very large particles (e.g., insects, plant detritus, and pollen). These large particles, which can be seen in the air near sources, have relatively short atmospheric lifetimes and typically do not transport more than a few tens or hundreds of meters. In contrast, these large particles are not measured by typical air quality sampling instruments. Thus, the type of sampling equipment and the proximity to local PM sources can drastically affect measurements and interpretations of the data.

A series of dust experiments that were conducted between the shoreline and a road demonstrated that particle number concentrations, especially for larger particles, decline significantly from the roadway to the shore. Although deposition and dispersion from roadways to the shoreline and potentially to mid-lake are not completely characterized by these spatially and temporally limited measurements, it is clear that local emission sources and their proximity to the lake are important. Additional characterization of spatial variations in particle number and concentration and the resulting refinement of annual deposition estimates would require additional measurements.

8.3 Nitrogen

8.3.1 Findings

Total nitrogen concentrations (both gaseous and particulate) were observed at the four in-basin TWS sites. At all these sites, particulate N amounted to no more than 5% to 10% of the TSP mass. However, the particulate N accounted for roughly 30% of the total N observed in high-traffic, populated areas but an even greater 60% of the total N observed in the less populated receptor areas. Inversely stated, gaseous N (i.e., ammonia and nitric acid) comprised 60% to 80% of the total N at the high N sites while only 40% of total N was gaseous N at the low N site.

Ammonia concentrations were highest at SOLA, followed by Sandy Way, Lake Forest, and lowest at Thunderbird Lodge. Nitric acid concentrations followed a similar pattern. At the locations with the highest concentrations (SOLA, Sandy Way, and Lake Forest),

ammonia concentrations peaked during winter and fall, were lower during summer, and lowest during spring. At the site with low ammonia concentrations (Thunderbird), ammonia concentrations peaked during summer-fall and were lowest during spring-winter. Much higher ammonia concentrations were measured in South Lake Tahoe. Nitric acid concentrations in the southern Tahoe Basin were highest in winter, lower in fall, lower still in summer, and least in spring. Nitric acid concentrations in the northern Tahoe Basin were highest in summer-fall and lowest in spring-winter. Thus, substantial seasonal differences were seen between nitric acid concentrations at Lake Forest and South Lake Tahoe.

Particulate nitrogen (ammonium and nitrate ions) concentrations from the TWS and MVS networks were difficult to compare because TWS was equipped with back-up filters for catching nitric acid (but not ammonium ion) and MVS was not. Nevertheless, observed particulate nitrogen concentrations differed between the southern, northern, and remote locations. The particulate N concentrations were 25% higher at South Lake Tahoe (SOLA & Sandy Way) than at Lake Forest and Thunderbird, where the study-average concentrations were roughly the same. West shore (Wallis Residence & Coast Guard) and east shore sites (Zephyr Cove) had generally lower particulate nitrogen concentrations than mid-lake buoys. Mid-lake particulate nitrogen concentrations most resembled concentrations at the south shore (Timber Cove).

8.3.2 Insights

Ammonia and nitric acid measurements are technically difficult and the denuder method provides no exception to these difficulties. Separate measurements were not made for nitrous acid, but nitrous acid concentrations are a positive artifact in the HNO_3 measurements. Thus, nitrous acid was represented in the HNO_3 measurements and the subsequent estimates of nitrogen deposition. The stability of ammonia measurements over the two-week sampling period was a significant unanswered issue. No mid-lake gaseous nitrogen data were collected.

Particulate nitrogen observations were limited by lack of a back-up filter for ammonium ion and no back-up filters for other volatile species. For samples collected with the MVS, almost half of the ammonium ions and likely a molar equivalent amount of the nitrate ions may have been lost because back-up filters are not feasible with this instrument.

8.4 Phosphorus

8.4.1 Findings

From over six hundred possible (TWS & MVS) ambient samples, zero samples were observed with concentrations above the measurement uncertainty limits. Interestingly, the four highest concentrations greater than 15 ng/m^3 (minimum detection level) were recorded for Thunderbird Lodge (27.3 ng/m^3; invalid due to low air flow), the Coast Guard pier (21.0 ng/m^3), Lake Forest (16.4 ng/m^3), and SOLA (15.1 ng/m^3).

Based on reanalysis of the filters by UC Davis using a different X-Ray Fluorescence (XRF) method with better limits of detection, it appears that the originally quoted limits of P detection (based on a pure sample) were two or more times lower than under real-world conditions where silicon (Si) and sulfur (S), which have XRF signals that overlap with that of P, are common elements in the PM sample. Often when the original data indicated high concentrations, the reanalysis indicated low concentrations and vice versa. Thus, there was difficulty in detecting P, not only for ambient samples but also for source samples.

Although staff attempted a number of different methods, it is apparent that atmospheric phosphorus is very difficult to measure. With XRF, the primary method used in LTADS, the P measurement is subject to interference from overlapping signals of other, much more abundant elements in ambient PM samples, which have a large soil component. Furthermore, the x-ray emissions can be self absorbed by other P atoms in the particle. The magnitude of the correction for this self absorption depends strongly on the size and composition of PM greater than 2.5 µm. Based on analyses of measurement uncertainties, source profiles, P concentrations reported for other non-urban areas of the State, and so forth, staff concluded that the average P concentration in the Tahoe Basin is between 20 and 40 ng/m^3, with the upper limit very unlikely to be exceeded as an annual average for the Basin.

8.4.2 Insights

Using standard methods, P measurements are difficult in ambient PM due to interferences from S and Si. LTADS attempted alternative methods to measure P such as the Inductively Coupled Plasma Mass Spectrometry (ICPMS); however, this alternative method was not helpful. The synchrotron XRF method used by UCD showed improved measurement sensitivity but did not detect a higher maximum P concentration than reported by standard XRF. Additional review indicated that the current analytical quantification techniques, which are reasonable for small particles (PM2.5), are likely not appropriate for large particles due to greater self absorption of the x-rays. The self absorption corrections depend strongly on the size, composition, and distribution of P (also Si and S) within the particle, information not generally available.

8.5 Air Pollution Transport

8.5.1 Findings

The transport of pollutants in any significant measure from the San Francisco Bay Area and Sacramento Valley air basins to the Tahoe Basin is counter-indicated by meteorological processes. Upslope surface winds are typically too slow to transport significantly high concentrations of pollutants the full distance to the Tahoe Basin before surface winds reverse in the evening (due to density-driven drainage flow as the mountain slopes cool). Big Hill was established as a comprehensive monitoring site upwind of the Tahoe Basin during LTADS. This site was also located well away from local influences and well situated to provide a good indication of any potential for

regional and global transport impacts. However, because Big Hill is below and west of the crest of the Sierra Nevada, it is possible for pollutants to reach Big Hill but still not reach the Tahoe Basin. Furthermore, any air flow over the Sierra crest, whether at the surface or aloft, would also need to be mixed vertically down to the lake surface; this mixing with typically cleaner air would dilute pollutant concentrations before reaching the Lake.

In addition to the physical (geographical and meteorological) constraints, deposition and chemical reactions also act to reduce the impact of pollutant transport. Although the mountain counties receive some air parcel transport from Sacramento, Bay Area, and San Joaquin Valley air basins, reactive nitrogen species, such as nitric acid, nitrates, and total reactive nitrogen (NO_Y) probably do not survive sufficient time to be transported in significant measure from the San Francisco Bay Area, San Joaquin, and Sacramento air basins to the Tahoe Basin. Organic nitrates tend to have longer lifetimes in the atmosphere than other nitrogen species but they also have low deposition velocities. In general, when local pollutant sources are present, they will exert more influence on ambient concentrations than do upwind NO_Y sources.

Measurements during UCD aircraft flights over the lake in late summer and fall of 2002 indicate the possibility of ammonia transport. During a boat sampling transect along the western shore of the Lake late one afternoon, a spike observed in ozone and PM_fine concentrations indicated the possibility that an aged, polluted air mass was transported through a col in the Sierra Nevada crest.

The peak TSP concentrations at Big Hill occurred during summer and fall (50% higher than the rest of the year). During summer and fall, the southern and northern regions of Tahoe had 25% more TSP than Big Hill. These seasons have potential for both transport (due to longer days and solar induced upslope air flows) and local dust emissions (due to increases in traffic with dry conditions).

8.5.2 Insights

Local emissions account for most of the observed concentrations of air pollutants that are higher than typical regional and global background levels in the Tahoe Basin. However, some primary pollutants (such as ammonia) that have abundant and ubiquitous upwind anthropogenic and natural sources and secondary pollutants, such as ozone, may survive the transport processes (e.g., mixing, dilution, deposition). Transport may contribute to increased background concentrations of ammonia and ozone in the Tahoe Basin. Meteorological process and ambient air quality data do not support the concept of 1-day transport to the Tahoe Basin of highly polluted air masses.

No significant wildfires occurred during LTADS and so staff collected no ambient data to address the magnitude of the impact of smoke from wildfires on N, P, and PM deposition to the Lake. Wildfires undoubtedly input a large amount of these pollutants into the atmosphere as has been confirmed by specie profiles of source samples as well as limited ambient measurements in smoke plumes. However, the magnitude of the actual impact depends on the size, location, and duration of the fires as well as the

associated meteorology (elevated plumes, inversion layers, wind direction). The actual deposition to the lake of these emissions, which are limited in time and space relative to year-round processes, is not easily known. It is not obvious to staff that smoke plumes from episodic large-scale fires outside the basin, although impressive in their immediate impact, are likely to contribute much to the annual loading of PM, P, or N to the lake itself.

8.6 Source Characterization

LTADS source characterization efforts were intended to improve understanding of a few selected sources with potentially significant contributions to atmospheric deposition. The LTADS efforts related to the Tahoe emission inventory in no way represent a comprehensive assessment or characterization for emissions within the Tahoe Basin. With this in mind, staff cautiously offers the following summary.

8.6.1 Findings

LTADS provided detailed (though by no means definitive) characterization of particles associated with road dust and wood smoke from prescribed fires and wood stoves. On average for wood smoke (PM10 & PM2.5 filter) samples, nitrate concentrations were 0.15%, ammonium ion was 2.55%, and P was below 0.01%, while organic carbon comprised 49% and elemental carbon nearly 9% of the mass. The source specific wood smoke results are very similar to the neighborhood wood smoke results.

On average for roadside dust samples, PM nitrate concentrations were 0.25%, ammonium ion was 0.46%, and P was not detected, while organic carbon was 34%, elemental carbon was 8%, aluminum was 3%, and silicon was 12% of the mass on the filters (PM10 & PM2.5).

Multiple experiments and data analyses indicated that motor vehicles and population centers exerted a strong influence on PM, ammonia, and NO_y concentrations. The BAM PM2.5 measurements on the rooftop at Sandy Way exhibited a clear impact of wood smoke during winter evenings.

8.6.2 Insights

Very low concentrations of P and particulate nitrate in the wood smoke samples support the hypothesis that wood smoke is not likely a significant source of P and particulate nitrate. Ammonia might be emitted in significant quantities in wood smoke but these measurements did not include gaseous data collection. LTADS source characterization efforts had insufficient resources to properly compare particulate nitrate and ammonia emissions from these natural combustion sources versus motor vehicles.

The December 14, 2005 LTADS workshop at Tahoe concluded that gathering basic information in both California and Nevada (e.g., population, land use, prescribed burning, wildfire, visitor information, and hotel/motel occupancy data) was still an unmet need for developing proper emission inventories for the Tahoe Basin.

8.7 Meteorology

LTADS meteorological instrumentation included remote sensing equipment to characterize the upper air, including mini-sodars (measuring horizontal winds within 100 meters of the ground level), radar wind profilers (vertical and horizontal winds from 100 meters up to several kilometers above ground level), and radio acoustic sounding systems (temperatures from 100 meters to nearly one kilometer above ground level). In work not sponsored by LTADS but applicable to addressing LTADS issues, the Desert Research Institute (Professor Gayle L. Dana) conducted micrometeorological measurements (vertical flux of heat, water vapor, and momentum) within a few meters of the Lake surface. All of these data are in the early stages of analysis.

8.7.1 Findings

Winds observed at surface sites in the Tahoe Basin display temporal regularity with daily oscillation between onshore and offshore flow due to the mesoscale influences. However, spatial variations are important as well. In particular, the on-shore and off-shore flows have complexities in terms of their horizontal extent and their depth which are not defined by point observations. In some areas of the Lake (e.g., east and northwest), the interaction of meso- and synoptic scale influences can regularly result in flows parallel to the shore with little transport of air pollutants from the shoreline onto the Lake.

8.7.2 Insights

Characterizing the spatial variability of the winds at Tahoe is a challenge due to the forested nature of the Basin and the small scale terrain influences that limit the spatial representativeness of any near ground measurements. Because the mini-sodars are much quieter and require less space and power, they are easier to site than radar wind profilers with RASS, but they do not serve the same purposes. The vertical range of mini-sodars is much less and depends in part on the specific humidity, which is limited by the cooler temperatures at Tahoe compared to lower elevations. The vertical range of the mini-sodar is also limited by ambient noise. Flows below a few tens of meters, which are critical for estimating atmospheric deposition to the Lake, are strongly influenced by the most local terrain features, especially during drainage flows. Flows to a few hundred meters or more above ground level can be strongly influenced by the thermal differences between land and lake surfaces and by the larger scale terrain features.

8.8 Surrogate Surface Deposition Methods

LTADS included a special study to compare surrogate surface methods of measuring dry deposition. It was hoped that the analysis would provide consistent relationships that would permit deposition measurements among surrogate surface samplers to be reconciled. However, the limited and variable results in the surrogate surface methods comparison precluded definitive relationships and adjustment of historical data to better characterize the actual deposition associated with the most representative method. Wet

and dry deposition assessments based on ambient air quality data and meteorological conditions provided in this report were in crude agreement with measurements during 2003 by the TRG bucket method.

8.8.1 Findings

The continuous water surrogate surface deposition sampler (WSS), which conceptually would provide the most representative measurement of dry deposition to a water surface, will require upgrades to increase its robustness for field comparisons with the "buckets." Wind action, deposits of plant and insect materials, and desiccation all create difficulties in interpreting surrogate surface deposition data or making comparisons with deposition estimates calculated from meteorological and air quality data.

8.8.2 Insights

Improved siting of the "bucket" samplers would improve comparability with air quality measurements. An improved operational design for the WSS would include shorter periods for sample collection (e.g., 24-hour) and sample analysis (e.g., weekly).

8.9 Potential for Future Research and Utility of Narrowing Uncertainty in Deposition Estimates

The primary purpose of LTADS was to provide an independent estimate of the direct atmospheric inputs to Lake Tahoe of air pollutants potentially reducing water clarity. These estimates were used in developing a TMDL that incorporates pollutant inputs to the lake from air, streams, land, and underground. The ranges of the lower, central, and upper estimates of atmospheric deposition incorporate both uncertainties in the measurements and scientific judgments of the possible effects of poorly known sources of variation, such as particle size distributions. The range of estimates provided in the main body of the report (Chapters 4, 5, and 8) and in Appendix M also reflect judgments about spatial variability of concentrations and deposition velocities as they may differ from the conditions at the monitoring sites, due to the distribution of sources, drainage winds around the lake, and upper level winds over the lake.

The significance of uncertainties in the deposition estimates is not the numbers themselves but the relative benefit it would make to the TMDL and Tahoe Basin water quality control programs if the ranges for the estimates of deposition were narrowed. More specifically, the range of estimated deposition rates is only an issue for those pollutants for which the TMDL interpretation or list of possible control options is different for the upper and lower estimates. For example, if even the lower estimate for a pollutant's input to the lake is deemed excessive in the TMDL, then narrowing the range would have no regulatory significance. Conversely, if even the upper estimate for a pollutant's input is deemed insignificant in the TMDL, then narrowing the range also would have no regulatory significance. Similarly, if the list of potential emission control strategies for a particular pollutant would not be different at either end of the range, then

narrowing the range of deposition estimates for that pollutant would have no regulatory significance.

If the TMDL review or subsequent development of water quality control strategies determines that strategies should differ substantially if the actual atmospheric deposition rate falls at one end of the range of estimates versus the other, then there is practical reason to attempt to narrow the range of estimates. In this case, the potential for additional research to narrow the range of estimates would presumably be critically considered along with the cost and the probability of successfully delivering more definitive information. The following paragraphs summarize and comment upon potential research approaches, some of which the LTADS investigators believe, based on their experience, would be productive avenues to narrow uncertainties in the atmospheric deposition estimates.

As air quality specialists, the LTADS investigators cannot anticipate how the current estimates will be used in the TMDL process, nor can they anticipate which, if any, of the ranges of estimates will leave uncertainty in the selection and priority of potential strategies for mitigation. Indeed, some of the choices for mitigation strategies may be entirely dependent on best available controls and independent of the current range of deposition estimates.

The following discussions are intended solely as informal guides to help the responsible agencies understand the types of research efforts that the LTADS investigators believe would be more or less productive for narrowing uncertainties *assuming such a narrowing is deemed necessary*.

8.9.1 Potential Approaches for Narrowing Estimates of Nitrogen Deposition

If refinement of nitrogen deposition estimates would lead to changes in mitigation methods, there are several potential approaches that could be considered. Better spatial and temporal resolution of ammonia and nitric acid concentrations through land-based measurements might be less valuable than making on-lake measurements. However, land-based measurements would probably be more feasible and would improve the estimates of deposition and increase understanding of the possible sources. This information could also be important to planning the locations of on-lake measurements, if those are pursued. Some attention to South Lake Tahoe as the location with higher concentrations of gaseous nitrogen concentrations and possible nitric acid measurements at northern Tahoe basin might be warranted. In spite of the logistical difficulties, if nitrogen deposition estimates need to be narrowed, then collection of gaseous nitrogen concentrations over mid-lake areas would be an important additional measurement.

Particulate nitrogen concentrations could also be considered but appear to be much less important to the total nitrogen input. Although particulate nitrogen was not a large contributor to the estimated deposition of total nitrogen, simultaneous observations of gaseous and particle nitrogen would provide a better view of the overall nitrogen

chemistry. Similarly, back-up filters for volatilized ammonium and nitrates would be warranted, if additional particulate nitrogen measurements are needed.

A more difficult and less useful approach to quantifying concentrations over the Lake would be to directly measure the advection of nitrogen species across the shoreline. This would be difficult due to requirements for vertical resolution and also because of the limited temporal resolution of the current measurement methods for ammonia and nitric acid. The following is not necessarily recommended but is included as a cautionary note. If multi-hour sampling times were required to acquire sufficient sample volume or control analytical costs, then longer term sampling, conditioned on wind direction, should be considered. It would be unwise to commit to such a program, however, prior to the demonstration of its feasibility through rigorous pilot projects.

8.9.2 Potential Additional Research on Phosphorus

If a narrowed range of estimates of phosphorus deposition would alter mitigation decisions, then the first need would be for better quantitative measurement of P concentrations in particles and source materials. For improved measurement methods, additional preparatory research would be needed to quantify the self absorption correction factors appropriate for large particles that are typically found in road dust. Pilot studies to ascertain the implications of field and lab blank concentrations on a site-by-site basis would also be required.

Improved characterization of the spatial variations in phosphorus concentrations would also be a key element of refined estimates of deposition. Thus, collection of samples over the Lake would be very important.

More definitive information on the P content of Tahoe-specific soils, pollen, plant detritus, wood smoke, prescribed fires, and motor vehicle emissions are all potential avenues for improvement of P deposition estimates and water quality control decisions.

Improved characterization of the size and sources of particles could potentially supply phosphorus to the Lake would also be a key element in the refinement of deposition estimates. We note that there is a potential mismatch between sampling methods due to differences in collection efficiencies based on particle size. Air quality monitoring is generally not intended to collect the very large particles with relatively high gravitational settling velocities. On the other hand, P deposition estimates with wet/dry bucket surrogate surface sampling, if located near a source of large particles, would likely collect those larger particles (and if very near such a source might over-represent such particles). Larger particles may include natural materials such as plant detritus or pollen.

8.9.3 Potential Additional Research on Wind Fields

Three-dimensional wind fields for the Tahoe Basin could be developed to resolve more of the complexities of transporting particulate matter and nutrients from the shoreline to mid-lake. If wind field development is undertaken with modeling, it should be with the

recognition that the existing upper air measurements, although ambitious and not previously available for Tahoe, are still very limited compared to the spatial complexity they are intended to represent. In particular, within the Basin, only one measurement location (South Lake Tahoe Airport) provides wind or temperature data at heights above the limited vertical range of the three mini-sodars. Thus, extensive evaluation of the performance of meteorological models is probably not possible with the existing data. However, the LTADS RWP/RASS and mini-sodar data are available for comparison with the 2003 wind and temperature fields developed by the MM5 modeling that was conducted to create the historical database of precipitation and freezing levels necessary for the watershed runoff modeling. Such a comparison effort would provide spatial and temporal reference points for characterizing the general performance of the MM5 model used in the precipitation runoff analyses.

The LTADS meteorological data and the previously collected flux data, such as Professor Dana's work, should be fully analyzed and evaluated before additional measurements are considered. Using these data, we recommend a fuller exploration of wind trajectories and the fluxes at the lake surface-air interface.

If future studies attempt the ambitious task of more fully characterizing 3-dimensional meteorological fields, then additional upper air measurements, such as additional radar wind profilers with RASS or episodic deployment of rawinsondes, should be considered to provide more complete spatial coverage for areas around the lake where RWP/RASS cannot not be sited. With additional measurements, there would be the potential for a robust evaluation of the performance of meteorological models; for example, evaluations for simulations overlapping periods with supplemental upper air (e.g., rawinsonde) observations. Such a program might include instrumentation on additional buoys and releasing rawinsondes from multiple piers. If well-designed, there might be a potential for co-funding for such a measurement program from parties with a purely meteorological interest.

8.9.4 Potential Additional Research for Direct Observation of Air-Water Fluxes

Although an ambitious meteorological program may not be justified solely for refinement of deposition estimates, there would be benefit in obtaining simultaneous flux measurements of the exchange of momentum, heat, and water vapor between the atmosphere and the lake. Consideration of a more complete suite of measurements could potentially attract expertise and funding from the boundary layer meteorology community.

A very useful observation would be direct measurements to characterize vertical fluxes over the lake (i.e., the exchange of some trace gases or particles between the atmosphere and the water surface). Such measurements, possibly by eddy covariance method, would require great care for site selection and evaluation of spatial representativeness. If eddy covariance observations of trace gas or particle fluxes are not logistically or financially feasible, eddy covariance measurements of meteorological (momentum, water vapor, and heat) fluxes, could still be possible. They would be useful for comparison with those values inferred in the course of estimating deposition

velocities. The realities of constraints on access to potential sites and limitations of those sites with respect to representative results should be considered along with their implications for the usefulness of the resulting measurements. Only with such a view could the potential value of flux measurements be realistically weighed against the direct costs and opportunity costs.

8.9.5 *Potential Additional Research* of Surrogate Surface (Bucket) Samplers

The relative loading of surrogate surface samplers, compared with the rate of dry deposition to water, may differ with environmental conditions such as wind speed and with particle size or chemical characteristics of gases. The dependencies and variability are complex and have not been quantified. Thus, interpretation of results is problematic. These issues are universal to many studies beyond Tahoe and have not been resolved. An additional controlled experiment with a water surface sampler, the "buckets," and air quality measurements could be considered to provide a rough guide for comparisons. However, because multiple variables are likely important, such a comparison should not be expected to provide a formula for translating results between methods. Equally, or perhaps more significant, for any deposition sampling with surrogate surface samplers in the Lake Tahoe Basin are the practical issues of siting the samplers to ensure better spatial representativeness of the measurements.

8.9.6 Potential Additional Research of Atmospheric Budgets by Direct Observations

In theory, atmospheric budgets based on measurements could be helpful to constrain the estimates of deposition to the lake. Some have suggested observation-based budgets to characterize the advection of pollutants into and out of the Tahoe Basin. However, the spatial complexity of the Basin boundaries and logistical constraints (e.g., lack of potential sites with electrical power), and potential differences in concentration in and above the forest canopy make such an endeavor logistically infeasible. The spatial and temporal complexity of winds, vertical mixing, and concentrations would also make it very difficult to construct an observationally based pollutant budget for a mass balance of advection and deposition over the lake. Although a pollutant budget for the atmosphere over the Lake might be possible, significant uncertainties (e.g., due to undefined variation in vertical mixing with distance downwind from the shoreline) would remain despite large expenditures for a reasonable density of observations. Such an atmospheric budget would require a vast increase in monitoring resources compared to those utilized in LTADS.

To illustrate the complexity and resources required, note that vertical profiles of pollutant concentrations and winds would be needed to characterize advection (horizontal flux across a vertical plane near the shoreline) as one element of such a program. A high density of measurements would be required due to the spatial complexity of the terrain, meteorological fields, and concentrations. Vertical profiles are difficult and expensive to determine and ideal measurement heights to characterize profiles of concentration could be expected to differ between pollutants. Temporal differences associated with wind shifts are also a concern. Some species are currently only measured with filters or

denuders that require relatively long sample times for sufficient sample volume. Thus, for some chemical species, it might only be feasible to sample conditionally, based on wind direction, to provide some inference of temporal variations necessary to characterize horizontal fluxes. The possible benefits of such measurements should only be considered in the context of the resources required and realistic acknowledgement of the uncertainties that would likely remain. They should not be undertaken without successful demonstration of methods via smaller pilot studies.

8.9.7 Potential Additional Research of Transport

Although literature reviews and additional analysis of the historical and LTADS data could provide more insights on the relative importance of local and transported emissions, the results are unlikely to be as quantitative as desired due to the limited number of monitoring sites and the complex topography and meteorology.

Definitive direct monitoring of transport above the surface layer is difficult and expensive in any setting. Further, for the Tahoe Basin, the complex meteorological setting and the relatively clean air near and within the Basin makes it difficult to differentiate a transport component from the natural and local components. Observational studies with sufficient horizontal and vertical resolution to more accurately quantify transport would be very expensive, if feasible at all. The cost seems far out of proportion to any benefit of small improvements in quantification. For these reasons, staff has not recommended additional air pollution measurements to assess transport.

8.9.8 Potential Additional Research of Emission Sources

Atmospheric phosphorus that could participate in deposition appears to be primarily of geological origin. However, natural input of phosphorus from plant detritus may also be important. Possible contributions of phosphorus by smoke from residential wood combustion, planned fires, and wildfires are likely minor compared to geological sources. However, despite this basic understanding of likely phosphorus sources, collection of more source profiles for refining pollutant emission factors may be useful to add certainty and guide control strategies. Additional enhancement of the fire database for the Tahoe Basin, including statistics such as acres burned (prescribed and wild fire), fuel condition, etc., could support more comprehensive analyses. Literature reviews and analyses of global air pollution transport may be of scientific interest and provide information on the possibility of P transport (e.g., in Asian dust) but is unlikely to be relevant to the selection of control strategies for phosphorus in the TMDL.

Compared to particulate nitrogen, gaseous ammonia and nitric acid appear to be far more important contributors to the total direct atmospheric deposition of nitrogen to the Lake. The emission sources for these compounds or their precursors have not been fully characterized and future investigations should also consider measurement difficulties.

8.9.9 Potential Additional Research to Improve Measurement Methods

Because ambient concentrations are low in the Tahoe Basin, many of the measurements were at, or below, the sensitivity of the measurement methods. Improved measurements of phosphorus, ammonia, nitric acid, and speciation of particulate matter would be helpful to the Lake Tahoe efforts. Improvement of measurement methods is a more general scientific need which, if addressed by the larger scientific community, could provide opportunity for further investigations in the Tahoe Basin. With improved sensitivities, better characterization of ambient concentrations and emission rates would be possible, especially for phosphorus, ammonia, and nitric acid.

8.10 Summary

LTADS was a multi-million dollar effort with contributions of funds and efforts by many agencies and groups. LTADS addressed issues of relevance to the TMDL stakeholders, providing refined atmospheric deposition estimates and improved understanding of emission sources and atmospheric processes. LTADS was the first atmospheric study to collect detailed ambient air quality samples continuously throughout a year. LTADS also featured continuous meteorological measurements aloft to better characterize atmospheric processes in the Tahoe Basin and enhance the data analyses and interpretations. LTADS thus collected a spatially and seasonally comprehensive database of atmospheric (air quality and meteorological) data which staff was unable to fully analyze and utilize in the preparation of this report. The LTADS approach provided estimates of dry deposition by a different method than previously used, confirming the N deposition estimate, refining the P deposition estimate, and providing a new PM deposition estimate. The estimates are based on observations representing the seasonal and diurnal variability of ambient concentrations and deposition velocities were calculated from hourly observations of meteorology and water temperature. In addition, to deposition estimates, the LTADS data allow important insights into probable sources of atmospheric deposition to the Lake. LTADS improved the understanding of many atmospheric issues relevant to development of the water clarity TMDL, but many issues may require further study. Staff summarized their LTADS efforts and participated in a forum to guide future research at a workshop in December of 2005. Presentations from this workshop are available on ARB's LTADS website (http://www.arb.ca.gov/research/ltads/ltads.htm).

ARB staff has also worked with the State Water Resources Control Board to sponsor a joint workshop on Atmospheric Deposition and Water Quality in February of 2006. Staff shared their insights and the presentations of this workshop are available on the State Water Resources Control Board's website (http://www.swrcb.ca.gov/workshops/atmos_pres.html). The ARB staff continues to work with the State and local Water Boards regarding the role of air pollution in additional water quality concerns.